APL-UW Deep Water Propagation:
Philippine Sea Signal Physics and North Pacific Ambient Noise

Final Report
Award Number N00014-13-1-0009

Dr. Rex K. Andrew, Principal Investigator

Applied Physics Laboratory

University of Washington

1013 NE 40th St.

Seattle WA 98105

phone: (206) 543-1250 fax: (206) 543-6785

`rex@apl.washington.edu`

Prepared for:
Dr. Robert H. Headrick
Program Officer, Code 322OA
Ocean Atmosphere and Space Research
Office of Naval Research
875 N. Randolph Street
Arlington VA 22203

Date: October 15, 2015

Abstract

We proposed a program involving two inter-related components of ASW: signal and noise. Deep water signal propagation is largely thought to conform to existing physics models, whereas theories of signal statistic propagation are much less developed. We utilized the datasets from the Philippine Sea 2009 and 2010 experiments to investigate where some of these theories break down and where theory development is necessary. Our analysis showed that (1) there are small biases in the Munk-Zachariasen and Flatté-Dashen predictions of log-amplitude variance at 284 Hz at 107 km, (2) the Flatté-Dashen prediction of pulse spread at 200 Hz and 300 Hz at 510 km was quite accurate, unlike findings reported at lower frequencies and larger ranges, and (3) the observed pulse intensity distribution at 200 Hz and 510 km (near exponential) did not obviously follow from the observed pulse spread at 200 Hz and 510 km (very small). Two technical reports were written to document supporting advances in (1) modeling internal waves for long range acoustic propagation calculations, and (2) estimating internal wave strength using a single CTD cast. Our program to collect and quantify trends in the anthropogenic component of low-frequency ambient noise, generally attributed to distant shipping, produced some previously unpublished results from datasets spanning roughly 1994-2007 for seven low-frequency systems throughout the N. Pacific. These findings confirm that there has been a decrease in the ambient noise over this period. The primary data collection program was suspended early in the grant by order of the U.S. Navy. All archived data — some 18 years old — was upgraded to new media for long-term storage.

Objectives

Our primary objectives during this grant were to understand how the fundamental statistics of broadband low-frequency acoustical signals evolve during propagation through a dynamically-varying deep ocean, and how the oceanic ambient noise field varies throughout deep ocean battlespaces. Current models of signal randomization over long ranges in the deep ocean were developed for and tested in the North Pacific Ocean gyre. The first objective of this research is to determine the validity of these models in a region with different oceanographic features, specifically the Philippine Sea. The second objective is to continue an 18-year long experiment utilizing the North Pacific Ambient Noise Laboratory to determine whether models of oceanic ambient noise capture the spatial and temporal trends observed across the basin.

Summary of Results

Philippine Sea Analysis Our approach utilized a combination of at-sea measurements, theoretical modeling and computational simulations. Our primary measurement was a 54 h transmission exercise over a range of roughly 510 km. We transmitted the signals: the acoustic receptions (and associated receiver details) were provided by Worcester at Scripps, and the environmental measurements at the receiver provided by Colosi at the Naval Postgraduate School. The exercise used the "multiport" source and two simultaneous signals with carriers at 200 and 300 Hz. Each multiport signal had its own m-sequence law, allowing complete separation of the two signals in code space. Dr. Andrew White, an ONR Postdoctoral Fellow at APL-UW, conducted corresponding Monte Carlo parabolic equation simulations under ONR grant N00014-14-1-0218 which were reduced and analyzed under this grant for comparison to the at-sea measurements and the theoretical predictions.

North Pacific Ambient Noise Laboratory (NPANL) Our primary approach was to involve ambient noise collections 24/7/365 except for outages, on APL computers located at a remote facility. The hydrophones are located in the North Pacific basin. Data collection was suspended indefinitely in March 2014 by direction from the U.S. Navy.

The original budget breakdown for this grant is shown in Fig. 1. The primary objective was to spend most of the effort analyzing Philippine Sea 2009 and 2010 data. This was our first major experience working with the data from the Scripps "distributed vertical line array" (DVLA), which itself was an instrument embodying some new technologies. NPANL support was expected to be minimal; collecting data has only a minor on-going cost, but substantially more effort was expected to bring the existing raw datasets up-to-date. We envisioned using a combination of undergraduate and graduate students to assist.

The final cost breakdown is shown in Fig. 2. The effort envisioned for NPANL support was smaller than expected for two reasons: (1) data collection was suspended by the U.S. Navy, and (2) we decided not to archive the existing datasets to M●DISC technology. M●DISC technology uses special inorganic optical media which purportedly has a shelf life of 1000 years (as opposed to COTS organic optical media, which has a shelf life of 3-5 years per the manufacturers.) However, the M●DISC writers did not seem reliable. All ATOC-NPAL datasets were re-archived only to standard organic optical media. Almost all the NPANL-associated costs involved moving the deep water laboratory from one floor to another within APL-UW, and copying the ATOC-NPAL datasets. Minimal use of student support and retiree tech support occurred. No graduate student could be attracted to the proposed electrical engineering project because there was no associated path to a graduate degree,
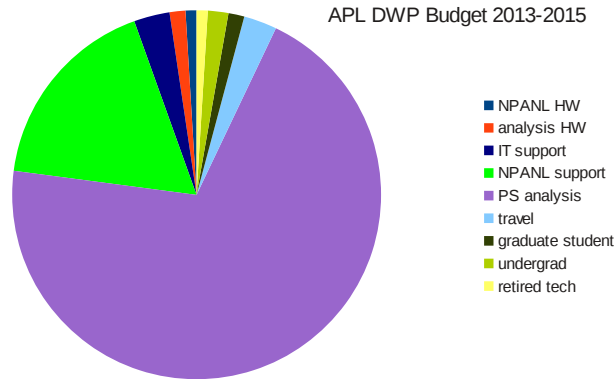
APL DWP Budget 2013-2015

- NPANL HW
- analysis HW
- IT support
- NPANL support
- PS analysis
- travel
- graduate student
- undergrad
- retired tech

Figure 1: Original grant funding breakdown.

(i.e., it was just a "job"), and therefore that project was delayed until data collection could be resumed.

Almost all travel costs supported Philippine Sea analysis. Information technology costs (e.g. administering our workstations and our computer cluster) were handled by grant performers. Most of the undergraduate student effort went into the first phase of DVLA data processing.

Numerous journal papers were produced during this grant period involving one or more grant performers as co-authors. Most of these papers appeared in a special issue of the *Journal of the Acoustical Society of America* on long range deep water propagation. These papers are cited at the end of this report.

Papers, articles and reports written primarily by performers under this grant are appended.

Detailed Results

Philippine Sea Analysis

- Our manuscript on a three-way comparison between the White *et al.* (2013) at-sea measurements of log-amplitude variance and Monte Carlo predictions of log-amplitude variance and Munk-Zachariasen theory predictions was accepted at the *J. Acoust. Soc.*

APL DWP Actual 2013-2015 Allocations

- NPANL HW
- analysis HW
- IT support
- NPANL support
- PS analysis
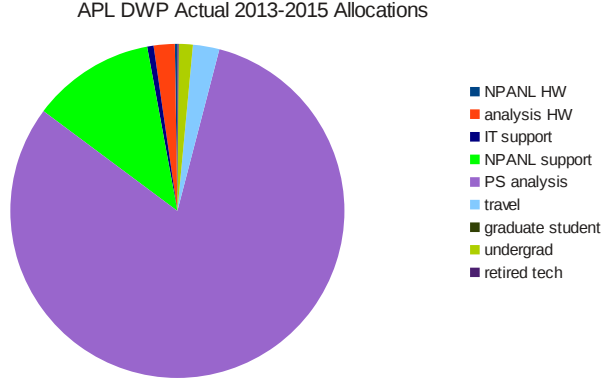- travel
- graduate student
- undergrad
- retired tech

Figure 2: Approximate final grant expenditure breakdown.

Am. [Appended.]

- An undergraduate student, Mr. Robin Mumm (junior, physics), was hired for some repetitive routine data-organization tasks. First, he computed the hourly spectrogram for every hour that APL transmitted to the VLA, in order for us to visualize and identify any interfering acoustic events. Second, he built a "database" for post-processed data products related to the APL PhilSea2010 acoustic experiments for sharing among researchers. Since the APL experiments utilized (after pulse compression) pulsed interrogation of the ocean, the primary database elements are the pulses themselves. He completed the population of databases for the red (200 Hz) and violet (300 Hz) multiport signals and the associated red and violet Monte Carlo parabolic equation simulation datasets provided by Dr. Andrew White, APL-UW.

- Ganse prepared a manuscript for the *JASA Express Letters* describing intensity and pulse spread statistics for the 510 km ocean acoustic transmissions at 200 Hz. The intensity distribution is near-exponential, indicative of the saturated scattering regime. The pulse spread is very small, indicative of the partially saturated regime. These two features should not occur together under the current theory. The underlying mechanism for this conjunction is not known.

  The manuscript presenting these results has been sent to co-authors for review. [Appended].

- We computed the spread of pulses observed during PhilSea10 for both the "red" and "violet" signals radiated simultaneously by the APL-UW multiport transmitter. These

5

two signals are m-sequences with carrier frequencies of 200 Hz and 300 Hz that correspond to the two multiport resonance frequencies of 210 Hz and 320 Hz. Multiple sections of branches of the timefront observed on the Scripps vertical line array at range 509 km could be resolved, yielding a rich dataset of pulses. Roughly 9000 pulses were transmitted for both the red and violet signals over 50 hrs. I compared the observed pulse spread against spread predictions obtained from CAFI. Additionally, Dr. Andrew White, APL-UW, conducted Monte Carlo parabolic equation simulations of the PhilSea10 scenario at 200 and 300 Hz, and my student extracted pulses from the simulated timefronts. This resulted in a dataset of 240 realizations for either 200 or 300 Hz for all corresponding sections of the timefront. Based on Gaussian-fits to the observed averaged wander-corrected intensity pulses, these results suggest that CAFI calculations are quite accurate for 19 to 20 total turning points. This is contrary to results published for much larger ranges. However, for increasing total turning points, the CAFI predictions seem to be developing an increasing over-prediction. This may be related to the longer range over-predictions.

A manuscript describing these findings has been submitted to the *J. Acoust. Soc. Am.* [Appended].

- We sent the entire RR1006 CTD dataset (this was the APL 2010 Philippine Sea cruise) to Peter Worcester. This included 55 CTDs in both original "raw" SeaBird format and a format post-processed at-sea to the Colosi NPAL specification.

- We ported the Henyey-Reynolds internal simulation code (Henyey and Reynolds, 2013) from Fortran to C++ for use in computer simulations. The underlying mathematics and several key test cases were described in an APL-UW technical memo. [Appended.]

- We compared the Henyey-Reynolds internal wave simulation code (Henyey and Reynolds, 2013) to the Colosi-Brown internal wave simulation code (Colosi and Brown, 1998) and found that the Colosi-Brown algorithm produces an internal wave field with a slightly bias in energy. This was found to be due to the shape in the horizontal wavenumber domain of the support for the random spectral components, which had been optimized for use with 2-D DFTs (Colosi, personal communication.) This result was presented at the 2013 Pacific Rim Underwater Acoustics Conference, Hangzhou, China. [Appended].

- We developed a method to estimate the strength of an internal wave field using a single CTD cast. Traditionally, the estimation of internal wave strength requires a mooring with autonomous CTDs deployed for roughly one month or more. (Colosi *et al.* (2013).) This method filters the single cast data into a high wavenumber component (indicative of small-scale internal wave fluctuations) and a low wavenumber component, which is

indistinguishable from the background sound speed profile and gives no information on the large scale internal wave fluctuations. Using this method, Henyey and Ganse analyzed data from the 2004 LOAPEX experiment and the 2009 and 2010 Philippine Sea experiments. The internal wave energy in the Philippine Sea was generally seen to be higher than in the LOAPEX experiment. Spice fronts were also evident.

This method and the results are fully described in an APL-UW technical memo. [Appended.]

North Pacific Ambient Noise Laboratory

- Undergraduate student M. Sven, Physics, processed all the data for seven receivers (previously never processed) located throughout the North Pacific in order to support a special session talk at the Acoustical Society of America on ambient noise trends, San Francisco, 2013.

- Undergraduate student B. auf der Springe (Electrical Engineering) assembled an interface box for fanning out a single GPS clock to multiple clock-driven systems at NAVOCEANPROFAC.

- Andrew moved our hardware laboratory to a new room at APL-UW.

- Andrew moved our CUI Data Center to a new room at APL-UW.

- Andrew moved our Secure Data Center to a new secure room at APL-UW.

- At the request of NAVOCEANPROFAC, we removed all our APL-UW equipment from a blockhouse in Coos Bay, OR.

- Andrew met with N2N6F24 to discuss the status of authorization for the NPANL ambient noise collections. Related to this, we researched our old ATOC files and assembled a package of relevant CNO letters, emails and agreements to support an N2N6 inquiry into the current status of our collection program.

- Andrew re-archived all the ATOC/NPAL/NPANL optical media. Some of these discs are 15+ years old, and there is a considerable concern that some of these data could "evaporate". (Low-cost organic dye optical media is thought to have a shelf-life of about 3 - 5 years.) The first step in this process loaded the data onto the computer hard drive. The data were reorganized into DVD-sized directories, effecting a compression for the early CDs of about 7 input discs to 1 output disc. The second step wrote the content to fresh DVDs.

- Andrew was invited to give a lecture at the International Whaling Commission Scientific Committee Workshop on Predicting Sound Fields, in Leiden, Netherlands on "Collecting and Curating 20+ years of Low-Frequency Ambient Sound", 15-16 April 2014.

- Andrew teamed with Wilcock, Stafford and Odom to write an Annual Review article on low frequency (1 - 100 Hz) ambient noise in the ocean. [Appended.]

- Andrew wrote a short article on an apparent "noise hole" in the Northeast Pacific, based on APL-UW measurements. This appeared in the *J. Ocean Technology*, 2014. [Appended.]

- The science plan for the International Quiet Ocean Experiment finally passed all reviews and was published by SCOR-POGO. Andrew was one of the co-authors. [Appended.]

Publications

The following is a list of publications from this grant involving at least one performer from this grant as a co-author. Papers containing significant content provided by a grant performer are appended and noted as such.

[1] RK Andrew, AW White, JA Mercer, PF Worcester, MA Dzieciuch and JA Colosi, "A test of deep water Rytov theory at 284 Hz and 107 km in the Philippine Sea", *J. Acoust. Soc. Am.* **138**(4) pp 2015-2023, October 2015. [Appended].

[2] RK Andrew, "Is there a "Noise Hole" in the Northeast Pacific", *The Journal of Ocean Technology*, **9**(1), pp 48-49, (2014), [published, refereed]. [Appended.]

[3] WSD Wilcock, KM Stafford, RK Andrew, RI Odom, "Sounds in the Sea at 1-100 Hz", *Ann. Rev. Mar. Sci.* 6, pp 117-140 (2014) [published, refereed]. [Appended.]

[4] HC Song, BM Howe, MG Brown, RK Andrew, "Diversity-based acoustic communication with a glider in deep water (L)", *J. Acoust. Soc Am.* **135**(3), pp 1023-1026, (2014), [published,refereed]

[5] FS Henyey, JA Mercer, RK Andrew and AW White, "A method to determine small-scale internal wave and spice fields from a single CTD profile with application to three long-range ocean acoustics experiments", Technical Memo TM 1-14, Applied Physics Laboratory, University of Washington, 2014 [published,non-refereed]. [Appended.]

[6] RK Andrew, "Comparisons of Methods for Numerical Internal Wave Simulation in Long Range Acoustical Propagation", 4th Pacific Rim Underwater Acoustics Conference 2013, October 11-13, 2013, Hangzhou China. [submitted] [Appended.]

[7] AW White, RK Andrew, JA Mercer, PF Worcester, MA Dzieciuch, and JA Colosi, "Wavefront intensity statistics for 284-Hz broadband transmissions to 107-km range in the Philippine Sea: observations and modeling I", *J. Acoust. Soc Am.* **134**(4), pp 3347-3358, (2013), [published,refereed]

[8] TK Chandrayadula, JA Colosi, PF Worcester, MA Dzieciuch, JA Mercer, RK Andrew, and BM Howe, "Observations and transport theory analysis of low frequency, long range acoustic mode propagation in the Eastern North Pacific Ocean", *J. Acoust. Soc Am. J. Acoust. Soc Am.* **134**(4), pp 3144-3160, (2013), [published,refereed]

[9] TK Chandrayadula, KE Wage, PF Worcester, MA Dzieciuch, JA Mercer, RK Andrew, and BM Howe, "Reduced rank models for travel time estimation of low mode pulses", *J. Acoust. Soc Am.* **134**(4), pp 3332-3346, (2013), [published,refereed]

[10] RA Stephen, ST Bolmer, IA Udovydchenkov, PF Worcester, MA Dzieciuch, RK Andrew, JA Mercer, JA Colosi, and BM Howe, "Deep seafloor arrivals in long range ocean acoustic propagation", *J. Acoust. Soc Am.* **134**(4), pp 3307-3317, (2013), [published,refereed]

[11] IA Udovydchenkov, MG Brown, TF Duda, PF Worcester, MA Dzieciuch, JA Mercer, RK Andrew, BM Howe, and JA Colosi, "Weakly dispersive modal pulse propagation in the North Pacific Ocean", *J. Acoust. Soc Am.* **134**(4), pp 3386-3394, (2013), [published,refereed]

[12] PF Worcester, RK Andrew, AB Baggeroer, JA Colosi, GL D'Spain, MA Dzieciuch, KD Heaney, BM Howe, JN Kemp, JA Mercer, RA Stephen, and LJ Van Uffelen, "The North Pacific Acoustic Laboratory (NPAL) deep-water acoustic propagation experiments in the Philippine Sea", *J. Acoust. Soc Am.* **134**(4), pp 3359-3375, (2013), [published,refereed]

[13] FS Henyey and SA Reynolds, "A numerical simulator of ocean internal waves for long range acoustics", Technical Memo TM 1-13, Applied Physics Laboratory, University of Washington, 2013. [Appended.]

Attached papers and reports.

A test of deep water Rytov theory at 284 Hz and 107 km in the Philippine Sea
by Rex K. Andrew, Andrew W. White, James A. Mercer, Matthew A. Dzieciuch, Peter F. Worcester, and John A. Colosi

A test of deep water Rytov theory at 284 Hz and 107 km in the Philippine Sea

Rex K. Andrew,[a)] Andrew W. White, and James A. Mercer
Applied Physics Laboratory, University of Washington, Seattle, Washington 98105, USA

Matthew A. Dzieciuch and Peter F. Worcester
Scripps Institution of Oceanography, La Jolla, California 92037, USA

John A. Colosi
Naval Postgraduate School, Monterey, California 93943, USA

Predictions of log-amplitude variance are compared against sample log-amplitude variances reported by White, Andrew, Mercer, Worcester, Dzieciuch, and Colosi [J. Acoust. Soc. Am. **134**, 3347–3358 (2013)] for measurements acquired during the 2009 Philippine Sea experiment and associated Monte Carlo computations. The predictions here utilize the theory of Munk and Zachariasen [J. Acoust. Soc. Am. **59**, 818–838 (1976)]. The scattering mechanism is the Garrett–Munk internal wave spectrum scaled by metrics based on measured environmental profiles. The transmitter was at 1000 m depth and the receivers at nominal range 107 km and depths 600–1600 m. The signal was a broadband *m*-sequence centered at 284 Hz. Four classes of propagation paths are examined: the first class has a single upper turning point at about 60 m depth; the second and third classes each have two upper turning points at roughly 250 m; the fourth class has three upper turning points at about 450 m. Log-amplitude variance for all paths is predicted to be 0.04–0.09, well within the regime of validity of either Born or Rytov scattering. The predictions are roughly consistent with the measured and Monte Carlo log-amplitude variances, although biased slightly low. Paths turning in the extreme upper ocean (near the mixed layer) seem to incorporate additional scattering mechanisms not included in the original theory.
© 2015 Acoustical Society of America. [http://dx.doi.org/10.1121/1.4929900]

I. INTRODUCTION

In a previous paper, White *et al.*[1] reported on acoustical fluctuations that were observed in broadband signals centered at 284 Hz and transmitted for over 60 h during a 2009 experiment in the Philippine Sea. The low-latitude sound speed profile and the range of 107 km supported several distinct wholly refracted paths having one, two, or three upper turning points. Paths confined to and below the main thermocline had small log-amplitude variances of 0.04–0.09. The propagation regime suggests that a theory advanced by Munk and Zachariasen[2] (hereafter, referred to as MZ), which itself is an extension of an underlying theory that assumes weak fluctuations, might accurately model the observations. This paper shows that MZ calculations of log-amplitude variance are roughly consistent within observation error with the actual log-amplitude variance for these paths, although biased slightly low. A path turning very near the surface had twice as much log-amplitude variance and appears to be in a different propagation and/or scattering regime.

The underlying theory belongs to Rytov.[3] When the index of refraction inhomogeneities along a propagation path are weak and smoothly varying in space, Rytov *et al.*[3] found an approximate solution to the fundamental scattering equations called the method of smooth perturbations. Conditions for validity of this approximation occur in a number of practical cases, and Rytov theory is used today in characterizing scattering in, for example, terrestrial microwave links and infrared and optical paths.[4]

Adaptation of Rytov theory to underwater acoustics, however, has not been straightforward. In contexts where the propagation path is more or less straight, Rytov theory has proven accurate enough. These configurations generally involve short ranges and high frequencies, e.g., probing turbulent scales of mixing in a coastal underwater channel[5] over 670 m at 67 kHz, or using ultrasound in a fluid test cell[6] over 30 cm at 100 kHz.

For longer ranges, the depth dependence of the sound speed causes the propagation path to refract upward, or downward, or both. In order to accommodate these additional propagation features, Munk and Zachariasen applied Rytov theory locally, invoking the local depth and angle of the unperturbed ray (i.e., the ray theoretic solution in an ocean having only a non-stochastic background sound-speed profile.) Statistics were computed by integrating local scattering contributions along the unperturbed ray path from transmitter to receiver.

a)Electronic mail: rex@apl.washington.edu

Predictions from MZ theory (and others) were compared to observations made during several experiments conducted in the 1970s. In the first set of experiments, called here the Cobb Seamount experiments,[7,8] Ewart[7] used signals from 2 to 8 kHz over a range of 17.2 km with lower paths characterized by upward turning depths of about 975–1500 m. Desaubies[9] showed that MZ theory incorporating an appropriately parameterized Garrett–Munk (GM) internal wave spectrum yielded reasonably accurate measures of log-amplitude variance at 4 kHz, but not at 8 kHz, and showed significant discrepancies explaining the log-amplitude auto-spectra for both frequencies.

In a second experiment, Worcester[10] analyzed signals at 2250 Hz transmitted over 25 km via both an upper and lower path. The lower path turned upward at a depth of 1471 m, and the upper path turned downward at 185 m. The analysis showed that fluctuations along both paths were not inconsistent with MZ theory using a version of the GM spectrum. Comparisons of intensity auto- and cross-correlation functions were, however, ambiguous because the experiment duration spanned only 15 h.

It is important to note that in both of these experiments, the acoustic paths can be characterized by eigenrays having shallow launch angles $|\theta_0| \lesssim 4°$ (with respect to horizontal). We will return to this issue in Sec. VI.

Following these experiments, the focus of deep water research shifted for more than a decade to much longer ranges and much lower frequencies. Rytov theory, in general, and the deep water adaptation of MZ theory in particular, were not expected to be valid in these configurations. Recently, however, Colosi et al.[11] demonstrated that MZ predictions had reasonable agreement with several signal statistics for an 87 km path at 75 Hz at a mid-latitude site in the North Pacific. This regime is longer in range than the earlier Ewart and Worcester experiments, but at a much lower frequency.

White et al.[1] describe a scattering experiment in the Philippine Sea with a similar range—107 km—but a signal frequency (284 Hz) nearly two octaves higher. Corresponding a posteriori theoretical Monte Carlo calculations were remarkably accurate for most of the reception configurations. (The calculations are a posteriori in the sense that the calculations are made after the experiment using oceanographic measurements obtained during the experiment.) This paper provides associated a posteriori MZ theory predictions, completing a three-way comparison between at-sea measurements, Monte Carlo simulations, and theoretical predictions. MZ theory represents an analytical approach to predicting acoustic field statistics, and can provide greater physical insight to mechanisms of randomization than can Monte Carlo simulations. In addition, the MZ calculations are much faster to obtain compared to Monte Carlo results. [In the case presented here, a single MZ calculation required about 1 min, and a Monte Carlo parabolic equation (MCPE) simulation with 226 realizations required several weeks.] This effort therefore serves to further delineate the regions where MZ theory makes reasonably accurate predictions and where the theory develops some discrepancies.

This report is organized as follows. Section II outlines the structure of the calculations used here, including a Fresnel tube computation that is an alternative to that used in Colosi et al.[11] Section III summarizes the key features of the experiment. Section IV summarizes the theoretical Monte Carlo calculations reported by White et al.[1] Section V provides the comparison between the observed acoustical log-amplitude variance and the corresponding a posteriori MZ predictions. The theoretical expressions require several environmental profiles and a parameter—the scattering strength—which must be determined from oceanographic measurements. Provenance and construction of these are described in this section. Some of these are common and some are not. Estimation of the scattering strength parameter is not well-known: Sec. V also describes this calculation and, importantly, the error in the estimate. A discussion of the apparent regimes of validity of MZ theory and directions for further investigations are provided in Sec. VI.

II. MUNK-ZACHARIASEN THEORY

There are three key constructs in MZ theory: the eigenray, the associated Fresnel tube, and the space-time spectrum of sound-speed anomalies. Eigenrays have been thoroughly treated in the literature and will not be reviewed here. The theory is, in principle, agnostic with respect to the exact form of the sound-speed anomaly field, but here, as in most previous applications to the open ocean, the sound-speed anomalies are assumed to be due to fluid displacements caused by internal waves, with the space-time internal wave displacement field given by the GM model. This derivation is briefly summarized in Sec. II A. Construction of the Fresnel tube is described in Sec. II B, and Sec. II C describes the numerical calculation required for this study.

MZ theory writes the field $\psi = \psi_0 \exp(\chi + i\phi)$, where ψ_0 is the field in the absence of sound-speed anomalies, and χ is the (zero-mean) log-amplitude fluctuation and ϕ is the zero-mean phase fluctuation. Write $X = \chi + i\phi$. Then

$$\text{var}(\chi) = \langle \chi^2 \rangle = \frac{1}{2}\left(\langle |X|^2 \rangle + \text{Re}\{\langle X^2 \rangle\} \right). \tag{1}$$

Using MZ Eq. (66) for $\langle |X|^2 \rangle$ and MZ Eq. (74) for $\langle X^2 \rangle$ [note that this equation has a sign error; see MZ Eq. (75)] one can obtain

$$\langle \chi^2 \rangle = \frac{2}{\pi} k_0^2 N_0 b \int_0^R dx \sum_{j=1}^{\infty} \frac{1}{j} \int_{\omega_L}^N d\omega \, \frac{S_{\mu\mu}(\omega,j)}{\sqrt{\omega^2 - \omega_L^2}} \frac{\sin^2\gamma}{\cos^2\theta}. \tag{2}$$

Quantities θ, ω_L, and γ are all functions of the unperturbed eigenray path depth $z_{\text{ray}}(x)$, which in turn is parameterized by range x from 0 to R. Wave number $k_0 = 2\pi f/c_0$, where f is the acoustical frequency in Hertz and c_0 is a reference sound speed. The product $N_0 b$ incorporates the Brunt-Väisälä frequency scale N_0 and a depth scale b, and is $\int N(z)\,dz$ where $N(z)$ is the Brunt-Väisälä or buoyancy frequency profile; however, N_0 and b always appear together, and therefore $N_0 b$ will always be treated as a single

quantity.[12] Angle θ is the path inclination relative to the horizontal. The term $\omega_L{}^2 = f_C{}^2 + N(z)^2 \tan^2\theta$, where f_C is the local Coriolis parameter (here, in radians/s). $S_{\mu\mu}(\omega, j)$ is the spectrum (described more fully in Sec. II A) of fractional sound-speed anomalies μ ($\equiv \delta c/c$) as a function of internal wave frequency ω and mode number j. The term γ is given in MZ by

$$\gamma = \frac{\pi}{4} \frac{j^2}{(N_0 b)^2} \left((\omega^2 - \omega_L{}^2) R_{Fy}^2 + N(z)^2 R_{Fz}^2 \right), \quad (3)$$

where $R_{Fy}^2 = 2\pi x(R - x)/k_0 R$ is the horizontal Fresnel radius, and R_{Fz}^2 is the vertical Fresnel radius. Since the horizontal correlation length of the sound-speed anomalies is much greater than the vertical correlation length, the first term is generally much smaller than the second and is neglected. This leaves

$$\gamma \approx \frac{1}{4\pi} \left(\frac{\pi j N(z)}{N_0 b} \right)^2 R_{Fz}^2 = \pi \left(\frac{j N(z) R_{Fz}}{2 N_0 b} \right)^2. \quad (4)$$

A. Spectrum of sound-speed anomalies

The spectrum of fractional sound-speed anomalies $S_{\mu\mu}(\omega, j)$ due to internal wave displacements requires a mapping $\mu = \mathcal{T}\zeta$ between fractional sound-speed anomaly μ ($= \delta c/c$) and vertical fluid displacement ζ. The standard transformation is given by MZ as

$$\mathcal{T}_c = (1/\bar{c})(\partial_z \bar{c}_P). \quad (5)$$

Here and below, the term $\bar{c}$ denotes the depth-dependent background sound-speed profile; explicit depth dependence will be omitted. The potential sound-speed gradient is

$$\partial_z \bar{c}_P = \partial_z \bar{c} - \partial_z c_A. \quad (6)$$

Here, c_A is the adiabatic sound speed, such that $-\bar{c}^{-1}\partial_z c_A \equiv \gamma_A = 1.14 \times 10^{-5}$ m^{-1} [Flatté et al.,[13] Eq. (1.1.10)].

Given this mapping, the spectrum of fractional sound-speed anomalies is

$$S_{\mu\mu}(\omega, j) = \mathcal{T}_c^2 S_{\zeta\zeta}(\omega, j). \quad (7)$$

The most mature version[14] of the GM spectrum of vertical fluid displacements can be written as[12]

$$S_{\zeta\zeta}(\omega, j) = b E_0 \frac{N_0 b}{N(z)} \frac{\omega^2 - f_C{}^2}{\omega^2} H(j) B(\omega). \quad (8)$$

Here $H(j) = H_0^{-1}(j^2 + j_*^2)^{-1}$ is the modal spectrum and H_0 is such that $\sum_0^\infty H(j) = 1$, and $B(\omega)$ is

$$B(\omega) = \frac{2}{\pi} \frac{f_C}{\omega} \frac{1}{\sqrt{\omega^2 - f_C{}^2}} \quad (9)$$

and is normalized so that $\int_{f_C}^{N(z)} B(\omega)\, d\omega \approx 1$ for $N(z)/f_C \gg 1$. The product bE_0 incorporates the energy scale E_0 and the depth scale b; however, these two terms always also appear

together, and like $N_0 b$ will be considered a single quantity.[12] Combining Eqs. (7)–(9) yields

$$S_{\mu\mu}(\omega, j) = \mathcal{T}_c^2 b E_0 \frac{N_0 b}{N(z)} H(j) D(\omega), \quad (10)$$

where the function $D(\omega)$ is

$$D(\omega) = \frac{2 f_C}{\pi} \frac{\sqrt{\omega^2 - f_C{}^2}}{\omega^3}. \quad (11)$$

The normalization of $B(\omega)$ provides $\int_{f_C}^{N(z)} D(\omega)\, d\omega \approx \frac{1}{2}$ for $N(z)/f_C \gg 1$.

B. Fresnel tubes

The line of sight in ocean acoustics is the eigenray, which is generally not straight over any typical range. Let the eigenray be the parametric curve $z_{\rm ray}(x)$; there is no loss of generality in restricting the path to the two-dimensional system with range x and depth z. The transmitter is at point $\mathcal{S} = (0, z_{\rm ray}(0))$ and the receiver at point $\mathcal{R} = (R, z_{\rm ray}(R))$. The Fresnel tube is defined as that volume around the eigenray whose boundary points $\mathcal{B}$ satisfy

$$\frac{1}{2}T = |[\tau(\mathcal{B}, \mathcal{S}) + \tau(\mathcal{B}, \mathcal{R}) - \tau(\mathcal{R}, \mathcal{S})]|, \quad (12)$$

where $\tau(\mathcal{B}, \mathcal{A})$ is the travel time from point $\mathcal{A}$ to point $\mathcal{B}$. The eigenray does not formally have an associated frequency, but the Fresnel concept is frequency-dependent, and therefore T is the period of the propagating field, assumed here to be monochromatic. Equation (12) says that the Fresnel tube boundary is defined when the difference in travel time between the travel time along the eigenray and the travel time along an alternate nearby path to and from a boundary point is $\pm$ half a wave period. (Some authors use $\pm$ quarter wave period.[15])

Flatté et al.[13] give a prescription for computing the boundary of the Fresnel tube. An alternate approach is taken here, utilizing dynamic ray tracing theory.[16] In addition to producing Fresnel tubes for simple propagation paths such as those defined here, dynamic ray tracing can handle more complex situations such as range-dependent media and reflections from interfaces. The approach uses a local coordinate system in which one axis (say, the third axis, $\hat{\mathbf{q}}_3$) is aligned along the local tangent to the ray. The first axis, $\hat{\mathbf{q}}_1$, is then located in the (x, z) plane (i.e., in the vertical plane), and the second axis, $\hat{\mathbf{q}}_2$, is directed out-of-plane.

The derivation of the Fresnel tube is thoroughly described in the dynamic ray tracing literature[17]; only key points are mentioned here. In the paraxial approximation, one obtains

$$\frac{1}{2}T = \frac{1}{2}\mathbf{u}^T [\mathbf{M}(\mathcal{O}, \mathcal{S}) + \mathbf{M}(\mathcal{O}, \mathcal{R})]\mathbf{u}, \quad (13)$$

where $\mathbf{u} = [u_1 \hat{\mathbf{q}}_1 + u_2 \hat{\mathbf{q}}_2]$. $\mathbf{M}$ is a 2×2 propagator matrix. Equation (13) is solved for (u_1, u_2) at every point $\mathcal{O}$ on the eigenray. Due to the anisotropic nature of the sound-speed

anomaly inhomogeneities, the influence of u_1 dominates that of u_2, and therefore Eq. (13) can be simplified to

$$\frac{1}{2}T = \frac{1}{2}u_1^2 \big([\mathbf{M}(\mathcal{O},\mathcal{S})]_{1,1} + [\mathbf{M}(\mathcal{O},\mathcal{R})]_{1,1} \big), \quad (14)$$

which only requires the first element of the propagator matrix. The boundary of the Fresnel tube (under the paraxial approximation) in the $\widehat{\mathbf{q}}_1$ direction is then given by

$$u_1^{-1} = \sqrt{f}\sqrt{[\mathbf{M}(\mathcal{O},\mathcal{S})]_{1,1} + [\mathbf{M}(\mathcal{O},\mathcal{R})]_{1,1}} \quad (15)$$

for an acoustical frequency f.

For a cylindrically symmetric ocean model, the propagator matrix is particularly simple and is completely described in this case by Porter and Bucker.[18] The computations are implemented in the propagation code BELLHOP. In practice, there are two complications. BELLHOP uses an adaptive step integrator and therefore solutions for the propagator elements and, hence, solutions u_1 do not occur on a regular x-axis grid. Second, the boundary point $\mathcal{B}$ for each solution $u_1(x)$ does not occur on a regular x-axis grid either, because the local coordinate system is generally rotated relative to the local Cartesian (x, y, z) system. Both problems are easily circumvented via interpolation.

An example tube calculation (for one of the paths described later) is shown in Fig. 1.

C. Numerical details

Equation (2) is the general MZ expression. For the specific case involving the GM spectrum,[14] $S_{\mu\mu}(\omega, j)$ is separable and the integration over ω can be done analytically. The numerical evaluation of Eq. (2) proceeds by writing

$$\langle \chi^2 \rangle = A \sum_{j=1}^{J} j^{-1}H(j)I_j, \quad (16)$$

where the summation upper limit has been truncated at J, $A = (4/\pi^2)bE_0(N_0b)^2 f_C k_0^2$ and I_j is the one-dimensional integral
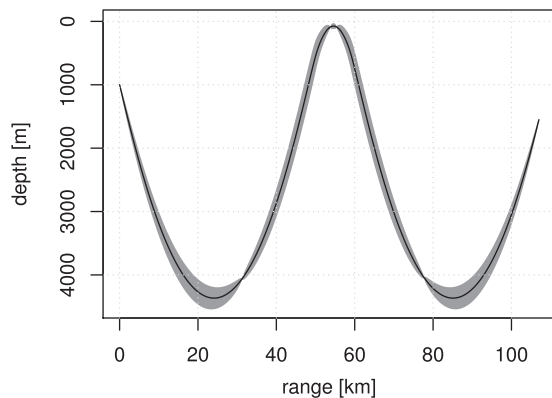

FIG. 1. Fresnel tube (vertical slice), 284 Hz, Philippine Sea 2009 experiment. The eigenray is the solid black line, the tube is represented by the shaded region.

$$I_j = \int_0^R dx\, Q_j(x) = R\int_0^1 d\alpha\, Q_j(\alpha R), \quad (17)$$

with integrand

$$Q_j(x) = Q(x;j) = \frac{\mathcal{T}_c^2}{N}\frac{\sin^2\gamma}{\cos^2\theta}W. \quad (18)$$

All terms are implicit functions of range via a dependence on $z_{\text{ray}}(x)$. The term $W(x)$ is

$$W(x) = \int_{\omega_L}^{N(z)} \frac{d\omega}{\omega^3}\frac{\sqrt{\omega^2 - f_C^2}}{\sqrt{\omega^2 - \omega_L^2}}. \quad (19)$$

This integral has branch points at $|\omega| = \omega_L$ (which are also singular points.) Generally, $\omega_L > f_C$ except for $\theta = 0$. Using the branch cut $[-\omega_L, \omega_L]$, a closed form solution was found for $\theta \neq 0$ by Colosi et al.[11] An equivalent expression for $\theta \neq 0$ is

$$W(x) = \frac{\sqrt{1 - f_C^2/N(z)^2}\sqrt{1 - \omega_L^2/N(z)^2}}{2\omega_L^2}$$
$$+ \frac{1}{2\omega_L^2}\left(\frac{\omega_L}{f_C} - \frac{f_C}{\omega_L}\right)\coth^{-1}\left(\frac{\omega_L}{f_C}\frac{\sqrt{1 - f_C^2/N(z)^2}}{\sqrt{1 - \omega_L^2/N(z)^2}}\right)$$

$$(20)$$

and at $\theta = 0$ the solution follows directly from Eq. (19) and is

$$W(x) = [1 - f_C^2/N(z)^2]/2f_C^2.$$

Romberg quadrature is used for the numerical estimation of the integrals of Eq. (17).

III. EXPERIMENTAL MEASUREMENTS

The at-sea data were collected during the 2009 Philippine Sea experiment (PhilSea09). Worcester et al.[19] has given an overview of the entire Philippine Sea effort. White et al.[1] provided a comprehensive description of this experiment, so only a summary will be provided here.

An electro-acoustical transmitter was suspended at 22°16.95′N, 126°19.77′E to a depth of 1000 m from the R/V *Melville*. The transducer has sharp resonances at about 210 Hz and 320 Hz. The transmitted signal was a 1023-bit m-sequence[20] with a carrier frequency of 284 Hz and 2 cycles per bit. The transducer drive signal was equalized to mitigate the distortion induced by the doubly peaked system transfer function, yielding a reasonable facsimile of an m-sequence with a 130 Hz bandwidth and pulse resolution of 7.7 ms. The root-mean-square (RMS) source level was roughly 183 dB re 1 μPa at 1 m.

The receiver was located at 21°21.90′N, 126°01.02′E and involved a 5 km mooring suspended from a subsurface float at a range of 107 km and a bearing of 198° from the transmitter. The mooring included two autonomous subarrays of hydrophones, each consisting of 30 hydrophones and

one controller.[21] The upper subarray had an inner inter-element spacing of 25 m for 25 hydrophones and of 75 m for two hydrophones above and three hydrophones below the inner hydrophones. It spanned the deep sound channel (centered around about 1040 m). Wavefield statistics from the lower subarray were not reported by White *et al.*[1] and therefore the lower subarray will not be described further. The mooring was also outfitted with Sea-Bird SBE37-SMP pumped conductivity-temperature-pressure microCAT conductivity-temperature-depth (CTD) recorders,[22] Sea-Bird SBE39 temperature recorders,[23] and a long-baseline acoustical navigation system.

The *m*-sequences were transmitted beginning roughly at 10:00 UTC on yearday 117 and continued for 60 h. Each *m*-sequence was 7.2 s in length. Sequences were transmitted continuously in a schedule of 10 min on, 5 min off, 10 min on, 5 min off, 15 min on, and off for the remainder of each hour. Data records heavily contaminated by in-water signals from unidentifiable sources were removed.

After pulse-compressing the raw data, White *et al.*[1] mapped eigenray path identifiers to individual branches of the acoustical time front. Subsections of four branches could be resolved, each involving roughly a dozen receiver depths. In every receiver time series where a particular branch could be isolated, a short time segment containing the complex pulse waveform was extracted for that branch. This yielded sample sets over the duration of the experiment of ~15 700 pulses for every depth and branch combination, excluding combinations where branches overlapped or crossed. Each pulse was transformed into the Fourier domain. The data record for each available sensor depth and time front branch combination then consisted of the time series of squared magnitudes (i.e., the intensity) of the Fourier coefficient corresponding to the carrier frequency. White *et al.*[1] do not give the sample variances of these records themselves, but rather the span of the corresponding 95% confidence interval; see their paper for a discussion of how this confidence interval was estimated. The log-amplitude variance spans used here are taken directly from their Fig. 8 (where they give RMS log-intensity in decibels.)

White *et al.*[1] analyzed four time front branch subsections. Eigenray paths for each subsection were similar: (a) three turning points initially launched downward, denoted ID−3; (b) four turning points launched upward (ID+4); (c) four turning points launched downward (ID−4); (d) five turning points launched upward (ID+5). Representative paths are shown in Fig. 2.

IV. MONTE CARLO CALCULATIONS

The commonly accepted standard for wave-theoretic solutions in the paraxial approximation for weakly range-dependent channels is the parabolic equation, particularly for long-range, deep-water ocean acoustic scenarios where bathymetric interaction is minimal or absent, and only fields propagating near horizontal are important. This approach integrates well with the Monte Carlo method for simulating the distribution of wavefield statistics. White *et al.*[1] used this MCPE approach in an *a posteriori* prediction of
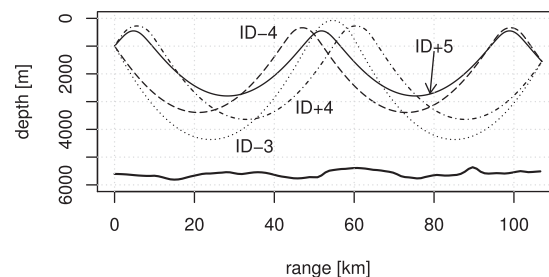

FIG. 2. Example eigenrays. The transmitter was at depth of 1000 m. Paths are shown to sensor HM028 at a nominal depth of 1550 m at range 107 km. The thick solid line at the bottom is the Smith-Sandwell bathymetry (Ref. 24). Note that paths ID+4 and ID−4 have very similar characteristics—numbers of upper and lower turns, upper turning depth—but path ID−3 is quite different.

log-amplitude variances. Details on the parabolic equation computation are given by White *et al.*[1] Each Monte Carlo realization built an acoustic channel on the background sound speed $\bar{c}(z)$ by adding a random range-depth realization of sound-speed anomalies constructed using the Henyey–Reynolds algorithm.[25] White *et al.*[1] set the strength of the sound-speed anomalies by analyzing the original receiver mooring microCAT CTD data to obtain a GM strength of ≈ 1.6. (More on this in Sec. V.) This value is similar to the value of ≈ 1.4 found by Colosi *et al.*[26] Since the MCPE method is computationally intensive, only 226 realizations were obtained.

V. ANALYSIS

In an *a posteriori* prediction, there are several environmental quantities that must be estimated and/or constructed from measurements made during the experiment prior to the primary calculation. The background sound speed profile $\bar{c}(z)$, Brunt-Väisälä frequency profile $N(z)$, and $\partial_z \bar{c}_P$ profile were the same profiles used by White *et al.*[1] in their MCPE simulations.

Estimation of the product bE_0, required in Eq. (10), is less straightforward. Colosi *et al.*[26] provide a thorough discussion of the random oceanographic fields during PhilSea09, but do not provide an explicit estimate of bE_0. Alternatively, White *et al.*[1] describe the estimation of the GM strength coefficient in terms of a ratio $\hat{r}$ of observed integrated spectral energy $\hat{s}$ to integrated spectral energy s_{GM1} based on the standard GM79 model at unity strength. Under the paradigm that $s_{GM1} = \frac{1}{2}(bE_{GM1})(N_0 b)$ [using their Eq. (1) and our notation], one can define

$$\hat{r} = \widehat{bE_0}/bE_{GM1}. \tag{21}$$

As with bE_0, the product bE_{GM1} is considered a single variable. Under the standard model, one has[25]

$$\frac{1}{2}(bE_{GM1})(N_0 b) = 0.277 \text{ m}^2\text{rads/sec} \tag{22}$$

and hence $bE_{GM1} = 0.056$ m for the value of $N_0 b$ in effect here. White *et al.*[1] describe depth-averaged lower and upper bounds on $\hat{r}$, derived by examining one month records of

Andrew *et al.*   2019

sound-speed time-series as measured by the 12 pumped microCATs on the receiver mooring. A lower bound of 1.6 is derived by ignoring tidal peaks in the spectra, under the assumption that tidal processes have insignificant effects on intensity fluctuations. This assumption is commonly made because tidal effects are considered to be large vertical scale perturbations, and large scale perturbations affect primarily the travel time. The intensity, however, is affected mainly by the small scale perturbations. Using their Fig. 8, the apparent standard error on this lower bound is 0.12 (assuming 12 independent measurements.) From Eq. (21), this implies $\widehat{bE_0} = 0.089 \pm 0.007$ m, ignoring tidal energy. An upper bound of 3.33 is also given, which includes tidal energy. The lower bound is used by White et al.[1] in reporting their MCPE calculations (Sec. IV). We address both bounds in the discussion below.

With this value of $\widehat{bE_0}$ and the other parameters shown in Table I, the log-amplitude variance equation (2) can now be computed and compared to the actual measurements. The integrals of Eq. (17) were estimated numerically with Romberg quadrature. Romberg quadrature is an adaptive algorithm whose result will be interpreted below as a random variable with a uniform distribution of $U_{[I_* - \delta, I_* + \delta]}$, where the estimated integral (i.e., at a given mode number j) is I_* and $\delta = \epsilon I_*$. Here, ϵ is the relative estimated error, which is preset in the algorithm to 1 part in 10^6. The variance of a random variable with distribution $U_{[a,b]}$ is $(b - a)^2/12$; hence, the RMS error is $\delta/\sqrt{3}$. This value is considered the standard error. In order to compare to the 95% confidence interval error bars used by White et al.,[1] each integration was assigned an error of twice this RMS value. Errors for the entire calculation (i.e., over all modes) used a quadrature sum of the individual errors. The final error was obtained by the quadrature sum of the total quadrature estimation errors and the error for $\widehat{bE_0}$. In all cases, the error on $\widehat{bE_0}$ dominated.

The ranges of MZ log-amplitude variance for each class of path are shown in Table II. Also given are the corresponding values for the scintillation index and the RMS log-intensity. The full comparison of at-sea measurements, Monte Carlo calculations, and MZ predictions versus depth for all four path classes is shown in Fig. 3.

TABLE I. Parameters used in the calculation. The term $N_0 b = \int N(z)\, dz$ and is computed to be roughly 9.98 rads-m/s. (The integral is over the entire water column.)

Parameter	Symbol	Value
Latitude		21.5°
Buoyancy frequency	$N(z)$	See text
	$N_0 b$	See below
Coriolis parameter	f_C	5.33×10^{-5} rad/s
Modal bandwidth	j_*	3
Maximum modes	J	120
Reference sound speed	c_0	1480 m/s
Background sound speed	$\bar{c}(z)$	See text
Acoustical frequency	f	284 Hz
Strength	$\widehat{bE_0}$	0.089 ± 0.007 m

TABLE II. Comparison of typical log-amplitude and log-intensity fluctuation statistics from the MZ computations. The scintillation index (SI) is approximately $4\,\mathrm{var}\,\chi$ for $\mathrm{var}\,\chi \ll 1$. The RMS log-intensity (RMS ι) is given in units of decibels, following Colosi et al. (Ref. 11); these are the same units as those used in Fig. 3.

Path	var χ	SI	RMS ι
ID−3	0.038–0.043	0.15–0.17	1.7–1.8
ID+4	0.067–0.074	0.27–0.30	2.3–2.4
ID−4	0.067–0.076	0.27–0.30	2.3–2.4
ID+5	0.080–0.090	0.32–0.36	2.5–2.6

VI. DISCUSSION

These comparisons indicate that a posteriori MZ theory is largely consistent with at-sea measurements and MCPE calculations of log-amplitude variance at the 5% level of significance for paths ID+4, ID−4, and ID+5 at 284 Hz over 107 km. This conclusion is reinforced by the power of the three measurement campaigns:

- The duration (60 h) and pulse repetition rate (500/h) guaranteed a formidable at-sea dataset; assuming an intensity correlation time of 5 m and a 50% gap loss, White et al.[1] still obtained roughly 360 independent samples.
- The MCPE calculations used 226 independent samples; while more would be preferable, this is commensurate with the actual data.
- The numerical estimation of integrals equation (17) continually refines its estimate of the integral until it reaches the pre-defined error bound 1 part in 10^6.

The three-way comparison reported here is remarkably consistent. Even though the actual measurements were mediated by a mixture of oceanographic processes and the MCPE predictions were driven solely by GM-style internal waves, the correspondence between the actual measurements and the MCPE predictions is excellent. The correspondence between the MCPE and MZ predictions is also very good, which should follow because both calculations used the same scattering model. The results also suggest that MCPE calculations are more accurate predictions of the measurements than MZ predictions (using the scattering strength lower bound), with MZ slightly underpredicting the log-amplitude variance. More stringent error bounds would be needed to firmly support this conclusion.

The results for paths ID+4 and ID−4 are similar, which should be expected since the two paths themselves have similar characteristics. Agreement between observed data and either MZ predictions or MCPE calculations is not as good for path ID−3, but this is not unexpected. Figure 2 shows that this path has an upper turning depth of roughly 60 m. This near-surface region experiences considerable oceanographic variability (mixed layer dynamics, convective turbulence, etc.) not included in the GM model. This variability can cause a variety of effects not represented by the simplistic eigenray solution shown in Fig. 2, such as a surface duct or even surface reflections. White et al.[1] consider possible hypotheses in more comprehensive detail: here, it should suffice to note that inspection of the intensity record for path
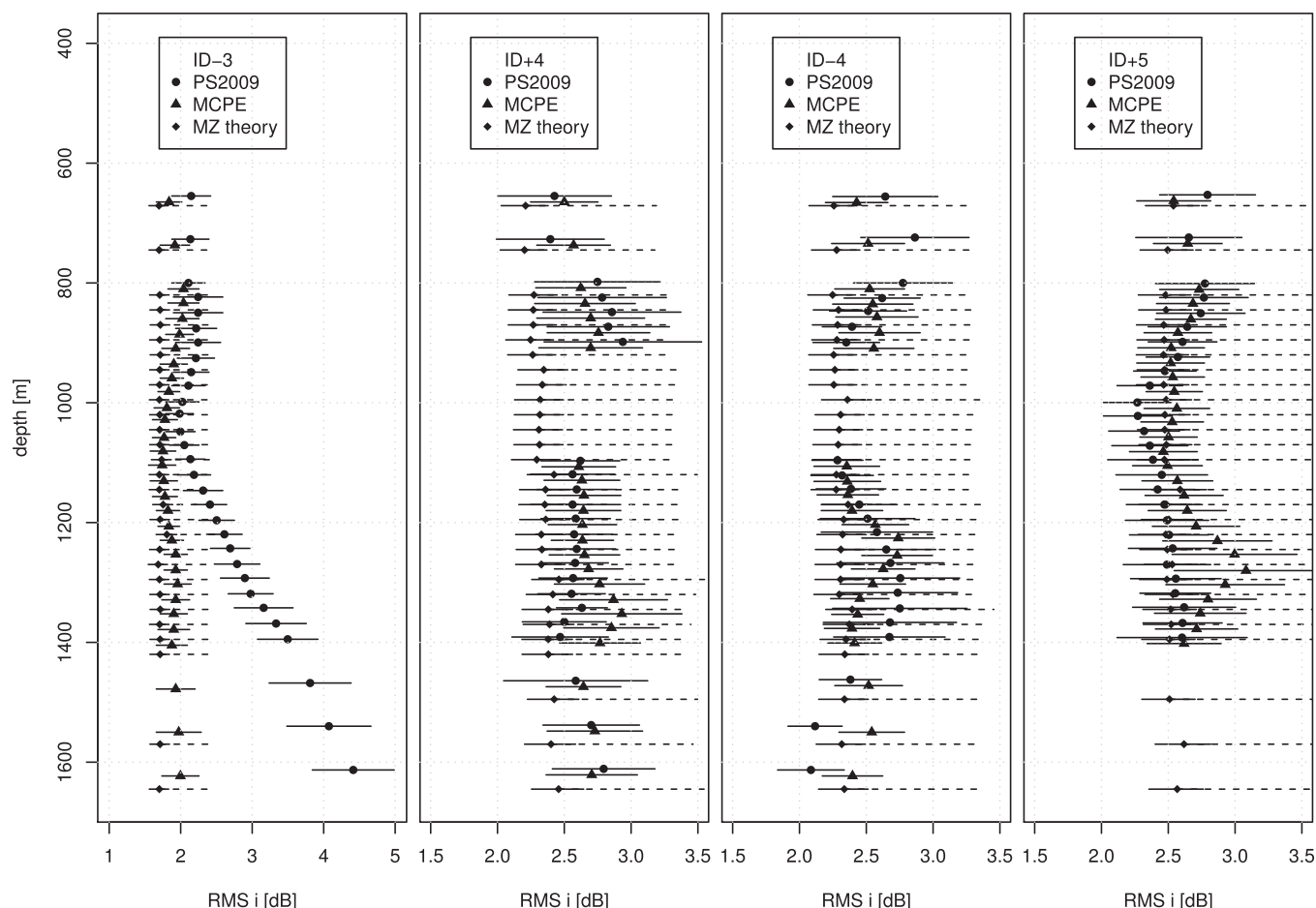
FIG. 3. Comparison of log-intensity variances (presented as RMS log-intensity ι) for the Philippine Sea 2009 experiment, 107 km, 284 Hz. Panels left to right correspond to ray path geometries ID−3, ID+4, ID−4, and ID+5. Error bar spans for at-sea measurements (PS2009) and Monte Carlo estimates (MCPE) are taken from White *et al.* (Ref. 1) and are two standard errors. The at-sea and Monte Carlo error span center points are merely the span midpoints and are only provided for reference; they are not given *per se* by White *et al.* See the text for a discussion of the solid MZ prediction error bars. The dashed MZ error bars reflect the lower (left endpoint) and upper (right endpoint) bounds given by White *et al.* MCPE results offset downward by 10 m, MZ results by 20 m for clarity. Note that the left panel has a different abscissa scale to accommodate the at-sea measurements below about 1000 m. Since var $\iota = 4$ var χ, RMS $\iota = (10/\ln 10)\sqrt{\text{var}\,\iota} = (20/\ln 10)\sqrt{\text{var}\,\chi}$ in decibels.

ID−3 (their Fig. 4) seems to indicate that the intensity fluctuations were modulated by a strong non-GM diurnal process. MZ theory incorporating the GM model has no mechanism to include this.

White *et al.*[1] allowed for internal wave strength to be between GM strength parameter 1.6 and 3.33, largely because it is not well understood how tidal spectral energy, a significant component in the PhilSea09 environment, influences acoustic signal fluctuations. Tidally forced sound-speed fluctuations are considerably unidirectional and have no representation in the GM model, which assumes horizontally isotropic internal waves. MZ predictions using GM strengths [1.6,3.33] span all measurements for paths ID+4, ID−4, and ID+5: this level of uncertainty supports only the broadest of conclusions on the model. White *et al.* speculated that the lower bound (vice the upper bound) was a better estimate of scattering strength for intensity fluctuations because it provided a better spectral fit at high frequencies, away from the strong tidal peaks. Indeed, the results presented here can be used in a rudimentary inverse problem: the MZ predictions suggest that the scattering strength is at or perhaps slightly higher than the lower bound provided by

White *et al.*[1] The scattering strength upper bound is clearly not appropriate. These acoustic results can therefore be used to reduce the uncertainty in the ocean model.

In a more general sense, questions surrounding the validity of the Rytov approximation have had a durable longevity. This issue has been debated in the western literature long after Pisareva showed in the Russian literature that the issue depended on a wave parameter D, and that when this wave parameter was small, the Rytov approximation was valid when the log-amplitude variance was less than unity.[27,28] The wave parameter was $2\lambda R/\pi L^2$, where λ is the acoustic wavelength, R is the propagation distance, and L is a correlation length scale (e.g., in a spherical isotropic medium.) For PhilSea09, the wave parameter is $\mathcal{O}(10^{-2})$ using order-of-magnitude estimates. This suggests that this experiment involved only the Fresnel scattering regime and, therefore, only the bound on log-amplitude variance is relevant. Since the observed log-amplitude variance is less than unity, the Rytov approximation would be valid.

Scattering in the deep ocean is much more complex than the scenarios assumed in the early Russian literature due to the refraction of unperturbed paths and the anisotropy of the

sound speed inhomogeneities and, therefore, the wave parameter used by Pisareva should be inappropriate. Correlation length scales in the horizontal and vertical differ considerably. Flatté–Dashen theory,[13] which develops moment expressions starting with the path integral formalism, was built specifically to accommodate the additional complexities of the ocean scenario. In Flatté–Dashen theory, the scattering regime is categorized by the product $\Lambda\Phi^2$ involving a diffraction parameter Λ and a strength parameter Φ. Under Flatté–Dashen theory, the Rytov approximation is valid when $\Lambda\Phi^2 < 1$. (See, e.g., Fig. 8.6 in Flatté et al.[13]) For the PhilSea09 experiment, calculations from CAFI[29,30] (which implements Flatté–Dashen expressions) show that $\Lambda\Phi^2$ ranges from 0.3 to 0.6 using the parameter values of Table I and an effective GM strength of 1.6 for the four rays considered here. Hence, under Flatté–Dashen theory, the Rytov approximation should be valid. (As an aside, the Pisareva condition is therefore not misleading.)

Even though Flatté–Dashen theory is a more complete theory[11] and supercedes MZ theory, the literature[31,32] indicates that MZ theory and Flatté–Dashen theory are the same when $\Lambda\Phi^2 < 1$, at least to first order in the Rytov series. Flatté–Dashen theory dictates that the log-amplitude variance in the geometrical-optics approximation is given approximately by $\frac{1}{4}\Lambda\Phi^2$ (Flatté et al.[13], Eq. 8.3.2). Table III shows the depth-averaged values of log-amplitude variance predictions from MZ theory and from Flatté–Dashen theory (implemented via CAFI) for the four eigenrays studied here. These are compared to MCPE calculations, which here are considered the benchmark result. This comparison shows that MZ theory slightly underpredicts the MCPE result. While it is not the purpose of this paper to compare Flatté–Dashen theory or CAFI against MCPE calculations, Table III shows that CAFI overpredicts the MCPE result, and that the CAFI result for $\frac{1}{4}\Lambda\Phi^2$ is almost twice the MZ result within the observed error. [This is, however, consistent with comments offered by Flatté et al.:[13] the log-amplitude variance in the geometric region is $\mathcal{O}(\frac{1}{4}\Lambda\Phi^2)$, an assertion which proves true here.] The value of MZ theory is therefore that it provides Rytov-based expressions for the log-amplitude variance and, by extension, the scintillation index, which, within the limits of its validity, appear to be more accurate than the CAFI-based Flatté–Dashen theory results.

Calculations of $\Lambda\Phi^2$ for the Worcester experiment[10] at 2250 Hz and the Cobb Seamount experiments[13] at 4 and

8 kHz dictate that the Rytov approximation (hence, MZ theory) remains valid for these scenarios. This is consistent with the lower frequency Worcester measurements,[10] but not the higher frequency Ewart measurements.[8,9] Both of these experiments analyzed near-horizontal propagation paths. Thus, measurements covering a sparse set of scenarios from high angle, low frequency, hundred kilometer range (Colosi et al.,[11] White et al.[1]) to low angle, mid frequency, ten kilometer range may have delineated the boundaries of valid Rytov and MZ theory application. In an effort to probe the sensitivity of the phase and log-amplitude variance and spectral predictions of MZ theory versus frequency, range, and propagation path steepness, Tombul conducted an unpublished numerical study to compare MZ predictions against direct MCPE simulation.[33] Individual eigenrays were simulated using beams with launch angles of $0°$, $5°$, $10°$, and $14°$. Ranges varied from 50 to 200 km. Frequencies were 75, 200, and 400 Hz. The medium profiles were analytic models scaled for good correspondence with typical oceanographic data. For shallow launch angles, he found good agreement for log-amplitude variance. For steeper launch angles, he observed discrepancies. The MZ results failed completely at 400 Hz and $14°$ ray angles. At 200 Hz and $10°$, which compares closely with these data, he found that MZ underpredicted MCPE results to the extent that he concluded that MZ theory was no longer valid for these and higher frequencies at this angle. Tombul's results are generally consistent with the results presented here: Fig. 3 and Table III show that MZ calculations are underpredicting the MCPE results. Tombul's conclusion may be too severe; MZ theory is largely consistent with measured and MCPE results, but it does appear that a higher order correction is required to eliminate the prediction bias. Simulations were not conducted at the frequencies used by Worcester[10] and Ewart.[7,8]

The transition region from Rytov/MZ theory to the more comprehensive Flatté–Dashen theory seems to be bounded by a couple of experiments and simulations performed over the past several decades, but several gaps remain in these boundaries. In order to eliminate these gaps, MCPE simulations should be pushed to higher frequencies, and careful ocean experiments pursued at low mid-frequencies for steeper propagation paths.

ACKNOWLEDGMENTS

TABLE III. Comparison of Rytov-based predictions of log-amplitude variance from MZ and Flatté–Dashen theory against MCPE calculations for the four eigenrays studied here. The MCPE, MZ, and $\frac{1}{4}\Lambda\Phi^2$ columns are the depth-averaged values. The final row provides the eigenray-averaged ratios of MZ predictions against the MCPE calculations and the CAFI predictions against the MCPE calculations.

Ray ID	MCPE	MZ	MZ/MCPE	$\frac{1}{4}\Lambda\Phi^2$	$\frac{1}{4}\Lambda\Phi^2$/MCPE
-3	0.0473	0.0389	0.82	0.075	1.59
$+4$	0.0961	0.0705	0.73	0.133	1.38
-4	0.0832	0.0725	0.87	0.148	1.78
$+5$	0.0940	0.0830	0.88	0.113	1.20
		Average	0.83	Average	1.49

[1]A. W. White, R. K. Andrew, J. A. Mercer, P. F. Worcester, M. A. Dzieciuch, and J. A. Colosi, "Wavefront intensity statistics for 284-hz broadband transmissions to 107-km range in the Philippine Sea: Observations and modeling," J. Acoustic. Soc. Am. 134, 3347–3358 (2013).

Andrew et al.

[2]W. H. Munk and F. Zachariasen, "Sound propagation through a fluctuating stratified ocean: Theory and observation," J. Acoust. Soc. Am. **59**, 818–838 (1976).

[3]S. M. Rytov, Y. A. Kravtsov, and V. I. Tatarskii, *Principles of Statistical Radiophysics 4, Wave Propagation Through Random Media* (Springer, Berlin Germany, 1989), pp. 49–50.

[4]A. D. Wheelon, *Electromagnetic Scintillation 2, Weak Scattering* (Cambridge University Press, Cambridge, UK, 2003), pp. 1–9.

[5]D. Di Iorio and D. M. Farmer, "Path-averaged turbulent dissipation measurements using high frequency acoustical scintillation analysis," J. Acoust. Soc. Am. **96**, 1056–1069 (1994).

[6]T. A. Andreeva and W. W. Durgin, "Experimental investigation of ultrasound propagation in turbulent, diffractive media," J. Acoust. Soc. Am. **115**, 1532–1536 (2004).

[7]T. E. Ewart, "Acoustic fluctuations in the open ocean—A measurement using a fixed refracted path," J. Acoust. Soc. Am. **60**, 46–59 (1976).

[8]T. E. Ewart and S. A. Reynolds, "The mid-ocean acoustic transmission experiment—MATE," J. Acoust. Soc. Am. **75**, 785–802 (1984).

[9]Y. J. F. Desaubies, "On the scattering of sound by internal waves in the ocean," J. Acoust. Soc. Am. **64**, 1460–1469 (1978).

[10]P. F. Worcester, "Reciprocal acoustic transmission in a midocean environment: Fluctuations," J. Acoust. Soc. Am. **66**, 1173–1181 (1979).

[11]J. A. Colosi, J. Xu, P. F. Worcester, M. A. Dzieciuch, B. M. Howe, and J. A. Mercer, "Temporal and vertical scales of acoustic fluctuations for 75-Hz, broadband transmissions to 87-km range in the eastern North Pacific Ocean," J. Acoust. Soc. Am. **126**, 1069–1083 (2009).

[12]F. S. Henyey, D. Rouseff, J. M. Grochocinski, S. A. Reynolds, K. L. Williams, and T. E. Ewart, "Effects of internal waves and turbulence on a horizontal aperture sonar," J. Ocean. Eng. **22**, 270–280 (1997).

[13]S. M. Flatté, R. Dashen, W. H. Munk, K. Watson, and F. Zachariasen, *Sound Transmission through a Fluctuating Ocean* (Cambridge University Press, Cambridge, UK, 1979), pp. 6–7.

[14]W. Munk, "Internal waves and small-scale processes," in *The Evolution of Physical Oceanography*, edited by C. Wunsch and B. Warren (MIT Press, Cambridge, MA, 1981), pp. 264–291.

[15]I. I. Rypina and M. G. Brown, "On the width of a ray," J. Acoust. Soc. Am. **122**, 1440–1448 (2007).

[16]V. Červený, *Seismic Ray Theory* (Cambridge University Press, Cambridge, UK, 2001), pp. 102–235.

[17]V. Červený and J. E. P. Soares, "Fresnel volume ray tracing," Geophysics **57**, 902–915 (1992).

[18]M. B. Porter and H. P. Bucker, "Gaussian beam tracing for computing ocean acoustic fields," J. Acoust. Soc. Am. **82**, 1349–1359 (1987).

[19]P. F. Worcester, M. A. Dzieciuch, J. A. Mercer, R. K. Andrew, B. D. Dushaw, A. B. Baggeroer, K. D. Heaney, G. D. D'Spain, J. A. Colosi, R. A. Stephen, J. N. Kemp, B. M. Howe, L. J. V. Uffelen, and K. E. Wage, "The North Pacific Acoustic Laboratory deep-water acoustic propagation experiments in the Philippine Sea," J. Acoustic. Soc. Am. **134**, 3359–3375 (2013).

[20]W. H. Munk, P. F. Worcester, and C. Wunsch, *Ocean Acoustic Tomography* (Cambridge University Press, Cambridge, UK, 1995), pp. 190–195.

[21]P. F. Worcester, S. Carey, M. A. Dzieciuch, L. L. Green, D. Horwitt, J. C. Lemire, and M. Norenberg, "Distributed vertical line array (DVLA) acoustic receiver," in *Proc. 3rd International Conf. on Underwater Acoustic Measurements*, edited by J. S. Papadakis and L. Bjørnø (Foundation for Research and Technology Hellas, Nafplion, Greece, 2009), pp. 113–118.

[22]Sea-Bird Electronics, Inc., "MicroCAT C-T (P optional) recorder SBE 37-SMP," Technical Report, Sea-Bird Electronics, Inc., 13431 NE 20th Street, Bellevue WA (2012), available at http://www.seabird.com/products/spec_sheets/37smpdata.htm (Last viewed 6/11/2012).

[23]Sea-Bird Electronics, Inc., "Temperature and pressure recorder SBE 39," Technical Report, Sea-Bird Electronics, Inc., 13431 NE 20th Street, Bellevue WA (2012), available at http://www.seabird.com/products/spec_sheets/39data.htm (Last viewed 6/11/2012).

[24]W. H. F. Smith and D. Sandwell, "Global seafloor topography from satellite altimetry and ship depth soundings," Science **277**, 1956–1962 (1997).

[25]F. S. Henyey and S. A. Reynolds, "A numerical simulator of ocean internal waves for long-range acoustics," Technical Report No. APL-UW TM 1-13, Applied Physics Laboratory, University of Washington, Seattle, WA (2013).

[26]J. A. Colosi, L. J. van Uffelen, B. D. Cornuelle, M. A. Dzieciuch, P. F. Worcester, B. D. Dushaw, and S. R. Ramp, "Observations of sound-speed fluctuations in the western Philippine Sea in the spring of 2009," J. Acoust. Soc. Am. **134**, 3185–3200 (2013).

[27]V. V. Pisareva, "O granitsakh primenimosti metoda 'plavnykh' ozmush-cheni\u{i} v zadache o rasprostranenii izlucheniya cherez sredu s neodnorod-nostyami" ("Limits of the applicability of the method of 'smooth' perturbations in the problem of radiation propagation through a medium containing inhomogeneities"), Akust. Zh. **6**, 87–91 (1960).

[28]A. D. Wheelon, *Electromagnetic Scintillation 2, Weak Scattering* (Cambridge University Press, Cambridge, UK, 2003), pp. 23–30.

[29]S. M. Flatté and G. Rovner, "User's guide to CAFI" (1998), available at http://oalib.hlsresearch.com/Other/cafi/CAFI_Guide.pdf (Last viewed 3/29/2015).

[30]S. M. Flatté and G. Rovner, "Calculations of internal-wave-induced fluctuations in oceanacoustic propagation," J. Acoust. Soc. Am. **108**, 526–534 (2000).

[31]R. Dashen, "Path integrals for waves in random media," J. Math. Phys. **20**, 894–920 (1979).

[32]D. R. Palmer, "An introduction to the application of Feynman path integrals to sound propagation in the ocean," Naval Research Laboratory Report No. 8148, Naval Electronic Systems Command, Washington, D.C. 20360 (1978).

[33]S. Tombul, "A numerical study of the validity regimes of weak fluctuation theory for ocean acoustic propagation through random internal wave sound speed fields," Master's thesis, Naval Postgraduate School, Monterey, CA, 2007.

J. Acoust. Soc. Am. **138** (4), October 2015

Andrew *et al.*   2023

Deep fades without destructive interference in the Philippine Sea long-range ocean acoustic experiment by Andrew Ganse, Rex K. Andrew, Frank S. Henyey, James A. Mercer, Peter F. Worcester, and Matthew A. Dzieciuch

(submitted to co-authors for review, targeted to the *JASA Express Letters*)

Deep fades without destructive interference in the Philippine Sea long-range ocean acoustic experiment

Andrew A. Ganse, Rex K. Andrew, Frank S. Henyey, James A. Mercer

Applied Physics Laboratory, University of Washington, Seattle, WA.

aganse@apl.uw.edu, rex@apl.uw.edu, frank@apl.uw.edu, mercer@apl.uw.edu

Peter F. Worcester, Matthew A. Dzieciuch

Scripps Institution of Oceanography, University of California - San Diego, La Jolla, CA

pworcester@ucsd.edu, mdzieciuch@ucsd.edu

July 3, 2015

Abstract

Acoustic pulses (f_c=200 Hz) received across 510 km in the Philippine Sea 2010 experiment show deep fading. Tntensity fluctuations are near-exponentially distributed and scintillation indices are high (1.1-1.9). According to prevailing theory, destructive interference between micro-multipaths causes deep fading, and random interference of randomly-phased micro-multipaths causes the exponential distribution of intensity. However, most measured pulse spreads in this dataset are not even half the carrier period, failing to support either mechanism. Further, the subset of received pulses with less than a quarter carrier period of spread still show deep fades and near-exponentially distributed intensities. Neither result presently has a theoretical explanation. © 2015 Acoustical Society of America

PACS numbers: 43.30.Re, 43.30.Qd

1   Introduction

A major scientific interest in the ocean acoustic research community is to better understand the limits of fluctuation theories for long-range ocean acoustic scattering, which seek to explain the phenomenon of deep fading in long-range ocean acoustic receptions. Pulse propagation records from the Philippine Sea 2010 ("PhilSea10") experiment show a fundamental mismatch between measurements of ocean acoustic scattering effects and those predicted by current theory. This work reports acoustic intensities and pulse spreads in these measurements. Histograms of the intensity fluctuations are approximately exponential, with the lowest intensities the most common (i.e. deep fading), and scintillation indices are high (1.1-1.9). According to micro-multipath theory,[1] destructive interference between superimposed micro-multipaths causes the deep fading and random interference of many randomly-phased micro-multipaths causes the exponential distribution of intensity. However, as will be presented, only a minority of pulse spreads in this measured dataset are even as large as half the carrier period, failing to support either mechanism. Additionally, received pulses with less than a quarter carrier period of spread are still found to be near-exponentially distributed, again without an obvious mechanism. Observed statistics are also compared to model predictions made by the "Computation of Acoustic Fluctuations from Internal waves (CAFI)" code.[2]

"Micro-multipathing" is defined as the splitting of the ray on one arrival branch (ray ID) into many sub-rays due to perturbations in the water column; these would all be the same single arrival in the range-independent case. The concept is distinct from the macro-scale multipath caused by the range-independent background waveguide and reflections. The use of "path" in the term micro-multipath also should not be confused with the "path" of path integral theory, in which a path is any path and not just a ray.

In single phase screen theory[3] in a single-scale medium, there is a rigorous mathematical connection between micro-multipathing and the intensity statistics described above. Given the assumption that the mean square phase shift $\Phi^2 >> 1$ radian so that the acoustic field is

incoherent, then at long ranges the scattering yields an exponential distribution of acoustic intensity. The many different micro-multipaths in that case offer a multitude of destructive interference possibilities, so the lowest acoustic intensities are the most probable. The phase is fully randomized so the spread of an acoustic pulse should be much greater than half its carrier period. In testing for micro-multipath interference in this work, we examine the extreme case of whether the pulse spread is less than a half carrier period. In fact one expects that spread to be well beyond a half carrier period if the exponentially distributed intensities are due to micro-multipath random interference, and at least a half carrier period if deep fades are due to destructive interference.

We clarify that the processing and results in this work are all on the post-pulse-processed signals. Previous reports[4,5] analyze statistics of intensities and pulse spreads in deep ocean acoustics experiments, but without examining the validity of the micro-multipath interference hypothesis. In fact, reference 4 shows the same patterns in pulse shape, pulse spreads, and intensity statistics as are reported here, and the same conclusions could be drawn from results shown in that paper as are shown here. Also note that recent work by other researchers[6] investigates this same issue in a shallow water regime.

An observed reception $s(t)$ on a uniquely identifiable branch of the timefront is modeled as a superposition of replicas of the transmitted pulse $p(t)$ propagating from the source along one or more eigenrays to the receiver, as in Eq. (1). The observed waveform is the transmitted pulse convolved with a sum of shifted and scaled delta functions.

$$s(t) = p(t) * \sum_{j}^{N} a_j \delta(t - \tau_j) \tag{1}$$

For destructive interference, two or more arrivals must be separated in time by at least half the carrier period T_c. As the time separation between pulses increases, the intensity of their sum fluctuates with the interference pattern, and the width of the total pulse $s(t)$ increases according to the time separation of the constituent pulses. If the width of $s(t)$ is

not greater than $p(t)$ by at least half the carrier period, then the constituent pulses are not separated by enough to support destructive interference.

2   Methods

The PhilSea10 experiment took place in the West Philippine Basin, on the order of 500 km east of Taiwan and Luzon.[7] Coded signals were sent for 54 hours from the ship-dipped MP200 "multiport"[8] source lowered to 998 m depth at 19.0 N, 130.2 E. The signals were 20.46 second M-sequences with a center frequency of 200 Hz, transmitted for the duration of the experiment aside from five-minute windows near the end of each hour for acoustic navigation. The unknown transfer function of the source distorted the drive signal so signal processing based on the monitored in-situ signal at the source is used to correct the distortion effects.[9] 510 km northwest of the source ship stop, at 21.3624 N, 126.0132 E, a distributed vertical line array (VLA) spanned virtually the whole water column with 150 hydrophones. Fig. 1a shows the geometry of the experiment and Fig. 1b depicts the arrivals and depths of the four hydrophones analyzed in this paper, in the context of the received acoustic timefront.

For each hydrophone, acoustic arrivals A-F (see Fig. 1b) are windowed out and time variations due to VLA motion are removed using a VLA tracking solution. The time-varying (over the 54 hour experiment) widths of the pulses in these windows form the basis for the pulse spread analysis, and the intensity Fourier component corresponding to the center frequency of the signal is extracted from these windows for the intensity analysis.

Pulse widths in this work are calculated by using spline interpolation to find the peak intensity, and then noting the two times at which the interpolant crosses half the peak intensity.

3   Variations in pulse spread and intensity

The fluctuating measured pulse spread δW_m is the difference between the random received pulse width W_{rx} and the deterministic transmitted pulse width W_{tx}. It is expressed in Eq.

(2) as a sum of a random pulse width fluctuation δW_o due to oceanic fluctuations that affect propagation and another random pulse width fluctuation δW_n due to additive ambient noise, which perturbs the pulse width because the noise distorts the pulse. The mean spread $\langle \delta W_o \rangle$ due to the ocean is $\langle \delta W_m \rangle - \langle \delta W_n \rangle$.

$$\delta W_m = \delta W_o + \delta W_n \tag{2}$$

The statistics of δW_o depend upon those of δW_n. Fig. 2a shows a Monte-Carlo-generated probability density function (PDF) of δW_n based on receptions of the mean background noise well away from the accordion structure of the timefront arrivals. A single transmitted pulse measured by the source-monitor hydrophone (fluctuations of this pulse over experiment time are incredibly small) has 43470 instances of random noise added to it, which is five times the number of measured receptions. These random noise instances are simulated with the same spectrum as the actual background noise measured at the respective receiver hydrophone on the VLA. The noise instances distort the source-monitor pulse, causing a fluctuating pulse spread, which is measured in the same way as described above for the measured pulses. The width at half-maximum of this PDF of δW_n is used to set an upper bound of measured pulse spreads to use in analyses of intensities.

The PDF of the measured pulse spreads δW_m is shown in Fig. 2b. Negative measured spreads are due to ambient noise, which distorts the pulse whose width is being measured. Only a minority of the PDF is greater than the half carrier period of T_c=2.5ms. The CAFI-predicted and measured pulse spreads, as well as the percentage of spreads greater than half a carrier period, are listed in Table 1 along with those for all six of the arrival branches on four hydrophones depicted in Fig. 1b. CAFI actually predicts the spread at $1/\sqrt{e}$ ($\approx$0.6) rather than half the maximum intensity, but that difference is small compared to the difference between predicted and measured spreads.

The results in the figure above focus on just one arrival branch on one hydrophone, but they are consistent with many other arrivals and hydrophones in the experiment, as shown by the table. Overall, the 200 Hz centered signal transmitted from the source had after pulse compression a pulse width of 20.5 ms, which when received 510 km away was only very slightly spread out (per Table 1 and Fig. 2b) due to additive ambient noise as well as scattering in ocean fluctuations.

Since the measured pulse spreads do include a portion which are greater than or equal to half the carrier period $T_c/2$, the complete dataset does potentially include some fading caused by destructive interference. So we next analyze measured intensities with pulse spreads less than a certain threshold, selectively filtering out those larger pulse spreads entirely. As represented by the shaded regions in Figs. 2a and 2b, this upper threshold is set to half the carrier period ($T_c/2 = 2.5$ ms) minus the half-width Δ_n at half-maximum of the PDF of δW_n. For arrival D on hydrophone #057, $\Delta_n = 1.3$ ms. Half the period of the carrier is required for destructive interference, but the threshold is even further reduced by the half-width of the noise PDF because the measured spreads are contaminated by the noise, which smears the pulse spread information across the $T_c/2$ boundary. The subset of measurements with pulse spreads less than 1.2 ms ($= T_c/2 - 1.3$, the shaded region in Fig. 2b) has no destructive interference and thus no deep fading.

Fig. 3a shows histograms of single-frequency intensities for all the measured pulse spreads, as well as for the subset of pulse spreads less than 1.2 ms (the shaded region in Fig. 2b). That subset has no spreads large enough to account for the destructive interference necessary for fading. However, both histograms of intensity display a near-exponential distribution, at least for the lower 95% of the data; the intensities in the highest tail (last 5% of data) are higher than exponentially distributed. This description is made more specific by the Q-Q plot shown in Fig. 3b. That plot represents a theoretical exponential distribution on the abscissa and the distribution of the measured data on the ordinate axis, so if the points followed exactly along the diagonal with slope=1 then the measured distribution would be

exactly exponential. As with the histogram in Fig. 3a, this Q-Q plot shows that for both the complete and the thresholded datasets, the lowest 95% of the intensities are close to exponentially distributed, and the highest one percent of the intensities are significantly higher than exponentially distributed.

As before, these figures show only statistics from a single arrival branch (ray ID) on a single hydrophone, but this result is consistent across many arrival branches on many hydrophones in the 54 hour dataset. Table 2 lists predicted and measured scintillation indices for the same arrivals and hydrophones listed in Table 1 regarding pulse spreads. The measured scintillation index is defined as SI $= \langle \mathrm{I}^2 \rangle / \langle \mathrm{I} \rangle^2 - 1$, where I is the carrier-frequency spectral component of the intensity. Both predicted and measured SI are greater than one in all cases; the Q-Q plot in Fig. 3b shows that this is caused by the high tails of the last percent or so of the data – if SI is recalculated for the measured $\mathrm{I}/\langle \mathrm{I} \rangle < 4$, the SI values are 0.9-1.1 (and 1.0 for the case plotted here). The standard error of the measured SI values is calculated by block bootstrap (blocking by the correlation time of the intensities), assuming that the time variability of the SI is greater than the sampling error so that the latter is neglected.

4   Summary and conclusions

The majority of observed pulse spreads are too small to allow for destructively interfering or randomly phased micro-multipaths. In the model of Eq. (1), in-phase signals sum to large amplitudes, whereas out-of-phase signals sum to low amplitudes. The preponderance of small spreads should therefore suggest a preponderance of large amplitudes. The measured intensity distributions, however, fail to support this proposition. This contradiction applies in general, but more significantly it also applies for a sub-population of measurements selectively filtered to only include spreads less than a quarter carrier period. There is presently no theoretical explanation for these phenomena.

The pulse spreads predicted by CAFI for this experiment are also less than a half carrier period and comparable to the mean δW_o of the data, and the CAFI-predicted scintillation indices are large and comparable to the measured ones. These together suggest that path integral theory (via CAFI) and the data agree more with each other than they do with the micro-multipath hypothesis. The CAFI predicted SI is 1.3-1.7 which is in partial saturation, so significant destructive interference is to be expected, but this does not bear out in the pulse spread observations.

The figures in this paper focus on a single arrival branch on a single hydrophone, but as the tables show, these results are consistent across many arrival branches and many hydrophones. Comparison of the mean pulse spreads with scintillation indices for the six arrivals on four hydrophones in Tables 1 and 2 supports the same conclusions.

Acknowledgements

References

[1] Flatté, S.M., R. Dashen, W.H. Munk, K.M. Watson, F. Zachariasen, *Sound Transmission Through a Fluctuating Ocean*, Cambridge University Press, Cambridge, England, (1979).

[2] Flatté, S.M., and G. Rovner, "Path-integral expressions for fluctuations in acoustic transmission in the ocean waveguide," in Methods of Theoretical Physics Applied to

Oceanography, P. Müller, ed., pp. 167-174 (Proceedings of the Ninth Aha Hulikoa Hawaiian Winter Workshop, 1997).

[3] Uscinski B.J., *The Elements of Wave Propagation in Random Media*, McGraw-Hill, London, (1977).

[4] Colosi J.A., E.K. Scheer, S.M. Flatté, B.D. Cornuelle, M.A. Dzieciuch, W.H. Munk, P.F. Worcester, B.M. Howe, J.A. Mercer, R.C. Spindel, K.Metzger, T.G. Birdsall and A.B. Baggeroer, "Comparisons of measured and predicted acoustic fluctuations for a 3250-km propagation experiment in the eastern North Pacific Ocean", J. Acoust. Soc. Am. 105 , 3202-3216 (1999); http://dx.doi.org/10.1121/1.424650

[5] Colosi, J.A., F.Tappert and M.A. Dzieciuch, "Further analysis of intensity fluctuations from a 3252-km acoustic propagation experiment in the eastern North Pacific Ocean", J. Acoust. Soc. Am. 110 , 163-169 (2001); http://dx.doi.org/10.1121/1.1369100

[6] Tang, D., D. Rouseff, F.S.Henyey, and J.Yang, "Single-path acoustic scintillation results from the Shallow Water 2006 Experiment", J. Acoust. Soc. Am. 126, 2172 (2009).

[7] Worcester P.F., M.A. Dzieciuch, J.A. Mercer, R.K. Andrew, B.D. Dushaw, A.B. Baggeroer, K.D. Heaney, G.L. D'Spain, J.A. Colosi, R.A. Stephen, J.N. Kemp, B.M. Howe, L.J. Van Uffelen and K.E. Wage, "The North Pacific Acoustic Laboratory deep-water acoustic propagation experiments in the Philippine Sea", J. Acoust. Soc. Am. 134 , 3359-3379 (2013); http://dx.doi.org/10.1121/1.4818887

[8] Andrew, R. K., "The APL-UW Multiport Acoustic Projector System", Technical Report APL-UW TR 0902, December 2009.

[9] White, A.W., R.K. Andrew, J.A. Mercer, P.F. Worcester, M.A. Dzieciuch, J.A. Colosi, "Wavefront intensity statistics for 284-Hz broadband transmissions to 107-km range in the Philippine Sea: Observations and modeling", J. Acous. Soc. Am. 134 (4), 3347-3358 (2013).

Table 1: Predicted and measured statistics of pulse spread variations over 54 hours for six arrivals on four hydrophones, for pulses centered at 200 Hz. CAFI-predicted pulse spread $\widehat{\delta W_o}$, mean pulse spread $\langle \delta W_o \rangle$, and percentage $\%_m$ of measured pulse spreads greater than half the carrier period. Pulse spread units are milliseconds. Arrival designators A-F correspond to arrivals marked on timefront in Fig. 1b.

| arr | #023 ($\bar{z}$=750m) | | | #057 ($\bar{z}$=1391m) | | | #090 ($\bar{z}$=1991m) | | | #111 ($\bar{z}$=2794m) | | |
	$\widehat{\delta W_o}$	$\langle \delta W_o \rangle$	$\%_m$	$\widehat{\delta W_o}$	$\langle \delta W_o \rangle$	$\%_m$	$\widehat{\delta W_o}$	$\langle \delta W_o \rangle$	$\%_m$	$\widehat{\delta W_o}$	$\langle \delta W_o \rangle$	$\%_m$
A	1.2	1.6	31.4	1.2	1.6	31.1	1.4	1.6	29.1	1.4	1.7	28.6
B	1.0	1.7	31.7	1.1	1.6	29.7	1.0	1.8	33.0	1.3	1.6	28.8
C	1.0	1.7	30.1	1.0	1.8	31.1	0.9	1.7	30.7	1.0	1.9	32.4
D	1.0	1.4	29.8	1.0	1.7	32.5	0.9	1.6	29.2	1.8	1.9	33.7
E	2.5	1.9	34.5	1.9	2.0	36.5	1.9	1.9	34.6	1.8	2.2	36.0
F	2.3	1.8	32.4	1.9	1.8	33.9	1.9	1.9	33.3	2.0	2.3	36.8

Table 2: Predicted and measured statistics of intensity variations at 200 Hz over 54 hours for six arrivals on four hydrophones: predicted scintillation index $\widehat{SI}$ from CAFI model, measured SI $\pm$ one standard error as calculated via block bootstrap. Arrival designators A-F correspond to arrivals marked on timefront in Fig. 1b.

arr	#023 ($\bar{z}$=750m) $\widehat{SI}$	SI	#057 ($\bar{z}$=1391m) $\widehat{SI}$	SI	#090 ($\bar{z}$=1991m) $\widehat{SI}$	SI	#111 ($\bar{z}$=2794m) $\widehat{SI}$	SI
A	1.5	1.3±0.2	1.5	1.4±0.2	1.5	1.3±0.1	1.5	1.1±0.1
B	1.7	1.3±0.2	1.7	1.3±0.1	1.7	1.2±0.2	1.6	1.4±0.1
C	1.6	1.6±0.2	1.7	1.5±0.2	1.6	1.3±0.2	1.6	1.4±0.1
D	1.7	1.5±0.1	1.7	1.4±0.3	1.7	1.5±0.2	1.5	1.9±0.3
E	1.3	1.3±0.2	1.4	1.9±0.2	1.4	1.6±0.2	1.4	1.2±0.1
F	1.5	1.7±0.3	1.5	1.8±0.4	1.5	1.9±0.3	1.6	1.6±0.2

(a)

(b)
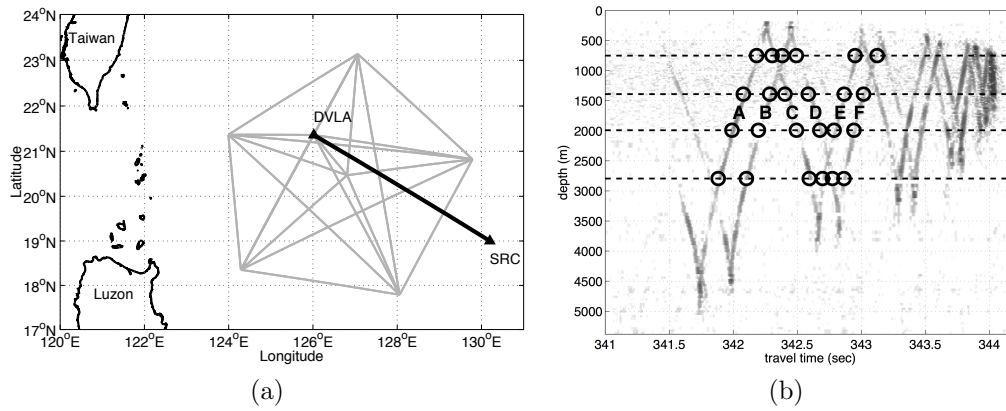
Figure 1: (a) Geometry for the experiment. (b) Measured timefront showing acoustic intensities of a single pulse-compressed M-sequence, with the six arrivals and four hydrophones discussed in this paper (serial# 023, 057, 090, and 111, at depths 750 m, 1391 m, 1991 m, and 2794 m respectively).
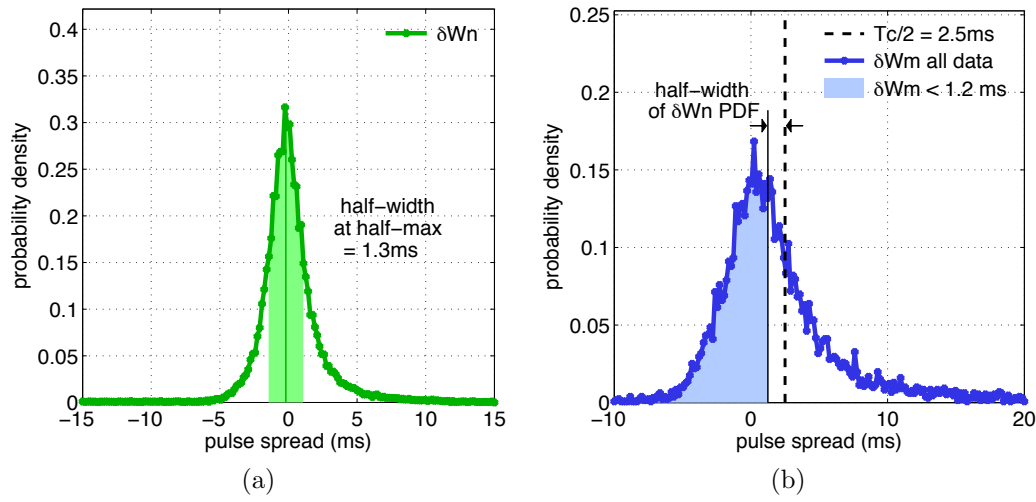
Figure 2: Pulse spreads for arrival D on hydrophone #057. (a) Monte-Carlo-generated PDF of the ambient noise-induced component of the pulse spreads. (b) PDF of measured pulse spreads δW_m (dark blue) and the subset of them thresholded at 1.2 ms (light blue). (Color online)
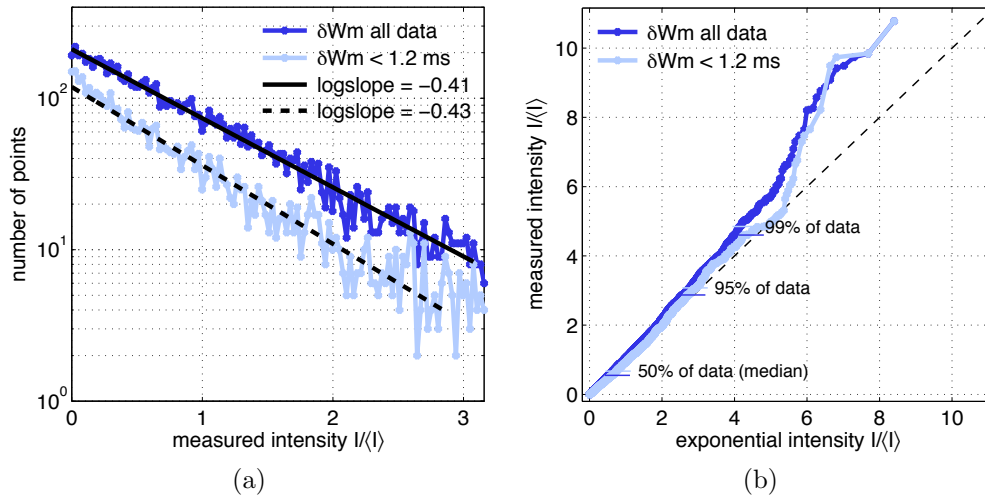
Figure 3: Intensity statistics for arrival D on hydrophone #057. (a) Histograms of all measured intensities (dark blue) and the subset of them with pulse spreads thresholded at 1.2 ms (light blue), i.e. in the shaded region of Fig. 2b. Fit lines estimating the slopes of the two histograms cover the lowest 95% of the intensities. (b) Q-Q plots for the two histograms in (a). Note there are a small number of data (a few percent) with intensities greater than the upper boundary of the abscissa shown in (a); the complete ranges are shown in (b). (Color online)

Low-frequency Pulse Propagation over 510 km in the Philippine Sea: A Comparison of Observed and Theoretical Pulse Spreading by Rex K. Andrew, Andrew Ganse, Andrew W. White, James A. Mercer, Matthew A. Dzieciuch, Peter F. Worcester, and John A. Colosi

(submitted to *J. Acoust. Soc. Am.*)

Low-frequency Pulse Propagation over 510 km in the Philippine Sea:

A Comparison of Observed and Theoretical Pulse Spreading

Rex K. Andrew,[a)] Andrew Ganse, Andrew W. White, and James A. Mercer

Applied Physics Laboratory,

University of Washington,

Seattle,

WA 98105

Matthew A. Dzieciuch and Peter F. Worcester

Scripps Institution of Oceanography,

University of California at San Diego,

La Jolla,

California,

92093

John A. Colosi

Department of Oceanography,

Naval Postgraduate School,

Monterey,

California,

93943

(Dated: draft compiled: September 22, 2015)

Abstract

Observations of the spread of wander-corrected average intensity pulses propagated over 510 km for 54 hours in the Philippine Sea are compared to Monte Carlo predictions using a parabolic equation and path-integral predictions. Two simultaneous *m*-sequence signals are used, one centered at 200 Hz, the other at 300 Hz; both have a bandwidth of 50 Hz. The internal wave field is estimated at slightly less than unity Garrett-Munk strength. The observed spreads in the early ray-like arrivals are much less than the pulse width. Spreads for the 200 Hz signal are roughly 1 ms; spreads for the 300 Hz signal are substantially smaller and hence almost unmeasurable. Monte Carlo predictions are accurate for 21 and 22 turning points but show increasing over-prediction for decreasing turning points. Path-integral theory prediction of spread is accurate for 17 and 18 total turning points, contrary to results reported for much longer ranges. However, path-integral predictions appear to be increasingly biased high with increasing numbers of turning points.

I. INTRODUCTION

Time-domain statistics of low frequency long range sonar signals are important for underwater acoustic communication and navigation, but the current theory that predicts these statistics is not as broadly verified as the theory for frequency-domain statistics. This study presents observations of the spread of averaged intensity pulses propagated over 510 km for 54 hours in the Philippine Sea, and compares the measured spread again simulations from Monte Carlo predictions using a parabolic equation, and path-integral predictions. Two simultaneous m-sequence signals are used, one centered at 200 Hz, the other at 300 Hz; both have a bandwidth of 50 Hz. Intensity pulses are isolated in the early ray-like part of the timefront, and collected on several dozen hydrophones on a water-column-spanning mooring. The observed spread in the early ray-like arrivals is much less than the pulse width. Spreads for the 200 Hz signal are roughly 1 ms; spreads for the 300 Hz signal are substantially smaller and hence almost unmeasurable. Monte Carlo predictions are accurate for 21 and 22 turning points but show increasing over-prediction for decreasing turning points. Path-integral theory prediction of spread is accurate for 17 and 18 total turning points, contrary to results reported for much longer ranges. However, path-integral predictions appear to be increasingly biased high with increasing numbers of turning points.

Pulsed signals and underwater propagation studies have had a long acquaintanceship in acoustics. In 1827, Colladon and Sturm used an impulse-like subsurface bell strike in Lake Geneva to measure the sound speed in water[1]. Impulse-like sound was later used by Ewing and Worzel in 1948 to study the propagation properties of the deep sound channel using 1 kg TNT explosive charges[2]. Explosive charges were ideal for deep sound channel studies: indeed, Bergmann extols the virtues of explosive charges in a dated U. S. Navy underwater acoustics manual[3]

> Explosive sound . . . consists of one or more pulses of extremely short duration [and] can be useful . . . in that it can supply valuable additions to our information about . . . causes of many of the phenomena observed in sound transmission.

a)Electronic address: `rex@apl.washington.edu`

Very large explosives could be used to explore very long range propagation: a significant example is the 1960 Perth-Bermuda experiment, in which 140 kg depth charges were used to ensonify a propagation path almost 20 Mm long[4]. Underwater ordnance, however, is significantly hazardous, and explosive pulses are poorly controlled waveforms at best. The development of electro-acoustic sources permitted much greater control over radiated waveforms, but practical sources lack the source level of explosive charges. Alternate techniques are required to provide adequate signal-to-noise ratio (SNR) at long ranges. The seminal long-range low-frequency effort was the 1991 Heard Island experiment[5], in which pulse-compression was used on *m*-sequences to achieve adequate SNR gain at ranges as great as 18 Mm; as a by-product, pulse-compression produces pulses in the post-processed data.

Appreciation for the features of propagation through a stochastic medium has been motivated by the timeless problem of the fluctuating intensity of starlight. Efforts to find quantitative solutions for these and related statistical features began in earnest using celestial sources in the mid-20th century. Celestial objects were considered to be always "on" (vice pulsed) and therefore it was natural to start with the Helmholtz equation, which is a single-frequency "always on" equation with no sense of a time domain. For problems with only weak forward scattering, the paraxial approximation could be applied, and considerable progress was made for low-order single-frequency statistical field moments. Treatment of pulsed sources, driven by improvements in transmitting and receiving instrumentation, quickly followed for radar ranging and pulsars, which were discovered in 1967. The common approach for solutions of pulse propagation statistics is to use Fourier synthesis on single frequency solutions, and this development is included in standard textbooks[6].

The extension of these solutions to problems of acoustical propagation in the ocean was not successful due to the unique properties of the oceanic sound channel and the anisotropy of the scattering mechanisms. The evolution of underwater solutions has been thoroughly described elsewhere (c.f. Flatté *et al.*[7].) Development paralleled earlier efforts, starting with the Helmholtz equation and applying the paraxial approximation, and reasonable solutions have been found for the phase and, to a lesser degree, the amplitude and intensity of phasors for a few typical scenarios. Phasors are single-frequency constructs; the extension for wideband waveforms, i.e., pulses,

followed the same prescription as for optical and radio propagation problems in the atmosphere, but apparently has not been as successful. In 1999, Colosi *et al.*[8] noted that pulse spread predictions for the ATOC Engineering Test were nearly two orders of magnitude too large and Colosi *et al.*[9] concluded that wideband (i.e., pulse) propagation predictions remains an unsolved problem in ocean acoustics. Further efforts bore out that assessment. In 2000, Flatté and Rovner[10] suggested that the pulse-spread prediction from Flatté-Dashen theory did not seem to be well-understood in long-range low-frequency regimes. Finally, in 2003, Flatté and Vera conducted a comparison of Flatté-Dashen theory to Monte Carlo parabolic equation (MCPE) simulations at 250 Hz and 1000 km, and offered evidence that Flatté-Dashen theory over-predicted the MCPE pulse spread by an order of magnitude[11].

More recently, the desire to send communication and navigation information over long ranges in the ocean has increased the importance of utilizing time-domain waveforms. Communication theory has a long history in understanding and developing fading multipath channels. The confluence of communication theory concepts with underwater acoustical propagation appears now to be the logical evolution of stochastic wave propagation research in underwater acoustics.

Whereas a single-frequency phasor has two parameters — amplitude and phase — a complex broadband pulse has essentially an infinite number of parameters, providing a much richer set of potential statistical descriptors. The central effort in this study contracts that set to a single important statistic, the observed spread of average pulses. Based on the recent literature, this topic alone involves a mismatch between theory and observation, and therefore should benefit from a comprehensive treatment. Precise definitions of "average" and "pulse" are given in the following sections.

The analysis presented here involves a three-way comparison between measurements made in the Philippine Sea, extensive MCPE simulations, and theoretical calculations. The definitions themselves are provided in section II. Section III describes the background for the three datasets. Each dataset consists of depth- and path-indexed pulse spreads and associated statistics. First, the actual experiment is described, followed by the data processing used on the at-sea data necessary to calculate the spreads. Second, the MCPE simulations are described, including the input param-

eters, which were tuned to mimic at-sea conditions as closely as possible. Data processing on the MCPE simulations was intentionally as similar as possible to that applied to the at-sea data. Third, the input parameters and the physical interpretation of the calculated measures are described for corresponding theoretical calculations, which implement Flatté-Dashen theory. The definitions of pulse spread used here is given in section IV , and then section V provides the three-way comparisons of pulse spread for the Philippine Sea 2010 experiment.

In general, we find that the pulse spread in the early ray-like arrivals is much less than the pulse width, and in some cases is less than the sample period (roughly 1 ms) and hence almost unmeasurable. As expected, there is no significant dependence on the sign of eigenray launch angle at the source. MCPE predictions are quite accurate for 20 and 21 turning points, and are biased slightly larger for fewer turning points, i.e., for paths which may be interacting with a shallow warm core eddy. Predictions from Flatté-Dashen theory show a greater sensitivity on the number of turning points than do the observations or the MCPE simulations. This bias can be almost an order of magnitude high for very small pulse spreads, but generally only a factor of 2 or 3 when the pulse spread is of order 1 ms.

II. PULSE SIGNAL MODEL

The early part of the acoustic field at receiver location $\mathbf{r}_S$ and frequency ω due to a source at location $\mathbf{r}_R$ can be written

$$\tilde{p}_0(\omega; \mathbf{r}_S, \mathbf{r}_R; l) = \tilde{h}(\omega)\tilde{g}_0(\omega; \mathbf{r}_S, \mathbf{r}_R; l), \tag{1}$$

where $\tilde{h}(\omega)$ is the transfer function of the transmitter system. Subscript 0 denotes an ansatz without stochastic perturbations. Under a paraxial approximation, $\tilde{g}_0(\cdot; \cdot, \cdot, l)$ represents the Green function for the lth distinct stationary phase propagation solution from $\mathbf{r}_S$ to $\mathbf{r}_R$. In the unperturbed scenario, this solution will be called the unperturbed eigenray. Typically, the early part of the acoustic field admits multiple unperturbed eigenray solutions. (This is a fundamental difference between the underwater scenario and optical and radio scenarios in the atmosphere.)

In the "image formulation" of Tolstoy and Clay[12], the Fourier transform of Eq. 1 is

$$p_0(t) = h(t) * g_0 \delta(t - t_0),$$ (2)

where $h(t)$ is the transmitter impulse response, g_0 is an amplitude, t_0 is a delay and $*$ denotes convolution. (The spatial notations have been dropped. Additionally, development below will isolate the features of a single unperturbed eigenray solution, and therefore the designator l become superfluous and will be left out as well.) This representation, using a simple retarded time-domain Green function, will be adequate for the development below. From Eqs. 1 and 2, the received acoustic intensity is

$$|p_0(t)|^2 = \iint d\omega_1 \, d\omega_2 \, e^{i(\omega_1 - \omega_2)t}$$
$$\times \tilde{h}^*(\omega_2)\tilde{h}(\omega_1)\tilde{g}_0^*(\omega_2)\tilde{g}_0(\omega_1).$$ (3)

In the presence of random propagation conditions, $\tilde{g}_0$ will be a random function, represented by $\tilde{g}$, the received intensity will be a non-negative stochastic waveform, and one considers the ensemble average of Eq. 3:

$$\langle |p(t)|^2 \rangle = \iint d\omega_1 \, d\omega_2 \tilde{h}^*(\omega_2)\tilde{h}(\omega_1)\Gamma(\omega_1, \omega_2)e^{i(\omega_1 - \omega_2)t},$$ (4)

where

$$\Gamma(\omega_1, \omega_2) = \langle \tilde{g}^*(\omega_2)\tilde{g}(\omega_1) \rangle$$ (5)

is the frequency-frequency mutual coherence function (F-FMCF) and the notation $\langle \cdot \rangle$ throughout denotes an ensemble average.

The F-FMCF is a Fourier domain function which plays a central role in the analysis of pulse propagation experiments. Traditionally, derivations for it are sought first, and then predictions on the time-domain dual, which is an ensemble-averaged pulse, are computed using a Fourier or Fourier-like synthesis. Dashen *et al.*[13] derived expressions for the F-FMCF for the stochastic ocean propagation problem, using a path integral treatment. Flatté and Stoughton[14] provided an alternate expression using Floquet theorems to exploit the periodicity inherent in vertically cycling eigenray paths. More recently, Kalugin *et al.*[15] used local transformations of the parabolic equation, a technique originally introduced by Mazar and Felsen[16].

In this study, the probe signal bandwidth was not wide enough to ensonify the dominant Fourier domain region of the F-FMCF directly, and therefore the analysis pursues features of the time-domain pulses.

Since this is a pulse propagation experiment, it is at this point germane to define the term "pulse". While a pulse is an obvious construct, it nevertheless appears in the literature in many guises. A "pulse" is generically an L^2 integrable function with compact and finite support. Generalized pulses have essentially an infinite number of descriptors. As this is unwieldy, pulses are often either represented by a analytical function with a small number of parameters, or characterized by a small number of descriptors, such as moments and central moments. Other descriptors may include the mode, the width (e.g., the full width at half maximum), or other summary measures. When the waveform is modeled by a parametric curve, descriptors either involve the parameters directly or some function of the parameters. Recourse to some of these summary descriptors will occur in the analysis and interpretation sections.

None of the pulses encountered here meet this rigorous definition. The transmitter impulse function $h(t)$ is bandlimited due to practical hardware constraints, and therefore cannot formally have finite time-domain support. The unperturbed received waveform $p_0(t)$, which in this model is a scaled and shifted replica of $h(t)$, inherits this difficulty. The Dirac delta function in Eq. 2 is a pathological example, and by itself does not meet the L^2 criterion. Furthermore, the ubiquitous Gaussian function, which does have a finite second moment, fails because it is neither time nor frequency-limited.

Stochastic wave propagation introduces more complexity. Following Flatté-Dashen theory[7], the stochastic received waveform can be modeled as

$$p(t) = h(t) * \sum_{m \in \mathcal{M}} g_m \delta(t - t_m), \tag{6}$$

where g_m and t_m are now random amplitudes and delays of micro-multipath ray paths near the unperturbed eigenray. The $\mathcal{M}$ notation represents the index set identifying the micro-multipath components, of which there are a random number per realization. (The micro-multipath index m is different than the multipath index l associated with unperturbed eigenrays: the set $\mathcal{M}$ is considered

8

here to involve only those paths associated with a single, isolated, unperturbed eigenray.) Eq. 6 is the fundamental signal model for the analysis below. While $p(t)$ usually does not have the same appearance as $h(t)$, $p(t)$ (and $|p(t)|$ and $|p(t)|^2$ and so on) inherits the inconsistency in mathematical rigor associated with $h(t)$ via the model Eq. 6. Furthermore — and here terminology becomes very flexible indeed — averages, such as Eq. 4, have also been called pulses for the case where $h(t)$ is a true impulsive pulse $\delta(t)$[6]. This will be addressed in section III.C.

Fortunately, for the type of waveforms observed here, intuition allows us to sidestep questions of mathematical rigor. As shown in section III.A.3, the radiated waveform (after equalization and pulse-compression) appears for all practical purposes to have compact finite time-domain support. If time-domain sidelobe structures exist, they are buried in noise. We will take the approach that all significantly peaked features have compact time support and are legitimate pulse entities This approach breaks down when the pulse is faded, particularly deeply faded; adaptations for these cases are discussed in section III.A.4. The construct Eq. 4 has special importance and has been called the ensemble-averaged pulse[13,17]. To avoid confusion with the other pulses discussed here, it will be called below the ensemble-averaged intensity pulse (EAIP).

In this work, the observed and predicted properties of the EAIP are examined.

For the particular case where $h(t)$ is the impulse response $\delta(t)$, Eq. 6 gives

$$C(t) = \sum_{m \in \mathcal{M}} g_m \delta(t - t_m) \tag{7}$$

which plays a prominent role in communication theory where Eq. 7 is known as the time-variant impulse response[18]. (The "time-varying" nature of the response refers to the change in the set $\{g_m, t_m, \mathcal{M}\}$ with change in the evolution time of the channel, i.e., from realization to realization, and is not indicated explicitly in Eq. 7, which only shows a dependence on the signal time t.) Various quantities, such as the multipath intensity profile[18] and its Fourier transform, the spaced-frequency correlation function[18], can be developed from the channel impulse response, and these functions are fundamental for determining the communication capacity of fading multipath channels such as the PhilSea10 channel.

FIG. 1. Geographic configuration in the deep Philippine Sea for the pulse propagation experiment.

III. METHOD

A. Philippine Sea Data

1. The 510 km Pulsed Propagation Experiment

The at-sea observations were obtained during an experiment conducted 5-29 May 2010 in the Philippine Sea. This effort was part of a larger multi-cruise, multi-institution "PhilSea10" experiment[19] to investigate the deterministic and stochastic properties of long-range deep ocean sound propagation in a region of energetic oceanographic processes. The assets for this experiment are shown in Fig. 1. A transmitter package was suspended from the R/V *Roger Revelle* at location "SS500" at $19°00.00'$N, $130°12.00'$E to a depth of 998 m. The acoustic data was collected by an autonomous vertical line array (VLA) receiver deployed to the seafloor at nominally $21°21.7418'$N, $126°0.7867'$E, at a bearing of $302°$ and a range of 509783 m from the transmitter. Typical eigenrays are shown in Fig. 2: depth excess along the propagation path allowed a significant number of non-boundary interacting paths from transmitter to receiver. The range of upper turning point depths for the paths with unique, resolvable pulses are shown in Table I.

The transmitter package has been described by Andrew[21] and White *et al.*[22]. Briefly, the package consisted of the experimental double-ported doubly resonant electro-acoustic MP200/TR1446 transducer (designed by ImageAcoustics Inc. and manufactured by Massa Products, Inc.), a matching auto-transformer/tuner manufactured by Coiltron, Inc., a tracking pinger, auxiliary sensors, a monitor hydrophone attached to the deployment cable 20 m above the MP200/TR1446 and a

FIG. 2. Left panel: four representative eigenrays. The transmitter was at depth 998 m. Paths are shown to a typical receiver depth of 1200 m. Eigenrays launched upwards are ray ID $+18$ and $+22$; eigenrays launched downward are -17 and -22. The thick solid line is bathymetry from SRTM30_PLUS[20]. The right panel shows the range-averaged sound speed profile. This was also the sound speed profile used in the MCPE and CAFI calculations.

SeaBattery for sensor electronics power. The transmitter is synchronized to GPS for precision drive waveform delivery to the power amplifier. A long baseline acoustical navigation array was established at SS500 to track the 3-D location of the transmitter package. Additionally, the R/V *Roger Revelle* used dynamic positioning driven by a high-precision C-Nav GPS to maintain station at the transmit location. Measurements indicated that the package did not deviate from the target transmit location by more than a couple of meters throughout the experiment.

The VLA concept has been described by Worcester *et al.*[23] and the PhilSea10 configuration by Worcester *et al.*[19]. The instrument was designed to capture as much of the full-water-column acoustic field in deep water as possible. The PhilSea10 mooring included five autonomous sub-arrays of hydrophones for a combined total of 150 hydrophone modules. Each subarray had one controller. Each hydrophone module was an intelligent sensor package containing the transducer, signal conditioning and digitizing circuitry, a microcontroller, a local clock, flash memory and a battery. The modules were commanded by their associated controller using inductive modems

11

communicating over the mooring wire itself. The number of hydrophone modules and the inter-element spacing varied within and between subarrays. Nominal configurations are shown in Table II. The inter-element spacing throughout the middle of the deep sound channel was designed to resolve low-frequency low-order modes, while the shallower and deeper sensor spacings were larger to achieve (nearly) full water column coverage. The mooring was also outfitted with Sea-Bird SBE37-SMP pumped conductivity-temperature-pressure microCAT CTD recorders[24], Sea-Bird SBE39 temperature recorders[25] and a long-baseline acoustical navigation system which navigated the controllers on the mooring once per hour. The hourly position solutions were considered accurate to within a couple of meters. Positions between hours used linear interpolation between adjacent hours: positions of hydrophone modules used linear interpolation between adjacent controller positions.

2. Environmental Section

From May 15 to May 21, the R/V *Roger Revelle* obtained a CTD section along the nominal acoustic propagation path between SS500 and the VLA. Casts were made about every 10 km to a depth of about 1500 m, starting from the VLA. Every fifth cast was to within several hundred meters of the bottom, roughly 5000 to 6000 m, depending on location. This section involved 51 casts. The difference between the derived sound speed and the corresponding WOA2009 May climatology[26–28] in the upper ocean is shown in Fig. 3. There was a significant warm-core eddy down to roughly 300 m towards SS500, but colder than usual water closer to the VLA. These are typical time-varying mesoscale features of the Philippine Sea not captured by the standard oceanographic climatologies.

3. The At-Sea Pulsed Signals

The transducer has sharp resonances at about 210 Hz and 320 Hz. In the PhilSea09 Pilot Study/Engineering Test[22], the transducer was treated as a device with a single passband from below 210 Hz to above 320 Hz, and a 130 Hz-wide drive signal was centered between the two
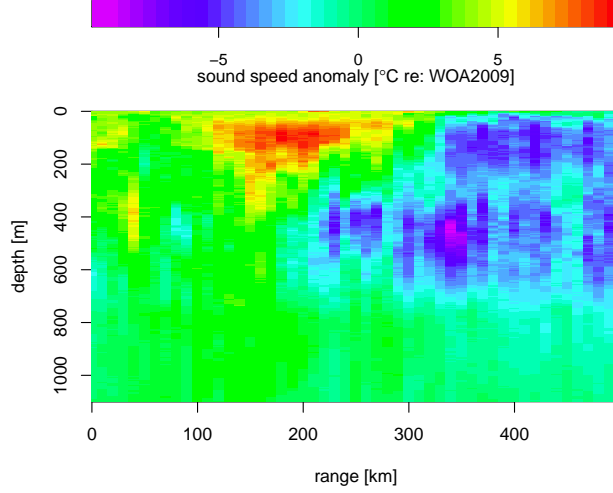
FIG. 3. Section sound speed difference from the WOA2009 climatology. The reference sound speed computed from May WOA2009 temperature and salinity, converted to sound speed using TEOS-10[28]. Range is section distance from SS500.

resonances. In the PhilSea10 experiment, the transducer was treated as two separate devices with passbands around each resonance. The drive signal was a superposition of two m-sequences[29] with carriers of 200 and 300 Hz. Based on an optical analogy, the 200 Hz (longer wavelength) signal was denoted the "red" signal, and the 300 Hz (shorter wavelength) signal was denoted the "violet" signal. Parameters for these signals are shown in Table III: the parameters were selected so that each m-sequence was 20.46 s in duration in order to superpose exactly.

Transmissions began 2010 May 8 at 16:48:10 UTC and continued for 54 hours. Each transmission involved a guard m-sequence followed by 161 continuous science sequences. A transmission gap occurred at the end of each 161 sequence block to allow the transmitter to resynchronize data capture files, rest the power amplifier, and provide an ensonifcation-free time window at the VLA for mooring navigation. The source level, measured in the water with the monitor hydrophone, was roughly 191 dB re: 1 μPa @ 1 m, corrected to broadside.

The sharp resonances of the transducer induced considerable unacceptable distortion to the radiated signal spectra, and therefore equalization was required to obtain sharp pulses after pulse-compression. The equalization filters were designed using the actual radiated waveforms as mea-

13
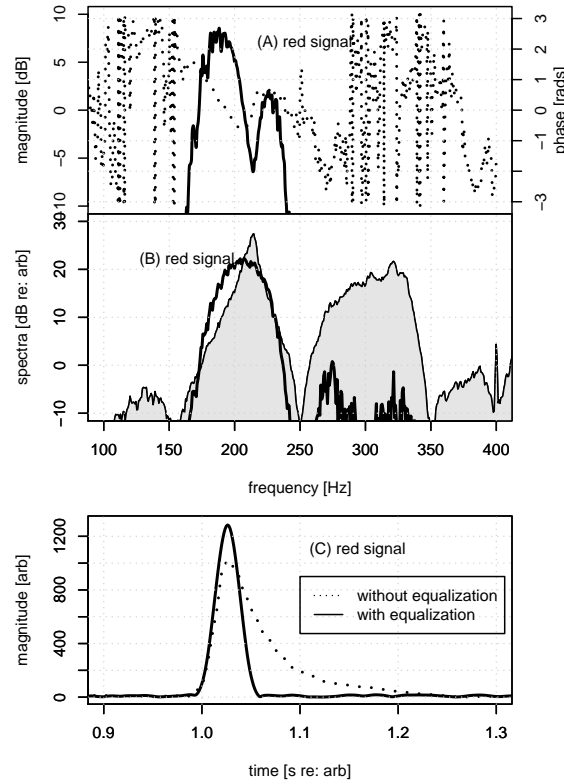
FIG. 4. PhilSea10 "red" signal features. (top) The Fourier domain magnitude (black line) and phase (dashed line) of the red equalization filter; (middle) the autospectra over 30 s of the radiated signal (grey-filled) and after application of the red signal filter (black line); (bottom) the pulse-compressed pulse before and after equalization.

sured on a monitor hydrophone attached to the suspension cable and located 20 m above the transducer. The Fourier characteristics of the filters and their effects are shown in Figs. 4 and 5. The filters eliminate a trailing "afterglow" and deliver clean, narrow, triangular pulses typical in *m*-sequence processing.

4. *Data Processing and Reduction*

The data records from each hydrophone were first processed to yield pulse-compressed data frames. Processing involved (a) correction (via a depth-, unit- and frequency-invariant transfer
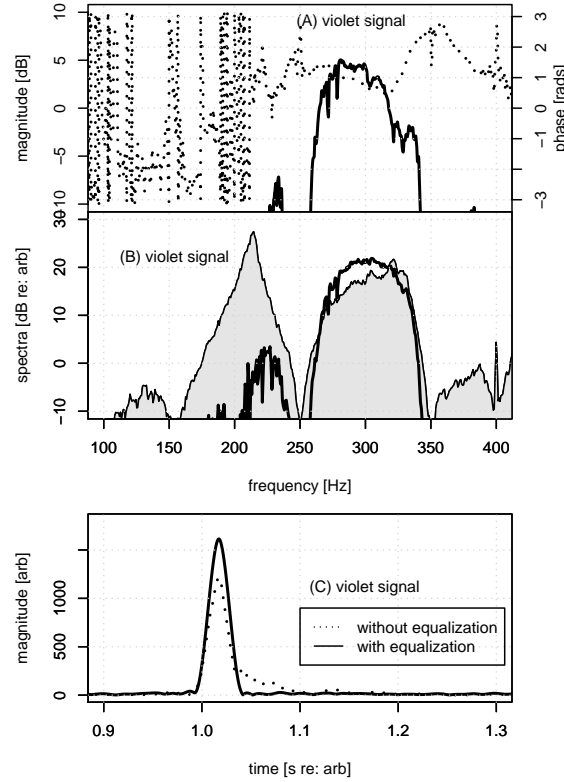
FIG. 5. PhilSea10 "violet" signal features. (top) The Fourier domain magnitude (black line) and phase (dashed line) of the violet equalization filter; (middle) the autospectra over 30 s of the radiated signal (grey-filled) and after application of the violet signal filter (black line); (bottom) the pulse-compressed pulse before and after equalization.

function) to in-water units of μPa, (b) data compression or expansion via a chirp-Z transform to counter any local hydrophone module timebase dilation, (c) forward-backward bandpass filtering with second order Butterworth filters with red/violet bandwidths of 175/220 Hz to mitigate out-of-band noise, (d) resampling to a standard m-sequence frequency of four times the carrier frequency, (e) filtering (in the frequency domain) by the appropriate post-equalizer filter function, and (f) pulse-compression. Additionally, the hydrophone module records are time-shifted to account for timebase drift between the Maxim DS4026 TCXO module clock and the controller Q-Tech MCXO QT2002 clock, and the QT2002 and the controller Symmetricom X72 rubidium frequency standard, which had been disciplined to UTC via a GPS link prior to deployment and

15

represents UTC. Finally, each frame is time-shifted to the surveyed center position, based on the 3-D navigation solution for the mooring at each frame time. No timebase corrections were made for the transmitter position error because deviations of the transmitter from its design target location were deemed too small to be significant. This processing resulted in 161 frames per hour per hydrophone, for a total of 8694 frames for either the red or violet signal.

The composition of each frame for all hydrophones yields the measured timefront: the unparalleled size of the VLA provides nearly complete full-water-column resolution of the timefront. An example timefront using the red signal is shown in Fig. 6. A 10-hour record of red and violet pulses for ray ID-17 on hydrophone module 57 is shown in Fig. 7: the records are somewhat identical, but the fades and twinkles are slightly different. It should be noted that both signals travel through the same path to the receiver; any loss of correlation is therefore directly indicative of a decrease in the F-FMCF between (roughly) 200 and 300 Hz. A more complete frequency domain analysis of the F-FMCF spanning the red and violet signals will be pursued in a future paper.

The noise level associated with each frame was required. The ambient noise at the receivers varied throughout the experiment due to nearby shipping, local weather conditions and other interfering in-water signals. Rather than estimate the actual ambient noise levels, a representative level was determined from the final pulse-compressed frames. The frames were time shifted so that the finale appeared approximately in the middle of each 20.46 s frame. The early arrivals appear prior to this time. After this time, the data dropped to about 10 s of more-or-less stationary complex noise of constant character, which we consider to be the background noise process in the context of the pulse-compressed waveforms. The final 4 s of this complex noise were extracted and processed into autospectral estimates via the Welch method using 1024-pt blocks with 50% overlap. The DC value was then used as a representative background level *NL*.

The first stage of data reduction followed that of White *et al.*[22]: two-dimensional regions of the timefront were identified that contained distinct, non-overlapping sections of branches. These are shown for the red signal in Fig. 6. The (complex) waveforms for each region for all associated hydrophone records were extracted. These waveforms formed the sample pulse population. The
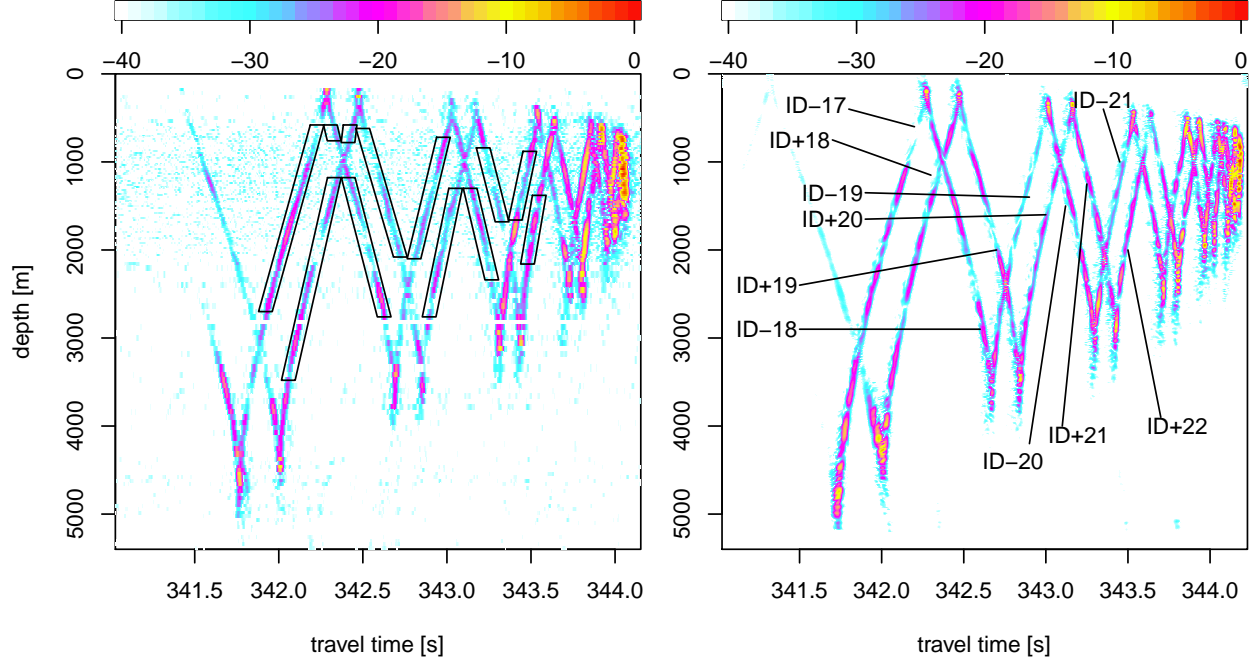
FIG. 6. Example timefronts. Left side: entire (149 hydrophones) observed timefront after post-equalization and pulse compression, red signal, *m*-sequence transmitted 2010/05/08 16:48:10. Polygons show roughly the timefront regions extracted for analysis. The violet signal timefronts had a similar appearance; the polygons for the violet signal pulses were nearly identical to those of the red signal timefront. Right panel: Predicted MCPE timefront realization for the 300 Hz simulation (corresponding to the violet signal.) The 200 Hz timefront simulations were similar. The original solution was produced on a 1 m depth grid: the timefront was resampled to a 10 m grid for plotting. The branches are labeled with their corresponding ray identifiers. Each timefront has been normalized by its largest value. The color scales shown on top are decibels.

timefront branches were easily identified with downward-launched ray identifiers -17, -18, -19, -20, -21, and upward-launched identifiers $+18$, $+19$, $+20$, $+21$, and $+22$. Waveforms were only extracted where there was an unambiguous branch: regions at the cusps and at the branch crossings were therefore excluded in order to avoid introducing the additional complexity of interpreting and decomposing interfering pulses. The consistency of the polygon boundaries along the branches made it feasible to identify and extract the waveform containing the pulse, even if
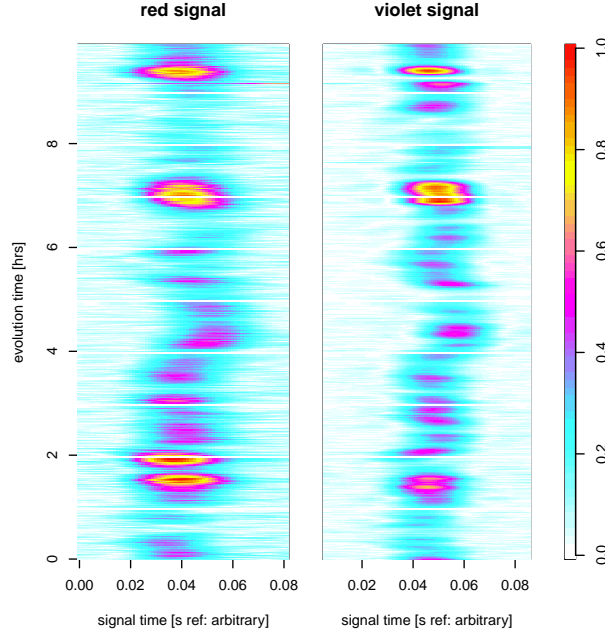
FIG. 7. Pulse-by-pulse records after timing correction, post-equalization and pulse compression for 10 hours starting (at the transmitter) at 2010/05/08 16:48:10. Gaps occur hourly for VLA navigation. Left side: red signal. Right side: violet signal. Ray ID−17. Both signals were in the water at the same time and were separated in post-processing in code space. The color scale is linear in amplitude.

the pulse itself was deeply faded and buried in noise. Such deeply faded and barely recognizable pulses (if recognizable at all) were generally down-weighted in subsequent analysis as being too corrupted by noise. (More on this below.)

In the second stage of data reduction, the EAIP was estimated. Notionally, the EAIP can be represented by an arithmetic average of the observed data. Although each data frame is synchronized to GPS and synthetically time-shifted to eliminate arrival time offsets due to differences from the nominal transmitter-receiver distance, the arrival times of the observed pulses still wander forward and backward due to random ocean propagation influences. Correcting for this ocean-induced wander has consequences regarding the interpretation of some theoretical constructs. This will be addressed in section III.C. Following Colosi *et al.*[8], each waveform was wander-corrected with an alignment algorithm.

It should be noted that the majority of strong pulses observed in the data were unimodal and not seriously misshapen. In other words, if some decomposition algorithm would produce a set $\mathcal{M}$ consisting of multiple components, any probable set of delays $\{t_1, t_2, \ldots\}$ would be tightly clustered within an unresolvable span of say half a carrier period or less. This is unlike the much longer range data of Colosi *et al.*[8].

Arithmetically averaging the resulting sample of wander-corrected waveforms still retained an inconsistency. During fades, particularly deep fades, the pulse signature is easily obscured by the background noise structure. The background noise structure in $|s(t)|^2$ is all-positive, and it does not average to zero. It was therefore desirable to down-weight the contribution of those waveforms representing a faded pulse. noise level in the ith frame. Including this weighting, the estimated wander-corrected intensity pulse, more properly termed the weighted average intensity pulse (WAIP), is

$$\text{WAIP}(t) = \frac{\sum_i w_i |s_i(t)|^2}{\sum_i w_i}, \tag{8}$$

where w_i is the weighting on the ith pulse and is a function of the noise level in the ith frame. As an example, Fig. 8 shows this calculation for the timefront branch ID-17 for hydrophone module S/N 57, the population of observed pulses, and the associated WAIP over the entire experiment for both the red and violet signals. WAIPs were calculated for all receiver depth and timefront branch combinations for which unique and distinct pulses could be extracted. There were 10 branches and nearly 100 hydrophones. About half of all possible permutations yielded distinct pulses. There were roughly 8694 timefronts (a few were discarded due to noise contamination). The total number of pulses processed was roughly 4.9 million for either the red or violet signals.

Presentations of the observed wander-corrected WAIPs versus the transmitted intensity pulses for both signals are shown in Fig 9. The comparisons are catalogued by MP200 signal color and eigenray ID. All the WAIPs for a given eigenray ID —i.e., for a single timefront branch — are normalized and overlaid. The radiated intensity pulse is also normalized and overlaid.

The first thing to note is that the WAIPs are very closely the same shape as the radiated intensity pulse. The red signal WAIPs seem to have a slightly elevated trailing tail. The violet WAIPs are fit very well by the radiated intensity down to a local minimum near the bottom; further
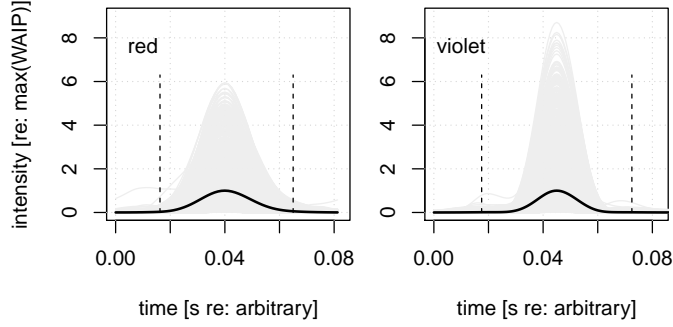
FIG. 8. Wander-corrected WAIPs from HM S/N 57 ID−17. The individual wander-corrected sample pulses are shown in grey. There are 8692 red sample pulses and 8694 violet sample pulses. The WAIPs are shown by black curves. All pulses are normalized by the maximum value of the associated WAIP. Vertical dashed lines indicate the boundary outside of which the waveforms are smoothly attenuated with cosine tapers to zero during the coarse alignment step. Left panel: red signal. Right panel: violet signal.

out, the WAIPs have some low-level structure. This is characteristic of all comparisons except for ID−17 and ID+19. The spread in the WAIPs versus the radiated intensity pulses is very small and is difficult to gauge by eye. Numerical methods estimated the spreads at one or two sample periods. (More on this in section IV.)

B. Monte Carlo PE Calculations

Standard wave-theoretic solutions in the paraxial approximation for the typical weakly range-dependent channels encountered in mid- to low-latitude long range deep water ocean acoustic scenarios (where bathymetric interaction can be neglected, and only fields propagating near horizontal are important) are defined by the parabolic equation. Monte Carlo methods are then used on top of the parabolic equation solutions to simulate the distribution of the wave field statistics. Each Monte Carlo realization builds an acoustic channel on the background sound-speed field by adding a random realization of sound-speed anomalies. Following Colosi-Brown[30], the anomalies

20
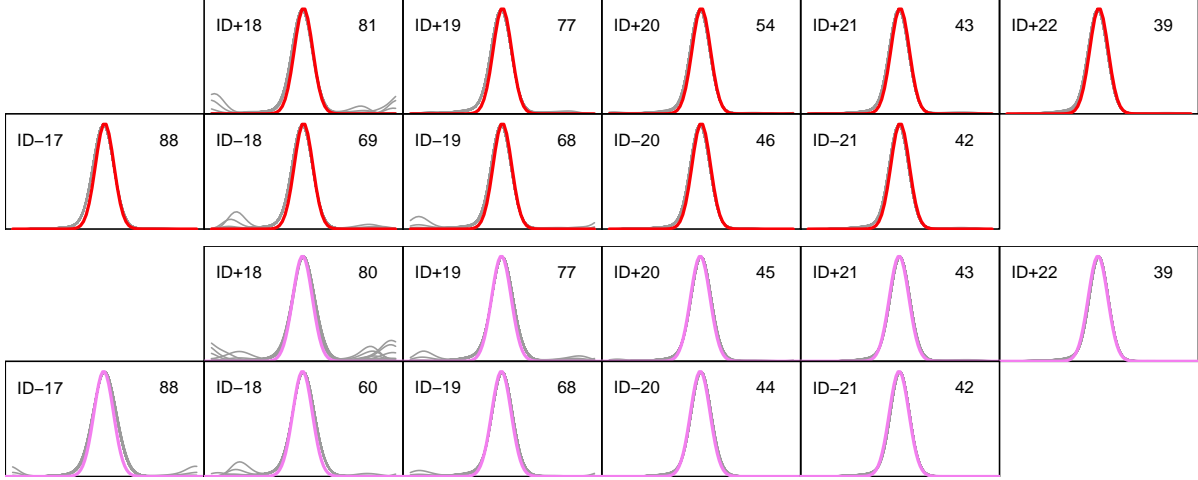
FIG. 9. Shape-by-shape comparison of MP200 WAIPs as measured on the transmitter package monitor hydrophone, and the weighted-averaged intensity pulses (WAIPs) observed on the receiver. The timefront branch identifier is given in each panel in the upper left corner. The WAIPs are all normalized to unity maximum and drawn in grey: the number of WAIPs in each panel is given in the upper right corner or each panel. The radiated intensity pulse has also been normalized to unity and has been time-shifted by eye in order to align roughly with the WAIPs. Top: "red" signal, 66 points at 800 samples/s, spanning 82.5 ms. Bottom: "violet" signal, 110 points at 1200 samples/s, spanning 91.7 ms.

are defined as

$$\delta c(x, z) = \frac{\partial \bar{c}_P}{\partial z} \zeta(x, z) \tag{9}$$

where $\bar{c}_P$ is a background potential sound speed, and $\zeta(x, z)$ is a random vertical fluid displacement field due to internal waves. The theory for devising an anomaly field from an ocean with range-dependent background temperature and salinity fields is not well-established. Therefore, following White *et al.*[22], the problem is simplified by considering the slowly varying background $\bar{c}(x, z)$ to be a range-independent function $\bar{c}(z)$ In this ansatz, the internal wave field can be defined with the well-known Garrett-Munk GM79 model[31].

The key environmental factors required for the simulation of the $\zeta(x, z)$ field under the GM79 model are described in section III.B.1. The full Monte Carlo calculation is briefly reviewed in
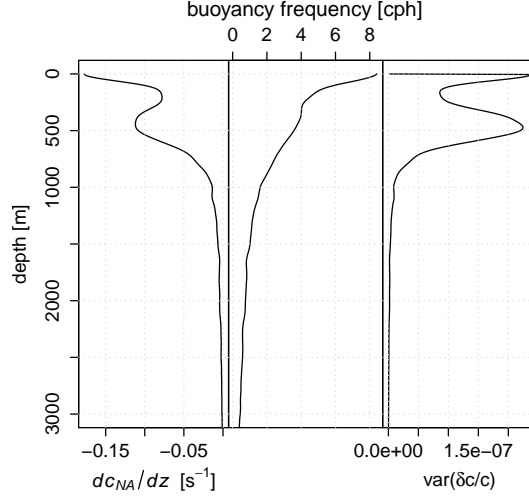
FIG. 10. Profiles for the internal wave simulations. Left panel: the non-adiabatic sound-speed gradient, used to convert the vertical fluid displacement to sound-speed anomaly; center panel: the Brunt-Väisälä buoyancy frequency profile; right panel: the profile of the variance of the fractional sound-speed anomalies. The first two profiles were used in the MCPE simulations, the latter two profiles in the CAFI calculations. Only the top 3000 m of the water column are shown.

section III.B.2.

1. Vertical Displacement Field

The vertical fluid displacement field was constructed using the Henyey-Reynolds algorithm[32]. In addition to the background sound speed profile $\bar{c}(z)$, the Henyey-Reynolds algorithm requires the Brunt-Väisälä frequency profile $N(z)$, the potential sound-speed gradient $\partial_z \bar{c}_P$, and the strength product $bE_{GM:x}$ for a Garrett-Munk field with strength x. (The product $bE_{GM:x}$ always appears as a single term, and will be treated below as such.) The profiles were all derived by smoothing and averaging the CTD casts, described in section III.A.2, made along the section. The buoyancy frequency and potential sound-speed gradient profiles are shown in Fig. 10. The term $bE_{GM:x}$ is a key scalar parameter whose estimation is not as straightforward. This is given briefly next.

White *et al.*[22] describe the estimation of the Garrett-Munk strength from month-long records

of sound-speed measured on the VLA mooring during the PhilSea09 Pilot Study/Engineering Test. A similar procedure was applied to the VLA mooring microCAT CTD records for the period encompassing this pulse propagation experiment. The procedure involves the ratio $\hat{r}$ of observed weighted integrated spectral energy $\hat{s}_{GM:x}$ of the inferred vertical fluid displacement at strength x to the weighted integrated spectral energy $s_{GM:1}$ of vertical fluid displacement based on the unity strength GM79 model. The weighting is the Brunt-Väisälä frequency profile $N(z)$; the product of the profile $N(z)$ and the vertical fluid displacement spectrum is depth-invariant. Under the paradigm that this depth-invariant quantity $s_{GM:x} = \frac{1}{2}(bE_{GM:x})(N_0 b)$ one has

$$\widehat{bE}_{GM:x} = \hat{r}(bE_{GM:1}). \tag{10}$$

The hat notation (̂) represents an estimated value. Here, the product $N_0 b$ is the integral of $N(z)$ over the water column, and will be treated as a single term. Under the standard model[32]

$$\tfrac{1}{2}(bE_{GM:1})(N_0 b) = 0.277 \text{ m}^2\text{rads/sec} \tag{11}$$

for a unity strength Garrett-Munk internal wave field, and hence $bE_{GM:1} = 0.055$ m for the value of $N_0 b = 10.13$ m-rad/s computed from the CTD data. This defines the unity strength energy level. The ratio $\hat{r}$ was estimated to be 0.93 ± 0.078 (for 13 CTDs) and therefore $\widehat{bE}_{GM:x} = 0.051 \pm 0.004$ m.

The Henyey-Reynolds algorithm[32] uses this value of $\widehat{bE}_{GM:x}$ and the other parameters shown in Table IV to generate realizations of the $\zeta(x, z)$ field.

2. MCPE Calculation

The PE calculations were carried out using the split-step Padé algorithm in the Navy Standard Parabolic Equation.[33] Use of the NSPE in the analysis of the PhilSea09 experiment was outlined in White *et al.*[22]: application here was similar. Computation time scales with the number of Padé coefficients, and therefore convergence tests were conducted on the number of Padé coefficients: six coefficients were found to given reasonable convergence. White *et al.*[22] found that a range step of 25 m also provided reasonable convergence, and that was used here as well. Each NSPE

computation produced an acoustic field solution $\psi(z, r = R; f)$ at the range R of the VLA for frequency f. A full-ocean depth grid with 1 m spacing was used. Solutions were generated on a grid of frequencies, weighted with a spectral shaping curve, and then inverse Fourier transformed to synthesize the time-domain timefront. The spectral shaping followed that used by White *et al.*[22]: a Gaussian pulse was sought in the time-domain via a Gaussian shaping function in the frequency domain. The frequency domain weighting was defined to correspond to the red signal (but identical for both) as

$$S(f) = \exp\left(\frac{-(f - f_o)^2}{2\sigma^2}\right). \tag{12}$$

In order to match the time-domain shape of the pulse observed on the monitor hydrophone, $S(f)$ was required to be $1/e$ at $f_\pm = f_o \pm B/2$, where f_o is the carrier frequency, $B = f_o/N_Q$ and N_Q is the number of cycles per digit. Hence, $\sigma = f_o/(2N_Q\sqrt{2})$. For the red signal ($f_o = 200$ Hz), this located the -3 dB points of the amplitude spectrum at roughly 180 and 220 Hz. A similar procedure was followed for the simulations corresponding to the violet signal ($f_o = 300$ Hz.) As an example, the violet signal timefront is shown in Fig. 6: the red signal timefront was similar.

Since the MCPE method is computationally intensive, only 240 realization were obtained.

3. Simulation Data Processing

The MCPE timefronts were basebanded prior to data reduction. The first stage of data reduction sought to mimic the operations on the at-sea data; uniquely identifiable sections of each timefront were selected, corresponding to the at-sea ray paths ID-17, $+18$, -18, $+19$, -19, $+20$, -20, $+21$, -21 and $+22$. These were similar to those used for the at-sea timefronts. Complex waveforms were extracted for those depths that corresponded to the nominal hydrophone depths on the VLA. These waveforms formed the sample pulse population for the simulated data. In the second stage of data reduction, the pulses were similarly wander-corrected, squared and averaged. Since there is formally no additive ambient noise in the simulation data, the weighted average utilized unity weighting on all pulses: this is then a true EAIP. Roughly 144,000 pulses were processed for either the red or violet MCPE simulations. Example EAIPs are shown in Fig. 11.
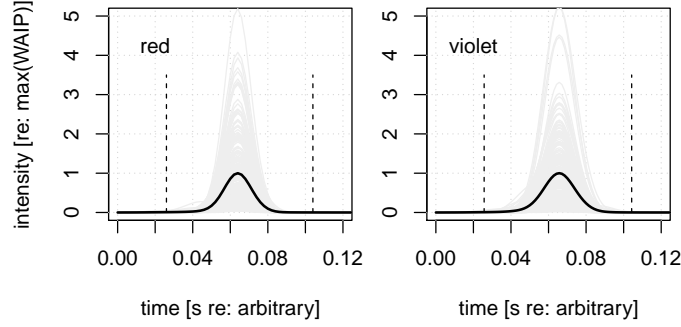
FIG. 11. MCPE ensemble averaged intensity pulses (EAIPs) from depth $z = 1360$ m, corresponding to the nominal depth of VLA hydrophone S/N 057. Timefront branch corresponding to ID-17. 240 pulses. The pulses are normalized by the maximum value of the EAIP. Vertical dashed lines indicate the boundary outside of which the waveforms are smoothly attenuated to zero during the coarse alignment step. Left panel: red simulations. Right panel: violet simulations.

C. CAFI Calculations

The EAIP is often written as the Fourier transform of $\Gamma(\omega_1, \omega_2)$ as a function of $\Delta\omega$:

$$\langle I(t) \rangle \propto \int d\Delta\omega \, \Gamma(\Delta\omega) e^{i\Delta\omega t}. \tag{13}$$

This is a well-known result[6,7]. It can be derived, following Uscinski[6], by using the change of variables $\Delta\omega = \frac{1}{2}(\omega_2 - \omega_1)$ and $\bar{\omega} = \frac{1}{2}(\omega_2 + \omega_1)$ in Eq. 4. Thus,

$$\langle |p(t)|^2 \rangle \propto \iint d\Delta\omega \, d\bar{\omega} \tilde{H}(\bar{\omega}, \Delta\omega) \Gamma(\bar{\omega}, \Delta\omega) e^{i2\Delta\omega t}, \tag{14}$$

where

$$\tilde{H}(\bar{\omega}, \Delta\omega) = \tilde{h}^*(\bar{\omega} + \Delta\omega) \tilde{h}(\bar{\omega} - \Delta\omega). \tag{15}$$

Under the assumptions that $\Gamma(\bar{\omega}, \Delta\omega)$ does not vary significantly with $\bar{\omega}$ and therefore can be written approximately as $\Gamma(\Delta\omega)$, and that $\tilde{H}(\bar{\omega}, \Delta\omega)$ is approximately constant (say equal to $\tilde{H}_0(\bar{\omega})$) over the essential region of support of $\Gamma(\Delta\omega)$, the EAIP becomes

$$\langle |p(t)|^2 \rangle \approx \int d\bar{\omega} \tilde{H}_0(\bar{\omega}) \int d\Delta\omega \, \Gamma(\Delta\omega) e^{i\Delta\omega t}, \tag{16}$$

25

from which the well-known standard form Eq. 13 can be obtained.

Flatté-Dashen theory assumes that $\Gamma(\omega_1, \omega_2)$ is described by the model

$$\Gamma(\bar{\omega}, \Delta\omega) = e^{-(\Delta\omega^2/2\bar{\omega}^2)\Phi^2} Q(\Delta\omega) e^{-i\delta\omega\tau_1} \tag{17}$$

at least for small $\Delta\omega$. Here, Φ^2 is the phase variance (of a single frequency phasor) due to wander, and τ_1 represents a mean bias or delay in arrival time. The Q function represents the additional decoherence when more than one path reaches the receiver.

In order to interpret the Flatté-Dashen result in the context of the wander-corrected averaged intensity pulses estimated in sections III.A.4 and III.B.3, one observes that wander-correction eliminates the variability represented by Φ^2. Furthermore, referencing the averaged intensity pulse to an arbitrary origin renders unnecessary any considerations of a mean delay. Under these conditions,

$$\Gamma(\bar{\omega}, \Delta\omega) \approx Q(\Delta\omega). \tag{18}$$

Flatté-Dashen theory uses path integral techniques to evaluate the Q function[13,17]. The resulting expression is complicated in the general case; Dashen *et al.*[13] offers a simpler parametric approximation

$$Q(\Delta\omega) \approx e^{-\frac{1}{2}(\tau_0\Delta\omega)^2}. \tag{19}$$

The code "Calculations of Fluctuations in Internal Waves" (CAFI)[10,34] provides τ_0.

Under approximation Eq. 18, the equation for $\langle |p(t)|^2 \rangle$ can be rewritten as

$$\begin{aligned}
\langle |p(t)|^2 \rangle &\propto \int d\Delta\omega \left[\int d\bar{\omega} \tilde{H}(\bar{\omega}, \Delta\omega) \right] Q(\Delta\omega) e^{i\Delta\omega t} \\
&= \mathcal{F}^{-1}\{\mathcal{F}\{H(t)\}\mathcal{F}\{q(t)\}\}
\end{aligned}$$

where $q(t) \leftrightharpoons Q(\Delta\omega)$ are Fourier duals and $H(t) \leftrightharpoons \int d\bar{\omega} \tilde{H}(\bar{\omega}, \Delta\omega)$ are Fourier duals and $\mathcal{F}\{\cdot\}(\mathcal{F}^{-1}\{\cdot\})$ is a forward (inverse) Fourier transform. $H(t)$ is just $|h(t)|^2$. Using the Fourier duality of convolution and multiplication, the expression for $\langle |p(t)|^2 \rangle$ becomes

$$\langle |p(t)|^2 \rangle \sim |h(t)|^2 * q(t). \tag{20}$$

Thus, for wander-corrected data, there is a simple convolution interpretation to the Fourier synthesis of the ensemble averaged intensity pulse. For reference, the Fourier transform of Eq. 19 is

$$q(t) \sim e^{-\frac{1}{2}t^2/\tau_0^2} \tag{21}$$

and is also a Gaussian function.

The input profiles for CAFI are shown in Fig. 10. The input parameters are given in Table V. Typical scattering regime values for these calculations are $\Phi \approx 4$, $\Lambda\Phi \approx 0.8$, $\Lambda \approx 0.2$ and $\Lambda\Phi^2 \approx 3.4$ at 200 Hz. Values for 300 Hz are similar. The regime is classified as partially saturated.

IV. ANALYSIS

Pulse spread will be defined as a width measure of the EAIP (or WAIP) minus the same measure of the radiated pulse squared. That is, the spread of an arbitrary pulse waveform $p(t)$ based on a reference pulse $p_0(t)$ will be defined as $\mathcal{S}(p; p_0) \equiv \mathcal{W}(p) - \mathcal{W}(p_0)$ where the width of a pulse p is $\mathcal{W}(p)$. In all cases presented here, Gaussian functions were fitted to the data, and the corresponding width metric derived from the estimated dispersion parameter. For a Gaussian function $G(t) = e^{-(t/a)^2}$, one has $\mathcal{W}_G(G) = \frac{1}{2}a^2$.

Although the radiated pulse is considered to have (theoretically) a triangular shape after equalization and pulse-compression, the WAIPs (as shown in Fig. 8) are fit very well with a Gaussian function. In the MCPE simulations, the input pulse spectrum is given a Gaussian taper, and therefore the theoretical time-domain shape also possesses a Gaussian form. Furthermore, consistent with the bandlimited response of the transducer and the Gaussian-like characteristics of the observed radiated signal, the width $\mathcal{W}_G$ for the squared equalized radiated red (violet) pulse was determined to be 17.38 ms (14.04 ms). Comparisons of spreads for red and violet wavefields are shown in Fig. 12 and Fig. 13.

Since the at-sea records are serially correlated, the error in each WAIP width estimator was estimated using the block bootstrap[35] with a block size of 50 samples resampled 50 times. The estimated errors were not sensitive to greater block sizes. The MCPE records, however, are inde-
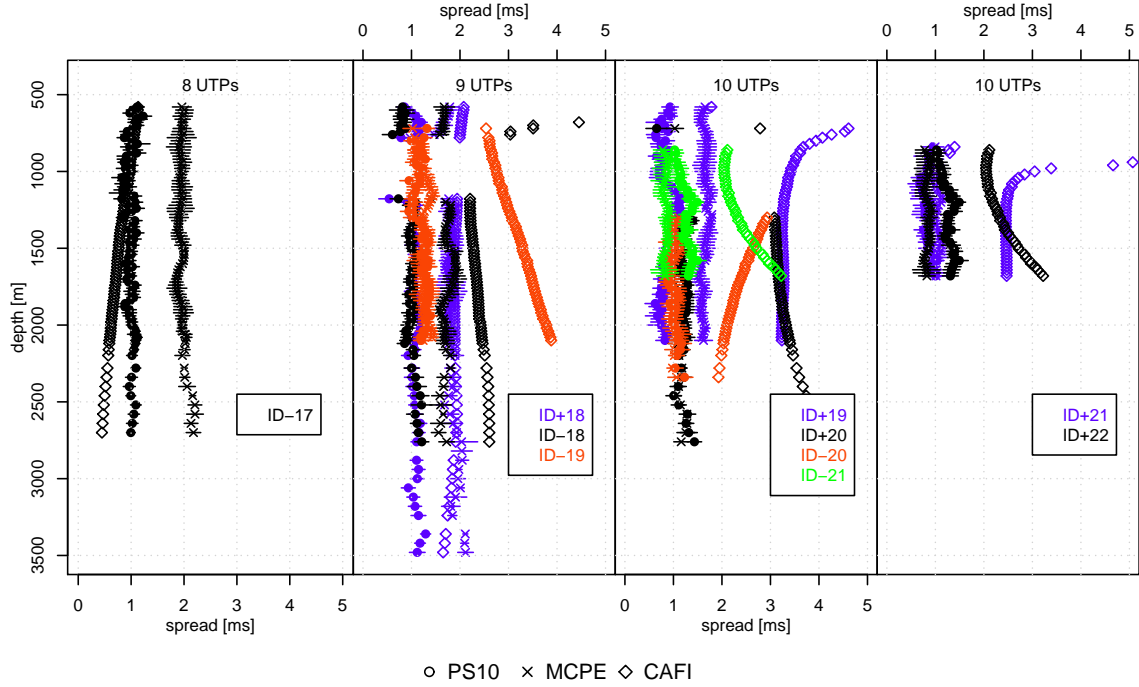
FIG. 12. Pulse spreads for the "red" signal in the PhilSea10 experiment. Panels grouped by total number of upper turning points (UTPs) along the path. Path identifiers shown in the inset. Symbols denoting observed measurements, MCPE predictions and CAFI calculations shown at the bottom.

pendent, and therefore the error in each EAIP width estimator was estimated using the standard bootstrap with 50 resamplings. Two standard error bars are shown for both the at-sea data and the MCPE data in Figs. 12 and 13: many of the error bars are too small to see in these figures.

V. DISCUSSION

The use of electro-acoustic sources has enabled controlled and highly repeatable pulse waveforms for underwater propagation studies. In the PhilSea10 experiment, the transmission protocol of 161 pulses/hour for 54 hours yields a rich dataset for time-domain research. The three-way comparison here between the measured PhilSea10 data, MCPE simulations and Flatté-Dashen calculations provides several comparative insights. First, the MCPE simulations were designed to mimic the PhilSea10 scenario as well as possible. Second, the MCPE and CAFI calculations
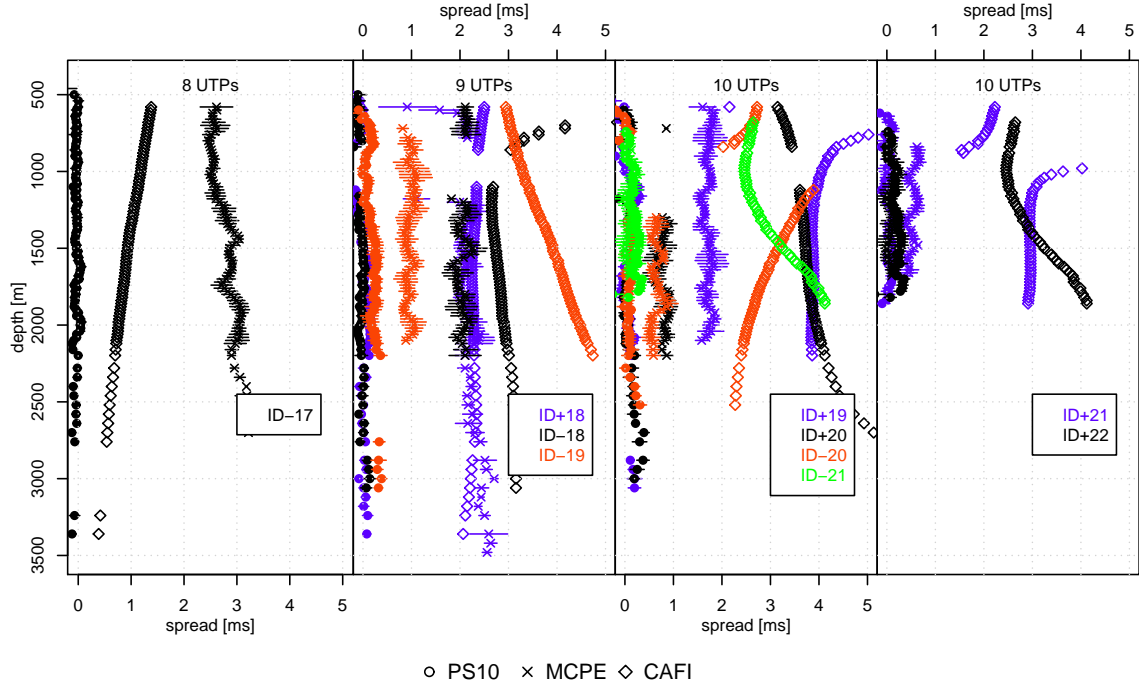
FIG. 13. Pulse spreads for the "violet" signal in the PhilSea10 experiment. Panels grouped by total number of upper turning points (UTPs) along the path. Path identifiers shown in the inset. Symbols denoting observed measurements, MCPE predictions and CAFI calculations shown at the bottom.

used exactly the same input profiles. While it is not the purpose of this study to test Flatté-Dashen theory, this comparison should lead to further insight into the prediction performance of the path-integral approach.

Figures 12 and 13 show that the wander-corrected averaged pulse spread incurred over this 510 km section was very small, much less than the pulse width. It has been noted before that the early timefront contains pulses that retain a high degree of similarity with the original radiated pulse, and these results bear this out. The wander-corrected averaged spreads for the red signal are only about 1 ms, and the spreads for the violet signal are almost unmeasurable against the sample period of approximately 833 μs. There does not seem to be a dependence on the sign of the initial launch angle of the path.

The MCPE results over-predict the wander-corrected averaged spread for the earlier paths (i.e.,

ID-17, ID±18, ID$+19$), but are generally quite accurate for the paths with more turning points. This could be due to mismatches in the simulation background profile for the near-surface regions, a region which will preferentially affect the earlier paths which vertex closer to the sea surface. The PhilSea10 section involved range-dependent mesoscale features that are not represented in the range-independent background profiles in the MCPE simulations, particularly a strong, warm-core eddy in the upper 200 m. (See Fig. 3.) The experiment duration (54 hours) also involved evolution of the upper ocean profiles due to near-surface mixed layer growth and decay and also barotropic and baroclinic tides. None of these quasi-diurnal processes are represented in the simulation range- (and time-) invariant background profiles. The MCPE predictions should therefore not conform exactly to the measured statistics.

There is a trend for CAFI calculations in which the error is small for the earlier paths but the over-prediction seems to grow with the number of turning points. This is consistent with the observations of Colosi *et al.*[8] that the pulse spread predictions were much larger — by as much as an order or two — for experiments at longer ranges (and hence many more turning points.) The over-prediction measured here, for up to 22 turning points, is about a factor of 3 for the red signal, but about a factor of 10 for the violet signal. (The significance of this latter factor is uncertain because this factor relies heavily upon the fact that the violet signal WAIP spread is very small.)

Propagation through a randomizing medium is known to produce a trailing tail in the averaged intensity pulse[36]. In the oceanic case, where there exists a sound channel, Dashen *et al.*[13] argued that a precursor could also exist. After equalization and pulse-compression, leading or trailing sidelobes outside the triangle are not evident in the radiated signal (Figs. 4 and 5.) From Fig. 9, it can be seen that there is a slight trailing edge for the red signal WAIPs. There appears to be no such feature for the violet signal WAIPs. No precursors are evident. However, corresponding figures for the MCPE EAIPs (no shown) do display precursors (but no trailing edges), confirming the Dashen assertion, at least for controlled simulation data.

Several authors[37,38] have reported an additional feature in simulations in the averaged intensity timefront: a low-level background or plateau or pedestal extending far from prominent pulses. From Figs. 8 and 11, the PhilSea10 observations have almost all of the pulse amplitude concen-

trated within twice $\mathcal{W}_G$ from the mode of a given pulse. The low-level background, however, is described as extending much further, i.e., many times $\mathcal{W}_G$, from the mode of a given pulse. Hegewisch[38] noted this feature in her simulations and called it a "fluctuation front". Beron-Vera *et al.*[37] also observed a "cloud" of very faint (i.e., very low amplitude) arrivals extending far from the prominent main arrivals. It should be noted that these observations were made using simulated data, in which there is no additive ambient noise, only numerical noise. It is not clear that this front or cloud is strong enough to be seen in the weak SNR situations encountered in long-range actual measurements.

If this front or cloud is some kind of scattering leakage from an individual pulse, then the convolutional kernel operator in Eq. 20 is responsible for a much greater morphological change than currently believed, and, indeed, the very definition of pulse width would need serious revision. Such a feature cannot be a consequence of the convolution of a Gaussian kernel with the radiated magnitude-squared pulse, as indicated in Eq. 20. While it is true that a Gaussian kernel has infinite support, and that convolution against any finite support waveform will result in infinite support, the Gaussian tails fall off too fast to resemble the features reported by Hegewisch[38] and Beron-Vera *et al.*[37]. Additionally, it has been noted by Dashen *et al.*[13] that the quadratic exponential dependence of the F-FMCF is only valid for small frequency differences: the tails of $\Gamma(\Delta\omega)$ are not well described by current theory, and it is these tails which would contribute most strongly to an extended low-level feature. Dashen *et al.*[13] has indicated that the quadratic exponential model of Eq. 19 may be improved, particularly in the tails, by a higher order expansion in the underlying path integral treatment, and this improvement may explain a broader low-level EAIP pedestal or background.

These results suggest that MCPE simulations provide more accurate predictions of observed wander-corrected averaged pulse spread for the later ray-like paths than the earlier ray-like paths. These later ray-like arrivals are more concentrated toward the central sound channel. CAFI calculations appear to over-predict the pulse spread as the number of turning points increase. The assessments of Flatté[39], Colosi *et al.*[9], Colosi *et al.*[8], and Flatté and Rovner[10] are not accurate at this range: Flatté-Dashen theory as implemented in CAFI characterizes wander-corrected broad-

band behavior well, at least with regard to the average pulse spread, for 8 upper turning points. Low-frequency experiments should be conducted at ranges from 500 km to more than 1 Mm to determine if Flatté-Dashen theory indeed has an increasing discrepancy with increasing turning point.

The F-FMCF was not estimated directly in this study because the signal bandwidths used in this experiment were not broad enough to ensonify the full coherent bandwidth of the channel. MCPE simulations should be used at these and greater ranges in order to image the actual F-FMCF. MCPE simulations can implement signal spectra with unrealizably large bandwidth, and also do not suffer from additive ambient noise. Direct estimation of the F-FMCF would permit a careful comparison of the relationship of the EAIP and F-FMCF.

References

[1] H. Medwin and C. S. Clay, *Fundamentals in Acoustical Oceanography*, 4–5 (Academic Press, San Diego, US) (1998).

[2] M. Ewing and J. L. Worzel, "Long range sound transmission", in *Propagation of Sound in the Ocean* (Geological Society of America, New York) (1948), Memoir 27.

[3] P. G. Bergmann, "Explosions as sources of sound", in *Physics of Sound in the Sea*, 173–191 (Department of the Navy Headquarters Naval Material Command, Washington D.C.) (1969), NAVMAT P-9675.

[4] B. D. Dushaw, "Another look at the 1960 Perth to Bermuda long-range acoustic propagation experiment", Geophys. Res. Let. **35**, L08601: 5pp (2008).

[5] W. H. Munk, R. C. Spindel, A. B. Baggeroer, and T. G. Birdsall, "The Heard Island Feasibility Test", J. Acoustic. Soc. Am. **96**, 2330–2342 (1994).

[6] B. J. Uscinski, *The Elements of Wave Propagation in Random Media*, 38–40 (McGraw-Hill, Nwe York USA) (1977).

[7] S. M. Flatté, R. Dashen, W. H. Munk, K. Watson, and F. Zachariasen, *Sound Transmission through a Fluctuating Ocean*, 6–7 (Cambridge University Press, Cambridge UK) (1979).

[8] J. A. Colosi, E. K. Scheer, S. M. Flatt, B. D. Cornuelle, M. A. Dzieciuch, W. H. Munk, P. F. Worcester, B. M. Howe, J. A. Mercer, R. C. Spindel, K. Metzger, T. G. Birdsall, and A. B. Baggeroer, "Comparisons of measured and predicted acoustic fluctuations for a 3250-km propagation experiment in the eastern North Pacific Ocean", J. Acoustic. Soc. Am. **105**, 3202–3218 (1999).

[9] J. A. Colosi, A. B. Baggeroer, T. G. Birdsall, C. Clark, B. D. Cornuelle, D. Costa, B. D. Dushaw, M. A. Dzieciuch, A. M. G. Forbes, B. M. Howe, D. Menemenlis, J. A. Mercer, K. Metzger, W. Munk, R. C. Spindel, P. F. Worcester, and C. Wunsch, "A review of recent results on ocean acoustic wave propagation in random media: basin scales", J. Ocean. Eng. **24**, 138–155 (1999).

[10] S. M. Flatté and G. Rovner, "Calculations of internal-wave-induced fluctuations in ocean-acoustic propagation", J. Acoustic. Soc. Am. **108**, 526–534 (2000).

[11] S. M. Flatté and M. D. Vera, "Comparison between ocean-acoustic fluctuations in parabolic-equation simulations and estimates from integral approximations", J. Acoustic. Soc. Am. **114**, 697–706 (2003).

[12] I. Tolstoy and C. S. Clay, *Ocean Acoustics; Theory and Experiment in Underwater Sound*, 250–253 (American Institute of Physics, New York, NY) (1987).

[13] R. Dashen, S. M. Flatté, and S. A. Reynolds, "Path-integral treatment of acoustic mutual co-

herence functions for rays in a a sound channel", J. Acoustic. Soc. Am. **77**, 1716–1722 (1985).

[14] S. M. Flatté and R. B. Stoughton, "Predictions of internal-wave effects on ocean acoustic coherence, travel-time variance and intensity moments for very long-range propagation", J. Acoust. Soc. Am. **84**, 1414–1424 (1988).

[15] A. Kalugin, A. Bronshtein, and R. Mazar, "Propagation of the two-frequency coherence function inan onhomogeneous background medium", Waves in Random Media **14**, 389–409 (2004).

[16] R. Mazar and L. B. Felsen, "High-frequency coherenec functions propagated along ray paths in the inhomogeneous background of a weakly random medium: I-Formalism and evaluation of the second moment", J. Acoustic. Soc. Am. **81**, 925–937 (1987).

[17] S. A. Reynolds, S. M. Flatté, R. Dashen, B. Buehler, and P. Maciejewski, "AFAR measurements of acoustic mutual coherence functions of time and frequency", J. Acoustic. Soc. Am. **77**, 1723–1731 (1985).

[18] J. G. Proakis, *Digital Communications*, 454 – 543 (McGraw-Hill, Inc.) (1983).

[19] P. F. Worcester, M. A. Dzieciuch, J. A. Mercer, R. K. Andrew, B. D. Dushaw, A. B. Baggeroer, K. D. Heaney, G. D. D'Spain, J. A. Colosi, , R. A. Stephen, J. N. Kemp, B. M. Howe, L. J. V. Uffelen, and K. E. Wage, "The North Pacific Acoustic Laboratory deep-water acoustic propagation experiments in the Philippine Sea", J. Acoustic. Soc. Am. **134**, 3359–3375 (2013).

[20] D. T. Sandwell, R. D. Müller, W. H. F. Smith, E. Garcia, and R. Francis, "New global marine gravity model from CryoSat-2 and Jason-1 reveals buried tectonic structure", Science **346**, 65–67 (2014).

[21] R. K. Andrew, "The APL/UW Multiport Acoustic Projector System", Technical Report APL/UW TR-0902, Applied Physics Laboratory, University of Washington, Seattle WA (2009).

[22] A. W. White, R. K. Andrew, J. A. Mercer, P. F. Worcester, M. A. Dzieciuch, and J. A. Colosi, "Wavefront intensity statistics for 284-hz broadband transmissions to 107-km range in the Philippine Sea: observations and modeling", J. Acoustic. Soc. Am. **134**, 3347–3358 (2013).

[23] P. F. Worcester, S. Carey, M. A. Dzieciuch, L. L. Green, D. Horwitt, J. C. Lemire, and M. Norenberg, "Distributed vertical line array (DVLA) acoustic receiver", in *Proc. 3rd International Conf. on Underwater Acoustic Measurements*, edited by J. S. Papadakis and L. Bjørnø, 113–

118 (Foundation for Research and Technology Hellas, Nafplion Greece) (2009).

24 Sea-Bird Electronics, Inc., "MicroCAT C-T (P optional) Recorder SBE 37-SMP", Technical Report, Sea-Bird Electronics, Inc., 13431 NE 20th Street, Bellevue WA (2012), `http://www.seabird.com/products/spec_sheets/37smpdata.htm`: last accessed 2012.06.11.

25 Sea-Bird Electronics, Inc., "Temperature & Pressure Recorder SBE 39", Technical Report, Sea-Bird Electronics, Inc., 13431 NE 20th Street, Bellevue WA (2012), `http://www.seabird.com/products/spec_sheets/39data.htm`: last accessed 2012.06.11.

26 R. A. Locarnini, A. V. Mishonov, J. I. Antonov, T. P. Boyer, H. E. Garcia, O. K. Baranova, M. M. Zweng, and D. R. Johnson, "World Ocean Atlas 2009, Volume 1: Temperature", Technical Report, U.S. Government Printing Office, Washington, D.C. (2010), NOAA Atlas NESDIS 68, S. Levitus, Ed.

27 J. I. Antonov, D. Seidov, T. P. Boyer, R. A. Locarnini, A. V. Mishonov, H. E. Garcia, O. K. Baranova, M. M. Zweng, and D. R. Johnson, "World Ocean Atlas 2009, Volume 2: Salinity", Technical Report, U.S. Government Printing Office, Washington, D.C. (2010), NOAA Atlas NESDIS 69, S. Levitus, Ed.

28 "Thermodynamic Equation of Seawater-2010 (TEOS-1)", `http://www.teos-10.org`, last accessed 2015.03.29.

29 W. H. Munk, P. F. Worcester, and C. Wunsch, *Ocean Acoustic Tomography*, 190–195 (Cambridge University Press, Cambridge UK) (1995).

30 J. A. Colosi and M. G. Brown, "Efficient numerical simulation of stochastic internal-wave-induced sound-speed perturbation fields", J. Acoustic. Soc. Am. **103**, 2232–2235 (1998).

31 W. Munk, "Internal waves and small-scale processes", in *The Evolution of Physical Oceanography*, edited by C. Wunsch and B. Warren, 264–291 (MIT Press, Cambridge MA) (1981).

32 F. S. Henyey and S. A. Reynolds, "A numerical simulator of ocean internal waves for long-range acoustics", Technical Memorandum APL-UW TM 1-13, Applied Physics Laboratory, University of Washington, Seattle (2013).

33 "Navy Standard Parabolic Equation,(NSPE), version 5.3", Part of the Oceanographic and At-

mospheric Master Library, Naval Oceanographic Office, `CSO.navo.fct@navy.mil`. Last viewed September 5, 2015.

[34] S. M. Flatté and G. Rovner, "User's Guide to CAFI", `http://oalib.hlsresearch.com/Other/cafi/CAFI_Guide.pdf`: last accessed 2015.03.29 (1998).

[35] A. C. Davison and D. V. Hinkley, *Bootstrap Methods and their Applications*, chapter 8, 385–436 (Cambridge Series in Statistical and Probabilistic Mathematics, Cambridge University Press, Cambridge UK) (1997).

[36] B. J. Uscinski, *The Elements of Wave Propagation in Random Media*, 37–50 (McGraw-Hill, Nwe York USA) (1977).

[37] F. J. Beron-Vera, M. G. Brown, J. A. Colosi, S. Tomsovic, A. L. Virovlyansky, M. A. Wolfson, and G. M. Zaslavsky, "Ray dynamics in a long-range acoustic propagation experiment", J. Acoustic. Soc. Am. **114**, 1226–1242 (2003).

[38] K. Hegewisch, "A random matrix approach to long range acoustic propagation in the ocean", Ph.D. thesis, Washington State University (2010).

[39] S. M. Flatté, "Wave propagation through random media: Contributions from ocean acoustics", Proceedsings of the IEEE **71**, 1267–1294 (1983).

[40] J. B. Bowlin, J. L. Spiesberger, T. F. Duda, and L. F. Freitag, "Ocean Acoustical Ray-Tracing Software RAY", Technical Report WHOI-93-10, Woods Hole Oceanographic Institution (1992).

[41] J. A. Colosi, L. J. van Uffelen, B. D. Cornuelle, , M. A. Dzieciuch, P. F. Worcester, B. D. Dushaw, and S. R. Ramp, "Observations of sound-speed fluctuations in the western philippine sea in the spring of 2009", J. Acoustic. Soc. Am. **134**, 3185–3200 (2013).

ray ID	+18	+19	+20	+21	+22
depths	139-195	221-242	308-335	354-364	422-432

−17	−18	−19	−20	−21	ray ID
106-150	183-218	294-311	335-351	409-420	depths

TABLE I. Upper turning point depth spans in meters for those paths which yielded unique, resolvable pulses in the timefront. Eigenray paths computed using the sound speed profile in Fig. 2 and the computer code RAY.[40]

subarray	depths [m]	spacing [m]	number of modules
1	180-540	40	10
	580-1180	20	31
2	1200-2120	20	47
	2160-2200	40	2
3	2280-3240	60	17
4	3360-4320	60	17
5	4383-5381	40	26

TABLE II. Hydrophone module subarray population, inter-element spacing and nominal depths for the five VLA subarrays.

parameter	red	violet
carrier	200 Hz	300 Hz
law	2033	3471
sequence length	1023	1023
cycles/digit	4	6
digit length	20.00 ms	20.00 ms
sequence length	20.46 s	20.46 s
phase mod angle	88.209°	88.209°
bandwidth	50 Hz	50 Hz
science sequences	161/hr	161/hr
total sequences	8694	8694

TABLE III. MP200/TR1446 dual *m*-sequence signal parameters. The drive signal was the superposition of both red and violet signals. See section III.A.4 for details regarding pulse widths. Neither red nor violet signal was equalized prior to transmission.

parameter	symbol	value
latitude		$21.3624°$
buoyancy frequency	$N(z)$	See text
	$N_0 b$	See below
inertial frequency	f_C	5.2980×10^{-5} rad/s
modal bandwidth	j_*	6
maximum modes	J	200
reference sound-speed	c_0	1481.81 m/s
background sound speed	$\bar{c}(z)$	See text
signal carrier frequencies	f	200 or 300 Hz
strength	$\widehat{bE}_{GM:x}$	0.051 ± 0.004 m
GM strength		0.93 ± 0.078

TABLE IV. Sound speed perturbation field parameters used in the MCPE calculations. The term $n_0 B = \int n(z)\, dz$ and is computed to be roughly 10.129 rads-m/s. (The integral is over the entire water column.) The value of j_* was taken from Colosi *et al.*[41].

parameter	value
carrier f_o	200 Hz or 300 Hz
adiabatic gradient γ_A	1.119×10^{-5} m^{-1}
extrapolated buoyancy frequency N_0	3 cph
integrated buoyancy frequency $N_0 b$	5812 m-cph
modal bandwidth j_*	6.0
reference displacement ζ_0	7.01 m

TABLE V. Input parameters for CAFI calculations.

List of Figures

"A numerical simulator of ocean internal waves for long range acoustics", by Frank S Henyey and Stephen A Reynolds, Technical Memo TM 1-13, Applied Physics Laboratory, University of Washington, 2013.

A Numerical Simulator of Ocean Internal Waves for Long-Range Acoustics

by Frank S. Henyey and Stephen A. Reynolds

Applied Physics Laboratory   University of Washington
1013 NE 40th Street   Seattle, Washington 98105-6698

ACKNOWLEDGMENTS

ABSTRACT

In combination with an appropriate background ocean model, simulations of internal waves are necessary to create realistic scenarios for use in acoustic propagation studies. Our approach employs contemporary understanding of internal wave statistics with a simulator that produces two-dimensional (range/depth) slices of internal wave displacements. The method produces statistical realizations for acoustic studies that are true to ocean measurements with nominal computational cost.

1 Introduction

This report describes a numerical simulator that produces realizations of internal wave displacements for use in studies of long-range acoustic propagation. The goals of any simulator are twofold: first to produce simulations that are realistic, and second, to do so efficiently.

There are a variety of numerical simulators for internal waves. Like the one described here, most are spectral models. These models commonly utilize the formulation for the Garrett and Munk (GM) spectrum and in particular, the formulation based on a simplified Wentzel–Kramers–Brillouin (WKB) approximation [6]. In shallow water or near the surface, these WKB approximations are not valid. Taking a non-WKB approach improves simulation realism with little cost, and provides an algorithm valid in both deep and shallow water.

For several years, the simulator described as a starting field in Winters and D'Asaro [7] (hereinafter WD97) was employed to model situations involving relatively short-range acoustic transmission experiments, i.e., less than 50 km. The fields may be incremented in time consistent with the internal wave dispersion relationship and the method is almost free of the WKB limitation. For shallow water and short-range situations, their approach was extended to relax this limitation. However, because the code is three-dimensional, the approach is computationally intensive. And, to minimize memory usage, strict limits are imposed on the smallest and largest wave numbers that may be represented.

An attempt was made to use 3-D fields from the WD97 technique for long-range propagation studies. Two-dimensional depth-range fields were obtained by slicing through the 3-D field along an angle, then interpolating the field onto the desired grid. This allows continuous slices to any range to be formed. In WD97, 2-D horizontal fast Fourier transforms (FFTs) are taken at each depth so the fields are periodic about the boundaries. Unfortunately, periodicities related to the size of the box inevitably are produced in the output fields. So WD97 produces reasonably realistic fields within its domain. However, it is computationally intensive and when extended to long range, the resulting fields are not realistic. The WD97 approach was not designed for long-range propagation studies.

It was realized that by sampling in k_x and $k = \sqrt{k_x^2 + k_y^2}$ rather than the traditional k_x and k_y, only a moderate number of k-values are required. But a trade-off is made: the problem reduces to a single Fourier transform in x providing a field at one (or a few) y-values. The resulting internal wave simulator is very efficient and meets our requirements of producing displacement fields that (1) have megameter or greater periodicities, (2) are not constrained by the WKB approximation, and (3) contain a broad range of vertical and horizontal scales. Hence the simulator generates realistic fields to very long ranges (megameters). In section II, the formulation is described. In section III, examples and results from tests are shown. An appendix presents a pseudo-code for reference by those wishing copies of the software.

2 Method

Much of our formalism develops from Henyey et al. [4] (hereinafter H97). The numerical simulator follows the presentation in WD97, where a general method for a five-variable simulation is presented. Here, obtaining sound speed variations requires only the internal wave displacement field. Depict this field in two dimensions as $\zeta(x, y, z; t)$. The third dimension $y = 0$. Note that throughout this discussion, time is considered a parameter. For convenience consider the displacement field in terms of the component horizontal wave number k_x, where x and k_x are Fourier transform pairs, then

$$\zeta(k_x, y, z) = \int e^{iyk_y} \sum_{j=1}^{M} \{G_- e^{-i\omega_{jk}t} + G_+ e^{i\omega_{jk}t}\} \varphi_{j,k}(z) dk_y \tag{1}$$

which is analogous to Eq. 18 in WD97.

We evaluate this expression at a given $y = y_0$. An inverse Fourier transform at each depth provides $\zeta(x, y_0, z; t)$. In an ocean modeled as horizontally infinite in both directions, G_- and G_+ are generalized functions of a continuous wave vector. From this point we will, as an approximation, treat them as ordinary functions of a discrete wave vector. Each of the discrete wave vectors is representative of a small area of continuous wave vector surrounding the discrete value. These areas fill up the whole space without overlapping. The value of G_- or G_+ at one of the discrete points is the average of the corresponding generalized function over the area surrounding that point.

For a finite depth ocean, there is a decomposition in the wave field in vertical modes $\varphi_{j,k}(z)$, where mode number $j = 1, 2, \ldots, M$. The modes $\varphi_{j,k}(z)$ and their frequencies are functions of the horizontal wave number k, where $k^2 = k_x^2 + k_y^2$ (cf. WD97 Eq. 8 ff.). The modes and frequencies ω_{jk} are obtained by a method that has been passed from researcher to researcher for many years. We map the problem onto finding the eigenvalues and eigenvectors of a symmetric, tri-diagonal matrix. In terms of eigenfunctions $\psi = \sqrt{n^2 - f^2}\varphi$, Eq. 8 of WD97 for the vertical modes may be written as

$$\frac{1}{\sqrt{n^2 - f^2}}(k^2 - \partial_z^2)\frac{1}{\sqrt{n^2 - f^2}}\psi = \lambda\psi \tag{2}$$

The eigenvalues

$$\lambda = k^2/(\omega^2 - f^2) \tag{3}$$

and eigenfunctions are obtained using a tri-diagonal mode solver. In this mapping, the mode normalization

$$\int_{-L_z}^{0} (n^2 - f^2)\varphi_{j,k}(z)\varphi_{j',k}(z) \, dz = \delta_{jj'} \tag{4}$$

and boundary conditions, $\varphi_{j,k}(-L_z) = \varphi_{j,k}(0) = 0$ are preserved.

To obtain the displacement field in two dimensions for a given depth as a function of horizontal wave number, there is a summation over j and over k. This differs from WD97. The reduction to two dimensions requires us to define k_y in terms of k and k_x.

The wave amplitudes are determined by G_- and G_+. These are complex random deviates generated separately to allow independent right- and left-going waves. G_- and G_+ have zero mean, with a variance given by the internal wave spectrum defined below and by the wave number area represented by one wave vector. The variance is proportional to 1/area because of the averaging of delta-correlated quantities.

The technique defined in Eq. 1 is common. Realizations are obtained via Monte Carlo method on the weights, G_- and G_+. A displacement realization is generated in the wave number domain, with amplitude determined by the model spectrum. Note that the depth dependence is specified by the amplitudes of the vertical modes. (This property is one step in freeing us from the WKB approximation.) At this stage, WD97 uses a 2-D inverse Fourier transform at each depth and obtains the field in the 3-D spatial domain.

Our method uses the full spectral model. This is reduced to one dimension in the horizontal by summing over circles or annuli in horizontal wave number space. Once generated in the wave number domain, only a one-dimensional inverse FFT is needed to obtain the field in range. The result is an efficient and accurate algorithm.

Consider the differential displacement variance in frequency, mode number, and horizontal wave number

$$S(\omega, j)d\omega dj \frac{d\theta}{2\pi} \tag{5}$$

Though the mode number increment, dj, equals 1, we leave it in for completeness. We assume the spectrum and the vertical modes are independent of horizontal direction (i.e., the field is horizontally isotropic). In Eq. 5, θ is the direction of the horizontal wave number. Writing the variance in terms of increments in horizontal wave numbers gives

$$S(\omega, j)d\omega dj \frac{d\theta}{2\pi} = \frac{S(\omega, j)d\omega}{2\pi k dk} dj dk_x dk_y \tag{6}$$

Recognizing the group speed, $v_g = d\omega/dk$, and folding the k_y integral to the positive k_y side, the differential variance becomes

$$var = \frac{S(\omega, j)v_g}{\pi k} dj dk_x d|k_y| \tag{7}$$

In terms of the annulus $k_i < k < k_f$,

$$dk = k_f - k_i \tag{8}$$

$$d|k_y| = \sqrt{k_f^2 - k_x^2} - \sqrt{k_i^2 - k_x^2} \tag{9}$$

At this point, our derivation has diverged from H97. Finally, using Eq. 6, with $\langle \cdot \rangle$ denoting an expected value,

$$\langle |G_+|^2 \rangle + \langle |G_-|^2 \rangle = \frac{S(\omega, j)v_g}{\pi k} dj dk_x d|k_y| \tag{10}$$
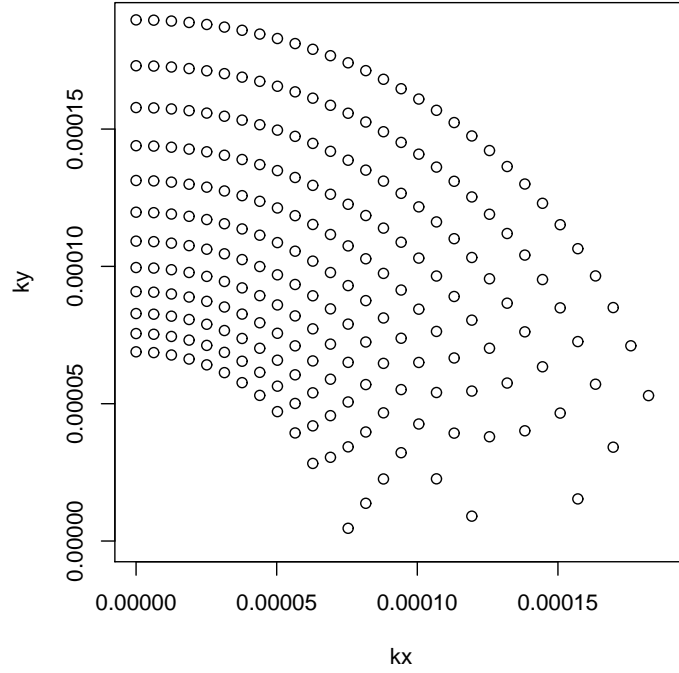
Figure 1: Example of the sampling in the first quadrant of the (k_x, k_y) plane. Only the first 12 values of horizontal wave number k are shown, corresponding to $m = 0, 1, 2, \ldots, 11$. The logarithmic spacing in k is already evident. The gridding is uniform in k_x. Only 12 modes need be computed to support this constellation of sample points in (k_x, k_y) space.

This assumes a two-sided spectrum in k_x. The Jacobian

$$J = \frac{v_g}{\pi k} \tag{11}$$

arises from the conversion of $d\omega d\theta$ to $dk_x d|k_y|$.

Due to horizontal isotropy, the computational effort of calculating the modes can be significantly reduced over that involved in a standard sampling of the (k_x, k_y) plane by only computing the modes on a grid of $k = \sqrt{k_x^2 + k_y^2}$ values. The sampling here is also chosen to have logarithmic spacing with the first increment in each decade equal to about 10% over the first value. This puts about 25 sample points in each decade. Thus, the horizontal wave number spacing is given as $k_m = k_0 r^m$, $m = 0, 1, 2, \ldots$ with $r = 10^{0.04}$. The lowest mode wave number is set as $k_0 = 2\pi/L_{kh0}$, where L_{kh0} is the length scale of this mode.

The conversion from sampling in (k_x, k_y) to sampling in (k, k_x) on annuli of constant k results in non-uniform contributions to the simulation along the k_y axis (Fig. 1). Here, the sample (k_x, k_y) locations for the first 12 "rings" ($m = 0, 1, 2, \ldots, 11$) are shown, and $L_{kh0} = 1 \times 10^5$ m and $\Delta k_x = 2\pi/L_x$ with $L_x = 1 \times 10^6$ m. Only the (k_x, k_y) sample locations corresponding to positive $k_y^2 = k^2 - k_x^2$ are valid. This results in sparse samping near the k_x
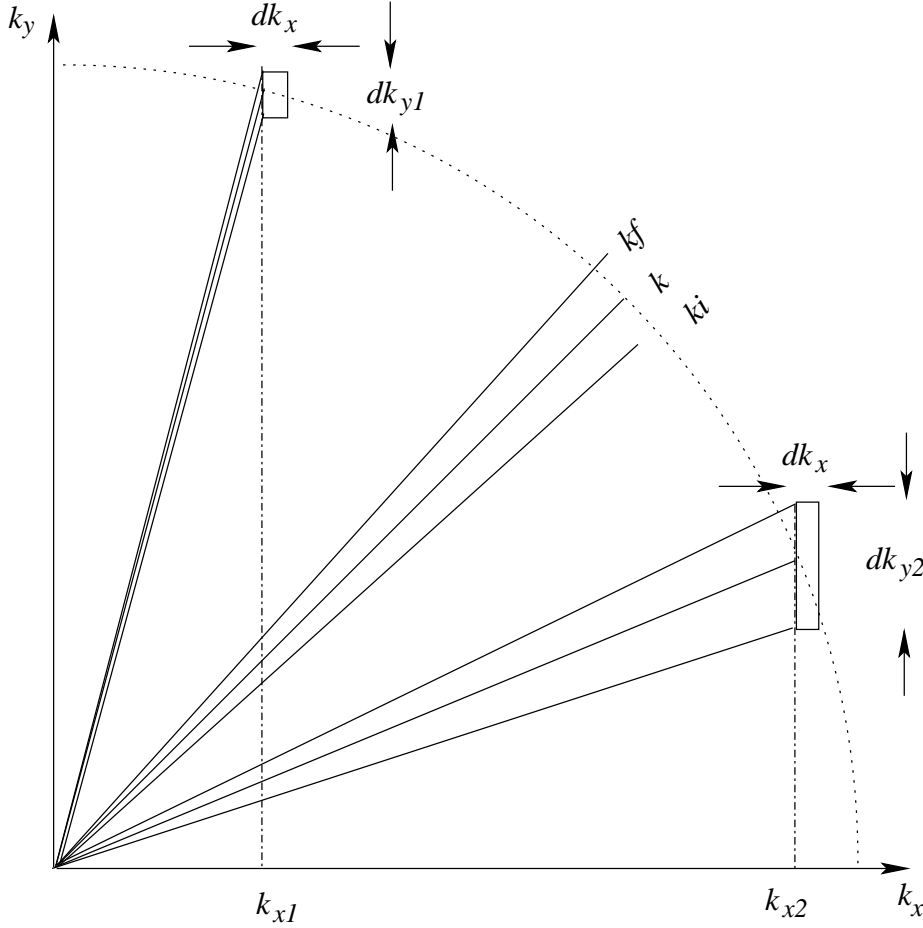
Figure 2: Examples of the differential areal tiling based on the (k, k_x) sampling scheme. The example presents only the sampling in the first quadrant of the (k_x, k_y) plane.

axis. This scheme is designed for accurate simulations along the x axis, but not the y axis.

The differential variance contributions defined by Eq. 9 result in a non-uniform $k_x - k_y$ tiling of the (k_x, k_y) plane (Fig. 2). A small correction to the differential variance contribution (Eq. 9) is required for the first ring, or differential elements adjacent to the k_x axis. If $m = 0$ or $k_i \leq k_x$, then $d|k_y| = \sqrt{k_f^2 - k_x^2}$. This essentially models the contribution as coming from a triangle with an apex at the origin (instead of a rectangle).

The group speed $d\omega/dk$ is obtained directly using the Hellmann–Feynman theorem [2,3].

Using Eq. 3,

$$\frac{d\omega}{dk} = \frac{1}{2}\frac{k}{\omega\lambda}\left[2 - \frac{k}{\lambda}\frac{d\lambda}{dk}\right] \tag{12}$$

The term $d\lambda/dk$ can be computed from Eq. 2. Differentiating both sides of Eq. 2 by k yields

$$\frac{2k}{n^2 - f^2}\psi = \frac{d\lambda}{dk}\psi \tag{13}$$

Multiplying both sides by ψ and integrating over depth yields

$$2k\int\varphi^2(z)\,dz = \frac{d\lambda}{dk}\int(n^2 - f^2)\varphi^2(z)\,dz \tag{14}$$

using the definition of ψ. However, from Eq. 4, $\int(n^2 - f^2)\varphi^2\,dz = 1$. Hence

$$\frac{d\omega}{dk} = \frac{k}{\omega\lambda}\left[1 - \frac{k^2}{\lambda}\int\varphi^2\,dz\right] \tag{15}$$

$$= \frac{\omega^2 - f^2}{\omega k}\left[1 - (\omega^2 - f^2)\int\varphi^2\,dz\right] \tag{16}$$

Thus, once the modes φ and the eigenfrequencies ω have been computed, the group speed $d\omega/dk$ can be determined directly. No WKB approximations are required in this step.

To this point, any spectrum could be used. We follow H97 who utilize a GM spectrum modified so as not to include WKB approximations. This model decomposes into frequency and vertical mode number. In this representation the spectrum is separable. H97 defines the spectrum as

$$S(\omega, j) = (BE_{GM})(n_0 B)^2 H(j)\frac{2}{\pi}\frac{f}{\omega^3}\sqrt{\omega^2 - f^2} \tag{17}$$

where

$$n_0 B = \int n(z)dz \tag{18}$$

and

$$H(j) = \frac{H_0}{j^2 + j_*^2} \tag{19}$$

The constant H_0 normalizes to unity the summation of $H(j)$. The WKB limitation is removed from the traditional GM spectral model. Density does not enter this formulation; the spectrum is in terms of energy per unit mass. Note BE_{GM} is a single parameter and j_* is the traditional characteristic (vertical) mode number. Both BE_{GM} and j_* must be specified in each simulation. GM neglected the contribution of the deeper part of the ocean in the integral of Eq. 18, resulting in a significant underestimate of $n_0 B$. If a corrected value of $n_0 B$ is used, both BE_{GM} and j_* should be appropriately adjusted. Note also that Eq. 1 is written as a function of y. At this time, we have only implemented the code to evaluate the field at a single value of y_0. For convenience, we have selected the plane $y_0 = 0$.
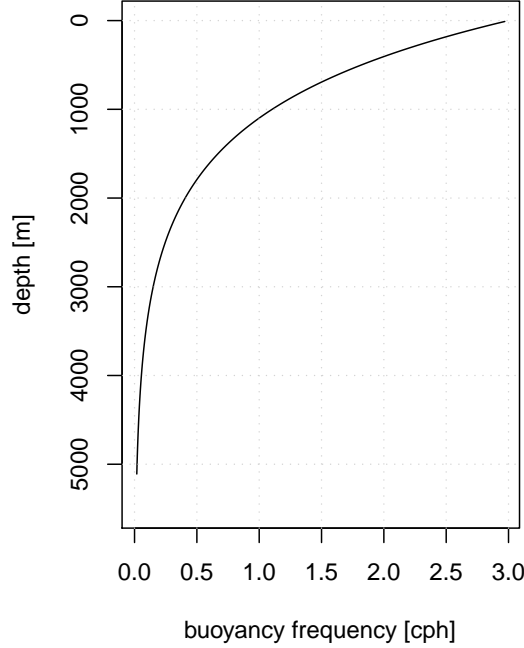
Figure 3: Buoyancy profile used in the tests. The profile is the "Munk canonical profile" modified by the Coriolis frequency at 25°.

3   Tests

We present two tests to demonstrate both the validity and viability of the method. First we examine the variance of the simulated internal wave variability. The second explores the distribution of energy in horizontal wave number. In both cases, the numerical results are compared with predictions from WKB theory that are readily calculable.

In the following tests, a test buoyancy profile was constructed using $n^2(z) = n_{\mathrm{Munk}}^2(z) + f^2$, where $n_{\mathrm{Munk}}(z) = n_0 e^{-z/B}$, and $n_0 = 3$ cph and B is a vertical scale length here assigned 1300 m. The Coriolis frequency was based on a latitude of 25°. This profile is shown in Fig. 3.

With the buoyancy profile specified, the other parameters found in the spectrum (Eq. 17) must be set. The computed values of $N_0 B$ and BE_{GM} are 6.67 m s^{-1} and 8.32×10^{-2} vice the canonical values of 6.81 m s^{-1} and 8.20×10^{-2}. The differences are due to numerical
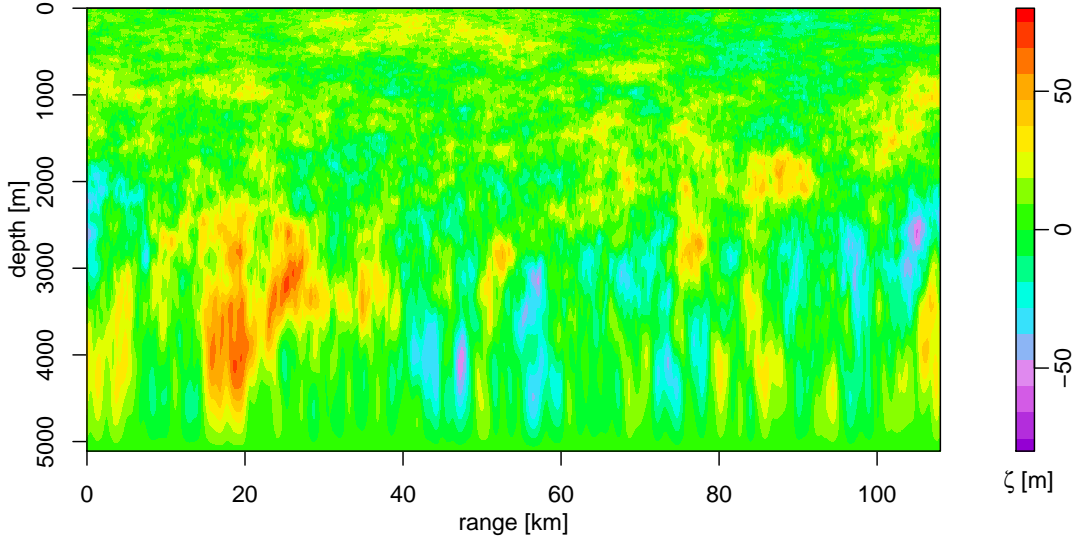
Figure 4: Color contour plot for a typical single realization of internal wave displacements. A range of 100 km is plotted (corresponding to an n/f aspect ratio of 20). `iseed` was -1 and `t0` was 0.0.

error in the quadrature of $n(z)$. The low-mode cutoff was assigned the value of the canonical model, $j_* = 3$. The computational domain was 1000 km in range and 5.5 km in depth with sampling of 8192 points in the horizontal and 512 points in the vertical. In the program a base 2 FFT is used in the horizontal. This can be changed. A vertical sampling of 512 steps was chosen for convenience. This may be increased for larger j_*. The total number of internal wave vertical modes was chosen to be 80.

A portion of a typical realization is shown in Fig. 4. Note that because of the aspect ratio the contours are distorted. In reality the displacement contours form pancake-like structures stretched out in the horizontal.

VARIANCE

The simplest test is to estimate the displacement variance for a given depth and compare with WKB theory. The variance given by Munk [6] is

$$\langle \zeta^2 \rangle_{\text{WKB}} = \tfrac{1}{2} B E_{GM} \frac{n_0 B}{n(z)} \tag{20}$$

Multiplying both sides by $n(z)$ removes the depth dependence from the Munk variance, and one obtains

$$n(z)\langle \zeta^2 \rangle_{\text{WKB}} = \tfrac{1}{2} B E_{GM} n_0 B \tag{21}$$

which we compare to $n(z)\langle \zeta^2 \rangle$. The comparisons between Eq. 21 and the result from five
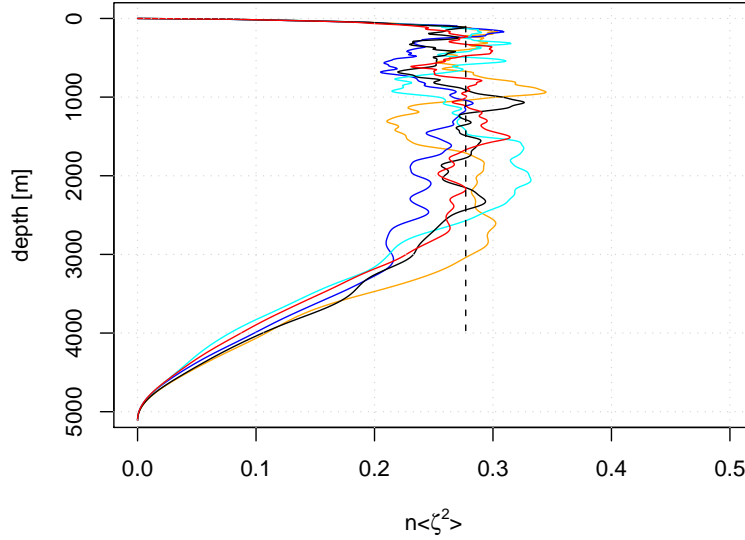
Figure 5: Five simulation realizations of $n\langle\zeta^2\rangle$ using `iseed` $= -1, -2, -3, -4, -5$. The vertical line is the WKB result at 0.277. This figure tests Eq. 21.

simulations are shown in Fig. 5. The simulations all used time `t0` $= 0$, and random number generator seeds, `iseed`, of -1, -2, -3, -4, and -5. Over mid-depth, the simulated results are within $\pm 20\%$ of the WKB prediction. The comparison above 2500 m is especially good. Very near the surface and toward the bottom, WKB is not expected to be valid.

TOWED DISPLACEMENT SPECTRA

We turn now to compare displacement spectra of (one-dimensional) horizontal wave number. Referred to as "towed," these spectra may be estimated from measurements using horizontal tows of sensors that are suspended at fixed depths from a ship steaming in one direction. The displacement may be inferred from temperature measurements, for example, by using the vertical temperature gradient and assuming a linear relationship.

From the simulations, we have the displacement data directly. A sample spectrum is shown in Fig. 6 from one of the simulations. There is considerable variability at low wave number. The theoretical spectrum can be obtained from Eq. 1 and is

$$TS_\zeta(k_x) = \int \sum_j \frac{S(\omega_{jk}, j)v_g}{\pi k} \varphi_{jk}^2(z) \, d|k_y| \tag{22}$$

Both spectra generally follow a k_x^{-2} dependence at high wave number. This is expected from WKB theory where for convenience, we obtain predictions by evaluating numerically an expression (Eq. 19) from Levine et al. [5]. This expression is complicated but may be
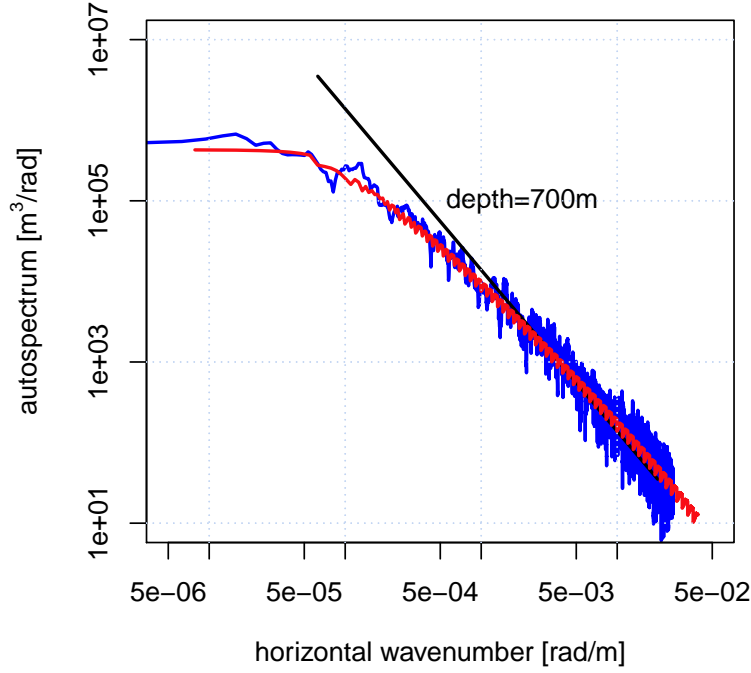
Figure 6: Comparisons of horizontal "towed" spectra at depth 700 m. A single realization is used (iseed = −1). The sample variance was 92.74. The autospectrum was estimated using the multitaper method with 8 tapers and a time-bandwidth product of 4. This is shown in blue. The estimated integral of the sample autospectrum was 93.77. The full theoretical expression (using 101 modes) is shown in red — this is Eq. 22. The discretization of the sampling in wave number space is evident as a "stair-step" appearance in the theoretical curve at higher wave numbers. The predicted variance based on an estimated integral of this curve is 83.97. Additionally, the Levine et al. [5] approximate expression is shown with a solid black line. This figure tests Eq. 22 and Eq. 23.

interpreted by considering the approximate formula given by Desaubies [1] for high wave number:

$$TS_\zeta(k_x) = \pi \left(\frac{2}{\pi}\right)^3 BE_{GM} \frac{j_* f}{n} \left(\ln \frac{n}{f} - \frac{n^2 - f^2}{2n^2}\right) k_x^{-2} \qquad (23)$$

There is an $n(z)^{-1}$ dependence in depth and a k_x^{-2} dependence in wave number.

We expect from Fig. 5 that spectra near the surface and bottom will not follow the WKB behavior. We select a mid-depth of 700 m for the comparison. The sample spectrum is shown in Fig. 6 along with the WKB prediction. The model and data spectra are consistent

with each other and confirm the horizontal wave number behavior in the simulation.

Both the total variance and the horizontal spectral behavior of the simulations are consistent with the underlying model. Each simulation is an independent realization. The variability observed between simulations is typical for Monte Carlo experiments and demonstrates the acceptability of the method.

4 Summary

This report describes a numerical simulator for creating two-dimensional range/depth slices of sound speed variability associated with ocean internal waves. The simulator is both efficient and realistic. Designed for studies of internal wave effects on megameter acoustic propagation, it may also be used for short and intermediate ranges. The algorithm does not depend on WKB approximations, and therefore remains accurate in shallow water or near the ocean surface. Combined with the appropriate deterministic background profiles, the statistical model for the internal waves produces realizations that are true to ocean measurements while the method is easy to implement with low computational cost.

The method also can be extended to simulations wherein an accurate random wave field is needed for arbitrary values of x and y — i.e., fully 3-D simulations, not only simulations along a section $y = y_0$. In such cases, the tiling in the (k_x, k_y) domain should be square, so that dk_x and dk_y are the same everywhere. Gridding of the k_x and k_y axes then becomes uniform. Efficiency is retained as the contributions $\{k, dw_{jk}/dk, \varphi_{jk}(z)\}$ are assigned to be the contributions from the annulus for k' closest to the point (k_x, k_y).

References

[1] Desaubies, Y.J.F., Analytical representation of internal wave spectra, *J. Phys. Oceanogr.*, **6**, 976–981, 1976.

[2] Feynman, R.P., Forces in molecules, *Phys. Rev.*, **56**, 340, 1939.

[3] Hellmann, H., *Einführung in die Quantenchemie*, Franz Deuticke, Leipzig und Wien, 1937, p. 285.

[4] Henyey, F.S., D. Rouseff, J.M. Grochocinski, S.A. Reynolds, K.L. Williams, and T.E. Ewart, Effects of internal waves and turbulence on a horizontal aperture sonar, *IEEE J. Ocean. Eng.*, **22**, 270–279, 1997.

[5] Levine, M.D, J.D. Irish, T.E. Ewart, and S.A. Reynolds, Simultaneous spatial and temporal measurements of the internal wave field during MATE, *J. Geophys.. Res.*, **91**, 9709–9719, 1986.

[6] Munk, W.H., A survey of internal waves and small scale processes, in *Evolution of Physical Oceanography*, B.A. Warren and C. Wunsch, eds., Cambridge, MA, MIT Press, 1981.

[7] Winters, K.B., and E.A. D'Asaro, Direct simulation of internal wave energy transfer, *J. Phys. Oceanogr.*, **27**, 1937–1945, 1997.

Appendix: Pseudo-code

The pseudo-code for an implementation of the method (Fig. 7) and input parameters (Table 1) are given. Where appropriate, these parameters were used in the results described in this report.

```
loop over kh { kh = k0*r**m; m=0, 1, ..., nkh }
   compute modes, frequencies, and group velocities for each kh

   loop over kx { kx = 0, 1/Lx, ..., Nx/(2Lx)
      zero accumulator at kx and depth z
      compute d|ky|

      loop over j {1,2,...JMAX}
            compute variance Var = S(omega,j)*vgp/(pi*kh)*dj*dkx*d|ky|
            generate G+ from CN(0, Var)
            generate G- from CN(0, Var)

            loop over z
                accumulate [G+*e^(i*omega*t) + G-*e^(-i*omega*t)]*mode_j(z)
            endloop (z)
      endloop (j)
   endloop( kx )
endloop( kh )

loop over depth z
   zeta(z) = IDFT{ accumulant(kx;z) }
endloop (z)
```

Figure 7: Pseudo-code for a simulator.

Parameter	Description	Current Value	Pseudo-code
L_x	x-dimension (total range)	1×10^6 m	Lx
N_x	number of points in x-direction	8192	Nx
N_z	number of points in z-direction	512	
j_{max}	number of vertical displacement modes j	80	JMAX
t	evolution time for the realization	time [s]	t
N_k	number of horizontal wavenumber modes m	80	nkh
L_{kh0}	length of largest horizontal mode	1×10^5 m	2π/k0
iseed	initializes random number generator	integer (< 0)	
j_*	vertical displacement mode bandwidth	3	in S()
f	inertial frequency, $4\pi\Omega\sin(\text{latitude})$ [rad/s]	latitude dependent	in S()
Ω	rotation rate of Earth's surface	1 cycle/day	
BE_{GM}	strength [m]	8.32×10^{-2}	in S()
$n(z)$	buoyancy frequency profile [rad/s]	profile dependent	in S()
r	log-step increment, horizontal wavenumbers	$10^{0.04}$	r

Table 1: Parameters required in the algorithm.

REPORT DOCUMENTATION PAGE

1. REPORT DATE *(DD-MM-YYYY)*	2. REPORT TYPE	3. DATES COVERED *(From - To)*

4. TITLE AND SUBTITLE

5a. CONTRACT NUMBER

5b. GRANT NUMBER

5c. PROGRAM ELEMENT NUMBER

6. AUTHOR(S)

5d. PROJECT NUMBER

5e. TASK NUMBER

5f. WORK UNIT NUMBER

7. PERFORMING ORGANIZATION NAME(S) AND ADDRESS(ES)

8. PERFORMING ORGANIZATION REPORT NUMBER

9. SPONSORING/MONITORING AGENCY NAME(S) AND ADDRESS(ES)

10. SPONSOR/MONITOR'S ACRONYM(S)

11. SPONSOR/MONITOR'S REPORT NUMBER(S)

12. DISTRIBUTION/AVAILABILITY STATEMENT

13. SUPPLEMENTARY NOTES

14. ABSTRACT

15. SUBJECT TERMS

16. SECURITY CLASSIFICATION OF:			17. LIMITATION OF ABSTRACT	18. NUMBER OF PAGES	19a. NAME OF RESPONSIBLE PERSON
a. REPORT	b. ABSTRACT	c. THIS PAGE			
					19b. TELEPHONE NUMBER *(Include area code)*

A Method to Determine Small-Scale Internal Wave and Spice Fields from a Single CTD Profile with Application to Three Long-Range Ocean Acoustics Experiments

by F.S. Henyey, J.A. Mercer, R.K. Andrew, and A.W. White

Technical Memorandum
APL-UW TM 1-14
March 2014

Applied Physics Laboratory   University of Washington
1013 NE 40th Street   Seattle, Washington 98105-6698

ACKNOWLEDGMENTS

ABSTRACT

The smaller vertical scales of sound speed variability of several recent deep water Pacific Ocean acoustic experiments are extracted from individual conductivity, temperature, depth (CTD) casts taken along the acoustic paths of these experiments, close to the times of the experiments. The sound speed variability is split into internal wave variability and spice variability, as these two parts obey very different dynamics – the internal waves move through the water and the spice field moves with the water. Larger scales are mostly responsible for acoustic travel time fluctuations, but smaller scales are mostly responsible for other important phenomena such as intensity and arrival angle fluctuations. A method is presented to determine when the two components are separable. The internal wave properties are consistent with a spectral model such as a generalized Garrett–Munk model, whereas the spice is very intermittent, and the measurements are not extensive enough to confidently make a spice model for acoustic propagation purposes. Both the internal wave results and the spice results are summarized as vertical wavenumber spectra over a selected vertical depth interval, but with the spice, it must be understood that a spectral model would be very different from the data, and that the three-dimensional horizontal–vertical spectrum would be pure conjecture. The spectral level of the (small-scale) spice, averaged over all the profiles, is comparable to that of the internal waves, suggesting that it is not significantly less important to acoustic propagation than are the (small-scale) internal waves.

This page is blank intentionally.

1 Introduction

In several recent low-frequency, long-range acoustic propagation experiments, a number of deep conductivity, temperature, depth (CTD) profiles were taken to characterize the propagation environment. The characterization of the environment in acoustics experiments is, of necessity, incomplete; the acoustics is the primary concern. In particular, deep CTD profiles are time intensive, and multiple deep profiles at one location are rarely taken. Thus, the time dependence of the measured profile is not known directly. Time dependence, when available, is used to extract sound speed fluctuations from a background sound speed profile. Here, a method is developed to estimate the smaller scale fluctuations from single profiles. Moored CTD instruments provide a complementary view of fluctuations. For these measurements, time series are obtained, but the vertical resolution is necessarily much coarser than with a CTD profile. For example, in one of the experiments considered here moorings deployed had inter-sensor spacings of 30–140 m over our depth range of interest; fluctuations with wavelengths twice those scales and larger were extracted from the sensor data [3]. In contrast, our largest scale is on the order of 100 m in the vertical.

Experimental data considered here are from the Long-Range Acoustic Propagation Experiment (LOAPEX [12]), 10 September – 10 October 2004; the Philippine Sea pilot study (PhilSea09), 14 April – 1 May 2009; and the Philippine Sea Experiment (PhilSea10) [16], 5–29 May 2010. Here, we analyze acoustically relevant fluctuations in the profiled CTD measurements made during these experiments. Both internal waves and spice are of interest. The internal waves and spice are put on a comparable quantitative scale in terms of their influences on the sound speed. Specifically, we calculate a vertical displacement of density from an equilibrium background density stratification and a vertical displacement of sound speed from a background sound speed profile.

LOAPEX includes seven CTD profiles taken at acoustic source stations along a 3200-km path from a receiver mooring. In addition, there was a profile taken north of the island of Kauai. PhilSea09 includes 19 CTD profiles taken during three cruises between acoustics moorings. PhilSea10 includes 51 CTD profiles taken every 10 km along a 500-km path from a receiver mooring. Every fifth PhilSea10 profile samples the entire water column, while the other four extended to about 1500 m depth. The receiver moorings in PhilSea09 and PhilSea10 were in the same place, and were the southwest end of the PhilSea09 CTD line and the northwest end of the PhilSea10 CTD line. This report presents results in the form of spectra for a few of the profiles, and several average spectra. The complete set of available spectra is presented in the Appendix.

The primary goal of our method is to extract the small-scale internal wave and spice fields from a single profile. The small scales are defined here to have vertical wavelengths smaller than about 100 m. Larger scale features, in a single CTD profile, cannot be distinguished from structure in the background. The larger scales are mostly responsible for acoustic travel time fluctuations, but the smaller scales are mostly responsible for other phenomena such as the intensity and arrival angle fluctuations. The assumption is made that the

smaller scales in density and sound speed are the internal waves and spice of interest. This assumption is tested at every place and time, as described below. It is possible that the background stratification at some places and times has smaller structures, requiring the test to be done everywhere.

The method described here is based on the familiar approximate relation that the density ρ differs from a reference background density profile ρ_0 by the density displacement ζ_ρ times the non-adiabatic density gradient

$$\rho - \rho_0 = \zeta_\rho \left(\frac{\partial \rho_0}{\partial z} \right)_{\text{na}} \tag{1}$$

and a corresponding relation based on sound speed

$$c - c_0 = \zeta_c \left(\frac{\partial c_0}{\partial z} \right)_{\text{na}}. \tag{2}$$

Formal measurements of the 'reference' quantities cannot be determined from single CTD casts, and therefore the following approximations are made. Given only a single cast, the background sound speed (treatment for the density is identical) is approximated by the low-pass filtered sound speed, and the non-adiabatic background sound speed gradient is approximated with the vertical derivative of the low-pass filtered sound speed. Because the low-pass filtering cannot distinguish between the background structure and the low-mode perturbations, the approximate ζ_c represents, at best, the high-mode components of the perturbation field. However, as mentioned previously, the quantities of interest here are the smaller scales of the internal wave and spice fields. Unfortunately, the approximation for the reference sound speed gradient does not work well in all cases, as the non-adiabatic gradient can be small or even negative. The method presented here cannot be used for profiles in which that is the case.

2 Processing

The initial stages of the processing were done with Seabird software [15]. This processing converted the raw data to conductivity, temperature, and pressure, adjusted the measurement time constants, and calculated the practical salinity. (Unfortunately, some salinity spiking remained, which can overwhelm legitimate small-scale fluctuations at high wavenumbers.) The outputs used from the Seabird software were pressure, temperature, and salinity. The next step of the processing uses the thermodynamic equation of state for seawater [8]. This equation of state has two very important properties:

1. It is consistent thermodynamically. The fundamental expression is for the Gibbs free energy G as a function of pressure, temperature, and practical salinity. All other state quantities are calculated in terms of derivatives of this function. (See, for example,

Müller [13].) Automatically, the adiabatic lapse rate of density is the reciprocal of the square of the sound speed. (Here, the adiabatic lapse rate of any quantity Q means the adiabatic derivative of Q with respect to pressure, which we write as $(\partial Q/\partial P)_{\text{ad}}$.)

2. The formula for G was based on a least squares fit of various data, and that data included the Del Grosso sound speed [6], which is thought to be the most accurate sound speed formula in the deep ocean [7]. This makes all quantities more accurate in the deep ocean.

Various derivatives of the Gibbs function representation [8] up to third order were calculated. (Some third order derivatives are needed for the adiabatic lapse rate of sound speed.) The depth was calculated by integrating the hydrostatic equation. The results are interpolated onto a uniform depth grid. The outputs of this step are depth, pressure, density, sound speed, and the adiabatic lapse rates of density and sound speed. A consistent depth interval of 50 m to 1480 m was selected for all profiles. This depth interval is, or contains, the depths of most acoustical interest, which are the regions of the acoustic upper turning points. The choice of 50 m for the top was made to avoid the observed surface mixed layer. Many of the profiles did not go below 1480 m, determining our lowest depth.

Next, sloping straight line trends are removed from the density and sound speed profiles, leaving detrended curves that vanish at the end points. Further processing is performed in the vertical wavenumber Fourier domain. The density and sound speed are not stationary Gaussian processes, so the common practice of using windowed exponential Fourier transforms would weight different parts of the depth range unequally. Instead, we use sine and cosine transforms as described below, which weight different regions more equally. Of the various types of such transforms, type I transforms [10] are appropriate when data are specified on equally spaced points that include the top and bottom points. The detrended curves are sine transformed: the trend line will be associated later with the value at vertical wavenumber $k_z = 0$.

The next step is to split the density and sound speed data into a low-pass part and a high-pass part. To prevent ringing, a taper in wavenumber space was applied. The taper is $\cos^2(\pi k_z/4k_c)$, $0 \leq k_z \leq 2k_c$ where $k_c = 2\pi/100$ m is the half-amplitude cutoff wavenumber. The derivative of the low-pass component is calculated by multiplying the tapered sine transform by k_z, and inverse cosine transforming after including the slope of the separated straight line as the $k_z = 0$ part. The adiabatic derivative of density is the adiabatic lapse rate times the numerically calculated derivative of the pressure with respect to depth. The non-adiabatic derivative of the low-pass part is the difference between the derivative of the low-pass part and the adiabatic derivative of the low-pass part. The buoyancy frequency squared ([13], Eq. 6.83) is the non-adiabatic derivative of the low-pass filtered density multiplied by $-g/\rho$, or equivalently,

$$N^2 = g^2 \left(\frac{d\rho}{dP} - \left(\frac{\partial \rho}{\partial P} \right)_{\text{ad}} \right). \tag{3}$$

The high-pass part is defined as the inverse sine transform of the total minus the low-pass part. We postulate that the high-pass part contains primarily the fluctuations due to internal waves and spice, while the derivative of the low-pass part is dominated by the derivative of the background (and the large-scale fluctuations, which cannot be separated from the background.)

Following (1) and (2) the density and sound speed displacements are calculated by dividing each high-pass component by the non-adiabatic derivative of the corresponding low-pass component. The Garrett–Munk (GM) model predicts the high-pass internal wave spectrum to be stationary. However, we do not want to assume this model result in our analysis, and moreover we do not have any expectation for the spice displacements, so a sine transform is appropriate. By construction, the displacements vanish at the top and bottom. The sine transforms are calculated and squared to yield periodograms of the displacements (hereinafter spectra), and multiplied together to yield cross-periodograms (hereinafter cross-spectra) between the density and sound speed displacements. These periodograms are pre-whitened by multiplying by k_z^2; this essentially yields strain periodograms. The spectral estimates are obtained by smoothing the strain periodograms. Each sine periodogram value, considered as a spectral estimate, has a variance equal to twice the square of the spectral value. The particular smearing used reduces the variance of the spectral estimates by more than a factor of 20 from that of the periodogram. If the displacements and strains are not stationary processes, the spectra must be understood as power spectra averaged over the depth range.

The displacement spectra are rapidly decreasing, so one gets a much smaller dynamic range with the strain spectra (i.e., by pre-whitening), allowing plots that show much more detail. The less variable spectrum decreases the severity of aliasing and distortion of the spectrum due to the smearing. The second reason only applies to the internal waves. The GM spectrum, which makes a Wentzel–Kramers–Brillouin (WKB) approximation, gives a very simple description of the strain spectrum: the vertical wavenumber spectrum, except for the first few modes, is constant in wavenumber and depth.

For the "GM79" version [5] of the GM spectrum, the strain spectrum has the value 0.275 m for wavenumbers in rad/m, or 1.73 for wavenumbers in cpm. Munk describes a saturation cutoff, empirically at a 10-m wavelength, where the shear rate variance divided by N^2 is "of order 1." Beyond that cutoff, the shear or strain spectrum falls proportional to $1/k_z$. The strain variance in the GM79 model is one-third the variance of the ratio of shear to buoyancy frequency. As a result, the strain spectral level times the cutoff is 0.173, given the Munk values. Beyond the cutoff, the strain spectrum is $0.173/k_z$ (where k_z is in cpm).

Fig. 1 shows the effects of the high-pass filter and the spectral smoothing on the GM79 spectrum. Results from the data must be interpreted with the high-pass filter in mind. The sound speed displacement can be thought of as made up of the sum of two parts, the spice and density displacements. If the water parcel were moved adiabatically to a depth at which its density is the reference density, it would be moved by the negative of its density
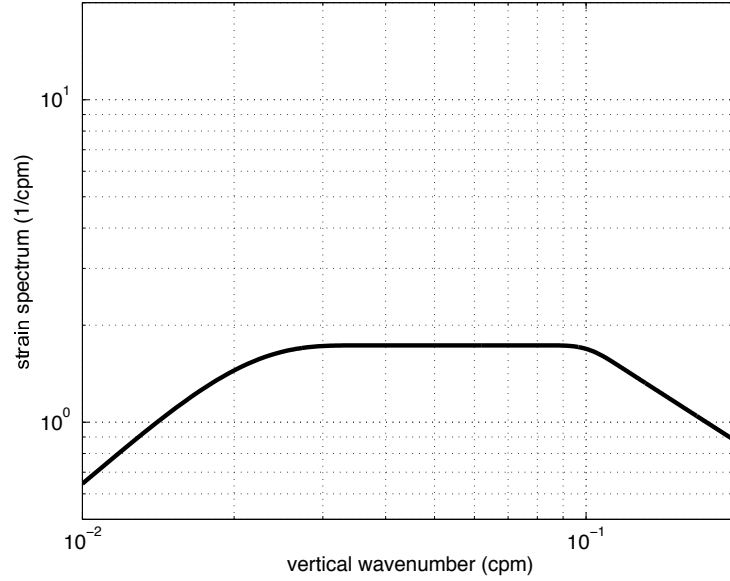
Figure 1: The effect of our processing method on the Garrett–Munk internal wave strain spectrum. The normalization is the GM79 version [5]. The low wavenumbers are suppressed by the high-pass filter, and the suppression is spread to somewhat higher wavenumbers by the smoothing of the spectrum. The Munk cutoff at high wavenumbers is included.

displacement. However, it still might not have the reference sound speed. It would have to be moved adiabatically an additional negative of the spice displacement to make its sound speed equal to the reference sound speed. Internal waves move through the water, while spice fluctuations move with the water. The phase of the waves changes linearly with time relative to the spice, so one expects no correlation between the density displacement and the spice displacement. This pair of assumptions, that the density fluctuations are internal waves and that these waves are uncorrelated with spice, can be tested. The displacements are

$$\zeta_\rho = \zeta_{\mathrm{IW}}$$
$$\zeta_c = \zeta_{\mathrm{IW}} + \zeta_{\mathrm{spice}}.$$

Under the assumptions made above, the correlation functions are

$$
\begin{aligned}
\langle \zeta_\rho(z_1)\zeta_\rho(z_2)\rangle &= \langle \zeta_{\mathrm{IW}}(z_1)\zeta_{\mathrm{IW}}(z_2)\rangle \\
\langle \zeta_\rho(z_1)\zeta_c(z_2)\rangle &= \langle \zeta_{\mathrm{IW}}(z_1)\zeta_{\mathrm{IW}}(z_2)\rangle + \langle \zeta_{\mathrm{IW}}(z_1)\zeta_{\mathrm{spice}}(z_2)\rangle \\
&= \langle \zeta_{\mathrm{IW}}(z_1)\zeta_{\mathrm{IW}}(z_2)\rangle \\
\langle \zeta_c(z_1)\zeta_c(z_2)\rangle &= \langle \zeta_{\mathrm{IW}}(z_1)\zeta_{\mathrm{IW}}(z_2)\rangle + \langle \zeta_{\mathrm{IW}}(z_1)\zeta_{\mathrm{spice}}(z_2)\rangle \\
&\quad + \langle \zeta_{\mathrm{spice}}(z_1)\zeta_{\mathrm{IW}}(z_2)\rangle + \langle \zeta_{\mathrm{spice}}(z_1)\zeta_{\mathrm{spice}}(z_2)\rangle \\
&= \langle \zeta_{\mathrm{IW}}(z_1)\zeta_{\mathrm{IW}}(z_2)\rangle + \langle \zeta_{\mathrm{spice}}(z_1)\zeta_{\mathrm{spice}}(z_2)\rangle.
\end{aligned}
$$

These relations can be Fourier transformed into spectra. The density displacement spectrum and the density–sound speed cross spectrum are predicted to be equal, both equal to the internal wave displacement spectrum. The imaginary part of the cross spectrum should be zero. The sound speed displacement spectrum is larger, and is equal to the sum of the density displacement and spice displacement spectra. This is the fundamental test. In some cases, these tests would fail. For example, in the C-SALT area [14] off the northeast coast of South America, a double-diffusive process mixes the water in steps sufficiently rapidly to overcome the dynamical effect of internal wave propagation. Thus, on the scale of the steps, the density displacement and spice displacement are correlated.

Submesoscale vortices [11] typically have a spice signature as well as a small vertical density displacement relative to the surrounding water, so they would also yield a small correlation. Larger vortical-mode features, such as mesoscale eddies, also have both spice and density variability, but we consider these much larger features to be part of the background; in any case, they are eliminated by the high-pass filter. These examples show that the tests of the assumptions should be made in every case.

In addition, the tests may be successful, but the results would still not be valid. Spice fronts temporarily reversing the general trend of the sound speed profile can violate the use of low-pass derivatives to estimate sound speed displacements. Several profiles from the experimental data considered here had such fronts (Fig. 2), but were eliminated from analysis so as to have consistent processing for the remainder. The density profile, when low-pass filtered, has a nearly constant derivative in the depth interval shown, so density displacements are estimated accurately, but if the sound speed is low-passed, the derivative is very small, and is sensitive to the parameters of the low-pass filter, so the corresponding displacements are very large and meaningless.

These fronts are clearly relevant to acoustic propagation, but in a way different from the oscillating fluctuations that our method can handle.

3   Examples

3.1   LOAPEX

Eight CTD profiles were taken at locations where the acoustic projector was deployed to transmit to a pair of vertical line arrays (VLA) of receivers. The first seven locations were along a great circle. The location of the VLA was 33.4°N 222.3°E and the farthest station was at 34.6°N 187.5°E. These transmission stations are identified by their distance in kilometers from the VLA as T50, T250, T500, T1000, T1600, T2300, and T3200. The last profile was taken a short distance north of the island of Kauai.

Each of the first four profiles had spice fronts leading to unrealistic 'sound speed displacements'. Therefore, these profiles are excluded from this study, even though a modified

Sound speed (heavy line) and –density (light line) [arbitrary units]
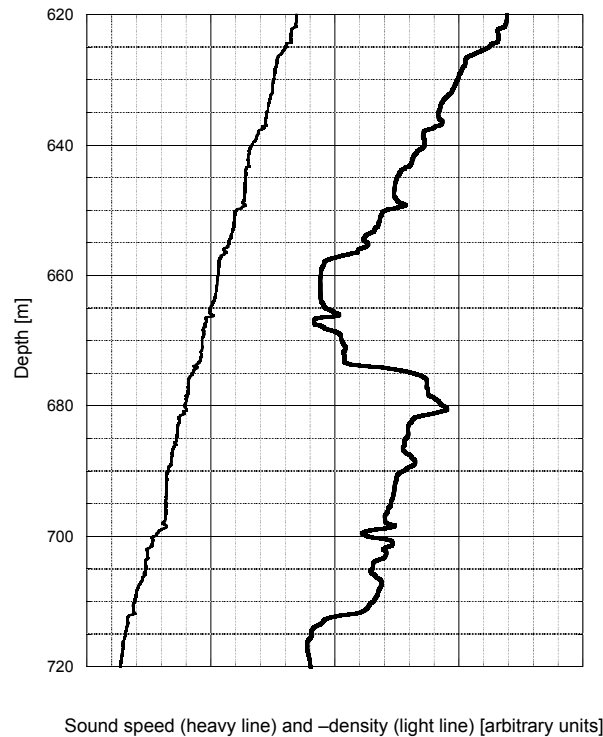
Figure 2: A 100-m section of a CTD profile, showing a spice front that invalidates the derivative formula for sound speed displacement. The density profile shows no features at this front, so the density displacement is given correctly by the corresponding formula. Profiles such as this are excluded from the analysis presented here.

algorithm could yield meaningful results.

The T1600 profile was taken at a station located at 35.3°N, 154.9°W. It is about several hundred kilometers away from either of the two major North Pacific fronts, the subpolar and subtropical fronts. Thus, it might be expected to have less spice than locations close to one of these fronts.

An upper section (400–500 m) from the vertical profiles of the density and sound speed displacements at station T1600 shows that the two are approximately the same (Fig. 3a); little spice is evident. A lower section (900–1000 m) shows that the two displacements differ (Fig. 3b). Although the (high-pass) density displacements resemble a stationary Gaussian process, the spice is very intermittent, being present in one of these sections, but almost non-existent in the other. This spatial intermittency occurs throughout all profiles. Plots of strain spectra (Fig. 4) show density and cross-spectra as approximately equal, completing the test successfully, and the sound speed spectrum is consistently larger than the others.

The density spectrum rises initially, due to the high-pass filter of the processing, looking similar to the reference GM79 curve (Fig. 1). Beyond the rise, it is roughly constant. The
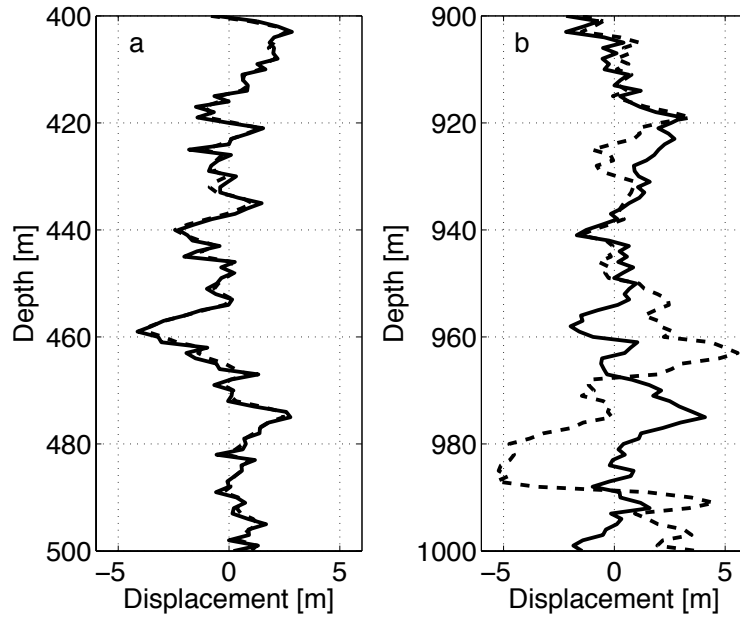
Figure 3: Sections of the LOAPEX T1600 displacement profiles, showing spice intermittency. The density displacement is the solid curve and the sound speed displacement is the dashed curve. From 400 m to 500 m (a), the two curves are almost identical, showing almost no spice fluctuations. From 900 m to 1000 m (b), the curves are very different, showing the presence of significant spice fluctuations.

level in the rise and beyond is about half the strength of the GM model, which has been found to apply generally to the Northwest Pacific [2, 4]. Munk's arguments imply that the break for a half-strength spectrum should be at twice the wavenumber shown in the comparison curve, or about 0.2 cpm. This delayed break is consistent with the data. No spectra are shown beyond 0.2 cpm, as salinity spiking becomes important at about that value. The sound speed strain spectrum is about 50% larger than the density displacement spectrum at smaller wavenumbers, rising to about twice the density displacement spectrum at larger wavenumbers. If we take the spectral levels as an indication of the importance to acoustics, the spice is about half as important to equally important as the internal waves averaged over this profile. However, as can be seen by comparing the two displacements (not shown), there is very little spice between 200 m and 900 m. The minimum sound speed is around 750 m deep, so any acoustic propagation with an upper turning point below 200 m is affected very little by spice at this location.

T2300 and T3200 are on about the same latitude as T1600, and the spectra are similar to those of T1600, but for these profiles, there is significant spice in the 200–900-m region. The average of the three spectra are shown in Fig. 5. All four strain spectra results are provided in Appendix 1.1. The density strain spectral level is about half of GM79, and the spice strain is slightly larger than the density strain. The Kauai station is in a different oceanographic region than the stations described previously. The internal wave spectral
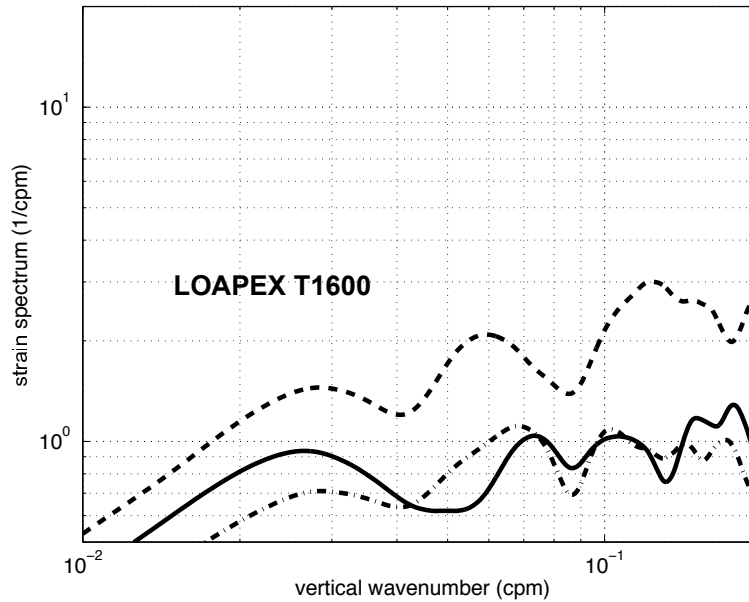
Figure 4: The spectra from LOAPEX T1600. The solid curve is the density strain spectrum, the dashed curve is the sound speed strain spectrum, and the dot-dash curve is the cross spectrum. From the assumption of the lack of correlation between internal waves and spice, the density strain spectrum and the cross spectrum should both equal the internal wave spectrum, and therefore be equal, which is approximately true. Their level is about half the GM79 level (Fig. 1). The spice spectrum is the difference between that of the sound speed and that of the density. The level of the spice spectrum is close to that of the internal wave spectrum for this profile.

level is larger, more than twice the GM79 value (Fig. 6). There appears to be a break in the spectrum at about the wavenumber 0.04 cpm, in agreement with Munk's prediction.

3.2   PhilSea09

The main acoustic VLA mooring was located near 21.4°N, 126°E. The CTD profiles taken during PhilSea09 extended in a NNE direction to near 22.96°N, 126.56°E, a distance of 182 km at a compass heading of 18°.

Nineteen CTD casts made during the 2009 Philippine Sea Pilot Study/ Engineering Test [16] are analyzed. These casts were made from the R/V *Melville* during three instrument deployment and recovery cruises. (See Fig. 7.) These casts spanned the period 2 April – 12 May 2009, and sampled a 183-km section.

Several types of spectra were calculated from the CTD data. Spectra indicating very little spice are evident (Fig. 8). Other spectra had stronger contributions, e.g., cast G
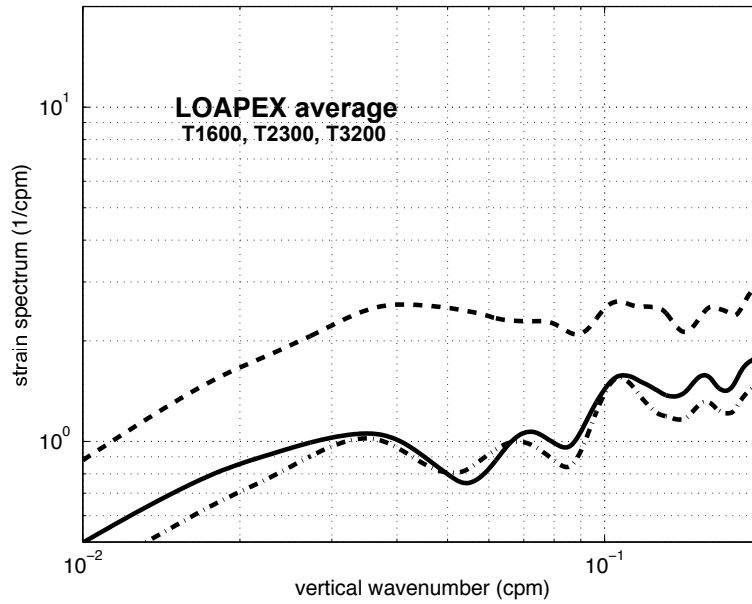
Figure 5: The average of the three spectra from LOAPEX stations near 35° latitude without spice fronts. The curves in this and other figures represent the same spectra as in Fig. 4. The cross spectrum is closer to the density strain spectrum than it was for a single station. The internal wave level is about half GM79. The spice spectrum (the difference between the dashed and solid curves) is larger than the internal wave spectrum.
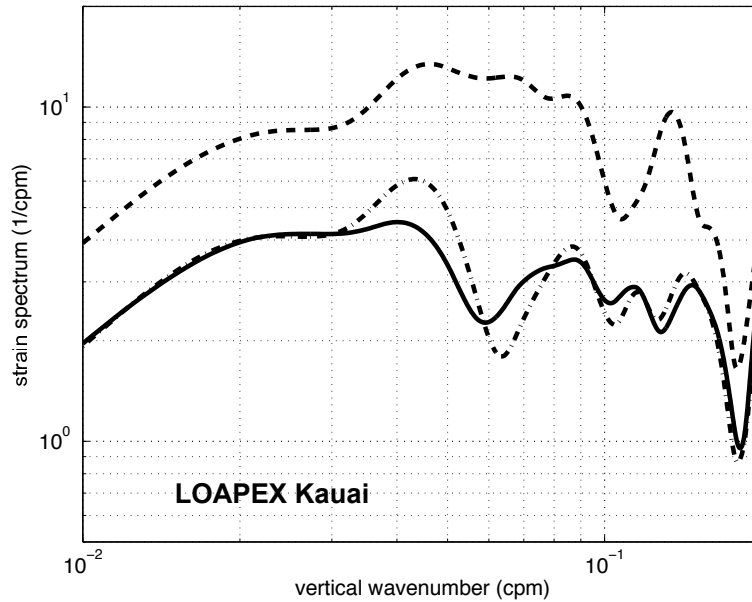
Figure 6: The spectra from the Kauai station. The internal wave level is more than twice the GM79 level, and there is an apparent spectral slope change at about 0.04 cpm, consistent with Munk's argument.
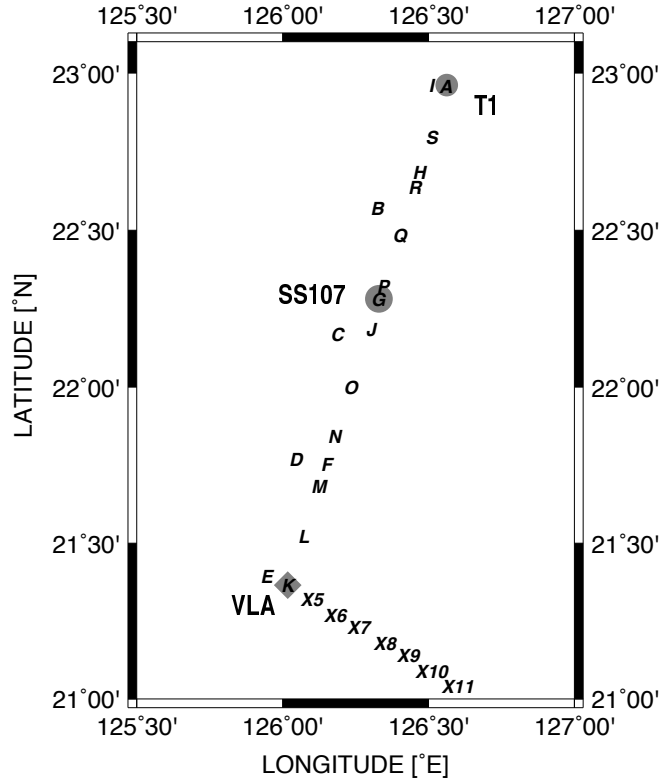
Figure 7: The positions of the PhilSea 09 CTD stations, labeled A through S, and a few of the PhilSea 10 stations labeled X5 through X11 (X4 and K were in almost the same place).

(Fig. 9). For this cast, the spice contribution is almost as strong as the internal wave contribution. Little is known about the spatial structure of spice, other than that it is 'intermittent'. Casts made near the VLA measured consistently low levels of spice intensity. Casts made further north generally measured higher levels of spice. Colosi and coworkers [3] suggest that spice contributions to sound speed anomalies were small at the VLA, in agreement with our analysis (Fig. 8). Relative density and sound speed anomaly maps made from all the CTD profiles along the section (Fig. 10) do not in general show a clear pattern of fronts, eddies, or intrusions that might suggest the presence of spice. This is expected because the cast programs on the three cruises were not organized into a regular space–time sampling program, and further, the casts span more than one month.

The average spectra for the entire set, excluding several that had distinct identifiable fronts, is shown in Fig. 11. All the strain spectra are provided in Appendix 1.2. The cross spectrum is almost exactly the same as the density spectrum (except for the small salinity spiking effect), showing that the assumptions of our processing are valid. Though spice level is less than the internal wave level, it is substantial.
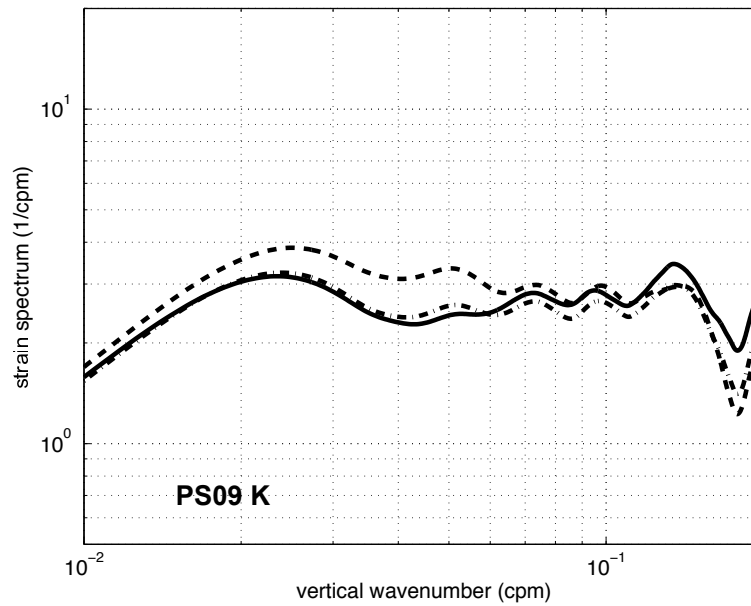
Figure 8: The spectra for a profile measured at the receiver mooring, PhilSea09. This profile has a small amount of spice fluctuations. The internal wave level is somewhat higher than GM79.
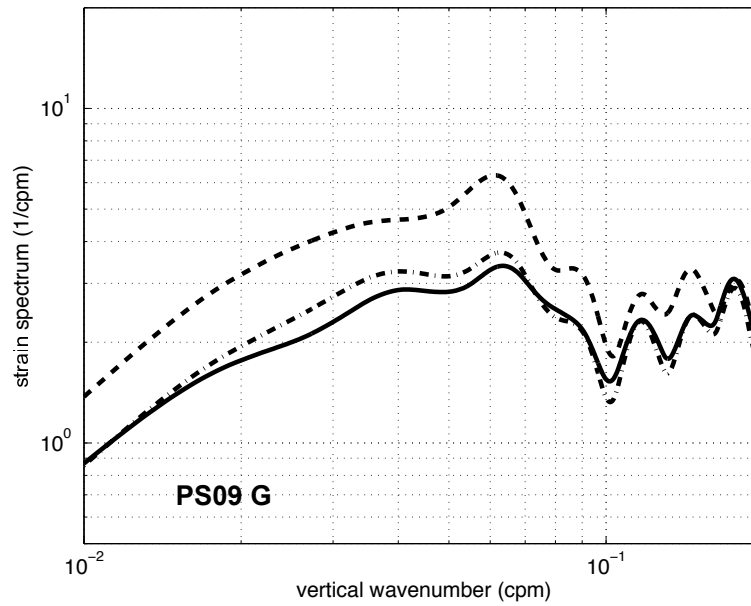
Figure 9: Spectra from PhilSea09 profile G. This profile has more spice, and its shape is somewhat different than the GM79 spectrum.
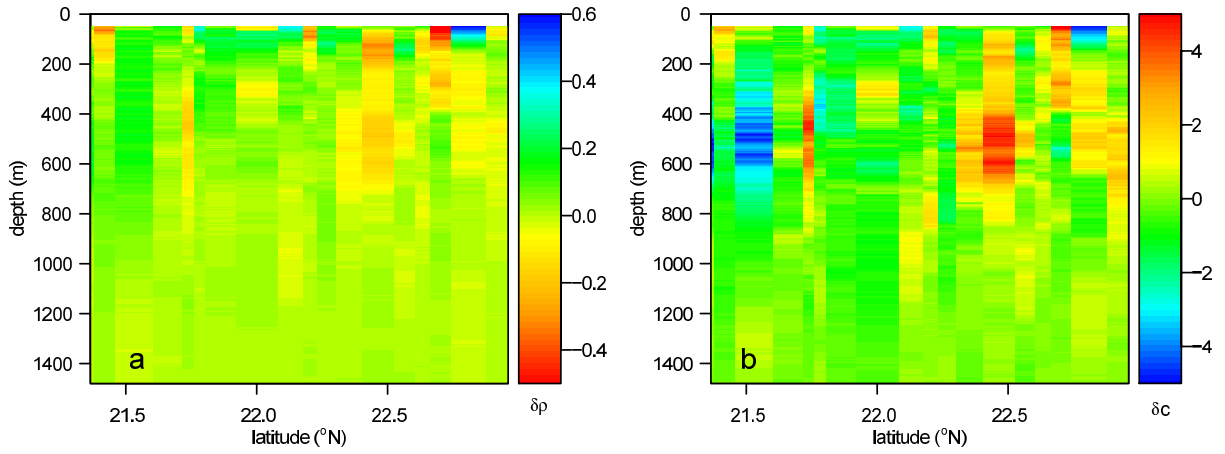
Figure 10: The large-scale density (a) and sound speed (b) anomaly fields in the PhilSea09 transect. The anomaly is defined as the difference between the measured values and the horizontal average at each depth. No clear pattern is evident, although the northern half of the observations suggests a more complex assembly of warm water parcels.
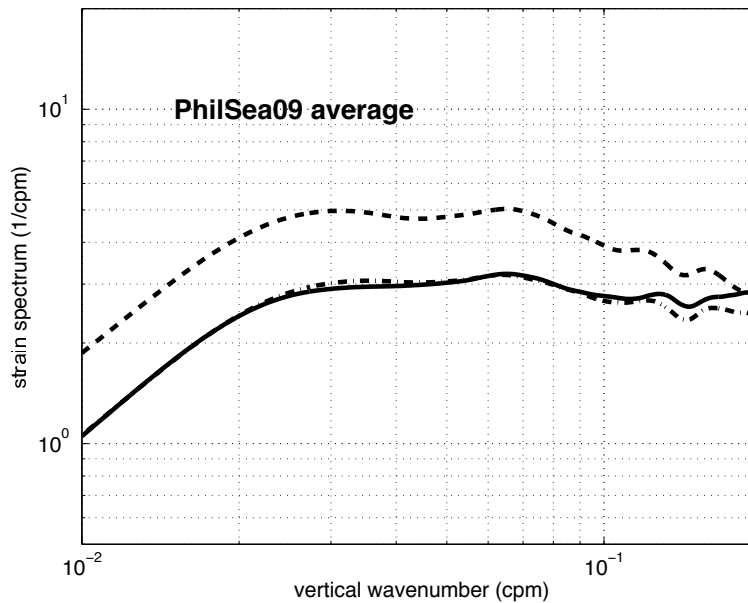
Figure 11: The average spectra from PhilSea09 profiles without spice fronts. The internal wave level is 1.7 times GM79, and the spice is 1.2 GM79.
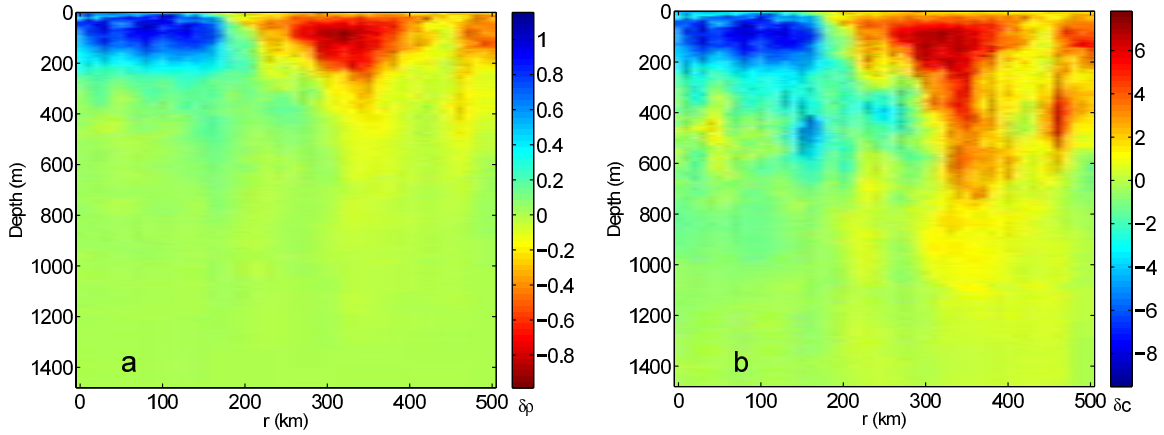
Figure 12: The large-scale density (a) and sound speed (b) anomaly fields in the PhilSea10 transect. The anomaly is defined as the difference between the measured values and the horizontal average at each depth. The western side is a relatively constant colder region, and there is a rather wide transition to a warmer and less constant region in the center and eastern part of the transect. The transition was verified to be in geostrophic balance using the measured current. The sound speed structure extends deeper than the density structure.

3.3 Philsea10

Fifty-one CTD profiles were taken every 10 km along a 500-km path at a compass heading of 121°, starting near the acoustic VLA mooring. Thus, the PhilSea09 and Philsea10 CTD lines almost coincided at their start points, and went in directions about 103° apart. There were several other profiles taken, which we do not discuss; the 500-km path consists of profiles numbered from #4 at range 0 to #54 at range 500 km.

The large-scale variability of sound speed and density along this path are characterized by a relatively uniform region for the first 170 km, with a much more variable contrasting region beyond that point (Fig. 12). The sound speed variability extends considerably deeper than the density variability. From the comparison with the ship's acoustic Doppler current profiler (ADCP) data and the density variation between these two regions, it was verified that the two regions are in geostrophic balance, as expected.

In the first 110 km (twelve profiles, #4 through #15), well within the relatively uniform region, very little spice fluctuation was observed. Profile #12 is the most spice-free of all (Fig. 13); the three spectra are almost identical. A small effect of salinity spiking is apparent on the density strain spectrum at the highest wavenumbers; it becomes larger at the wavenumbers beyond those plotted. The average of profiles taken in the first 110 km is shown in Fig 14. The density strain spectral level is about 75% larger than GM79. It is interesting that this region of little spice abuts the region of little spice observed one year earlier during PhilSea09.
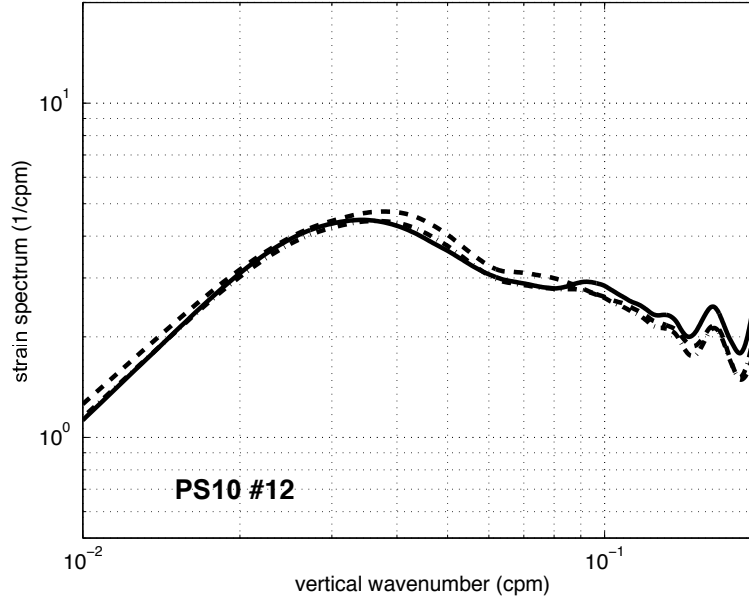
Figure 13: The PhilSea10 spectra from profile #12 with the smallest spice fluctuations.

Farther southeast, the amount of spice strain increases and the amount of density strain decreases. An example is profile #38 (Fig. 15). The average of the remainder of the profiles has a spectral level about 25% larger than GM79. The average for the entire set is shown in Fig. 16 and the entire set of strain spectra results is presented in Appendix 1.3. With this average of a large number of profiles, the cross spectrum is almost exactly the same as the density spectrum (except for the small salinity spiking effect), showing that the assumptions of our processing are valid. Though the spice level is less than the internal wave level, it is substantial.

Fig. 17 shows the spice field spatial characteristics along the PhilSea10 transect, plotting for each cast the difference between the strain spectrum calculated with the sound speed and the strain spectrum calculated with the density. Regions with little spice have a difference near zero. The bright red/orange regions indicate profiles (hence ranges) where there was considerable spice detected in the profile. This transect shows that spicy regions may be compact and localized.

4   Discussion

The processing to extract internal waves and spice from single CTD profiles satisfies validity tests, giving credibility to the spectra that have been calculated. The density strain spectrum measures the high-wavenumber internal wave strength, and the sound speed strain spectrum measures the sum of the internal wave and spice strengths.
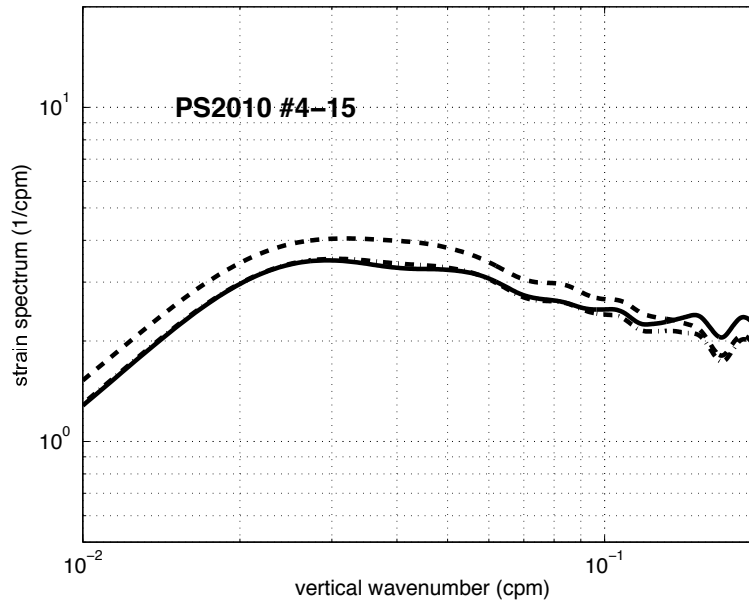
Figure 14: The average spectra of the first 12 profiles from the westernmost 110 km of the PhilSea10 transect. There is very little spice, and the internal wave spectral level is nearly twice the GM79 level. This region lies within the nearly constant colder region of the large-scale density and sound speed structure. Its west end is at the VLA mooring, where there was also very little spice in PhilSea09, one year earlier.
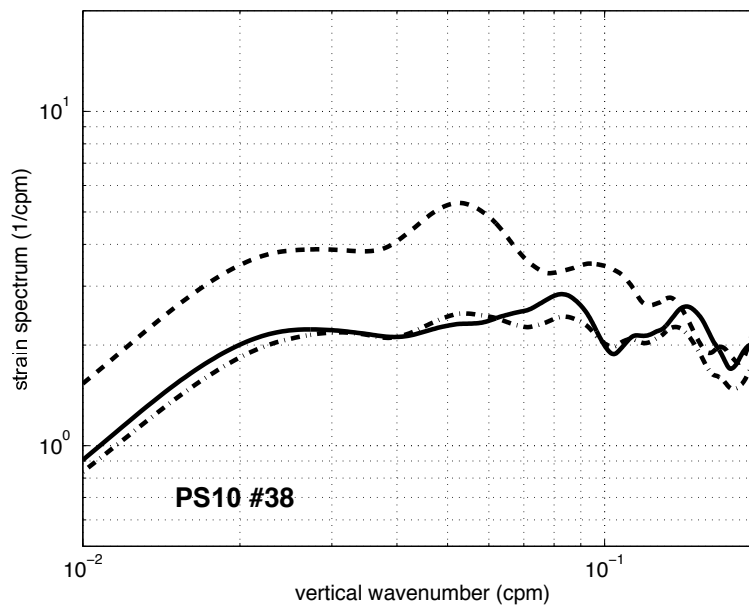
Figure 15: The spectra from profile #38 in the eastern part of the transect. Here the internal waves are only slightly above GM79, and the spice nearly equals the internal waves.
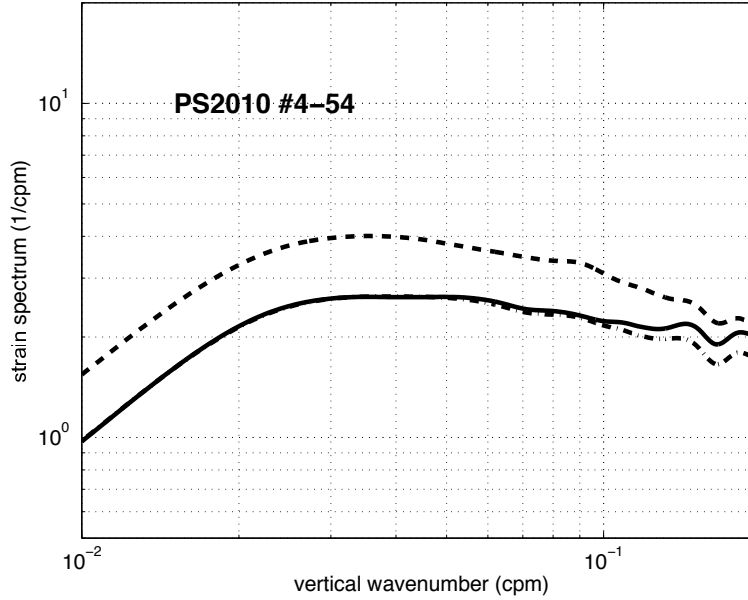
Figure 16: The average spectra from the PhilSea10 transect. The average internal wave level over the entire set is less than that over the first 110 km, but still above GM79. The level of the spice is close to the GM79 reference level.

The internal wave spectra are close to the GM79 shape, and their levels fit the GM assertion that they are mostly within a factor of two of their reference level. In this case, the strain reference level used is GM79, which differs from the reference level of the earlier GM model for the same total internal wave energy [9]. The internal wave level varies with geography, being small along the LOAPEX path and large in the Kauai region and in the Philippine Sea, with even a significant variation along the PS10 path.

The spice level is defined to reflect the importance of its acoustic effects. However, there is a significant uncertainty in such an identification. The spice is not well described by a spectral model. It is highly intermittent, and the response of the acoustics to this intermittency is not known. Moreover, the fluctuations in acoustic propagation depend on the simultaneous horizontal and vertical scales of the sound speed fluctuations, and the analysis presented here determines only the vertical scales. If the aspect ratio of the spice is about the same as the aspect ratio for internal waves, the spectral levels reported here are more likely to be useful in relating the relative importance of the two phenomena. We are far from being able to propose a model for the spice to be used in acoustic propagation calculations, but the levels found here suggest that it is comparable to the effects of internal waves.
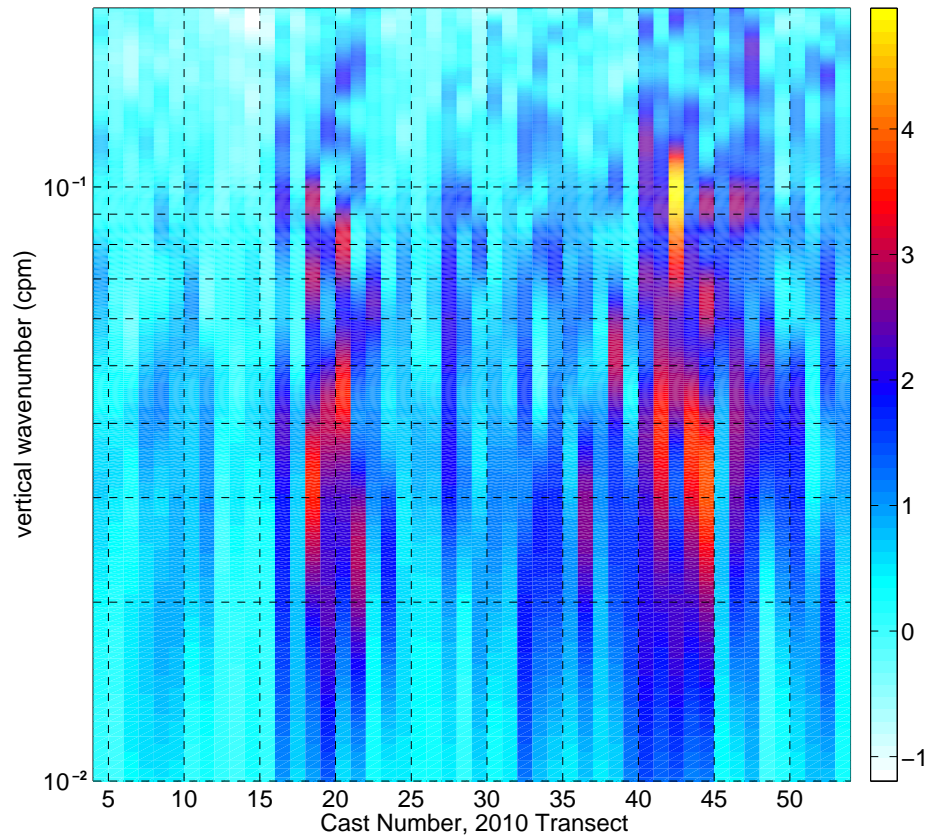
Figure 17: Spatial characteristics of this estimator along the PhilSea2010 transect. The figure shows the difference between the strain spectrum calculated from the sound speed and the strain spectrum calculated from the density. The horizontal axis is cast number: the casts are roughly 10 km apart. The leftmost cast is near the VLA, and the casts trend ESE. The color scale is in units of reciprocal cycles per minute.

References

[1] J.A. Colosi, 1999. *Data Report for NPAL Internal Wave Environmental Data, IW98 Cruise*, Woods Hole Oceanographic Institution, 54 pp.

[2] J.A. Colosi, 1997. Random media effects in basin-scale acoustic transmissions, in *Monte Carlo Simulations in Oceanography*, Proceedings of the 9th 'Aha Huliko'a Hawaiian Winter Workshop, University of Hawaii at Manoa, 14–17 January, P. Müller and D. Henderson, eds., pp. 157–166.

[3] J.A. Colosi, B.D. Dushaw, R.K. Andrew, L.J. van Uffelen, M.A. Dzieciuch and P.F. Worcester, 2103. Space-time scales of sound-speed perturbations observed in the Philippine Sea: Contributions from internal waves and tides, eddies, and spicy thermohaline structure, *J. Acoust. Soc. Am.*, 134, 3185–3200.

[4] J.A. Colosi, S.M. Flatté and C. Bracher, 1994. Internal-wave effects on 1000-km oceanic acoustic pulse propagation: Simulation and comparison with experiment, *J. Acoust. Soc. Am.* 96, 452–468.

[5] W.H. Munk, 1981. A survey of internal waves and small-scale processes, in *Evolution of Physical Oceanography*, B.A. Warren and C. Wunsch, eds., Cambridge, MA: MIT Press.

[6] V.A. Del Grosso, 1974. New equation for the speed of sound in natural waters (with comparisons to other equations), *J. Acoust. Soc. Am.*, 56, 1084–1090.

[7] B.D. Dushaw, P.F. Worcester, B.D. Cornuelle and B.M. Howe, 1993. On equations for the speed of sound in seawater, *J. Acoust. Soc. Am.*, 94, 255–275.

[8] R. Feistel and E. Hagen, 1995. On the GIBBS thermodynamic potential of seawater, *Progr. Oceanogr.*, 36, 249–327.

[9] A.E. Gargett, 1990. Do we really know how to scale the turbulent kinetic energy dissipation rate ϵ due to the breaking of oceanic internal waves? *J. Geophys. Res.*, 95, 15,971–15,974.

[10] S.A. Martucci, 1994. Symmetric convolution and the discrete sine and cosine transforms, *IEEE Trans. Sig. Proc.*, 42, 1038–1051.

[11] J.C. McWilliams, 1985. Submesoscale, coherent vortices in the ocean, *Rev. Geophys.*, 23, 165–182.

[12] J.A. Mercer, J.A. Colosi, B.M. Howe, M.A. Dzieciuch, R. Stephen and P.F. Worcester, 2009. LOAPEX: The Long-Range Ocean Acoustic Propagation Experiment, *IEEE J. Ocean. Eng.*, 34, 1–11.

[13] P. Müller, 2006. *The Equations of Oceanic Motions*, Cambridge University Press.

[14] R.W. Schmitt, H. Perkins, J.D. Boyd and M.C. Stalcup, 1987. C-SALT: An investigation of the thermohaline staircase in the western tropical North Atlantic, *Deep-Sea Res.*, 34, 1697–1704.

[15] Sea-Bird Electronics, Inc. *Seasoft V2: SBE Data Processing*, Bellevue, WA, `http://www.seabird.com/software/SBEProcforWindows.htm`, last accessed 2012.10.30.

[16] P.F. Worcester, R.K. Andrew, A.B. Baggeroer, J.A. Colosi, G.D. D'Spain, M.A. Dzieciuch, K.D. Heaney, B.M. Howe, J.N. Kemp and J.A. Mercer, 2013. Acoustic propagation and ambient noise in the Philippine Sea: The 2009 and 2010 – 2011 Philippine Sea experiments, *J. Acoust. Soc. Am.*, 134, 3359–3375.

A Spectra Results

This appendix provides the actual spectral characterizations of the small-scale vertical strain perturbations induced by internal waves and spice for all the appropriate single CTD casts in the LOAPEX, PhilSea09, and PhilSea10 experiments.

In all figures the solid curve is density strain spectrum, dashed is sound speed strain spectrum, and dot-dashed is the cross spectrum.

1.1 LOAPEX Strain Spectra
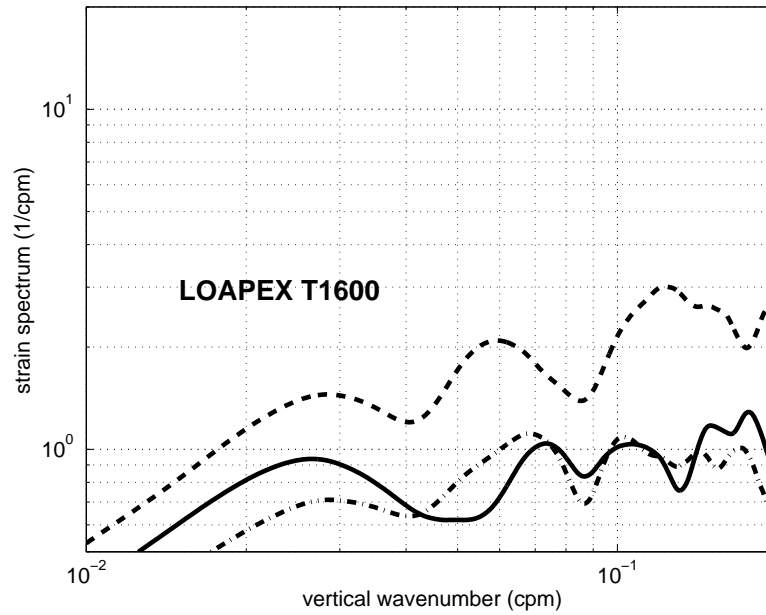
Figure 18: LOAPEX T1600.
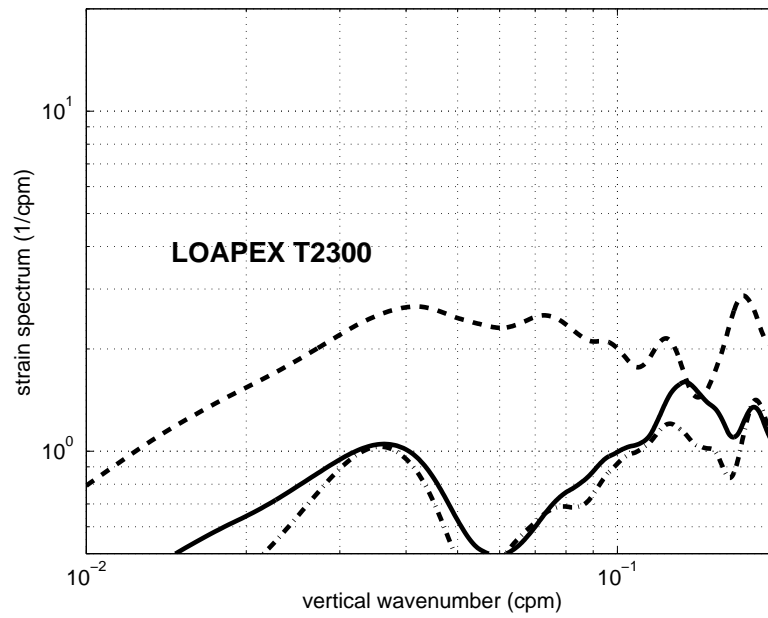
Figure 19: LOAPEX T2300.
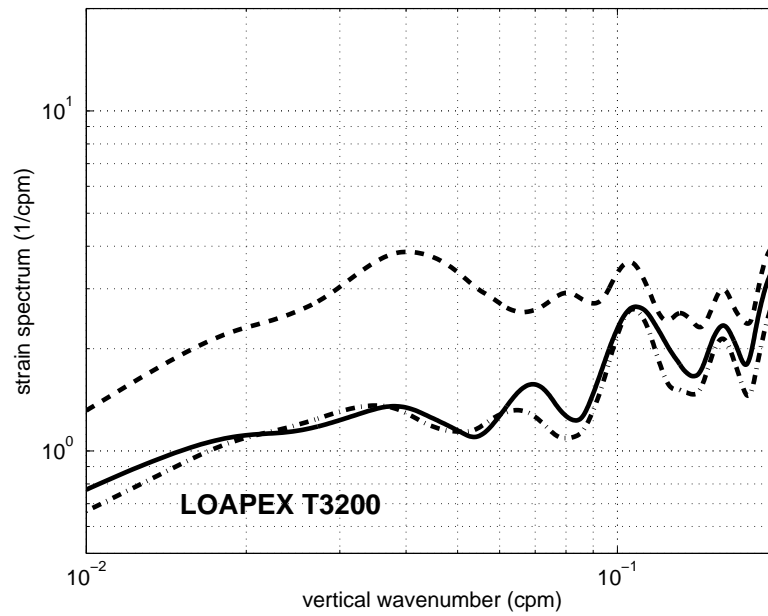
Figure 20: LOAPEX T3200.
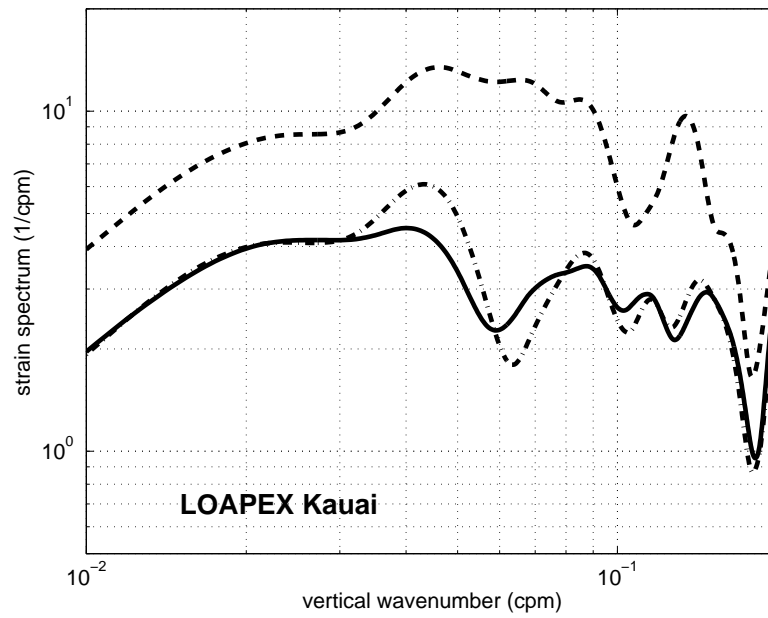
Figure 21: LOAPEX Kauai station.

1.2 PhilSea09 Strain Spectra
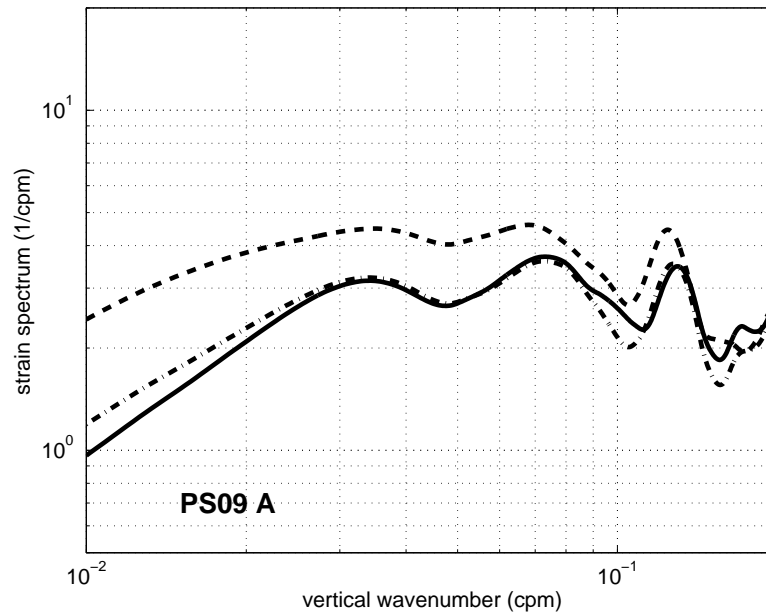
Figure 22: PhilSea09 CTD station A.
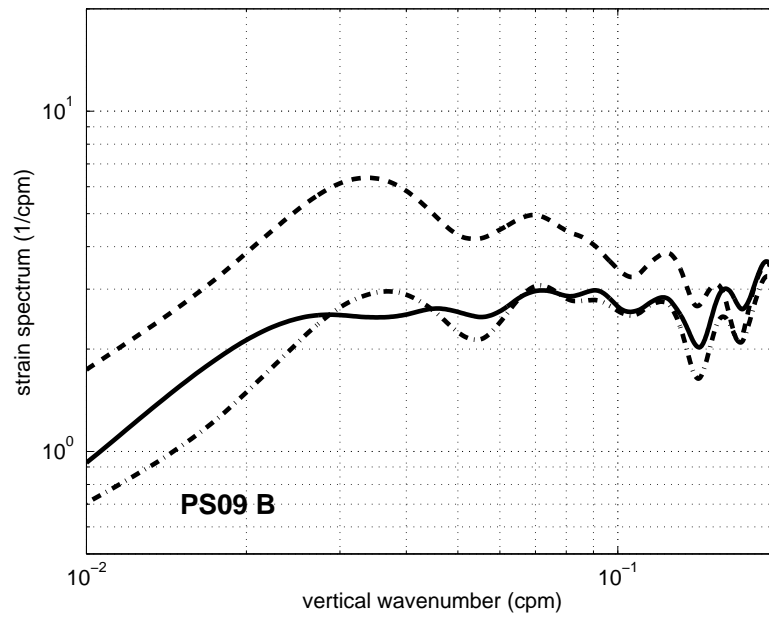
Figure 23: PhilSea09 CTD station B.
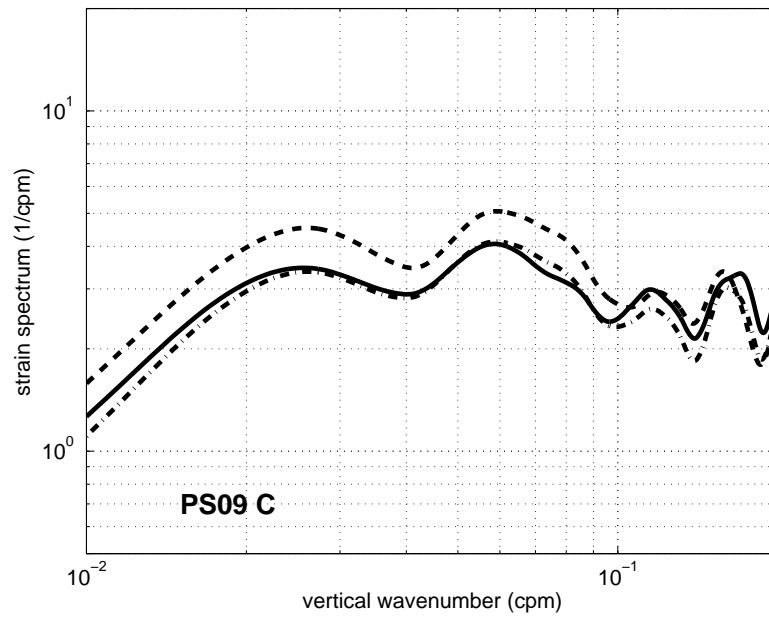
Figure 24: PhilSea09 CTD station C.
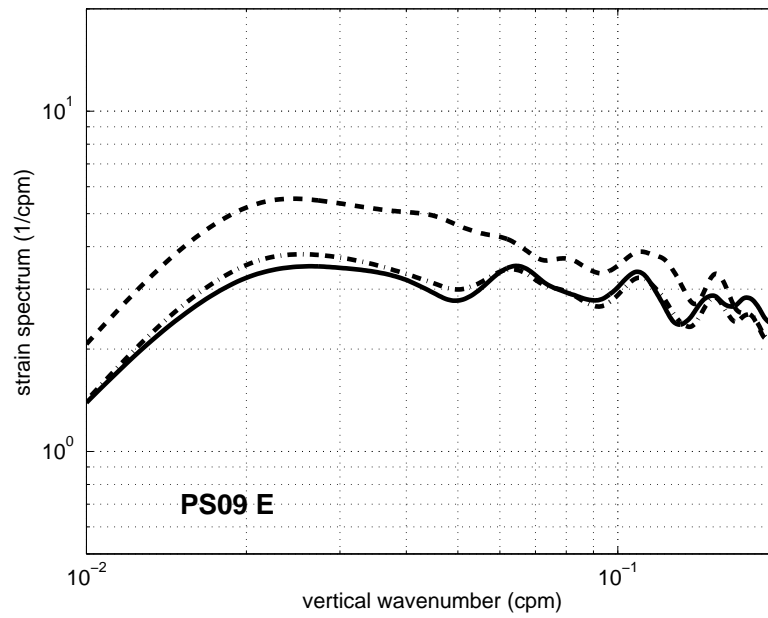
Figure 25: PhilSea09 CTD station E.
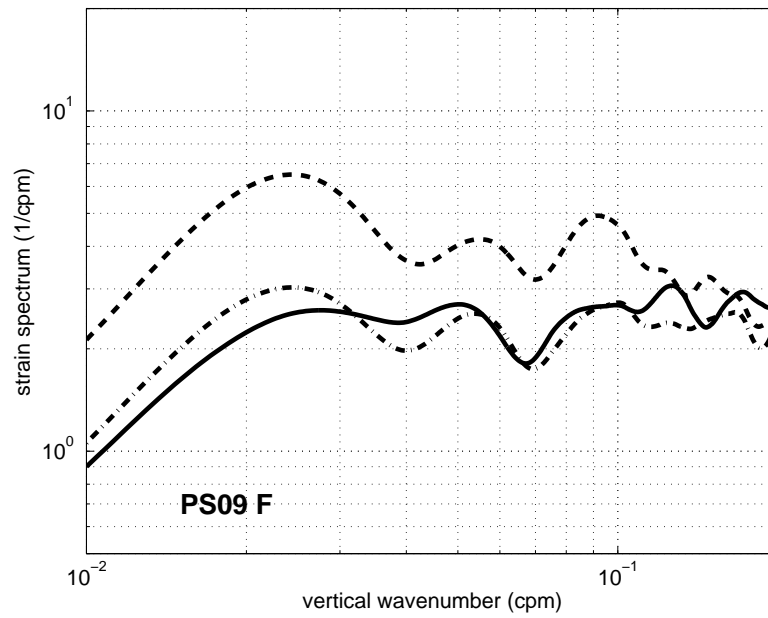
Figure 26: PhilSea09 CTD station F.
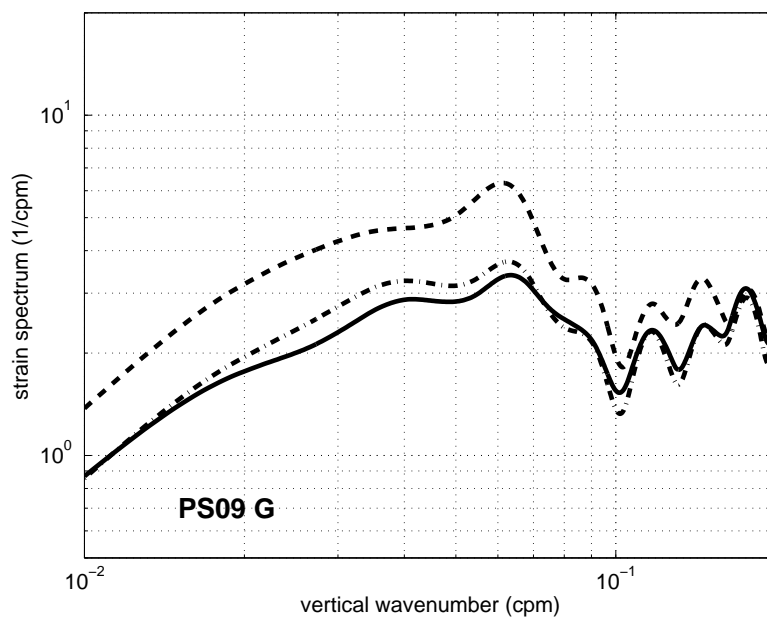
Figure 27: PhilSea09 CTD station G.
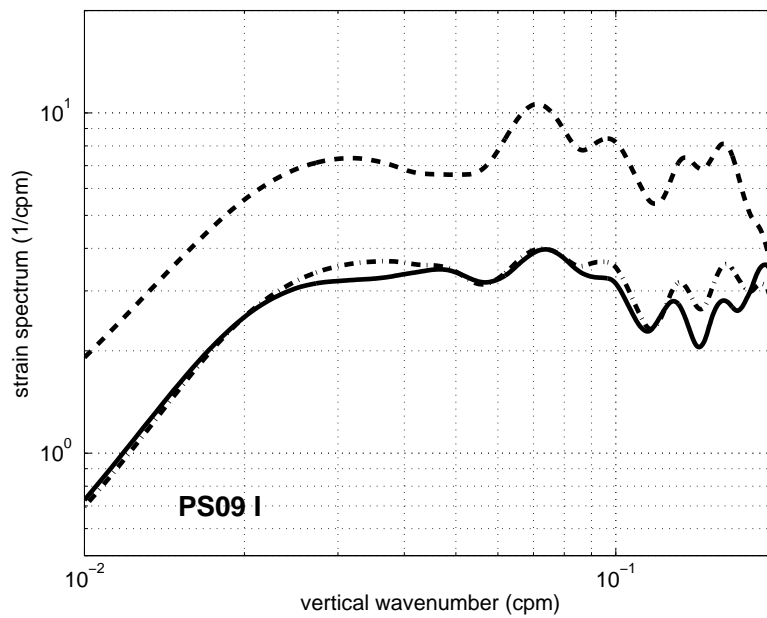
Figure 28: PhilSea09 CTD station I.
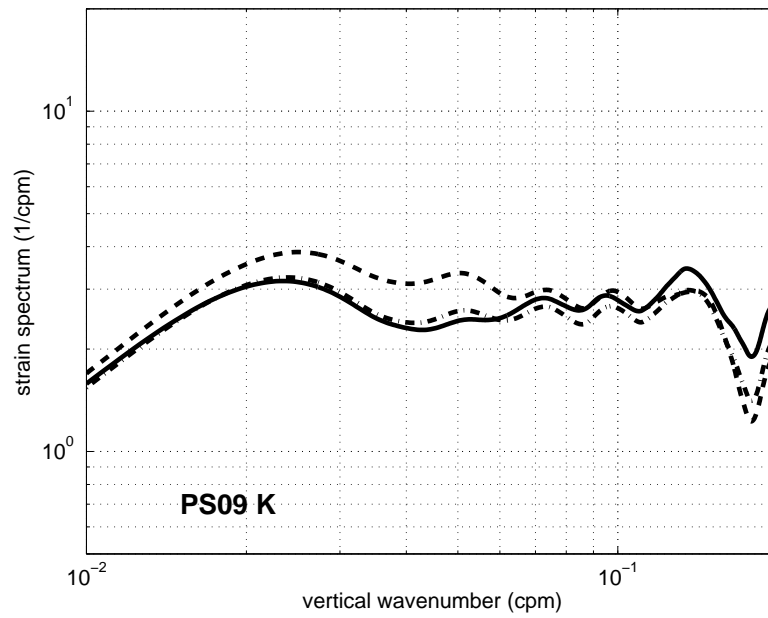
Figure 29: PhilSea09 CTD station K.
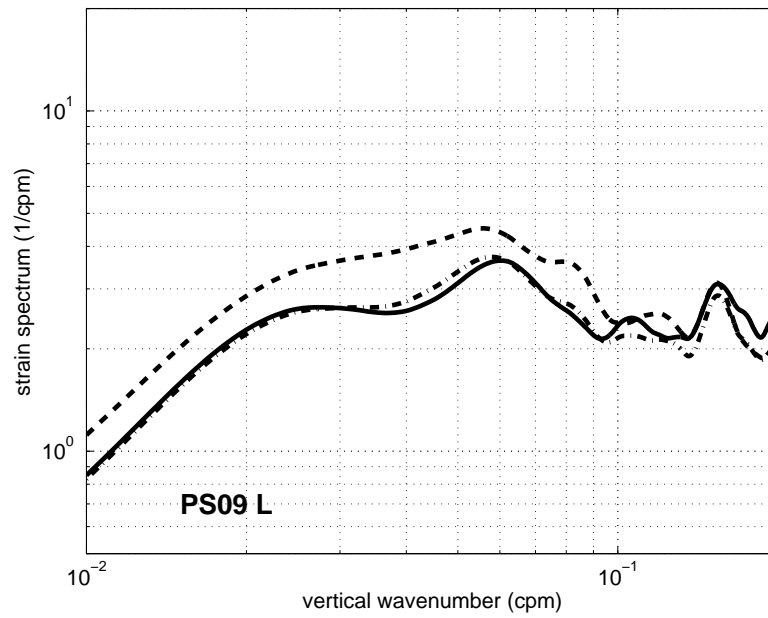
Figure 30: PhilSea09 CTD station L.
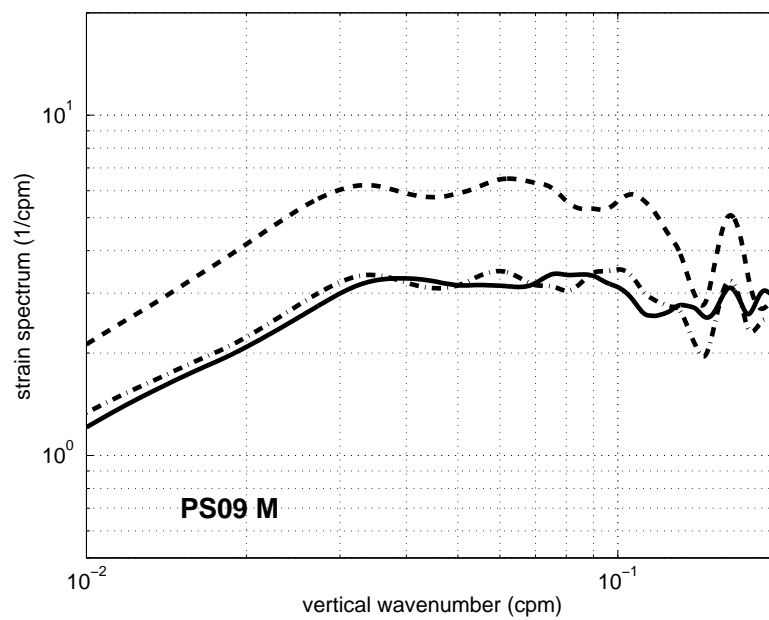
Figure 31: PhilSea09 CTD station M.
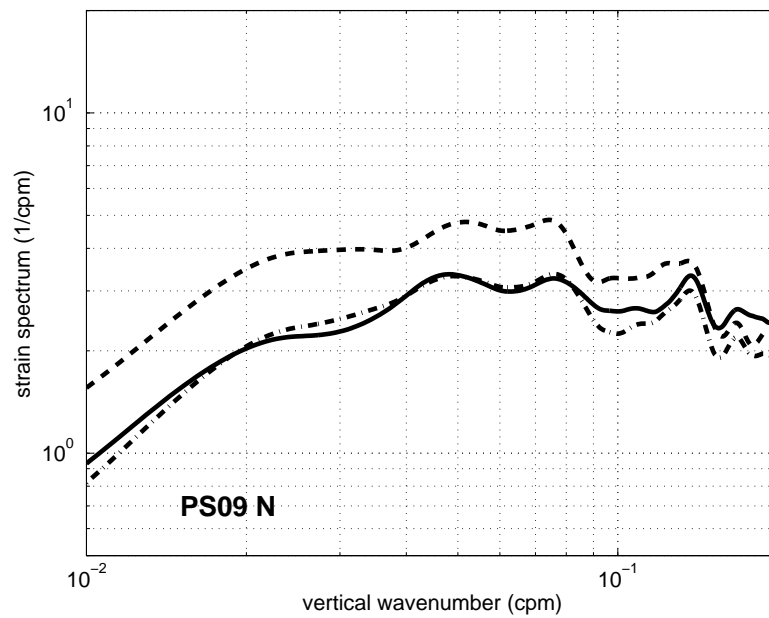
Figure 32: PhilSea09 CTD station N.
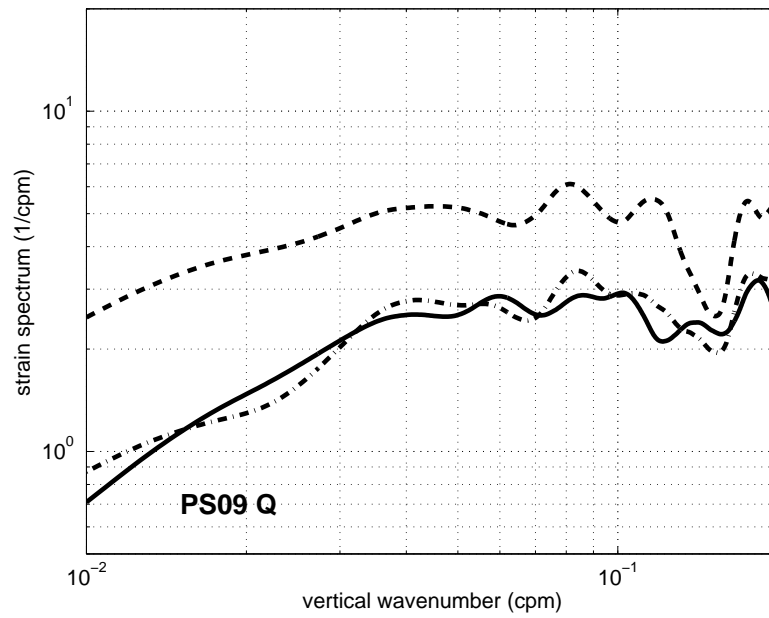
Figure 33: PhilSea09 CTD station Q.
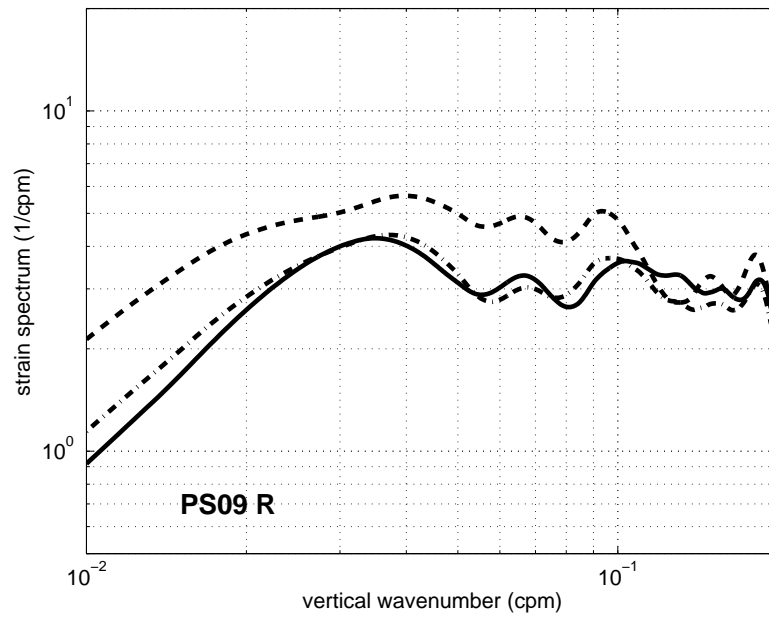
Figure 34: PhilSea09 CTD station R.

1.3 PhilSea10 Strain Spectra
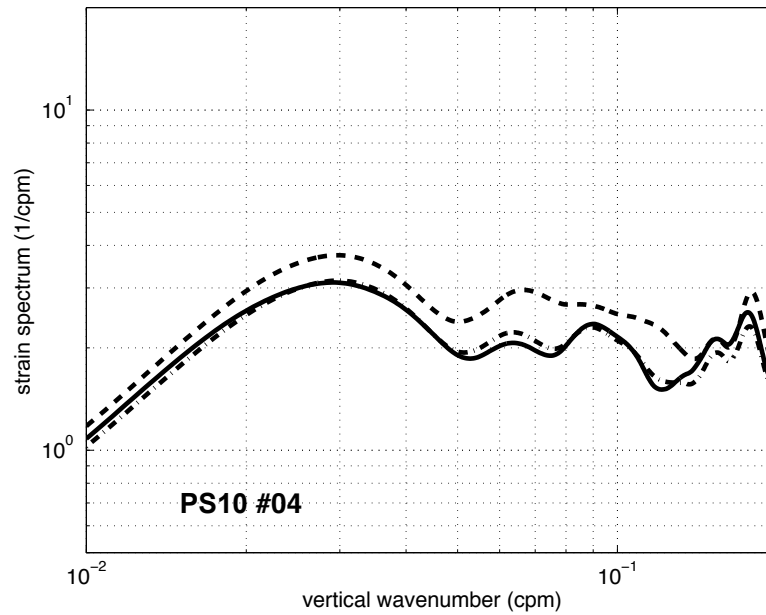
Figure 35: PhilSea10 cast dRR1006_004.
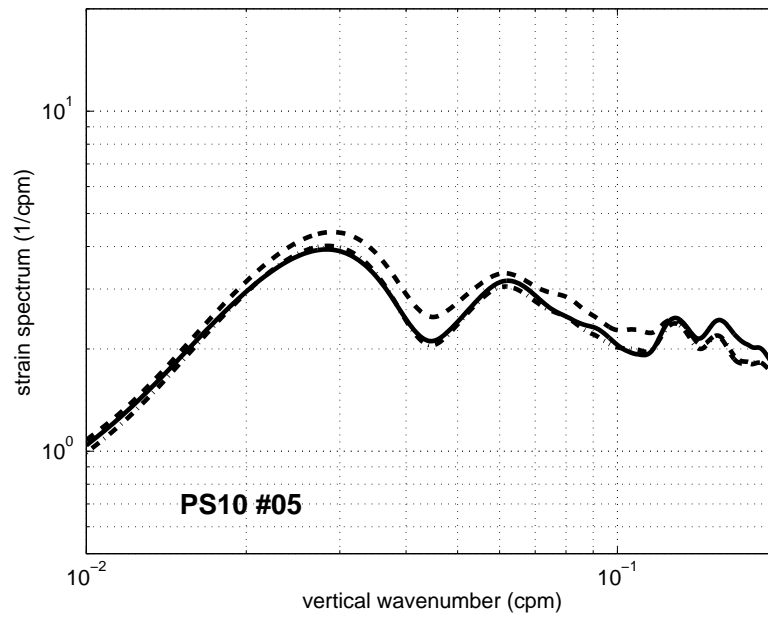
Figure 36: PhilSea10 cast dRR1006_005.
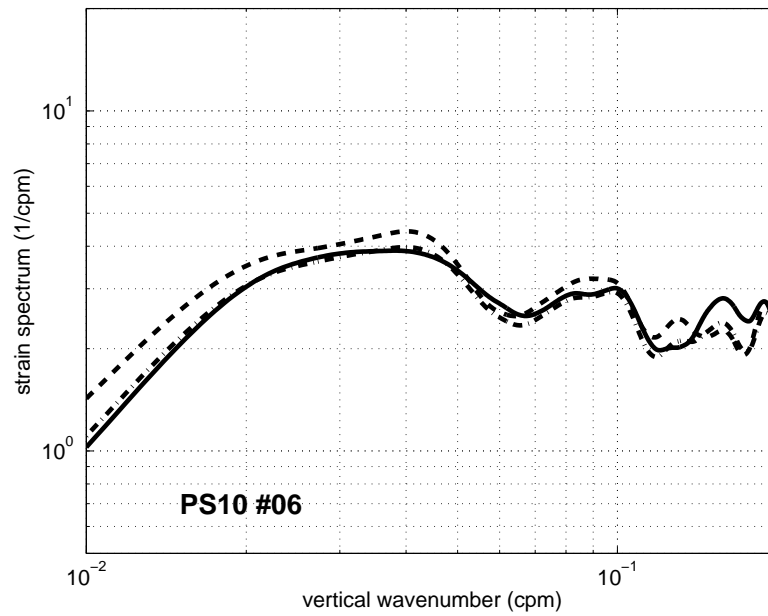
Figure 37: PhilSea10 cast dRR1006_006.
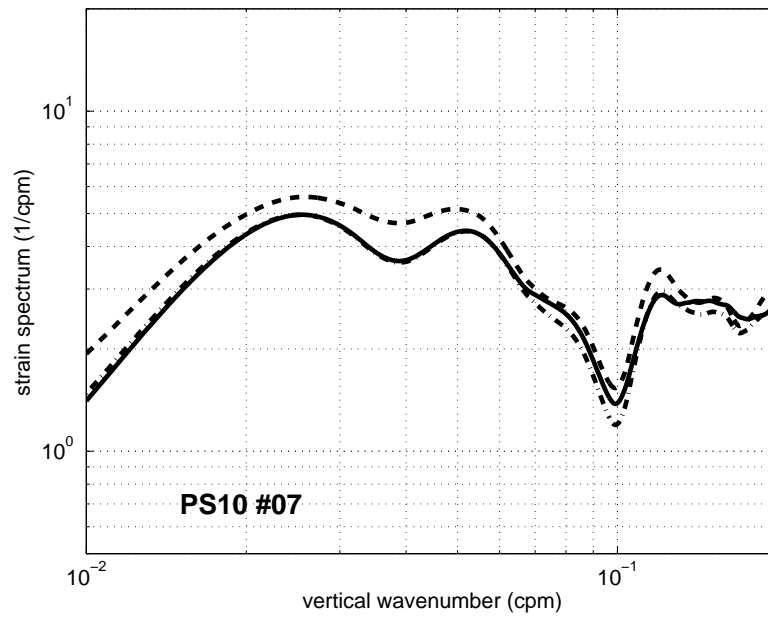
Figure 38: PhilSea10 cast dRR1006_007.
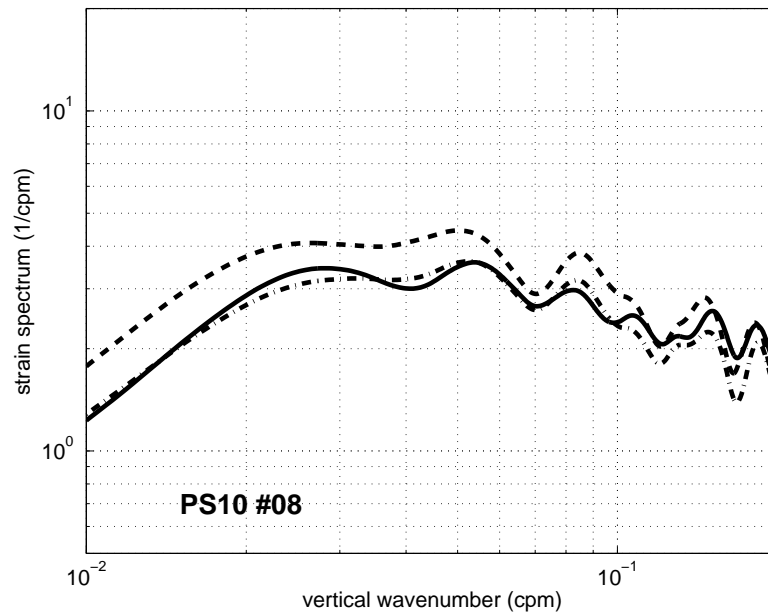
Figure 39: PhilSea10 cast dRR1006_008.
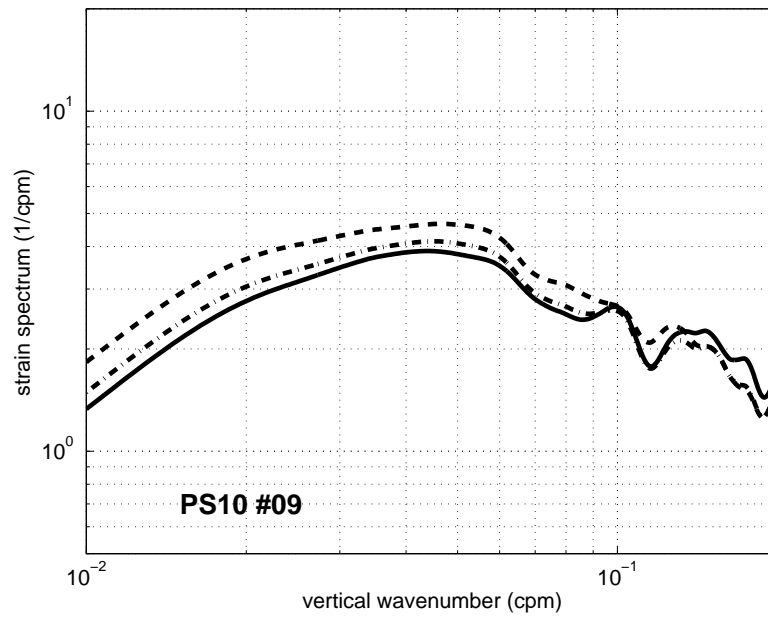
Figure 40: PhilSea10 cast dRR1006_009.
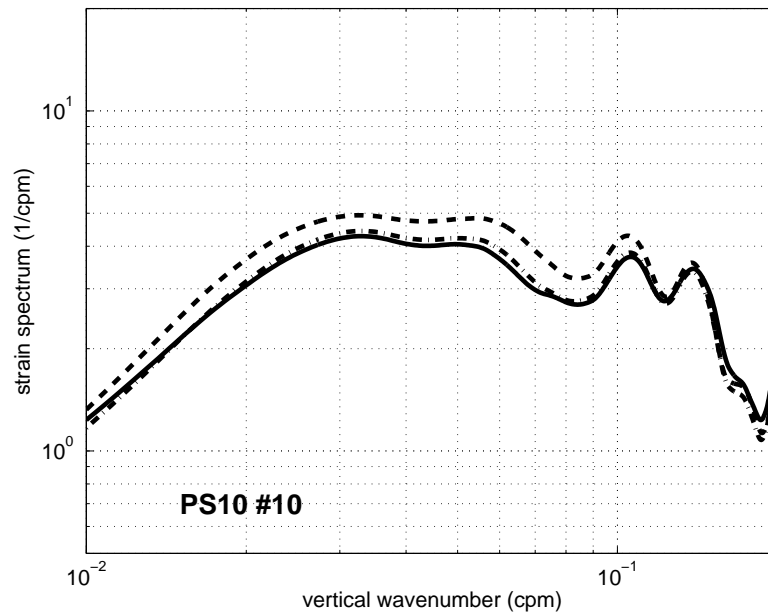
Figure 41: PhilSea10 cast dRR1006_010.
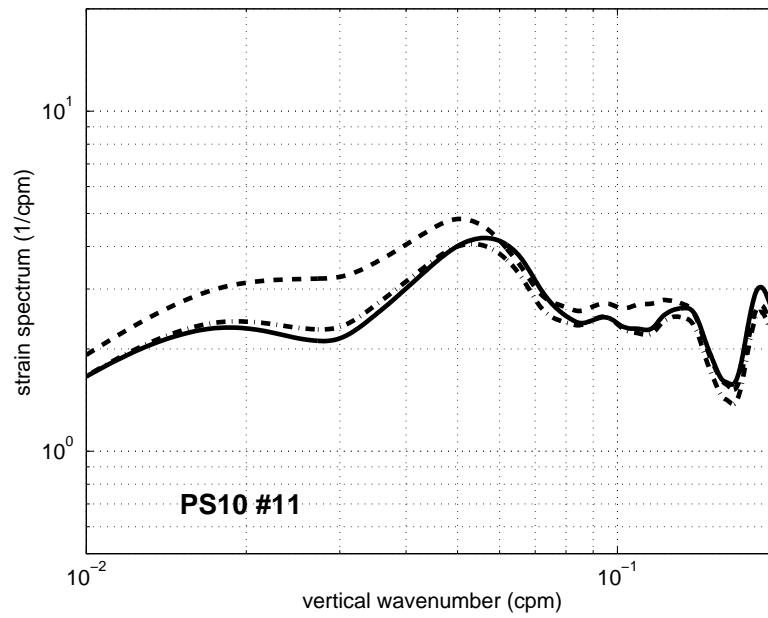
Figure 42: PhilSea10 cast dRR1006_011.
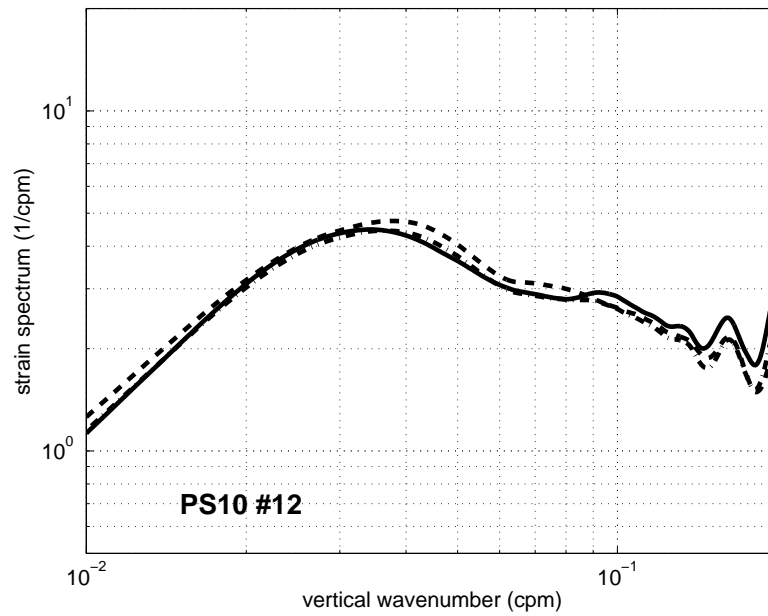
Figure 43: PhilSea10 cast dRR1006_012.
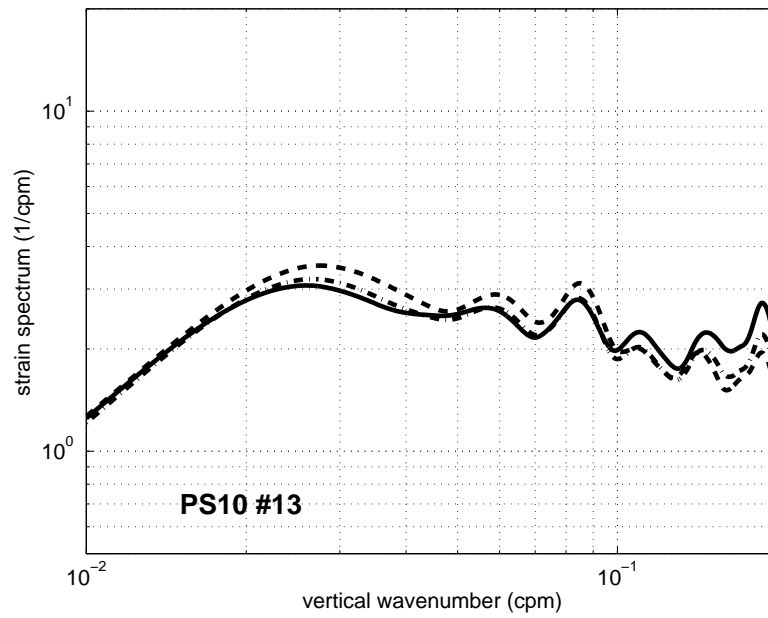
Figure 44: PhilSea10 cast dRR1006_013.
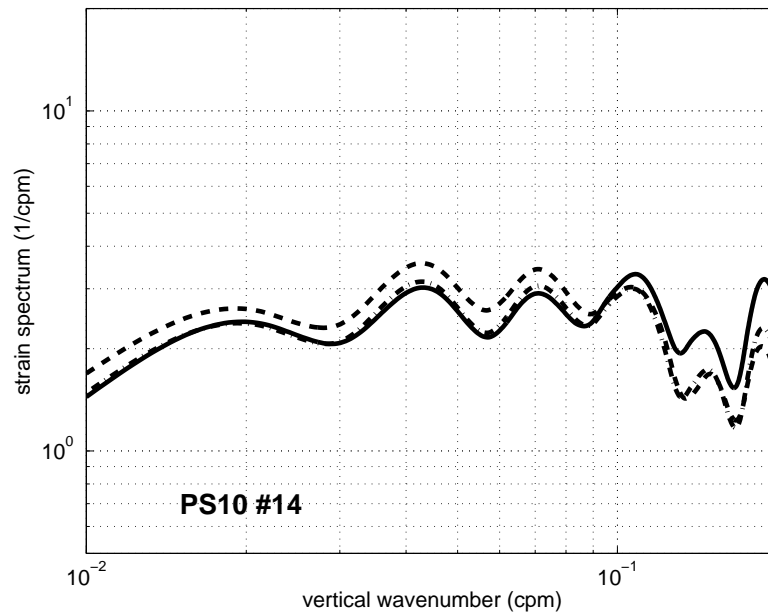
Figure 45: PhilSea10 cast dRR1006_014.
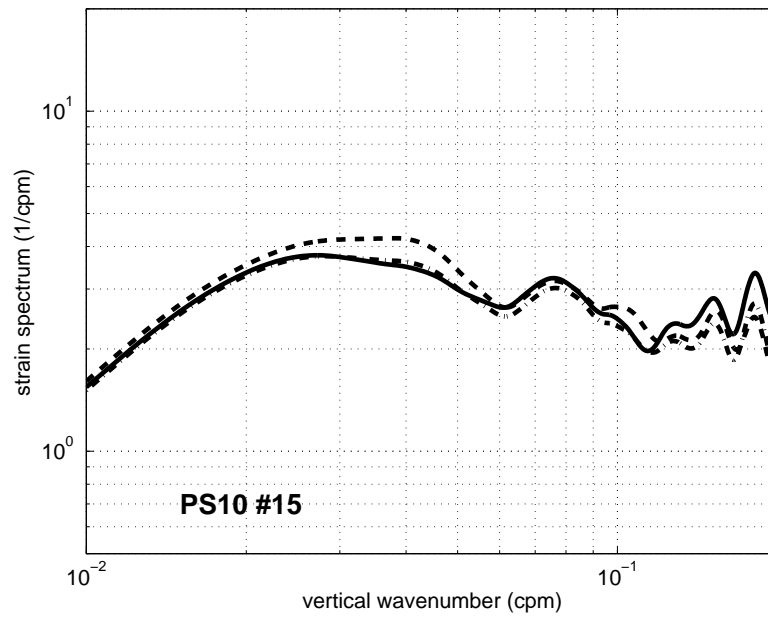
Figure 46: PhilSea10 cast dRR1006_015.
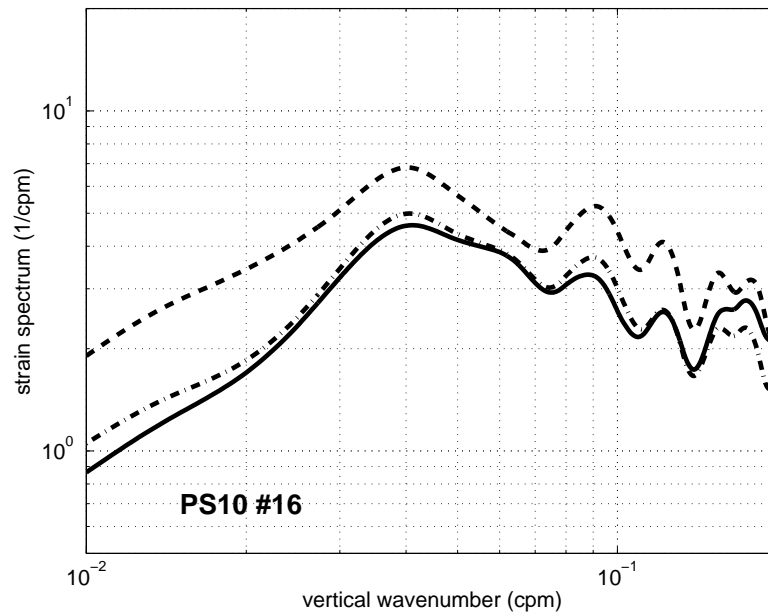
Figure 47: PhilSea10 cast dRR1006_016.
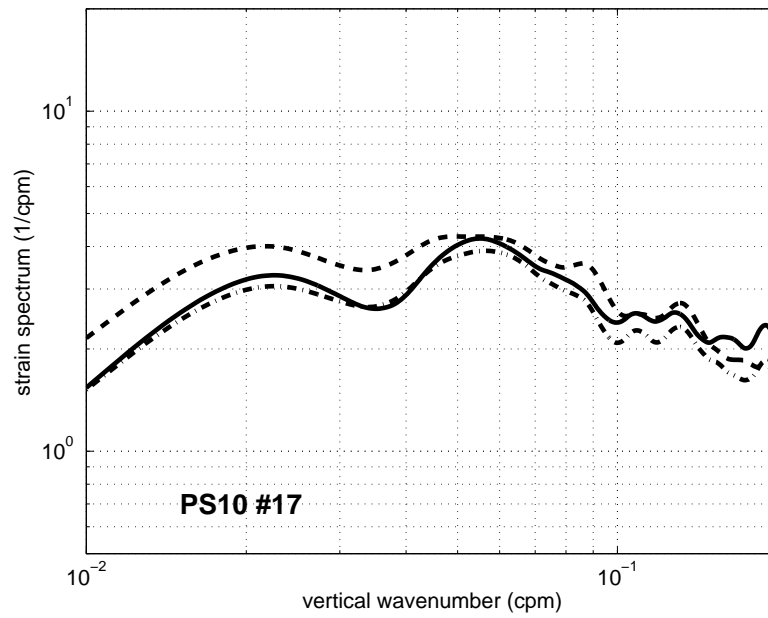
Figure 48: PhilSea10 cast dRR1006_017.
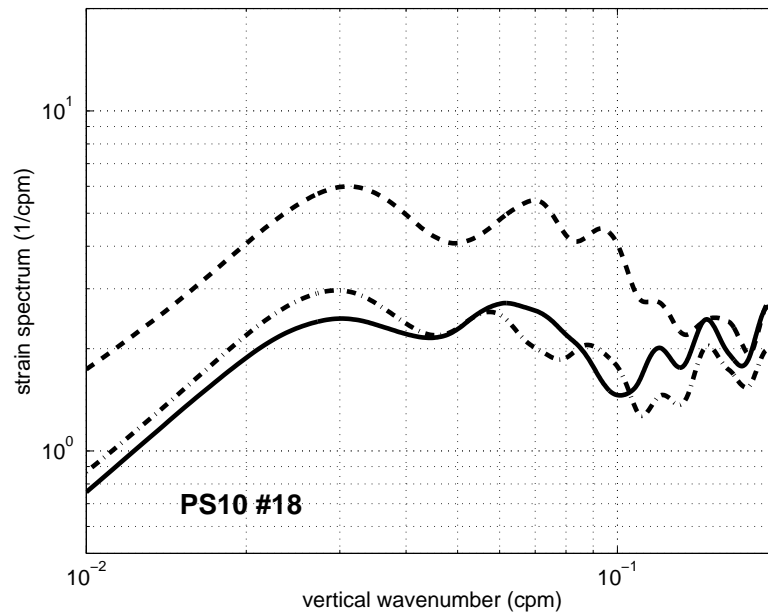
Figure 49: PhilSea10 cast dRR1006_018.
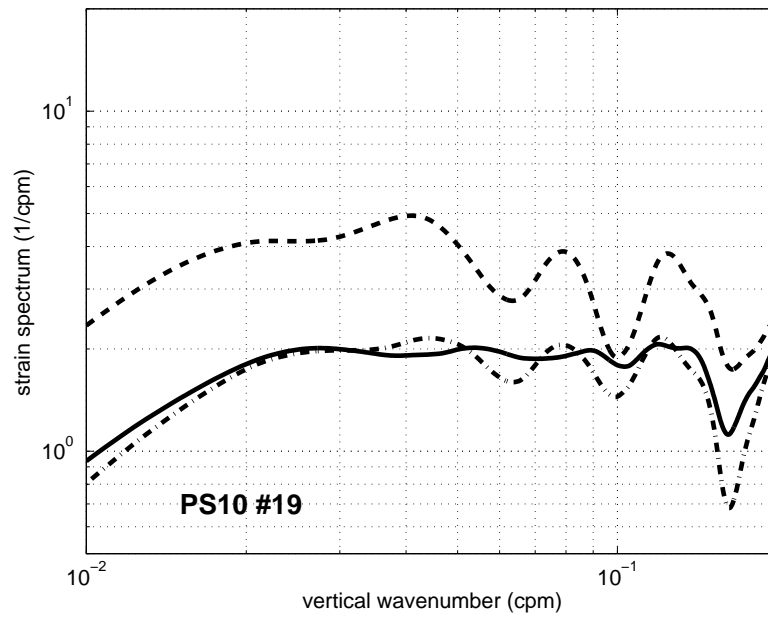
Figure 50: PhilSea10 cast dRR1006_019.
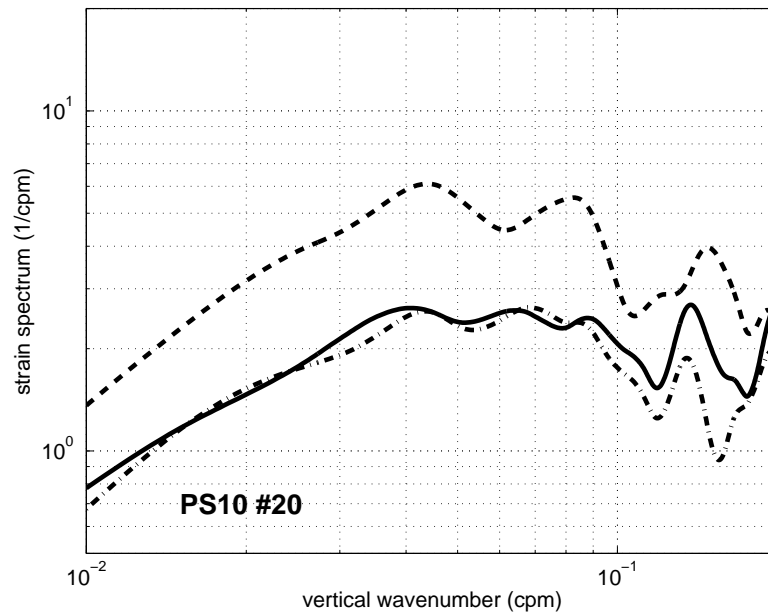
Figure 51: PhilSea10 cast dRR1006_020.
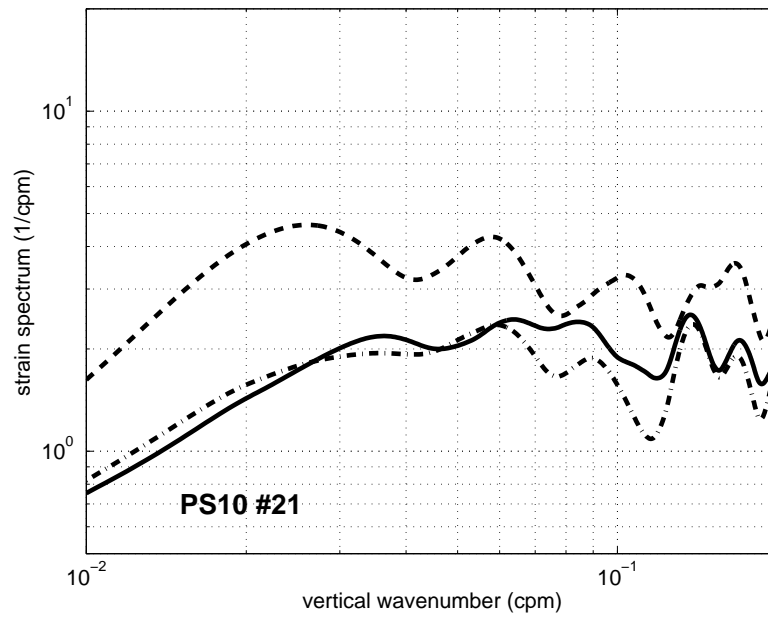
Figure 52: PhilSea10 cast dRR1006_021.
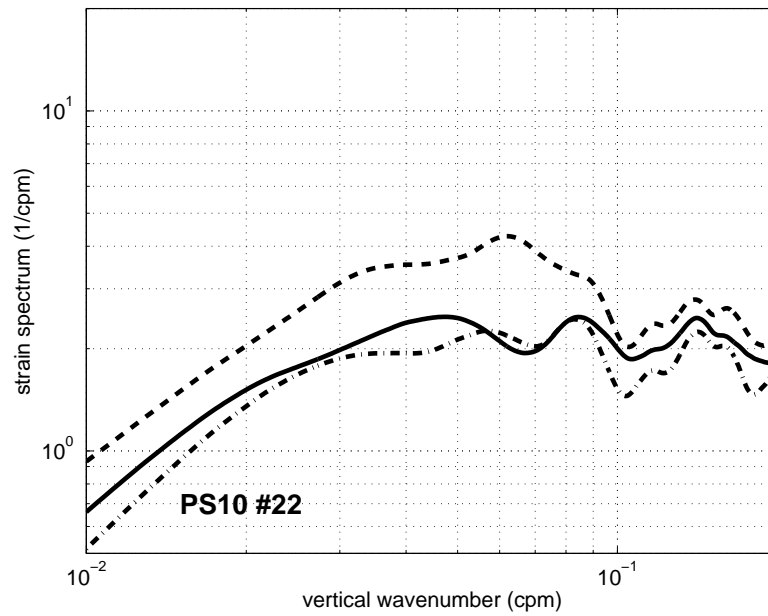
Figure 53: PhilSea10 cast dRR1006_022.
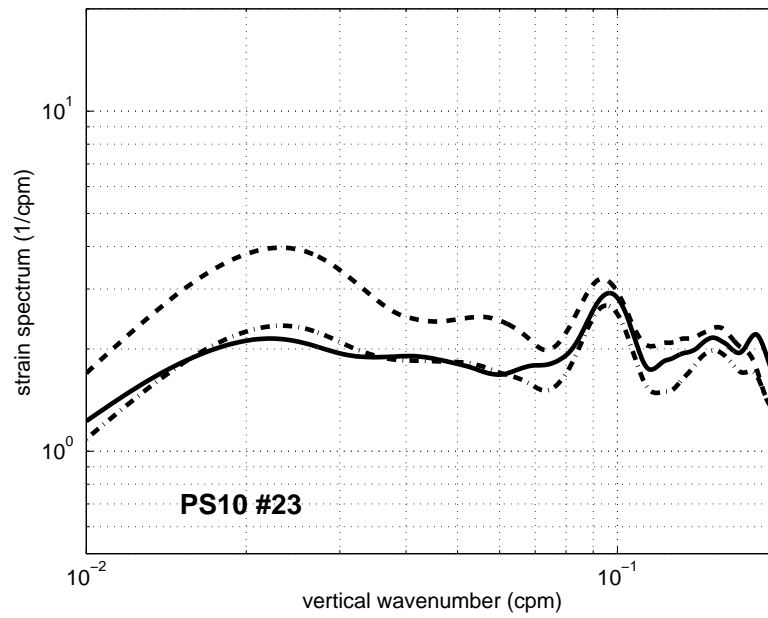
Figure 54: PhilSea10 cast dRR1006_023.
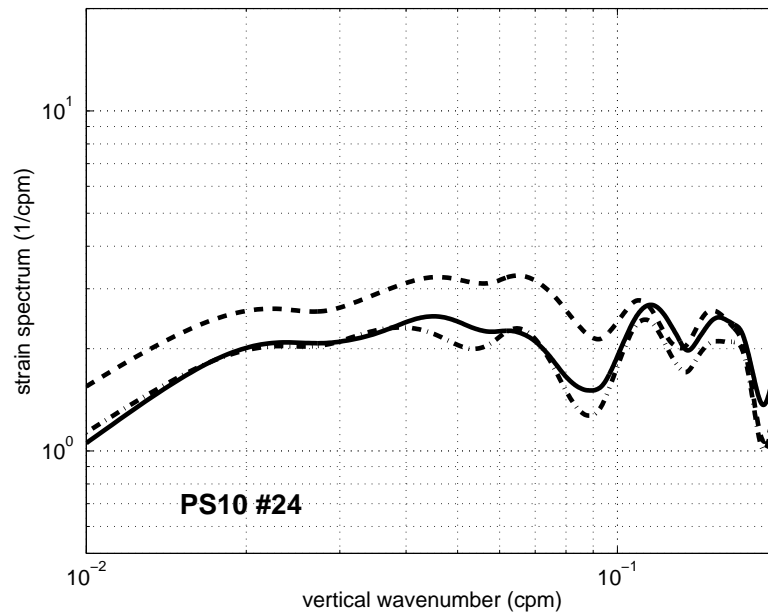
Figure 55: PhilSea10 cast dRR1006_024.
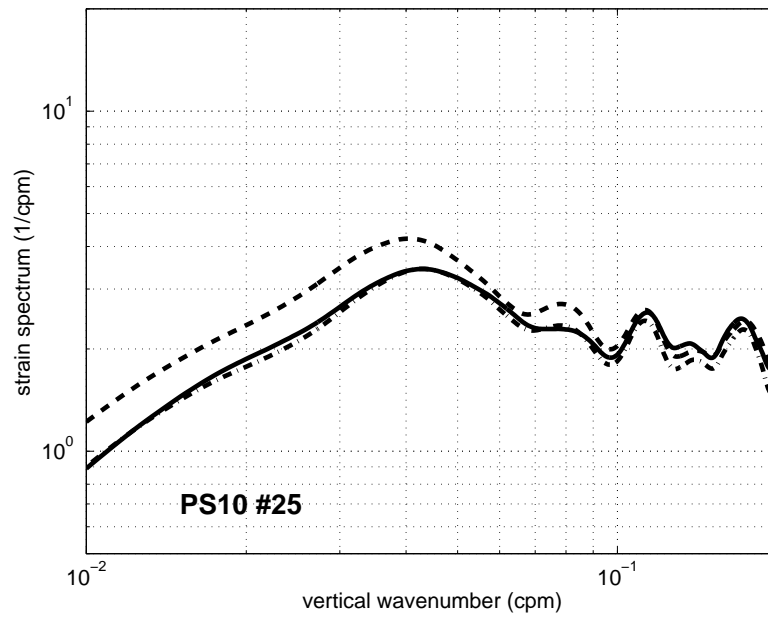
Figure 56: PhilSea10 cast dRR1006_025.
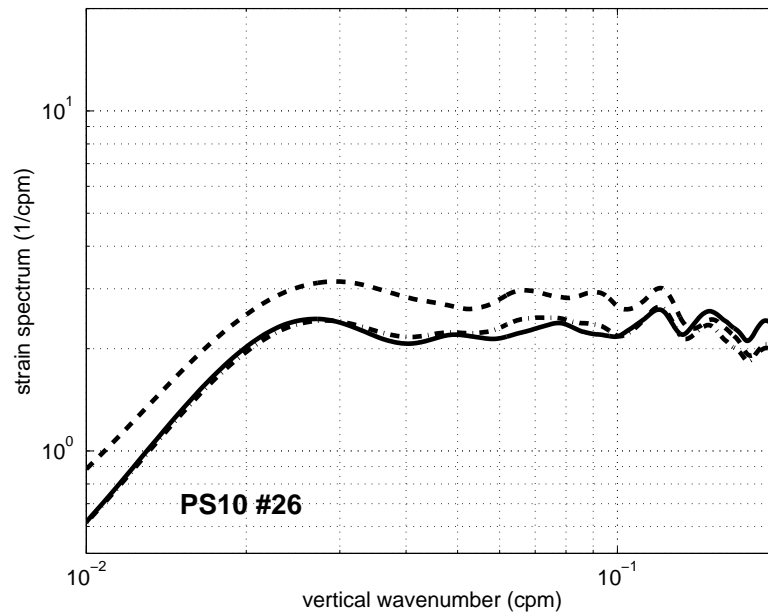
Figure 57: PhilSea10 cast dRR1006_026.
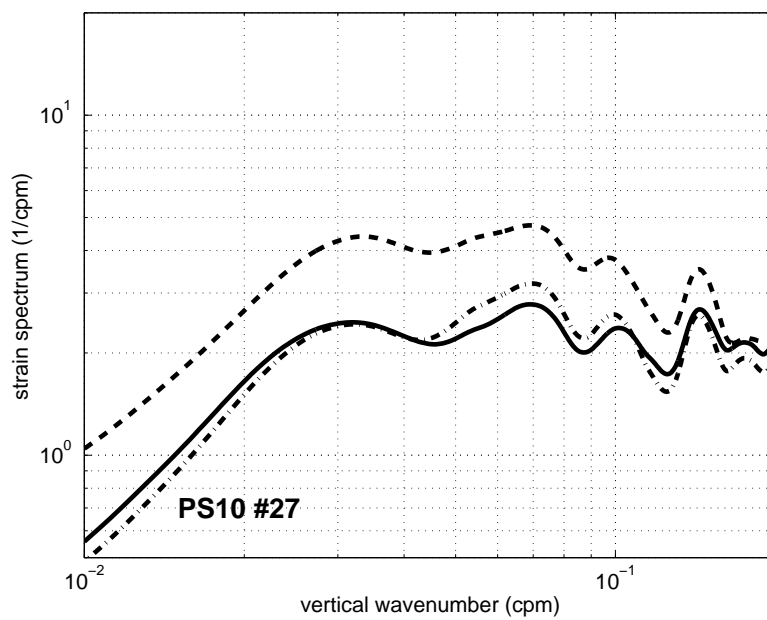
Figure 58: PhilSea10 cast dRR1006_027.
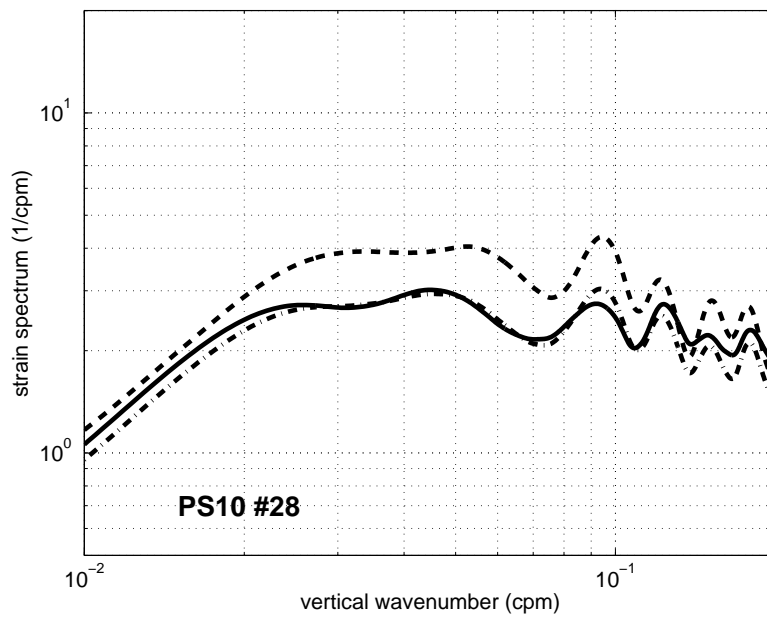
Figure 59: PhilSea10 cast dRR1006_028.
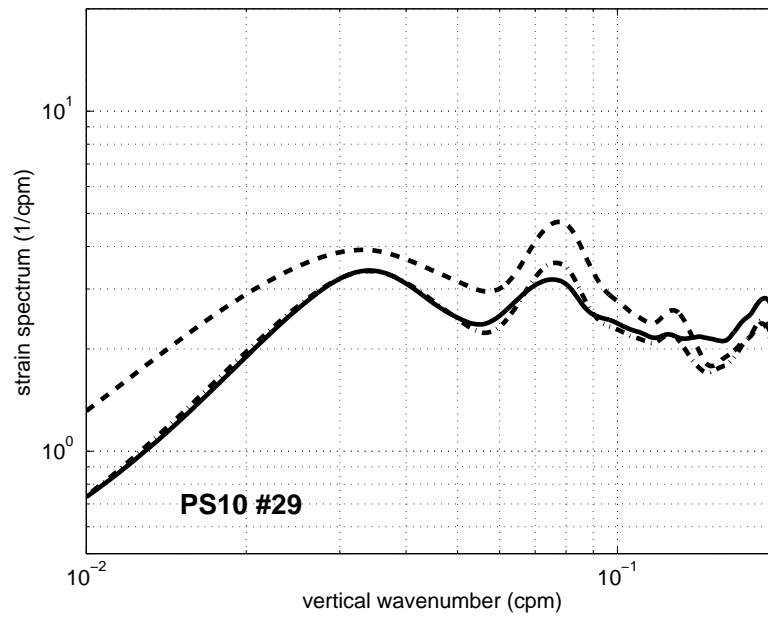
Figure 60: PhilSea10 cast dRR1006_029.
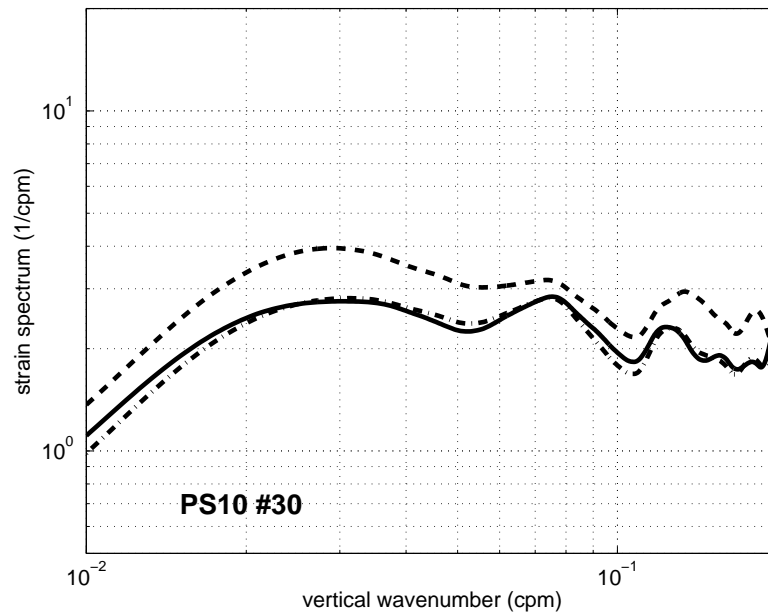
Figure 61: PhilSea10 cast dRR1006_030.
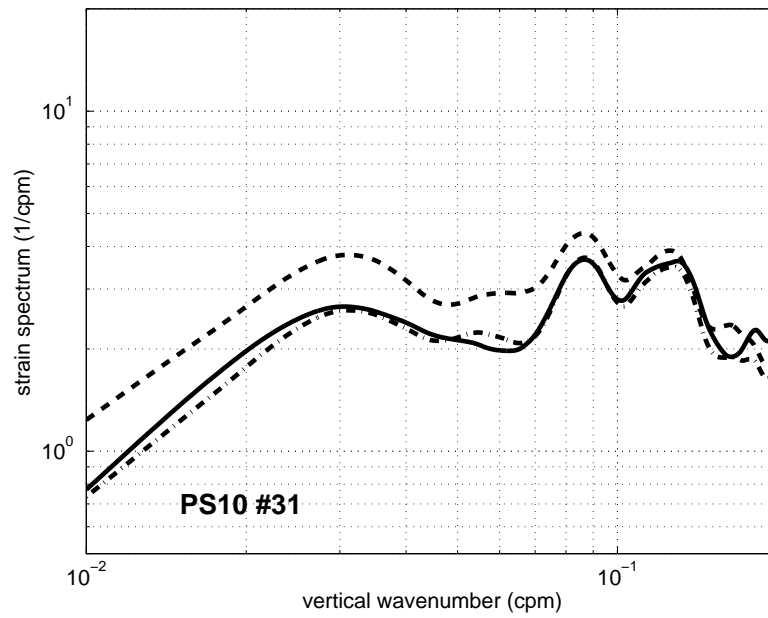
Figure 62: PhilSea10 cast dRR1006_031.
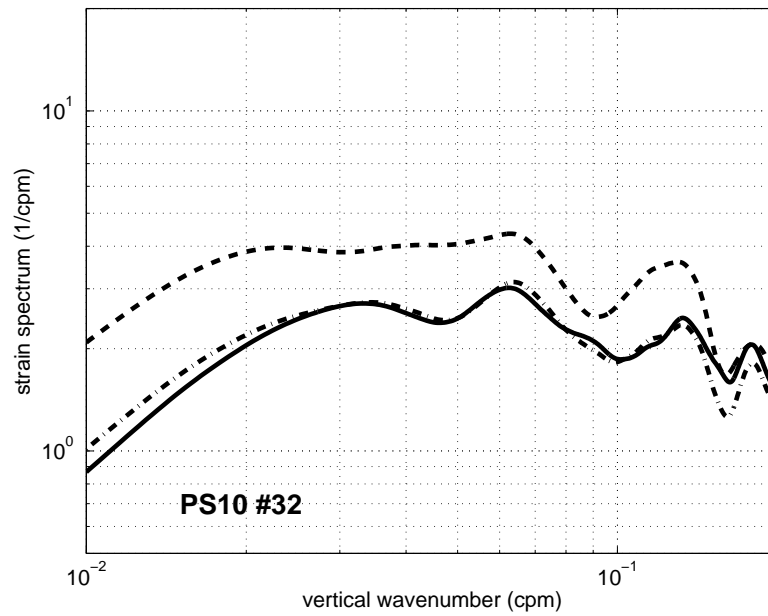
Figure 63: PhilSea10 cast dRR1006_032.
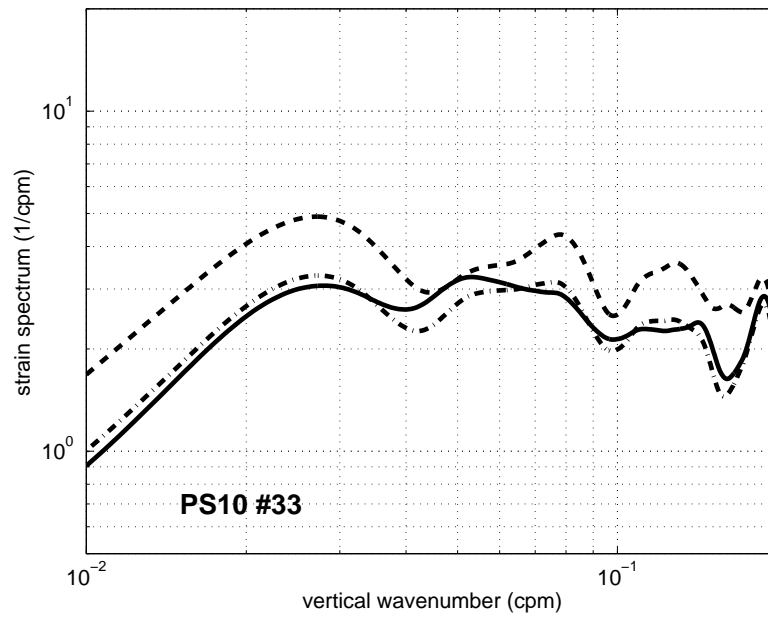
Figure 64: PhilSea10 cast dRR1006_033.
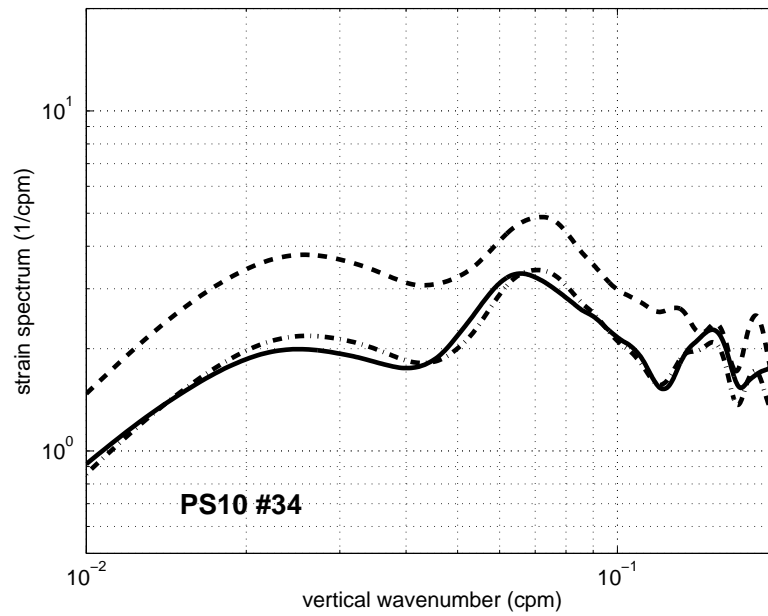
Figure 65: PhilSea10 cast dRR1006_034.
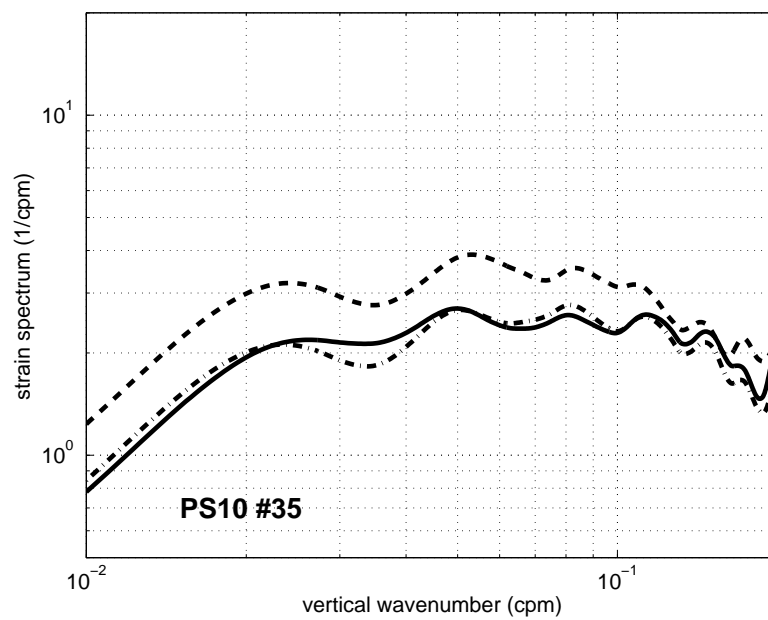
Figure 66: PhilSea10 cast dRR1006_035.
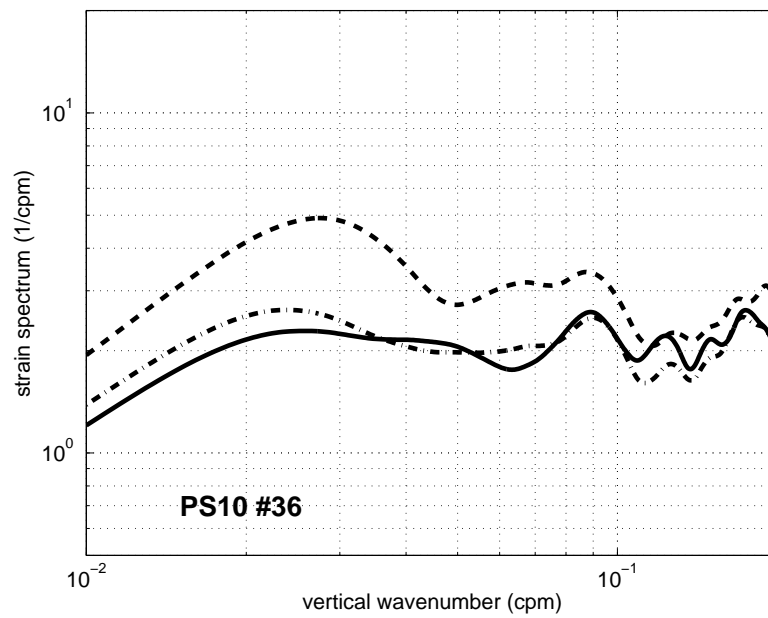
Figure 67: PhilSea10 cast dRR1006_036.
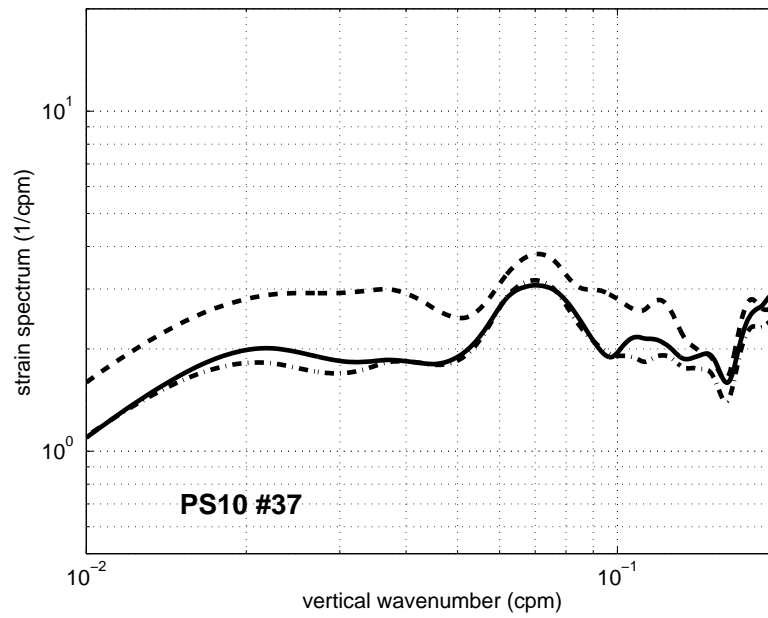
Figure 68: PhilSea10 cast dRR1006_037.
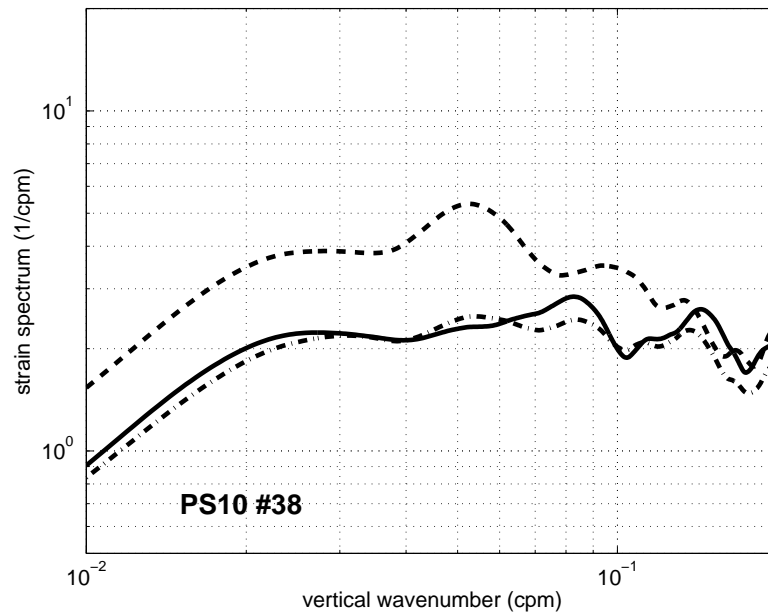
Figure 69: PhilSea10 cast dRR1006_038.
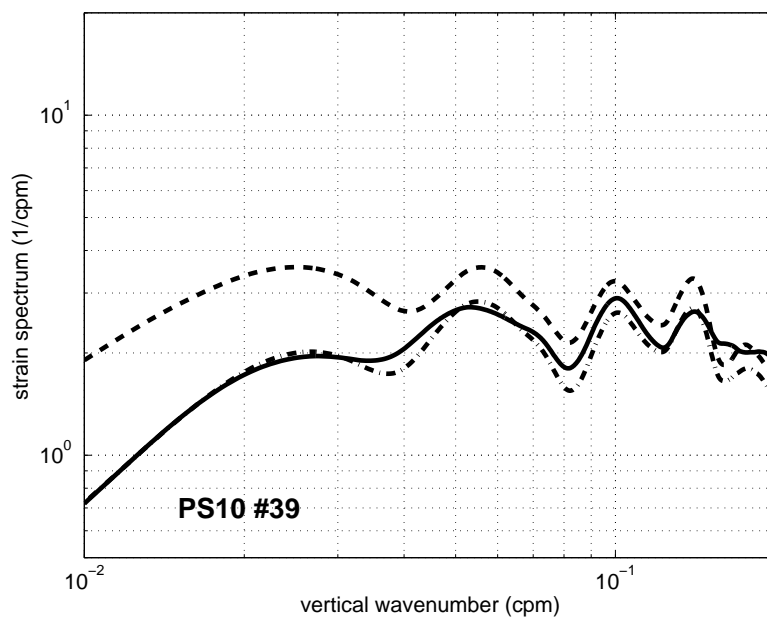
Figure 70: PhilSea10 cast dRR1006_039.
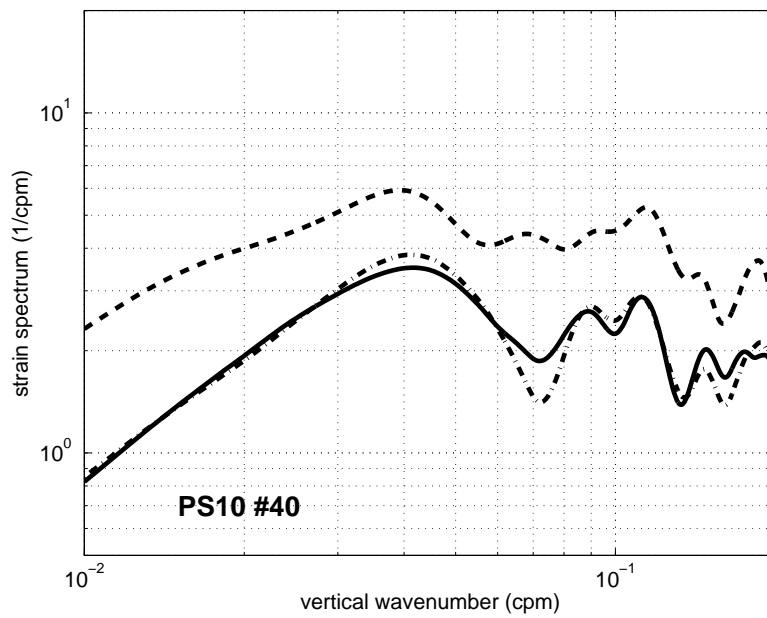
Figure 71: PhilSea10 cast dRR1006_040.
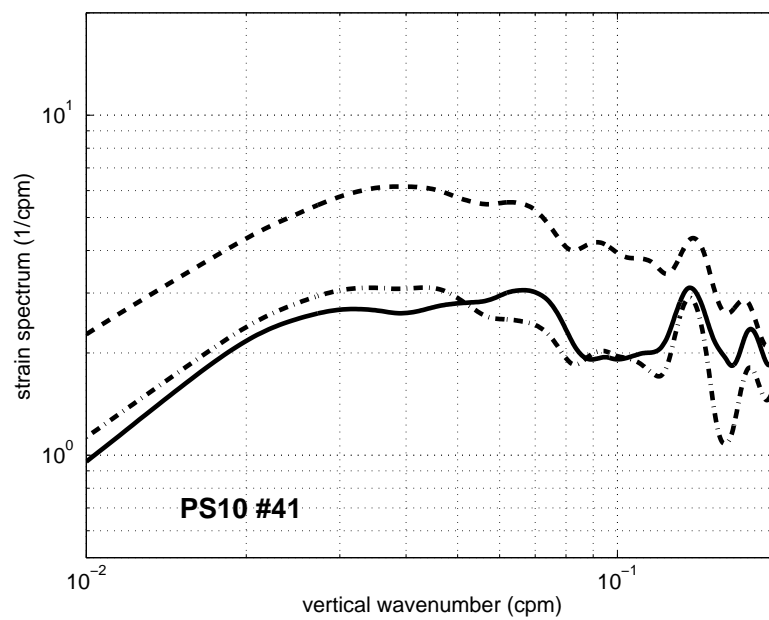
Figure 72: PhilSea10 cast dRR1006_041.
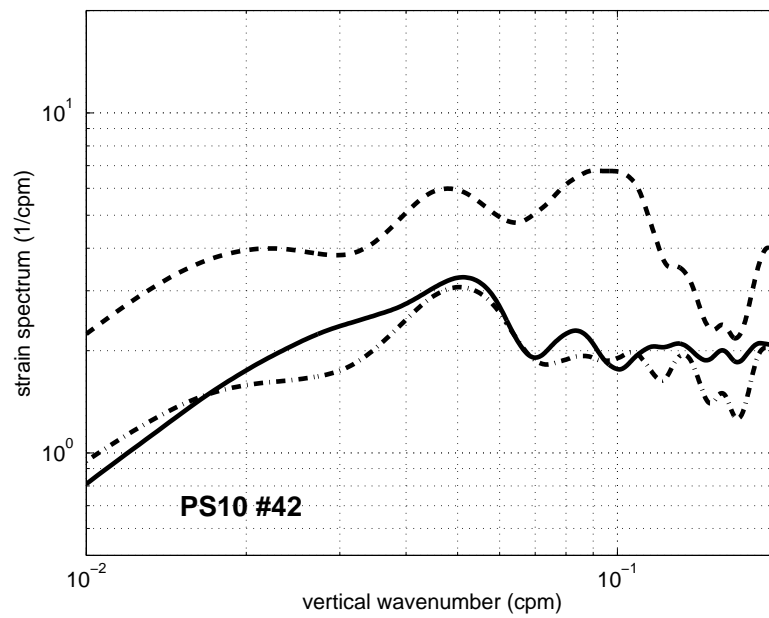
Figure 73: PhilSea10 cast dRR1006_042.
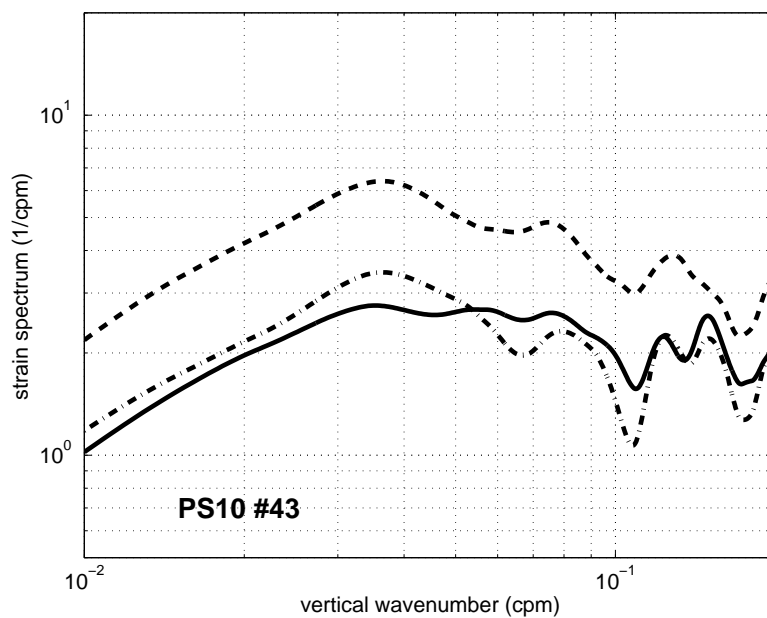
Figure 74: PhilSea10 cast dRR1006_043.
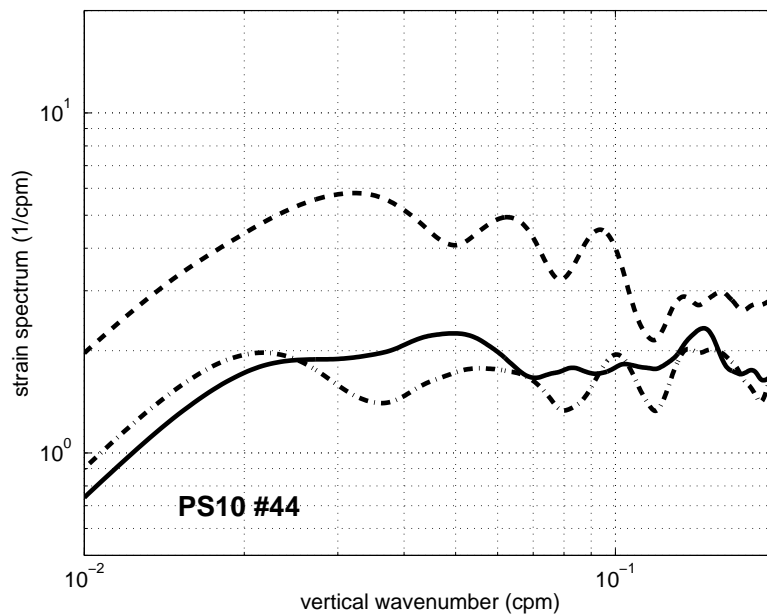
Figure 75: PhilSea10 cast dRR1006_044.
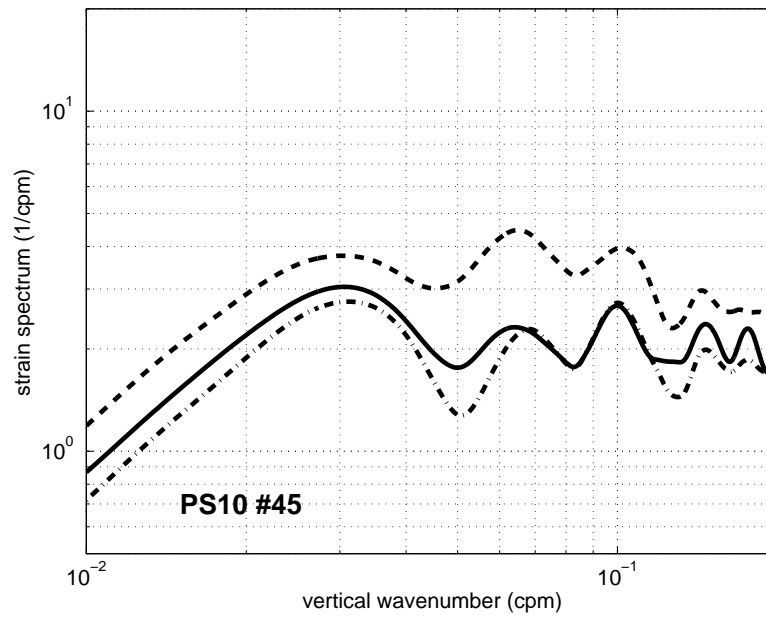
Figure 76: PhilSea10 cast dRR1006_045.
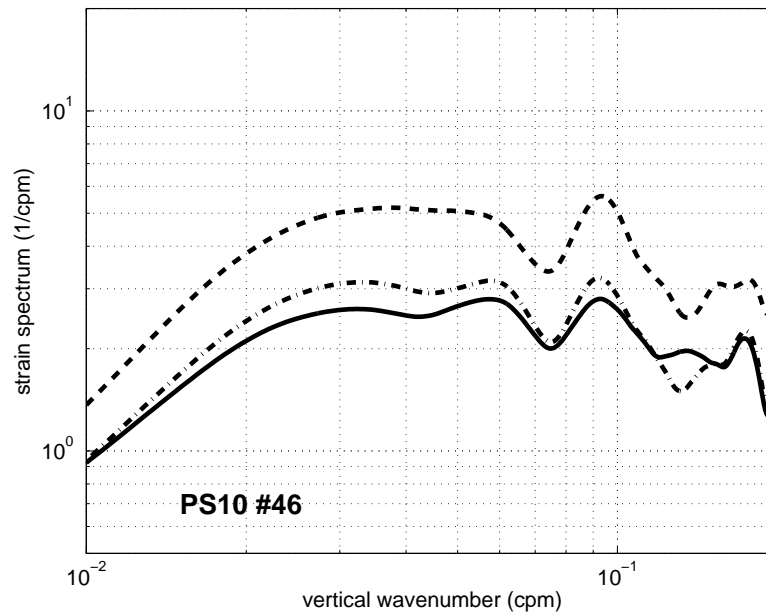
Figure 77: PhilSea10 cast dRR1006_046.
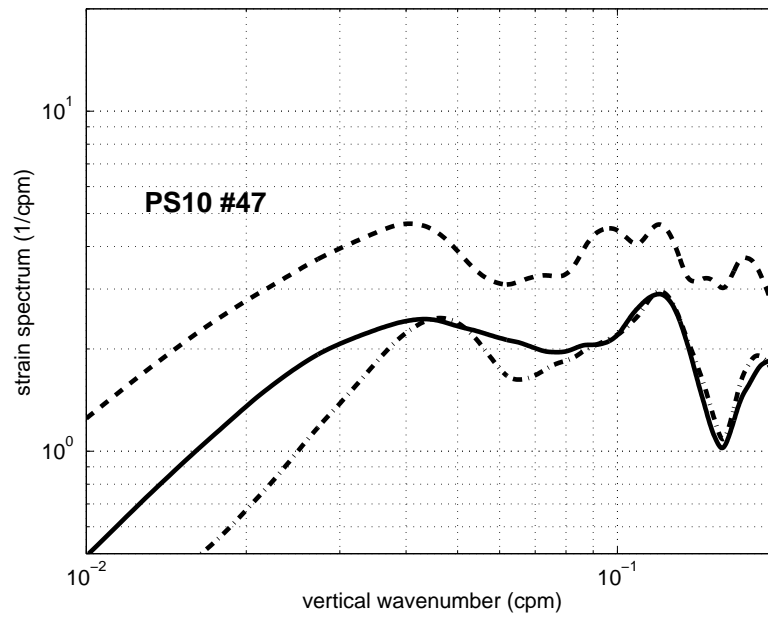
Figure 78: PhilSea10 cast dRR1006_047.
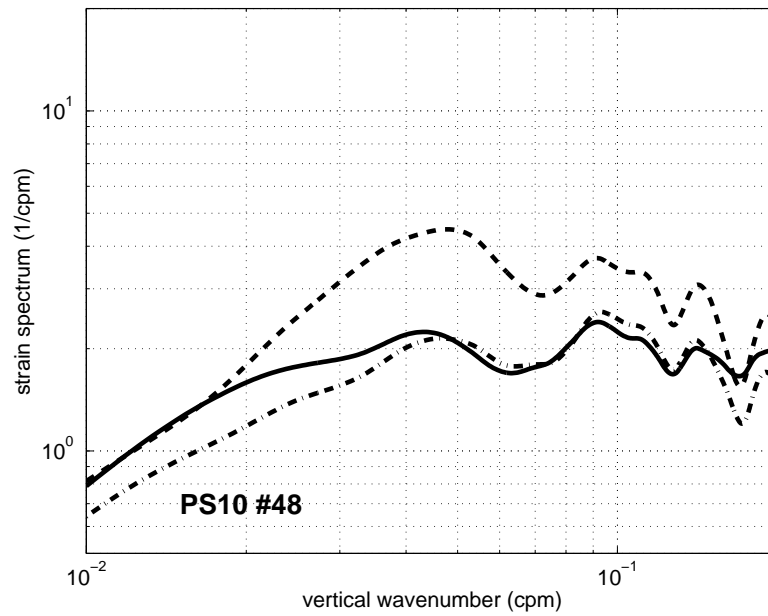
Figure 79: PhilSea10 cast dRR1006_048.
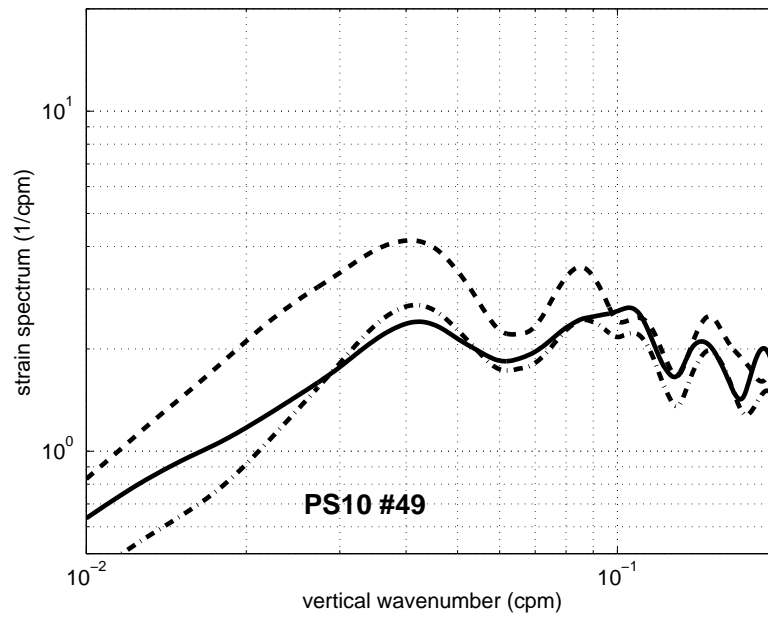
Figure 80: PhilSea10 cast dRR1006_049.
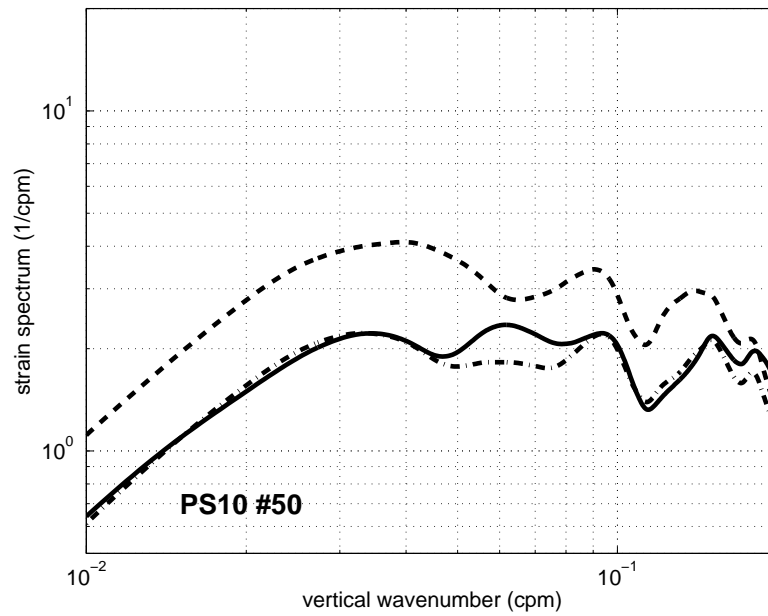
Figure 81: PhilSea10 cast dRR1006_050.
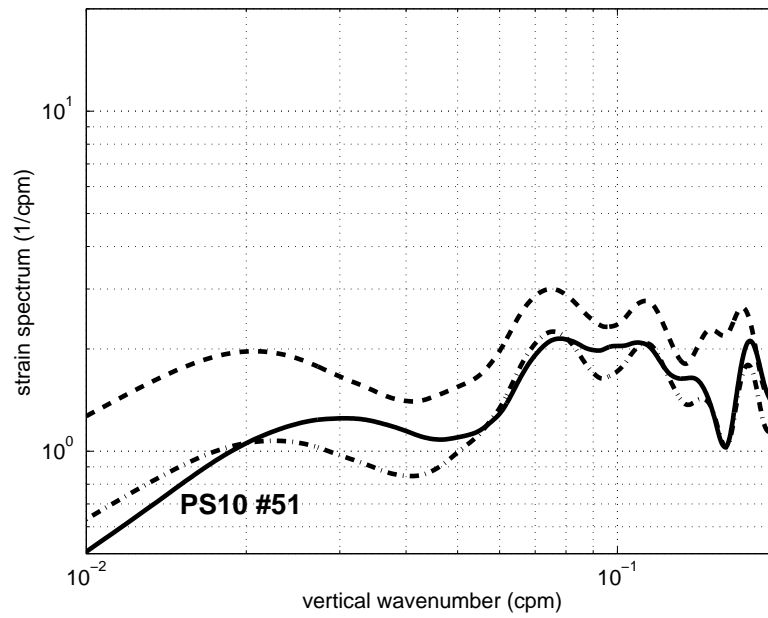
Figure 82: PhilSea10 cast dRR1006_051.
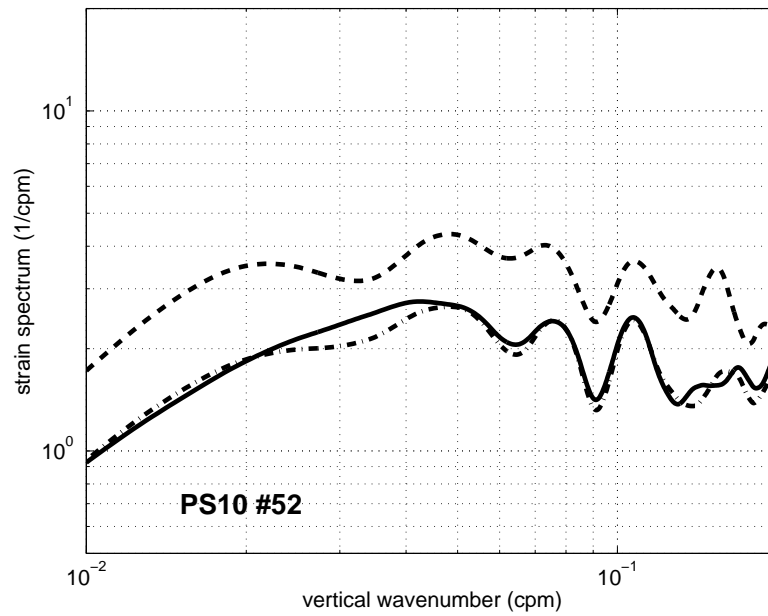
Figure 83: PhilSea10 cast dRR1006_052.
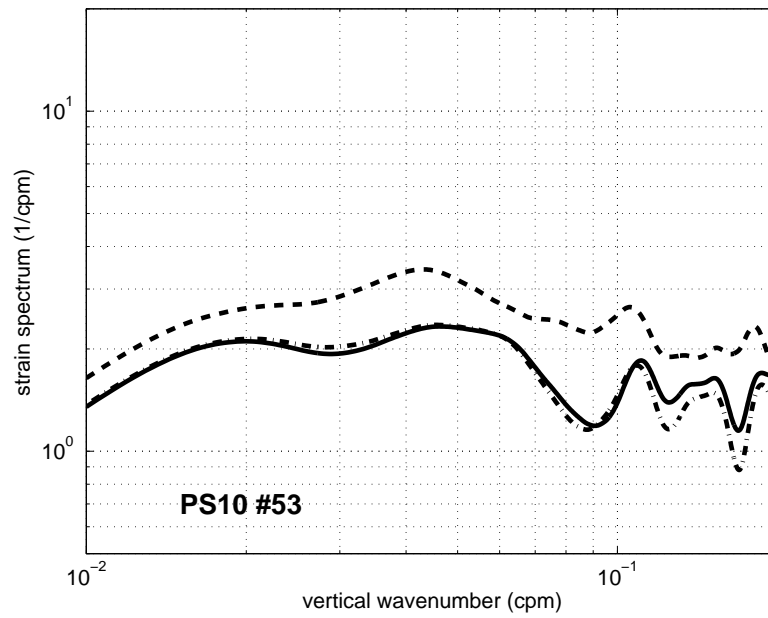
Figure 84: PhilSea10 cast dRR1006_053.
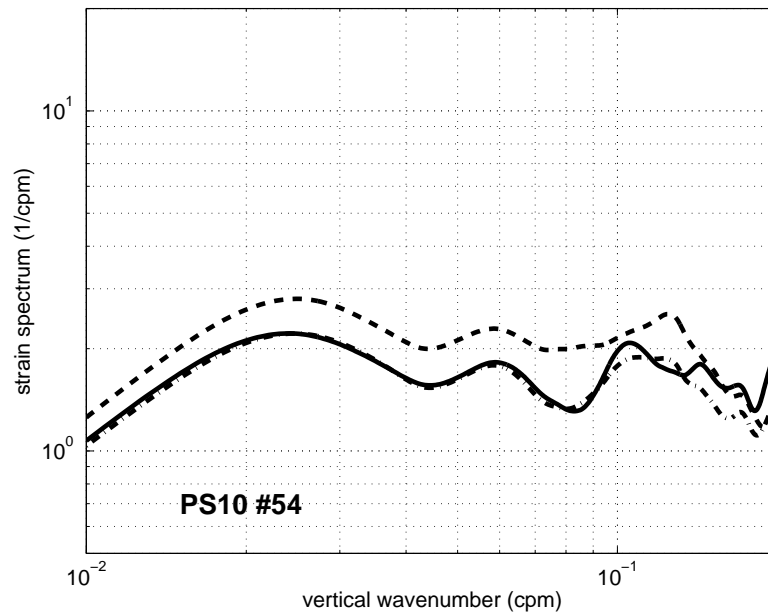
Figure 85: PhilSea10 cast dRR1006_054.

REPORT DOCUMENTATION PAGE

Form Approved
OPM No. 0704-0188

1. AGENCY USE ONLY *(Leave blank)*	2. REPORT DATE March 2014	3. REPORT TYPE AND DATES COVERED Technical Memorandum

4. TITLE AND SUBTITLE

A Method to Determine Small-Scale Internal Wave and Spice Fields from a Single CTD Profile with Application to Three Long-Range Ocean Acoustics Experiments

5. FUNDING NUMBERS
N00014-03-1-0181
N00014-07-1-0743
N00014-08-1-0843
N00014-06-1-0194
N00014-13-1-0009

6. AUTHOR(S)

F.S. Henyey, J.A. Mercer, R.K. Andrew, and A.W. White

7. PERFORMING ORGANIZATION NAME(S) AND ADDRESS(ES)

Applied Physics Laboratory
University of Washington
1013 NE 40th Street
Seattle, WA 98105-6698

8. PERFORMING ORGANIZATION REPORT NUMBER

APL-UW TM 1-14

9. SPONSORING / MONITORING AGENCY NAME(S) AND ADDRESS(ES)

Dr. Robert Headrick, Code 322OA
Office of Naval Research
One Liberty Center
875 North Randolph Street, Suite 4125
Arlington, VA 22203

10. SPONSORING / MONITORING AGENCY REPORT NUMBER

11. SUPPLEMENTARY NOTES

12a. DISTRIBUTION / AVAILABILITY STATEMENT

Approved for public release; distribution is unlimited.

12b. DISTRIBUTION CODE

13. ABSTRACT *(Maximum 200 words)*

The smaller vertical scales of sound speed variability of several recent deep water Pacific Ocean acoustic experiments are extracted from individual conductivity, temperature, depth (CTD) casts taken along the acoustic paths of these experiments, close to the times of the experiments. The sound speed variability is split into internal wave variability and spice variability, as these two parts obey very different dynamics -- the internal waves move through the water and the spice field moves with the water. Larger scales are mostly responsible for acoustic travel time fluctuations, but smaller scales are mostly responsible for other important phenomena such as intensity and arrival angle fluctuations. A method is presented to determine when the two components are separable. The internal wave properties are consistent with a spectral model such as a generalized Garrett--Munk model, whereas the spice is very intermittent, and the measurements are not extensive enough to confidently make a spice model for acoustic propagation purposes. Both the internal wave results and the spice results are summarized as vertical wavenumber spectra over a selected vertical depth interval, but with the spice, it must be understood that a spectral model would be very different from the data, and that the three-dimensional horizontal--vertical spectrum would be pure conjecture. The spectral level of the (small-scale) spice, averaged over all the profiles, is comparable to that of the internal waves, suggesting that it is not significantly less important to acoustic propagation than are the (small-scale) internal waves.

14. SUBJECT TERMS

internal waves, ocean spice, potential density, potential sound speed, Garrett–Munk spectrum, North Pacific Ocean, Philippine Sea

15. NUMBER OF PAGES
59

16. PRICE CODE

17. SECURITY CLASSIFICATION OF REPORT	18. SECURITY CLASSIFICATION OF THIS PAGE	19. SECURITY CLASSIFICATION OF ABSTRACT	20. LIMITATION OF ABSTRACT
Unclassified	Unclassified	Unclassified	SAR

"Comparisons of Methods for Numerical Internal Wave Simulation in Long Range Acoustical Propagation", by Rex K. Andrew, Pacific Rim Underwater Acoustics Conference 2013, Hangzhou, China

Comparisons of Methods for Numerical Internal Wave Simulation in Long Range Acoustical Propagation

Rex K. Andrew

Applied Physics Laboratory, University of Washington. Seattle, WA 98105 USA

randrew@apl.washington.edu

Abstract

The only technique currently known for estimating all the statistical properties of an acoustical field propagating through a randomizing ocean is Monte Carlo simulation. The standard model in deep ocean propagation asserts that the randomization is due to sound speed perturbations caused by the vertical fluid displacements of random internal waves. The Henyey-Reynolds algorithm [1] provides a computationally efficient method for generating these displacements for an ocean with range-independent stratification. This method, which is free from the Wentzel-Kramers-Brillouin approximation, uses vertical internal wave modes parameterized only by horizontal wavenumber magnitude --- i.e., along only one dimension, as opposed to throughout the two dimensional horizontal wavenumber plane. Results are shown for the standard horizontally-isotropic Garrett-Munk spectral model, and compared to the Colosi-Brown algorithm [2]. Accurate models of the oceanographic mechanisms causing sound speed randomization will be needed in the estimation of the parameters of ocean mixing processes via inversion of acoustical fluctuation statistics.

I. BACKGROUND

The most ubiquitous physical mechanism for randomizing the sound-speed in the deep ocean is the internal gravity wave field. Models of the internal wave fields evolved throughout the 1970's: the "standard model", known as GM79, was given in 1981 by Munk [3]. Internal waves were first invoked in Monte Carlo acoustical calculations by Dozier and Tappert in 1978[4]. In 1998, Colosi and Brown [8] (henceforth CB98) updated the Dozier and Tappert sound-speed simulation approach (e.g., to include GM79). Concurrently, Henyey and Reynolds developed an algorithm that has only recently been published [1] (henceforth HR13). Evans also produced a similar algorithm in an unpublished note [5].

The HR13 algorithm is described in section II, and its performance is compared in section III to two results from WKB theory. The HR13 algorithm is compared to the CB98 algorithms in section IV, including a summary of the benefits of the HR13 algorithm.

II. ALGORITHM

The sound-speed is represented as $c(\mathbf{r}) = c_0(\mathbf{r}) + \delta c(\mathbf{r}, t)$ where $c_0(\mathbf{r})$ is a "background" field and $\delta c(\mathbf{r}, t)$ is the randomizing component. Here, $\mathbf{r}$ represents field position. In the conventional approach, $\delta c = \zeta (dc/dz)_P$ where $(dc/dz)_P$ is the vertical gradient of "potential sound speed" [6]. ζ is a stochastic field representing the random vertical displacement of a fluid parcel. HR13 conceptualize the internal-wave field as horizontally-isotropic and model it with horizontal plane-wave modes and vertical standing-wave modes.

The vertical modes obey the linearized equation of motion

$$\frac{d^2W}{dz^2} + k^2 \frac{n(z)^2 - \omega^2}{\omega^2 - f^2} W = 0 \tag{1}$$

where f is the local inertial frequency and n(z) is the Brunt-Väisälä frequency profile due to ocean stratification. For a given value of horizontal wavenumber k, Eq. 1 defines a Sturm-Liouville problem. The solution consists of eigenfunctions $W_j(z)$ and associated eigenvalues $\lambda_j(k)$. The eigenvalues can be inverted to provide "eigenfrequencies" $\omega_j(k)$. HR13 solve Eq. 1 for eigenfunctions and eigenfrequencies by discretizing directly into a matrix eigenvalue problem and using a generalized tridiagonal solver. The group speeds $d\omega/dk$ will also be required. These can be calculated directly from the equation $\omega(\lambda)$ yielding

$$\frac{d\omega}{dk} = \frac{\omega^2 - f^2}{\omega k}\left[1 - (\omega^2 - f^2)\int W^2\, dz\right] \tag{2}$$

using the Hellman-Feynman theorem (see [1]) for $d\omega/dk$ in terms of the eigenfunctions $W_j(z)$. No approximations are required.

The literature provides two methods for synthesizing homogeneous pseudo-random wavefields. Both utilize an approach specifying the spectral properties of the wavefield. In two spatial dimensions, the first approach, due to Rice [7], incorporates random plane-wave coefficients:

$$\zeta(x,t) = \sqrt{\Delta_{kx}\Delta_{ky}}\sum_{kx}\sum_{ky}\sqrt{S_{zz}}\left[q_R\cos(k_x x - \omega t) + q_I\sin(k_x x - \omega t)\right] \tag{3}$$

where $S_{zz} = S(k_x, k_y)$ is the spectrum of the process, and $q_R \sim N(0,1)$ and $q_I \sim N(0,1)$ independently. The second approach, due to Shinozuka [8], uses randomized phase:

$$\zeta(x,t) = \sqrt{2}\sqrt{\Delta_{kx}\Delta_{ky}}\sum_{kx}\sum_{ky}\sqrt{S_{zz}}\cos(k_x x - \omega t + \phi) \tag{4}$$

where $\phi = \phi(k_x, k_y)$ is a uniform variate in $[0, 2\pi]$. The statistical distributions of these two methods differ: Katafygiotis et al [9] discuss this issue in detail. For our purposes, note that each method accumulates contributions over the (k_x, k_y) wavenumber plane. The two methods described above raster over a uniform grid in (k_x, k_y) space. HR13 chose an alternate scheme, rastering over k_x and $k = \sqrt{k_x^2 + k_y^2}$. This choice incurs variable-sized differential elements, as shown in Fig. 1.
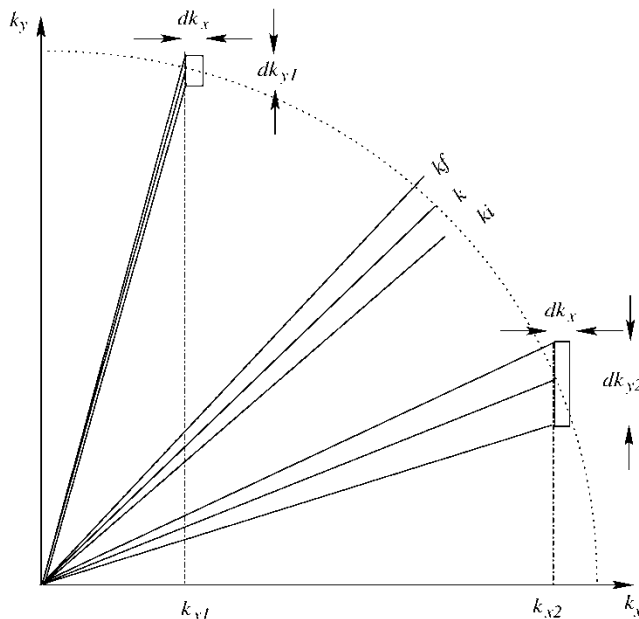
Figure 1. Example of the differential areal tiling based on the (k_x, k) sampling scheme. The example presents only the sampling in the first quadrant of the (k_x, k_y) plane.
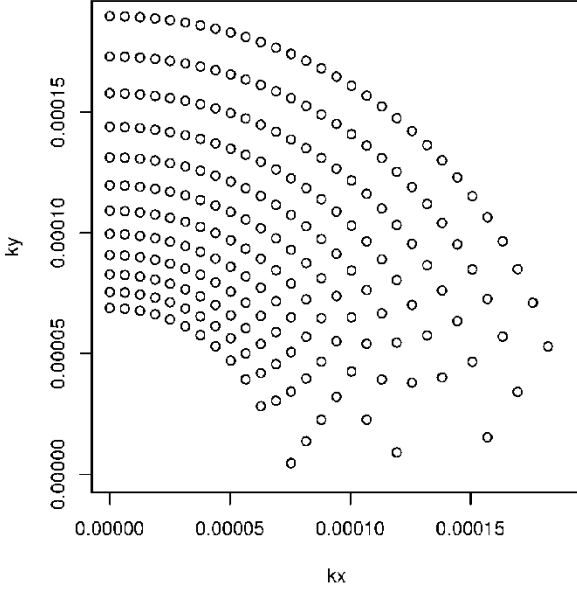
Figure 2. Example of the logarithmic sampling in the first quadrant of the (k_x, k_y) plane. Only the first 12 values of horizontal wavenumber k are shown, corresponding to m=0,1,2,….,11. The logarithmic spacing in k is already evident. The gridding is uniform in k_x. For a single mode number j, only 12 modes need be computed to support this constellation of sample points in (k_x, k_y) space.

Given independent sampling in k, HR13 utilize logarithmic spacing, $k_m = k_0 r^m$, m=0,1,2,3,….. Here, k_0 is the minimum wavenumber (maximum spatial scale), and r defines the number of samples per decade. HR13 use $r = 10^{1/25}$, i.e., 25 samples per decade. A representative diagram of this sampling scheme is shown in Fig. 2.

The displacement spectrum is derived from GM79 by removing the WKB approximations (see [1]) and is

$$S_{zz}(\omega, j) = \frac{2E_0 B(N_0 B)^2}{\pi M(j^2 + j_*^2)} \frac{f}{\omega^3} \sqrt{\omega^2 - f^2} \tag{5}$$

which is defined in terms of mode number j and frequency ω. This needs to be converted to a function of mode number j and horizontal wavenumber k, as follows:

$$S_{zz}(\omega, j) d\omega = S_{zz}(\omega, j) d\omega \frac{d\theta}{2\pi} = \frac{S_{zz}(\omega_j(k), j)}{2\pi k} \frac{d\omega}{dk} dk_x dk_y \tag{6}$$

where $M = \sum_{j=1}^{JMAX} (j^2 + j_*^2)^{-1}$. Then, using

$$\langle |G_+|^2 \rangle + \langle |G_-|^2 \rangle = \frac{S_{zz}(\omega_j(k), j)}{2\pi k} \frac{d\omega}{dk} dk_x dk_y \tag{7}$$

where G_+ and G_- are complex Gaussian variates, the final expression for the slice $\zeta(x, z; t)$ is

$$\zeta(x, z; t) = F^{-1} \left\{ \sum_{j=1}^{JMAX} \sum_{ky} \left[G_- e^{-i\omega t} + G_+ e^{+i\omega t} \right] W_j(z) \right\} \tag{8}$$

using an inverse Fourier transform in k_x.

III. VALIDATION

A key feature of any new algorithm must be an auxiliary definition of valid output. Two tests are provided. Input parameters are given in Table I. First, the product $n(z)\langle \zeta \rangle$ under WKB theory [3] should be depth invariant and, using the canonical test values, should equal 0.28. Five realizations of $n(z)\langle \zeta \rangle$ are shown in Fig. 3: throughout the main thermocline, this algorithm attains the WKB value

within sampling error.

Description	Value	Parameter
Maximum x range	1 000 000 m	
# grid points in x direction	8192	
# grid points in z direction	512	
Total modes	80	JMAX
# horizontal wavenumber grid points	100	
Maximum horizontal mode scale	100 000 m	$= 2\pi/k_0$
Minimum horizontal mode scale	1 000 m	
Brunt-Väisälä profile	Munk canonical profile	
Brunt-Väisälä profile scale	3.0 cph	N_0
Brunt-Väisälä profile depth scale	1300 m	B
GM strength	0.0832 m	$E_0 B$
Horizontal wavenumber gridding base	$10^{1/25}$	
Grid steps per decade	25	
latitude	20º	
Modal bandwidth	3.0	j_*

Table 1. Parameters used in the algorithm, with values used in the simulations.
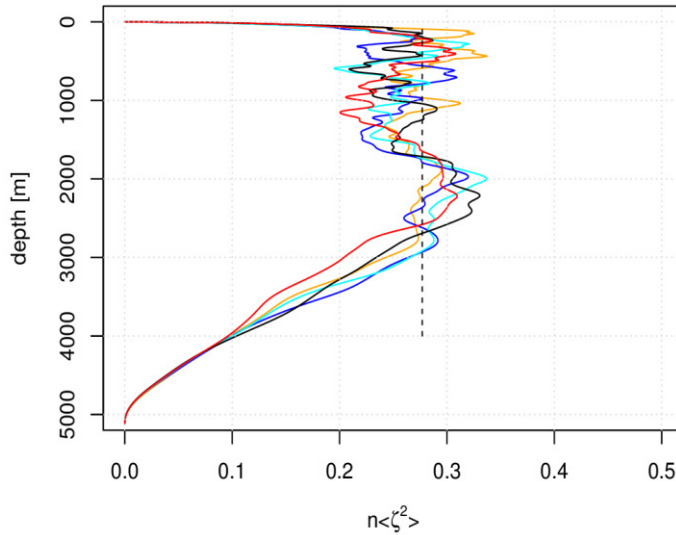
Figure 3. Simulation realizations of the product $n(z)\langle\zeta\rangle$ using the HR13 model and random number generator seeds of -1, -2, -3, -4, -5. The vertical line is the WKB result at 0.28.

The second test compares the horizontal wavenumber spectrum of vertical displacements. This is essentially a "towed" spectrum. The WKB result generally follows a k_x^{-2} dependence at high wavenumber. A sample spectrum estimated from a single horizontal series is shown in Fig. 4, and shows excellent agreement with the full theoretical expression. An approximate WKB solution derived by Levine et al [10] is shown as well. The WKB result has excellent agreement at high wavenumber, but considerable deviation at low wavenumber.
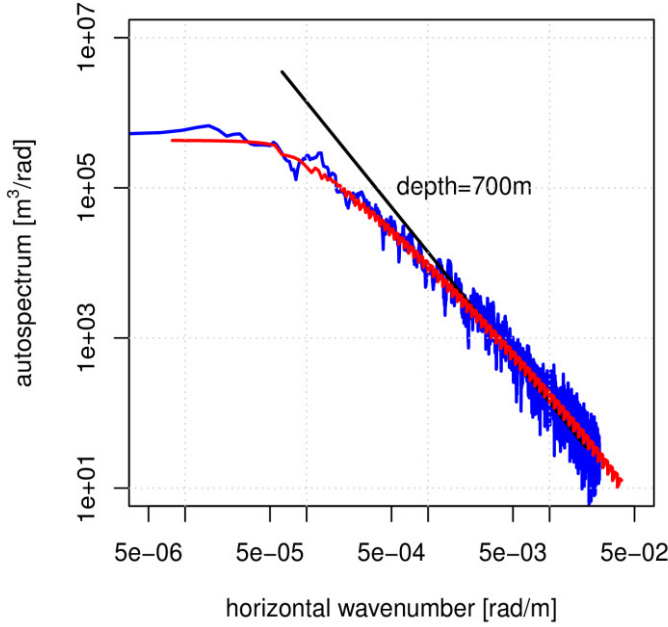
Figure 4. Comparisons of horizontal "towed" spectra, at depth 700 m. A single realization is used. The sample variance was 92.74. The autospectrum was estimated using the multitaper method with 8 tapers and a time-bandwidth product of 4. This is shown in blue. The estimated integral of the sample autospectrum was 93.77. The full theoretical expression (using 101 modes) is shown in red. The discretization of the sampling in wavenumber space is evident as a ``stair-step'' appearance in the theoretical curve at higher wavenumbers. The predicted variance based on an estimated integral of this curve is 83.97. The Levine approximate expression is shown with a solid black line.

III. COMPARISONS

CB98 provide a Rice method algorithm (Eq. 9) and a Shinozuka method algorithm (Eq. 19). They also provide simplifications for single (x,z) slice simulations. They use WKB stretching to substitute sinusoids for exact mode shapes. Sample spacing in the (k_x, k_y) wavenumber plane is uniform. The number of first quadrant wavenumber integrand sample points is roughly 1000*100 for HR13 and 1000*1000 for CB98. The number of modes for HR13 is 100*JMAX but only JMAX for CB98 because their modes are independent of horizontal wavenumber. CB98 specify the domain of integration as $k_{min} \leq |k_x|, |k_y| \leq k_{max}$. To compare with HR13, we use instead the domain $k_{min} \leq \sqrt{k_x^2 + k_y^2} \leq k_{max}$. The results for the product $n(z)\langle\zeta\rangle$ are shown in Fig. 5. Model parameters were taken from Table 1. HR13 simulations use 4 decades of wavenumbers; CB98 simulations use 2. Qualitatively, the results are similar; quantitatively, the HR13 method includes a correction for the region $\sqrt{k_x^2 + k_y^2} \leq k_{min}$ and thereby achieves the WKB result throughout the main thermocline and the deep sound channel.
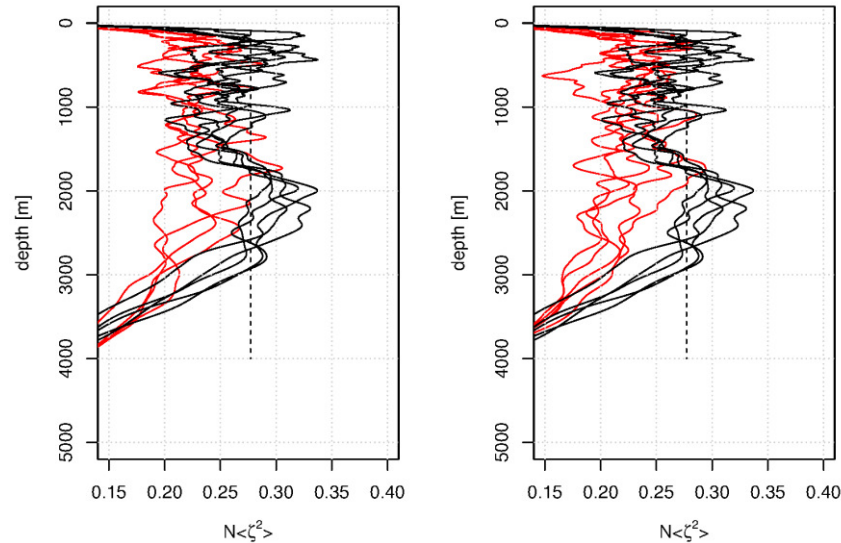
Fig 5. Comparison of $n(z)\langle\zeta\rangle$ for HR13 (black, Rice) versus CB98 equations 9 (left, Rice) and 19 (right, Shinozuka). CB98 results shown in red.

REFERENCES

[1] FS Henyey and SA Reynolds (2013). A Numerical Simulator of Ocean Internal Waves for Long-Range Acoustics, technical memorandum APL-UW TM 1-13, Applied Physics Laboratory, Seattle Washington.

[2] JA Colosi and MG Brown (1998). "Efficient numerical simulation of stochastic internal-wave-induced sound-speed perturbation fields", J. Acoust. Soc. Am, **103**(4), pp 2232-2235.

[3] WH Munk (1981). "A survey of internal waves and small scales processes", in Evolution of Physical Oceanography, BA Warren and C Wunsch, eds., Cambridge, MA, MIT Press.

[4] LB Dozier and FD Tappert (1978) "Statistics of normal mode amplitudes in a random ocean, I. Theory", J. Acoust. Soc. Am., **63**, pp 353-365.

[5] RB Evans, (2000). "Calculation of internal-wave eigen-frequencies and modes; displacement and sound speed realizations", unpublished technical note. http://oalib.hlsresearch.com/Other/wave/wave.doc, last accessed 8/2013.

[6] WH Munk and F Zachariasen (1976)."Sound propagation through a fluctuating stratified ocean: Theory and observation", J. Acoust. Soc. Am., **59**(4), pp 818-838.

[7] SO Rice (1954). "Mathematical analysis of random noise", Selected papers on noise and stochastic processes, N. Wax ed, pp 133-294.

[8] M Shinozuka (1987). "Stochastic fields and their digital simulation", Stochastic methods in structural dynamics, GI Schuëller and M Shinzuka, eds., Martinus Nijhoff, Dordrecht, the Netherlands.

 [9] LS Katafygiotis, A Zerva and AA Malyarenko (1999). "Simulation of homogeneous and partially isotropic random fields", J. Eng. Mech., October 1999, pp 1180-1189.

 [10] MD Levine, JD Irish, TE Ewart, SA Reynolds (1986). "Simultaneous spatial and temporal measurements of the internal wave field during MATE", J. Geophys. Res. **91**(C8), pp 9709-9719.

Technicalities

Is There a "Noise Hole" in the Northeast Pacific?

It is fairly well accepted that low-frequency (20-100 Hz) oceanic ambient noise has increased since the first measurements were made more than half a century ago. During this same period, commercial and industrial uses of the ocean, from merchant shipping to seismic exploration to luxury cruise ship travel, have also steadily expanded. Assuming human maritime activity produces a significant component of low frequency ambient noise, one might easily conclude that expanding utilization of the world's oceans will lead to increasing ambient noise.

While some measurements over the last two decades support this conjecture, measurements we have made in the Northeast Pacific suggest that ambient noise levels there are actually decreasing year to year. We routinely observe a seasonal dependence, with mid-depth noise levels dropping significantly in the late summer and early autumn. The year-to-year diminishing trend, however, is a new finding.

There could be several explanations for the seasonal dependence of ambient ocean noise in the Northeast Pacific. Under the assumption that a significant portion of noise is due to anthropogenic activity, seasonal dependence might reflect changes in shipping lanes, ship traffic, or seismic exploration scheduling. Geolocation data that could support this analysis exists, but mostly in proprietary databases: as yet, no study has aggregated these data into a comprehensive picture of the seasonality of open ocean sources.

The ocean climate may also play a significant role. There exists at low latitudes a "sound duct" in the deep ocean water column. Water supporting faster sound propagation sandwiches (above and below) a core of slower water. Sound entering downward into this "channel" refracts upward from the lower faster water; sound travelling upward in the channel refracts back downward from the upper faster water. The effect is like a hallway of mirrors – except the mirrors line floor and ceiling – and acts to duct sound efficiently over long distances.

The depth of the centre of this sound channel depends on the average temperature profile at each location of the ocean. At low latitudes, it reaches below 1,000 m. At high latitudes, it reaches the surface. Here, noise radiated southward by surface sources will be guided deeper and deeper as it propagates southward. It has been conjectured that most of the mid-depth noise we measure – say, in the Northeast Pacific – has originated at higher latitudes. Northern hemisphere trans-pacific shipping lanes follow high-latitude great circle routes, taking ships through regions that conduct their noise efficiently southward.

Ocean climate may modulate this effect in two ways. First, as the summer weather heats the ocean, the sound channel deepens. This moves the intersection of the sea surface and the channel centre further north, up against the Aleutian island chain. This decreases the region where ship noise can be captured and propagated southward. Second, wind provides energy to drive the ocean internal wave field. Internal waves are gravity waves – like sea surface waves – that exist throughout the ocean interior. They can scatter sound, most effectively in the vertical. One theory suggests that noise originating at the ocean surface at high to mid latitudes could be scattered into the sound channel by these internal waves and hence guided to long distances. And here it is curious to note that model predictions of internal wave energy show a significant hole in the Northeast Pacific, with a seasonal dependence that strengthens in the winter and decreases in the doldrums of late summer.

Merchant shipping might also not be the only high-latitude noise source. High-latitude storms can generate sea surface sound via breaking wind waves, and also via surf crashing on the Aleutians. These storms are more prevalent in the winter months and less so in the summer months – effectively contributing a seasonal non-anthropogenic component which may be enhanced by seasonal propagation conditions.

These factors may explain noise seasonality, which should be observable at mid-depths throughout the mid to low latitudes of the northern hemisphere. The mechanism driving the year-to-year trend is less obvious. It has been suggested that ocean warming could be gradually driving the intersection of the sound channel with the sea surface further and further north each year, thereby gradually reducing the areal capture of sea surface noise. Alternately, fleets may be phasing out older rattletrap freighters and tankers in favour of newer, sleeker designs that radiate less noise.

Plausible explanations can be made for noise level seasonality and increasing year-to-year noise levels. Indeed, we observe moderate to increasing year-to-year trends in the high north or Northwest Pacific. However, in the Northeast Pacific, between Hawaii and the North American west coast, we seem to have a "noise hole," where year-to-year levels are decreasing. The precise interplay of evolving anthropogenic contributions and ocean climate patterns and trends that cause this effect has yet to be understood.

Dr. Rex Andrew is Principal Engineer at the Applied Physics Laboratory University of Washington with over 25 years of experience either studying oceanic ambient noise or trying to mitigate it with signal processing techniques. His current research involves precise low-frequency long range sound propagation in the deep ocean using his laboratory's controlled acoustic transmitters, and characterizing the low-frequency oceanic soundscape due to sound radiated over long ranges from all the other sound sources in the ocean.

Sounds in the Ocean at 1–100 Hz

William S.D. Wilcock,[1] Kathleen M. Stafford,[2] Rex K. Andrew,[2] and Robert I. Odom[2]

[1]School of Oceanography, University of Washington, Seattle, Washington 98195; email: wilcock@u.washington.edu

[2]Applied Physics Laboratory, University of Washington, Seattle, Washington 98105; email: stafford@apl.washington.edu, rex@apl.washington.edu, odom@apl.washington.edu

Keywords

acoustics, ocean waves, earthquakes, marine mammals, shipping

Abstract

Very-low-frequency sounds between 1 and 100 Hz propagate large distances in the ocean sound channel. Weather conditions, earthquakes, marine mammals, and anthropogenic activities influence sound levels in this band. Weather-related sounds result from interactions between waves, bubbles entrained by breaking waves, and the deformation of sea ice. Earthquakes generate sound in geologically active regions, and earthquake T waves propagate throughout the oceans. Blue and fin whales generate long bouts of sounds near 20 Hz that can dominate regional ambient noise levels seasonally. Anthropogenic sound sources include ship propellers, energy extraction, and seismic air guns and have been growing steadily. The increasing availability of long-term records of ocean sound will provide new opportunities for a deeper understanding of natural and anthropogenic sound sources and potential interactions between them.

1. INTRODUCTION

**Noise (or sound)
level:** total acoustic
power expressed in
decibels relative to a
reference level, usually
normalized by the
bandwidth to yield a
spectral density
expressed in decibels;
in water, the reference
is 1 μPa²/Hz

Mode: a characteristic
harmonic acoustic
response; a weighted
sum of modes can be
used to model the full
acoustic field in the
ocean

Range: the magnitude
of a horizontal offset

Because sound waves propagate efficiently in water and electromagnetic waves do not, sound plays an important role in facilitating remote interactions in the ocean. Humans use ocean sound for communication and for imaging the ocean's interior, seafloor, and underlying crust. Sound is also a by-product of many anthropogenic activities in the ocean. Marine mammals use sound for communication and for echolocation.

The interval from 1 to 100 Hz coincides approximately with a frequency band that in ocean acoustics is termed the very-low-frequency (VLF) band. Because the wavelength of VLF sounds can be a significant fraction of the ocean depth, sound interactions with the seafloor are complicated, and their treatment requires an understanding of both acoustics and seismology. VLF sounds undergo little attenuation in water and thus propagate over large distances when trapped in the ocean waveguide. Sound levels are influenced over large regions by anthropogenic activities and marine mammals as well as by natural weather and geological processes. Records of VLF sounds from hydrophones and ocean-bottom seismometers are thus of multidisciplinary interest.

In this article, we aim to provide a broad review of scientific investigations of VLF sounds in the ocean. Section 2 presents an overview of the theory of acoustic propagation and the complications that arise at VLF frequencies from interactions with the seafloor. Section 3 then discusses the observation of sounds using hydrophones and seismometers. Sections 4–7 examine in turn the VLF sounds created by weather, earthquakes, marine mammals, and anthropogenic activities. Section 8 briefly discusses the interactions between low-frequency anthropogenic sounds and marine mammals and the difficulties associated with conducting robust studies to assess anthropogenic impacts. We conclude in Section 9 by outlining future research directions and needs.

2. THEORY

2.1. Acoustic Propagation

Typically, ocean acoustic propagation is a waveguide problem: The surface and bottom boundaries are much closer than any "side" boundary. The acoustic field $\psi(\mathbf{r}, t)$ as a function of space vector $\mathbf{r}$ (representing x, y, and z positions) and time t can therefore be decomposed into vertically trapped modes. If $\psi(\mathbf{r}, t)$ is decomposed into separate frequency components at Fourier (radian) frequency ω, the propagation of each component $\psi_\omega(\mathbf{r})$ is then governed (Munk et al. 1995, Brekhovskikh & Lysanov 2003) by the Helmholtz equation

$$\nabla^2 \psi_\omega(\mathbf{r}) + \frac{\omega^2}{c^2(\mathbf{r})} \psi_\omega(\mathbf{r}) = 0, \tag{1}$$

with appropriate boundary conditions at the ocean surface (where ψ is zero) and at the bottom (where the boundary condition is more complicated) (see Section 2.2). The dominant features of propagation are controlled by the sound-speed field $c(\mathbf{r}) = c_0(\mathbf{r}) + \delta c(\mathbf{r}, t)$, which may be decomposed conceptually into an average field $c_0(\mathbf{r})$ and a space/time-fluctuating part. The fluctuating part is usually much smaller than the average field and has timescales considerably longer than acoustic timescales, and it therefore has no significant role in the dominant features of propagation (Flatté et al. 1979, pp. 44–46).

For an ocean with properties that depend only on depth z, the acoustic field depends only on the range and depth. In this case, $c_0(\mathbf{r}) = c(z)$, the Helmholtz equation separates in depth and range, and the vertically trapped modes $\phi(z)$ obey the depth-only equation

$$\frac{\partial^2}{\partial z^2} \phi(z) + k_v^2 \phi(z) = 0, \tag{2}$$
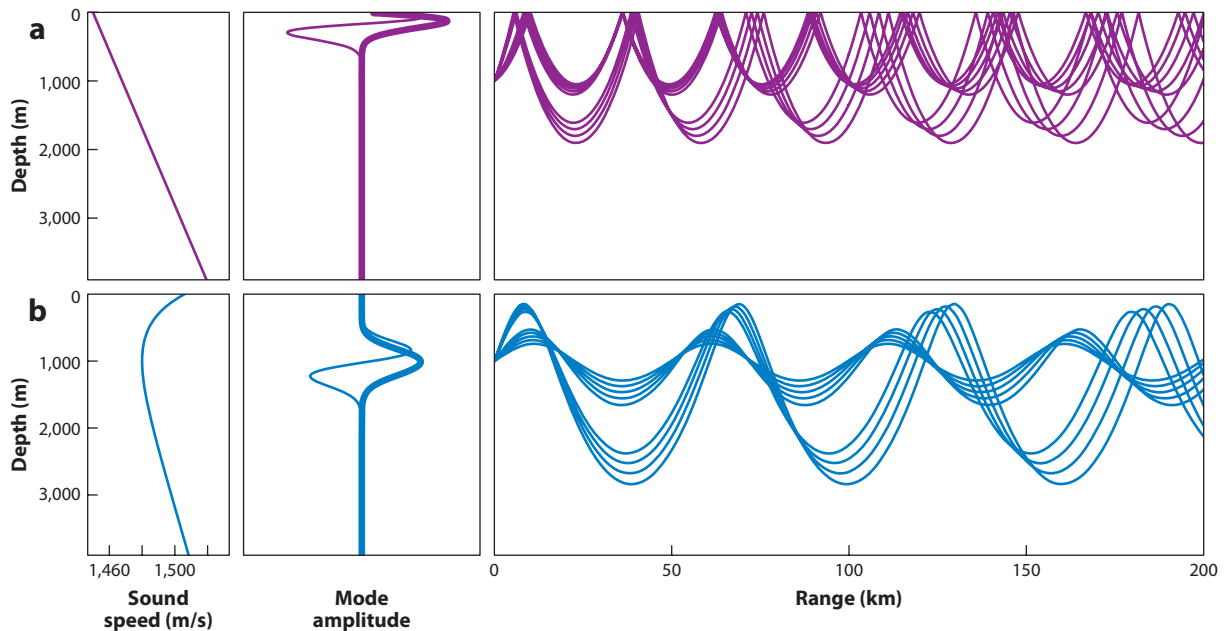
Figure 1

Two representative propagation regimes. (*a*) Polar regime. The left panel shows an idealized polar sound-speed profile, the middle panel shows modes 1 and 2 at 50 Hz (with mode 1 in *bold*), and the right panel shows two bundles of rays launched from an acoustic source at 1,000-m depth. The rays continually refract upward and skip off the surface. (*b*) Low-latitude regime. The left panel shows an idealized low-latitude sound-speed profile, the middle panel shows modes 1 and 2 at 50 Hz (with mode 1 in *bold*), and the right panel shows two bundles of rays launched from a source at 1,000-m depth. The rays cycle in the deep sound channel without interacting with the boundaries.

where k_v is the local vertical wavenumber (Munk et al. 1995). Each Fourier component can then be written as a weighted sum of all propagating modes.

Etter (2003, pp. 135–51) suggested that mode-theoretic models for shallow-water propagation become too computationally intensive above approximately 500 Hz. Very crudely, for a typical shallow depth H of 100 m and an average sound speed of 1,500 m/s, this frequency yields a value of roughly 30 for the nondimensional ratio $H/\bar{\lambda}$ of ocean depth to average acoustic wavelength $\bar{\lambda}$. This ratio can indicate a practical transition from mode-theoretic to ray-theoretic propagation regimes. At higher frequencies (i.e., larger values of $H/\bar{\lambda}$), the field can be visualized using rays (Munk et al. 1995), where rays indicate the sound propagation paths. The Helmholtz equation, in the high-frequency limit, yields ray equations that can be integrated forward for any $c_0(\mathbf{r})$, which makes ray diagrams particularly useful in regions with complex, range-dependent oceanography. For frequencies below 100 Hz in shallow water, mode representations are usually required. In the deep ocean, the transition ratio threshold is reached at approximately 10 Hz, which implies that higher VLF frequencies are adequately represented with ray diagrams.

The ocean's stratification makes $c_0(\mathbf{r})$ a strong function of depth but a weak function of range. Sound speed increases with hydrostatic pressure and temperature. Consequently, in isothermal and isohaline water, the sound speed increases with depth. A nearly isothermal example is the polar profile in **Figure 1a**, where surface and abyssal temperatures are similar. Alternatively, at low latitudes, solar heating of surface waters introduces a prominent temperature gradient; temperature decreases significantly with depth down to approximately 1,000 m and then decreases more slowly

Mode-theoretic:
a mathematical formalism that describes the acoustic field with modes

Ray-theoretic:
a mathematical formalism that conceptualizes the acoustic field with rays

Ray:
a path along which an acoustic or seismic signal travels

in the deep ocean. Sound speed is also proportional to temperature; in the upper ocean, the temperature effect dominates the pressure effect, and sound speed decreases with increasing depth. Pressure and temperature exchange dominant roles at approximately 1,000 m, producing a sound-speed minimum (**Figure 1***b*); below this depth, sound speed increases with depth as in a polar profile.

Figure 1 also shows the first few modes for both profiles. The lowest mode is concentrated near the surface for the polar profile and around the sound-speed minimum for the low-latitude profile (Munk et al. 1995). The ray picture for the polar profile shows propagation paths that continuously refract upward and bounce off the surface. In the low-latitude profile, fields initially refract downward until, significantly below the sound-speed minimum, they refract upward. The polar profile essentially ducts the sound along the surface, whereas the low-latitude profile ducts the sound about the deep sound-speed minimum. The deep duct is called the deep sound channel, or the sound fixing and ranging (SOFAR) channel (Urick 1983, p. 159).

2.2. Bottom Interaction

The bottom boundary between the ocean and the underlying crust is acoustically complicated. Much of the seafloor is sedimented with relatively muted topography, but near oceanic spreading centers, along continental margins, and in other volcanically and tectonically impacted regions, the topography can be rough. The properties of seafloor sediments and volcanic crust vary substantially with depth beneath the seafloor and can display substantial lateral heterogeneity. Energy from the acoustic wave field that interacts with the seafloor can be scattered, radiated into and out of the bottom, and absorbed by attenuation.

In the high-frequency limit, an acoustic wave with a planar wave front that is incident on a flat homogeneous sea bottom partitions into a reflected acoustic wave and transmitted compressional and shear body waves with amplitudes and phases given by the Zoeppritz equations (Ikelle & Amundsen 2005, pp. 92–95), which are dependent on the incidence angle and the seismic properties of the sea bottom. However, in the VLF band, the accuracy of these equations is limited even in areas of uniform seafloor, because wave-front curvature can be significant and the primary (P) and shear (S) wave velocities increase significantly with depth on the scale of the seismic wavelength (Ewing et al. 1992). Acoustic energy also couples into interface waves known as Scholte waves, which propagate along the seafloor and decay exponentially away from the boundary (Scholte 1947). At low frequencies, Scholte waves account for a large component of ocean noise near the seafloor (Nolet & Dorman 1996). Both P and vertically polarized S head waves (often referred to as lateral waves in the acoustics literature) propagate at the boundary and radiate into the water column (Brekhovskikh & Lysanov 2003).

The bottom boundary is further complicated by range dependence in the seafloor bottom/subbottom regions (Stone & Mintzer 1962, Smith et al. 1992). Fluctuations in acoustic wave speed can induce ray chaos in the water column that results in range-dependent waveforms (Smith et al. 1992, Tanner & Sondergaard 2007, Virovlyansky 2008). However, in shallow-water environments, the common causes of range dependence are related to the properties of the seafloor and the material beneath it. Variations in sediment composition and thickness, nonplanar boundaries, rough surfaces, strong density or velocity contrasts, and/or variations in water depth (Holland 2010) all add to the complexity of acoustic interactions with the seafloor. Even in areas of relatively simple geology, sediments can impose considerable range dependence on sound transmission over short ranges (Stoll et al. 1994).

Another source of complexity is elastic anisotropy, which is defined as the variation of elastic properties with direction. Possible sources of elastic anisotropy are the alignment of cracks and/or pores, preferred orientation of mineral grains, and lamination as a result of compositional layering

P wave: a longitudinal elastic body (or sound) wave in the Earth

S wave: a transverse elastic body wave in the Earth

Elastic anisotropy: elastic properties that are dependent on direction

(Carlson et al. 1984, Koesoemadinata & McMechan 2004, Valcke et al. 2006). Although many authors favor a ray-based approach to modeling range dependence within the water column, the elastic properties of anisotropic sediments require properly simulating polarization effects. In sedimentary layers, compressional (P) and vertically and horizontally polarized shear (SV and SH) waves combine to form propagating modes (Koch et al. 1983, Stoll et al. 1994, Godin 1998). Anisotropy induces these seismic modes to mix the polarizations of P, SV, and SH motions, even in the absence of range dependence in the media (Park 1996, Soukup et al. 2013).

The simplest model for anisotropy is associated with an axis of symmetry (Backus 1962) and is a natural model in the presence of layering or aligned planar cracks or pore spaces. Marine sediments often have transversely isotropic elastic symmetry, with fast velocity directions in the plane parallel to the bedding plane and slow velocity directions along the normal of the bedding plane. Horizontal bedding leads to a transverse-isotropic geometry with a vertical symmetry axis. This orientation does not couple acoustic signals with SH waves. Such coupling does occur with a horizontal symmetry axis that can be produced by the introduction of vertical parallel cracks. Layered sediments with nonhorizontal bedding require a tilted symmetry axis whose orientation may vary vertically in cross-bedded sediments (Martin & Thomson 1997).

SV wave: an S wave polarized in the vertical plane

SH wave: an S wave polarized in the horizontal plane

Decibel: a unit that describes differences in the power of acoustic signals (equal to 10 times the logarithm to base 10 of the ratio of the powers)

2.3. Attenuation

Propagating sound loses energy along its path by volume attenuation and volume and boundary scattering. Volume attenuation converts acoustic motion into heat primarily via bulk viscosity, owing principally to the presence of boric acid (Clay & Medwin 1977, pp. 96–102). For VLF sound, the attenuation is

$$\alpha(f) = (1.2 \times 10^{-7}) f^2 \text{ dB/km}, \tag{3}$$

where f is in hertz and is extremely low.

The acoustic impedance mismatch between seawater and seafloor sediment is often small, allowing a significant proportion of sound to propagate into the bottom. Attenuation levels are difficult to measure in the shallow subseafloor. They are likely frequency dependent and quite high, resulting in a loss of several decibels per kilometer for a 10-Hz signal; a significant portion of the sound propagating into the bottom does not radiate back out in the water column.

Scattering from rough boundaries also contributes to attenuation. The ratio of roughness scale to wavelength controls the amount of attenuation (Brekhovskikh & Lysanov 2003). Sea-surface roughness is negligible for VLF frequencies, but seafloor roughness such as undersea ridges and seamounts can be considerable, and further volume scattering occurs from heterogeneities beneath the seafloor. Although impedance contrast between seawater and basalt is relatively large, leading to reflected amplitudes that are higher than those in sedimented regions, the volcanic seafloor tends to be rough, and so much of the reflected energy is scattered.

In summary, fields ducted in the deep sound channel that avoid both the top and bottom experience only volume attenuation in the ocean and can propagate very long distances with very low loss. Sound fields that interact with the seafloor rapidly gain complexity but also undergo significant attenuation from scattering and absorption in the seafloor that limits their propagation distance.

3. OBSERVATIONS

Sounds in the ocean are detected with hydrophones that utilize piezoelectric transducers to generate electricity in response to pressure changes over a broad range of frequencies. Sounds can also be detected at the seafloor using three-component seismometers, in which each component records the velocity of the ground in one direction based on measurements of the motion or force required

to restrain an internal mass attached to a frame by springs. Recently, considerable effort has gone into extending the sensitivity of ocean-bottom seismometers to frequencies well below 1 Hz, but the technology to detect seismic signals on the seafloor in the VLF band is well established.

Most recordings of ocean sound by the academic community are presently made with autonomous instruments. Hydrophones are routinely deployed near the seafloor and on moorings within the water column, and more recently have been attached to drifters and autonomous underwater vehicles. Depending on the application, they may be deployed singly, in compact directional arrays, or in broadly spaced networks. Ocean-bottom seismometers are typically deployed in sites of geological interest, such as continental margins and tectonic plate boundaries. They are usually deployed in networks with an instrument spacing that may vary from ∼1 km to ∼100 km. The number of ocean-bottom seismometers in use by the academic community has grown significantly over the past decade, and there are presently upward of 1,000. As a result of advances in low-power electronics and digital storage, it is now relatively straightforward to record acoustic or seismic signals autonomously in the VLF band for a year or more. However, for hydrophone instruments designed to also record much higher frequencies, storage capacity limitations often mandate shorter deployments, duty cycling, or event detection.

Although deployments with a sea-surface expression can return data by satellite, the data rates are sufficiently high that continuous streams of VLF data are best supported by cables. The US Navy has operated the cabled Sound Surveillance System (SOSUS) networks of hydrophones in the Atlantic and Pacific Oceans and local hydrophone networks in test ranges since the 1960s. Following the end of the Cold War, SOSUS became available for scientific applications (Fox & Hammond 1994, Nishimura & Conlon 1994), but the data remain classified. A number of real-time hydrophones have also been deployed over the past 15 years at several locations in the oceans as part of the International Monitoring System of the Comprehensive Nuclear-Test-Ban Treaty (Hanson et al. 2001). An important development in recent years has been the establishment of deepwater cabled observatories for research operations. These include the North-East Pacific Time-Series Undersea Networked Experiments (NEPTUNE) Canada (Barnes & Tunnicliffe 2008) and Ocean Observatories Initiative Regional Scale Nodes (Delaney & Kelley 2013) observatories in the northeast Pacific, the European Sea Floor Observatory Network (ESONET) (Priede & Solan 2002), and the Dense Ocean Floor Network System for Earthquakes and Tsunamis (DONET) off Japan (Kawaguchi et al. 2008). Most of these systems are multipurpose, and nearly all include a hydrophone or seismic monitoring capabilities. The potential exists to use abandoned submarine cables to make observations in remote locations (Butler et al. 2000, Kasahara et al. 2006) or to install telecommunications cables for dual scientific and commercial use.

4. WEATHER

Weather has a considerable influence on VLF sound. Surface winds, both near and far, transfer energy into the sea surface and generate sound through several mechanisms. Radiative transfer of heat to and from the upper ocean moderates propagation conditions, which can cause long-range ducting of sound (see Section 2). Surface cooling can also cause the formation of sea-surface ice, which has its own distinctive acoustic signature. Carey & Evans (2011, pp. 54–97) provided a recent comprehensive treatment of the effects of weather on VLF sound. The following sections review the dominant influences of surface wind waves and ice.

4.1. Surface Wave Interactions

Surface winds act on the sea surface to build gravity waves. Nonlinear interactions of surface gravity waves traveling in opposite or nearly opposite directions generate an acoustic signal at twice the

frequency of the surface waves (Longuet-Higgins 1950). The sound level in the upper few hundred meters can be substantially higher than at greater depths because the generation mechanism includes a near-field term (Cato 1991). When the signals propagate beneath the seafloor, they are termed microseisms. The microseisms from the longest-period swell waves corresponding to large storms propagate efficiently around the Earth, resulting in a prominent global peak in seismic noise levels centered between 0.1 and 0.2 Hz (Webb 1998). At higher frequencies, the amplitudes of microseisms decrease, because the amplitudes of ocean wave-height spectra decrease with frequency and higher-frequency seismic signals are attenuated over shorter distances within the Earth. Above 1 Hz, the noise is generated locally, and noise levels measured in the ocean and on the seafloor are closely correlated with the local wind speed up to a saturation threshold (Dorman et al. 1993, McCreery et al. 1993, Webb 1998).

Microseismic noise showing a characteristic decrease in amplitude with frequency dominates the spectra in **Figure 2** at frequencies up to approximately 5 Hz, with intervals of low noise

Microseisms: seismic noise created by the nonlinear interaction of ocean waves (the term was coined before the mechanism was known)
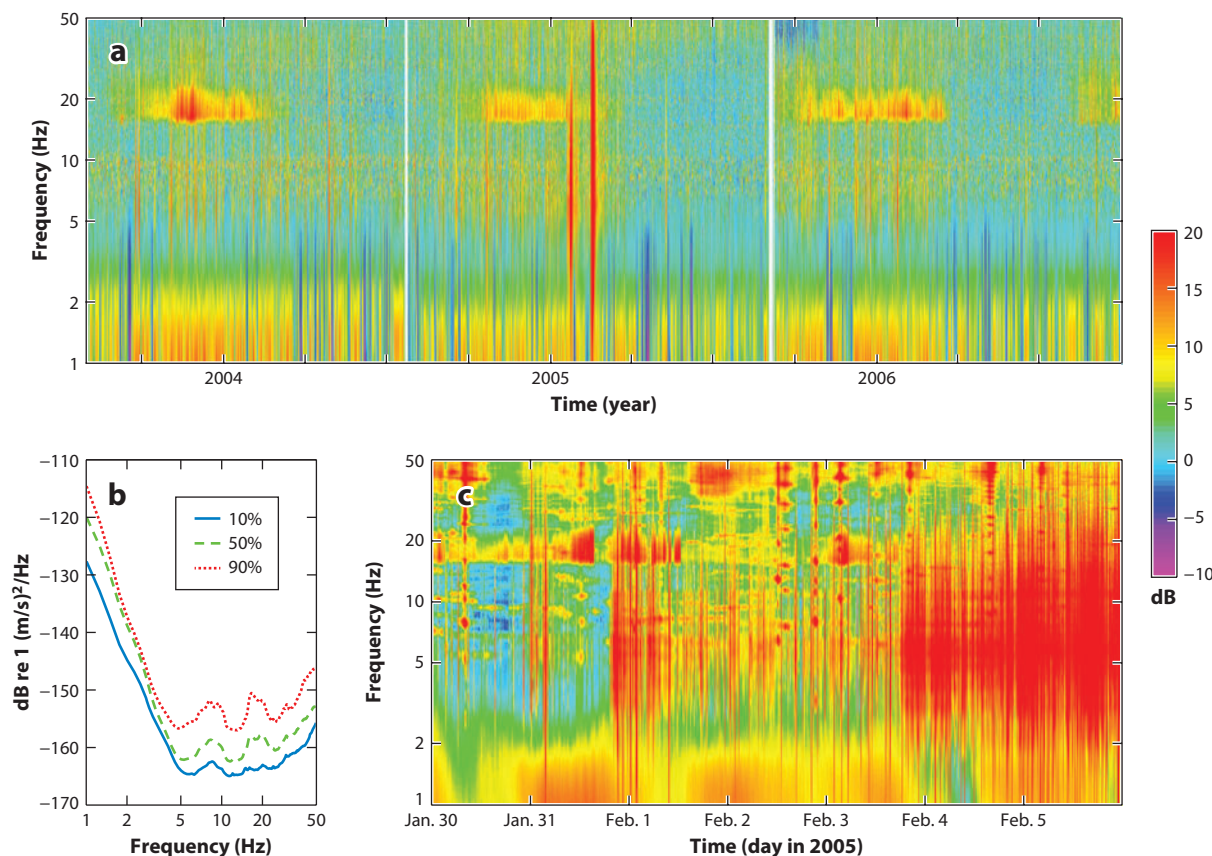
Figure 2

Seismic data collected in the very-low-frequency (VLF) band on the vertical channel of an ocean-bottom seismometer at 2,200-m depth on the Endeavor segment of the Juan de Fuca Ridge (Weekly et al. 2013). (*a*) Three-year velocity spectrogram. Each vertical raster line is a spectrum estimate averaged over 24 h. The 10th-percentile curve at each frequency has been removed to enhance the dynamic range. Two gaps mark annual servicing. (*b*) The 10th-, 50th-, and 90th-percentile curves. (*c*) Detailed spectrogram for one week in 2005 that includes a seismic swarm on the Juan de Fuca Ridge. The time-axis resolution is 10 min. Measurements are bounded at 50 Hz owing to the sampling rate.

corresponding to intervals of calm. The contribution from this mechanism may even extend to higher frequencies: Acoustic pressure spectra measured at the seafloor in deep regions of the North Pacific have features that can be matched to the spectra of ultragravity waves up to 30 Hz or more (Duennebier et al. 2012, Farrell & Munk 2013).

4.2. Surface Waves: Bubbles

When ocean waves break owing to instability mechanisms and then form (depending on the size of the wave) microbreakers, spilling breakers, or plunging breakers, the overturning fluid entrains air bubbles. Air bubbles are like simple mass-spring systems, with the highly compressible interior air acting like a spring and the fluid outside the bubble acting like a mass. Once excited, bubbles "ring" with characteristic oscillation frequencies f proportional to their radius, according to the Minnaert (1933) formula

$$ f = \frac{1}{2\pi R} \left(\frac{3\gamma P}{\rho} \right)^{\frac{1}{2}}, \tag{4} $$

where R is the bubble radius, P is the ambient pressure, ρ is the liquid density, and γ is the ratio of specific heats for air. Optical (Johnson & Cooke 1979, Deane 1997) and indirect acoustic resonance (Breitz & Medwin 1989, Farmer et al. 1998) measurements showed that the sizes of injected bubbles range from less than 20 μm to several centimeters; these bubbles consequently contribute to ambient sound at ringing frequencies of several hundred hertz to several hundred kilohertz.

Bubble entrainment and subsequent bubble ringing are therefore an accepted source mechanism for noise above the VLF range. Evidence supporting mechanisms that could generate noise within the VLF range is less decisive. Measurements are difficult owing to the pervasive contamination of anthropogenic noise (see Section 7). Nevertheless, studies in the Southern Hemisphere, where ship traffic is sparse (see Section 7.1), have found good correlation between local sound levels and wind speed (Cato 1976, Burgess & Kewley 1983). Because sea-surface energetics (whitecapping, gravity wave height, etc.) are related to wind forcing, these and similar studies dictate that source mechanisms be associated with sea-surface processes. Ultragravity surface waves (Section 4.1) provide at best a possible mechanism over only the lower end of the VLF range. Theories proposing individual ringing bubbles are discounted because bubbles with sizes large enough to resonate below 100 Hz have not been observed. An alternative theory proposes that the entire volume of bubbly fluid injected by a single breaking wave acts itself like one big bubble (Carey & Browning 1988, Yoon et al. 1991), with a corresponding resonance frequency much lower than that of its much smaller constituent bubbles.

Near coastlines, shoaling gravity waves generate considerable sound levels while breaking. Bubble oscillation is also a principal mechanism of sound generation here (Haxel et al. 2013). An auxiliary mechanism that can contribute acoustic energy over a broad frequency band is the current-induced transport of sediment (rocks, stones, and sand). Sound from shoaling waves breaking against a shoreline can propagate downslope away from the shore and out into open waters, and can make a significant contribution in coastal regions.

Weather effects are readily apparent at the higher VLF frequencies in the data captured near San Nicolas Island off the coast of Southern California (**Figure 3**). Above approximately 70 Hz, a prominent short-timescale striation pattern is evident. This signal correlates with (predominantly local) storms, which invoke bubble production via whitecapping and may persist for timescales of several days to a week.

Bannister (1986) has proposed high-latitude storms as a mechanism for generating distant sea-surface sound that can propagate to lower latitudes via the deep sound channel. At high latitudes,
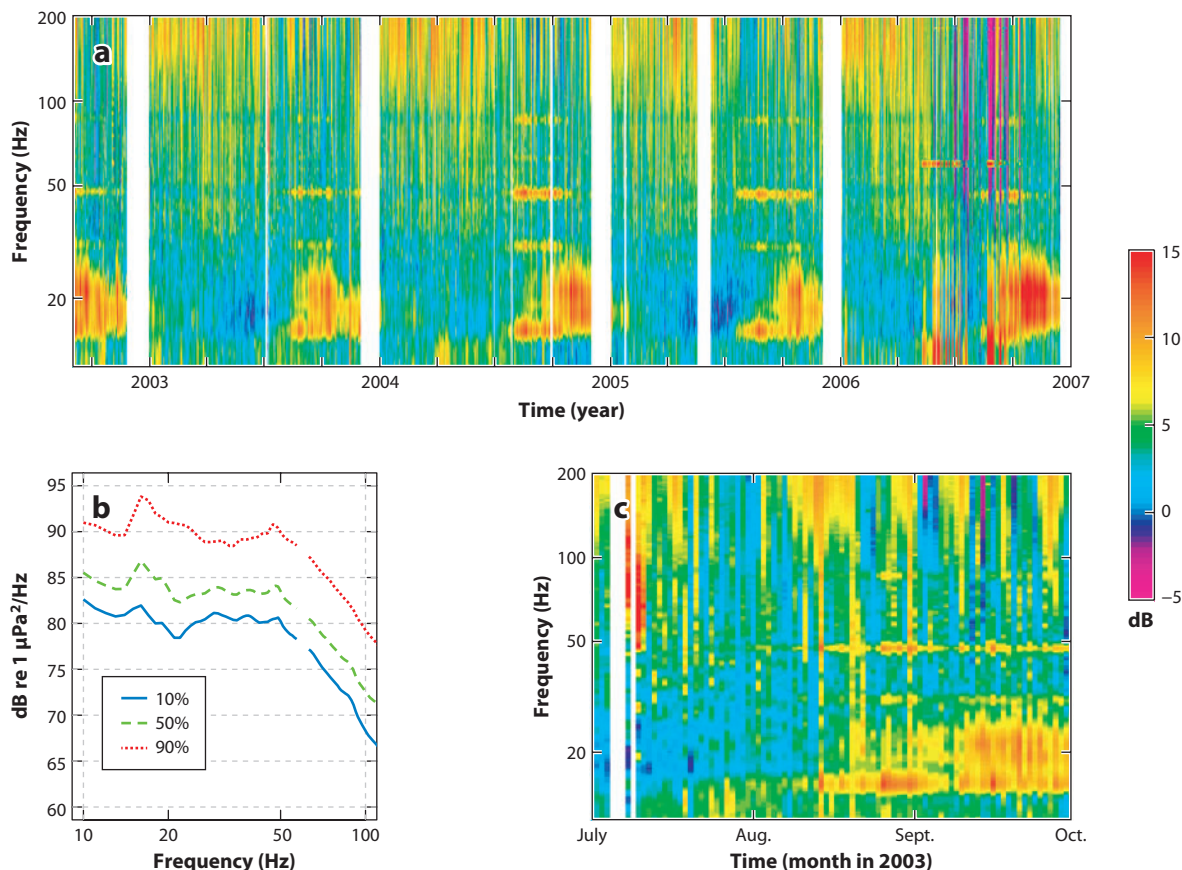
Figure 3

VLF sound collected off San Nicolas Island, Southern California (McDonald et al. 2006, Andrew et al. 2011). (*a*) Four-year spectrogram. Each vertical raster line is a spectrum estimate averaged over 24 h. The 10th-percentile curve at each frequency has been removed to enhance the dynamic range. Gaps represent equipment outages. (*b*) The 10th-, 50th-, and 90th-percentile curves. (*c*) Detailed spectrogram for several months in 2003. The time-axis resolution is 24 h. Measurements are bounded at 10 Hz owing to instrumentation calibration uncertainty at lower frequencies.

the deep sound channel is essentially at the surface, but it deepens toward the equator. At low latitudes, this provides a duct for confining the sound of distant surface energy to subsurface regions below a potentially quieter layer. Sufficiently accurate measurements do not yet exist to support this hypothesis.

4.3. Ice

Although the ice-covered Arctic would be expected to experience very low ambient noise levels owing to the lack of wind-driven waves, the dynamics of sea ice—including ice formation and deformation, pressure ridging, and cracking—greatly increase ambient noise levels over a broad range of frequencies (Lewis & Denner 1988, Farmer & Xie 1989). Below 100 Hz, ice cracks and fractures (**Figure 4*a***) caused by wind and stress contribute significantly to ambient noise levels, particularly in winter and spring months in ice-covered oceans (Dyer 1988, Roth et al. 2012).
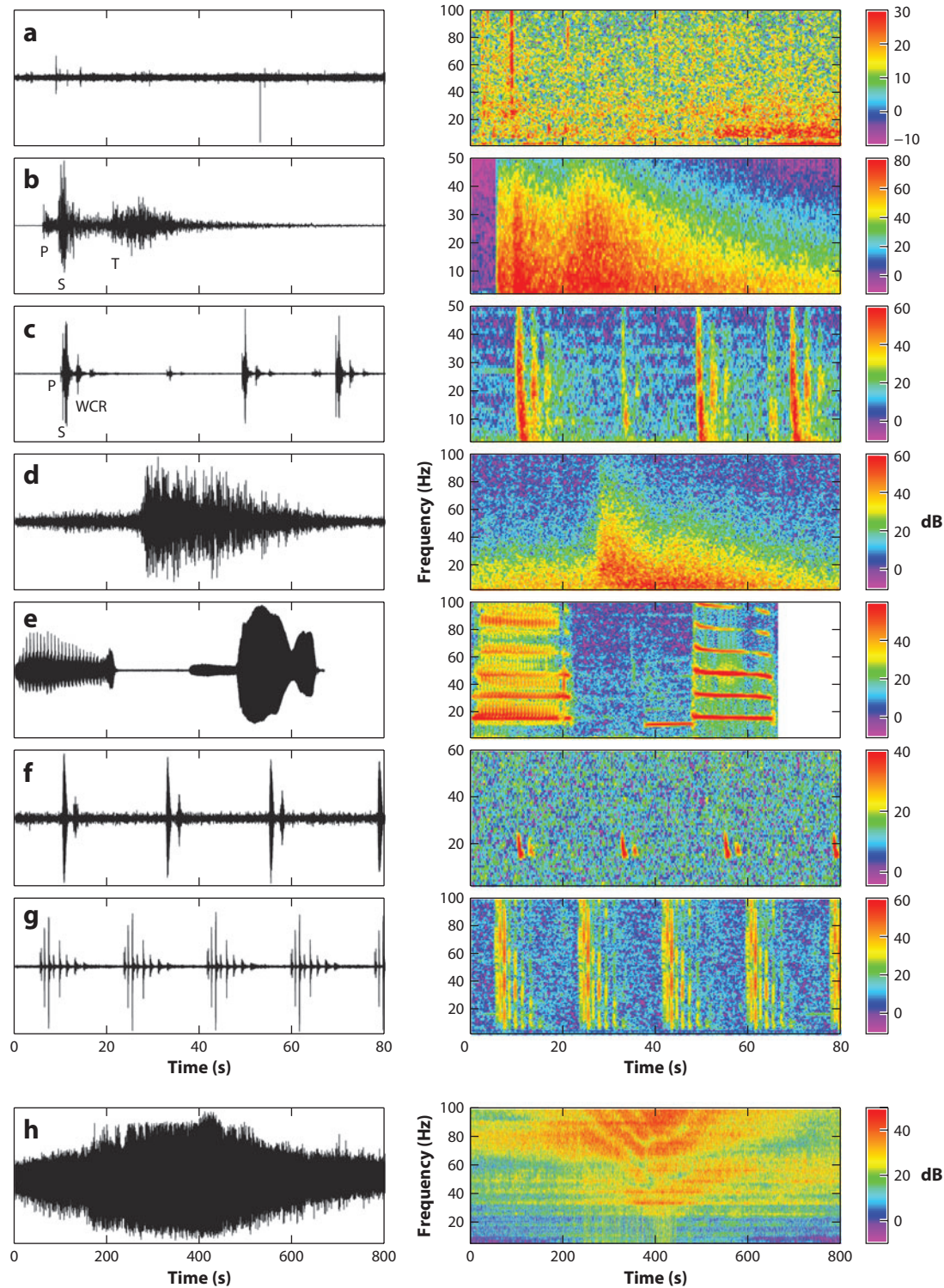
In the Antarctic, noise from rifting and breaking of icebergs in the frequency band from 2 to 35 Hz has been detected thousands of kilometers away from the event source, suggesting that these events have high sound source levels (~245 dB re 1 μPa at 1 m) (Chapp et al. 2005, Gavrilov & Li 2008). Other acoustic signals from icebergs include harmonically rich tremors with fundamental frequencies between 4 and 10 Hz. These so-called variable harmonic tremors can last from hours to days and have been associated with the movement of very large icebergs (Chapp et al. 2005). Shorter-duration low-frequency signals (so-called cusped pulse tremors, from 4 to 80 Hz) that are more pulsive and last only minutes to hours have been attributed to the internal resonance of smaller icebergs (Chapp et al. 2005). Low-frequency resonance may occur only when two icebergs collide or when very large icebergs ground on the ocean floor (Talandier et al. 2002). A further source for low-frequency sounds coming from the open ocean is internal resonance that occurs as very large icebergs are displaced when they encounter large eddies or the polar or sub-Antarctic fronts (Talandier et al. 2006). All of these signals from icebergs in the Southern Ocean can dominate low-frequency noise spectra at long distances (Chapp et al. 2005, Talandier et al. 2006).

Sound source level: the intensity of sound sources expressed in decibels relative to a reference sound measured at or corrected to a specific range; in water, the reference is 1 μPa at 1 m

T wave: a body wave from an earthquake that travels as a ducted wave in the ocean sound channel

5. EARTHQUAKES

Earthquakes are a significant source of discrete VLF sounds in the ocean; they are observed both as body waves that are transmitted across the seafloor at steep angles and as ducted waves known as T waves, which can propagate long distances horizontally within the sound channel. The spectrum of a seismic body wave reaching the seafloor is dependent on the earthquake source characteristics and the attenuation that occurs as the elastic wave propagates through the Earth (Shearer 2009, pp. 181–83). Earthquake signals in the VLF band are characterized by decreasing amplitudes at higher frequencies for two reasons. First, destructive interference reduces radiated amplitudes for frequencies exceeding a corner frequency that is approximately equal to the wave speed divided by the dimensions of the fault. Typical corner frequencies range across the VLF band from ~1 Hz for a magnitude-5.5 earthquake to ~100 Hz for a magnitude-1.5 microearthquake. Second, anelastic attenuation along the propagation path increases approximately linearly with frequency. Although shear (S) waves tend to have higher amplitudes at the source than compressional (P) waves, they are usually attenuated more strongly within the Earth and thus are observed at lower frequencies.

Body waves from teleseismic (distant) earthquakes are often not observed in the VLF band. Two notable exceptions are the P_n and S_n phases, which propagate with little attenuation in the lithosphere of oceanic plates and can be observed at frequencies extending to 20–30 Hz and distances up to 3,000 km (Walker 1981, Walker et al. 1983). Otherwise, the detection of body waves in the VLF band is limited to P waves near 1 Hz and is dependent on the characteristics of

←——

Figure 4

Examples of waveforms and spectrograms for various transient very-low-frequency (VLF) signals. The waveforms have been filtered with a 5-Hz high-pass filter, and the spectrograms have been normalized to the 5th-percentile value in the plotted frequency band. All but panel *h* are for an 80-s time interval, but the bandwidth and scaling of the spectrograms vary between signals. (*a*) Ice cracking noise recorded by a hydrophone. (*b*) A magnitude-4 earthquake recorded by an ocean-bottom seismometer at a 30-km range, showing P-, S-, and T-wave arrivals. (*c*) A swarm of local microearthquakes recorded by an ocean-bottom seismometer. The P- and S-wave arrivals are closely spaced for each earthquake, and two water column reverberations (labeled WCR) are visible for each earthquake spaced approximately 3 s apart. (*d*) A T wave for a distant earthquake recorded by a hydrophone. (*e*) The A and B calls of a northeast Pacific blue whale recorded by a hydrophone. (*f*) Regularly spaced 20-Hz fin whale pulses recorded by an ocean-bottom seismometer. Both the direct arrival and first water column reverberation are visible. (*g*) Air-gun shots spaced 18 s apart recorded on a hydrophone, showing multiple shallow-water reverberations. (*h*) Ship noise recorded by a hydrophone.

the earthquake and ambient noise levels (Webb 1998). Ocean-bottom seismometer experiments in some locations may fail to record any teleseismic P waves at ≥1 Hz (Wilcock et al. 1999).

Because they propagate over shorter distances and thus undergo less attenuation, local earthquakes near a receiver are a more significant source of VLF sounds than earthquakes at larger ranges. P and S waves are recorded by seafloor seismometers (**Figure 4b,c**), and the P waves are transmitted as coherent sound into the ocean. Because most earthquakes concentrate along tectonic plate boundaries, the number of local earthquakes is highly dependent on location. Seismic networks deployed on oceanic spreading centers (Tolstoy et al. 2006) and transforms (McGuire et al. 2012) may record tens of thousands of earthquakes per year. During earthquake swarm events, earthquakes and tremor can be the dominant sources of VLF noise (Tolstoy et al. 2006). In **Figure 2**, two large regional swarms are apparent in early 2005.

In most of the ocean, T waves are the most common earthquake sound (**Figure 4d**). T waves are characterized by emergent waveforms and are generated by two mechanisms. In regions with an inclined seafloor, such as continental slopes and the flanks of seamounts, successive reverberations between the sea surface and the seafloor propagating downslope lead to a progressive reorientation of acoustic rays toward the horizontal (Johnson et al. 1963, Okal 2008). This can lead to the generation of T waves that propagate into the ocean basin from sites on the seafloor that may be hundreds of kilometers away from the earthquake epicenter. In the absence of large-scale bathymetric features, abyssal T waves can be generated near an earthquake epicenter by scattering from seafloor roughness (Fox et al. 1994, de Groot-Hedlin & Orcutt 2001a, Park et al. 2001).

Because T waves propagate large distances in the ocean, they provide a means to monitor seismicity in the oceans using hydrophones at detection levels that are substantially lower than those of P and S waves recorded by the global seismic network. In the northeast Pacific, near-real-time analysis of data from the SOSUS network has provided a 20-year catalog of seismicity on the Juan de Fuca Plate (Dziak et al. 2011). One exciting result of this monitoring has been the real-time detection of several seafloor volcanic eruptions on the Juan de Fuca and Gorda Ridges (Fox et al. 1995, Dziak et al. 2011). This detection facilitated rapid ship-based responses that have contributed substantially to our understanding of seafloor spreading and subsurface hydrothermal and microbial processes (Delaney et al. 1998, Cowen et al. 2004). Regional networks of autonomous moored hydrophones have also been deployed in the deep sound channel in several other regions to create substantial catalogs of oceanic seismicity (Dziak et al. 2012).

6. MARINE MAMMALS

Marine mammals, particularly cetaceans (whales and dolphins), produce sounds over the largest range of any class of animal: from subsonic (large whales) to supersonic (porpoises and beaked whales) frequencies. The largest whales—the blue (*Balaenoptera musculus*) and fin (*Balaenoptera physalus*) whales—produce VLF sounds. Other species, such as humpback (*Megaptera novaeangliae*) and bowhead (*Balaena mysticetus*) whales, produce some sounds below 100 Hz, but these signals are only a small part of their acoustic repertoire. The sounds of blue and fin whales, by contrast, are almost all below 100 Hz. Both of these species produce long, loud bouts of calls, particularly in winter months, that contribute to overall regional ambient noise levels near 20 Hz (Curtis et al. 1999, Andrew et al. 2011, Nieukirk et al. 2012) (**Figures 2** and **3**). These long bouts, or songs, are thought to be male reproductive displays used to advertise fitness to other males, to attract females, or potentially to advertise a food resource (Payne & Webb 1971, Watkins et al. 1987, Croll et al. 2002, Oleson et al. 2007).

Blue whale calls (**Figure 4e**) generally consist of one to three units produced in a phrase, all of which have fundamental frequencies that are below 50 Hz and as low as 15 Hz. These units

are long (>10 s each) and may be frequency or amplitude modulated. Blue whale calls are also quite loud, with source level estimates ranging from 180 to 189 dB re 1 μPa at 1 m (Cummings & Thompson 1971, Thode et al. 2000, Širović et al. 2007). Although blue whale calls worldwide share these characteristics of being long, loud, and in the VLF band, whales from different areas produce sounds that are geographically distinctive (Stafford et al. 2001, 2011). The structure of blue whale songs remains stable over time, but there is evidence that the fundamental frequencies of the songs of some populations are decreasing, although a definitive reason for this decrease has not been found (McDonald et al. 2009, Gavrilov et al. 2012).

Fin whales also produce subsonic vocalizations (**Figure 4f**), but their calls are relatively short (1-s) pulses that are often slightly frequency modulated, spanning from ~40 down to 10 Hz. These "20-Hz pulses," as they are known, are repeated every 10–40 s and, like blue whale calls, may continue for hours or days at a time (Watkins 1981, Watkins et al. 1987). Fin whale calls are loud; source levels from 171 to 189 dB re 1 μPa at 1 m have been reported (Watkins et al. 1987, Charif et al. 2002, Širović et al. 2007, Weirathmueller et al. 2013). There is some evidence that the timing between successive pulses may vary geographically, but relatively few studies have examined this (Delarue et al. 2009, Castellote et al. 2011). In addition, some fin whale populations produce a higher-frequency pulse that sometimes accompanies the 20-Hz pulses; the frequency of this appears to vary geographically (Širović et al. 2009, Simon et al. 2010).

Although blue and fin whales produce other signals besides song notes in different behavioral contexts, these tend to be higher frequency and are produced less often than songs, and they therefore contribute less to overall ambient noise levels. Two other cetacean species produce signals with fundamental frequencies below 100 Hz: sei (*Balaenoptera borealis*) and Bryde's (*Balaenoptera edeni*) whales (Oleson et al. 2003, Rankin & Barlow 2007, Baumgartner et al. 2008). Relatively little is known about the acoustic behavior of these species, but the amplitudes of their signals are much lower than those of blue or fin whales, so these signals are unlikely to contribute significantly to global noise budgets (Cummings et al. 1986, Baumgartner et al. 2008).

7. ANTHROPOGENIC SOUNDS

Human utilization and exploitation of the ocean have resulted in additional components to VLF sound that did not exist before the nineteenth century. The usual catalog of sources includes at-sea structures, installations, and vessels; prominent categories are described below. Rarely considered—and poorly understood—are land-based sources. De Groot-Hedlin & Orcutt (2001b) suggested that sound from open-ocean acoustic sources could couple into the coastal crust and remain detectable some distance inshore. If the opposite is true (Collins et al. 1995), then the radiated noise from coastal cities might enter the marine soundscape. However, no definitive measurements exist, and this remains a speculative component.

7.1. Shipping Noise

One of the earliest uses of ambient sound was the passive detection of radiated noise from surface or subsurface vessels—a central military objective. Ships radiate a distinctive signal containing multiple harmonics over a diffuse broadband component (**Figure 4b**). The harmonics are related to the rotating machinery involved in the propulsion system: The fundamental frequency corresponds to the propeller blade rate, which is the rate that blades pass the shallowest depth (Ross 1976). For a propeller with N blades, this rate is N times the shaft rotation speed.

The primary noise mechanism appears to be cavitation occurring near the tip of the blade as the blade passes the top of its rotational arc (Ross 1976). The intensity of the radiated noise was
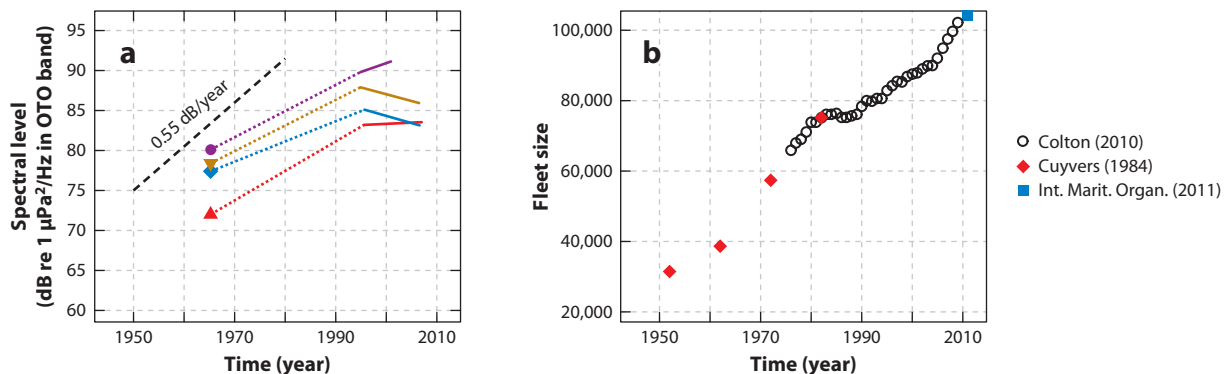
Figure 5

Merchant shipping contribution to acoustic noise. (*a*) Measurements at 32 Hz from four sites off the North American west coast. The symbols represent two-year averages at these sites from measurements made in the 1960s. The solid lines represent the durations and linear trends of a contemporary data set from the same sites (Andrew et al. 2011). Dotted lines connect the data from each site but are not intended to describe the ambient sound evolution during the intervening years. The dashed line with slope 0.55 dB/year is a linear regression described by Ross (1993) made from numerous measurements (not shown) at sites in the North Pacific and North Atlantic spanning roughly 1950–1970. (*b*) Size of the world merchant fleet over the same time period, compiled from several sources (Cuyvers 1984, Colton 2010, Int. Marit. Organ. 2011).

originally parameterized (using World War II ships) by ship speed and length (Ross 1976); recent studies (using newer ships) have suggested that ship draft, propeller size, and propeller tip depth might be better correlates (Wales & Heitmeyer 2002). Radiated levels are highly variable: Modern estimates of source level over 5–100 Hz for under-way vessels (Wales & Heitmeyer 2002, Leigh & Eller 2008, McKenna et al. 2012b) range from 171–190 dB re 1 μPa^2/Hz at 1 m for supertankers to 150–168 dB re 1 μPa^2/Hz at 1 m for small tankers, with levels decreasing with increasing frequency.

Early VLF sound observations (Wenz 1962) noted the signatures of individual passing ships, with amplitudes that increased as the ships approached and decreased as they receded. Wenz (1962) postulated that the ambient sound when a ship was not passing nearby was due to the distant armada of merchant ships, none of which were distinctly identifiable, and termed this contribution traffic noise. From a military perspective, this is the background noise that limits the performance of passive surveillance detection of hostile vessels. To first order, the size of the world's merchant fleet should be a positively correlated indicator of this contribution. Indeed, Ross (1993) showed that traffic noise increased throughout the middle of the twentieth century, when economic growth fueled an increase in transoceanic shipping. Measurements off the California coast (Andrew et al. 2002, McDonald et al. 2006, Chapman & Price 2011) showed that distant shipping noise levels have risen by approximately 10 dB compared with early reports. Statistics have indicated that the world merchant fleet size continues to grow (**Figure 5**); however, more recent high-resolution measurements off the North American west coast (Andrew et al. 2011) showed shipping noise trends that are level or even slightly decreasing. The discrepancy is not understood. Ainslie (2011) suggested that sea-surface temperature and/or ocean acidification changes may be introducing seasonal and interannual patterns in long-term records. Further complicating the issue is strong regional evidence that economic downturns, new regulations, and shipping lane relocation may be responsible (Frisk 2012, McKenna et al. 2012a).

The total contribution from shipping depends in part on the distribution of near and distant ships. The distribution is most heavily weighted in the shipping lanes crossing the Northern

Density (ships per thousand square nautical miles)
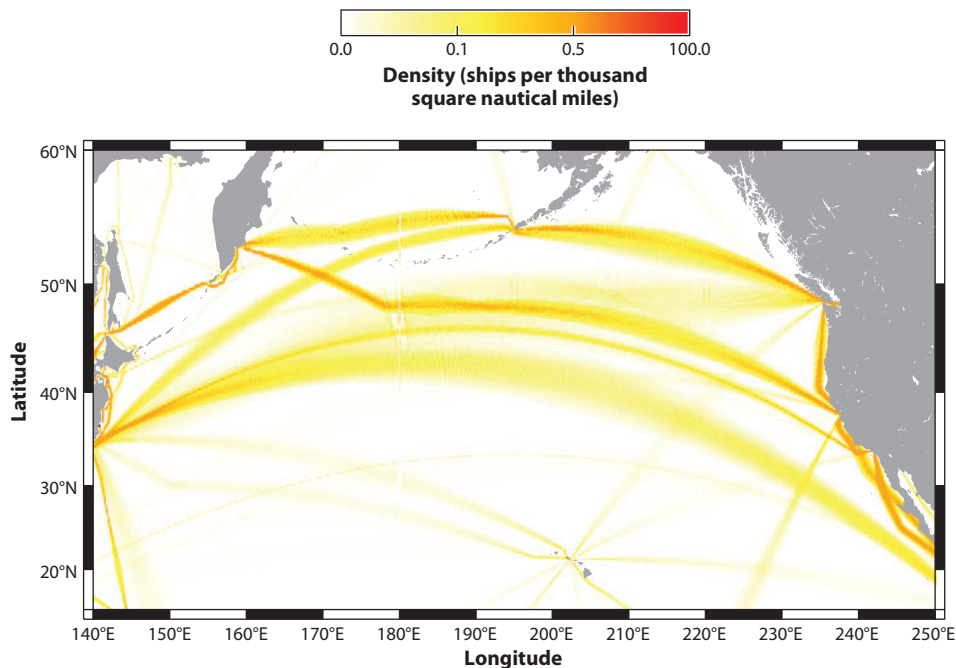
Figure 6

Shipping density in the North Pacific, compiled from 1998 records (Emery et al. 2001). The color scale is stretched at low densities to enhance trans-Pacific shipping lanes.

Hemisphere. **Figure 6** presents an estimate of ship density in the North Pacific for 1998 (derived from Emery et al. 2001). Shipping densities in the Southern Hemisphere are much lower, and the ship noise contribution there is much lower. Density maps such as **Figure 6** are key to understanding the spatial distribution of shipping noise and its regional impact on marine ecology, but density maps have been difficult and expensive to compile, and only two global maps have ever been constructed: one for 1998 (Emery et al. 2001) and one for 2010 (Walbridge 2013).

7.2. Energy Extraction

Civilization's increasing demand for energy has prompted an expansion of efforts to extract energy from ocean resources. Oil drilling is a well-known example, and recent projects include wind farms and tidal turbines. The VLF sound contributions from these initiatives may be space/time limited (as with pile driving for wind farm towers or oil rig decommissioning) or chronic (as with routine service vessel transportation to and from existing oil rigs). Additionally, the contributions are generally not well understood, possibly because the spatial and temporal extent of the activities is not well documented (e.g., for oil rig service vessel sizes, speeds, schedules, and routes) or the technology is too new (e.g., for undersea turbines). Several examples are given below.

Wind farms are a popular contemporary "green energy" technology. Wind turbines installed in the ocean radiate sound into the water and seabed from their foundations via structure-borne vibration owing to gearbox noise and turbulence on the fan blades. As more offshore wind farms are built, this technology will become a permanent addition to the VLF soundscape. Tougaard et al. (2009) measured radiated noise levels from individual turbines in shallow water and often observed a peak near 25 Hz at levels of 100–120 dB re 1 $\mu Pa^2/Hz$.

Hydrokinetic (tidal) turbines are a very new technology, and radiated levels are not available because no at-sea installations exist yet. Zampolli et al. (2012) used aerodynamic and turbulence models to postulate that the primary noise mechanism will be dipole radiation from the fan blades owing to unsteady flows originating from structures upstream of the blades. Most of the radiated noise is predicted to be below 20 Hz, with a level at 100 m of up to 100 dB re 1 μPa^2/Hz for a free stream velocity of 1.7 m/s.

Construction of wind farms, drilling platforms, and support infrastructure in harbors usually requires pile driving. The dominant radiation mechanism in impact pile driving is a Mach wave related to the radial expansion of the pile that propagates with supersonic speed down the pile after each impact (Reinhall & Dahl 2011). Typically, each impact radiates energy primarily above 100 Hz. Precise characterizations of source (or received) levels are generally not available owing to the vast differences in propagation conditions from site to site. Erbe (2009) reported sound exposure levels of 110–140 dB re 1 $\mu Pa^2 \cdot s$ over 10–40 Hz at a range of 320 m from a pier construction site (water depth 1 m); Bailey et al. (2010) reported levels of 10–120 dB re 1 μPa^2/Hz over 10–100 Hz at a range of 1,520 m during construction at an offshore (water depth 40 m) wind farm site.

7.3. Seismic Air Guns

An air gun generates an acoustic signal by releasing compressed air under high pressure from a pneumatic chamber. Arrays of air guns of different sizes can be tuned by adjusting their relative positions and discharge times to create an impulsive signal that is directed downward (Sheriff & Geldart 1995, pp. 211–18). A typical air-gun array signature (**Figure 4g**) extends across most of the VLF band, from a few hertz to well above 100 Hz. Air-gun arrays have high source levels; for example, the 36-element, 6,600-cubic-inch air-gun array on the R/V *Marcus G. Langseth* has a peak source level of 259 dB re 1 μbar at 1 m (Tolstoy et al. 2009). As a result, they can be recorded in the sound channel at distances of several thousand kilometers (Blackman et al. 2004; Nieukirk et al. 2004, 2012). During a seismic survey, they are discharged repetitively with an interval of ∼20 s.

There are approximately 150 seismic survey vessels worldwide (*Offshore* 2012) that operate on the continental shelves and slopes of rifted continental margins. Seismic surveys are more common in the Atlantic than in the Pacific. Like energy extraction projects (Section 7.2), individual surveys are sporadic and depend on the proprietary exploration schedules of the petroleum companies, although the overall activity can be remarkably persistent in some regions (Nieukirk et al. 2012).

7.4. Ocean Science

In the late 1980s, ocean acousticians proposed an ocean temperature measurement technique that uses long-range VLF signals. Pilot programs (Munk & Forbes 1989, Dushaw et al. 1999, Worcester & Spindel 2005) injected controlled phase-modulated signals at 57–75 Hz into the deep sound channel. The experiments of the Acoustic Thermometry of Ocean Climate (ATOC) project documented that the variability in basin-scale low-frequency sound transmission is due to seasonal changes in ocean temperature (ATOC Consort. 1998). These changes in temperature in turn influence sea-surface height measurements owing to thermal expansion as seawater warms. This methodology of producing low-frequency signals that are loud enough to be detected across ocean basins has been used in the Arctic with a 20.5-Hz signal to detect basin-scale warming of more than 0.5°C from 1994 to 1999 (Mikhalevsky et al. 1999, Mikhalevsky & Gavrilov 2001).

8. INTERACTIONS BETWEEN ANTHROPOGENIC SOURCES AND MARINE MAMMALS

Assessing whether anthropogenic sound has a negative impact on marine mammals is extremely difficult. Our understanding of the hearing responses of many marine mammals, particularly large whales, is incomplete. Determinations of whether they can hear certain signals and how loud the signals must be to be heard are often based on the frequency range of signals the marine mammals produce and potentially those produced by their predators. Further, to monitor the impacts of anthropogenic sound on marine mammals, visual observations of animals at the surface are most often used. Visual observations are limited to daylight hours and good weather, animals at the surface within visual range (which is much shorter than acoustic range), and a limited number of behavioral cues (e.g., changes in swim speed or direction and changes in respiration rate). Many marine mammal species spend >90% of their time underwater, and therefore responses to sound that occur below the surface cannot be documented. Finally, we still know so little about the ecology and behavior of most marine mammals that unless an animal washes up on a beach with obvious signs of acoustic trauma, it is extremely difficult to determine how, and for how long, exposure to underwater sounds impacts marine mammals on an individual- or population-level scale.

Reports of the impacts (or lack thereof) of low-frequency sources are relatively few, are often observational rather than experimental, and may arrive at different conclusions. For instance, fin whales exposed to air-gun surveys in the Mediterranean Sea moved away from the area and remained away for some time after the surveys ceased (Castellote et al. 2012). Blue whales increased their calling rate, potentially to compensate for increased ambient noise levels (Di Iorio & Clark 2010). McDonald et al. (1995) and Dunn & Hernandez (2009), in contrast, found no evidence of changes in the call rates of blue whales tracked from 28 to 100 km away from active air-gun operations or in the behavior of blue and fin whales near active operations. The ATOC experiments (see Section 7.4) were controversial when first conceived: The impacts, particularly on marine life, of injecting basin-spanning VLF sound into the deep sound channel were unknown. At the time, VLF levels of merchant shipping, nearshore construction, and geophysical exploration, which are generally much higher than ATOC signals, were either unmeasured or not publicly available. Some studies showed that the signals caused little or no behavior modification in cetaceans (Au et al. 1997, Mobley 2005), whereas others found that individual humpback whales spent less time at the surface when exposed to ATOC signal playbacks, although the overall distribution of humpback whales in the area did not change (Frankel & Clark 1998, 2000).

Although determining the interactions between anthropogenic noise sources and marine mammal life histories is fraught with difficulty and cannot be distilled into generalizations, it is important to take into consideration when discussing low-frequency noise. It is clear that shipping noise in the Northern Hemisphere, at least, has been increasing steadily (see Section 7.1), and this noise reduces the range over which species that use low-frequency sounds can communicate (Clark et al. 2009, Hatch et al. 2012). Low-frequency ship noise has been implicated in increased levels of stress hormones in North Atlantic right whales (*Eubalaena glacialis*) (Rolland et al. 2012). Noise from oil and gas exploration is pervasive year-round in the North Atlantic (Nieukirk et al. 2012). Seismic air-gun pulses overlap the frequency bands used by blue and fin whales (Nieukirk et al. 2004). The cumulative impact of these sources of increasing VLF noise on marine species that use sound as the primary means of sensing their environment may disrupt vital life history events, and this disruption may not be immediately obvious (Hatch et al. 2012).

9. FUTURE DIRECTIONS

Although the military has been observing VLF sound in the oceans for 50 years, long-term records of sound in the ocean obtained with hydrophones or seafloor seismometers are still scarce in the public domain. Advances in the capabilities and numbers of autonomous recorders and, more important, the move to establish long-term ocean observatories promise to substantially change this. An increasing number of ambient sound observations will provide enormous opportunities but will also bring additional challenges regarding collection protocols, data quality, record formats, metadata, and ease of access. These problems have been largely resolved within the academic seismic community through the development of global waveform databases and the tools to access them [the Incorporated Research Institutions for Seismology (IRIS) Data Management Center; **http://www.iris.edu/data**]; a similar approach is desirable for ocean acoustics data.

The dual use of SOSUS hydrophone data (Fox & Hammond 1994, Nishimura & Conlon 1994) has demonstrated the utility of long-term acoustic monitoring for studying weather-related noise, earthquakes, marine mammals, and shipping noise, and such studies will expand with open-access data. Seafloor seismic networks are also increasingly used to study marine mammals (McDonald et al. 1995, Rebull et al. 2006, Dunn & Hernandez 2009, Soule & Wilcock 2012). One particularly important opportunity is the prospect of more extensive and systematic studies of the impacts of anthropogenic sound on marine mammals. In addition to acoustics data, such studies will require assessing the contributions from a wide variety of existing transient and chronic anthropogenic sources. One such effort (Natl. Ocean. Atmos. Adm. 2012, Porter & Henderson 2013) required the integration of multiple databases for large commercial vessels, cruise ships, and roll-on/roll-off ferries, coupled with seismic survey track lines as stipulated in oil and gas exploration permits, service vessel activity models from government projection reports, and pile-driving noise models from environmental impact assessments for predictions in the US exclusive economic zone. The difficulties of assembling such data will only increase as the number and types of sources expand.

A global approach to handling ocean acoustics data is clearly needed, and the Sloan Foundation recently initiated such an effort. Denoted the International Quiet Ocean Experiment (Boyd et al. 2011), this project can perhaps serve as a framework for international collaboration in monitoring global ambient sound and estimating its effects on the acoustic ecology of the world's oceans.

DISCLOSURE STATEMENT

ACKNOWLEDGMENTS

LITERATURE CITED

Ainslie M. 2011. Potential causes of increasing low frequency ocean noise levels. *Proc. Meet. Acoust.* 12:070004

Andrew RK, Howe BM, Mercer JA. 2011. Long-time trends in low-frequency traffic noise for four sites off the North American west coast. *J. Acoust. Soc. Am.* 129:642–51

Andrew RK, Howe BM, Mercer JA, Dzieciuch MA. 2002. Ocean ambient sound: comparing the 1960s with the 1990s for a receiver off the California coast. *Acoust. Res. Lett. Online* 3:65–70

ATOC Consort. 1998. Comparison of acoustic tomography, satellite altimetry, and modeling. *Science* 281:1327–32

Au WWL, Nachtigall PE, Pawloski JL. 1997. Acoustic effects of the ATOC signal (75 Hz, 195 dB) on dolphins and whales. *J. Acoust. Soc. Am.* 101:2973–77

Backus GE. 1962. Long-wave elastic anisotropy produced by horizontal layering. *J. Geophys. Res.* 67:4427–40

Bailey H, Senior B, Simmons D, Rusin J, Picken G, Thompson PM. 2010. Assessing underwater noise levels during pile-driving at an offshore windfarm and its potential effects on marine mammals. *Mar. Pollut. Bull.* 60:888–97

Bannister RW. 1986. Deep sound channel noise from high-latitude winds. *J. Acoust. Soc. Am.* 79:41–48

Barnes C, Tunnicliffe V. 2008. Building the world's first multi-node cabled ocean observatories (NEPTUNE Canada and VENUS, Canada): science, realities, challenges and opportunities. In *OCEANS 2008: MTS/IEEE Kobe Techno-Ocean*, Kobe, Japan, April 8–11. Piscataway, NJ: Inst. Electr. Electron. Eng. **http://ieeexplore.ieee.org/xpl/articleDetails.jsp?arnumber=4531076**

Baumgartner MF, Van Parijs SM, Wenzel FW, Tremblay CJ, Esch HC, Warde AM. 2008. Low frequency vocalizations attributed to sei whales (*Balaenoptera borealis*). *J. Acoust. Soc. Am.* 124:1339–49

Blackman DK, de Groot-Hedlin C, Harben P, Sauter A, Orcutt JA. 2004. Testing low/very low frequency acoustic sources for basin-wide propagation in the Indian Ocean. *J. Acoust. Soc. Am.* 116:2057–66

Boyd IL, Frisk G, Urban E, Tyack P, Ausubel J, et al. 2011. An international quiet ocean experiment. *Oceanography* 24(2):174–81

Breitz ND, Medwin H. 1989. Instrumentation for in-situ acoustical measurements of bubble spectra under breaking waves. *J. Acoust. Soc. Am.* 86:739–43

Brekhovskikh LM, Lysanov YP. 2003. *Fundamentals of Ocean Acoustics*. New York: Springer-Verlag. 3rd ed.

Burgess AS, Kewley DJ. 1983. Wind-generated surface noise source levels in deep water east of Australia. *J. Acoust. Soc. Am.* 73:201–10

Butler R, Chave AD, Duennebier FK, Yoerger DR, Petitt R, et al. 2000. Hawaii-2 observatory pioneers opportunities for remote instrumentation in ocean studies. *Eos Trans. AGU* 81:157–63

Carey WM, Browning D. 1988. Low frequency ocean ambient noise: measurements and theory. In *Sea Surface Sound: Natural Mechanisms of Surface Generated Noise in the Ocean*, ed. BR Kerman, pp. 361–76. Dordrecht: Kluwer

Carey WM, Evans RB. 2011. *Ocean Ambient Noise: Measurement and Theory*. New York: Springer

Carlson RL, Schafternaar CH, Moore RP. 1984. Causes of compressional-wave anisotropy in carbonate-bearing, deep-sea sediments. *Geophysics* 49:525–32

Castellote M, Clark CW, Lammers MO. 2011. Fin whale (*Balaenoptera physalus*) population identity in the western Mediterranean Sea. *Mar. Mamm. Sci.* 28:325–44

Castellote M, Clark CW, Lammers MO. 2012. Acoustic and behavioural changes by fin whales (*Balaenoptera physalus*) in response to shipping and airgun noise. *Biol. Conserv.* 147:115–22

Cato DH. 1976. Ambient sea noise in waters near Australia. *J. Acoust. Soc. Am.* 60:320–28

Cato DH. 1991. Theoretical and measured underwater noises from surface wave orbital motion. *J. Acoust. Soc. Am.* 89:1096–112

Chapman NR, Price A. 2011. Low frequency deep ocean ambient noise trend in the Northeast Pacific Ocean. *J. Acoust. Soc. Am.* 129:EL161–65

Chapp E, Bohnenstiehl DR, Tolstoy M. 2005. Sound-channel observations of ice-generated tremor in the Indian Ocean. *Geochem. Geophys. Geosyst.* 6:Q06003

Charif R, Mellinger D, Dunsmore K, Fristrup K, Clark C. 2002. Estimated source levels of fin whale (*Balaenoptera physalus*) vocalizations: adjustments for surface interference. *Mar. Mamm. Sci.* 18:81–98

Clark C, Ellison W, Southall B, Hatch L, Van Parijs SM, et al. 2009. Acoustic masking in marine ecosystems: intuitions, analysis, and implication. *Mar. Ecol. Prog. Ser.* 395:201–22

Clay CS, Medwin H. 1977. *Acoustical Oceanography: Principles and Applications*. New York: Wiley & Sons

Collins MD, Coury RA, Siegmann WL. 1995. Beach acoustics. *J. Acoust. Soc. Am.* 97:2767–70

Colton T. 2010. *Growth of the world fleet*. **http://www.shipbuildinghistory.com/today/statistics/wldfltgrowth.htm**

Cowen JP, Baker ET, Embley RW. 2004. Detection of and response to mid-ocean ridge magmatic events: implications for the subsurface biosphere. In *The Subsurface Biosphere at Mid-Ocean Ridges*, ed. WSD Wilcock, EF DeLong, DS Kelley, JS Baross, SC Cary, pp. 227–43. Washington, DC: Am. Geophys. Union

Croll DA, Clark CW, Acevedo A, Tershy B, Flores S, et al. 2002. Only male fin whales sing loud songs. *Nature* 417:809

Cummings W, Thompson P. 1971. Underwater sounds from the blue whale, *Balaenoptera musculus*. *J. Acoust. Soc. Am.* 50:1193–98

Cummings WC, Thompson PO, Ha SJ. 1986. Sounds from Bryde, *Balaenoptera edeni*, and finback, *B. physalus*, whales in the Gulf of California. *Fish. Bull.* 84:359–70

Cuyvers L. 1984. *Ocean Uses and Their Regulation*. New York: Wiley & Sons

Deane G. 1997. Sound generation and air entrainment by breaking waves in the surf zone. *J. Acoust. Soc. Am.* 102:2671–99

de Groot-Hedlin CD, Orcutt JA. 2001a. Excitation of T-phases by seafloor scattering. *J. Acoust. Soc. Am.* 109:1944–54

de Groot-Hedlin CD, Orcutt JA. 2001b. T-phase observations in northern California: acoustic to seismic coupling at a weakly elastic boundary. *Pure Appl. Geophys.* 158:513–30

Delaney JR, Kelley DS. 2014. Next-generation science in the ocean basins: expanding the oceanographer's tool-box utilizing submarine electro-optical sensor networks. In *Seafloor Observatories: A New Vision of the Earth from the Abyss*, ed. P Favali, A de Santis, L Beranzoli. Chichester, UK: Springer Praxis. In press

Delaney JR, Kelley DS, Lilley MD, Butterfield DA, Baross JA, et al. 1998. The quantum event of oceanic crustal accretion: impacts of diking at mid-ocean ridges. *Science* 281:222–30

Delarue J, Todd SK, Van Parijs SM, Di Iorio L. 2009. Geographic variation in Northwest Atlantic fin whale (*Balaenoptera physalus*) song: implications for stock structure assessment. *J. Acoust. Soc. Am.* 125:1774–82

Di Iorio L, Clark CW. 2010. Exposure to seismic survey alters blue whale acoustic communication. *Biol. Lett.* 6:51–54

Dorman LD, Schreiner AE, Bibee LD, Hildebrand JA. 1993. Deep water seafloor array observations of seismo-acoustic noise in the eastern Pacific and comparisons with wind and swell. In *Natural Physical Sources of Underwater Sound: Sea Surface Sound (2)*, ed. BR Kerman, pp. 165–74. Norwell, MA: Kluwer

Duennebier FK, Lukas R, Nosal E, Aucan J, Weller R. 2012. Wind, waves and acoustic background levels at Station ALOHA. *J. Geophys. Res.* 117:C03017

Dunn RA, Hernandez O. 2009. Tracking blue whales in the eastern tropical Pacific with an ocean-bottom seismometer and hydrophone array. *J. Acoust. Soc. Am.* 126:1084–94

Dushaw BD, Howe BM, Mercer JA, Spindel RC, Baggeroer AB, et al. 1999. Multimegameter-range acoustic data obtained by bottom-mounted hydrophone arrays for measurement of ocean temperature. *IEEE J. Ocean. Eng.* 24:202–14

Dyer I. 1988. Arctic ambient noise: ice source mechanics. *J. Acoust. Soc. Am.* 84:1941–42

Dziak RP, Bohnenstiehl DR, Smith DK. 2012. Hydroacoustic monitoring of oceanic spreading centers. *Oceanography* 25(1):116–27

Dziak RP, Hammond SR, Fox CG. 2011. A 20-year hydroacoustic series of seismic and volcanic events in the northeast Pacific Ocean. *Oceanography* 24(3):280–93

Emery L, Bradley M, Hall T. 2001. *Database Description (DBD) for the Historical Temporal Shipping Database Variable Resolution (HITS), Version 4.0*. PSI Tech. Rep. TRS-301, Plan. Syst. Inc., Slidell, LA

Erbe C. 2009. Underwater noise from pile driving in Moreton Bay, Qld. *Acoust. Aust.* 37:87–92

Etter P. 2003. *Underwater Acoustic Modeling and Simulation*. London: Spon. 3rd ed.

Ewing J, Carter JA, Sutton GH, Barstow N. 1992. Shallow-water sediment properties derived from high-frequency shear and interface waves. *J. Geophys. Res.* 97:4739–62

Farmer DM, Vagle S, Booth AD. 1998. A free-flooding acoustical resonator for measurement of bubble size distributions. *J. Atmos. Ocean. Technol.* 15:1132–46

Farmer DM, Xie Y. 1989. The sound generated by propagating cracks in sea ice. *J. Acoust. Soc. Am.* 85:1489–500

Farrell WE, Munk WH. 2013. Surface gravity-waves and their acoustic signatures, 1–30 Hz, on the mid-Pacific sea floor. *J. Acoust. Soc. Am.* 134:3134–43

Flatté SM, Dashen R, Munk WH, Watson KM, Zachariasen F. 1979. *Sound Transmission Through a Fluctuating Ocean*. Cambridge, UK: Cambridge Univ. Press

Fox CG, Dziak RP, Matsumoto H, Schreiner AE. 1994. Potential for monitoring low-level seismicity on the Juan de Fuca Ridge using military hydrophone arrays. *Mar. Technol. Soc. J.* 27(4):22–30

Fox CG, Hammond SR. 1994. The VENTS Program T-phase project and NOAA's role in ocean environmental research. *Mar. Technol. Soc. J.* 27(4):70–74

Fox CG, Radford WE, Dziak RP, Lau T-K, Matsumoto H, Schreiner AE. 1995. Acoustic detection of a seafloor spreading episode on the Juan de Fuca Ridge using military hydrophone arrays. *Geophys. Res. Lett.* 22:131–34

Frankel AS, Clark CW. 1998. Results of low-frequency playback of M-sequence noise to humpback whales, *Megaptera novaeangliae*, in Hawai'i. *Can. J. Zool.* 76:521–35

Frankel AS, Clark CW. 2000. Behavioral responses of humpback whales (*Megaptera novaeangliae*) to full-scale ATOC signals. *J. Acoust. Soc. Am.* 108:1930–37

Frisk GV. 2012. Noiseonomics: the relationship between ambient noise levels in the sea and global economic trends. *Sci. Rep.* 2:437

Gavrilov AN, McCauley RD, Gedamke J. 2012. Steady inter and intra-annual decrease in the vocalization frequency of Antarctic blue whales. *J. Acoust. Soc. Am.* 131:4476–80

Gavrilov I, Li B. 2008. Long-term variations of ice breaking noise in Antarctica. *J. Acoust. Soc. Am.* 123:2989 (Abstr.)

Godin O. 1998. A note on differential equations of coupled-mode propagation in fluids. *J. Acoust. Soc. Am.* 103:159–68

Hanson J, Le Bras R, Dysart P, Brumbaugh D, Gault A, Guern J. 2001. Operational processing of hydroacoustics at the prototype international data center. *Pure Appl. Geophys.* 158:425–56

Hatch LT, Clark CW, Van Parijs SM, Frankel AS, Ponirakis DW. 2012. Quantifying loss of acoustic communication space for right whales in and around a U.S. national marine sanctuary. *Conserv. Biol.* 26:983–94

Haxel JH, Dziak RP, Matsumoto H. 2013. Observations of shallow water marine ambient sound: the low frequency underwater soundscape of the central Oregon coast. *J. Acoust. Soc. Am.* 133:2586–96

Holland CW. 2010. Propagation in a waveguide with range-dependent seabed properties. *J. Acoust. Soc. Am.* 128:2596–609

Ikelle L, Amundsen L. 2005. *Introduction to Petroleum Seismology*. Tulsa, OK: Soc. Explor. Geophys

Int. Marit. Organ. 2011. *International shipping facts and figures—information resources on trade, safety, security, environment*. Rep., Int. Marit. Organ., London

Johnson BD, Cooke RC. 1979. Bubble populations and spectra in coastal water: a photographic approach. *J. Geophys Res.* 84:3761–66

Johnson RH, Northrop J, Eppley R. 1963. Sources of Pacific T-phases. *J. Geophys. Res.* 68:4251–60

Kasahara J, Iwase R, Nakatsuka T, Nagaya Y, Shirasaki Y, et al. 2006. An experimental multi-disciplinary observatory (VENUS) at the Ryukyu trench using the Guam-Okinawa geophysical submarine cable. *Ann. Geophys.* 49:595–606

Kawaguchi K, Kaneda Y, Araki E. 2008. The DONET: a real-time seafloor research infrastructure for the precise earthquake and tsunami monitoring. In *OCEANS 2008: MTS/IEEE Kobe Techno-Ocean*, Kobe, Japan, April 8–11. Piscataway, NJ: Inst. Electr. Electron. Eng. **http://ieeexplore.ieee.org/xpl/articleDetails.jsp?arnumber=4530918**

Koch RA, Penland C, Vidmar PJ, Hawker KE. 1983. On the calculation of normal mode group-velocity and attenuation. *J. Acoust. Soc. Am.* 73:820–25

Koesoemadinata AP, McMechan GA. 2004. Effects of diagenetic processes on seismic velocity anisotropy in near-surface sandstone and carbonate rocks. *J. Appl. Geophys.* 56:165–76

Leigh CV, Eller AI. 2008. *Dynamic ambient noise model comparison with Point Sur, California, in situ data*. Tech. Memo. APL-UW TM 2-06, Appl. Phys. Lab., Univ. Wash., Seattle

Lewis JK, Denner WW. 1988. Arctic ambient noise in the Beaufort Sea: seasonal relationships to sea ice kinematics. *J. Acoust. Soc. Am.* 83:549–65

Longuet-Higgins MS. 1950. A theory for the generation of microseisms. *Philos. Trans. R. Soc. Lond. A* 24:1–35

Martin BE, Thomson CJ. 1997. Modelling surface waves in anisotropic structures II: examples. *Phys. Earth Planet.Inter.* 103:253–97

McCreery CS, Duennebier FK, Sutton GH. 1993. Correlation of deep ocean noise (0.4–30 Hz) with wind, and the Holu spectrum—a worldwide constant. *J. Acoust. Soc. Am.* 93:2639–48

McDonald MA, Hildebrand JA, Mesnick S. 2009. Worldwide decline in tonal frequencies of blue whale songs. *Endanger. Species Res.* 9:13–21

McDonald MA, Hildebrand JA, Webb SC. 1995. Blue and fin whales observed on a seafloor array in the Northeast Pacific. *J. Acoust. Soc. Am.* 98:712–21

McDonald MA, Hildebrand JA, Wiggins SM. 2006. Increases in deep ocean ambient noise in the Northeast Pacific west of San Nicolas Island, California. *J. Acoust. Soc. Am.* 120:711–18

McGuire JJ, Collins JA, Gouedard P, Roland E, Lizarralde D, et al. 2012. Capturing the end of a seismic cycle on the Gofar Transform Fault. *Nat. Geosci.* 5:336–41

McKenna MF, Katz SL, Wiggins SM, Ross D, Hildebrand JA. 2012a. A quieting ocean: unintended consequence of a fluctuating economy. *J. Acoust. Soc. Am.* 132:169–75

McKenna MF, Ross D, Wiggins SM, Hildebrand JA. 2012b. Underwater radiated noise from modern commercial ships. *J. Acoust. Soc. Am.* 131:92–103

Mikhalevsky PN, Gavrilov AN. 2001. Acoustic thermometry in the Arctic Ocean. *Polar Res.* 20:185–92

Mikhalevsky PN, Gavrilov AN, Baggeroer AB. 1999. The Transarctic Acoustic Propagation Experiment and climate monitoring in the Arctic. *IEEE J. Ocean. Eng.* 24:183–201

Minnaert M. 1933. On musical air bubbles and the sounds of running water. *Philos. Mag.* 16:235–48

Mobley JR. 2005. Assessing responses of humpback whales to North Pacific Acoustic Laboratory (NPAL) transmissions: results of 2001–2003 aerial surveys north of Kauai. *J. Acoust. Soc. Am.* 117:1666–73

Munk WH, Forbes AMG. 1989. Global ocean warming: an acoustic measure? *J. Phys. Oceanogr.* 19:1765–78

Munk WH, Worcester P, Wunsch C. 1995. The forward problem: range-independent. In *Ocean Acoustic Tomography*, pp. 30–114. Cambridge, UK: Cambridge Univ. Press

Natl. Ocean. Atmos. Adm. 2012. *Mapping cetaceans and sound: modern tools for ocean management.* Symp. Final Rep., Natl. Ocean. Atmos. Adm., Washington, DC. **http://cetsound.noaa.gov/pdf/ CetSound_Symposium_Report_Final.pdf**

Nieukirk SL, Mellinger DK, Moore SE, Klinck K, Dziak RP, Goslin J. 2012. Sounds from airguns and fin whales recorded in the mid-Atlantic Ocean, 1999–2009. *J. Acoust. Soc. Am.* 131:1102–12

Nieukirk SL, Stafford KM, Mellinger DK, Dziak RP, Fox CG. 2004. Low-frequency whale and seismic airgun sounds recorded in the mid-Atlantic Ocean. *J. Acoust. Soc. Am.* 115:1832–43

Nishimura CE, Conlon DM. 1994. IUSS dual use: monitoring whales and earthquakes using SOSUS. *Mar. Technol. Soc. J.* 27(4):13–21

Nolet G, Dorman LM. 1996. Waveform analysis of Scholte modes in ocean sediment layers. *Geophys. J. Int.* 125:385–96

Offshore. 2012. Worldwide seismic vessel survey. *Offshore* 72(3):36–41

Okal A. 2008. The generation of *T* waves by earthquakes. *Adv. Geophys.* 49:1–65

Oleson EM, Barlow J, Gordon J, Rankin S, Hildebrand JA. 2003. Low frequency calls of Bryde's whales. *Mar. Mamm. Sci.* 19:407–19

Oleson EM, Calambokidis J, Burgess WC, McDonald MA, LeDuc CA, Hildebrand JA. 2007. Behavioral context of call production by eastern North Pacific blue whales. *Mar. Ecol. Prog. Ser.* 330:269–84

Park J. 1996. Surface waves in layered anisotropic structures. *Geophys. J.Int.* 126:173–83

Park M, Odom RI, Soukup DJ. 2001. Modal scattering: a key to understanding oceanic T-waves. *Geophys. Res. Lett.* 28:3401–4

Payne RR, Webb DD. 1971. Orientation by means of long range acoustic signaling in baleen whales. *Ann. N. Y. Acad. Sci.* 188:110–41

Porter MB, Henderson LJ. 2013. Global ocean soundscapes. *Proc. Meet. Acoust.* 19:010050

Priede IJ, Solan M, eds. 2002. *ESONET: European Seafloor Observatory Network.* Rep. EVK3-EVK3-CT-2002-80008, Univ. Aberdeen, Aberdeen, UK

Rankin S, Barlow J. 2007. Vocalizations of the sei whale *Balaenoptera borealis* off the Hawaiian Islands. *Bioacoustics* 16:137–45

Rebull OG, Cusi JD, Fernandez MR, Muset JG. 2006. Tracking fin whale calls offshore the Galacia Margin, NE Atlantic Ocean. *J. Acoust. Soc. Am.* 120:2077–85

Reinhall PG, Dahl PH. 2011. Underwater Mach wave radiation from impact pile driving: theory and observation. *J. Acoust. Soc. Am.* 130:1209–16

Rolland RM, Parks SE, Hunt KE, Castellote M, Corkeron PJ, et al. 2012. Evidence that ship noise increases stress in right whales. *Proc. R. Soc. B* 279:2363–68

Ross DG. 1976. *Mechanics of Underwater Noise*. New York: Pergamon

Ross DG. 1993. On ocean underwater ambient noise. *Acoust. Bull.* 18:5–8

Roth E, Hildebrand J, Wiggins S, Ross D. 2012. Underwater ambient noise on the Chukchi Sea continental slope from 2006–2009. *J. Acoust. Soc. Am.* 131:104–10

Scholte JG. 1947. Range of existence of Rayleigh and Stoneley waves. *Geophys. J. Int.* (Suppl. S5) 5:120–26

Shearer PM. 2009. *Introduction to Seismology*. New York: Cambridge Univ. Press. 2nd ed.

Sheriff RE, Geldart LP. 1995. *Exploration Seismology*. New York: Cambridge Univ. Press. 2nd ed.

Simon M, Stafford KM, Beedholm K, Lee CM, Madsen PT. 2010. Singing behavior of fin whales in the Davis Strait with implications for mating, migration and foraging. *J. Acoust. Soc. Am.* 128:3200–10

Širović A, Hildebrand JA, Wiggins SM. 2007. Blue and fin whale call source levels and propagation range in the Southern Ocean. *J. Acoust. Soc. Am.* 122:1208–15

Širović A, Hildebrand JA, Wiggins SM, Thiele D. 2009. Blue and fin whale acoustic presence around Antarctica during 2003 and 2004. *Mar. Mamm. Sci.* 25:125–36

Smith KB, Brown MG, Tappert FD. 1992. Ray chaos in underwater acoustics. *J. Acoust. Soc. Am.* 91:1939–49

Soukup DJ, Odom RI, Park J. 2013. A modal investigation of elastic anisotropy in shallow water environments: a study of anisotropy beyond VTI. *J. Acoust. Soc. Am.* 134:185–207

Soule DC, Wilcock WSD. 2012. Fin whale tracks recorded by a seismic network on the Juan de Fuca Ridge, Northeast Pacific Ocean. *J. Acoust. Soc. Am.* 133:1751–61

Stafford KM, Chapp E, Bohnenstiel DR, Tolstoy M. 2011. Seasonal detection of three types of "pygmy" blue whale calls in the Indian Ocean. *Mar. Mamm. Sci.* 27:828–40

Stafford KM, Nieukirk SL, Fox CG. 2001. Geographic and seasonal variation of blue whale calls in the North Pacific. *J. Cetacean Res. Manag.* 3:65–76

Stoll RD, Bryan GM, Bautista EO. 1994. Measuring lateral variability of sediment geoacoustic properties. *J. Acoust. Soc. Am.* 96:427–38

Stone RG, Mintzer D. 1962. Experimental study of high-frequency sound propagation in a randomly inhomogeneous medium. *J. Acoust. Soc. Am.* 34:735–36

Talandier J, Hyvernaud O, Okal EA. 2002. Long-range detection of hydroacoustic signals from large icebergs in the Ross Sea, Antarctica. *Earth Planet. Sci. Lett.* 203:519–34

Talandier J, Hyvernaud O, Reymond D, Okal EA. 2006. Hydroacoustic signals generated by parked and drifting icebergs in the Southern Indian and Pacific Oceans. *Geophys. J. Int.* 165:817–34

Tanner G, Sondergaard N. 2007. Wave chaos in acoustics and elasticity. *J. Phys. A* 40:R443–509

Thode AM, D'Spain GL, Kuperman WA. 2000. Matched-field processing, geoacoustic inversion, and source signature recovery of blue whale vocalizations. *J. Acoust. Soc. Am.* 107:1286–300

Tolstoy M, Cowen JP, Baker ET, Fornari DJ, Fubin KH, et al. 2006. A seafloor spreading event captured by seismometers. *Science* 314:1920–22

Tolstoy M, Diebold J, Doermann L, Nooner S, Webb SC. 2009. Broadband calibration of the R/V *Marcus G. Langseth* four-string seismic sources. *Geochem. Geophys. Geosyst.* 10:Q08011

Tougaard J, Henriksen OD, Miller LA. 2009. Underwater noise from three types of offshore wind turbines: estimation of impact zones for harbor porpoises and harbor seals. *J. Acoust. Soc. Am.* 25:3766–73

Urick RJ. 1983. *Principles of Underwater Sound*. New York: McGraw-Hill. 3rd ed.

Valcke SLA, Casey M, Lloyd GE, Kendall J-M, Fisher QJ. 2006. Lattice preferred orientation and seismic anisotropy in sedimentary rocks. *Geophys. J. Int.* 166:652–66

Virovlyansky AL. 2008. Ray chaos in underwater acoustic waveguides. *Int. J. Bifurc. Chaos* 18:2693–700

Walbridge S. 2013. *Assessing ship movements using volunteered geographic information*. PhD thesis, Univ. Calif., Santa Barbara

Wales SC, Heitmeyer RM. 2002. An ensemble source spectra model for merchant ship-radiated noise. *J. Acoust. Soc. Am.* 111:1211–31

Walker DA. 1981. High-frequency Pn,Sn velocities: some comparisons for the western, central, and south Pacific. *Geophys. Res. Lett.* 8:207–9

Walker DA, McCreery CS, Sutton GH. 1983. Spectral characteristics of high-frequency P_N, S_N phases in the western Pacific. *J. Geophys. Res.* 88:4289–98

Watkins WA. 1981. Activities and underwater sounds of fin whales [*Balaenoptera physalus*]. *Sci. Rep. Whales Res. Inst.* 33:83–117

Watkins WA, Tyack P, Moore K, Bird J. 1987. The 20-Hz signals of finback whales (*Balaenoptera physalus*). *J. Acoust. Soc. Am.* 82:1901–12

Webb SC. 1998. Broadband seismology and noise under the ocean. *Rev. Geophys.* 36:105–42

Weekly RT, Wilcock WSD, Hooft EEE, Toomey DR, McGill PR, Stakes DS. 2013. Termination of a decadal-scale ridge-spreading event observed using a seafloor seismic network on the Endeavour segment, Juan de Fuca Ridge. *Geochem. Geophys. Geosyst.* In press

Weirathmueller MJ, Wilcock WSD, Soule DC. 2013. Source levels of fin whale 20 Hz pulses measured in the Northeast Pacific Ocean. *J. Acoust. Soc. Am.* 133:741–49

Wenz GM. 1962. Acoustic ambient noise in the ocean: spectra and sources. *J. Acoust. Soc. Am.* 34:1936–56

Wilcock WSD, Webb SC, Bjarnason IT. 1999. The effect of local wind on seismic noise near 1 Hz at the MELT site and in Iceland. *Bull. Seismol. Soc. Am.* 89:1543–57

Worcester PF, Spindel RC. 2005. North Pacific Acoustic Laboratory. *J. Acoust. Soc. Am.* 117:1499–510

Yoon SW, Crum LA, Prosperetti A, Lu NQ. 1991. An investigation of the collective oscillation of a bubble cloud. *J. Acoust. Soc. Am.* 89:700–6

Zampolli M, Nijhof MJJ, de Jong CAF, Ainslie MA, Jansen EHW, Quesson BAJ. 2012. Validation of finite element computations for the quantitative prediction of underwater noise from impact pile driving. *J. Acoust. Soc. Am.* 133:72–81

Contents

Errata

An online log of corrections to *Annual Review of Marine Science* articles may be found at
http://www.annualreviews.org/errata/marine

International Quiet Ocean Experiment Science Plan, edited by Peter Tyack, George Frisk, Ian Boyd, Ed Urban, and Sophie Seeyave
published jointly by the Scientific Committee on Oceanic Research (SCOR) and the
Partnership for Observation of the Global Oceans (POGO).

INTERNATIONAL QUIET OCEAN EXPERIMENT
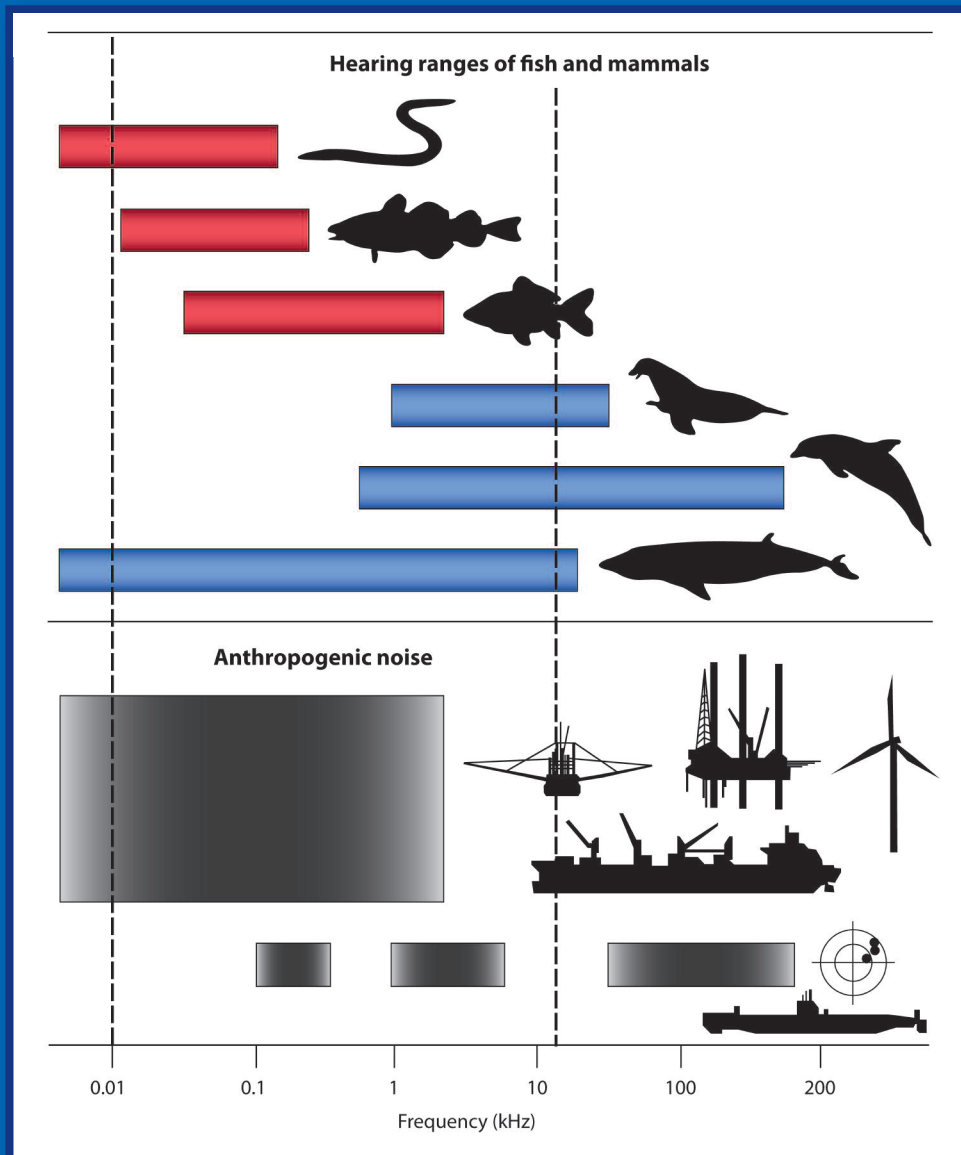
Science Plan

EDITED BY
Peter Tyack • George Frisk • Ian Boyd
Ed Urban • Sophie Seeyave

International Quiet Ocean Experiment
Science Plan

Editors: Peter Tyack, George Frisk, Ian Boyd,
Ed Urban, Sophie Seeyave

Preface

This Science Plan for an International Quiet Ocean Experiment (IQOE) is the result of a series of discussions that started at the joint meeting of the Scientific Committee on Oceanic Research (SCOR) and the Ocean Studies Board of the U.S. National Research Council in October 2008 at the Woods Hole Oceanographic Institution. At that meeting, Jesse Ausubel of the Alfred P. Sloan Foundation posed the question about what might be observed in the behavior of animals in the ocean if all human-generated sound in the ocean were stopped for some period. Ausubel expanded on his ideas in a November 2009 article in *SEED Magazine*:

> *I propose that scientists, environmentalists, and maritime industries organize an International Quiet Ocean Experiment in which humans refrain from adding noise to the oceans for a few hours. Because of the speed sound spreads in sea water, we might, fortunately, need to turn down the volume globally for only four hours or so to achieve a great diminuendo. During this time researchers would observe the behavior of many forms of life in the ocean that might respond to the quiet change.* (JH Ausubel. Broadening the scope of global change to include illumination and noise. *SEED Magazine* 23 Nov. 2009)

Through funding from the Sloan Foundation, Ausubel helped SCOR and the Partnership for Observation of the Global Oceans (POGO) convene an international workshop of ocean acousticians and marine mammal scientists at the University of Rhode Island (URI, USA) in October 2010, led by Ian Boyd (University of St. Andrews, UK) and George Frisk (Florida Atlantic University/Woods Hole Oceanographic Institution, USA). Participants at the URI meeting concluded that, although it was probably not feasible to turn off sound in the ocean for any significant period, an international project on sound in the ocean and its effects on marine organisms is needed to help document ocean sound as a form of global change with widespread impacts. The results of the URI meeting were presented in a paper in *Oceanography* magazine (Boyd et al. 2011. An International Quiet Ocean Experiment. *Oceanography* 24(2):174–181, doi:10.5670/oceanog.2011.37.)

One conclusion of the URI meeting was that it would be important to gather ideas and input from the broader community of scientists, navies, industry, and others at an open meeting. The Intergovernmental Oceanographic Commission hosted an open science meeting at its headquarters in Paris, France, in August 2011. This Science Plan is a distillation of the discussions at that meeting.

The scientific community, SCOR, and POGO owe a debt of gratitude to Jesse Ausubel, the Alfred P. Sloan Foundation, the Intergovernmental Oceanographic Commission, and academic and governmental institutions that made this Science Plan possible. We also thank Ed Urban (SCOR Executive Director) and Sophie Seeyave (POGO Executive Director) for the excellent staff support they have provided in the development of this IQOE Science Plan.

Peter Burkill
SCOR President

Karen Wiltshire
POGO Chair

Table of Contents

Chapter 1
Executive Summary

The International Quiet Ocean Experiment (IQOE) will create an international program of research, observation, and modeling to better characterize ocean sound fields and to promote understanding of the effects of sound on marine life. Our current knowledge is inadequate in relation to the effects of anthropogenic sound[1] on marine life; the resulting scientific uncertainty makes it difficult to balance the need for precaution in protecting marine ecosystems against the potentially large costs to socially important activities such as commercial shipping, offshore energy exploration and development, and military readiness.

A central feature of the IQOE will be an International Year of the Quiet Ocean (IYQO), which will focus the participating scientific, industrial, environmental, and naval communities on the goal of an intense period of scientific activity, coordinated across regions to create a global program. The IYQO will raise awareness of the effects of sound in the ocean within the participating communities and in the public realm. The IQOE aims to study effects of sound from an ecosystem perspective and longer time scale than most ongoing research. The project will focus broadly on soundscapes, defined by acoustic ecologists as all the sounds present in a habitat.

The IQOE will address five fundamental questions:

1. How have human activities affected the global ocean soundscape compared with natural changes over geologic time?
2. What are the current levels and distribution of anthropogenic sound in the ocean?
3. What are the trends in anthropogenic sound levels across the global ocean?
4. What are the current effects of anthropogenic sound on important marine animal populations?
5. What are the potential future effects of sound on marine life?

The IQOE is a response to evidence of increasing sound levels in the ocean from human activities. The human contribution to ocean sound has increased during the past few decades and anthropogenic sound has become the dominant component of marine sound in some frequency bands and geographic regions. Anthropogenic sound levels will increase as the ocean becomes more industrialized, thus making the measurement of ocean sound fields an important tool for assessing industrial presence in the ocean.

Sound is an important factor in the lives of many marine organisms. Evidence is accumulating that human-generated sound in the ocean is approaching levels that cause negative effects on marine life. Certain species already show symptoms of the effects of sound. Although some of these effects are acute, such as lethal strandings of beaked whales exposed to naval sonar, chronic sublethal effects may be more prevalent and therefore more important for populations, but are difficult to measure.

The IQOE will mobilize the participating communities to investigate sound in the ocean in a way that will be useful for management of sound sources to mitigate harm to marine life. The IQOE will (1) ensure that the measurement of the sound field becomes an integrated part of global ocean observations; (2) develop a global approach to investigating ocean sound, engaging the worldwide community of ocean scientists; (3) support innovation in passive ocean observing systems to detect, classify, and track marine organisms;

---

[1]*Throughout this document we usually use the term "sound" instead of the term "noise"; the term "noise" is used when the source of sound cannot be identified, or in contexts emphasizing the contrast between a "signal" and background "noise."*

(4) support data management and the development of data standards; (5) develop models of how sound travels in the ocean; (6) support the planning and implementation of regional experiments; and (7) ensure constructive engagement with industry, regulators, nongovernmental organizations, and the public.
To achieve these goals, the activities of the IQOE are planned around four themes:

Theme 1 - Ocean Soundscapes: Projects carried out under Theme 1 will describe *ocean soundscapes* from regional to global scales. This theme will include identification of the primary sound sources that contribute to each soundscape, empirical modeling of components of each soundscape, modeling of acoustic propagation, and validation of these models using ocean observation systems. This theme will be the main focus of efforts to measure trends in ocean sound levels and to define sound budgets within regions. It will also investigate soundscape diversity and examine the concept that the conservation of soundscapes may be an appropriate objective for integrated management of the marine environment.

Theme 2 - Effects of Sound on Marine Organisms: Theme 2 includes projects designed to plan and carry out experiments to study *the effects of sound on marine organisms.* This may include experiments to make regions quieter and to observe the responses of marine organisms to quieting. This theme will include the use of planned experiments as well as opportunistic studies using post hoc statistical modeling to test for effects. This theme is the main vehicle through which the biological significance of sound will be assessed and, where possible, this will be focused on estimating dose–response relationships so that assessments of the effects of sound can be predictive, with special emphasis on the effects of sound on populations and ecosystems. Much of this theme will rely on the use of a small set of representative species.

Theme 3 - Observations of Sound in the Ocean: *Observing sound in the ocean* will be the focus of work done under Theme 3 to coordinate and standardize existing acoustic observing systems, while adding sound measurements to existing and future observing systems, and to encourage technical innovation in the measurement of sound. This theme will develop data standards—where these do not already exist—and will promote observation of the key biological and physical variables. Much of the data management needed by the IQOE will be managed from within this theme.

Theme 4 – Industry and Regulation: Theme 4 develops the methodology for noise monitoring within regulatory regimes. This theme will include efforts to examine the operational management of sound in the ocean through risk analysis by, among other approaches, defining appropriate thresholds for disturbance, damage to marine life, and harm to marine ecosystems. It will also help regulators to measure compliance, and industry to maintain its activities, by providing innovative solutions to problems presented by regulation. This theme will integrate and apply the results from the other three themes.

Each of these four themes is important in preparations for the IYQO.

The IQOE will be implemented under the governance of the Scientific Committee on Oceanic Research (SCOR) and the Partnership for Observation of the Global Oceans (POGO). A Scientific Steering Committee will manage the project with the support of a secretariat. Working groups will be established to ensure that IQOE themes are implemented and to plan and implement particular activities. The Steering Committee will be responsible for international planning and coordination of contributing national activities funded from national sources over a period of at least 10 years. The IQOE will plan a series of workshops in its first three years, which will lay the foundation for IQOE implementation. Particular emphasis in the early years of the project will be given to characterizing global trends in ocean sound, gaining access to existing long time series of ocean sound, planning studies of effects, specifying standards for observations and experimentation, designing a data management system, and planning for pilot studies. As with other international research projects, the sponsors will seek funding for international planning and implementation, whereas it is expected that the national scientific communities interested in IQOE-related research and observations will solicit research funding from traditional national sources.

Chapter 2
Introduction and Overview

2.1 Purpose of the document

Underwater sound is important for many marine organisms. In general, marine species are more likely than terrestrial organisms to rely on sound to support life functions because the ocean is relatively opaque to light and is relatively transparent to sound. Ocean sound has many natural components, including naturally occurring events such as storms and breaking waves, the fracturing of sea ice, subsurface volcanoes and seismic activity, along with the calls and other sounds produced by a great variety of marine species. In the mid-19th century a new source of sound began to fill the ocean, driven by the rapid spread of mechanical propulsion in the shipping industry (Figure 2.1).
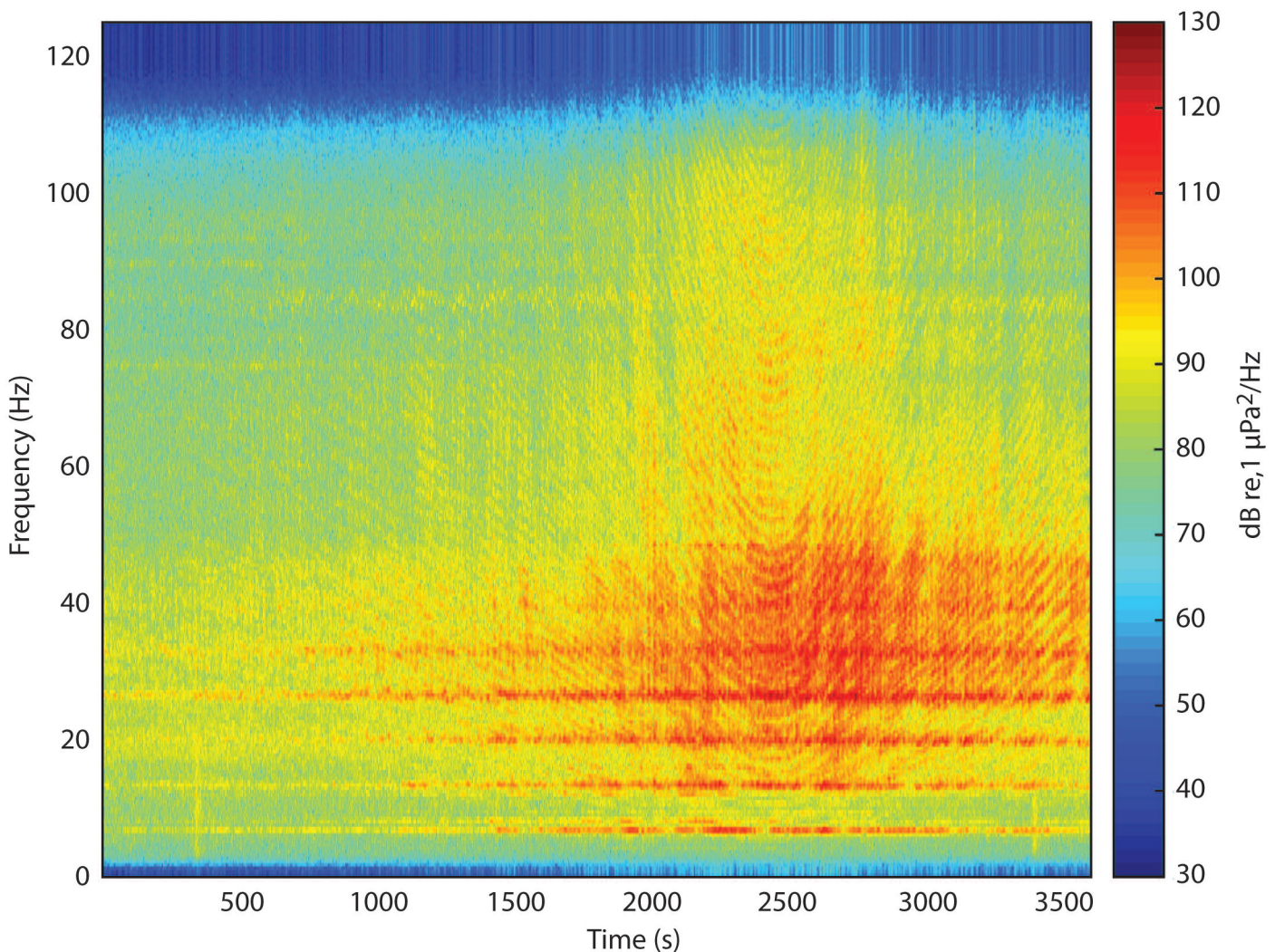
Figure 2.1. *Sound spectrogram of a large vessel passing by the Cape Leeuwin CTBTO observatory off southwestern Australia. Image courtesy of Centre for Marine Science and Technology, Curtin University, Perth, Western Australia.*

This human dimension to sound in the ocean is set against a backdrop of a complex natural sound field. For example, the deep ocean environment creates a sound channel (the SOFAR channel[2]) by which low-frequency acoustic waves can propagate over large distances, sometimes hundreds of kilometers and often much further (Figure 2.2). The multiple complex pathways taken by this sound affect the final received levels. When sound is averaged through time at the receiver, this provides an integrated signal defined by the relative locations of all the sound producers, the architecture of the ocean basin, and the properties of the water through which the sound has passed.
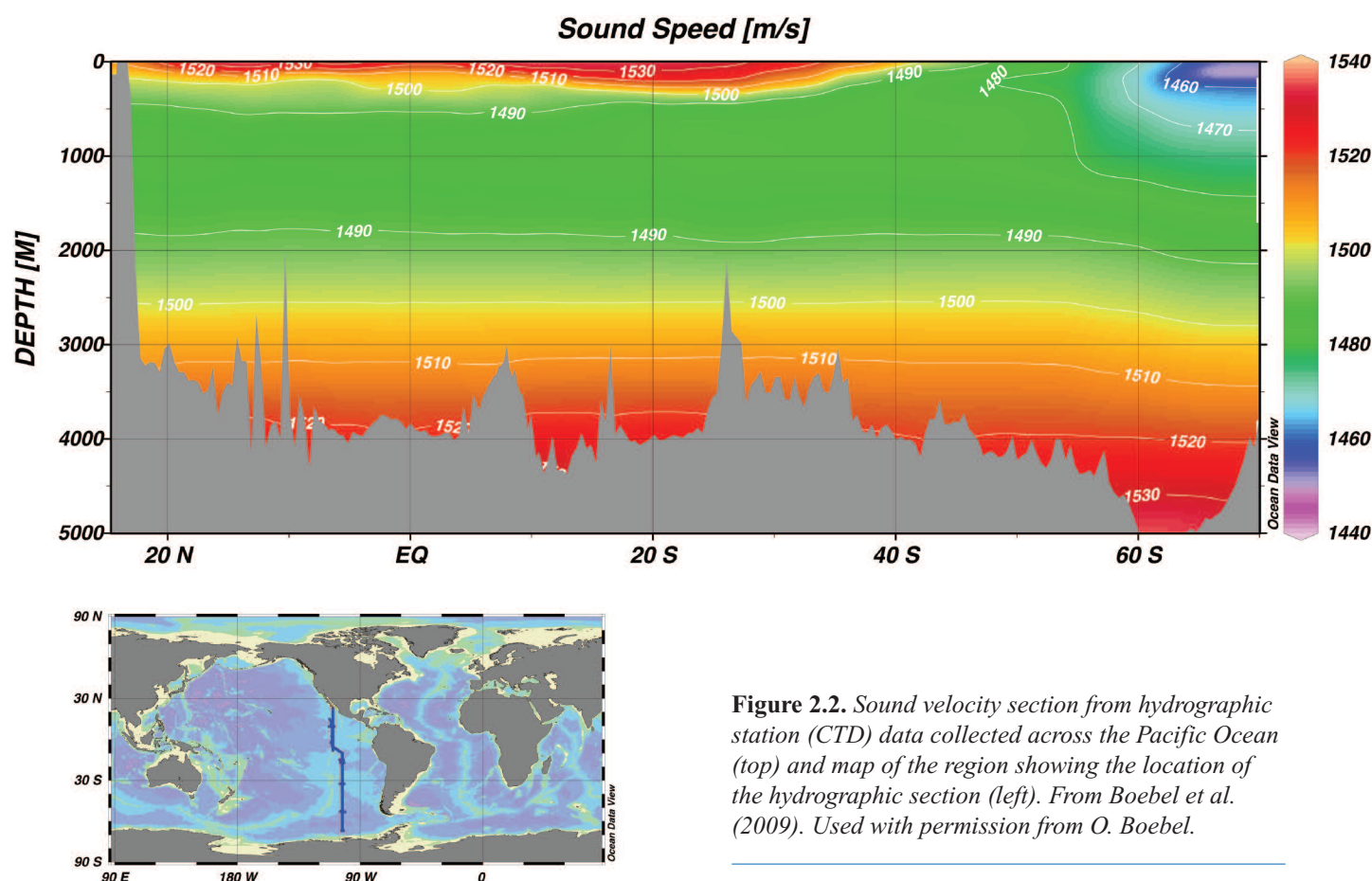
Figure 2.2. *Sound velocity section from hydrographic station (CTD) data collected across the Pacific Ocean (top) and map of the region showing the location of the hydrographic section (left). From Boebel et al. (2009). Used with permission from O. Boebel.*

The level of sound in the ocean may be linked to the global economy (Frisk, 2012). This is because most human activities in the ocean produce sound and many of these are increasing, including offshore construction, oil and gas exploration, fisheries, and recreational boating. Intense sound can have acute impacts on some animal life and it is assumed that low levels of continuous sound may lead to chronic effects, but little is known about the true extent of these chronic effects and whether they are likely to be a problem. However, if human activities resulting in increasing ocean sound levels continue on their current trajectory, they are likely to exceed thresholds of disturbance more often and in an increasing number of locations. Consequently, we can infer that chronic effects on marine life are likely to increase. This document develops the template for a global research project that will

---

[2] *The SOFAR channel is a horizontal layer of the ocean where sound speed is the slowest, because of the effects of temperature and pressure. Sound refracts toward areas of slower speed, so that sound, particularly low-frequency sound, can concentrate in this layer. In Figure 2.2, the SOFAR channel is roughly shown in green in the midlatitudes, with a shoaling (blue and purple colors) at higher latitudes.*

resolve the extent and significance of these effects and help to suggest mitigation approaches.

Human activity also has the potential to affect the levels of sound in the ocean in less direct ways. Intensive whaling and fishing have removed some biological producers of underwater sound, and global warming is altering the geographical distribution of other organisms. Some investigators have estimated that ocean warming has increased the strength and frequency of tropical storms (Knutson et al., 2010), which produce sound associated with rain, lightning, and breaking waves, and may influence the patterns of ice breaking in the polar regions. Even changes in the acidity of the ocean as it absorbs CO_2 affects its acoustic properties (Hester et al., 2008; Udovydchenkov et al., 2010), although there is still discussion of the magnitude of potential effects.

A scientific analysis of adverse effects from anthropogenic sound in the ocean is challenging because of the wide range of acoustic sources; variations in frequency, intensity, and occurrence; and the complexity of acoustic propagation, especially in strongly stratified and shallow waters. Even more significant is our ignorance of how animals respond behaviorally and physiologically to sound. Tackling the scientific problem of understanding underwater sound and its effects on organisms requires new interdisciplinary and international collaboration, and this document sets out how we are aiming to achieve this new objective.

The International Quiet Ocean Experiment (IQOE) provides a framework for a decade-long project of research, observations, and modeling, aimed at improving our understanding of generation, propagation, and reception of sound in the ocean and its effects on marine organisms. The project will include carefully designed observations exploiting situations of varying sound inputs in conjunction with detailed model analysis. The project will build toward a period of intensive study of sound in the ocean, an International Year of the Quiet Ocean (see Chapter 7).

2.2 Rationale for an IQOE

Benefits of an international program

A question often asked when planning international research projects regards the benefit of an international approach, instead of individual scientists and groups of scientists proceeding independently. There are many potential benefits of the IQOE:

1. IQOE will serve as a focal point to bring together a larger number of scientists and engineers to identify priority questions and promising approaches to answering the questions.

2. IQOE will provide a mechanism to bring together a critical mass of resources (expertise, equipment, finances) over an extended period to make progress on difficult observational, modeling, and research challenges.

3. IQOE will provide the necessity and resources for international standardization and intercalibrations for better comparison of the results of observations, modeling, and research worldwide.

4. IQOE will demonstrate the importance of ocean acoustics and biological effects to the public, managers, and policymakers.

5. IQOE will attract financial resources and staffing to provide critical infrastructural support for meeting planning, communication, development of scientific publications, and capacity building.

Scientific rationale

Does the sound made by humans harm marine life and, if so, how does it interact with other stresses resulting from human activities? At present, we can offer only preliminary answers to these important questions, and only for a few species. We know that as the ocean has become more industrialized, the sound levels associated with human activities have increased (NRC, 2003; Frisk, 2012). For example, in areas where measurements have been made (mainly off the west coast of North America), in the last three decades of the 20th century, anthropogenic sound in the ocean increased in the frequency range between 10 Hz and 200 Hz (Andrew et al., 2002; McDonald et al., 2008; Chapman and Price, 2011; Andrew et al., 2011) (Figure 2.3). However, given the spatial and temporal complexity and variability in sound sources, the relative contribution of anthropogenic sound is not always readily distinguishable. An intriguing feature of Figure 2.3 is the apparent leveling off or decrease of sound levels between 1995 and 2007 in this location. Research is needed to understand the cause of the decrease in this region, and to predict whether sound levels will begin increasing again.
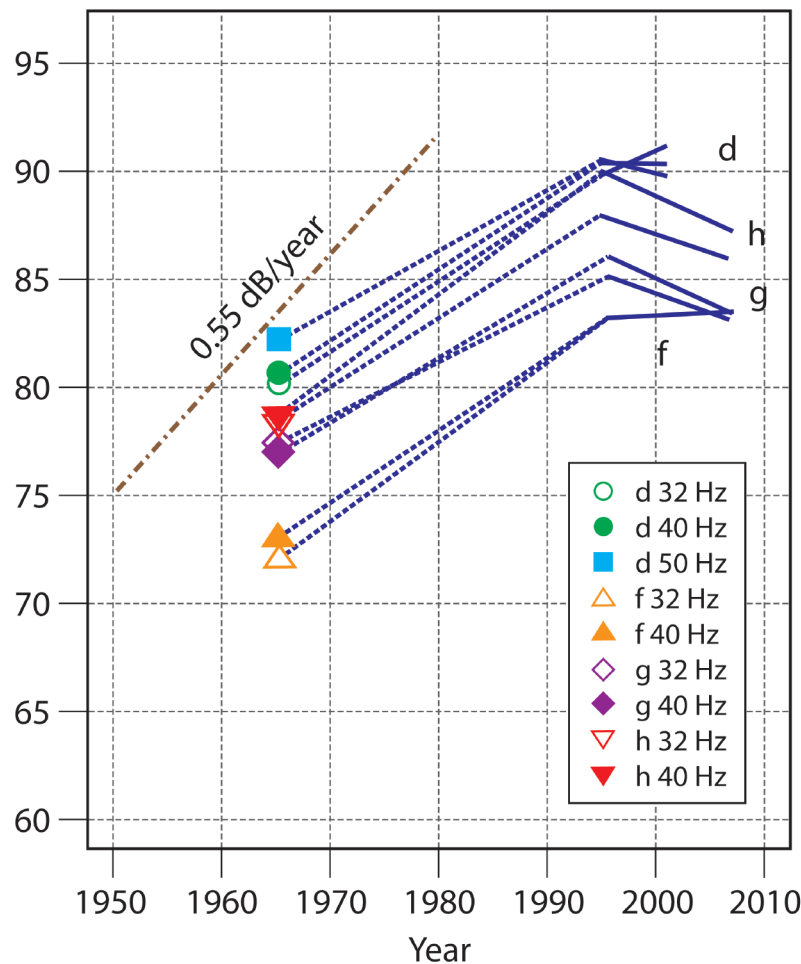
Figure 2.3. *Historical and contemporary shipping traffic sound levels along the west coast of North America from Andrew et al. (2011). Solid lines represent the trend lines fitted to the APL/UW data in Andrew et al. (2011), shown over the temporal span of the actual dataset. Thin dotted lines connect measurements for the same frequency band for each system. The heavy dashed line indicates the trend suggested by Ross (2005), which was based broadly on data from many systems in both the Atlantic and Pacific oceans, and not specifically on data from the systems used in Andrew et al. (2011). Reprinted with permission from R.K. Andrew, B.M. Howe, and J.A. Mercer. Copyright 2011, Acoustical Society of America.*

New sources of anthropogenic sound are being created. These include increasingly sophisticated sonar systems for characterizing the seabed, understanding the water column, and searching the ocean for hostile or lost vessels. They also include acoustic systems for geolocation and acoustic tomography used to study the physical properties of the ocean over very large scales. All of these add to new ship propulsion systems and to new technologies for drilling and mining in deep water to increase the potential challenges to marine life. Increasing our basic knowledge of the sensitivity of marine organisms to sound will allow more intelligent designs of these new technologies to minimize their impact on marine organisms.

The effect of sound on marine life is a knowledge gap in marine science. The human contribution to ocean sound has become the dominant component of the sound field in some marine environments (NRC, 2003; Hildebrand, 2009). Sound can strongly affect the lives of many marine organisms either because they have hearing sensitivity across a wide frequency range or because they produce sounds themselves. There is considerable overlap between the human contribution to ocean sound and the frequencies used by specific marine organisms (Figure 2.4). Theory and observations increasingly suggest that human sound could be approaching levels at which marine life may experience chronic negative effects (Rolland et al., 2012). We know the harmful levels for a few species, but have little information for the majority of species.
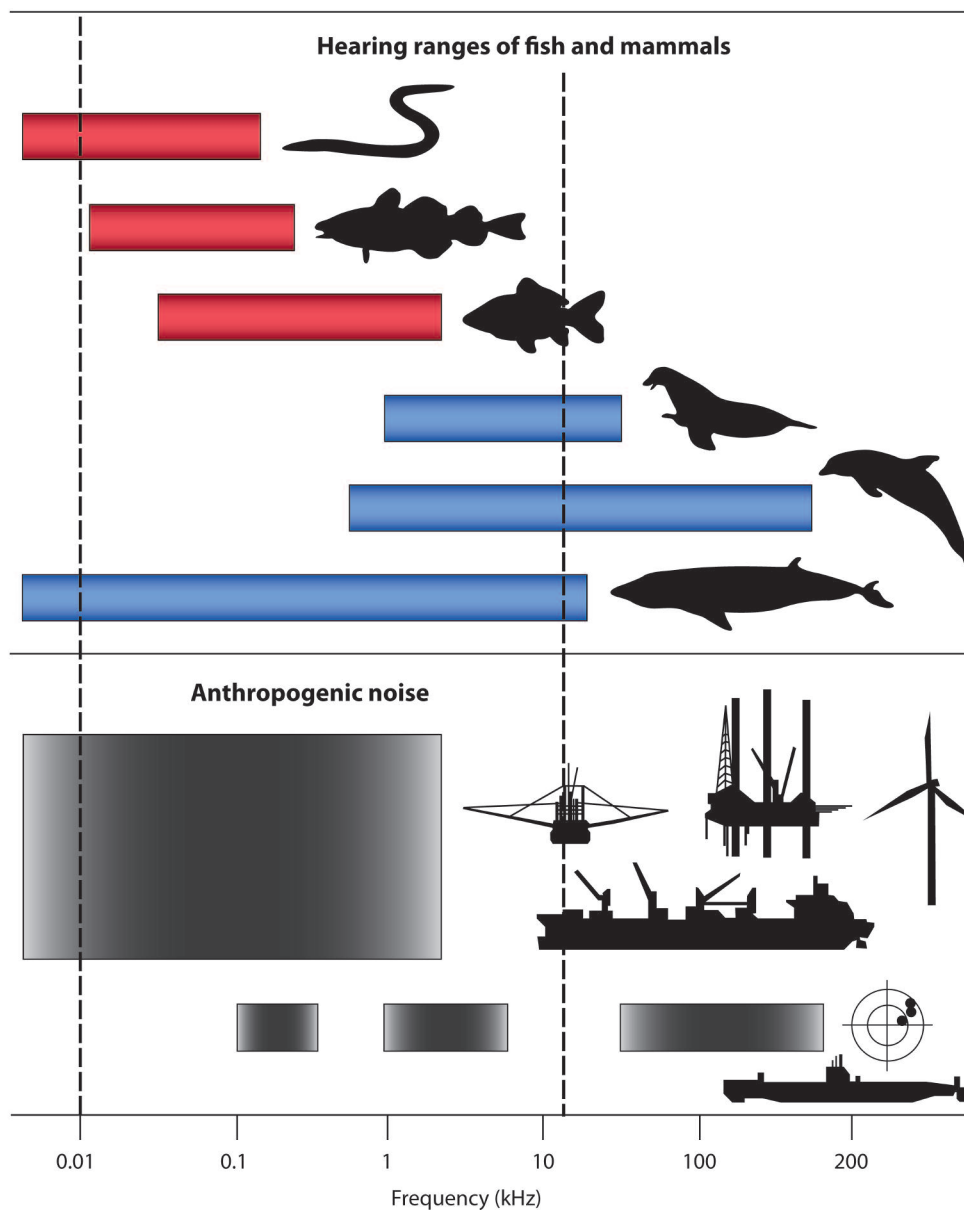
Figure 2.4. *Diagrammatic representation of the overlap between the hearing ranges of different kinds of fish and mammals and the frequency of sound produced by different human-generated sources (from Slabbekoorn et al., 2010). This is a considerable simplification of the Wenz curve (Wenz, 1962). The diagram does not reflect the changes in auditory sensitivity of each group of organisms, but simply represents the kind of auditory range over which sensitivity is likely to occur. Permission for reuse granted by* Trends in Ecology and Evolution.

Some marine mammals and fish show symptoms indicative of negative effects of sound, but it is currently impossible to determine whether other marine organisms are also harmed by sound because they have not yet been studied to the same extent. Although some of these effects are likely to be acute and rare in occurrence, chronic sublethal effects may be more prevalent, but are much more difficult to measure. This difficulty creates an important challenge because even if chronic effects are difficult to observe, this does not mean that they are not ecologically significant. Moreover, we need to ensure that keystone or indicator species within major, or important, ecological systems, as well as species already recognized as endangered, are not threatened by rising levels of marine sound. We need to identify the thresholds of such effects for different species and be in a position to predict how increasing anthropogenic sound will affect populations and the integrity of marine ecosystems. The IQOE is being developed with the

objective of coordinating the international research community to both quantify the intensity and distribution of ocean sound, and to examine the functional relationship between sound and the viability of key marine organisms and ecosystems. This has implications for the future exploitation and management of the marine environment and will inform global, regional, and local decision-making about the exploitation of marine resources.

2.3 Background

The potential impact of anthropogenic sound on marine life is a matter of societal concern. Most people are unaware of ocean sound, yet it is a vital part of the ocean environment, important not only to large marine mammals, but also to fish and other animal groups. Environmental nongovernmental organizations are more aware of the issue and can motivate action of various kinds, such as industrial guidelines, litigation, and possible regulation designed to reduce the impact of sound on marine life. Such action can be expensive and must therefore be based on robust scientific evidence. Moreover, the results of such understanding need to be effectively communicated to the public to foster rational discussion, informed policy development at national and international levels, and public support for meaningful and justifiable action.

The basic scientific foundations for management of sound in the ocean fall into two related categories. First, the contemporary ocean sound field should be described adequately. This description cannot be represented by a single number, but must rather be a quantitative description of the kinds of sound that exist, and their frequencies, intensities, and variations in both space and time. An important example of the value of long time series observations of key environmental parameters is the "Keeling Curve" that documents the changes in atmospheric CO_2 concentration (Keeling, 1960). Documenting changes in the ocean sound environment is more complex and will require long-term measurement with appropriate hydrophone stations across many regions, together with analysis that identifies trends in different contributions. Technological advancements allow such measurements to span a broad frequency range and to record or transmit the data in various forms. Existing systems such as hydrophones used for Comprehensive Test Ban Treaty Organization verification and various cabled ocean observatories designed principally for other functions could also provide the backbone of ocean observation for sound. Quantitative predictions of the underwater sound field will require better understanding of the different sound sources—both natural and anthropogenic—and the propagation characteristics within the ocean that contribute to the building of a "soundscape."[3]. This will require development of numerical models of ocean sound fields based on knowledge and measurements of the sources and of the propagation environment, and of statistical models that can be used to fit the numerical models to data obtained from calibrated acoustic measurements. This validation of numerical models through testing their predictions against observations is an important part of the IQOE. Once validated, the numerical models can be used to explore the relative significance of different sources, guide design of further measurements, and provide valuable tools for planning mitigation efforts where these are found necessary.

In addition to a basic characterization of ocean soundscapes, the biological impact of the sound must be studied to guide appropriate management of sound in the ocean. For a particular region this will include knowledge of the species that occur and their sensitivity to acoustic interference. Given the generally limited state of our knowledge of biological sensitivity to sound, this represents, by far, the most challenging aspect of the scientific and management problem. We are unlikely to resolve this challenge quickly or completely. Nevertheless, a good understanding of the effects of anthropogenic sound on marine life remains essential to rational decision-making and is a central goal of the IQOE. The long range at which sound spreads in the ocean emphasizes the need for study at large scales. In addition, human activities are adding noise throughout the global ocean. The IQOE is the first project to address questions and attempt to provide answers over hitherto unexplored scales. This ambition governs the international global scale of the IQOE and its proposed duration of at least a decade.

Humans introduce sound to the ocean through many different activities. Each source may have different effects, depending on the range of frequencies produced; the source's power output; whether the source radiates an intermittent, pulsed, or a continuous sound; and the degree to which the sound is radiated in certain directions (few sound sources are truly omnidirectional). Some anthropogenic sources—such as some military sonar, seismic air guns, pile driving, and explosions—are both impulsive and of high intensity. Götz and Janik (2011) showed that the rapid rise time of some high-intensity impulse sounds can elicit a reflex startle response that, because it is aversive, can result in sensitization to sound.

---

[3]*A soundscape is a detailed and comprehensive description of an* acoustic environment.

There is increasing evidence that these types of sounds can elicit strong negative reactions, or even physical injury, in some marine species. Concern about the possibility that sounds may lead to negative behavioral reactions or physical injury has led to higher levels of scrutiny for many of those sources. Recently, military sonars have been a particular focus of attention because of their association with atypical mass strandings of beaked whales (Cox et al., 2006). Nevertheless, sonar exercises occur in some areas of beaked whale presence with no recorded mass strandings (D'Amico et al., 2009). The acute effects of sonars on beaked whales probably depend on the context of the exposure (i.e., distance from sonar to whale, bathymetry, presence of surface temperature ducts, behavior, and number of naval vessels). Animal strandings are probably the most easily observed and extreme end point of a syndrome of behavioral responses to sound in these species (Boyd et al., 2007). There is increasing evidence that a similar syndrome of reduced capacity to perform normal life functions is present across a wide range of marine fauna, including fish (Slabbekoorn et al., 2010; Simpson et al., 2014) and marine mammals (Southall et al., 2007; Tyack, 2008).

Humans also influence ocean sound in an indirect way, through anthropogenic changes in the concentration of carbon dioxide and the temperature of the ocean. It has been suggested (Hester et al., 2008; Brewer and Hester, 2009; Ilyina et al., 2009) that increasing ocean acidity might increase low-frequency sound levels by increasing the ocean's transparency to sound, although theory suggests that this effect has been negligible to date (Joseph and Chiu, 2010; Udovydchenkov et al., 2010). Another possible issue is a decrease in sound due to increase in the average sea surface temperature (Ainslie, 2012). Research is needed to investigate whether this effect might explain the leveling off

seen in Figure 2.3 in the reception of ship sound.

A major question in almost all of these cases is whether the impact on the fitness of individual organisms is great enough to jeopardize the viability of their populations. One broad ecosystem-based approach would relate indices of ecosystem health, such as biodiversity (potentially using natural components of the soundscape – Sueur et al. 2008; Parks et al. 2013) to indices of noise and other stressors. This approach has the advantage of enabling a rapid and very broad-scale evaluation of effects of noise on marine ecosystems. On the other hand, this approach fails to test the causal links from sound exposure through disturbance of individuals to effects on vital rates to effects on populations. A 2005 report of the U.S. National Research Council developed an approach to identify all these links (Figure 2.5), which defines a rationale for developing assessments of the significance of sublethal effects and for identifying the most important gaps in our knowledge. The greatest challenge is to define the functional relationships between behavioral and physiological responses to sound and then the biological consequences for growth, reproduction, and survival—an essential requirement of this assessment process (Figure 2.5). Defining the transfer functions between the different boxes of the Population Consequences of Acoustic Disturbance (PCAD) framework (Figures 2.5 and 2.6) and building knowledge of biological significance will be challenging. However, it may be possible to make progress through a combination of modeling transfer functions, leveraging multiple datasets derived from ongoing observational studies, passive acoustic monitoring, and the direct measurement of the level of sound received by marine organisms, usually using tags temporarily attached to those organisms or using sensors that are located near the animals.
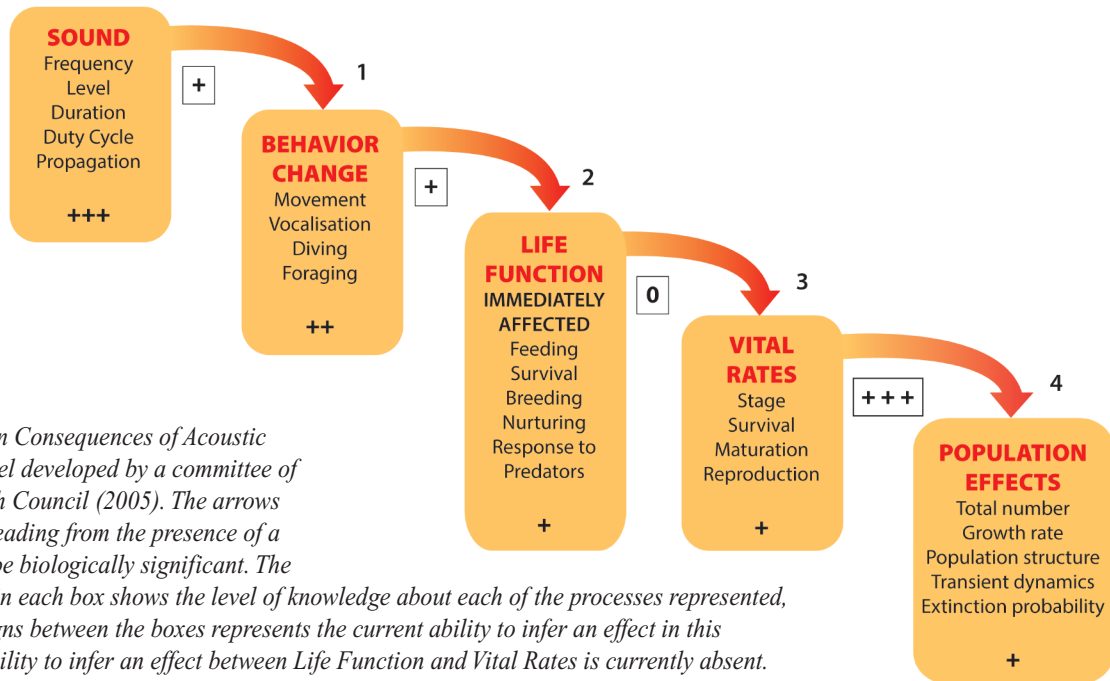
Figure 2.5. *The Population Consequences of Acoustic Disturbance (PCAD) model developed by a committee of the U.S. National Research Council (2005). The arrows define transfer functions leading from the presence of a sound to effects that may be biologically significant. The number of plus signs within each box shows the level of knowledge about each of the processes represented, and the number of plus signs between the boxes represents the current ability to infer an effect in this sequence. Note that the ability to infer an effect between Life Function and Vital Rates is currently absent. This diagram demonstrates why it is enormously difficult to infer significant effects of sound on marine life and also why, even if there are real effects of sound, demonstrating a connection to sound as the cause is also enormously difficult. Reprinted with permission from the National Academies Press, Copyright 2005, National Academy of Sciences.*
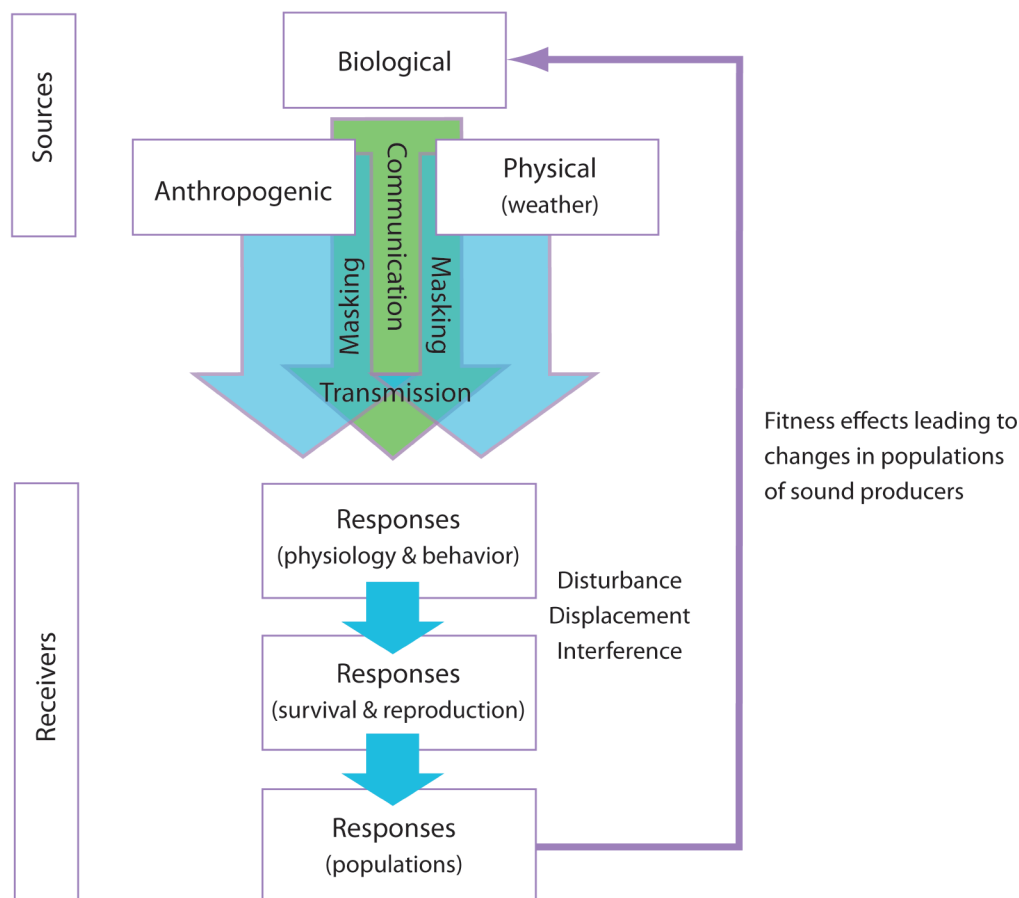
Figure 2.6. *A diagrammatic view of the issues being investigated by the IQOE (from Boyd et al., 2011). Permission for reuse granted by* Oceanography *magazine.*

Figure 2.6 defines three major sources of sound in the ocean: physical, biological, and anthropogenic. Physical sound sources include geophysical sources as well as sounds generated by ocean weather due mainly to wind and waves. Physical and biological sound sources can "mask" the sounds involved in marine animal communication and echolocation. Animals that rely on sound are likely to have evolved mechanisms to cope with this type of masking (Tyack, 2008). However, overlaid on this soundscape is new sound added by humans, and marine animals may not be able to handle the additional masking to the same extent. The characteristics of the sound received by organisms ("receivers") will determine responses that could cascade through physiological or behavioral effects on an animal's ability to feed, migrate, and breed and which, in turn, may lead to changes in reproduction and survival of the individual. The physiology and behavior of individuals are affected by changes in sound levels. If enough individuals are affected, the distribution, abundance, and dynamics of populations can be affected. Some fish and invertebrates rely on acoustic cues to find suitable habitat and to make the decision to switch from their larval planktonic form to settle on a substrate (Simpson et al., 2005; Montgomery et al., 2006). If noise interferes with settlement, this could have broader ecosystem effects.

Shipping has long been recognized as an important anthropogenic sound source (Wenz, 1962). The volume of cargo transported by sea has been doubling approximately every 20 years (http://www.marisec.org/shippingfacts/ worldtrade/volume-world-trade-sea.php), resulting in an increase in anthropogenic sound from this source. Although the measurement of sound in relation to these changes has been mostly local and is incomplete, the current estimate is that increased shipping has been accompanied by an increase in anthropogenic sound at frequencies below 500 Hz. From 1950 to 2000, the shipping contribution to ambient sound of some locations increased by as much as 15 dB, corresponding to an average rate of increase of approximately 3 dB per decade (Andrew et al., 2002, 2011; Hildebrand, 2009; Chapman and Price, 2011; Frisk, 2012). We also know that offshore oil and gas exploration and production, as well as renewable energy developments, have expanded during the same period, as has the fishing industry.

These changes could be important to the many marine organisms that use sound either passively to listen and orient relative to their surroundings, or actively by producing sound themselves to search for prey or other objects, communicate, or in some cases as a by-product of other activities. The active production of sound is relatively easy to detect, but passive use of sound is not. It is likely that most multicellular marine organisms use sound passively as a way of sensing their environment, including listening for prey and predators, and changing behavior in relation to weather and obstacles (including moving ships or stationary human-made objects). The idea that animals may use something analogous to "acoustic daylight" (Buckingham et al., 1992) to gain an image of their surroundings is gaining momentum, even if it is difficult to demonstrate empirically. The properties of sound in water and the low levels of light penetration below the surface in many circumstances mean that sound has essentially replaced light to sense distant objects, for some species, as the principal source of environmental information (Ausubel, 2009). Indeed, sound is so important for many species that understanding the acoustic environment amounts to describing their acoustic ecology.

Setting and defining a standard for soundscape quantification will be one of the first priorities addressed by the IQOE, to facilitate an internationally coordinated scientific effort. Several years ago the International Organization for Standardization/Technical Committee 43/Subcommittee 3 (ISO/TC 43/SC 3) on Underwater Acoustics was formed to establish standards in the field of underwater acoustics, including natural, biological, and anthropogenic sound. This international group is addressing topics that include measurement and assessment techniques associated with the generation, propagation, and reception of sound, as well as its reflection and scattering by the seabed, sea surface, and organisms. Soundscape quantification and the effects of underwater sound on the ocean environment, humans, and aquatic life are also being considered. The ISO and the IQOE will coordinate activities in this area and the IQOE will develop any additional standards needed to make measurements comparable worldwide. The IQOE will hold a workshop on standardization of observations early in the project.

2.4 Defining the questions

Much evidence indicates that sound in the frequencies below 10 kHz is most important for marine organisms, except in the case of some invertebrates (e.g., snapping shrimp, Alpheidae species) and some marine mammals (dolphins, some whales, and seals) that have developed the capacity to both produce and, in some cases, hear complex sounds at much higher frequencies (up to >120 kHz in smaller cetaceans). Our basic knowledge of the way in which marine organisms sense sound and then respond behaviorally to different sound stimuli is rudimentary for most species and groups. Similarly, the extent to which higher background sound levels mask the ability of marine animals to interpret sound signals from their environment is largely unknown, as is the extent to which they are

disturbed by loud human-produced sounds in their vicinity.

For example, we now know that several species of whales have adjusted their communication calls in a manner that suggests they are "raising their voices" or otherwise changing their calls to be heard in the context of potentially masking sounds (e.g., Au et al., 1985; Miller et al., 2000; Foote et al., 2004; Holt et al., 2008; Parks et al., 2010). This pattern of speaking louder in noise is known as the Lombard effect (Lombard, 1911), originally reported for humans, but also seen in terrestrial species such as birds that use sound in social activities (Lengagne, 2008; Slabbekoorn and Bouton, 2008). In the presence of high levels of background sound, some species simply stop vocalizing, either because they are being disturbed or because, like humans trying to talk in the presence of loud background sound, they give up because communication becomes ineffective. Acoustic masking of marine mammals from increased low-frequency ambient sound is of particular concern in species that rely on low-frequency sound, such as the large baleen whales (Clark et al., 2009), because low-frequency sound travels greater distances. Although it is possible that whales could be especially sensitive (and we know that not all whale species share the same sensitivities), the presence of masking and the Lombard effect leads to two questions: (1) how widespread are these effects among marine organisms, and (2) even if they are widespread, are they important to the function and survival of viable populations?

New research and observations also need to study biological and sensory mechanisms for increasing the detectability of signals, including waiting to call until noise decreases, increasing the rate of calling, increasing signal intensity, increasing the signal duration, shifting the frequency of a signal outside of the noise band, and the potential (energetic or fitness) costs associated with these adaptations (see Tyack, 2008 for review).

Based on the foregoing rationale, the IQOE will address the following fundamental questions:

1. How have human activities affected the global ocean soundscape compared with natural changes over geologic time?
2. What are the current levels and distribution of anthropogenic sound in the ocean?
3. What are the trends in anthropogenic sound levels across the global ocean?
4. What are the current effects of anthropogenic sound on important marine animal populations?
5. What are the potential future effects of sound on marine life?

2.5 IQOE objectives

The IQOE will last for 10 years, to provide sufficient time to ramp up the large international research effort required, for planning observations and experiments; designing and deploying acoustic sensors; developing the community of scientists and technicians necessary to carry out the planned work; and analyzing, synthesizing, and disseminating the data and information developed by the study. In broad terms, the IQOE will assess global sound characteristics in the ocean, determine whether there are trends in sound characteristics, and test the hypothesis that changes in sound characteristics affect marine habitats and species in ways that cause significant changes in their populations.

The IQOE will build a global scientific community with expertise across a broad range of disciplines and with the technologies and tools, including databases, necessary to support research in ocean sound as a core activity within future ocean science. The fundamental questions will be addressed through the organization of four research themes:

Theme 1: Ocean Soundscapes

- Characterizing soundscapes
- Identifying sound sources
- Modeling soundscapes
- Identifying trends in ocean sound levels
- Quantifying sound budgets
- Documenting soundscape diversity

Theme 2: Effects of Sound on Marine Organisms

- Identifying model species and habitats
- Employing experimental approaches, as well as comparative and baseline studies, and large-scale experiments
- Measuring effects
- Determining dose–response relationships
- Determining biological significance

Theme 3: Observations of Sound in the Ocean

- Establishing data standards
- Deploying new global and regional observing systems, including biological observations
- Integrating observing systems
- Conducting synthesis and modeling

Theme 4: Industry and Regulation

- Informing noise monitoring and regulation
- Defining thresholds
- Considering risk management
- Measuring compliance
- Communicating results

2.6 Anticipated benefits

The questions addressed by the IQOE are important for two main reasons. First, industrialization of the ocean is likely to increase in the next few decades. A large proportion of the manufactured goods and raw materials needed by a growing global economy are being shipped around the globe on the ocean. The demand for hydrocarbons is also pushing exploration and production farther offshore into deep waters at continental shelf edges, at depths from which sound can more easily enter the SOFAR channel. Energy extraction from the ocean wind, waves, and tides—although resulting in a relatively small amount of energy production at present—is expected to increase rapidly over the next few decades. In coastal areas, recreation is also leading to increasing sound levels from pleasure boats and cruise vessels. There are serious concerns that this process of increasing industrialization and recreation will lead us in small steps toward an intolerable acoustic environment for many marine organisms.

It is in the best interests of sound producers to help study the effects of sound on marine organisms, because the *precautionary principle* is slowly but progressively constraining the ability of sound producers to operate (Gillespie, 2007). Precaution in the face of uncertainty is rational and is an approach that is now deeply embedded in the way that environmental management operates in many countries, both nationally and through international agreements. Reducing uncertainty by increasing our knowledge and understanding of the effects of human-generated sound on marine organisms will help protect wildlife while avoiding excessive regulation.

A second and even more profound reason for giving attention to the issue of sound in the ocean is that industrialization of the ocean inevitably leads to negative effects that could perhaps be minimized with advanced planning. Humankind is slow to learn lessons from the negative impacts of the past industrialization of the ocean. The dangers of causing irreversible declines in the quality of the planet's self-regulating environment are tangible and real. The nonlinear, complex nature of the Earth system means that, although many parts of this system are self-regulating within broad boundaries, collapses could happen quickly and without much warning. At some point, small changes could lead to very large shifts in the state of ocean ecosystems. Although there is some evidence that many parts of the ocean show remarkable resilience to the direct exploitation of fish, whales, plankton, and other forms of biological productivity, there is increasing evidence that there are definite limits.

Ecological collapse is an emotive and poorly defined term. However, if viewed from a human perspective, as describing ecosystems that can no longer support normal goods and services, collapse has already happened locally as a result of direct exploitation (Bakun and Weeks, 2006; Thurstan and Roberts, 2010). The danger is that the uncontrolled increase of sound in the ocean—some of which could be avoided with appropriate design, planning, and technological innovation—could add significant stress to already-stressed oceanic ecosystems. Unless we improve our knowledge of the consequences of sound pollution, we may be cruising blindly toward consequences that could cost us much more than we will ever gain from ignoring them.

Therefore, the benefits of IQOE activities will accrue across many stakeholder groups:

- *Regulators* who codify emerging legal frameworks as constraints on the sound radiated by industrial activity.
- *Legislators* who design legal frameworks to regulate sound in the ocean.
- *Members of the public* who have an increasingly jaundiced view of the activities and motivation of industry, especially in the ocean, where experience of poor management in fisheries has sensitized the public to issues of marine management.
- *Managers* who need relatively simple and defensible targets and reference points to establish as objectives for managing anthropogenic sound in the ocean.
- *Scientists* because sound is usually overlooked as part of the physical structure of the ocean, and it is likely to have much more widespread importance than is currently appreciated.
- *Militaries* for which the ocean is both a barrier that aids national and international security and a challenge because it can provide cover for those with aggressive intentions. The importance of sound in the ocean has been appreciated by submariners, and those who wish to monitor submarine activity, for many decades, and much of our current knowledge of ocean acoustics derives from studies conducted to support defense and submarine warfare. We need to broaden the foundation for our knowledge of sound in the ocean.
- *Industries* that produce sound and technologists who are seeking ways to reduce the inputs of sound from commercial activities.

2.7 Activities

Experimental approaches

To address the challenging scale of questions posed by the effects of increasing ocean sound levels we need to ensure that science activities are coordinated across international boundaries and across disciplines. This is why the IQOE has been proposed. The IQOE will employ two approaches to help increase our understanding of sound in the ocean and its effects. One of these approaches will be to conduct experiments involving the active manipulation of anthropogenic sound sources, either through directed, temporary reductions of these sound sources at regional scales, or through planned lulls in sound production (e.g., due to planned shutdown of offshore construction, the diversion of shipping lanes, or the temporary presence and absence of sound sources). The second method will be to make opportunistic observations of the effects of anthropogenic sounds on marine ecosystems and species. These experimental approaches will require expanded observations and modeling.

Ocean soundscapes

A first step in this direction will be to define what we call *ocean soundscapes*. An ocean soundscape is a characterization of the acoustic environment that fully describes its spatial, temporal, and spectral characteristics. Although we have identified at least 30 sites or networks globally that have currently or recently collected data about ocean sound (see Appendix II), in almost all cases the monitoring stations involved have been established to perform specific functions. This is reflected in the disparity of sensor designs and of data collection and transmission protocols. We need to find ways to use these data in a unified framework and to establish other measurement systems to understand the complex global sound field in the ocean. Building a picture of this global sound field, even in a relatively unrefined form, is a high priority as a baseline for other studies. Sound propagation modeling—based on ship position and activity (from Automatic Identification System data, e.g., Hatch et al., 2008), data for wind and rainfall, and data for seismic surveying, sonars, pile driving, and explosions—may provide a general view of the sound fields across the global ocean.[4] The most challenging "unknown" in estimating the global soundscape will probably be the contribution of biological sound, which will require better understanding of animal vocal behavior, particularly when species vocalize in large numbers to produce "choruses." Refinement of the

quantification of sound fields will be possible with increasing knowledge of the sound production from ships and other human activities, many of which are currently poorly characterized.

The IQOE will promote the establishment of a network of stations making acoustical observations. This network will build on the existing and planned capability of the Global Ocean Observing System (GOOS) and on local and regional systems such as the U.S. Integrated Ocean Observing System and the Australian Integrated Marine Observing System, by helping to define standards and protocols for sensors and for the analysis, storage, and distribution of data across a global research community. Some elements of global ocean observation systems actively produce anthropogenic sounds that can be used for acoustic tomography or for global security, but the IQOE will focus on passive acoustic systems rather than active acoustics. This means that it is not envisaged that the IQOE will promote the use of active systems, such as Doppler profilers, swath bathymetry, tomography or seismic arrays unless they are a specific part of an experiment to understand their effects on marine life or are necessary for in situ acoustic calibrations.

> The IQOE will not introduce sound to the ocean at durations or levels that will produce long-range effects. Any introduction of sound will either be at high frequencies or at low enough sound levels and durations that the IQOE will not significantly add to global ocean noise pollution. An important aspect of the IQOE will be determination of the hearing capabilities of marine organisms and dose–response relationships, which will require limited and controlled addition of sound to the ocean. Such additions will be subject to normal permitting and animal care requirements. The IQOE will also take advantage of the noise-producing activities of industry and navies, where possible, to study the impacts of such noises on marine organisms.

Predicting sound fields and managing sound inventories

Characterizing the global ocean soundscape, with appropriate estimation of statistical uncertainty around variation in space, time, and frequency, is a necessary step toward predicting ocean sound fields in particular locations. These predictions can then be compared with in

---

[4] *The IQOE will explore with navies and exploration firms how to obtain useful information from their activities without compromising the security and proprietary aspects of their data.*

situ measurements from existing sites, and a process of tuning sound field models to maximize the fit to the empirical observations will eventually refine the descriptions of ocean soundscapes. This global analysis of ocean soundscapes may enable classification of soundscapes into types that may facilitate grouping experiments or data according to the sound environment in which they were conducted. The goal of the IQOE is to maintain a global long-term focus, which will inform local efforts in modeling and measuring both sound fields and effects of sound on marine organisms and ecosystems.

Predicting sound fields in this way will also feed directly into the emerging processes for the regulation of offshore human activities and general industrial development. In both the United States and Europe, for example, legislation is moving rapidly to embrace marine spatial planning and setting standards for sound exposure, principally on a precautionary basis. But existing information is not sufficient to build the rationale for spatial management of industrial activities to reduce potential sound impacts on sensitive species or habitats. Marine spatial planning faces particular problems for pollutants such as sound that can spread hundreds or thousands of kilometers, covering the global ocean (Hatch and Fristrup, 2009). The development of sound budgets[5] on the global scale will enable regional and local managers to refine these budgets to reflect their own needs at regional and local scales, and to help define the kinds of threshold values that managers often need in order to set legally binding conditions on use of the ocean. This spatially nested approach to model development and validation is necessary because characterization of sound in the ocean needs to be tackled initially at large scales given the long-range propagation of low-frequency sound. Even local models need to have specified boundary conditions to build local sound budgets and we intend to provide this capability.

Preindustrial sound levels

What was the soundscape of the global ocean like before large-scale industrial activities in the ocean? Many have explored this question with respect to the removal of marine mammals and fish, in particular, but we also want to know how noisy the ocean was in the past. In other words, can we back-cast the ocean soundscape to a preindustrial era? Given estimates that current baleen whale populations are only a small portion of pre-whaling levels, it is likely that the ocean had a much higher level of biological noise in the preindustrial era, particularly in the low frequencies.

Similarly, can we predict the ocean soundscape in the future if current trends continue? Given historical changes in sound levels, what is the cost-benefit trade-off if regulations are set to reduce the sound produced by human activities? These questions, though interesting in their own right, have most relevance if they are accompanied by robust functional relationships between sound and the growth or decline of populations of marine organisms.

2.8 Summary

The development of a body of knowledge that begins to flesh out the types of responses of individual organisms to different levels of sound—responses such as changes in the reproductive rate, growth rate, use of habitat, survival rate and benefits from the social structure—is an essential part of the strategy being adopted by the IQOE. The species that need to be included vary across the full range of marine organisms, but perhaps could focus principally on some of the keystone or indicator species within major, or important, ecological systems, as well as species already recognized as endangered. Many of the resulting "effects" studies will be small-scale in situ experiments, and some may be possible in controlled conditions in the laboratory. However, all experiments must be designed carefully with controls and also with a view to ensuring that the effects observed can be built into larger-scale strategic models of effects at population and ecological levels.

The challenge and opportunity of the IQOE is to coordinate scientific activities concerning the effects of ocean sound on marine organisms internationally, whether conducted in the academic, governmental, or industrial (e.g., Joint Industry Program) sectors. The framework set out in this document is intended to provide the template that will meet this challenge for the benefit of human society and the environment.

---

[5] *Sound budgets are defined as the overall distribution of sound energy at a particular location within a defined period of time. A budget may break down the total received sound level by source, but since not all sources will be known, this is not a prerequisite for the construction of a budget.*

Chapter 3
Theme 1: Ocean Soundscapes

3.1 Characterization of soundscapes

Quantitative description of the ocean sound field, which is how we define soundscapes, is fundamental to any analysis of trends in the levels of sound in the ocean and the effects of these trends. If we wish to understand the consequences of variation in sound within the ocean, it is essential to define variation in the sound field, spatially, temporally, and with respect to frequencies. The term soundscape used in the context of the ocean has resonance with a landscape. While light is the principal source of environmental information about a landscape for many terrestrial animals, water-dwelling animals rely to a much greater extent on sound, especially below the upper sunlit ocean layer. Use of the term *soundscape* reminds us of the central role of sound in providing cues to aquatic animals about their surroundings.

The term *soundscape* has developed recently within the terrestrial environment (Pijanowski et al., 2011) and has also been applied in a marine context (e.g., Cotter, 2008). A soundscape is a description of an *acoustic environment*. However, while an acoustic environment can be perceived from the various perspectives of receivers of signals, we follow Pijanowski and colleagues' (2011) definition of soundscape as a quantification of the ocean sound field and how it varies in a way that is unbiased by the method of measurement. This view recognizes that the acoustic environment of two colocated organisms (or receivers) that have different capacities for sound perception could be very different, but both are in identical soundscapes. We must take care to distinguish between soundscape and the way in which an individual receiver may sense different components of the soundscape.

Variation in the soundscape is central to almost every aspect of the IQOE. The soundscape is the context within which any field experiments (Theme 2) have to operate by observing the response of organisms to intentional or uncontrolled changes in it. It may also be used to document the contribution made to ocean sound by humans and as a measure of the extent of industrialization of the ocean.

At any time within a defined space, a soundscape may be described quantitatively in terms of different measures, such as

- the acoustic waveform as a function of time;
- the spectrum (sound intensity versus frequency over appropriate time scales; for example, narrow-band spectrum, 1/3-octave band levels);
- the spectrogram (time history of spectra); and
- sound energy over specified time scales, often referred to as sound pressure level (particularly to describe high-level transients).

Figure 3.1 illustrates a cross section through a soundscape (also illustrated in Figure 2.1), where a broad-band acoustic spectrum has been measured across time, in this case for three weeks, to form a spectrogram displaying acoustic energy as a function of frequency versus time. Presented in this form, which is the normal form for the depiction of the dynamics of ocean sound measured from a particular observation station, the soundscape can be rather difficult to interpret. It is difficult to verify independently the interpretations given in such figures, which rely on the experience of the observer. Spectrograms that use long-term spectral averaging often contain sounds for which there is no obvious source or explanation. Such displays can be useful for illustrating long time-varying datasets, but it is often difficult to ascertain the detailed structure of many signals, and short transients may not be visible at all. Use of detectors tuned for specific signals is a critical tool for fully describing these datasets.

The variation in the soundscape represented by the different sections in Figure 3.1 is remarkable. This kind of variability is what would normally be expected within ocean regions where there are a wide variety of different sound sources, including natural physical and biological sound, as well as human-generated sound. The increase in sound attenuation in the ocean as sound frequency increases means that the spatial scale reflected in a spectrogram such as that shown in Figure 3.1 changes from small scale (a few kilometers) at the top of the central diagram to a very large scale of hundreds of kilometers at the bottom of the central diagram. Soundscape analysis aims to present the distribution of acoustic energy within a defined region, with an ultimate goal of predicting the acoustic energy received at any point within the soundscape.
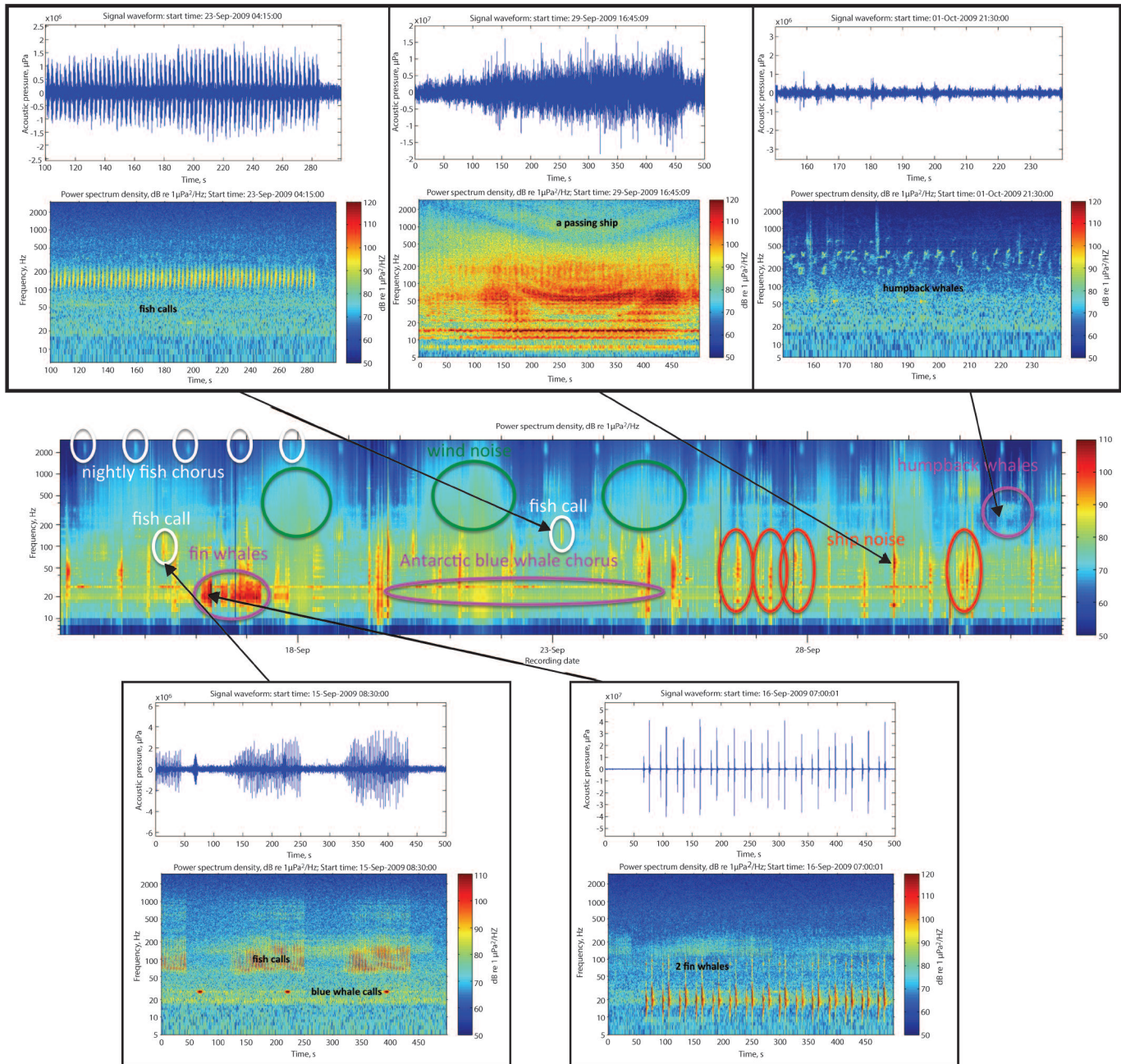
Figure 3.1. *The middle panel shows a 3-week spectrogram of the marine soundscape at the IMOS Perth Canyon acoustic observatory. The sounds of fish (individual fish calling and regular nighttime chorus of fish), Antarctic blue whales, fin whales and humpback whales, wind, as well as passing ships are detected and a few examples are labelled. The five panels (3 above and 2 below the 3-week spectrogram) show zoomed-in spectrograms of a few example sound signatures, and their pressure time series waveforms. Data and images courtesy of Centre for Marine Science and Technology, Curtin University, Perth, Western Australia.*

Characterization of a soundscape at a specific location first requires measurements of the received sound field over sufficient time to sample its diurnal and seasonal variation. Components of the ambient sound field may be identified (Cato, 2008) from these data, such as sound generated at the sea surface or by ships and marine organisms. These components can be related to other, more readily measured or estimated, variables such as wind speed (which is a very good predictor of sea surface sound), the distribution of ships, and the migrations and distributions of animals that produce sound. Sampling of the received sound field also can help to classify components of the soundscape that have no known source.

In addition, where a few individual sources make significant contributions to the soundscape it will be possible to model the contribution using a knowledge of source levels and directionality (sound output from the sources) and propagation loss. Examples include the contributions from passing ships and from whales. In particular, this approach will be useful for estimating the contribution of higher source level anthropogenic sounds, such as from seismic surveys and pile driving.

In some cases, it may be possible to use this modeling approach to estimate some components of the ambient soundscape. In few cases will the necessary knowledge of source levels and behavior be available for individual sources where many individuals are involved, such as in the sounds of distant shipping, but some source characteristics can be estimated through statistical approaches. For example, traffic sound may be modeled from averaged shipping densities and averaged source levels. Comparison with measurements of shipping sound would be required for validating the model and then adjusting it to maximize its fit. In other cases, such as biological choruses, so little is known about the distributions of animals that produce sound on the spatial scales required (i.e., close enough to contribute to the soundscape) or the source levels, or the sound-producing behavior, that modeling their contribution in this way has generally not been feasible. Greater success has been achieved with empirical modeling from the temporal and spatial variation of the measured biological components. In fact, this information can be coupled with information about calling rates to use sound to estimate the abundance of sound-producing animals (Marques et al., 2012).

Predictions of soundscapes can be extended to a wider range of locations by a combination of empirical modeling based on the measured characteristics and behavior of components with their relationship to readily available variables on which they depend (e.g., wind speed for sea surface sound) and modeling of the contribution of sources from their distributions, source levels and propagation loss, where this information is available.

The complete characterization of soundscapes can be achieved only to within certain bounds of accuracy. The uncertainty involved arises because of limitations in knowledge of the characteristics of the sources involved, their distributions, abundance and the spatial and temporal variation, as well as the limitations in modeling. Fundamental inaccuracies exist within sound propagation models, which are necessarily approximations of the physics involved, and there are limitations in the environmental knowledge needed in the propagation models. There are further limitations in our knowledge of marine animal distributions, their source

levels and behavior. These limitations will constrain our ability to predict soundscapes based on information about individual sources and it will be important to quantify uncertainties of IQOE soundscape models. Most natural and many human sources of sound have poorly known characteristics, and radiate sound power levels that vary over multiple time scales, growing louder, then quieter, and sometimes dying away completely. This variability can be characterized using probability functions, although it is likely that the actual variability of measured sound will be accompanied by quite high levels of uncertainty.

The difficulties associated with decomposing all elements of a soundscape to known sources at known ranges are so daunting that some biologists have proposed a radically simpler way to relate soundscapes to critical ecological parameters. Sueur et al. (2008) propose an acoustic entropy index that can be calculated from recordings of environmental sound with no requirement of knowledge of each source, and they suggest that this index correlates with biodiversity in terrestrial habitats that they recorded. They also propose an acoustic dissimilarity index, calculated for pairs of recordings, which they suggest correlates with the number of acoustically active species that are not shared between terrestrial habitats. Depraetere et al. (2012) critique the acoustic entropy index for changing with varying environmental noise of nonbiological origin, and they propose a different index for biodiversity called "acoustic richness." Parks et al. (2013) point out that noise can be an even greater problem in the marine environment, where sound propagates over longer ranges than in terrestrial environments. They analyzed acoustic data from three oceans, identifying known low-frequency calls from whale species. They then showed that noise-compensated entropy values correlate better with biological source data than with noncompensated entropies, which were strongly affected by anthropogenic noise. This radical simplification of the problem can enable first-order estimates of ecological status of habitats, but these will need to be validated over time with better biological data.

Sound levels are usually determined by measuring sound pressure levels, but many fish and invertebrates sense particle velocity representing the actual motions of fluid elements in response to the fluctuating pressure of the sound field. The particle velocity, which may be affected by turbulence, internal waves, and eddies, is a vector quantity that gives information about the proximity and direction of a sound source. As fish and many invertebrates detect particle motion, they may be especially capable of determining the direction of sources in the horizontal and vertical planes. Hence, methods of measuring or estimating particle velocity need to be included to characterize sound sources and

exposures for these species.

Key questions

Relevant questions related to the characterization of soundscapes include the following:

- What acoustic frequencies are relevant to the ocean soundscape?
- What quantities and metrics are useful to measure components of soundscapes?
- What are the contributing components of soundscapes?
- How should the contributing components be combined to characterize and differentiate soundscapes?

Research approach

The current state of knowledge allows us to approximate the sound propagation from particular sources if the sound characteristics (e.g., sound level, spectrum, directionality, transmission timing, location, movement, orientation) are known. We also have significant knowledge of components of ambient sound. The most productive approach to increasing knowledge of soundscapes would be to develop a framework for calculating soundscapes from local to global scales. Ideally, this would be at all scales in three dimensions and it would also illustrate how the soundscape changes through time, but we will need to structure the approach carefully to allow for progress within the current constraints of the data.

An approach combining a series of measurements at particular locations with models will allow us to characterize soundscapes at these locations, including the way in which they change diurnally and seasonally, with the weather and with migrations and behavior of marine animals. Measurements will be delivered through Theme 3, on Observations on Sound in the Ocean.

From observations and modeling we will move toward regional, ocean-basin scale and global characterization of soundscapes. We will use a nested approach by first focusing on the global or ocean-basin scale with relatively coarse spatial grids and also on local characterizations of the soundscape where high-quality data are available in some specific places from local sensors. Models to describe sound propagation and the ocean conditions to determine sound speed are both available at the large scale. These global-scale results can be used to define the boundary conditions for calculations of the soundscape at regional and local scales, both of which require much smaller grid sizes.

The global-scale characterization will use global

approximations for oceanic conditions, including seasonal variation and use of grid sizes commonly available for global oceanographic datasets. Datasets are available for the three additional layers required to describe a global soundscape, namely (1) weather as a physical sound source, using global weather and climate model outputs; (2) the distribution and density of biological sound producers within broad classes (e.g., toothed whales, baleen whales, snapping shrimp, demersal fish biomass); and (3) anthropogenic sound sources using the best available knowledge of the distribution of human activity. This approach should include the statistical uncertainty connected with those components (see Section 7, Example 1). Bottom-up approaches (i.e., small-scale studies to identify how various factors contribute to local soundscapes) might contribute to ground-truthing global model outputs. This approach may also drive the initiation of case studies in specific or characteristic soundscapes to capture information on local soundscape composition and variation for a set of representative "archetype" soundscapes.

Initial calculations of this global soundscape will include high levels of statistical uncertainty, but they will create a clearer view of where the greatest statistical uncertainties lie and also the most effective way in which this uncertainty can be reduced. Soundscape characterization is vital at an early stage of the IQOE because we need to identify those variables that lead to the greatest uncertainty. This process will lead in the remainder of the IQOE to a focus on assimilating or collecting the data that will contribute most to the reduction of statistical variance in soundscape calculations, much of which will be delivered through Theme 3 on Observations on Sound in the Ocean.

The output from this work will be a map showing the intensity of sound across the ocean. The method of representing this intensity will require more work; there are many different ways of representing sound intensity, but it is likely that the map will display the integrated total power throughout the global ocean. The integration intervals over space and time are an important research topic. The temporal integration could range from the integration time for mammalian hearing (less than 1 s) to decades, depending on the research question. Spatial integration can range from meters to thousands of kilometers and can depend on frequencies of interest. These issues of integration intervals are one aspect of standardization of measurement techniques that the IQOE will address.

Future iterations of the global soundscape characterization will include variations based on different scenarios associated with the physical, biological, and anthropogenic data layers. Three example scenarios follow:

1. The outputs from global circulation models and long-term weather prediction will be used to examine the impact of climate change on ocean ambient sound from weather and the way in which changes in ocean stratification, temperature, and pH may affect the intensity of ocean sound in particular regions.
2. Changing the biological layers to those more representative of an era before large-scale industrial fishing and whaling will allow us to test the hypothesis that the biological contribution to ocean ambient sound is considerably less now than it has been in the past.
3. Prediction of the changes on ocean ambient sound in the Arctic associated with ice retreat (including sound generated by iceberg calving and the progressive breakup of polar ice sheets) and increasing industrialization of the Arctic

Ocean (see Section 7, Example 2).

Ambient noise is the term sometimes used to describe background sounds that merge in such a way that their individual sources cannot be distinguished. More formally, it may be defined as sound in the ocean that, in the absence of a specified signal, is received by an omnidirectional sensor and does not result from the sensor or observing system. Consequently, the level of ambient noise is a function of several factors, including the number, source levels, and bandwidth of sound sources and their range from the detector. If different sound sources overlap in frequency, the signal received will be a merged signal from all the sources producing sound in that frequency band, and it may be impossible to untangle the different sources. Figure 3.2 shows this pattern of complexity involving overlapping sound sources.
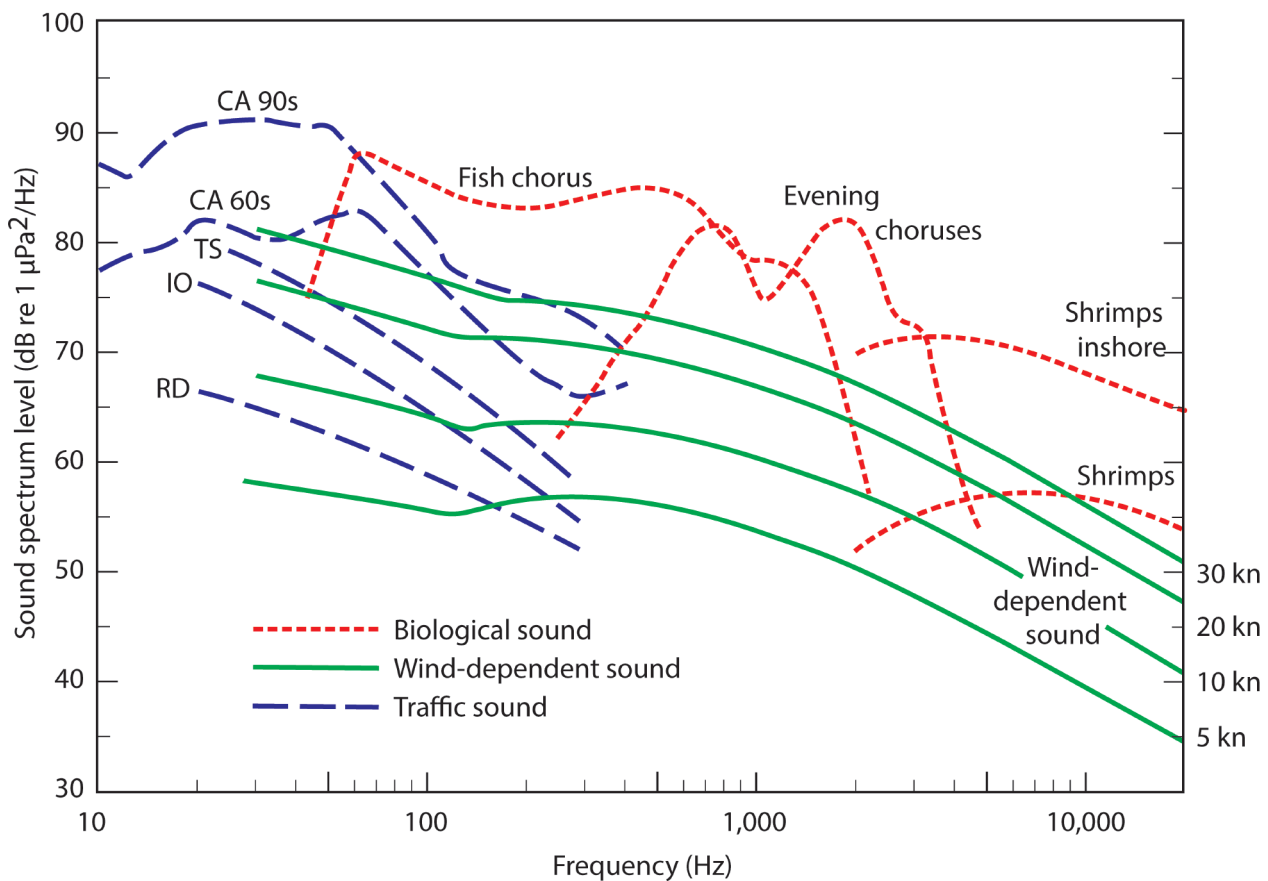
Figure 3.2: *Summary of ambient sound spectral density components shown as averages of sustained background sound levels. These components can be combined to predict soundscapes for particular conditions. Traffic sound is the sound of distant shipping and excludes close ships. "CA 90s" shows levels measured off California in the late 1990s (Andrew et al., 2002) at the same place and using the same methods as the curve "CA 60s" measured in the early 1960s (Wenz, 1969). Lower levels of traffic sound occur off Australia: "TS" Tasman Sea, SW Pacific, "IO" SE Indian Ocean, "RD" remote (from shipping lanes) deep water. Wind-dependent sound is from breaking waves for the wind speeds shown. The biological choruses vary with time of day and season (typical maximum levels shown). "Shrimps" refers to the sustained background sound from snapping shrimp in shallow water (modified from Cato, 1997). Permission for reuse of the figure is granted by The International Institute of Acoustics and Vibration.*

Finally, the IQOE aspires to make soundscape characterization the centerpiece of the assessment of the global trends in ambient sound. This goal is only aspirational at this stage because of the immense amount of work required before it can be achieved. For the immediate future the development of assessments of global trends in ambient sound needs to use time series of data that are, by definition, collected at single points. Since these points are relatively few in number, many have only short time series and, in most cases, it is difficult to filter out near-field transient sound sources. It will be challenging to compile an authoritative view of whether ambient sound is increasing, but soundscape characterization is one approach that can integrate data from many sources—physical, biological, human—to examine trends in sound based on a broad range of historical time series and forecasting mechanisms. Where there are individual time series of sparsely distributed observations (see Theme 3), it should then be possible to validate the resulting soundscape predictions against these observations. This approach has the potential to provide, eventually, a truly global integrated assessment of trends in ambient sound.

One imaginative approach to establishing long-term observation of trends in ocean sound would be to place an observatory in the sea below the landward end of an Antarctic ice shelf. Although technically challenging to implement, this would allow monitoring of a deep-ocean acoustic environment in the absence of near-field biological and weather sound. There would be a need to ensure that ice cracking sounds did not occur to such an extent that they were a significant influence on the capacity to measure the long-range sound field. Both the Ross and Filchner ice shelves would be appropriate for this purpose and would "look" out into the South Atlantic and South Pacific oceans, respectively.

A final added benefit of characterizing soundscapes is that it may be possible to identify areas with rare soundscapes that deserve protection. This approach has been suggested in terrestrial environments (Dumyahn and Pijanowski, 2011), but it is not known whether the

same approach will be feasible in ocean environments.

3.2 Ambient sound and the components of soundscapes

Ocean soundscapes are composed of a combination of *ambient noise* and sounds from sources that can be localized.[6] These are often transient or pulsed sounds, or occasionally they are from sources that are completely characterized in terms of their spectrum, and their contribution to ambient sound can be inferred or calculated. However, the term *ambient noise* may sometimes be used as a surrogate for a sound field in which there are no specific identifiable sources.

Ambient noise includes sound from the sea surface, sound from distant shipping (defined as *traffic sound* by Wenz, 1962) and biological choruses when animals are so numerous that the sounds of individuals merge into a continuous background. Localized individual sound sources include passing ships, other human activity (e.g., pile driving, seismic air guns, and sonar), as well as sounds of individual animals vocalizing. Soundscapes include both natural and anthropogenic components. Figure 3.3 gives an example of the sound spectrum from pile driving. The natural components can be further subdivided into physical sound sources, such as weather or ice, and biological sources, such as snapping shrimp, fish, and whales.

Ambient noise has been studied extensively for about 70 years so that we have substantial knowledge of the characteristics of ambient noise in general, and in many environments in particular. Historically, most of the measurements of ambient noise have been motivated by strategic naval considerations. Much of the research has been in areas near North America and Europe, where the highest density of human-induced sound is observed. This leaves significant deficiencies in knowledge for areas of the world where there is less or very little human activity, although there has been some work in areas with lower densities of sound from human activities, such as Australia, New Zealand, and the Antarctic.

---

[6] *Note that some people refer to ambient noise as all measureable sound that is not of specific interest, irrespective of whether it can be localized.*
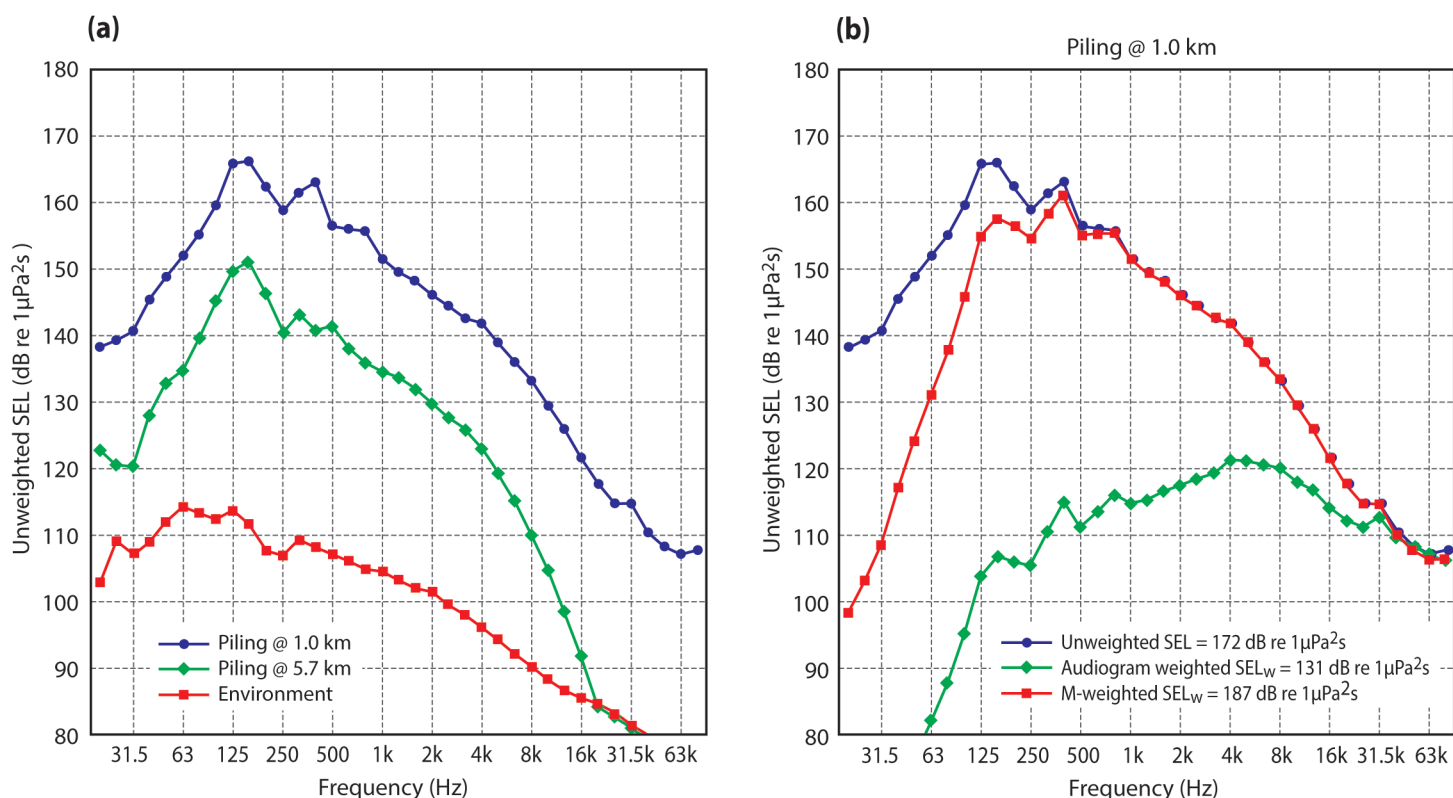
Figure 3.3. *(a) The average 1/3-octave band spectra of the sound exposure level (SEL) at two different distances from a piling operation, compared with the SEL of the average noise (ambient sound plus sound from measurement platform, integrated over one second duration) in the absence of the piling signal. (b) Shows the same 1/3-octave band spectra of the SEL after M-weighting the audiogram to compensate for the sensitivity of cetaceans that tend to hear best at higher frequencies. From De Jong and Ainslie (2008). Permission from the authors and from the Société Française d'Acoustique to reprint the figures.*

Sound associated with local weather conditions, especially wind, can form a substantial component of the sound field (Figure 3.2). In the absence of precipitation, wind speed can therefore be used as a proxy for the sea surface sound component of ambient sound because many studies have shown that the two are well correlated. Figure 3.4 shows results of a study carried out in the Tongue of the Ocean in the Bahamas, which is almost completely isolated from other background ocean sound and therefore provides a useful environment in which to calibrate the relationship between wind speed and ambient sound. The figure shows a consistent and linear pattern of wind speed and ambient noise level, raising the possibility that surface wind speed data can be translated into an ambient sound prediction, although this assumes similarity between the Tongue of the Ocean and other locations. Before using this type of relationship in a general sense, it would be useful to see this result replicated for other environments.
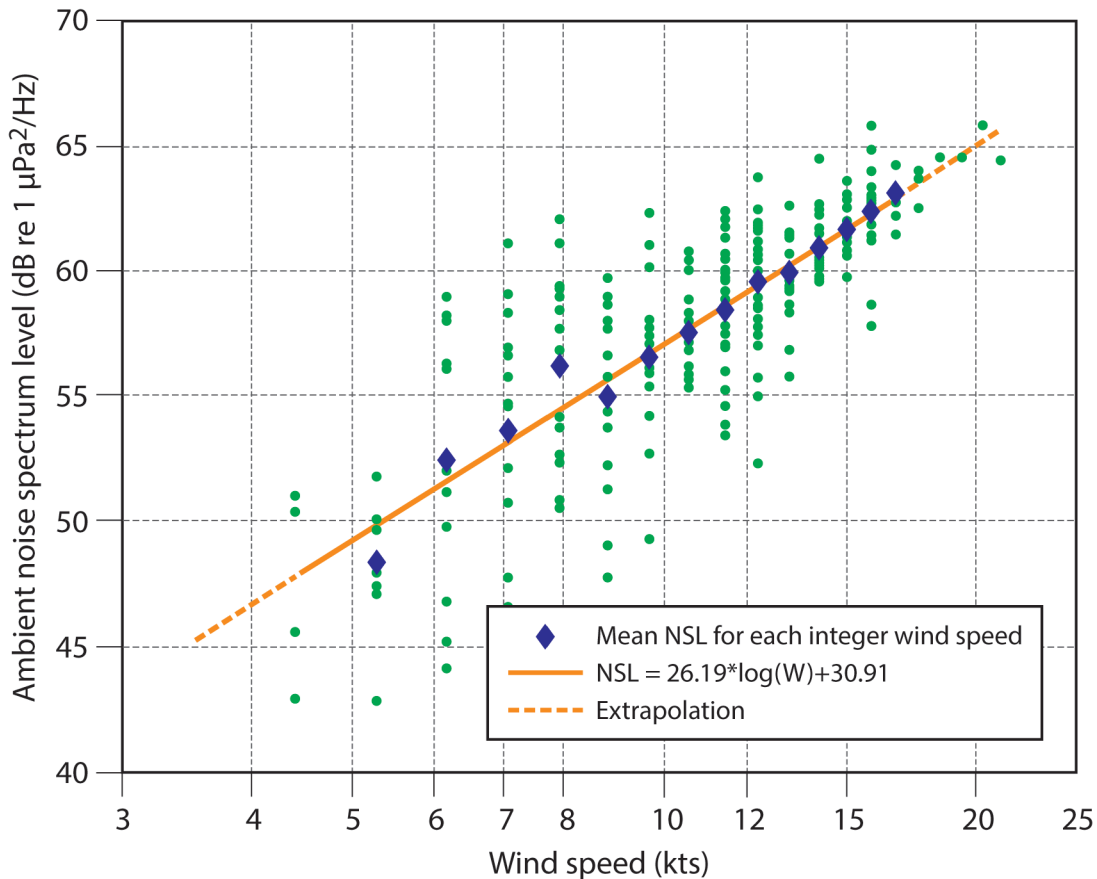
Figure. 3.4. *Ambient noise spectral density level (NSL) in relation to wind speed (knots) at frequency 1 kHz. Small data points depict 495 NSL values used to establish the correlation with integer values of the log of the wind speed. Diamonds depict mean values of NSL for each value of wind speed. The solid line indicates the linear regression based on mean values (diamonds). Dashed lines indicate regions of extrapolation of the regression. From Reeder et al. (2011). Used with permission from Acoustical Society of America, Copyright 2011.*

Temporal variation in ambient noise is substantial, typically around 20 dB, because of variation in weather and biological activity, with extremes of variation in excess of 30 dB. Localized individual sources can add substantially to the sound levels and variability in a soundscape. An example of the spectral and temporal variability of a soundscape off the Queensland coast is shown in Figure 3.5. Various natural and anthropogenic sources, continuous and transient, nearby and distant, contributed to this spectrum but, in general, only very specific sound sources, including two pingers, can be clearly distinguished. This type of plot showing the percentiles of variability in the amplitude of the ambient sound spectrum helps to summarize the ambient sound field.
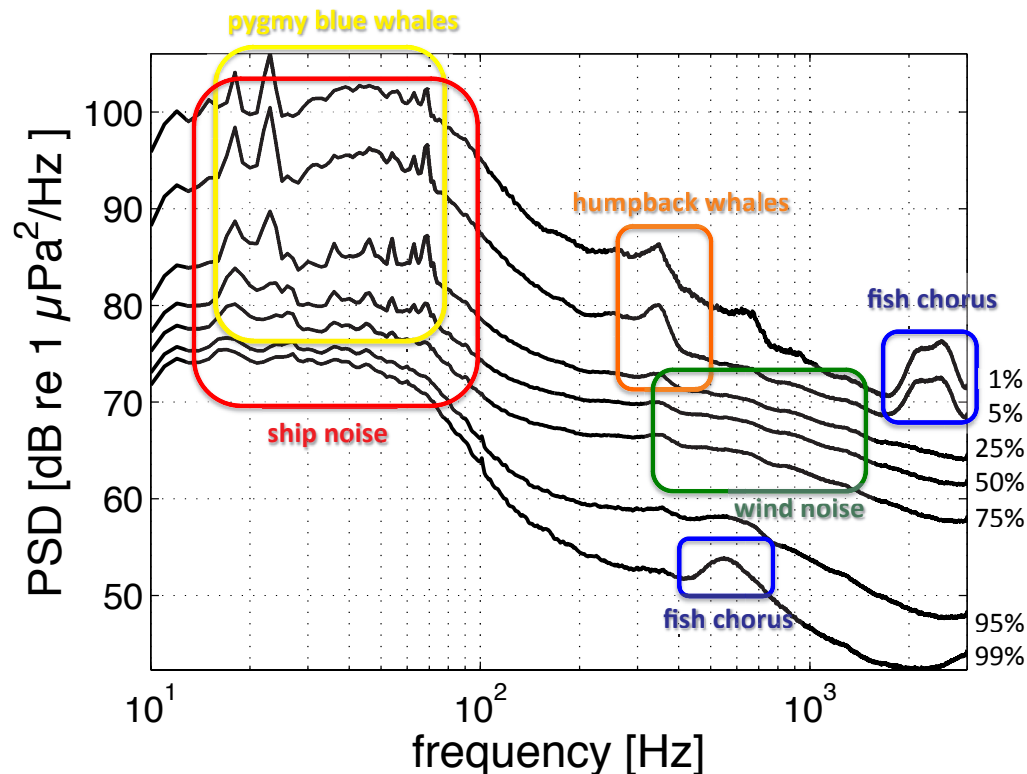
Figure 3.5. *Temporal variability of ambient sound spectral density (PSD) recorded over a full 12-month-period at the Integrated Marine Observing System (IMOS) acoustic recording station in the Perth Canyon off Western Australia. The nth percentile gives the level that was exceeded n% of the time. The 50th percentile is the median. Data and image from Centre for Marine Science and Technology, Curtin University, Perth, Western Australia.*

The identification, characterization, and localization of sources that contribute to a complex soundscape in a given location at a given time is a key factor in understanding soundscapes and their effects on marine life. "Source separation" can be spatial, temporal, spectral, or statistical (or a combination). It is important to appreciate the physical mobility and statistical nonstationarity of most of the sources of interest (at various scales) that often lead to using nonstationary descriptors such as spectrograms, in spite of their shortcomings.

As mentioned earlier, there are growing efforts to use environmental recordings to characterize the biodiversity of habitats, and differences between habitats. However, it is particularly important to separate nonbiological and anthropogenic sources of sound from the data used for these estimates, as this noise will bias the desired signal (Parks et al., 2013). The selection of time and location of recordings will also have to take into account temporal variation in signaling, propagation, and noise, and different ranges of propagation of sounds of different frequencies.

However, it is also important to understand why ambient sound amplitude and frequency vary through time. Sound profiles such as those illustrated in Figure 3.1 can provide clues about the sources of sound and, consequently, allow a certain amount of disentanglement of the ambient sound profile. For example, in regions where there is unlikely to be a large amount of local pleasure boat traffic, diel variation is very probably caused by biological sources that are often much more active at night than during daylight (see snapping shrimp in Figure 3.1). Diurnal variations in shipping noise have also been attributed to day-night differences in shoaling behavior of fish whose swim bladders absorb sound energy (Figure 3.6). Similarly strong seasonal trends in ambient sound in particular frequencies have been observed by the hydrophones deployed by the Comprehensive Test Ban Treaty Organization (CTBTO) in the Indian Ocean, and these are most likely associated with whale migrations. Annual changes with specific timings may also be related to weather, although there is evidence from some locations that the single most obvious signal is whale migrations on a seasonal time scale even compared with sound from wind and shipping (Burtenshaw et al., 2004).
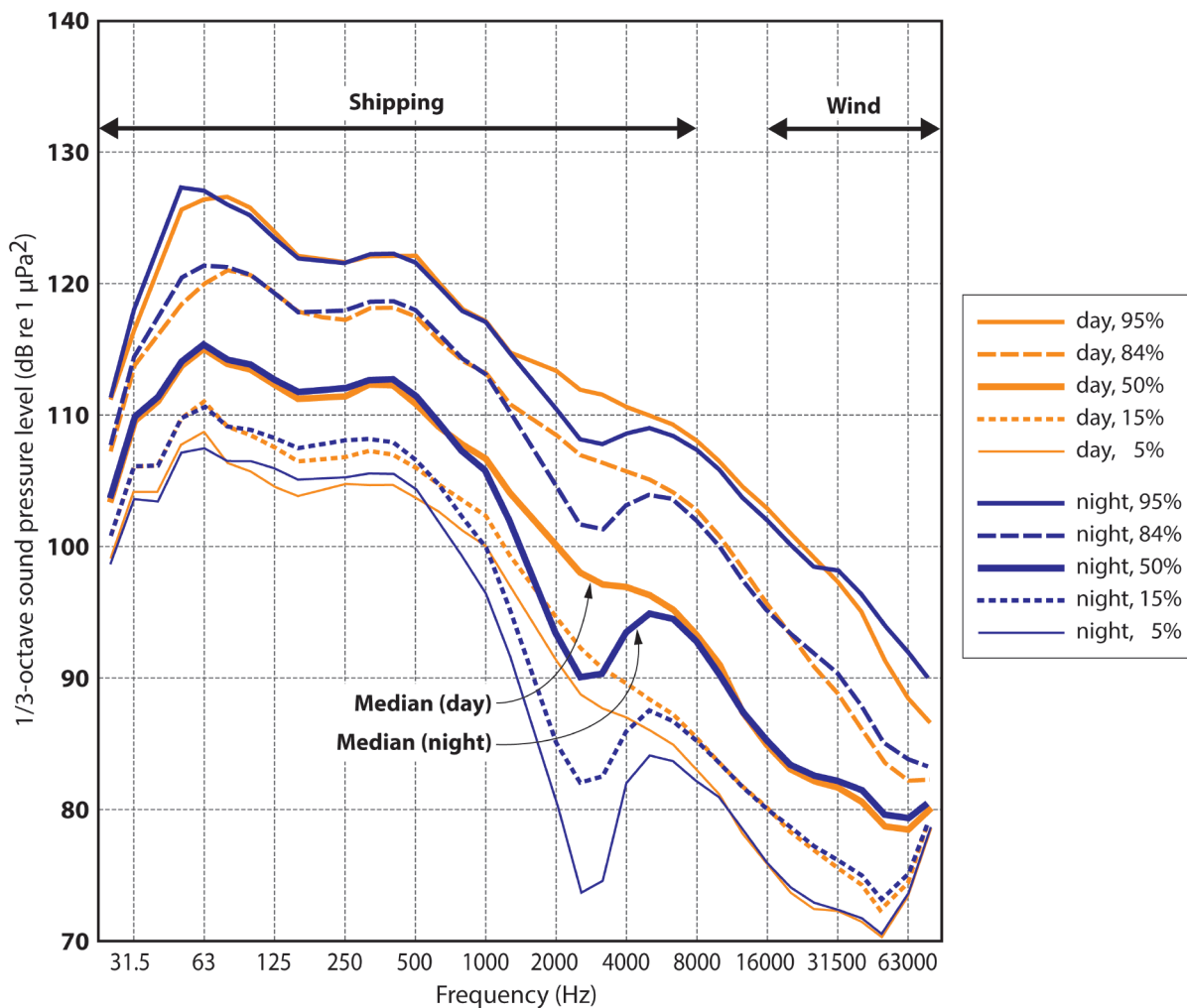
Figure 3.6: *Temporal variability in sound spectra (sound pressure level in 1/3-octave bands) during a one-week recording of ambient sound close to the Port of Rotterdam, including shipping-generated sound below 10 kHz, mostly due to dredging activity, and wind-related sound above 20 kHz. Strong diurnal changes in shipping sound are attributed to fish with air bladders, which absorb sound efficiently when dispersed at night (from Ainslie et al., 2011). Used with permission from the authors and the organizers of the Underwater Acoustic Measurement conferences.*

The intrinsic characteristics of the sources (in terms of factors such as spectral content, time evolution, radiation pattern) need to be characterized independently based on the way in which that sound is modified as it propagates through seawater, especially for physically large sources such as ships.

Nevertheless, in spite of our goal to characterize the sources that make up soundscapes, most existing studies represent soundscapes in terms of a spectrogram (e.g., Figures 3.1 and 3.5) and the motivation is to disaggregate the contributing components from a complex soundscape measured at a specific time and location. This approach has attracted a large amount of attention in the past because of the importance of localized sound sources in military applications used for detecting the signal of a submerged object from within the background ambient noise. Defining the position and main characteristics of contributing sources (in particular anthropogenic ones) relies on accurate modeling of sound propagation from the source to the measurement location, based on representative modeling of oceanographic features affecting sound propagation, such as wind speed (Figure 3.4; Nystuen et al., 2008), wave height, sound velocity profiles, ocean bathymetry, and sediment type.

It will be challenging to design systems that classify sound sources based on all available a priori information that could help in resolving the problem, such as oceanographic measurements, visual observations, ship tracks from the Automatic Identification System (AIS), and information about the presence of other industrial activities such as pile driving (Figure 3.3a) or seismic surveying. Access to

historical data may allow post hoc analysis. The identification of sound sources will need to rely on access to central libraries of recorded and identified sounds.

Automatic detectors and classifiers can be used for streamlined analysis of data. Classification systems will form an important part of the IQOE. Several commercial or open-source software tools are available for detecting, localizing, and classifying marine mammal sounds in real time or as a post hoc system for analyzing detections using WAV files. Individuals can design detectors for any sound source and load them into open-source software tools, broadening their applicability for the IQOE. Databases are also critical for validating detection and classification systems. For example, Mellinger and Clark (2006) describe an online database of low-frequency calls of baleen whales.

Key questions

Relevant questions related to understanding variation in ambient sound include the following:

- Can sound sources be classified into broad groupings that will provide sufficient detail to enable the construction of predicted ambient sound maps?
- What are the important sound sources for which we have insufficient information about both the sounds they produce and their distribution?
- What patterns in the behavior of sound sources and sound propagation are important to predict the underlying causes of ambient sound variation?

Research approach

The number and type of potential sound sources are almost limitless, making it impracticable to include every individual source in models to estimate soundscapes. In such situations, modelers often include a small number of representative elements in their models, scaling up individuals to populations based on estimated numbers or densities of individuals. The IQOE modeling activities will use such an approach, selecting a small number of representative examples of the three main classes of sound sources: physical, biological (Figure 3.7), and human-generated. For example, a model soundscape might include one or two species of baleen whales, one dolphin species, one fish species, a small number of storms in specific areas, and a few types of ships, naval sonars, and seismic surveys in specific locations.

Figure 3.7 *Examples of biotic contributors to ocean sound.*
(top) Blue whales (Balaenoptera musculus)*. Credit: NOAA: http://www.afsc.noaa.gov/nmml/gallery/cetaceans/blue-6.php,*
(lower left) Snapping shrimp (Alpheus lottini)*: http://smithsonianscience.org/2012/03/preventing-home-invasion-means-fighting-side-by-side-for-coral-dwelling-crabs-and-shrimp/, (lower right) Atlantic croaker* (Micropogonias undulatus)*: EFSC Pascagoula Laboratory; Collection of Brandi Noble, NOAA/NMFS/SEFSC. http://commons.wikimedia.org/wiki/File:Fish4327_-_Flickr_-_NOAA_Photo_Library.jpg*

For physical sources of sound, we will explore further examples of the use of wind data as a proxy for sound produced by weather and examine the extent to which the relationship between wind speed and ocean sound is consistent among these examples. A further factor determining sound levels in polar waters is that associated with ice movement and breakup. However, we will also test the hypothesis that this sound is related to wind speed. The sound produced by sea ice can take many forms. For example, during winter, thermal cracking is a major source, especially during clear nights (in this sense the sound is dependent on the weather). Ice fracture and compression-related cracks produce distinctive signals that depend on the larger-scale current and wind stresses. The closing of winter also produces a distinctive sound. Interaction of ice floes in the marginal ice zone is affected by wind and waves and is the source of significant sound. An important further source of sound is the noise generated by icebergs (Figure 3.8) as they calve and break up, and ice sheets as

they are moved by tides and winds.

Databases and libraries, or links to existing databases and libraries, of appropriate sounds will be created on the central data Web site for the IQOE by building on the Aquatic Acoustic Archive (http://aquaticacousticarchive.com/) and the MobySound (Mellinger and Clark 2006) archives that have already been created.

Furthermore, we will support the continuation of the *ad hoc* Detection-Classification-Localization (DCL) Workshop series, including researchers with a common interest in the detection and classification of marine biological sound, especially from marine mammals. Six workshops have been held in this series so far, the most recent in 2013 (see http://www.onr.navy.mil/reports/FY13/mbgilles.pdf). In this context, we will also support the further development of appropriate software systems for data collection and off-line analysis.

Figure 3.8. *The IQOE will estimate the contribution made to ambient sound by the breakup of Arctic ice floes. Photo by Brocken Inaglory, Creative Commons Attribution-Share Alike 3.0 Unported license.*

3.3 Modeling soundscapes (sources and propagation)

Information about ocean soundscapes can be used for different purposes. Biologists often want actual time-series data, representing precisely the sounds heard by whales, fish, and other organisms in the marine environment. This allows careful analysis, for example, of how shipping sound might mask communication between animals, or interfere with foraging. On a much broader scale, the sound power can be averaged globally and annually to describe trends (see Section 3.1) or determine sound budgets. The sound sources span a wide range of frequencies from the low-frequency rumble of earthquakes, the drumbeat of seismic air guns, and the churning sounds of ship propellers, to mid- or high-frequency sonar pings and the even higher frequency foraging clicks of marine mammals.

Significant effort has been devoted over the years to developing sound propagation models, mainly for naval applications. As a result, regions outside those of naval interest are sometimes poorly modeled; for example, an adequate model for range-dependent acousto-elastic environments (such as sandstone and limestone seafloors, or tropical reef environments) is still lacking. Furthermore, much of the navy-driven work has focused on detecting extremely quiet sources (submarines) by listening for them against the background of these other masking sources. Thus, the focus of modeling efforts essentially reverses foreground and background.

Modeling soundscapes is carried out using a variety of sound propagation models (Frisk, 1994). This requires information about sound sources (see Section 3.2) and about the structure of the ocean through which the sound is likely to travel. The prediction of propagation depends on the specific model used—and there are many from which to choose—and the characteristics of the environment. The models normally work by simulating the path of sound through water in two-dimensional slices radiating away from the sound source. As sound encounters different discontinuities, such as the surface, the seabed, or an ocean front, its path is determined by the characteristics of the discontinuity due to diffraction or reflection. The gradient and position of the thermocline as well as the density of the seawater, determined by measuring temperature and salinity changes with depth, therefore are important input variables within these models.

Consequently, to predict the propagation of a known sound in the ocean accurately, the following information is needed: (1) ocean "weather" or oceanography in terms of its temperature and salinity structure; (2) sea state in terms of surface wave and wind-generated bubble conditions; (3) water depth or bottom topography; and (4) geoacoustic sub-bottom structure in terms of the density, sound speed, shear wave speed, and attenuation of sound in the sediment. Sound speed in the ocean is also affected by pressure, creating areas of the ocean in which sound can be trapped in "waveguides" and propagated for long distances. Sound waves refract and reflect, much as light waves do.

Global bathymetry is probably the most readily available data, through sources such as the National Geophysical Data Center in the United States. International consortia (HYCOM, Mercator, and FOAM) provide global forecasts of oceanographic information. Global sources of information for the sea state need further investigation; however, satellite data often can give information about the roughness of the sea surface.

One of the biggest challenges in modeling soundscapes is to model the ocean bottom reflectivity accurately. Some limited global databases of ocean bottom composition are available. It may be possible to learn more about bottom reflectivity from existing sound sources (e.g., shipping traffic), reducing the need to add new sources. Exploiting this information to characterize the seabed, as well as the structure of the ocean, is an innovative challenge for the IQOE (Gervaise et al., 2007).

Overall, there will be a need to develop approaches to modeling that use approximations for information required. For example, we are uncertain how precisely variability in oceanic conditions will need to be specified for investigations of general questions at large spatial scales. Will it be necessary to specify ocean weather conditions precisely, or can functional relationships between ocean sound and wind speed provide an appropriate surrogate for ocean weather (see Section 3.2)? The precision of inputs necessary at any desired scale, and the uncertainties involved, will need to be specified.

Modeling the propagation of sound to characterize soundscapes is feasible at large scales within the open ocean. However, the complexity of shallow coastal environments will make it immensely difficult to develop useful predictive models in such areas. Instead, sound propagation models have been run on independent bearing lines assuming that the sound stays in a single two-dimensional vertical slice. The IQOE will encourage the development of modern advances in three-dimensional sound propagation modeling (Figure 3.9). A considerable factor in the uncertainty in these models is information about the sediment type and its acoustic reflectance and this uncertainty points to a need for improved integration of information about the geomorphology of the seabed to sound propagation models.
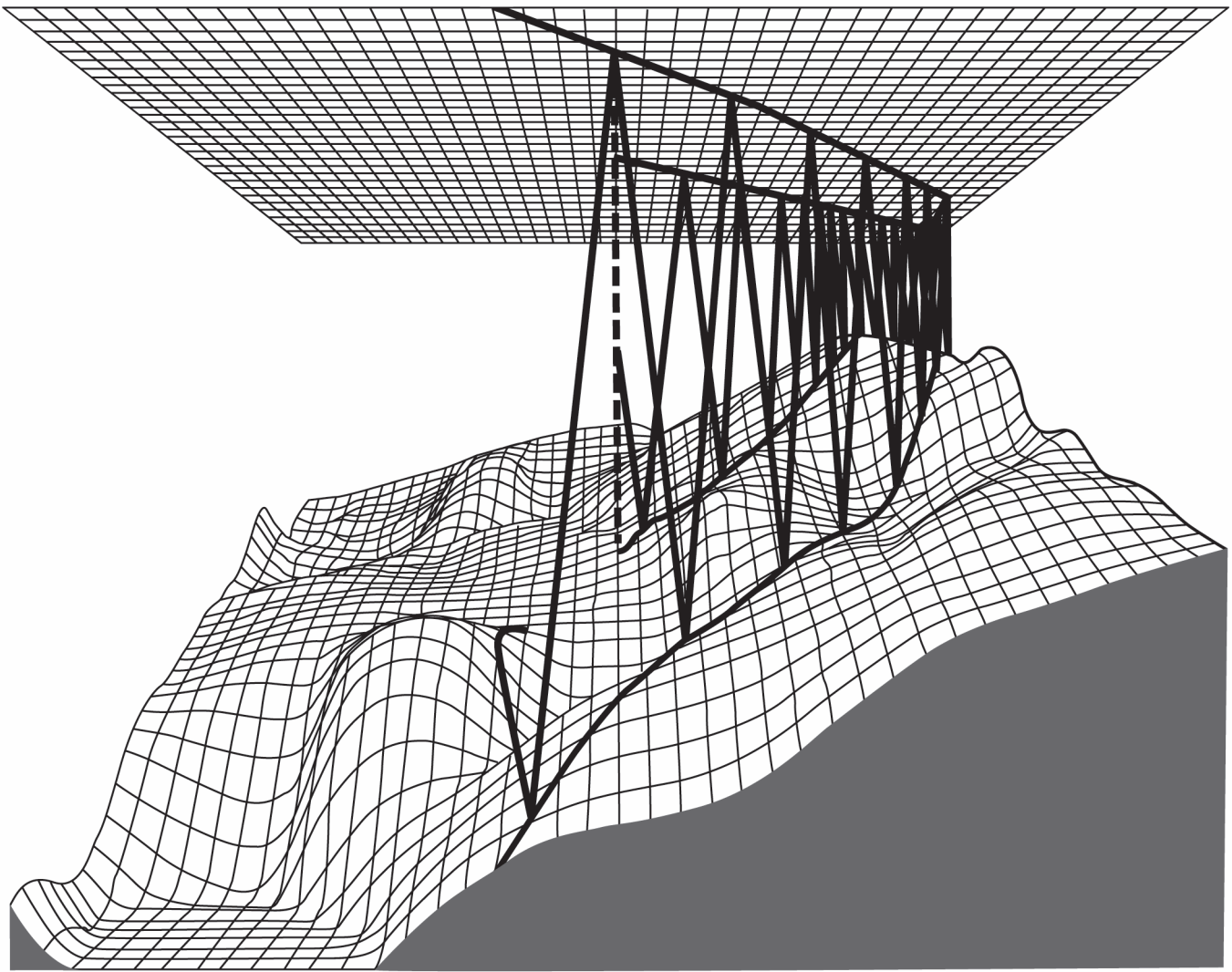
Figure 3.9. *Rays of sound, illustrating horizontal refraction, traveling over a complicated topography that produces three-dimensional effects, illustrating a model of a beam trace for shallow water near Hawaii. Permission from Bucker (1994). Copyright 1994, Acoustical Society of America.*

By making several broad assumptions, it should be relatively easy to generate soundscape models, but validation of these models will be much more difficult. The process of generating models will probably be most easily accomplished at large spatial and temporal scales but validation data, most probably generated through ocean observation (see Theme 3), will be most relevant to smaller spatial and temporal scales.

There will be a discrepancy between the spatial scales at which soundscape models are likely to be developed and those associated with data collection. This is because data are almost always collected at single locations and the extent to which that location can be used to validate models will vary with sound frequency. Point observations will be less effective for validation as frequency increases. Consequently, validation may most likely succeed initially at lower frequencies.

Model validation may be possible by fitting the model results to observations. Since the models themselves can be generated independently of the observations, it should be possible to establish Bayesian fitting procedures for soundscape models. Not only will this allow generation of an expression of the accuracy of models because the output will be a statistical distribution, but it will also help to further define the parameters in the soundscape models that provide most information.

Experimental validation is the ultimate test. To achieve

effective validation, it is necessary to be able to separate the individual components of the soundscape. This will require a variety of sensors, including horizontal and vertical line arrays, as well as vector sensors that respond directly to the particle velocity field sensed by many species of fish.

Site selection is also a key part of the validation. Sites in the Southern Ocean where human contributions are less important will be useful to assess the prediction of naturally occurring sound due to storms, lightning, wind, etc. In particular, a site under the Ross or Filchner ice shelves could provide a unique opportunity to establish conditions that would allow calibration of the ambient background sound level without contamination by local biotic or abiotic sounds. These sites are essentially 1000 km^2 caves isolated from anthropogenic sources of sound and that have their entrances pointing toward the South Pacific and South Atlantic oceans. However, specific recommendations about sites should emerge from a process that evaluates a set of alternatives and provides logic for the selection(s).

Key questions

Relevant questions related to modeling soundscapes include the following:

- To what extent can existing models be used to characterize global soundscapes and estimate the uncertainties within the models?
- What are the limits of modeling in terms of the scales at which it is possible to obtain reliable results and how does this vary between contrasting locations (e.g., offshore versus coastal)?
- What sampling is required for key parameters to characterize the main sources of sound?
- What sampling is required for key parameters to characterize the propagation medium?

Research approaches

We will establish a modeling working group to exploit situations in which it may be possible to test the validity, as well as the uncertainty, in different models. Ensemble modeling, the use of multiple models to evaluate specific scenarios, will be used to examine the influence of model structure and assumptions. This model validation may be carried out in conjunction with other studies in the Effects of Sound on Marine Organisms and the Ocean Observation themes (Themes 2 and 3, respectively). There may be areas, such as ice shelves in the Antarctic or isolated regions that are known in considerable detail and are acoustically quiet, like the Tongue of the Ocean, that provide opportunities for model development and validation. Indeed, the U.S. naval underwater ranges may be ideal for this purpose because of

the hydrophone arrays present and the high level of knowledge of acoustic propagation conditions in these locations. Some biologically important areas, such as shallow coastal areas, are particularly difficult to model and will require extra effort.

The IQOE also wishes to support the development of new models that include three-dimensional capability and that are dynamically linked to oceanographic models (Theme 3), as a way of developing improved real-time model performance.

3.4   Influence of climate change

The Earth's changing climate is resulting in increasing acidity and temperature of the upper ocean. The increasing temperature also is causing melting of polar ice caps and possibly increasingly frequent tropical storms. These changes can affect the soundscape in many different ways:

- Increasing average wind speed (Young et al., 2011) might lead to increasing contributions to noise from breaking waves and decreasing contributions from other sounds if these are weakened by surface scattering (Weston and Ching, 1989).
- The periods and areas for which sound is affected by melting ice will change. Changes in salinity will change sound propagation.
- Increasing acidity might lead to increased acoustic transparency (Hester et al., 2008; Brewer and Hester, 2009). Although theory suggests that pH changes have had a negligible effect to date (Joseph and Chiu, 2010), the possibility remains of a larger increase in the 21st and 22nd centuries (Ainslie, 2012).
- Increasing temperature might have at least two offsetting effects:
  - Increasing sound levels due to increasing transparency.
  - Decreasing sound levels due to increased average surface sound speed (Ainslie, 2012).

Key questions

Relevant questions related to the influence of climate change include the following:

- Does climate change influence the ocean soundscapes?
- If so, through which mechanisms?
- Is the effect likely to be an increase or a decrease in the level of sound, and over what time scales will any effects be observed?
- Can we control the rate of increase or decrease?

Understanding these influences would open up the enticing prospect of inferring key parameters associated with climate change from measurements of ambient sound.

Research approach

The IQOE will investigate the sensitivity of ambient sound to parameters related to climate change (wind, pH, temperature) through models, correlations, and experimentation. Identification of focus areas for regional studies will be based on interests of the scientific community and results of soundscape observations and modeling. A key area for studying climate change effects will be the Arctic Ocean.

Chapter 4
Theme 2: Effects of Sound on Marine Organisms

4.1 Introduction

Theme 1 projects will deliver comprehensive descriptions of soundscapes. These descriptions will make it possible to predict the sound environment to which organisms will be exposed in specific places at specific times, but this knowledge does not extend to the part of a soundscape that an organism can actually hear and, therefore, how it may be affected. Theme 2 projects will study the responses of marine organisms to their specific "acoustic environments," which are determined by the ability of an organism to hear specific frequencies and sound levels that are part of the soundscape. Each species experiences a different acoustic environment, although similar hearing abilities are often shared by different members of the same taxon. This theme will involve characterizing the hearing abilities of key species and then studying how these species are affected by changes in their acoustic environments, both in their physiology and in their behavior, and how these effects accumulate to produce population-level effects. The theme will include effects from both acute and chronic changes in noise levels.

Acoustic environment

Before studying how sound affects marine organisms, it is necessary to consider how a soundscape—the totality of the sound field within the close vicinity of an organism—translates into a specific organism's acoustic environment. This translation process depends on what organisms hear.

Sounds generated by human activities have changed the soundscape of the ocean, as discussed in greater detail in Theme 1, and modify the acoustic environment of many marine species. The acute, short-term impacts and chronic long-term influences of changes in soundscapes at biologically meaningful scales of time and space, and at meaningful frequencies, are poorly understood. However, there is increasing evidence that animals are responding to and behaviorally compensating for influences from anthropogenic sounds (Tyack, 2008).

Changes in the acoustic environment (primarily increases in human-produced noise) can affect several aspects of an organism's physiology and behavior:

- Increases in sound levels can negatively impact an organism's ability to communicate with others of the same species, its ability to navigate, and its ability to forage for food. The seriousness of the impacts depends on whether the frequencies of human-produced noise are the same as those of the sounds produced by the organism and on the levels of the human-produced noise. This general phenomenon is called "masking."
- Changes in sound levels may directly impact an organism's physiology, such as heart rate and breathing.
- Changes in sound levels may affect an organism's behavior, such as direction and speed of travel, avoidance of noisy areas (which may be preferred habitats), ability to find a mate and reproduce, etc. Changes in behavior may be so extreme as to lead to strandings. Note that sounds such as naval sonar can trigger strandings, even at frequencies far from those of best hearing and of those used by the species that strand (Cox et al., 2006).
- Loud sounds can potentially cause temporary or permanent damage to marine mammal ears or other body parts, although the evidence for such effects in wild populations is limited.

In some cases these changes can have a direct and acute impact on an individual (e.g., a beaked whale responding to mid-frequency sonar, Tyack et al., 2011). Changes in acoustic environment can also have a more indirect and long-term influence on a population, such as prolonged and large-scale reduction in communication space for northern right whales (Clark et al., 2009) and reduction in foraging efficiency in resident killer whales (Williams and Ashe, 2007).

Sound production by human activities becomes biologically significant to an individual animal when it affects an individual's survival or ability to reproduce (generally known as fitness). Because the acoustic environments experienced by different colocated organisms can be very different, sound at particular frequencies has the potential to elicit widely varying responses from organisms of different species and to change the relationships among species in ways that are more complicated than can be predicted by simple dose–response relationships. In some circumstances, sound can change the competitive balance among species, resulting in a cascade of effects within communities (Ruttenberg et al., 2011).

Sound in the ocean modifies the habitats and ecosystems of a broad suite of species, thus amplifying the ecological risk of disturbance and complicating our ability to detect cause-and-effect relationships between other stressors and the responses of organisms. This becomes a particular problem because the largest habitat modifications are likely to occur in the low-frequency range (<300 Hz), over large ocean areas (e.g., ocean-basin scales), and for long periods of time (e.g., months to decades).

Overall, therefore, more research should be focused on the acoustic environments of key marine organisms and how changes in sound affect interactions among individuals and species. The fundamental importance of empirical studies of reactions of species to sound is highlighted by the strandings of beaked whales caused by exposure to sonar. The naval sonars involved have fundamental frequencies well below the lowest frequencies of beaked whale vocalizations, and well below the frequencies of best hearing for beaked whales. On the basis of how beaked whales use and hear sound, environmental analysis might estimate low risk from naval sonars, but exposure to these sonars causes beaked whales in some contexts to strand and die (D'Amico et al., 2009).

How sound levels are expressed

An important task of an international project like the IQOE is to standardize how sound levels are measured and expressed by project participants. Acousticians use the decibel scale to represent sound levels; this is a logarithmic scale expressing a decibel value with respect to a reference value. The reference pressure for underwater measurements is 1 Pa, one millionth of a pascal (Pa). A pascal is the Standard International (SI) unit for pressure, expressed as a force per area, 1 Newton/m^2. Seawater and air differ so much in density and in the speed at which they transmit sound that it is difficult to compare levels of sound pressure in air with water. An additional complication is that different reference pressures are used for decibel measurements of sound in air and underwater. There is no general method to predict hearing abilities of animals underwater from their ability to hear in air, so attempts to assess the equivalence of sound pressure measurements in air and in water should be avoided.

A critical element of predicting and managing effects of sound on animals involves deriving dose–response functions that relate acoustic dosage to effects on animals. Different measures of sound waveforms have been associated with different effects on animals. The most common measure used in the literature is sound pressure level (SPL$_{rms}$), which is a root mean square (rms) level calculated for the duration of a sound. For effects of impulse sounds, such as

sounds of pile driving and explosions, on hearing, the peak pressure can be important. The peak-to-peak pressure is the difference between the maximum and minimum of the instantaneous sound pressure during a specified time interval and is denoted in pascals. The zero-to-peak pressure is the maximum absolute value of the instantaneous sound pressure measured during a specified time interval and also is denoted in pascals.

Invertebrates and most fish species detect the particle motion component of sound. This motion involves small displacement of particles and is often expressed in terms of nm/s^2. Some fish have anatomical specializations that allow them to detect sound pressure as well as particle motion (Popper and Fay, 2011). Auditory systems in these species include a connection between the ear and a gas-filled cavity. When sound hits the cavity, the pressure wave causes the cavity to move. These movements cause particle displacement that is then sensed by the fish ear.

Hearing capabilities and sensitivities of marine organisms

Marine mammals have ears that detect the pressure wave of sound. Cetaceans are adapted to hear sound underwater, but pinnipeds can hear both in air and underwater. Virtually nothing is known about the importance, if any, of sound to the early life stages of fish and invertebrates, but there is evidence of the capacity of young animals to use sound (Radford et al., 2011).

The sensitivity of hearing of an animal can be represented in an audiogram (Figure 4.1), which shows for each frequency tested, the lowest level of sound that the animal can detect. Audiograms are vital for translating soundscapes into the acoustic environment as sensed by a species. Figure 4.1 shows some audiograms for animals that hear sound pressure underwater. Invertebrates such as the squid or crustaceans do not have very sensitive hearing and cannot hear much above 1000 Hz, or 1 kHz. Invertebrates and most fish only hear the particle displacement component of sound, detecting sound energy as their body moves back and forth in the sound waves. A dense mass (the otolith for fish or statolith for invertebrates) sits on hair cells that sense the inertial force generated between the mass and the moving body. This means that they cannot hear sounds with wavelengths smaller than their body size. With a sound speed in seawater of about 1500 m/sec, this means that a 1.5 m fish would not be sensitive to sounds above about 1 kHz. Fish whose hearing is supplemented by connection to an air-filled cavity can hear higher frequencies, and the closer the connection between the cavity and the ear, the better their sensitivity to sound pressure. Figure 4.1 shows sensitivity to pressure in a variety of fish and mammal species. The codfish (*Gadhus*

morhua) detects particle displacement below 50 Hz and sound pressure at higher frequencies, so it is valid to display its hearing above 50 Hz on a pressure scale (Chapman and Hawkins, 1973). Popper and Fay (2011) argue that the goldfish (*Carassius auratus*), a much smaller fish, senses particle displacement below 500 Hz, but has a more direct anatomical connection between a gas-filled cavity and the ear. Comparing the audiograms for cod and goldfish shows that the goldfish with the more direct connection appears to be more sensitive and have better high-frequency hearing. Some clupeid fishes are sensitive to frequencies as high as those used by odontocetes for echolocation (Mann et al., 2001); this specialized hearing is thought to warn the fish of an oncoming predator.
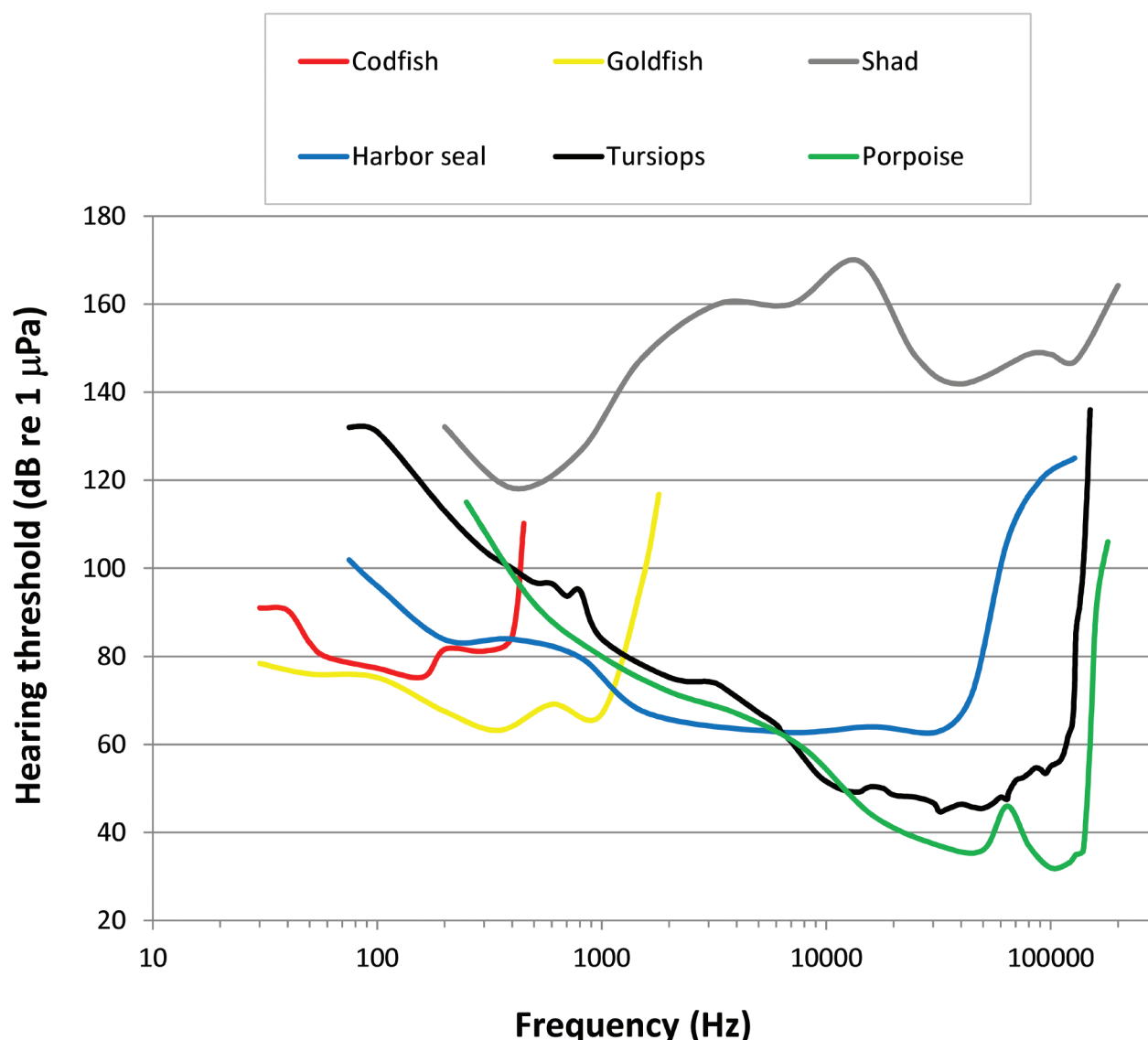
Figure 4.1. *Representative hearing thresholds (audiograms) of a range of marine organisms.*
Data from Johnson (1967: Tursiops: *bottlenosed dolphin); Møhl (1968: harbor seals); Fay (1969: goldfish); Chapman and Hawkins (1973: codfish); Mann et al. (1997: shad); Kastak and Schusterman (1995, 1998: harbor seals); and Kastelein et al. (2002: harbor porpoise).*

Pinnipeds are amphibious and have hearing adapted for listening in air as well as in water. The toothed whales use echolocation to orient, find, and capture prey. As with bats, echolocation has selected for high-frequency hearing; small porpoises are specialized for particularly high hearing ranges and delphinids for a medium range between that of the pinnipeds and that of porpoises. Hearing has never been measured in baleen whales, but their use of sounds in the 10-

1000 Hz range and the anatomy of their ears suggest that they are low-frequency specialists (Ketten, 2010). Seals can hear frequencies underwater ranging from about 75 Hz to 75 kHz, while most toothed whales and dolphins are thought to hear from about 200 Hz to 200 kHz. Their use of echolocation favors highly sensitive hearing at unusually high frequencies. The porpoises and several dolphin species use narrow-band high-frequency echolocation signals and appear to have hearing particularly specialized for high frequencies.

To correct sound exposure for the frequency range of hearing for different taxonomic groups of animals, it is possible to apply weighting functions to filter sound energy and predict the potential impact on these taxa (e.g., Southall et al., 2007; Figure 4.2). Other approaches have been suggested, such as Tougaard et al. (2014).
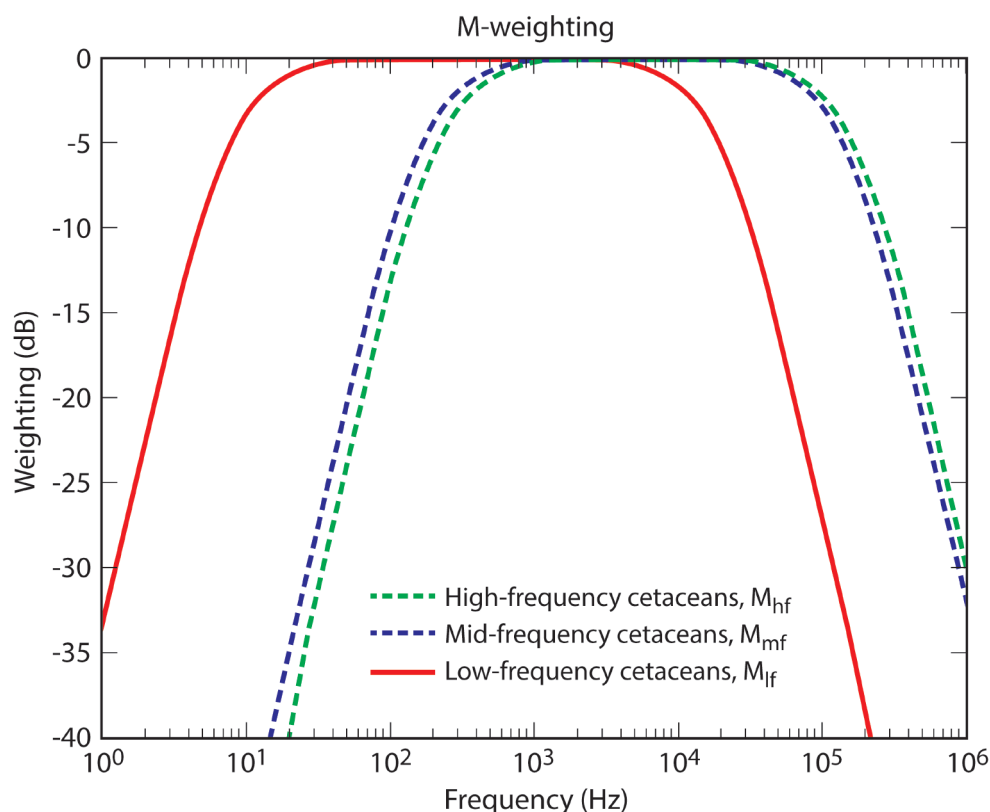
Figure 4.2. *Weighting curves suggested by Southall et al. (2007) to filter sound signals by the hearing capabilities of different cetacean taxa. Permission to reuse figure granted by the journal* Aquatic Mammals *and the authors.*

Sound exposure levels

To define criteria for sound exposures that damage hearing, Southall et al. (2007) reviewed experiments that quantified temporary reductions in hearing sensitivity after measured exposures to sound. The longer the exposures were, the lower the sound pressure levels required to cause the same hearing loss. The sound exposure level (SEL) is an acoustic measure that is useful for accounting for this relationship between level and duration. The sound exposure level for a sound of duration T is the equivalent sound pressure level (SPL) if the sound had a 1-second duration. Southall et al. (2007) advocate using an exposure criterion for hearing damage based on sound exposure level weighted by the frequency range of hearing. They also add a second criterion of peak pressure level unweighted by hearing curves, as sudden intense fluctuations of pressure can also damage the ears of marine organisms.

Effects of anthropogenic sound on marine organisms

Relatively little is known about the effects of anthropogenic sound on marine organisms, in relation to what we need to know. The hearing thresholds of most marine organisms have not been precisely described. Although there is considerable knowledge of the anatomy of auditory systems in marine vertebrates (Fay and Popper, 2000; Ketten, 2010) and of the mechanics of hearing, important uncertainties remain regarding the diversity of frequency-dependence of hearing capability, as well as hearing sensitivity, in many species. Even in species whose hearing capabilities have

been studied in considerable detail, mainly a few fish species and a small number of marine mammals, little is known about how hearing varies with age and other life-history features, such as sound exposure history.

Invertebrates—Most invertebrates are thought to detect particle motion (Budelmann, 1992), but there is relatively little understanding of their hearing capabilities.

Fish—Fish detect particle motion as well as sound pressure (Popper and Fay, 2011). Popper and Hastings (2009) reviewed the literature for fish and concluded that little is known about the effects of anthropogenic sounds on fishes, and that it is not yet possible to extrapolate from the results of one experiment to other parameters of the same sound, to other types of sounds, to other effects, or to other species. This is a typical situation.

Marine Mammals—More is known about effects of sound on marine mammals (Southall et al., 2007) than on invertebrates or fish. The earliest studies focused on behavioral responses that were obvious to visual observers. The most common response observed was avoidance. While avoidance can cause animals to leave preferred habitats, few studies have actually measured whether avoidance forced animals to move to suboptimal habitat. Other responses have been interpreted as disturbance responses. For example, U.S. permits for marine mammal research list "breaching, tail lobbing, underwater exhalation" as strong adverse reactions to vessels. Many papers report specific cases in which such behaviors were associated with some human activity, but there have been fewer studies structured to test whether the rate of these behaviors was actually higher during exposure to disturbance. The only case of lethal behavioral reactions of cetaceans to anthropogenic noise involves atypical mass strandings of beaked whales that occur during naval sonar exercises. Correlational studies have demonstrated a statistical association between these strandings and sonar exercises in several sites around the globe (D'Amico et al., 2009; Filadelfo et al., 2009). However, there has been growing understanding that disruption of critical activities

may be just as important as documenting acute responses. For example, Miller et al. (2009) found a reduction in swimming effort accompanied by an apparent reduction in foraging when sperm whales were exposed to seismic surveys, and Goldbogen et al. (2013) found a similar effect of naval sonar on foraging blue whales. Any disruption of critical activities—such as foraging, migrating, avoidance of predators, or group cohesion—could pose more significant risks to individual animals and populations. Acute effects have been summarized by Southall (2007), but there are few systematic studies on whether and how anthropogenic sound may disrupt critical activities. For example, the effects of masking of communication by anthropogenic sound and chronic disturbance of normal activities by sound are poorly understood.

Dose–response curves

Dose–response curves have also been estimated for behavioral responses of marine animals to underwater sound. For example, Miller et al. (2014) estimated the sound pressure level of naval sonar likely to cause avoidance reactions in killer whales. In an extensive review of the literature, Southall et al. (2007) found that SPL_{rms} was the most common acoustic parameter reported for sound exposures. The precise parameters of acoustic exposure that lead to response have seldom been tested, and are likely to vary depending on nonacoustic contextual parameters as well (Ellison et al., 2012). For perception of loudness, the mammalian ear tends to integrate sound energy over periods of 200-500 ms (Southall et al., 2007) and over frequency bands of about 1/3 octave. These results suggest parameters for estimating the loudness of a signal as perceived by a marine mammal. However, responsiveness to sound may depend on details of the waveform (e.g., does it sound like a predator?), the state of the animal (already stressed?), and the behavioral context (feeding? traveling?). In spite of our understanding that many factors influence behavioral responses, most studies of dose–response relationships emphasize a univariate response to an acoustic parameter like the one illustrated in Figure 4.3. The derivation of these types of relationships is central to predicting and managing the effects of anthropogenic sound on marine organisms.
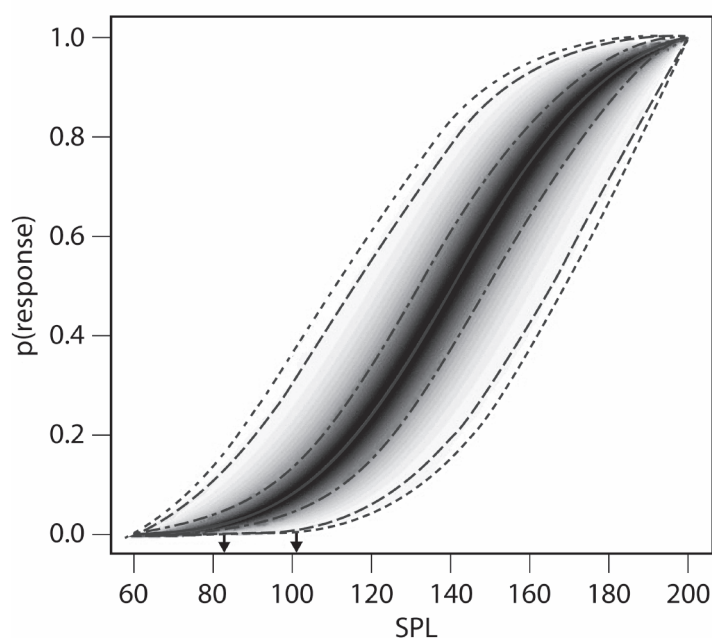
Figure 4.3. *Posterior dose-response curve showing the probability of onset of avoidance against received SPL (dB re 1 Pa). The solid central line represents the mean, followed by 50%, 95%, and 99% credible interval lines. The dose-response model assumes the signal is audible over the range, but the limited data on the threshold of hearing for 1−2 kHz signals by killer whales indicates that sensitivity ranges from 101 dB re 1 Pa at 1 kHz to 83 dB re 1 Pa at 2 kHz (marked in the figure with small arrows). Used with permission from the Acoustic Society of America.*

In some cases, responses are defined by physiological criteria, such as permanent or temporary threshold shifts (Southall et al., 2007). But functions relating behavioral responses to acoustic exposures, such as the black curve for avoidance responses of killer whales in Figure 4.3, are increasingly recognized as important. Exactly which threshold is most important will vary with the signal being tested and with species and circumstances, but in general, we need more information to create these kinds of response functions. Similarly, although Figure 4.3 shows "avoidance" as the response criterion, where this signifies a change in behavior as a result of sound exposure, many other criteria could be used; establishing which criterion is most important biologically, as opposed to which is most easily measured, will make a considerable difference to assessments of the effects of sound on the life functions of marine organisms (see Figure 2.4).

Regulatory use of noise measurements

A variety of jurisdictions have established regulatory criteria for the effects of sound on marine life. The regulator in the United States, the National Marine Fisheries Service (NMFS), has established criteria for "takes" under the Marine Mammal Protection Act (MMPA). For example, NMFS has established that exposure of harbor porpoise (*Phocoena phocoena*) to SPLs above 120 dB re 1 µPa are likely to cause behavioral harassment, a "level B take" under the MMPA. Similar exposures above 140 dB re 1 µPa are assumed to cause behavioral harassment in beaked whales. These takes of individual animals are prohibited by law, and are regulated whether they have long-term impacts on populations or not. By contrast, the Marine Strategy Framework Directive (MSFD) of the European Union (EU) focuses on measuring noise levels instead of actual effects of sound on animals (Van der Graaf et al., 2012). The MSFD proposes to monitor for good environmental status by measuring average SPL_{rms} in two-third octave bands at 63 and 125 Hz, thought to indicate noise from shipping that will propagate long distances. Management actions under the MSFD are likely to focus more on limiting noise exposure rather than limiting effects on wildlife as in the U.S. regulatory framework.

The kind of soundscape information provided by the IQOE from activities as part of Theme 1 should be helpful for managers to evaluate, support, and improve some of the noise monitoring requirements established by the European Union. However, effective protection of marine life from adverse effects of underwater sound will require an understanding of what sound exposures pose what kinds of risk. That kind of understanding will result from activities as part of Theme 2. The IQOE will make it a priority to improve the definition of the response functions for key species, especially keystone species within ecosystems, commercially important species, and species of conservation concern.

4.2. Hearing capabilities of key species and experimental methods for establishing functions relating acoustic exposure to behavioral responses

Key questions

- What are the hearing capabilities of key species?
- How can dose–response functions be created and expressed in forms that are scientifically accurate and meaningful for management decisions?

Fundamental to relating soundscapes to individual organisms and populations is to determine the acoustic environment for a species, the parts of the soundscape that the species can actually hear. The ideal way to objectively

quantify the hearing capabilities of any organism is to directly measure responses to a range of frequencies and sound levels, that is, to create an audiogram for the species. NRC (2000) recommended that U.S. federal agencies sponsor collection of audiograms from large samples of multiple individuals of different ages and both genders, including stranded and rehabilitating marine mammals.

Ideally, multiple individuals should be tested, over a range of ages, including both males and females, to describe an average or typical audiogram, and also the ranges in hearing abilities that may be present in a population. Most organisms cannot verbalize when they can hear or do not hear a sound, so other means of detecting whether a sound is audible need to be employed. Some marine mammals have been trained to indicate when they hear a sound. White (beluga) whales were trained by U.S. Navy scientists to indicate heard sounds at various depths in the open sea (Ridgway et al., 2001). Most other audiometric measurements that involve training have used animals in captive settings.

It is difficult or impossible to train most marine mammals, and particularly the larger toothed and baleen whales, to indicate what sounds they can hear. In these cases, it has occasionally been possible to test for "auditory evoked potentials" as the brains of organisms are exposed to sounds and brain reactions are measured. This technique, also used by physicians to test the hearing of newborn infant humans, has been used on stranded and rehabilitating marine mammals to test their hearing ability. For example, Nachtigall et al. (2005) determined the audiogram of an infant Risso's dolphin, Yuen et al. (2005) determined the audiogram for a false killer whale, and Castellote et al. (2014) used evoked potentials to test the hearing of beluga whales. Admittedly, the audiograms may represent the hearing of distressed individuals, but they correlate well with measures based on behavioral responses (Nachtigall et al., 2007).

Finally, the most widely used experimental method of testing whether specific sounds evoke specific behavioral responses of animals in the wild is to play sounds to a subject and look for behavioral responses. In free-ranging animals that are submerged at the time of exposure to sound, it may be difficult to observe behavioral responses directly and to obtain real-time feedback about the dosage given. A recent approach to resolving these problems has been the deployment of receivers on larger marine mammals that can both hear the sound sources (and thus measure received levels) and detect behavioral changes due to the sounds. This method often involves attaching a tag to each experimental subject. A typical tag for large whales is

described by Johnson and Tyack (2003), but may require modification for each species, and in many cases it may not be feasible to manufacture tags small enough to attach to the animals of interest. In these circumstances, alternative methods for recording the received sound and the animal's response will be required. The tag described by Johnson and Tyack (2003) was designed to record sound and behavior throughout the dive cycle of a whale even when animals are deep and out of view. Nonacoustic sensors also recorded depth, temperature, orientation, and acceleration of the whale. These nonacoustic sensors were sampled rapidly enough to capture fluke movements and swimming behavior, along with subtle changes in orientation. These types of tag are capable of simultaneous measurement of the dose of sound received and the behavioral response of the animal.

Under specific circumstances, there may be opportunities to conduct experiments that have a considerable level of control, for example, through controlled exposure experiments (CEEs). Although the IQOE will attempt to develop protocols that do not require the addition of sound to the ocean, some of the most successful recent studies have involved examining the response of animals to carefully controlled doses of sound (e.g., Tyack et al., 2011; DeRuiter et al., 2013). Controlled exposure experiments use well-established methods in the behavioral sciences to study the responses of animals to stimuli. When acoustic stimuli are used, the method is usually called a "playback experiment." An extensive literature documents the design of playback experiments (e.g., Kroodsma, 1989, 1990; Kroodsma et al. 2001; McGregor, 1992, 2000; Wiley, 2003). Classic playback experiments are only concerned with measuring and evaluating different responses to different stimulus types. The added features for controlled exposure experiments on sound involve controlling the level of exposure at the animal, and determining the minimum sound level that starts to elicit a response. The protocol normally achieves this goal by slowly increasing the received level at the animal from a level near what is just detectable until the animal responds, or a maximum planned level is reached (Tyack et al., 2011). This dose escalation ensures that the exposure at each animal is the minimum required to define the dose–response relation and to measure the response. If any such experimental studies are judged to be essential for resolving critical uncertainties about effects of sound on marine animals, for the IQOE to support them, they would have to involve sound exposures that are sufficiently limited in intensity, range of detection, and duration that they would be expected to have minimal effects beyond the specific question being studied, and the link between exposure and effect could not be demonstrated by using ongoing exposures.

Box 4.1 includes several detailed questions about effects of acoustic exposure.

Box 4.1. *Examples of questions to be addressed on the topic of dose–response relationships*

- **Physical and physiological effects**
    - Does background sound cause masking of animal communication and, if so, to what extent?
    - Do animals compensate for masking?
    - How do we measure or assess how the received sound is perceived by the animal? Does this change with environmental context?
    - Which animals are more susceptible to intense sounds, such as naval sonar or sounds used for seismic surveys? For example, are large whales more susceptible than small whales or fish?
    - What frequencies can be heard by various species of marine life? What are their audiograms?
    - How can we best estimate the hearing range of animals, for species where hearing cannot be measured directly?
    - Can hearing damage from sound be modeled?
    - What impact does long-term sound exposure have on the hearing ability of marine life? Is there an effective recovery period?
    - Could anthropogenic sound sources cause animals to become frightened, resulting in decompression sickness in the case of air-breathing marine organisms?
    - What are the impacts of industrial sounds on fish and turtles?
    - What are the impacts of industrial sounds on invertebrate species?
    - What is the relationship between equal loudness curves and audiograms?

- **Behavioral effects**
    - What aspects of the sound source are responsible for behavioral response: sound exposure level, peak pressure, frequency content, harmonic context, texture, etc.?
    - What behavioral responses occur when animals are exposed to anthropogenic sound sources?
    - How do anthropogenic sound impacts vary by species and environmental context?
    - Do long-term industrial operations have impacts on animal residency? If so, which species are most affected and to what extent?
    - What is the impact on animal populations of the masking of sound used for communication and echolocation?
    - Do animals become sensitized or habituated to repeated particular sound exposures?

Controlling the dose—Controlling the dose of sound received is an important component of a CEE. Since, for some species, high doses of sound could be damaging, the basic principles for achieving a balanced dose–response involve the following steps:

- Monitor response in real time.
- Establish a mechanism to cease exposure or prevent increases in the exposure level if response reaches a preset threshold.
- Evaluate the response for risk before increasing the duration or intensity of exposure.

Another concern is the need to control potential exposure for animals that are not the focal subjects. In free-ranging conditions it is possible that nonfocal individuals within a population will receive a greater dose than the focal animal. Monitoring efforts need to be put in place to reduce this risk.

Control subjects—Experimental designs require control subjects in addition to subjects exposed to a particular dosage range. Depending on circumstances, these could be unexposed individuals within the population or, probably more often, individuals will act as their own control. In these circumstances, the most critical part of most CEE designs is the ability to monitor specific animals' undisturbed behavior before exposure to a sound, followed by detailed monitoring of their responses during and after exposures. This before/during/after design is especially

useful where there is a high variance among individuals in expected behavior, but it requires in the subsequent analysis that the identity of each individual be included as a covariate.

Control stimuli—While an experiment may be designed to examine the response to a primary stimulus (such as sonar sound, ship sound, or pile driving), every controlled exposure experiment also requires control stimuli. One standard "silent" negative control stimulus would involve following the protocol in its entirety but without transmitting the signal of interest. There are also questions about how specific any observed response might be to the primary stimulus and, where this is important, a negative control stimulus should be used with the same timing and frequency range as the primary stimulus, but with band-limited noise instead of a specific waveform.

Research approaches

Hearing—The first task in approaching this key question is to compile all available data on hearing capabilities of marine organisms, including all the audiograms. A workshop will be held to discuss the available data, synthesize it, identify gaps in the data, discuss the potential list of representative species below, draft a review paper for the peer-reviewed literature, and develop an implementation plan for this key question.

A set of representative species, for which audiograms or other measures of hearing capabilities will be developed, should be identified. The following is a representative list of potential species. Audiograms for a few individuals already exist for some of these species, but more individuals should be tested. In some cases, this will require the development of new equipment and new techniques.

- Baleen whales: blue whale, northern/southern right whales
- Toothed whales and dolphins: killer whale, bottlenose dolphin, harbor porpoise
- Pinnipeds: harbor seal, ringed seal
- Sirenians: dugongs and manatees
- Birds: penguins, auks
- Fish: damselfish, tuna, plainfin midshipman
- Turtles: green turtle, leatherbacks
- Invertebrates (molluscs, crustaceans): squid, ghost crab, lobster, krill

Dose–response functions—Defining dose–response functions will require experimental studies of behavioral responses to sound exposure. Controlled exposure experiments may be performed under this theme to create

dose–response curves for these organisms, where these experiments will not endanger the test organisms or others. The IQOE will begin to answer the second key question (How can response functions be created and expressed in forms that are scientifically accurate and meaningful for management decisions?) by convening a meeting of scientists and managers to determine the kind of information that is both relevant to IQOE and possible for IQOE to provide, as well as meaningful for management discussions. This meeting will review and set priorities for cases of putative connections between sound exposure and behavioral responses where experimental studies are required to demonstrate the link and to define dose–response functions. The meeting will be held after the workshop on hearing capabilities.

4.3 Effects of changes in acute noise

Key questions

The key questions regarding the effects of changes in acute noise are the following:

- What frequencies, sound levels, and durations have effects on the physiology and behavior of key species?
- How do changes in sound levels affect interactions among species?

Section 4.2 discusses experimental methods for demonstrating the link between exposure to sound and acute behavioral reactions. The IQOE will, where possible, emphasize observational studies that do not require the introduction of new sounds. In uncontrolled experiments, significant effects of sound on marine organisms can be difficult to observe. Moreover, effects can be acute or chronic and, in general, it may be easier to observe acute rather than chronic effects. However, experience with some marine mammals (Cox et al., 2006) shows that the occurrence of certain extreme acute effects of sound exposure, such as stranding, can be classified as rare. Many organisms may have thresholds of response rather than a graded dose response (Figure 4.3) and when these thresholds are exceeded an acute intense response may suddenly occur. However, even in these circumstances, acute responses may be context-specific, so that the probability of an effect depends on both the probability of sound exceeding a threshold and the exposure happening in a context in which the animal is susceptible to the effect. Similarly, probability of response can be low at the low end of exposure for a dose–response function. In spite of this low probability, acute effects may still be biologically significant when they occur in species that have relatively low population resilience, such as marine mammals. The

majority of previous work on effects of sound has focused on acute effects on behavior that are relatively easy to measure. The IQOE will focus on selecting effects at spatial and temporal scales that are most important to populations and ecosystems.

Measuring stress—Behavioral responses to sound exposure or quieting are often observable and measurable responses to anthropogenic sound, but population-level effects of this sound will also be modulated through physiological stress responses. The main stress response in marine mammals is similar to the generalized stress response for other mammals, which is defined by activation of the hypothalamic–pituitary–adrenal (HPA) system in response to an internal or external stimulus (or stressor), resulting in elevated levels of glucocorticoid (GC) hormones (i.e., cortisol and corticosterone). Whether the response is beneficial or deleterious depends on the magnitude and duration of the response and the condition of the animal exposed to the stressor. Prolonged exposure to stress may result in immune system suppression, reproductive failure, accelerated aging, and slowed growth. If GCs are not the primary mechanism, they and other biomarkers may well be indicators of a cascade of effects leading from behavioral changes to alterations in reproduction and survival. However, even among well-studied mammal species, finding individuals exhibiting stress indicators outside the normal range of value for the species may not be indicative of widespread stress because different individuals have widely varying baseline levels of these stress indicators. A recent study suggested that symptoms of stress had been observed in right whales exposed to sound (Rolland et al., 2012), but the changes observed were within the normal range of variation and, while there was an association with a change in ambient ship sound, the relationship was weak. The IQOE will seek to use robust and verifiable measures of stress in organisms to obtain valid evidence of effects of sound on the physiological conditions of organisms.

Stress, measured in terms of similar hormonal indicators, is less well understood in fish and invertebrates. As in mammals, hormones are chemical signals that can have multiple functions operating with different potency on different receptor tissues. The function of hormones is modified through natural selection and through adaptation and acclimation. Consequently, their uses as signals of stress need to be validated carefully. But the concept of stress involving incapacity to adapt or acclimate to immediate environmental conditions is well understood. The ways in which marine species adapt or acclimate to stress are many and varied, and they reflect an underlying complexity of physiological function that may not yield

simple indicators of stress related to the effects of noise.

Interpreting point measures of endocrine responses to a stressor requires a good understanding of the natural variation in hormones associated with the generalized stress response. In free-ranging animals, where blood is difficult or impossible to sample, this understanding must rely on collecting biological materials that are more amenable to sampling. Although levels of hormones that potentially indicate stress, such as cortisol in the bloodstream, provide relevant information about stress, accumulation in other tissues and excretions such as blubber, skin, hair, feces, and exhaled breath may provide measures of chronic stress because they are integrated measures of the magnitude and duration of physiological stress responses. Thus, to use stress hormones from matrices beyond blood as indices of stress, the relationship between the levels and dynamics of hormones in blood and other matrices must be determined.

It remains to be seen whether it is possible to define "stress" with sufficient rigor and consistency to make it a general goal of the IQOE to measure stress in marine organisms as a general response variable. In its most general form, stress simply measures an aspect of an organism's physiology that is outside its normal range. Making and using such measurements will need to be judged based on individual cases and, in some specific circumstances, they may prove to be useful.

Research approach

Selecting key species—Since different animal taxa may show fundamentally different responses to sound, the IQOE will need to focus on key examples of several different species or taxa. These should be chosen to capture different lifestyles and population demographic features, while representing species for which we have good ancillary knowledge in a variety of study areas and situations, or that are especially amenable to study. Some animals may have a size and physiology allowing for large data loggers to be deployed on them for extended periods (e.g., seals), whereas deployment of large tags can be difficult for other species (e.g., fish, small odontocetes). Some species may have a lifestyle allowing for direct measures of fitness (e.g., damselfish), whereas it may be virtually impossible to measure this directly in others (e.g., baleen whales). Some locations may have patterns of disturbance that are favorable for opportunistic studies (long periods of silence, followed by long periods of activity). The optimal setting for these studies would include several of the best study species in sites where detailed information on soundscapes has been

and will continue to be collected. The list of representative study species should be based on a combination of the recommendations of the workshop on hearing capabilities and the results of Theme 1, so that the species with the best information in the best locations can be studied.

Baseline studies—Baseline studies provide a quantitative assessment of the normal, undisturbed state of organisms, communities, social structures, and populations. One of the greatest challenges to characterizing baseline conditions is that there may be high natural variability in the parameter(s) of interest. This natural variability makes the detection of changes resulting from the introduction of sound much more difficult because the effect must be differentiated statistically from natural variation. However, depending on what parts of the background variation are important to organisms, the low power of detection does not mean the effects of introducing sound are unimportant. Higher statistical power to detect changes can be obtained by either extending the duration of the baseline observations or by measuring a broad range of covariates alongside the baseline. These covariates could include other potential anthropogenic stressors that may change during the course of the study, but may also include indicators of the natural physical, chemical, and biological characteristics of marine systems. Including such variables within a statistical analysis to look for significant effects

from the acoustic exposure may greatly increase the chances of detecting these effects because the analysis controls for the effects of the covariates on the signal of interest. Nevertheless, even in circumstances where no "signal" is detected, there remains the possibility that the signal exists, but there is insufficient statistical power to detect it. Moreover, just because a signal cannot be detected by currently available technology and equipment does not mean it is not biologically significant, and conversely, even if a signal is detected this does not mean it is biologically significant. A key role of the IQOE will be careful selection of study situations that optimize our chances of detecting biologically significant effects at a range of spatial and temporal scales.

The IQOE will include many opportunistic studies. Most will be characterized by some form of observation of marine life and sound associated with a human activity that is generating sound. Observations of this type will be facilitated by the rapid increase in the availability of relatively inexpensive and mobile observation systems (Figure 4.4), which often collect and process data in real time on multiple channels. These multivariate time series, in which sample sizes can be very large, are amenable to the application of statistical modeling to discriminate among effects caused by changes in specific factors, including levels of anthropogenic sound.

Figure 4.4. *PAMBuoy is an example of a passive acoustic monitoring system mounted on a moored or drifting buoy that measures marine sounds and carries out acoustic detection and classification of different preprogrammed sound sources. It transmits these in near-real time by cell phone or satellite phone networks to base stations, including cell phones. Source: Sea Mammal Research Unit, University of St. Andrews (see http://www.pambuoy.co.uk/).*

It is probable that relatively few of these studies will provide clear statements of effects and in most cases any effects will be supported to different levels of probability. The value of these studies will be mainly felt through the cumulative weight of evidence they provide, often expressed through meta-analyses.

Ethical and practical constraints often make it difficult to carry out precisely planned experiments on the effects of acute sounds on marine life. Indeed, any experiment conducted in the field is likely to be more or less semiplanned because of the difficulties in ensuring that there are proper control treatments in place. Even in the laboratory, it may often be difficult to conduct fully controlled experiments because of limiting factors such as sample size where, especially for species like marine mammals, few individuals and species are available for study. This can result in biased results because it is impossible to control for individual variation, interspecies differences, and serial correlation within experiments.

Two main forms of unplanned or semiplanned experimental approach can be used. The *comparative approach* has been used traditionally as an empirical method in animal physiology and anatomy that has formed the basis of much of what we know about functional anatomy and physiology in noncaptive, nonagricultural species. The second approach is the a posteriori *opportunistic approach* in which observations made during some form of unplanned event allow the development of a functional explanation about a connection between the event and an organism's response.

Comparative approach—This approach uses comparisons between the responses of similar organisms in similar regions when exposed to different sound fields. Comparison provides the means by which an effect of sound may be measured against some form of control treatment. The control may be some measure of an organism's behavior or physiology before sound exposure or for the same species in a similar, but quieter or noisier, environment. In such studies the dose of sound is uncontrolled and the response variables being measured are usually unplanned and detected post hoc from a range of measurements because there is normally no a priori hypothesis about the exact nature of the

response to sound. Often, some form of multivariate statistical method (e.g., Bayesian techniques) is used to separate the signal in the data from noise associated with effects from uncontrolled variables.[7]

With the development of offshore industries that are increasingly regulated to limit the sound they produce, protocols are being developed to measure the impacts of these developments on some marine organisms. The required monitoring can often amount to studies conducted over many years and they may include several components:

1. Baseline assessment: documenting the state of the organisms of concern before the introduction of anthropogenic sound.
2. Impact monitoring: documenting any change in the state of organisms during the period when anthropogenic sound is produced.
3. Post-effects monitoring: documenting the return of the organisms to their original state after the period of anthropogenic sound production.

Variations on this approach include the capacity to compare the state of marine organisms in similar, and possibly contiguous, undisturbed and disturbed habitats simultaneously. In this case the "state" of organisms could include changes of behavior, physiology, social structure, or population density and population size. Ultimately, however, population size is likely to represent the end point of an accumulation of effects that result from acoustic and other stresses because this will reflect changes of fitness in individuals that accumulate at the population level to affect survival and/or reproduction. This means that measurements may have to be made over time scales of many years for species that have long generation times. Short-term changes in behavior, physiology, or social structure can be used as proxies for potentially significant (in terms of population trajectory) effects of acoustic stress. However, NRC (2005) points out the dearth of evidence relating repeated short-term changes and effects on growth, survival, and reproduction.

The following types of comparisons can be made:

a) Comparison across species and populations.

---

[7] *Uncontrolled or confounding variables are those factors that are not of direct interest, but cannot be considered to be the same in the control treatment and all experimental treatments. It is important to measure uncontrolled variables that are likely to have an effect on the variable(s) of interest.*

b) Comparison across habitats, locations, and time.
c) Comparison before and after sound exposure.
d) Comparison between pristine and noisy environments (and grades in between).
e) Comparison among treatments (e.g., pile driving, seismic, sonar, shipping sound).
f) Quieting as a treatment.

The IQOE will use opportunities to conduct studies on the effects of marine noise around the following sites:

1. Noisy and quiet environments

   Comparing animal behavior, abundance, and productivity between noisy and quiet environments reflects difficulties associated with attempting to ensure that the differences in the sites being compared are predominantly related to the soundscape. No two environments are identical and the differences in the soundscape may be small compared with other, unmeasured differences. However, research sites should be chosen carefully by the IQOE so that it is possible to compare the responses of animals across different soundscapes. This could be achieved using cross-sectional sampling of animals from resident populations within the locations being compared and longitudinally using the same individuals if they migrate among the contrasting acoustic habitats. Another opportunity occurs when sound exposure will move from one of the sites to another, with sufficient time to monitor both sites before and after the move.

2. Marine pile driving

   Offshore developments involving wind farms will result in pile driving on an unprecedented scale within some coastal regions. The effects of pile driving on marine life are poorly understood but, mainly as a result of the needs for industry to comply with regulation, research will be undertaken to examine the degree to which construction operations are compliant and to assess any effects on marine species. These research efforts would benefit from being included within the IQOE study design.

3. Seismic exploration

   The oil and gas industry has already done much

to advance knowledge about the effects of sound on marine life through the direct sponsorship of research through its Joint Industry Program (http://www.soundandmarinelife.org/). The IQOE will continue to undertake these kinds of studies of the effects of seismic survey sound on marine life. This will be conducted in collaboration with the oil and gas industry (see Theme 4). However, there are also important opportunities to undertake research in association with academic scientists undertaking seismic surveys for geophysical studies.

4. Shipping

   The IQOE will also examine the effects of the propulsion sound from ships, which is one of the most pervasive sources of anthropogenic sound. The approaches used will capitalize on the highly constrained nature of shipping lanes involving pinch points at which ship sound is likely to be greatest and the use of gradients in sound levels away from shipping lanes. Many of the most useful locations are easily defined, but circumstances will exist where habitat is shadowed from the acoustic effects of predictable ship tracks. Some of these shadow regions will be identified as outputs from the soundscape modeling described under Theme 1, but examples already exist of changes in shipping lanes that provide an opportunity for a natural experiment on the effects of sound from shipping on marine life. Shipping lanes were moved out of the Santa Barbara Channel off California to reduce the effects of local air pollution from shipping, changing noise levels significantly (McKenna et al., 2012). If future changes like this were known in advance, they would provide opportunities for observing the state of marine organisms before and after the change.

5. Explosions

   Explosions associated with disposal of unexploded ordnance, decommissioning of unwanted infrastructure, and navy exercises are responsible for high-amplitude sounds of short duration. In some areas, especially areas where much historical ammunition can be found—such as the Baltic and North seas—these activities could contribute significantly to sound budgets. A study in the Dutch North Sea concluded that the contribution from explosions to the annually averaged ambient sound in that area was comparable to that from pile driving (Ainslie et al., 2009).

6. Unusual events

The effects of sound on marine life have been brought to public attention mainly because of the unusual and extreme response of some species of beaked whales to military sonar (Cox et al., 2006). Indeed, much of the current knowledge of the effects of noise on marine mammals comes from behavioral response studies (or controlled exposure experiments) conducted on behalf of the U.S. Navy to help resolve this problem. These types of studies will mainly be dealt with in the following section, but there remains considerable interest in the occurrence of unusual events, especially the stranding of cetaceans, in relation to offshore industrial activities. The IQOE will undertake analyses, where appropriate, of the circumstances under which unusual events have happened as a way of potentially identifying evidence for causes and effects in relation to anthropogenic noise.

Opportunistic approach—The opportunistic approach to gathering experimental data is the most extreme form of unplanned experimental design. Often the data have been collected before any research question has been developed, and there is a need in these circumstances to rely on post hoc statistical analyses to examine relationships between the responses of organisms and sound levels. In many circumstances, this will involve the use of statistical models to help partition the variance in the states or responses of organisms to particular causes. Often, Bayesian statistics can be used in this context.

The IQOE will improve the strength of opportunistic monitoring studies by establishing common protocols for data collection that could allow comparison across studies at different times with different stressors in the same site or at different sites with different natural and anthropogenic stressors. The IQOE is based on the idea that, rather than introducing additional sound and observing the effects of this introduced sound, there is a need to examine the responses of organisms to quieting. Comparative and semi-unplanned

approaches provide an opportunity to make progress with this ambition.

4.4 Effects of changes in chronic noise

Key questions

- How can noise be observed over time to create a biologically meaningful measure of chronic noise?
- What are the effects of prolonged increases or decreases of noise on the physiology and behavior of key species?

The first question will be influenced by the results of Theme 1. The second question will require the IQOE to develop recommendations for long-term monitoring of the effects of chronic noise on marine organisms, probably in conjunction with long-term measurements of ocean soundscapes. This will be a "legacy activity" of the IQOE, which will hopefully extend far beyond the life of the project.

Research approach

A key goal of the IQOE will be to explore the effects on marine life of both increasing and decreasing sound, using independent controls. Although experiments in which sound exposure is controlled will be much more constrained in their extent and generality than opportunistic studies, the establishment of planned experiments will complement the more opportunistic comparative and semicontrolled approach described above.

Although large-scale manipulations (up to ocean-basin scale) will be important, such as moving shipping lanes, there will be an important trade-off between the spatial and temporal scales at which experiments take place and the feasibility of those experiments (Figure 4.5). Opportunities where the sound exposure can be changed over a 5- to 10-year period need to be identified. At present, the establishment of many marine reserves presents an opportunity to establish the capability to measure biological changes associated with changing levels of sound.
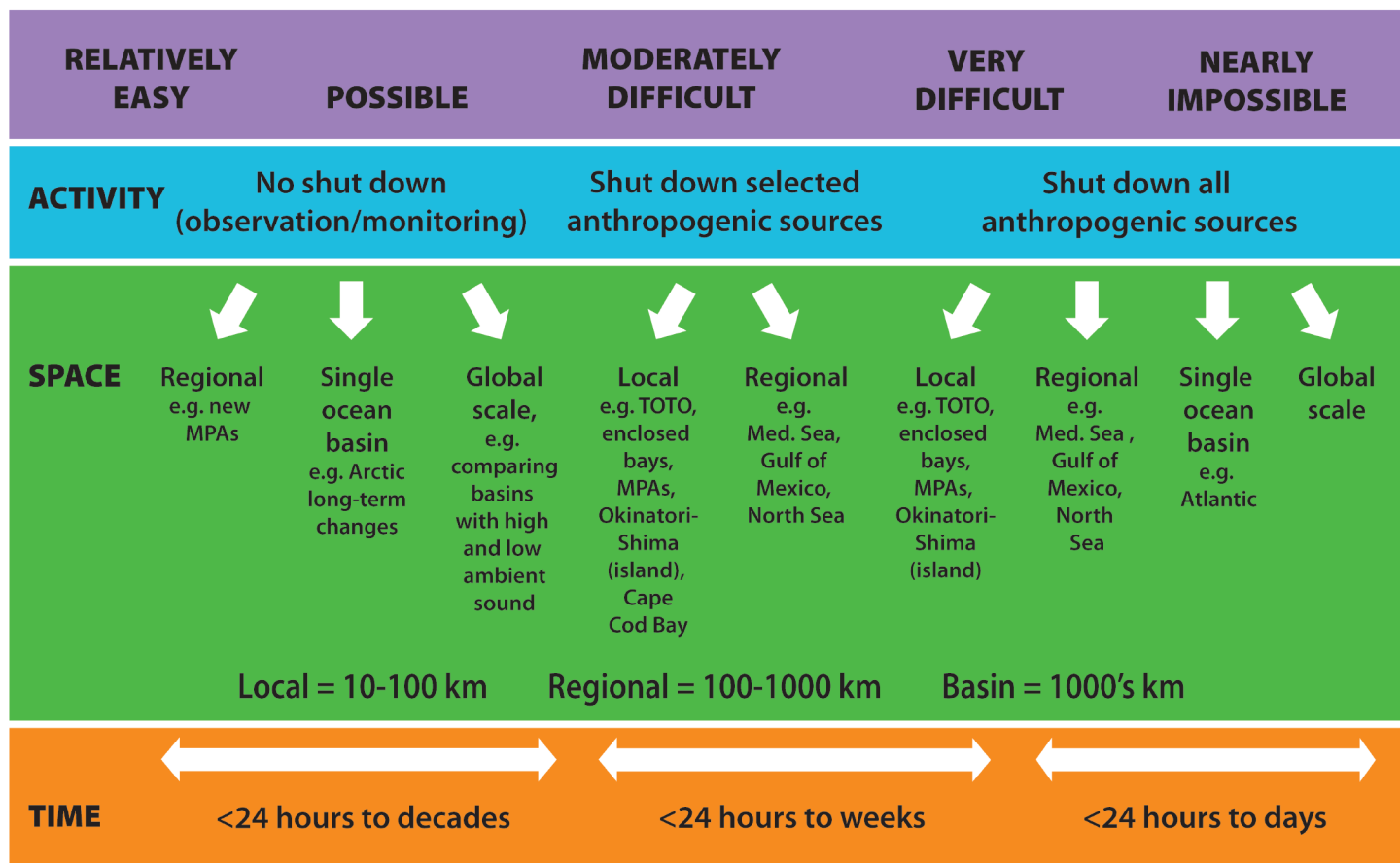
Figure 4.5. *Matrix of quieting feasibility. The difficulty and financial cost of a shutdown of noise sources increases from left to right in the matrix. The feasible time that a noise shutdown could be accomplished decreases from left to right (orange row). Different experimental activities (blue row) might be possible at different spatial scales (green row). The goal of the IQOE will be to conduct activities at many different scales. The relationship of the different temporal and spatial scales means that the most feasible approaches are likely to be several experiments carried out over long durations at small scales (i.e., toward the left of the diagram). Two roles that the IQOE will play will be (1) to help reduce the difficulty of experiments as one moves to the right in this diagram, and (2) to coordinate experiments of the type defined to the left of the diagram so that their data can be combined to deliver some of the benefits that will emerge if we were able to carry out experiments lying to the right of the diagram (from Boyd et al., 2011). Used with permission from the Oceanography Society.*

In ideal circumstances the most appropriate protocol will be to move sound sources to create contrasting (increased and decreased) sound conditions, and a key element to make this approach work will be to have enough advance notice (up to five years) to establish baseline observations before changes are made for other reasons. In the previous section, we also described a similar situation with opportunities associated with the introduction of sound because industry is expanding into new areas. The proposal here is similar, but in this case the experimenter has control of the sources and the study will be designed to detect effects of a shift from a noisy to a quiet environment and vice versa.

Long-term experimental studies are essential; short (weekly to monthly) studies are unlikely to capture the vital life-history effects except in short-lived species with rapid turnover, and they are often not the main focus of concern. The observations should include population counts and survival for short-lived species, and at least reproductive cycles for longer-lived species. In general, experiments should also include measurements of ecosystem covariates.

Experiments should not assume that a directional change in sound will produce proportional change in the response; nonlinear responses should be expected and sampling should be designed to capture such responses.

Design of experiments—A large-scale, long-term (lasting from months to years) experiment is proposed. This experiment will test the hypothesis that changes in chronic sound levels have biologically significant effects on individual target species (see above). In this case, biological

significance is defined by its meaning described in Figure 2.5 and the related text.

To achieve the experimental controls, chronic sound conditions will be experimentally changed within defined study areas. Each area should ideally contain three subsites, one in which the exposure is increased, one in which it is decreased, and a third in which the level remains relatively unchanged (Figure 4.6).

Within each site, a targeted set of observations will be made and models will be constructed to quantify treatment variables (chronic background sound levels), response variables (to individual species and ecosystem dynamics), and potentially confounding variables (physical and biological oceanographic conditions). Although it is likely to be introduced initially at a regional or local scale because of the practicalities involved, this design could be used as a blueprint for an ocean-scale experiment.

Predicting outcomes—Although we have identified a general hypothesis to test, careful consideration will need to be given to developing a framework to predict outcomes of

manipulations and the capacity to do this will have a strong influence on the location, species, and general situation chosen for an experiment. The general assumption underlying the design of IQOE experiments is that reducing sound will cause improvement in vital rates because sound as an external stressor is expected to have negative consequences for marine life. However, we should also consider the following factors:

1. How do animals use background sound, and have they become acclimated to higher sound levels or even experienced selection to sustain high performance under those conditions? Under these circumstances, it is possible that removing sound will lead to negative consequences.
2. Sound may alter predator–prey interactions. Changes in sound could have nonlinear consequences for community structure because even small changes in competitive interactions could have large effects on the dynamics in marine ecosystems. The same applies to predator–prey interactions.
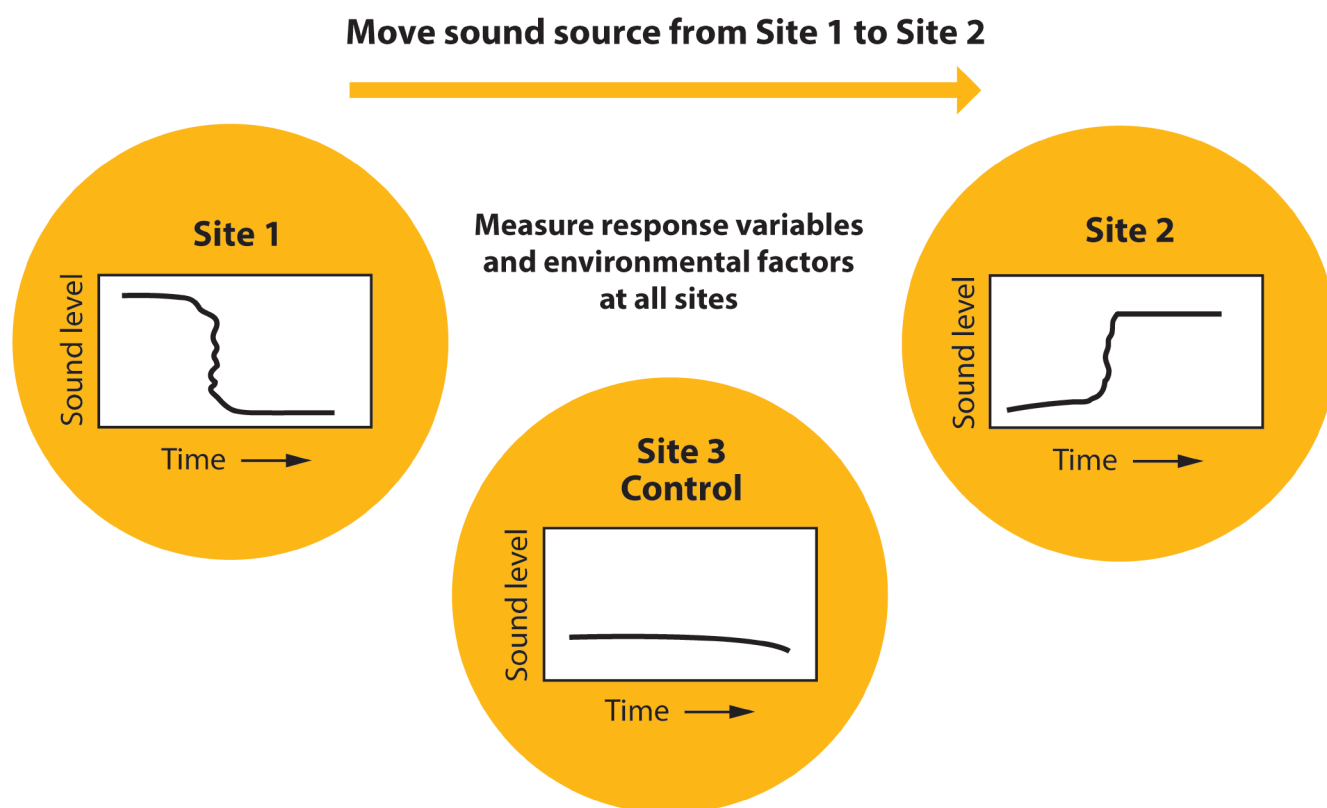
Figure 4.6. *Experimental design involving three locations. The time scales shown here will depend on the location and circumstances, and especially on the variance within the measured response variables, but they would normally require a minimum of two years, one year before a sound source was moved and one year after. Alternative, and simpler, approaches to this experimental design would be to compare loud and quiet areas or to measure effects over time in relation to changes in the levels of sound in small localized areas.*

The outputs from Theme 1 on Ocean Soundscapes will be important as inputs to this element of the IQOE. However, biological models of the system being studied will need to be developed in advance to predict the effects of experiments. The exact nature of these models will depend on the circumstances, but they could include population dynamics models or end-to-end ecosystem models. However, whatever model is chosen will need to be validated in advance of the experiments.

Study species—Ideally, study species should include a range of taxa—including invertebrates, fish, and mammals—each of which will provide different challenges to study. Organisms could be divided into categories by the role of sound in their lives, and their ability to hear and produce sound at frequencies of most interest. For example, if our focus is low-frequency sound, this defines the types of focal taxa as those with sensitivity to those frequencies.

The criteria for selecting species for inclusion in experiments might include the following:

- High sensitivity of the species to sound.
- Resident individuals should be preferred over migratory species and individuals.
- There should ideally be a high level of

background knowledge of the species, and even individuals, if long-lived species are involved. For example, some individual whales are known by marking patterns and have been monitored over years.
- The species is important in the ecosystem, or is commercially important, or it has some specific significance to the stakeholder community.
- The species needs to be accessible, and measuring responses must be feasible. It will also be important to distinguish among treatment, confounding, and response variables.

The species selected may be different from those selected as target species for the studies on hearing capabilities, but there would be obvious benefits to using the same species.

Given these constraints, there are relatively few species that will fit all of these criteria. In particular, pinnipeds (Figure 4.7), because of their size and propensity to return predictably to breeding colonies, and some long-lived resident fish species within reef habitats, would be appropriate candidates.
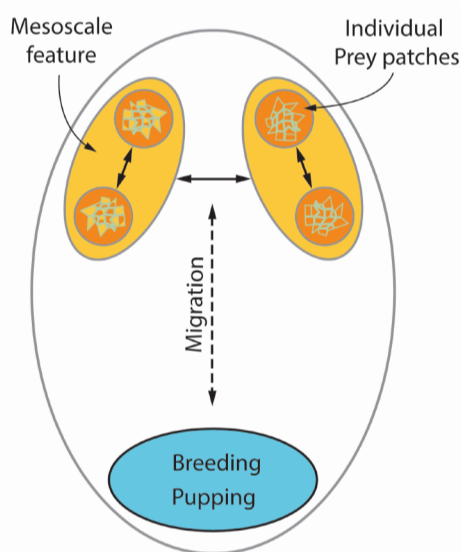
Figure 4.7. *Pinnipeds are likely to be appropriate for experimental studies. They are large enough to carry instruments, have predictable migration routes to and from predictable feeding locations, and return to specific locations on land, making individuals and populations feasible to monitor. They are also often a component of the marine fauna that carries specific legislation for their protection and management. Photo from Barbara Walsh (https://www.flickr.com/photos/barbarawalsh/5517303759/). Used under Creative Commons Attribution 2.0 (see https://creativecommons.org/licenses/by/2.0/legalcode).*

However, these types of experiment could be carried out at small spatial scales with species that are short-lived and accessible, perhaps using natural mesocosms in which species composition and ecosystem structure are well defined and possibly also controlled. This type of design also has the potential to include multiple species.

Site selection—The study sites will depend on the species being studied and the specific outcomes predicted for the experiment. A secondary feature will be the availability of baseline data from the site, to reduce uncertainty. Ideally, selected locations should have a long history of data collection on the species concerned. This type of criterion narrows the possibilities considerably.

Additional considerations include the following:

- Is there industrial activity in the area that could be used as the exposure and control? In some settings, it might be possible to shift the sound in a systematic way, but scientists need to work with industry to develop a consensus plan. For example, it may be possible to divert shipping for several years at a time, with enough advance notice, if this did not entail additional cost. In some cases, some shipping companies may decide to change their operating procedures for other reasons, affecting the routes used by its ships.
- Can the studies be replicated? If there were multiple independent sites (e.g., separate seal colonies) that could be monitored over a long period of time, this would provide an opportunity for replication. The choice of sites could lead to the development of different exposure scenarios for each site, for example, (1) increased sound, (2) decreased sound, and (3) no change in sound levels.

Variables to be measured

1. Dose or treatment variables

Measurement standards will be developed across different regions and species to make it possible to extrapolate beyond individual study sites and to determine global implications.

The most important dose or treatment variable is the sound received by the study animals (Boyd et al., 2008). Ideally, this should be measured directly from an instrument placed on or near the experimental animals, but also could be modeled based on information from the sound field (Theme 1).

2. Response variables

For each dose, the experiment will include defined response variables. Responses will be measured at different levels of the PCAD model (Figure 2.5), depending on the targeted organisms, for example, for short- versus long-lived species. With short-lived species, research will focus on vital rates as much as possible. For other species, it will be necessary to measure parameters that will allow estimation of vital rates. Individuals or species that leave the area and others that recolonize can also be measured by how they change their migration routes in relation to the sound sources. A combination of tracking and survey techniques may be applied, including mark-recapture studies and tracking of a subset of individuals. Tracking a subset of individuals over the observational period could also be used to study habituation and sensitivity.

3. Confounding variables

Confounding variables are those that can affect the responses to a specific dose or treatment in an experiment in a way that makes it hard to understand the results, particularly if the confounding variables are not measured. Some examples of confounding variables include ocean currents, temperature, salinity, chlorophyll, depth, bottom types, turbidity, and ice cover.

By using variation in the background sound levels, including intermittent noisy and quiet periods, it is possible to examine responses to a broad range of sound levels and types (e.g., chronic or acute conditions). This is as much about responses to quiet conditions as about those to the noisy conditions. Statistical models applied to these data can then be used to predict the effects of reduction in noise. An important goal of this element of the IQOE is to enable studies to identify areas where anthropogenic sound is already having deleterious effects. In such cases, quieting should have a beneficial effect. The duration of quieting windows should be carefully selected to be long enough to allow animals exposed chronically for years to return to a pre-exposure baseline.

4.5 Summary

Theme 2 aims to be the main driver for developing a deeper understanding of the connection between soundscapes and animal responses to the soundscapes. Therefore, it is important that considerable effort is committed to the tasks set out here.

When complete, these tasks should deliver representative dose–response functions relating the effects of anthropogenic sound for key species. Although, ideally, these should be in the form of classical dose–response

curves, it is much more likely that they will amount to a mixture of these types of precise functional relationships between animal responses and sound levels and heuristic assessments of the effects of sound at various levels from behavioral response to effects on populations. These types of assessments are most likely to constitute a body of knowledge that, through appropriate combination with risk analysis (see Section 6 and Figure 6.3), will meet the needs of managers and decision-makers. Given the current poor state of knowledge, these assessments will represent a major step forward and, when combined with the outcomes of Theme 1 on Ocean Soundscapes, will also form the basis for making predictions about the potential effects of future changes in anthropogenic sound in the ocean.

Chapter 5
Theme 3: Observations of Sound in the Ocean

5.1 Introduction

Sound in the ocean is challenging, both to detect and to visualize. This problem is one that requires measurements in many dimensions: three spatial dimensions, plus time and acoustic characteristics, which might be considered as adding three additional dimensions—amplitude, frequency, and variability over time. The process of measuring ocean soundscapes (see Theme 1) is concerned with characterizing these dimensions to form a coherent picture. In Theme 3, we address the requirements of the instruments and observing systems needed to provide the raw data to allow the measurement of soundscapes at a very wide range of spatial and temporal scales. The theme also addresses the need to observe sound fields from the perspective of the marine life that may be affected by sound. Being able to observe the sounds that organisms are exposed to, and that they can hear, has been identified as one of the most critical first steps toward being able to measure the effects of sound on organisms (Boyd et al., 2008).

Only limited data are available on ocean soundscapes. Information on long-term changes in ocean sound levels, whether anthropogenic or natural in origin, is available at only a few locations in the world ocean, for a limited period. Measurements of underwater sound also provide data that can be used to track, count, and study the behavior of vocalizing marine mammals and fish, which can be used to help determine the effects of anthropogenic sound on marine life. Finally, active acoustic measurements, using instruments such as high-frequency scientific echo sounders or low-frequency ocean waveguide remote sensing (Makris et al., 2006), can provide information on aspects of the ocean environment, such as the density and distribution of marine life, especially within the water column.

In recent years, there has been a strong emphasis on the development of ocean observation systems (Kite-Powell, 2009). System development has been enabled partly by increasing technological capability, but also by recognition of the need for new data about the ocean, that sometimes need to be delivered in real time, as in tsunami warning systems. These requirements have driven innovation and it is likely that the need for observation systems and their capabilities will increase greatly in the next decade. Traditional ocean observatories using moored systems of sensors are being augmented by mobile sensors on floats (Roemmich et al., 2009), autonomous underwater vehicles (Nicholls et al.,

2008), gliders (Johnson et al., 2009), and even instruments carried by marine mammals (Grist et al., 2011). Acoustic observation has not, in general, been a part of many of these systems and, when present, it is usually recording at very low acoustic frequencies that may be of greatest interest for observing seismic events or other physical changes, such as sea ice breakup, but is of less concern in frequencies that are important to most marine organisms.

5.2 Acoustic observation networks

Wherever possible, acoustic observations need to be included in ocean observing systems designed for other observations. This approach will contribute both to providing the information required to characterize the global ocean soundscape and make use of current and future infrastructure with minimum additional cost.

Hydrophone systems are already deployed for recording sound in the ocean, and many of these are listed in Appendix II. Other observing systems have been deployed for specific oceanographic, biological, chemical, or other environmental purposes, but have not included ocean acoustic sensors. One key benefit of integrating acoustic capabilities into such systems is that they would acquire diverse oceanographic and atmospheric data concurrent with the acoustical signals. These ancillary environmental data may be essential in determining the relationship between sound, the ecology of target organisms, and the environment. Some systems under development are cabled observatories, such as the U.S. Ocean Observatories Initiative, and offer unique platforms with power, timekeeping, and communications capabilities, thus providing opportunities for acoustical instrumentation. The IQOE has begun to identify and catalog existing and planned acoustical observation systems (see Appendix II). These systems have been described and tabulated according to several important criteria. The aims of this effort were to show what systems are available to address specific IQOE questions and to identify new acoustical capabilities that need to be developed for IQOE studies.

The remainder of this chapter places the IQOE into the context of the larger ocean observing systems; addresses the existing observation systems that either directly support acoustical measurements or could be configured to do so; suggests some examples of new technologies that would augment existing acoustical measurement capabilities; and recommends investigating the incorporation of acoustic measurements into ocean observation systems and their data

management processes, either archived from prior monitoring activities, or collected by contemporary or planned regulatory activities. Finally, the theme addresses the issues of standardization of data in quality, calibrations, formats, and management to enable the comparison of results among international collaborators.

5.3 Acoustics and global and regional ocean observing systems

The IQOE cannot, and does not need to, unilaterally deploy global ocean observing systems because of the resources, experience, and effort already expended in establishing and operating global and regional ocean observing systems (OOSs). Available ocean observing systems already include a wide range of observing technologies, from satellite observations of a variety of oceanic variables (e.g., surface height and temperature, wind, ice coverage, and chlorophyll-a concentrations) to standard National Oceanic and Atmospheric Administration (NOAA) weather buoys and some Argo floats providing upper ocean sound profiles and some even featuring acoustic rain gauges.

As the IQOE evolves, it needs to evaluate the relevance of ancillary data from readily available OOSs and ensure the continuous accessibility of such data throughout the project. Time-synchronized multivariate sensing systems will be increasingly important as attention focuses on interpreting the potential ecological impacts of sound. Consequently, the application and integration of OOSs as contributors to the IQOE monitoring and experimental efforts is preferred over solely acoustic measurements. However, the type and nature of these ancillary data streams depend on the specific question and the environment in which measurements are made. Indeed, information and data missing from existing systems, but essential for addressing IQOE science questions, will require deployment of additional instrumentation. Some of these deployments will probably transition into operational components of OOSs.

Experience and technologies to promote good data management and communication (DMAC) have grown out of the OOSs. The IQOE will need to take advantage of DMAC technology, and begin a dialog with observing organizations to help incorporate acoustical data streams within OOSs, where possible.

The ocean observing systems include within their mandate educational and public outreach efforts. These efforts would naturally extend to any acoustical activities related to these systems (see Chapter 7).

5.4 Integration within existing systems

Most or all of the envisioned IQOE monitoring and experimental efforts should use data from existing capabilities or promote the integration of acoustics into existing observing systems. An early objective of the IQOE will be to complete an initial draft of what is envisioned as a continually updated survey of the known systems (included in Appendix II and online at http://www.scor-int.org/IQOE/Appendix II.pdf). The survey matrix will be available for public contributions on the IQOE Web site and related to a global map showing locations of existing acoustic observing systems (an incomplete example is shown in Figure 5.1).
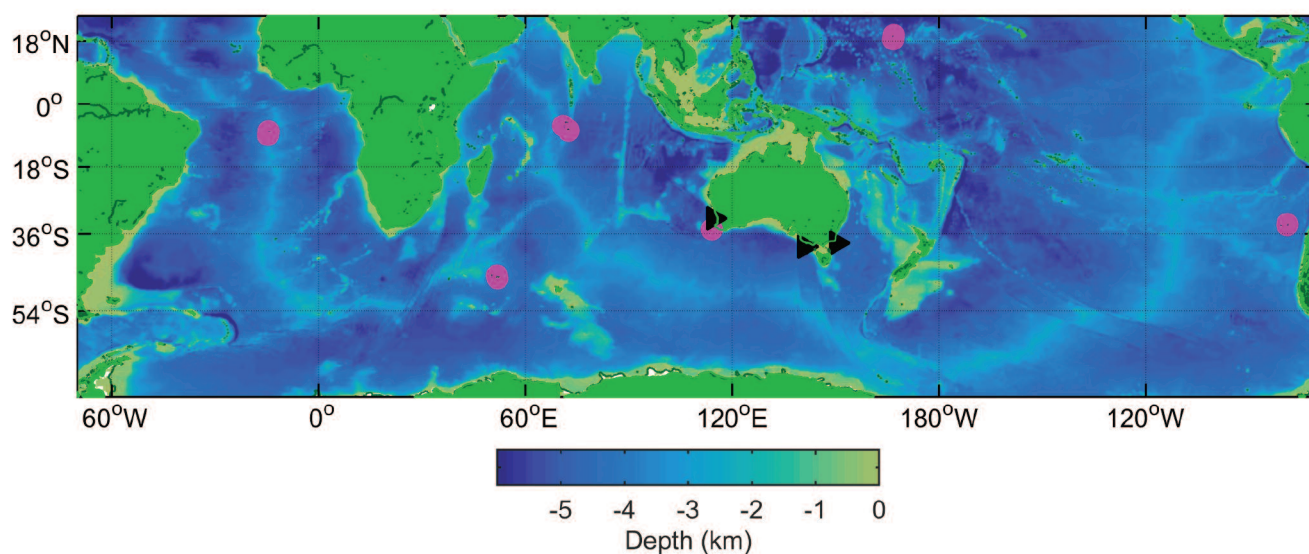
Figure 5.1. *Comprehensive Test Ban Treaty Organization (CTBTO) (magenta circles; see also Figure 5.2) and the regional Australian hydrophone facilities (black triangles) with ocean bathymetry derived from the Smith-Sandwell atlas (Smith and Sandwell, 1997). Each CTBTO receiver consists of a triplet of hydrophones to make it possible to determine the direction of acoustic signals. Data are recorded, processed, and transmitted to shore in real time from these arrays. From Dushaw et al. (2010). Permission to reuse figure granted by authors.*

Appendix II categorizes observing systems as cabled arrays (e.g., fiber-optic systems), remotely deployed archival systems (e.g., bottom-mounted recorders), and mobile systems (e.g., drifting buoys, gliders, animal-borne instruments). Each system was assessed relative to

- geographic location;
- whether acoustics is a current operational capability;
- various system characteristics;
- the inclusion and type of ancillary (nonacoustic) data;
- relative accessibility of data from each system;

- potential integration with other systems;
- sponsoring entity;
- general societal benefit or product of each system; and
- installation duration and life expectancy.

The derivation of the system matrix in Appendix II according to these criteria was intended to provide a basis for system selection when the experimental/monitoring areas and objectives are chosen (e.g., in Theme 2). The anticipated process would be the consideration of specific experiments, each with its own time-space resolution and objectives.
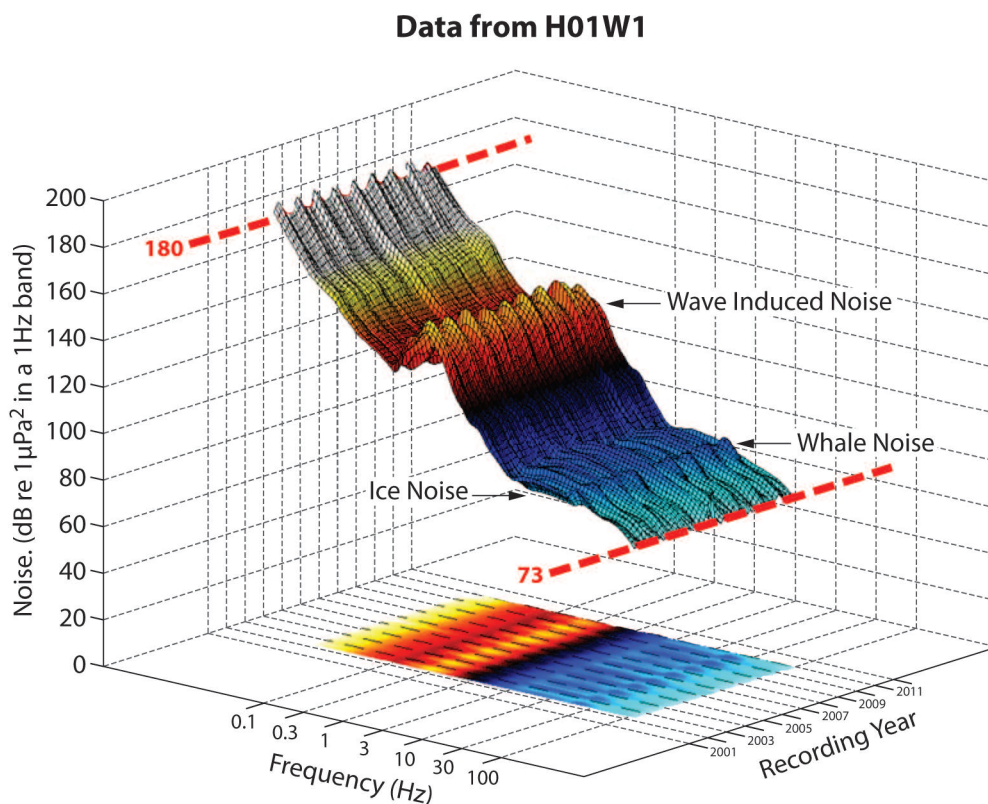
Figure 5.2. *Ambient sound spectral density level in relation to frequency through time recorded at one of the CTBTO sites in Western Australia (see Figure 5.1). The seasonal peaks at low frequencies are related to Antarctic ice breakup and at the higher frequencies these relate to seasonal calling by baleen whales. This is an example of the kind of depiction of the soundscape that could be achieved across many OOS sites. From Prior et al. (2012). Reproduced with permission from the Comprehensive Test Ban Treaty Organization.*

5.5 New systems designed for the IQOE

It should be possible to use existing passive acoustical technologies within existing and planned ocean observation systems. However, it appears unlikely that sufficient monitoring systems with passive acoustic capabilities exist in enough areas of the ocean to accomplish the broad and sustained monitoring

objectives of the IQOE. There is a need to conduct a detailed assessment, probably through one or more workshops, of the observation capacity that is required to meet the objectives of the IQOE, and to assess the extent to which modification of current and planned capabilities in ocean observation are likely to fulfill these objectives.

Although it is preferable to use and improve on the capabilities of existing systems, there will be instances where integration of currently available sensors into existing systems will not be possible, or existing system nodes may not be located in the appropriate geographical area(s) targeted for program experiments. In such cases, the IQOE may need to establish dedicated monitoring. The development of technology that would enhance the information available from existing systems and sensors has been identified in six areas:

1. *Particle motion/vector sensors*—Research has shown that a majority of fish species studied are more sensitive to the particle motion component of sound than to the pressure component (Popper and Fay, 2011). The need to measure this parameter is important for providing the proper environmental context for fish in response to sound exposure.

2. *Portable system designed for the IQOE (single hydrophone)*—In areas where OOS networks do not have regional nodes or coverage, it will be necessary to provide small, inexpensive, portable systems designed to provide required acoustic, and where necessary, other measurements. Many of these are already being developed and are available, although they may not have all the essential characteristics required. These portable systems need to provide information relating to the survey of global ocean soundscapes and short-term experiments, and they need to be compatible in their sensitivity and the way in which data are presented. Such portable and inexpensive devices will encourage wider international participation in the IQOE.

3. *Modular hydrophones to assemble horizontal and vertical line arrays*—The ability to assemble modular arrays quickly and efficiently will enhance our capability to provide directional acoustic data to the global soundscape survey effort and short-term experiments.

4. *Data transmission technology*—The limited bandwidth of current satellite transmissions is often a bottleneck for the transfer of high-volume acoustic data. Developments in this area on the recording hardware, processing, or data transfer aspects would be beneficial to the IQOE effort.

5. *Acoustic backscatter sensors, echosounders, and acoustic waveguide remote sensing*—Existing OOS and satellite networks provide valuable information on physical ocean properties and primary productivity. Passive acoustic monitoring (PAM) provides information on the presence of vocalizing animals (mammals and fish). The development and incorporation of scientific echosounders (for example) into OOS networks would provide the capacity to measure zooplankton and fish distribution and concentration in the water column, and to study the predator–prey dynamics of an area, which is needed to provide proper context for interpreting the effect of changing sound levels on marine animals. NEPTUNE and VENUS already have active acoustics capabilities, but this is not a widespread capability across OOS networks.

6. *Compliance monitors*—A simple sound management tool might be needed to monitor and report the acoustic state of a vessel. This could provide real-time information of the ship's acoustic state via the Automatic Identification System (AIS), which indicates a ship's identity, position, course, and speed.

5.6 Extracting useful scientific information from data collected for regulations

So far, we have considered only scientific OOS networks, but there will be a need for observation systems that assess compliance with limits on the additional sound in the ocean from anthropogenic sources. The need for these systems is developing quickly in various jurisdictions. In Europe, this is a specific requirement of the Marine Strategy Framework Directive (MSFD, 2010). Some of these observation systems may be in place for short periods when industrial development is proceeding, but there may also be other networks operated by coastal nations to demonstrate national compliance with targets for sound production from human activities.

The IQOE could adopt two different approaches to building on this opportunity. One would involve the analysis of acoustic data obtained in the course of regulatory monitoring of industrial developments. Alternatively, as regulation of ocean acoustical pollution is initiated throughout the world, the associated monitoring systems could be sources of future datasets, and the IQOE has an opportunity to influence the design and placement of such systems.

A survey of historical data to establish the nature of soundscapes of the past

Trends of sound are considered in more detail under Theme 1, but it is recognized that the assessment of trends needs to link with observing systems. Time series of acoustical data have been collected at multiple locations in multiple regions over the past 50 years. Many of these datasets were

generated by private industry, military, research institutions, and regulatory agencies for regulatory compliance, exploration, research, and targeted surveillance. Some of these data are proprietary or have national security classifications; whereas other datasets are openly available. For example, the U.S. Office of Naval Research (ONR) has supported the acquisition of acoustic data through its research programs, while the Naval Oceanographic Office (NAVOCEANO) has acquired extensive acoustic datasets through its survey efforts. However, these data are often not readily accessible to the scientific community because of either security restrictions or practical issues associated with processing and interpreting data recorded on various media and archived in a wide range of formats. Similar situations exist in other nations. At an early stage, the IQOE will undertake a comprehensive survey of historical data. This task will need to be undertaken by an IQOE group made up of providers and users of the data. A database will be established on the IQOE Web site to allow input of historical data, as well as new data (see the discussion of DMAC in Section 7.3). For these data to be useful, they must have been adequately calibrated, which may limit the amount of historical data that will be useful.

Historical data may not be in the format agreed upon by the IQOE, but targeted datasets could be reprocessed for contribution to the IQOE. The information resulting from the historical data survey and new data acquisition will provide information to the IQOE about historical soundscapes in areas of interest for comparison with the present and for validating contemporary acoustic models. Coordinating independent teams working on these problems simultaneously will help to provide cross-validation where it is not possible to validate using data.

Sources of future data for the IQOE

Government-mandated regulation of either radiated sound from individual sources or cumulative anthropogenic sound contribution in a targeted region will require monitoring instrumentation that may be a source of acoustic data for the IQOE. As an example, the U.S. National Marine Fisheries Service held a workshop to estimate a comprehensive sound budget for the ocean, with a special focus on the U.S. Exclusive Economic Zone, as part of the NOAA Cetsound project (NOAA, 2012). In the EU, the Marine Strategy Framework Directive (see Tasker et al., 2010) specifies that all EU member states monitor their marine environments to regulate the contribution of anthropogenic sound energy. This directive will require new monitoring systems throughout European waters. While the actual legally binding monitoring requirements are likely to be very narrow, the instruments being used to provide this information will have the capacity to collect considerable

additional data about sound. Consequently, the IQOE should establish data-sharing agreements that permit continuous delivery of these data to an IQOE data assembly center. An important task of the IQOE will be to involve data generators and managers globally to take advantage of the widest range of data available.

Since these kinds of data will be formatted primarily to meet the needs of regulatory agencies, it will be critical for the IQOE to coordinate with the agencies as early as possible to influence the data formats, and subsequently to devise any necessary reformatting procedures to transform the available data products into the IQOE formats. Technical contacts representing the IQOE will need to be appointed to interface with regulatory agencies, and the details of the data interface and any subsequent data reformatting may profit from attention as a subtopic at an IQOE technical workshop (if the issue arises early in the IQOE). We propose that a standing committee on data management should emerge from this workshop. Although these examples are specific to the United States and Europe, the IQOE should investigate whether similar opportunities or initiatives exist in other regions of the world and ensure effective liaison between those initiatives and the IQOE. An important activity of the IQOE will be to work with navies and all offshore engineering industries, including those in oil and gas exploration and production, wind-farm deployment and operation, bridge and tunnel construction, offshore mining, etc., for access to proprietary and classified data in a way that will advance the science without compromising the interests of those providing the data.

5.7 Data collection (including standardization), quality control, analysis, reporting, management, and accessibility

Of similar importance to synoptic measurements is the use of standards and the application of a systematic and standardized data management structure. Information and potentially important trends and observations are likely to be lost or unused unless an explicit strategy is implemented for data archiving, analysis, and sharing. Data acquisition and reporting standards are an important part of data management, as is the development of data sharing agreements that ensure the rights of individual data originators. As with ancillary data measurements, data management strategies require considerable deliberation and planning, and will vary depending on the systems employed and questions asked.

We recommend that a technology workshop be convened to define standards that will lead to a proposal for the global

soundscape project. This workshop will include representatives from the major observing systems but will necessarily follow specification by IQOE acousticians regarding experimental design. These specifications will strive to provide data acquisition and management standards and protocols for (at least) the following variables:

- Bandwidth
- Bits, resolution
- Sensitivity
- Units
- Sample rate
- Data format
- Analysis methods
- Calibration
- Metadata and data accessibility

The workshop is necessary to (1) enable agreement on terminology, (2) enable agreement among the acousticians on the standards for data and metadata, and (3) compile the acoustical data available from individual ocean observing systems.

5.8 Biological observing systems

The development of biological components of the OOSs have lagged behind the physical components, but the biological components were highlighted during OceanObs'09 (e.g., Gunn et al., 2010). An important class of acoustical system consists of those that employ passive acoustics for monitoring marine life, including distribution, abundance, and behavior (Mellinger et al. 2007; Van Parijs et al. 2009; André et al., 2011). Satellite observations of some biological variables are also available.

Biological observations collected for the IQOE may demonstrate their long-term importance and consequently transition to operational status and become elements of ocean observing systems. Combining biological observation with observations of sound will have two specific advantages. First, this will make it possible to develop experiments that relate the general bioscape (i.e., the acoustically determined distribution and abundance of components of marine communities, most probably in pelagic habitats) to other ocean sound variations. This will enable some options for developing *effects studies* as described under Theme 2.

Second, combining biological and acoustic measurements will enable identification, classification, and possible estimation of the abundance of organisms that are the sources of sound (Marques et al., 2009).

Software to achieve such goals is in a fairly advanced state of development (Figure 5.3), but the IQOE will stimulate the development of open-source software for the automated identification, localization, and classification of biological sound sources from ocean observation platforms.

5.9 Synthesis and modeling: physical, biological, and acoustic

Modeling will be an essential component of the IQOE for predicting ocean sound levels across the globe, estimating acoustic propagation of sound over space and time, and assessing impacts of changing sound on animal populations. Theme 1 concerning ocean soundscapes and Theme 2 concerning the response of marine life to sound both require the application and further development of models of how sound travels in the ocean.

A three-input modeling approach will be needed to integrate the acoustic, biological, and oceanographic data necessary to relate sound to biological dynamics because the three separate datasets are interrelated when assessing the impacts of acoustic change at the population level of animal groups. There are currently no models that predict the effects of chronic sound on marine animals, and much will be learned by an ongoing review of models now used to predict impacts of acute acoustic exposures. The Population Consequences of Acoustic Disturbance (PCAD) model will be a major conceptual tool for the IQOE (see Figure 2.5), but other modeling approaches will also be encouraged and used.

Models used within the IQOE will help project scientists understand how soundscapes change over space and time, using measurements made worldwide. To develop the most appropriate models, more accurate characterization and measurement of sound sources (biological and anthropogenic) is needed. Calibrated historical data (e.g., decades of data from navies, data from industry, data resulting from regulatory requirements) will be valuable for validating models and testing model predictions. However, there will also be a need for high-quality bathymetric data and integration with regional oceanographic models to enable accurate predictions of the sound field in particular locations. Consequently, there is a need for the IQOE to take an active and leading role in the development and implementation of new acoustic models that better integrate or set parameters for fine-scale details derived from new data and oceanographic modeling. See Theme 1 for further discussion of modeling and model validation.
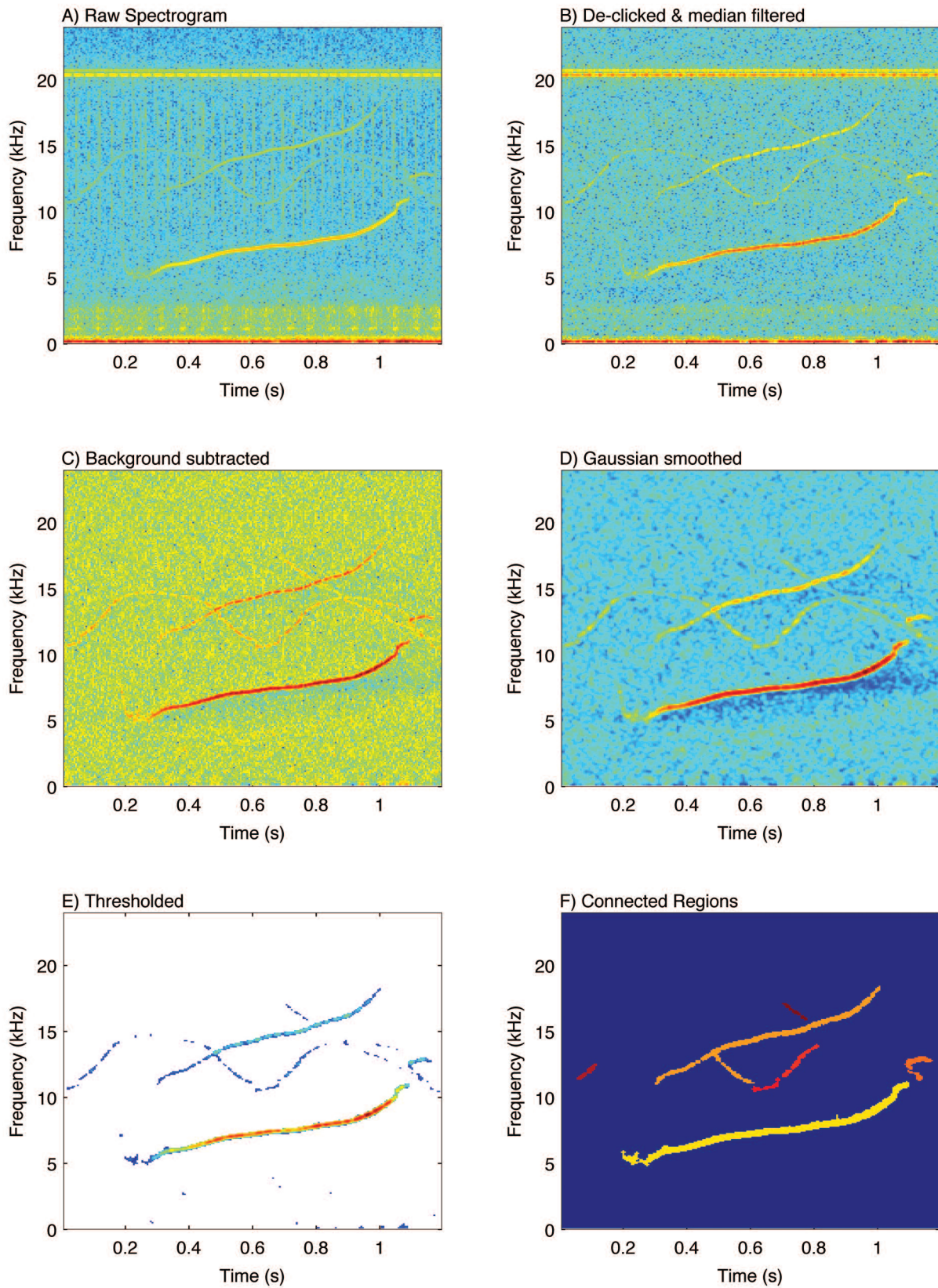
Figure 5.3. *Spectrogram of a typical dolphin whistle, showing the effects of the various processing stages of whistle contour extraction. This is typical of the processing carried out within whistle analysis software to enable identification of species. From Gillespie et al. (2013). Used with permission from the Acoustical Society of America, Copyright 2013.*

5.10 Recommendations

Monitoring/experiments for the IQOE

Five specific, though not mutually exclusive, types of monitoring or experimental efforts are recommended:

1) International Year of the Quiet Ocean

The International Year of the Quiet Ocean (IYQO) lies within the broader concepts of the IQOE, but there are opportunities to use a focused period of activity to make important progress. What is envisioned is a high-visibility international effort with coordinated observations around the globe over a short period to compare with modeling results. This yearlong activity would represent just the beginning of such coordinated observations and modeling. The intention is that this approach will produce a global map of soundscapes, and that these point measurements will inform subsequent models (see Theme 1). To establish a baseline of the soundscapes of the world's ocean basins, international coordination will be required to obtain comparable data in different locations. Ocean soundscape models are being developed through programs of U.S. agencies and others, and a workshop was held in the Netherlands in April 2014 to discuss progress on these modeling efforts (http://scor-int.org/IQOE/Leiden_Report.pdf). The data collection started in the IYQO will need to be continued to address the effects of seasonal, annual, and decadal environmental variability on ocean soundscapes.

2) Long-term measurements of sound

A high-priority effort for the IQOE should be the initiation of long-term monitoring of sound, particularly at low frequencies, over ocean-basin scales. Monitoring will also be required at a relevant vertical resolution because, while sound may travel considerable distances when the receiver is in the SOFAR channel, most biological receivers are not at that depth. The intent will be to focus in a sustained way on characterizing variability in overall sound, human contributions, and biological use of areas and possible impacts of anthropogenic sound. Low frequencies will be a particular focus because of the propagation of low frequencies over ocean basins and the likelihood that many of the animals that might respond to sound are those that use low-frequency sound (e.g., whales, fish). Observation systems are available in many likely study areas, but will probably need to be augmented for more complete coverage, particularly in abyssal areas of an ocean basin and within coastal regions where the patterns of sound transmission can be complex and difficult to predict with existing models. The Global Ocean Observing System (GOOS) is now engaging in identification of Essential Ocean Variables that would be monitored by GOOS into the future, and the IQOE will aim to provide input to this process as part of Theme 3.

3) Observation efforts to support regional "experiments"

We envision a geographically focused study with potentially short-term changes in the sound field. This study could include comparison of two similar habitats in an area of somewhat rapid change or contrasting anthropogenic activity, such as comparing the Gulf of Mexico with the Gulf of California. Such an experiment will occur over a regional spatial scale (e.g., tens to hundreds of kilometers) on weekly to decadal time scales, and will necessarily consider a broader frequency range than long-term measurements. It will consider a larger number of individuals of the target species and possibly also examine community-level effects.

This approach could include opportunistic studies such as those done in relation to the changes in shipping lanes around the California Channel Islands (see Theme 2), and could focus on areas of planned changes in shipping regulations, for example, the no-boat zone in San Juan Islands (before/during/after), and designation of Particularly Sensitive Areas (PSA) (subcommittee within IMO) involving rerouting of ships. The potential rerouting of shipping from Asia to the United States to pass farther south of the Aleutian Islands is a further opportunity. Another opportunity involves the presence of transient industrial noise, such as pile driving for the construction of wind farms. Other opportunities could exist on new gas platforms installed off Russia, in new leases in the Barents Sea, and in changes in maritime traffic in the Canary Islands area due to logistic and overload issues at large container-ship harbors in the Mediterranean Sea and Suez Canal area. The Suez Canal authority is developing a project to increase the depth of western channels of the Suez Canal from 48 ft. to 52 ft. This project is expected to affect traffic, some of which would have to be redirected temporarily along the west coast of Africa. The Las Palmas harbor in the Canary Islands can handle large container ships and thus it is expected that during these project periods, which may be repeated in the course of the IQOE project, a notable increase in traffic may occur and would be monitored by the PLOCAN observatory station and at the ESTOC site (see http://estoc.plocan.eu/en/).

Teilmann and Carstensen (2012) provide an example of how such opportunistic studies can be conducted. They monitored the acoustic activity of harbor porpoises before

a wind farm was installed, during construction, and for a long period after construction. The observations demonstrated decreased acoustic activity (and presumably reduced presence of porpoises) during construction of the wind farm, but gradual reoccupation of the area by porpoises during the regular operation of the wind farm.

The IQOE will establish an appropriate mechanism for interacting with the organizations and agencies involved in observations. To this end, the IQOE will appoint and fund a representative to attend meetings and make the case for participation of the IQOE in observation activities.

4) Arctic study comparison

The increasing retreat of the Arctic ice cover is opening up that region to increases in human activity, which is expected to bring profound changes to the natural (but not quiet) soundscape. Because of expected climate changes there is a unique opportunity to observe the effects of increasing levels of anthropogenic noise in this region. The Northwest Passage may in this context provide a specific area of interest to monitor soundscape changes given the increased presence of passing ships. A challenge for the IQOE will be to design experiments that can distinguish between the effects of changes in sound levels from other environmental change, such as change in ice cover.

The ecological changes in response to a changing soundscape are not expected to occur instantaneously, but rather are expected to occur over at least the duration of the IQOE and probably decades into the future; therefore, in addition to programs of short-term autonomous measurements, this suggests that the IQOE press for a long-term monitoring effort.

5) Antarctic study comparison

Numerous observational efforts are also underway in the Antarctic using autonomous systems (Figure 5.4), and the IQOE should coordinate with these efforts. However, if we wish to develop a system for making long-term measurements of the background ocean ambient sound, then placing sound observatories under Antarctic ice sheets would enable the collection of data that is free of near-field interferences. Although technically challenging, both the Ross and Filchner ice shelves would be appropriate for this purpose and would "look" out into the South Atlantic and South Pacific oceans, respectively.

Figure 5.4. *The Perennial Acoustic Observatory in the Antarctic Ocean (PALAOA) continuously records the underwater soundscape near the ice shelf edge, 12 km from the German Neumayer-Station III. Photo: Thomas Steuer, Alfred-Wegener-Institut (see http://www.awi.de/fileadmin/user_upload/News/Press_Releases/2013/3._Quartal/Buckelwale_Ilse/2011Palaoa_TSteuer_p.jpg).*

Chapter 6
Theme 4: Industry and Regulation

6.1 Introduction

The societal response to concerns about the effects of underwater sound generated from human activities has been to introduce legislation and establish regulations to govern sound-generating activities. Although still at an early stage in development, mainly because of the limited evidence for effects of sound on marine life, the legislative frameworks currently in existence tend to give government policymakers the option to introduce highly precautionary regulations. This tendency toward caution is mainly the result of high scientific uncertainty. As examples, both Europe and the United States have these types of legislative frameworks.

The legislative basis for most U.S. regulation focuses on the protection and recovery of particular species (Hatch and Fristrup, 2009), whereas European Union legislation is focused mainly on reducing the introduction of sound energy into the water (Tasker et al., 2010). EU regulation also includes aspects of species protection, directed at listed species and at the protection of critical habitats, within the Habitats Directive. Under the U.S. Endangered Species Act (ESA), acoustic injury or disturbance of any listed marine species or population is considered when determining whether an activity will "jeopardize" the existence of the species or population. The ESA also may consider whether human-generated sound will destroy or adversely modify habitats that are critical to the listed species. The U.S. Marine Mammal Protection Act (MMPA) prohibits "taking" marine mammals, where "take" is interpreted as to kill, injure, or harass individuals. The MMPA requires that human activities that could violate this prohibition, including harassment of marine mammals by sound, are subject to a permitting process. Exposure thresholds relevant to the MMPA have been established by the National Marine Fisheries Service of the U.S. National Oceanic and Atmospheric Administration (NOAA) to regulate potential impacts of sound on marine mammals. For whales exposed to sequences of pulsed sounds, the threshold at which harassment begins, as defined by regulators, is a received level at the animal of 160 dB re 1 Pa. For continuous sounds, the threshold is lower: 120 dB re 1 Pa. For seals and sea lions, the thresholds are 180 dB re 1 Pa and 160 dB re 1 Pa, respectively (NOAA, 2005; Hatch and Fristrup, 2009). These simple numerical thresholds imply zero response below the threshold and 100% response above the threshold. Moretti et al. (2014) used response data to develop more realistic, gradual dose–response functions for predicting impacts of sonar sounds on beaked whales (see Theme 2). The effectiveness of these types of regulatory approaches relative to the costs to human activities that produce sound in the ocean has been debated extensively and inconclusively.

The global commercial shipping fleet expanded from about 30,000 vessels (of about 85,000,000 gross metric tons) in 1950 to more than 85,000 vessels (about 525,000,000 gross metric tons) in 1998 (NRC, 2003). About 90 percent of world trade (in gross tonnage) depends on ship transport and, apart from declines during global economic downturns, the gross tonnage of goods transported by sea has steadily increased since the early 1970s. A theory has been proposed by Frisk (2012) that quantitatively links increasing low-frequency ambient noise levels to commercial shipping activity, which in turn, can be correlated with global economic trends (Figure 6.1).
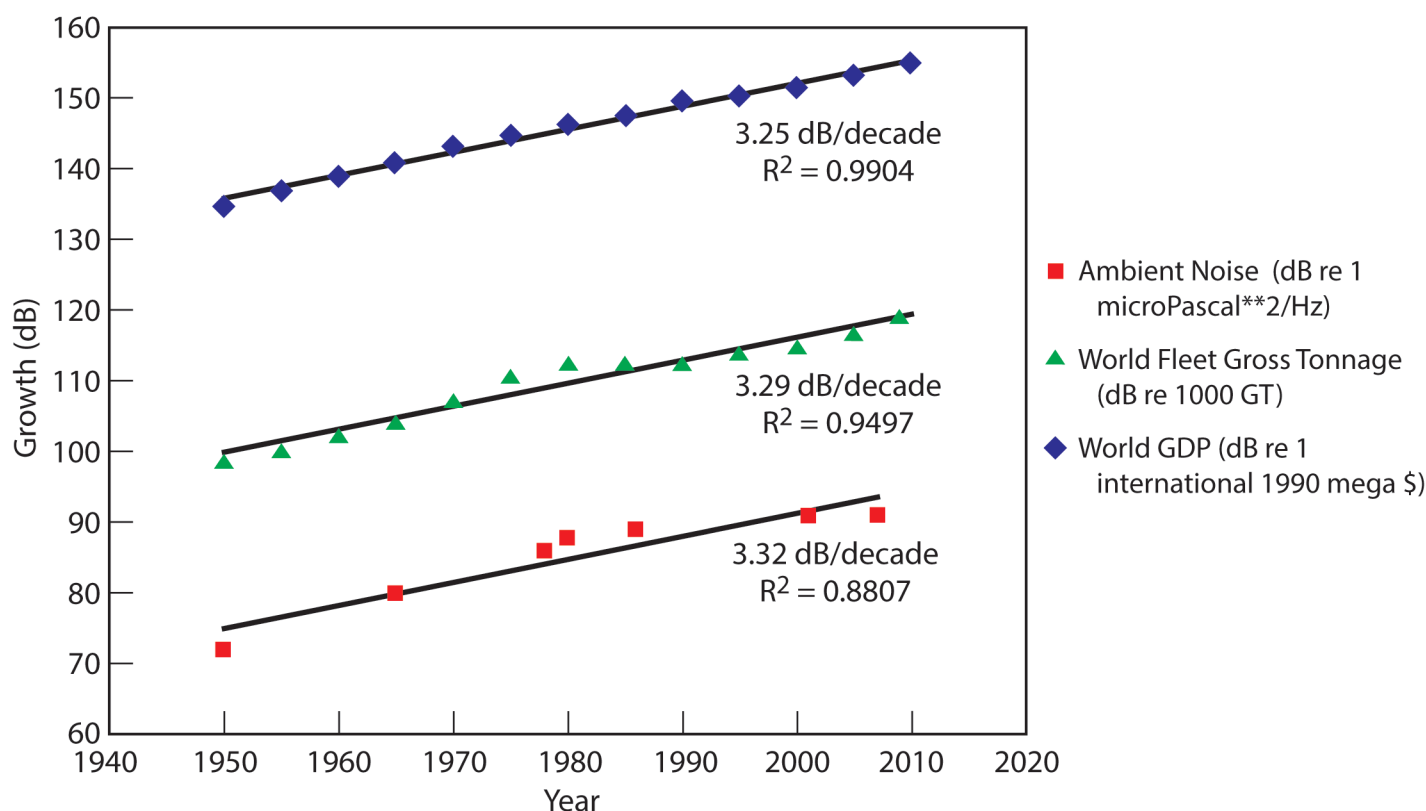
Figure 6.1. *Measurements of ambient noise levels, world fleet gross tonnage, and world gross domestic product are plotted as decibel (dB) quantities for the period 1950-2010. Linear fits to the data for all three quantities show similar slopes of 3.3 dB per decade with high goodness of fit (R^2) factors (Frisk, 2012). Used from Frisk, G.V. 2012. Noiseonomics: The relationship between ambient noise levels in the sea and global economic trends.* Nature Scientific Reports *2, Article number 437, doi:10.1038/srep00437, with permission from George V. Frisk, as allowed under the Creative Commons license.*

A continuing increase in shipping traffic is not certain because there could be an upper limit in the growth of ship transportation of goods brought about by (1) periods of slow or stagnant economic growth, as happened in the mid-1980s (Figure 6.1); (2) increased efficiency of the movement of goods; (3) reduced availability of raw materials or more efficient local sourcing of raw materials; and in the very long term (4) slower increases in demand because of leveling out of the global human population and especially the population of richer Northern Hemisphere nations. Nevertheless, all of these scenarios are uncertain, and it is possible that the recent growth of shipping will continue for the immediate future. Alternatively, technological improvements in engine and hull design could result in the sound produced by ships not increasing in proportion to either the number of ships or the tonnage of goods moved. This may be an explanation for the difference between the rapid increase in shipping since 2000 shown in Figure 6.1 and the decline in apparent shipping sound in the ocean shown in Figure 2.3 (Andrew

et al., 2011). Theme 1 on Ocean Soundscapes will help resolve whether there is a relationship between low-frequency omnidirectional ambient sound and shipping.

Changes in ocean sound will also be caused by other key human activities, such as oil and gas exploration and other offshore engineering. The IQOE is aimed principally at resolving some of the critical scientific uncertainties associated with our understanding of how sound travels in the ocean from these kinds of human activities to organisms, and how organisms react, both individually and as populations. Only partial progress will be made during the IQOE, and considerable uncertainties will remain. It is important, therefore, that the IQOE has the capacity to maximize its effectiveness in the long term within the arenas of policy and regulation by rendering current approaches to regulating marine sound more effective. In other words, the IQOE needs to have a legacy that will be effective far beyond its completion.

This theme will develop the applied axis of the IQOE research activities to complement the more fundamental research of the other themes. Some of this theme's approach will include specific research that could provide the basis for more informed approaches to regulation, such as those used by NOAA for regulating effects on marine mammals (NOAA, 2005), but much of the work in this theme will involve weaving an applied thread through the activities defined in Themes 1, 2, and 3, and increasing the likelihood that the knowledge gained is used in future regulatory activity. Consequently, some of the activities mentioned in this theme refer to those in other themes.

Managers, industry representatives, and government scientists have been involved in IQOE planning from the start and were responsible for creation of this section of the Science Plan. The IQOE will continue to seek to involve managers, regulators, industry representatives, and environmental NGOs in planning for IQOE observations and research, most likely through a subcommittee of the IQOE Steering Committee.

6.2 Risk frameworks

General description of risk frameworks

Exploitation of the ocean and its resources is a necessary part of human economic and social development. Continued expansion of the global human population, together with declines in the availability of basic raw materials, including energy resources, creates an imperative to continue to exploit ocean resources at least at current levels and probably much more in the future.

Therefore, industrial development will continue

even in the face of increasing regulatory constraints. In these circumstances, it can be costly to wait until scientific knowledge catches up to help ensure that industry can move forward with a high degree of certainty that the options chosen for future development will not significantly decrease the sustainability of the ocean environment. Consequently, we need a framework within which progress can be made in a measured manner, while simultaneously minimizing risks to the environment and the costs to industry in both direct financial costs and those related to lost opportunities. Such a framework will explicitly assess risk and incorporate adaptive management of the industrial process and development (Boyd et al., 2008; Figure 6.2).
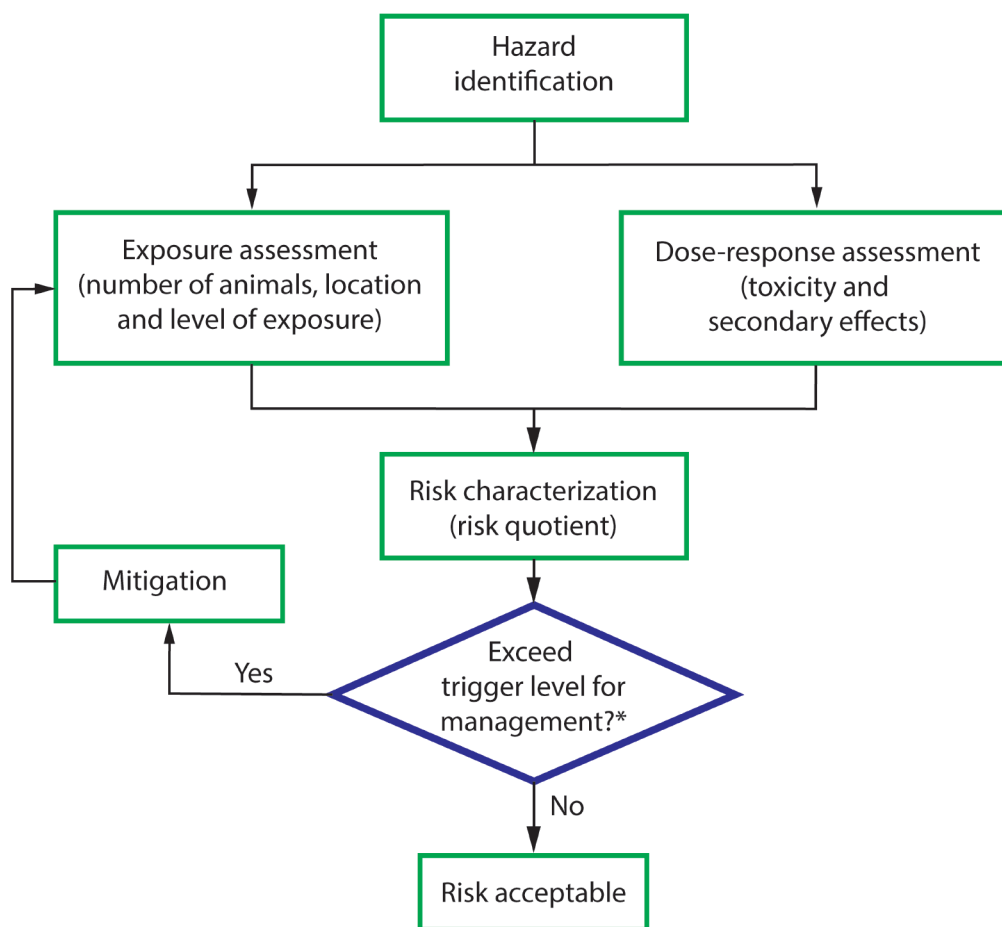
*Trigger level defined by legislation, value judgement or biological significance

Figure 6.2. *An illustration of the information flow and decision pathway for a risk assessment process. This shows a feedback process involving mitigation when the risk exceeds the trigger level for management action. This is an adaptive approach to managing risk. Redrawn from Boyd et al. (2008).*

The advantage of a science-based framework for regulation of sound in the ocean is that it allows industrial activity to proceed in a precautionary manner and establishes procedures for collecting information about its effects as activity proceeds. Effects are then assessed against predetermined objectives. If those objectives are not met, mitigation is introduced, the mitigated activity is allowed to continue and is again assessed against specific objectives. This procedure is continued until a satisfactory operating procedure or design is found for the industrial activity. Many circumstances lend themselves to this approach, but some activities will always be found to be too harmful to continue.

The following sections expand on the activities needed to populate the risk framework illustrated in Figure 6.2.

Hazard identification

The main questions that will need to be addressed are

- Which sound sources need additional characterization?
- What can we do to develop acceptable (by industry, regulators, and stakeholders) standards and methods for measurement?
- Can we develop alternative sound sources to reduce impact where intense sounds are required (e.g., air guns replaced explosive sources for seismic surveys. Would it help to replace seismic air guns with marine vibrators?)
- What impacts do alternative sound sources have on the environment?
- What can be done to existing sound sources to reduce unwanted sound?
- How does industry measure its contribution to the ocean sound budget?
- What do we need to do to better understand the global background sound status?

Dose–response assessment

Quantifying the relationship between dose (i.e., received sound characteristics) and response (behavioral response, masking, TTS, PTS, injury) will be a task for Theme 2 (see Section 4.2).

Exposure assessment

Exposure assessment involves specifying the population that might be exposed to the hazard, identifying routes through which exposure can occur, and estimating the magnitude, duration, and timing of the dose that marine mammals might receive as a result of exposure. The information needed in this category includes the following:

- Distribution and abundance of specific organisms, such as fish and marine mammals, over long time periods to identify overlap between sources and receivers
- Quantification of industrial activity in the areas under question
- Assessment of how industrial activity translates into sound budgets
- Identification of stressors other than sound that act on the population of interest

Some of this information should already be available from management agencies, although the translation of industrial activities into sound budgets will be addressed in this theme (Section 6.3).

Risk characterization

Risk characterization involves the overall assessment of risk and is achieved by integration of information from the first three steps in the risk assessment process shown in Figure 6.2 (hazard identification, dose–response assessment, and exposure assessment) to develop a qualitative or quantitative estimate of the likelihood that any of the hazards associated with the sound source will occur. The information needs in this category include the following:

- Determination of whether any effects are biologically significant
- Definition of biological "hot spots" for animal production or especially sensitive species that should be avoided at times
- Measurement of the population growth in areas where sound is prevalent
- Definition of cumulative impacts in terms of how specific sounds can interact with other pressures

Again, management agencies should be able to provide some of this information, and Theme 2 will help define which effects of sound are biologically significant.

6.3 Routine sound monitoring

Although issues concerning the observation of sound are dealt with in detail by Theme 3 for the scientific purposes of the IQOE, Theme 4 also requires an element of sound measurement, particularly to characterize human-generated sound sources. Measurement of the characteristics of the sources of human-generated sound is required so that these can be used within sound propagation models (see Theme 1). Figure 3.3 shows the amplitude of different frequencies with distance from a pile driver. However, not only is it necessary to examine amplitude as in this case, but other characteristics of the sound also need to be determined, such as directionality, bandwidth, particle motion, pulse width, height, and rise time. The sound radiated from a source can vary with orientation and, for ships, their speed and whether they are loaded. In addition, a fuller understanding of how the characteristics of these sounds may

change with propagation over larger ranges is required.

Even though sound from shipping is probably the greatest single source of human-generated sound in the ocean, this will not always be the case on local or regional scales. Pile driving is a fast-growing activity in some coastal regions, mainly because of the construction of offshore wind farms. Seismic surveys using air guns are also widespread. Other sources of marine sound include—but are not limited to—construction, dredging, acoustic communications, supersonic aircraft, ammunition, explosives, seismic exploration for scientific purposes, marine mining, cable laying, and naval training and surveillance sonars. The many types of sources and their associated sounds make it necessary to identify a way of quantifying them to make meaningful comparisons. One proposal for doing so is to determine their contribution to the total acoustic energy in the sea (Ainslie et al., 2009; Ainslie and Dekeling, 2011). Although sound spectral characteristics for many of these sources are available as examples that may (or may not) typify those types of sources, there is a need to compile information about these different sources and the extent to which they can be described by typical examples. The compilation then needs to be made available and the IQOE will promote this by developing a Web-based repository for spectral information about sound sources.

The IQOE will also adopt and promote standards for characterizing the sound from different sources, such as helping to develop and promote an International Standards Organisation (ISO) standard for radiated sound from ships in deep water. Such a standard is being developed by an ISO subcommittee devoted exclusively to underwater sound, and its effect on aquatic life. The IQOE will collaborate with the subcommittee in the adoption of appropriate standards for ships in shallow water as well as for sounds from other sources such as air guns, impact pile drivers and explosions, and for ambient noise (Cato, 1997; Carey and Evans, 2011). An essential prerequisite for all of these standards is the development of an acoustical terminology standard (Ainslie, 2011). The IQOE will promote these standards through the provision of Web tutorials about their application.

In many regions, statutory monitoring of sound levels is taking place around offshore developments or is being implemented by regional management authorities in response to wide-ranging legislation concerning management of the marine environment. This includes the Marine Strategy Framework Directive in European waters, where there is a commitment to establish guidelines to

regulate human-generated sound in the ocean even though there is considerable debate about what these guidelines should be.

Methodological standards need to be developed for ambient sound measurements over long periods, to allow legislative standards to be established and enforced. The outcomes of both Themes 1 and 3 will support this requirement, and the presence of observatories established for the statutory monitoring of marine noise also presents opportunities for low-cost data collection in support of research with broader objectives.

Sound recording systems of this type are likely to become routine in the future, and the IQOE has the opportunity to influence the design of monitoring protocols, the hardware systems for carrying out monitoring, and the data storage and analysis systems, and also to benefit from these systems. However, to achieve these goals, the IQOE will need to engage closely with those who are responsible for establishing sound monitoring to maximize these benefits. Figure 6.3 illustrates a system of sound monitoring on a local scale that has been developed by both regulators and ship operators to solve a conflict caused by ship strikes on northern right whales. This system uses acoustic detection of the right whales to alert the ships to their presence.
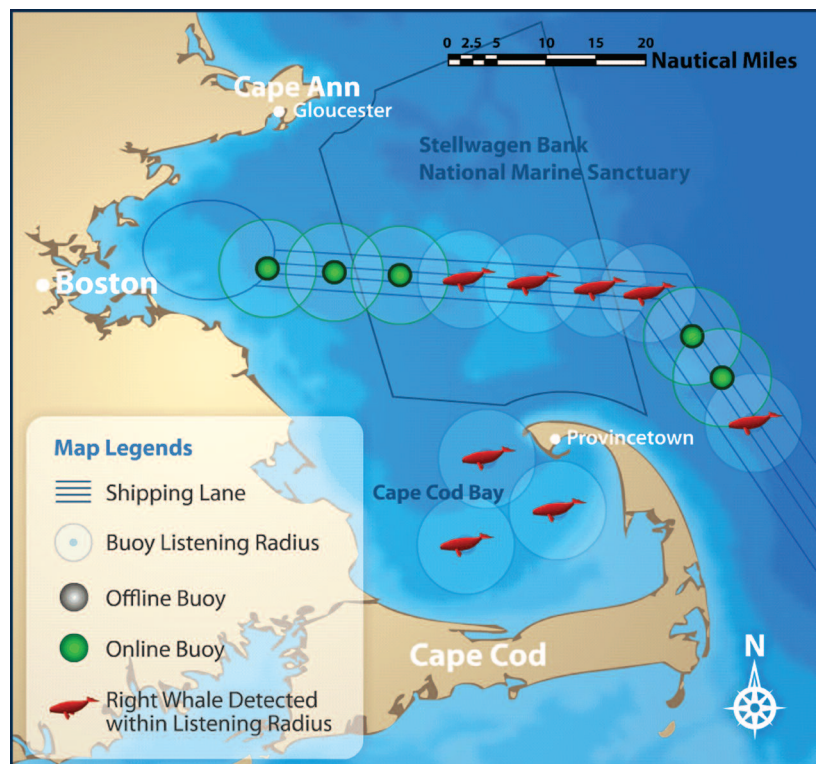
Figure 6.3 *Diagram showing a real-time auto buoy system that is operational off the northeast coast of the United States. The system alerts mariners to the presence of right whales to reduce the probability of ship strikes. From Van Parijs et al. (2009). Used with permission from Inter-Research Science Center.*

6.4 Research priorities for regulators and industry

Develop practical solutions, useful to industry and regulators, to monitor and mitigate human-produced sound

The effects of specific doses of sound on protected species—as well as other species that may have ecological or economic value—is important for regulators and, therefore, also for industry. From an industry and regulatory point of view, while it would be ideal to understand the mechanisms underlying adverse effects such as permanent loss of hearing (permanent threshold shifts: PTS), there is a greater need to move quickly to develop precautionary indicators of significant effects, such as using temporary threshold shifts (TTS) as a safe indicator for risk of PTS. This will facilitate studies that define simple, but robust, empirical relationships between sound and responses in marine organisms. For example, the behavioral responses of beaked whales to sonars (Tyack et al., 2011) are an indicator of potential harm. Translating the probability of behavioral disturbance into a probability of a significant population effect can probably be achieved relatively easily, but with low levels of confidence. Additional work will then be necessary to increase the confidence around the estimated level of effect. However, for the time being, the thresholds of behavioral disturbance found in this case are the precautionary threshold that may be used by regulators.

Studies concerning individual impacts can deal with behavioral response, masking, TTS, and auditory or nonauditory injury. Although it has been shown that, in some cases, sound can injure or even kill individual organisms, population-level consequences would be unlikely if only a small proportion of the population is affected. In contrast, behavioral and masking effects can occur at lower sound levels and over vastly larger areas, and therefore may affect a larger and potentially significant portion of the population.

The effects of multiple sound exposures (both sequentially and simultaneously) may accumulate and add to the effects of other stressors, such as of ship collisions with northern right whales (Figure 6.3); the IQOE needs to consider such cumulative effects. Therefore, the program will undertake modeling to examine how the measured, usually adaptive, responses of animals to underwater sound can be rescaled to develop realistic representations of risk to populations. Much of this will be done within the PCAD modeling framework (Figure 2.5).

The research needed to define biological significance of sound for marine organisms can be summarized as follows:

- Better identify the effects of underwater sound on individual marine animals, to make it possible to scale up the problem through the accumulation of effects on individuals to populations. This could involve investigations of the following:
  - Temporary threshold shift (TTS): More studies are needed to assess temporary threshold shifts for risk assessments;
  - Behavioral effects: There is very little understanding on the behavioral effects of sound on marine life; and
  - Masking of sound signals used by animals for communication: Experimental evidence of consequences of masking is required, rather than relying on predictions based on modeling.
- Determine the spatial distribution of sensitive species and how this changes through time as a way of defining critical habitats for industry to avoid.
- Determine whether the PCAD approach can provide practical solutions to the problem of regulating sound production by industrial activity. Both industry and regulators may need solutions that are less precise, but more tractable.
- Provide key information to make feasible a risk-based approach to adaptive management of industrial activity when faced with high uncertainty about the effects of sound.

Key questions—Industry and regulators have identified the following important questions:

- What is the effectiveness of existing monitoring techniques and tools and how can they be improved?
- What additional monitoring tools (short- and long-term) can be developed to assist in marine mammal observations?
- Can International Maritime Organization (IMO) data be used as an analysis tool on a local and regional basis?
- Are "soft-start" or "ramp-up" effective mitigation techniques?
- Are there other ways to mitigate unwanted sound, for example, air bubble curtains?

For all industrial activities, a fuller understanding of existing and projected trends in industrial activity levels and sounds produced by these activities is important. While the IQOE will not aim to use active acoustics, a potential

research topic for the project will be to help industry and regulators evaluate the impacts of active acoustic methods they use or intend to test.

In spite of its apparent prevalence, the importance of shipping sound for marine life is largely unknown. Shipping sound has the potential to mask the communication signals of marine mammals and fish, and both taxa have been shown to change behavior in reaction to these sounds. However, even though predictions based on theory indicate that communication ranges can be decreased as a result of increased sound levels, understanding the true extent of this effect is critically important. Many, if not most, species have developed mechanisms to compensate for masking, for example, increasing the source level of their sounds when located in an increased noise environment (Parks et al., 2010). There are also large differences in potential effects between deep and shallow waters and among the taxonomic groups affected.

Cavitation sound by propellers is an important source of shipping sound, so mitigation attempts could be targeted there. The Marine Environmental Protection Committee (MEPC) within IMO has formed a correspondence group on sound from commercial shipping that deals with mitigation measures such as ship-quieting technologies. Propellers are likely to be redesigned as a response to requirements to make more efficient propulsion. Sound radiation should be considered as part of the design process from the start.

Impact pile driving, used particularly for installation of offshore wind farm turbines, has been shown to lead to wide-ranging behavioral impacts on small odontocetes, such as harbor porpoises, and can injure marine life close to the source. This issue has been addressed in some regulations such as the EU *Marine Strategy Framework Directive* (also see OSPAR, 2009). Although marine pile-driving is generally well regulated in many regions and Environmental Impact Assessments (EIAs) are often required, cumulative effects of multiple piling activity, or cumulative effects of piling with other stressors (acoustic and nonacoustic) are not well understood and are beyond the scope of individual EIAs. Furthermore, particle acceleration is a primary concern for fish, especially in the near field, and should be measured directly in situ.

In examining the effects of seismic air guns on marine life, the International Oil and Gas Producers (OGP) has set a commendable example of the engagement of industry in researching acoustic impacts through the Joint Industry Program (OGP-JIP). While there are currently ongoing studies of the source characteristics of seismic air gun arrays, among a range of other studies (e.g., behavioral response study of Australian humpback whales to seismic air gun exposure), there remains a need for further research on the topics of behavioral effects, masking, and efficacy of mitigation measures.

Additional sound sources to be considered include naval sonars, cable laying, acoustic mapping, seismic exploration, deep-sea mining, wave- and tide-energy generation, new exploration technology, dredging, echo sounders, active positioning systems, and acoustic deterrent devices used in fish farming, among a range of others. Development of new technologies, such as marine vibroseis, that replace, where possible, existing sources, is strongly encouraged if there is evidence that the new source has lower impact.

Research approaches—Research needed by industry and regulators to determine how best to conduct routine sound monitoring can be summarized as follows:

- Define what is meant by "routine sound monitoring." For example, it is not always clear whether this should include measurements of specific activities, monitoring of ambient noise, or both.
- For ambient sound monitoring, it is necessary to identify the objective of meaningful and valued outcomes. Monitoring ambient sound can produce sound maps and sound budgets, and can identify trends of ambient sound over predetermined time scales in specific areas. This last objective is required, for example, by the EU Marine Strategy Framework Directive. Each of these objectives could require different approaches.
- Modeling sound propagation will be an important approach in designing monitoring networks and also for analyzing data.
- The development of compliance monitoring for sound levels at regional scales will require several steps, including
  - Identification of existing ambient sound measurement data within the study area.
  - Identification of suitable measurement systems (there is a database on suitable devices).
  - Identification of existing ocean observatories in the study area.
  - Assessment of the feasibility of using existing observatories for ambient sound monitoring.
  - Identification of representative sites

(including pressure areas or areas of high sensitivity) and the possibility of establishing reference areas where there is little human-generated ambient sound to describe natural fluctuations.

- ◦ Development of a work plan, including a maintenance schedule and data analysis reporting cycle.

- • If ambient sound monitoring is attempted in sensitive areas, the distribution and abundance of sensitive receivers (marine mammals and fish sensitive to the source in question) need to be documented to a higher standard than elsewhere so that there is sufficient statistical power to detect important changes in population status, and to be able to report these in sufficient time for management action to be taken.

- • Sound frequencies that are most biologically important should be monitored. Consequently, it is necessary to define these frequencies.

- • An investigation of the costs and benefits of monitoring is needed to ensure that the outcomes lead to a net benefit for society.

These tasks will need to be coordinated with the activities of Themes 1 and 3.

Measuring the relationship between industrial activities and sound levels

Compiling sound budgets (Nystuen et al., 2010) for a region is an approach used to establish or regulate the contribution made to the sound field by different industrial sources. It is likely that regulators could establish levels of anthropogenic sound within regions that cannot be exceeded and different industrial users of the ocean may have to work to remain within this limit. In this case, sound budgets, and perhaps allocation of sound credits to different ocean users may become commonplace. Compiling inventories of anthropogenic sound in a region may, therefore, be an important factor in establishing whether regulatory targets have been met. Industry will need to have simple and cost-effective tools for demonstrating compliance as well as real-time feedback to allow optimal decision-making during marine operations. For example, if the captain of a container ship knows the radiated, speed-dependent sound profile of the ship and also knows the contribution that the ship is allowed to make to the sound budget of the region, the captain can make a judgment about the speed at which the ship can travel, while also knowing that if the ship exceeds this speed, its excess contribution to the sound budget may be detected. Regulation is moving toward developing sound budgets, but we do not currently have the mechanisms in place for

monitoring and feedback to optimize human behavior in a way that matches aspirations to control sound levels.

Some progress may be made through the compilation of sound inventories that quantitatively assess the contribution and characteristics of different sources to the overall sound field in a given region. Such compilations can be used to identify research and regulation priorities. Furthermore, sound inventories might help in determining whether, and to what degree, human activities contribute to the ambient sound field. Thus, they are tools that can be used in marine management.

Robust, validated models of ambient sound are also likely to be a tool for marine spatial planning and informed regulation. The need extends from regional areas of heavy traffic to ocean-basin scales.

Key question—The key question for this topic is:

- • How can the observed sound field in specific locations be accounted for, based on known sources and propagation conditions?

To answer this question will require the development of models that will depend on

- • establishing long-term sound measurements (see Theme 3),
- • cataloging sound sources (see Section 6.2.2),
- • integrating these into propagation models (see Section 3.3), and
- • validating these models with direct observations (see Section 5.1).

Validated models can be used to evaluate the effectiveness of sound-constraining regulation to allow planners to examine the implications of different options for offshore development.

6.5 Implementation approaches

The IQOE will work with the IMO to further address the issue of shipping sound as one of the main contributors to undersea sound. The IQOE will work in collaboration with industry groups to develop a joint working group on the issue of underwater sound to strengthen the links between industry and research. This should be supported by a clear communication and outreach plan to convey the results of the IQOE to global stakeholders, policymakers, and the public (see Chapter 7).

The IQOE will, as far as possible, promote the use of scientific results to harmonize national regulations. There is

a danger of different standards being applied by different countries, resulting in confusion and adding unnecessary costs for industry. Although the regulation of human activities is a policy decision that is based on more than scientific facts, the same results could be used very differently across national boundaries. For example, many EU member states set priorities for underwater sound in very different ways. Researchers operating within the context of the IQOE have an opportunity to help harmonize the foundation of scientific information behind the decisions of environmental management. Wherever possible, environmental management should be based on empirical studies and standardization of measurement techniques globally. Standardized soundscape measurements developed through the IQOE can provide the long-term data that could be used to assess and monitor soundscape parameters in ecologically significant areas, such as marine protected areas.

Chapter 7
Implementation

7.1 Introduction

The preceding chapters present a case for a decade-long program of observations, modeling, and research related to sound in the ocean and its effects on marine organisms. Key questions are presented, as well as some general approaches for addressing these questions. The project priorities were developed based on an open science meeting. As with many international research projects, implementing this project will require additional discussions, meetings, and documents. However, the following will outline enough details of implementation to provide the sponsors (organizational and financial) and project scientists with a foundation on which to build the project.

7.2 Fundamental questions

Underlying the IQOE are five fundamental questions:

1. How have human activities affected the global ocean soundscape compared with natural changes over geologic time?
2. What are the current levels and distribution of anthropogenic sound in the ocean?
3. What are the trends in anthropogenic sound levels across the global ocean?
4. What are the current effects of anthropogenic sound on important marine animal populations?
5. What are the potential future effects of sound on marine life?

Questions 1-3 will be addressed by Themes 1 and 3, which focus on soundscape modeling and acoustic observations, respectively.

Questions 4 and 5 will be addressed primarily by Theme 2 (effects on sound on marine organisms), although the work carried out within Themes 1 and 3 will also be relevant. Theme 4 addresses how the results of the new research and observations will apply to management and regulations. Theme 4 will need to integrate information from Themes 1-3.

Each theme is divided into key questions and research approaches to each of these questions. Each theme will attract a different kind of scientist, but there will need to be an unprecedented level of cooperation among ocean acousticians, marine biologists, engineers, observing system specialists, data experts, and communication specialists to ensure the success of the IQOE.

7.3 Timeline

An approximate 10-year timeline is planned for the IQOE. This is the usual duration for large-scale ocean research projects, providing enough time to conduct detailed planning and foundational activities, raise funding for research, conduct new research and observations, and synthesize the results obtained. The community of scientists involved at the IQOE Open Science Meeting was enthusiastic about a decadal project. It is recognized that a project lasting only one decade will not be able to characterize how the effects of sound change with climate cycles—such as the El Niño – Southern Oscillation and North Atlantic Oscillation—that are repeated only one to a few times per decade. However, most funding agencies are reluctant to commit to projects longer than 10 years' duration.

The project will be implemented in four phases:

1. Laying the foundation (Years 1-3)
2. Pilot projects (Years 4-6)
3. International Year of the Quiet Ocean (Year 7)
4. Synthesis (Years 8-10)

The phases will not be strictly sequential. For example, planning for later phases will begin before Phase 1 is completed. In addition, some national programs have already begun implementing new observing systems in anticipation of the IQOE.

Phase 1. Laying the foundation
As with other international research projects, it will be important in the first few years to establish standards and data management mechanisms, and to synthesize as much available information as possible to provide a foundation for new observations and research, and to identify gaps in information that can help guide new activities.

Standards and intercalibrations—It will be important to come to agreement among project scientists regarding standards for acoustical and biological measurements before any large-scale observations and experiments are conducted. Standards are important so that data collected by different scientists in different locations can be compared and compiled into global databases. Establishing standards may require meetings of individuals who possess expertise in making observations and experimental

measurements. Intercalibrations may need to be conducted related to equipment and methods for observations. Intercalibration exercises are especially important when different research groups or observation systems use different equipment and techniques. Intercalibration may require workshops in which the most common systems and methods are tested against each other in the same location with the same acoustic and biological signals. Standardization and intercalibration may also be improved through training workshops.

Data management—The IQOE will establish a data management and communication (DMAC) activity, which will be responsible for establishing procedures and guidelines for data collection and assembly, and communication of data to users. Well-designed data management is crucial so that properly standardized and intercalibrated data are stored in a common location to create global datasets that can be analyzed by project scientists and eventually be openly available for reuse by other scientists and managers.

Synthesis of available data—A great volume of acoustical data and data from experiments on biological effects have been published in the peer-reviewed literature, as well as in government and industry documents. Compiling and synthesizing such data will provide a foundation for IQOE research and observations, avoid unnecessary duplication of scientific activities, and lead to identification of gaps in existing data and information.

It is envisioned that the first three years of the project will focus on the above three areas and they will be approached through a series of small workshops:

- Synthesis of activities on soundscape modeling: The IQOE cosponsored a workshop on Predicting Sound Fields, held on 15-16 April 2014 in Leiden, Netherlands (with the International Whaling Commission, the U.S. National Oceanic and Atmospheric Administration, the U.S. Office of Naval Research Global, the Netherlands Organisation for Applied Scientific Research, and the Netherlands Ministry of Infrastructure and the Environment). The report of the workshop can be found at http://scor-int.org/IQOE/Leiden_Report.pdf.
- Workshop on design of IQOE data collection, management, and access. Issues related to standardization of data collection and storage will need to be addressed early in the project. The goal of this workshop will be to agree to standards and procedures that would guide the

IQOE to make observations and research conducted in different locations comparable. The workshop will involve representatives from as many existing observing systems as possible, and will include members of existing standards groups such as the ISO ISO/TC 43/SC 3 on Underwater Acoustics.
- Workshop to synthesize data on the hearing capabilities of marine organisms.
- Workshop to set standards for ocean acoustic observations and experiments with marine organisms. The ISO ISO/TC 43/SC 3 on Underwater Acoustics will be consulted to plan this work.
- Meeting with industry representatives regarding their participation in the IQOE. The goal of this meeting will be to produce one or more memoranda of agreement between the IQOE and industry groups. This meeting also could result in the creation of an industry advisory group to the IQOE. The meeting may result in a standing working group of the IQOE that will focus on industry engagement. Such a working group will be necessary to ensure that Theme 4 is linked properly with the other themes and that the project is generating the information to answer the questions in Theme 4.
- Workshop on access to proprietary and classified information, past, and future. Success of the IQOE will depend on access to past data collected by navies, commercial oil and gas exploration companies, and the Comprehensive Test Ban Treaty Organization. Data collected as part of the IQOE will need to take into account sensitivities of stakeholders about collection and public access to acoustic data. The goal of this workshop will be to identify potential providers of information, what data they will make available, under what circumstances. The workshop will also discuss a process for developing written agreements about data sharing.

Other potential workshop include the following:

- Workshop to develop a world map of anthropogenic ocean sound (see Example 1 below). This workshop will work as far back in time as possible to determine whether it is possible to develop time series for ocean sound similar to the time series for atmospheric CO_2 concentrations known as the Keeling Curve (Keeling, 1960). This workshop will produce a paper for a high-profile journal.

- Workshop to plan an Arctic Ocean acoustic survey (see Example 2 below). This workshop will need to bring together scientists involved in acoustics of the Arctic Ocean, as well as organizations involved in Arctic Ocean science and observations. This workshop will produce a plan for an Arctic Ocean experiment that will be part of the IQOE.
- Workshop on the use of sound as an indicator of environmental status. This workshop will maintain close ties with the EU's Marine Strategy Framework Directive and will provide a world forum in which to discuss the meaning of "Good Environmental Status," how it is affected by underwater sound, and how changes in environmental status might be monitored using sound as a tool (see Example 3 below). The workshop will critically evaluate acoustic measures proposed for Good Environmental Status on an international basis and relating cost and reliability to effectiveness of different measures.
- Workshop on global ocean acoustic observations. The workshop will seek commitments from observation systems to install and support suitable hydrophones, as well as to identify areas of the global ocean where new hydrophone systems should be deployed. The workshop will produce a white paper that might be published in the peer-reviewed literature.
- Workshop on opportunistic observations. It will be necessary early in the project to establish mechanisms to identify opportunities related to changes in shipping lanes, planned large-scale pile driving activities, and other opportunities to study before, during, and after noise levels and effects on marine organisms. This workshop will conduct detailed planning for opportunities that have already been identified, as well as look forward to identify future approaches. The goal of this workshop will be to produce detailed plans for IQOE observations and experiments related to known opportunities, as well as a document that will specify how future opportunities will be approached.

Phase 2: Pilot projects
The information available from Phase 1 of the project will make it possible to proceed to Phase II, consisting of pilot projects. The purpose of the pilot projects will be to test the approaches described in this Science Plan in specific well-studied locations, with the intention of scaling up the approaches to more locations or a wider geographic range in Phase 3. This phase will also include planning for Phase 3.

Phase 3: International Year of the Quiet Ocean (IYQO)
An objective of the IYQO will be to conduct intensive and coordinated research, observations, and modeling worldwide and at large scales simultaneously. Phase 3 will be an intensive 12-18 months of acoustic observations and experiments worldwide, based on the information developed in Phase 1 and the experience gained from Phase 2. The IYQO will be used as a focus of public attention on sound in the ocean. Planning the IYQO for a single year has precedents in the International Geophysical Years (IGYs) and International Polar Years (IPYs). These events have resulted in both intensive research and observations in the focal year (or 18 months for IPYs) and sustained research and observational focus beyond the focal period of time.

Phase 4: Synthesis
Synthesizing data from the IYQO and reporting on studies carried out during Phase 3 will require several years to complete, partly because of the potential complexity of the data that will emerge and also because of the time that required to analyze them. It is likely that an open science meeting will be held toward the end of this period to report on the accomplishments of the IQOE and to discuss legacy activities.

7.4 Operating approach

The IQOE will be structured as a coordinating mechanism for all researchers with an interest in underwater sound and its effects on marine organisms and who are willing to pursue IQOE objectives within the boundaries of IQOE standardization and data sharing requirements.

Research will be funded through traditional national, regional, and international funding sources, such as agencies that fund research and observations (such as the National Science Foundation in the United States, the European Commission and national funding agencies worldwide, possibly through groupings of agencies such as the Belmont Forum). Any research that will be part of the IQOE will need to be approved by an IQOE Steering Committee (see Section 7.6). The Steering Committee will apply standards associated with the planning, data collection and reporting and will monitor progress of the collected set of IQOE-endorsed scientific activities. In return for complying with IQOE standards, researchers organizing specific studies will benefit from being a part of the process that defines the data standards, organizes outputs into common formats, and provides central coordination of data management and modeling. In addition, they will be a part of a community that achieves

the critical mass sufficient to sustain a high profile within the stakeholder community and that provides representation for their scientific outputs to policymakers, industry, and the public.

7.5 Governance

The IQOE will derive its authority from its organizational cosponsors, the Scientific Committee on Oceanic Research (SCOR) and the Partnership for Observation of the Global Oceans (POGO). These organizations also provide the international context within which the IQOE will operate. However, it is possible that national or regional subsections of the IQOE may develop, especially through collaboration in regional experiments.
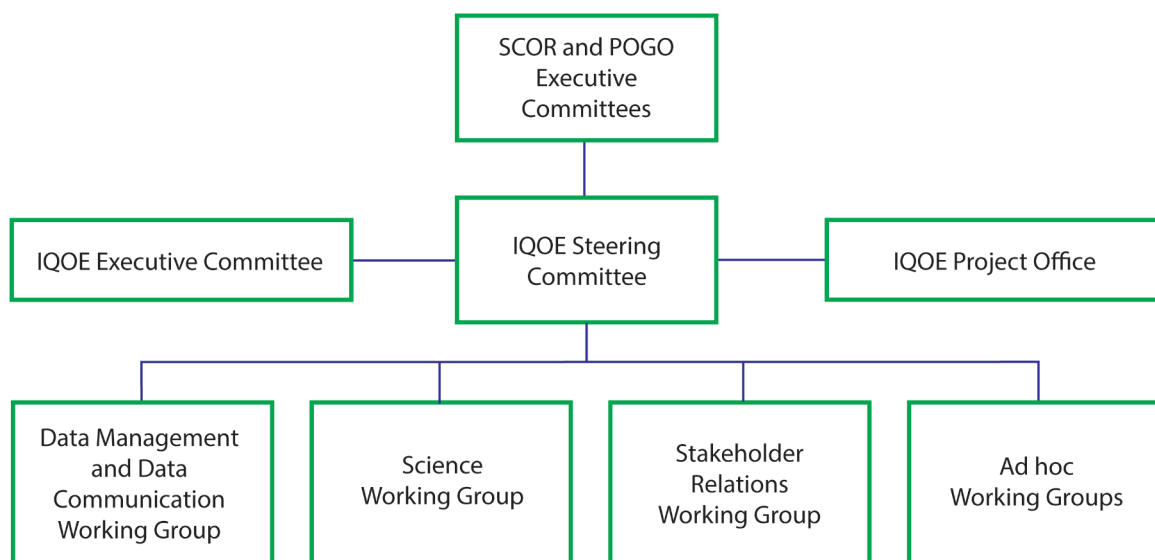
Figure 7.1. *The governance structure of the IQOE. The IQOE is established within the authority of SCOR and POGO. Lines on this diagram show routes of communication within the overall structure.*

Operational governance of the IQOE will be the responsibility of the Steering Committee (Figure 7.1). This committee and its chair(s) will be appointed by SCOR and POGO. The chair(s) of this Steering Committee will report annually to SCOR and POGO about all aspects of the IQOE, including progress in implementing the Science Plan, outreach, and stakeholder engagement. The SC may have joint chairs, particularly representing biological and acoustical expertise. The SC will be formed of its chair, the chairs of the permanent working groups, and as many as 10 additional members. The current plan is to have three standing working groups:

(1) *Working Group on Data Management and Communication* will have responsibility for defining the standards of data collection and managing the various systems used by the IQOE for data communication, including the Web site and associated data portal.

(2) *Science Working Group* will have responsibility for determining whether projects proposed by the research community should be included within the IQOE.

(3) *Stakeholder Relations Working Group* will establish communication with the shipping industry, oil and gas developers, navies, the CTBTO, and other groups with interests in IQOE science and could provide access to new sources of data.

Much of the international coordination and planning of the IQOE will be conducted by ad hoc working groups, each of which will be established to perform a specific task related to the IQOE objectives. Such tasks could be to conduct a specific experiment or study, but could equally be associated with coordination of public outreach or stakeholder engagement.

Appointments to working groups will be the responsibility of the Steering Committee. The IQOE will be managed on a day-to-day basis by the IQOE Executive Committee, which will be a subset of the IQOE Steering Committee.

7.6 Project management

Following review and approval of the Science Plan by the sponsors, the Steering Committee will be selected by project sponsors. The Steering Committee will have the following responsibilities:

- Manage implementation of the IQOE Science Plan and coordinate IQOE activities among different nations.
- Oversee the budget of the project.
- Establish appropriate policies for data management and sharing, and for standards and intercalibration to ensure that IQOE data collected by different investigators are comparable and to promote sharing and preservation of IQOE-related data.
- Collaborate, as appropriate, with other related programs.
- Create and implement the communication strategy (see Section 7.7).
- Report annually to SCOR, POGO, and any subsequent sponsors, on the state of planning and accomplishments of the IQOE.

SCOR will provide the primary administrative support for the IQOE, at least initially. The project may eventually require two or more staff persons (one person specializing in data issues and the other in logistics) to help implement and represent the IQOE. Duties that will need to be handled by an IQOE International Project Office include

- helping the Steering Committee with logistics for meetings and publications,
- representing the project at various meetings,
- fund-raising for project activities, working with the Steering Committee and sponsors,
- communications and outreach, including Web site and newsletter, and
- management of data.

Many international projects benefit from the creation of national committees, which can lead national efforts for planning science activities, fund-raising for these activities from national sources, promoting national data management activities, promoting capacity building, etc. The IQOE will investigate the formation of national and regional project committees. These could be particularly relevant in relation to basin-scale observations and experiments. The chairs of these national and regional committees will be ex officio members of the IQOE Steering Committee.

7.7 Communication and outreach

The IQOE Steering Committee will develop a communication strategy at an early stage. This strategy will identify all the major stakeholder groups and define the methods that will be used to communicate the purpose and results of the IQOE, as well as to encourage the involvement of stakeholders, when appropriate. This strategy will lead to the provision of publications and other materials that will allow those associated with the IQOE to provide a consistent and clear message.

The broader objectives of the IQOE include improved public appreciation of the ocean, the life within it and pressures upon it. Opportunities exist to stimulate the development of "citizen science" projects by streaming spectrograms in real time from observatories and by providing possibilities for the public to record sounds of marine organisms (e.g., through an iPhone application) and to upload these recordings to a Web site with an accompanying photograph. Links with Google and social networking will be important to encourage broad uptake of IQOE activities and information.

A comprehensive plan for the engagement of stakeholders and the public will be a priority for the IQOE. This plan will include targeted activities that reach policymakers, industry representatives, the media, and other stakeholders. Strategic activities will build awareness of the IQOE's research portfolio and encourage the participation of important industries in research activities.

Program "launch"

To accomplish IQOE goals within an international framework, it is essential that the program becomes widely known as a credible and trustworthy source of authoritative information and a basis for new measurements and new understanding of the effects of sound on marine life. An initial outreach and communications effort should reach professionals and scientists working on related research, print, and broadcast news media; the scientific community at large; stakeholders (e.g., policy and decision-makers, fishers, oil and gas industry representatives, and the environmental community); and the public to increase awareness of the IQOE, its mission, and potential projects. Public trust and confidence in the IQOE is critical and will be advanced as these parties become convinced of the scientific integrity of the research being conducted by the program's participants and discover the utility and timeliness of the products created by this significant international research effort.

The long-term viability of the IQOE will depend on

broadly based funding from government, industry, and private sources. This funding will only come if the program achieves broadly based public support. A highly focused and vigorous outreach program to develop the credibility of IQOE activities and eventually inform stakeholders and the public of the program's achievements will play a fundamental role in building this support and ensuring the program's long-term viability. To help achieve this credibility, the IQOE will work to develop a consistent image and a consistent message.

It is recommended that the program be "launched" with a suite of activities that include a scientific symposium and public lectures to engage the public, scientific community, and other stakeholders.

Central Web portal

A Web portal will provide a convenient "entry point" for the internal project participants and external community. It should reflect and highlight the state-of-the-art research by IQOE scientists. It should provide overviews and links to and from each field project. The portal should include a password-protected section for IQOE project participants, as well as openly available resources that will be useful for public purposes. Integrated social media should be considered in developing the site. Provisions will also be necessary for cataloging image, audio, and video files.

Interactive online database

An online database must be developed to allow for the cataloging, sharing, and archiving of program data. It should provide open data access for public uses. Periodic online training on how to use the data tools and contribute to the database will be important.

Media relations

The ongoing work of the IQOE will be brought to the attention of the international news media, and relationships between media and project representatives must be established. Resources such as "backgrounders" on important issues and new findings should be available on the central Web portal for the media, as well as audio and video material.

Highlights reports

Stakeholder and public interest can be developed through the sharing of new discoveries and research findings in well-publicized annual "highlights" reports. The release of these reports should be timed to coincide with an annual international media campaign.

Partner resources

It is essential that the IQOE gains the attention and support of public officials and other stakeholders worldwide. To help facilitate this attention and support, a suite of informational materials should be developed, which can be easily replicated, translated, and distributed by program participants. Common resources will assist project partners in communicating about the program and engaging stakeholders in their regions. These resources could include fact sheets, maps highlighting ongoing research, and reproducible graphics. It is also important that the program have a consistent "graphic identity" that is print and Web friendly. Other resources could include PowerPoint presentations, archived webinars, print materials, applications, and graphic visualizations.

Engagement of stakeholders is critical in all these processes. In fact, many data are already available, for example, as recorded in various environmental assessments, and these data should be made more widely accessible. Initiatives engaging the industry such as the International Oil and Gas Producers (OGP) Joint Industry Program and the recently formed working group on underwater sound within the Central Dredging Association (CEDA) are important first steps. In general, important roles will be played by the industry associations such as OGP and crucial international bodies such as the IMO and NATO to help us fill the knowledge gaps.

As an example of what should be possible on a larger scale, the Discovery of Sound in the Sea (DOSITS http://www.dosits.org/) program has developed a public Web site and an educational program for students and teachers from primary school through college. The Web site introduces the full range of science and issues associated with sound in the ocean. Ecological Acoustic Recorders (EARs) were developed by the Census of Coral Reefs project of the Census of Marine Life for monitoring of coral reefs, including the appraisal of coral reef biodiversity, activity of sound-producing organisms, and human activities in reef areas (Lammers et al., 2008). Sounds recorded by EARs can be heard at http://www.pifsc.noaa.gov/cred/ear_sounds.php. A variety of Web sites such as that described by André et al. (2011) aggregate real-time and archived acoustic data from a range of sites worldwide, making them available online. There are many other examples of sound from marine organisms available through the Aquatic Acoustic Archive (http://aquaticacousticarchive.com/) and DOSITS. Coordination with these kinds of established and successful outreach programs will be important for rapid ramp up of IQOE activities in these areas.

Promotion of the use of acoustics within the wider marine science community should be a further spin-off from the

IQOE. Researchers often do not use acoustics where it could actually benefit their research (and conversely their research can benefit the overarching questions being addressed by this project). These missed opportunities are largely because specialized acoustic technologies used to be complex and costly, which limited their accessibility. However, the means now exist to make cost-effective acoustic recording and data logging devices that can be readily used by other researchers without recourse to specialized technical knowledge.

7.8 Education and capacity building

An important aspect of large-scale international research projects is to help build capacity for science related to the project. In part, this is accomplished through involvement of graduate students in the work of their advisors. However, the sponsors also expect their projects to encourage the development of science capacity in developing countries. Research on sound in the ocean and its effects on marine organisms can be carried out anywhere that hydrophones could be deployed, but it will be important to provide opportunities for scientists from developing countries to participate in the IQOE and to receive training as a result of the project. SCOR and POGO conduct a great deal of capacity building through their various programs. Some specific opportunities that could relate to IQOE topics include the following:

- POGO Visiting Professorships—POGO offers the opportunity for institutions in developing countries to host scientists from other countries (developed or developing) for periods of about six months, to serve as teachers and mentors, and potentially to conduct joint research (see http://ocean-partners.org/index.php/training-and-education/pogo-visiting-professorship).
- POGO/SCOR Visiting Fellowships for Ocean Observations—POGO and SCOR cofund a program that provides an opportunity for students, technicians, postdoctoral fellows, and other early-career scientists to visit an institution in another country to learn how to deploy and operate, and analyze data from, observing systems (see http://www.ocean-partners.org/training-and-education/pogo-scor-fellowship).
- SCOR Visiting Scholars—SCOR operates a program similar to the POGO Visiting Professorship program, the major difference being that the terms of SCOR Visiting Scholars are shorter (2-8 weeks) and SCOR does not require the host and scholar to be prematched (see http://www.scor-int.org/SCOR_Visiting_Scholars.pdf).

7.9 Relationship with other organizations, programs, and activities

The IQOE is being established in the context of organizations, other projects, and observing system activities concerned with sound in the ocean and its effects on marine organisms. The IQOE will make connections with these entities by inviting individuals involved in them to serve on the SC or other IQOE groups, through workshops of the project, and through regular communication. Some particularly important relationships will include the following:

- Observing systems—This report catalogs ocean observing systems that the community believes could be important for implementation of the IQOE (see Appendix II). These include the Global Ocean Observing System (GOOS)—which is a global consortium of national, regional, and international observing systems—as well as specific systems that may or may not consider themselves part of GOOS, but which either currently include hydrophones or to which hydrophones could be added. The IQOE will also contribute, where relevant, to the "Oceans and Society: Blue Planet" program, which is the marine task within the Group on Earth Observations (GEO), an intergovernmental body dedicated to the use of Earth observations for the benefit of society.
- Industry and regulators—The major sources of human-generated sound arise from industries such as shipping, oil and gas exploration and production, energy production, and disposal of unexploded munitions. It will be important through the life of the project to keep contact with the relevant ocean industries to ensure that their needs for information are being met and to gain access to sound data from industry that could be useful for IQOE implementation. The project will work with industry groups, as appropriate. Both POGO and "Oceans and Society: Blue Planet" are creating working groups for industry engagement, and the IQOE will link to these groups as they develop. Regulators of industrial activity and environmental quality are also major potential users of IQOE results, and the project will ensure communication with such organizations.
- Scientific community—Members of the Steering Committee will provide the primary linkage to the relevant portions of the scientific community, including acousticians, marine biologists,

physical oceanographers, and others. The IQOE will present information about the IQOE and its progress at international ocean science and acoustic meetings.
- Related projects—The IQOE is being developed in the context of other research projects that are seeking to understand the global ocean and how it is changing. This is the first international project with a general focus on effects of sound in the ocean on marine life, and there are no closely related research programs on this international scale. The IQOE will coordinate with national research programs on marine mammals and sound. On the international scale, other SCOR-sponsored projects are focused on ocean biology, and projects sponsored by other organizations are interested in aspects of physical oceanography and climate. These projects will be kept informed about the IQOE.

7.10 Work streams and workshops

The IQOE will build its activities around work streams defined by the scientific requirements of this Science Plan. Establishing where synergies and dependencies lie within the program structure will be an early task for the Steering Committee, but many of these relationships will only emerge as the IQOE develops. There are, for example, strong dependencies between progress in defining soundscapes and progress in observing and modeling ocean sound.

7.11 Funding

Funding for the IQOE Open Science Meeting was provided by the Alfred P. Sloan Foundation. Two kinds of financial support will be necessary to implement the IQOE. First, support for planning and coordination will provide a basis for science activities. Support for planning and coordination will be sought from national science agencies and other national sources, industry, other foundations, and nongovernmental organizations. This funding will be used to support activities of the Steering Committee and the International Project Office, and for the activities during Phase 1 of the project. The second kind of financial support will be national and multinational funding to conduct the research, observations, and modeling described in this Science Plan. This kind of support will be sought and obtained from traditional sources and will leverage the much smaller planning and coordination support. It may be possible to obtain industry support to a greater extent than is typical for international research projects.

For the Census of Marine Life, the funding provided by nations through traditional channels for science activities was approximately 10 times the amount of funding for planning and coordination provided by the Sloan Foundation. To implement the IQOE successfully, it will be necessary for individuals to use this Science Plan and subsequent documents as a basis for proposals to their usual national and multinational (in some regions such as the EU) funding agencies. The SCOR Secretariat will provide logistic support (with help from the POGO Secretariat) to the project until it can arrange funding for staffing.

Example 1
World map of anthropogenic ocean sound

Objectives:

- Produce a map of the Earth's oceans showing total acoustic energy (over a meaningful duration, e.g. one year) from human sources.
- Create layers for the different sources: shipping, seismics, pile driving.
- The map will highlight regions characterized by high levels of sound (hot spots) and other regions that are still relatively unaffected by human-generated sound.
- The map will be made publicly available (in print and in GIS data).

Background and context:

Several studies indicate that ambient sound in the ocean has increased significantly over the past 50 years (Andrew et al., 2011; Chapman and Price, 2011; Frisk, 2012) at frequencies below 500 Hz. Sound at such low frequencies travels across ocean basins with little loss of energy. These studies attributed the increases to distant shipping. The U.S. National Oceanic and Atmospheric Administration sponsored a workshop and project to develop a regional map similar to that proposed here, but for the U.S. EEZ (NOAA, 2012). A world noise map will begin to expand our understanding of the spatial and temporal variation in sound within important ecological regions that are changing rapidly, such as the Arctic Ocean.

Approach:

1. Identify key people who will be able to produce this map.
2. Identify the types of anthropogenic sources that can and should be included in this map.
3. Identify data needs and sources.
4. Devise modeling approach.
5. Arrange peer review of both the approach and the input data (e.g., through a workshop).
6. Write software and run the model.
7. Arrange peer review of the results.
8. Write and publish report and map in a high-impact journal (*Nature* or *Science*).

A model will be used to impose a grid on the Earth's oceans. The total number of hours that each source operated within each cell needs to be extracted from the underlying databases. Source levels need to be assigned to each source. Transmission loss models will be applied (varying by acoustic zone) to populate cells with received energy. Maps of cumulative energy will be produced for each source type (shipping, seismics, pile driving) and as a cumulative total. Validation of the map with field measurements will use long-term recordings and error analysis that will consider the effects on the modeled received level as a function of source depth and receiver depth, uncertainty in source level, variability in sound speed profile, uncertainty in seafloor geoacoustics, and other relevant factors.

The layers of the map will look similar to the shipping density map by Halpern et al. (2008), illustrated in Figure 7.2. The map will be in units of energy. The transform from a shipping density map to a cumulative energy map, however, will not be linear.
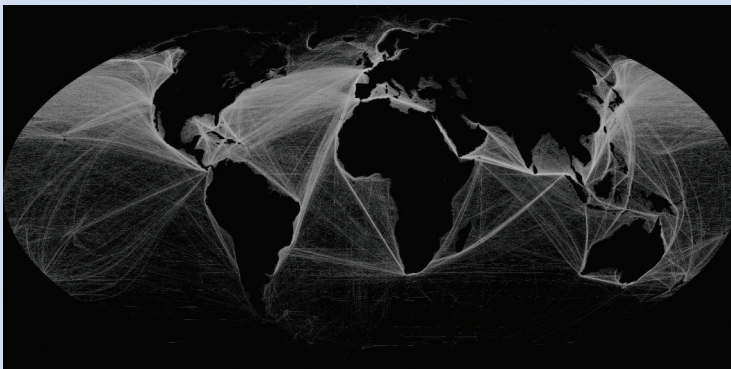
Figure 7.2. *Shipping density map. From Halpern et al. (2008). Reprinted with permission from AAAS.*

Example 2
Acoustic ecology of the Arctic Ocean: A survey along the ice edge

Objectives:
- Make recordings of ambient sound conditions in the Arctic Ocean, differentiating, when possible, anthropogenic, physical, and biological sound sources.
- Identify sounds from specific target study organisms, which may play an important role in ocean food webs. The goal here is to survey across the entire ecosystem (zooplankton-nekton), but also to target highly valued species like whales.
- Examine how the changing level of activities will change sound levels and where there is likely to be an intersection between the biology and sounds.

Background and context:

The Arctic Ocean is likely to be one of the most changed biomes as a result of climate warming. Loss of sea ice during summer and reduced ice cover in winter present opportunities for economic development that have hitherto been technologically impossible or not economically viable. In particular, the expansion of shipping traffic and the extension of oil and gas explorations and production into the Arctic Ocean are likely to be the main anthropogenic stressors. This is exemplified by the Shtokman gas field that exploits gas condensates and is estimated to be one of the world's largest natural gas deposits. These activities cause significant sound pollution (OSPAR, 2009). Considerable uncertainty exists around how these activities should be regulated in order to reduce their environmental effects.

Approach:
1. Assemble a team of acoustic and biological experts as a project steering group.
2. Determine the appropriate observation platform.
3. Conduct observations starting after the period of maximum ice extent in March, but before the minimum in September (see Figure 7.3) using a vessel transit of the NE passage back and forth close to the retreating ice edge.
4. Use dipping hydrophone arrays, towed hydrophones, bottom-mounted drifting buoys, and high-frequency scientific echosounders and profiling imaging systems.
5. Data from buoys and dipping stations will be used to quantify ambient sound levels.
6. Conduct targeted acoustic recordings of specific target species.
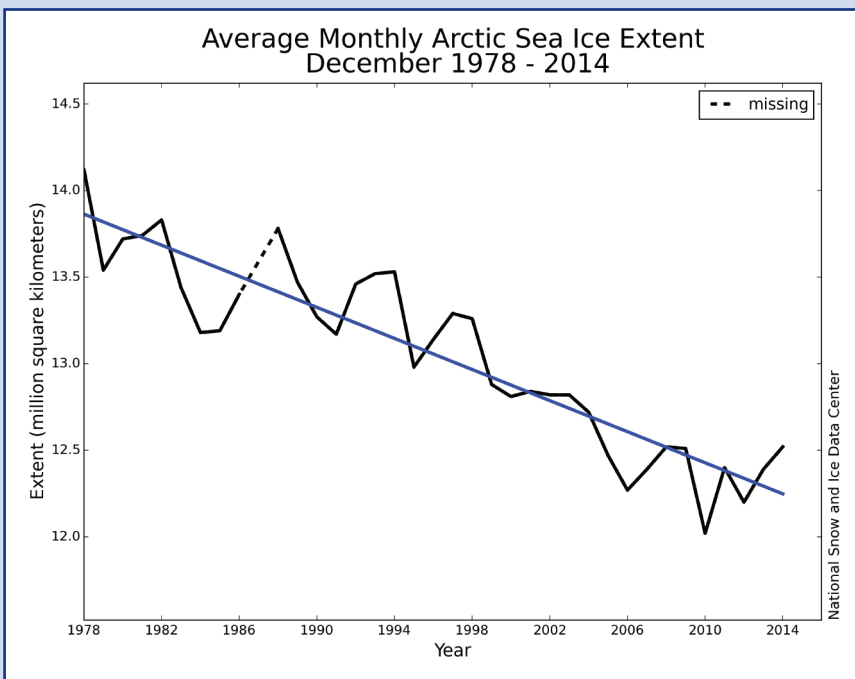
Figure 7.3. *Changes in Arctic sea ice extent over time. From U.S. National Snow and Ice Data Center, http://nsidc.org/arcticseaicenews/*

Example 3

Average ocean noise as environmental status indicator

Objectives:
- Monitor globally averaged low-frequency sound ("ocean noise").
- Identify observations to monitor key components of ocean noise budget.
- Detect changes in the key components from measured ocean noise.

Background and context:

Several studies (e.g., Andrew et al., 2011) indicate that the level of ambient sound in the ocean has increased significantly since the 1960s at frequencies below 500 Hz. The level of ocean noise is sensitive to the number and strength of the sources (mainly ships; also whales and air guns) and to propagation conditions. Monitoring the globally averaged low-frequency sound ("ocean noise") provides a useful indicator in its own right because of its possible impact on communication ranges of baleen whales (Parks et al., 2007; Stafford et al., 2007; Clark et al., 2009). It also offers the prospect of monitoring climate change through the propagation conditions (e.g., average temperature or wind speed) and changes in sources of sound (e.g., total sound power radiated by all ocean-going ships).

Approach:
1. Identify team able to monitor and interpret ocean noise collaboratively.
2. Develop instrumentation requirements.
3. Identify suitable site(s) for study.
4. Identify and gather key input data for feasibility study.
5. Model sound sources and propagation at site(s).
6. Measure sound field at site(s) and relate to key model input parameters.
7. Peer review (e.g., through a workshop) before proceeding to ocean scale.
8. Identify suitable ocean (suitable basin; suitable monitoring network).
9. Identify and gather key input data for selected ocean basin.
10. Model sound sources and propagation in ocean basin (see also Example 1, "World map of anthropogenic ocean sound").
11. Identify and bridge critical gaps in hydrophone network.
12. Measure sound field in ocean basin and relate to key input parameters.
13. Assess feasibility for detecting changes in key parameters.
14. Write and publish results in a peer-reviewed journal.

Feasibility study: The purpose of the feasibility study is to mitigate the risk of an ocean-scale experiment by identifying and testing the methods in advance. An important aspect of the feasibility study is understanding how the geometry and frequency would scale up to a larger (ocean-scale) experiment.

Ocean basin study: After a progress review, monitor sound on an ocean scale. The choice of a suitable ocean depends on having a hydrophone network with wide coverage, for which best use will be made of existing CTBTO stations, Station ALOHA http://aco-ssds.soest.hawaii.edu/ALOHA/, and The PerenniAL Acoustic Observatory in the Antarctic Ocean (PALAOA) http://www.awi.de/en/news/background/palaoa_what_does_the_southern_ocean_sound_like/, as well as newly installed stations (EU Member States are required to monitor trends in low-frequency underwater noise from 2014). Additional hydrophone stations might be needed. To provide an indication of any trend, ocean noise will be monitored for a period of several years. The first result is the ocean noise itself, a possible proxy for global economic activity (Frisk, 2012). Because propagation conditions also depend on parameters related to climate change (e.g., sea surface temperature, pH), the possibility also exists of monitoring climate change through changes in the ocean noise (see Figure 7.4).
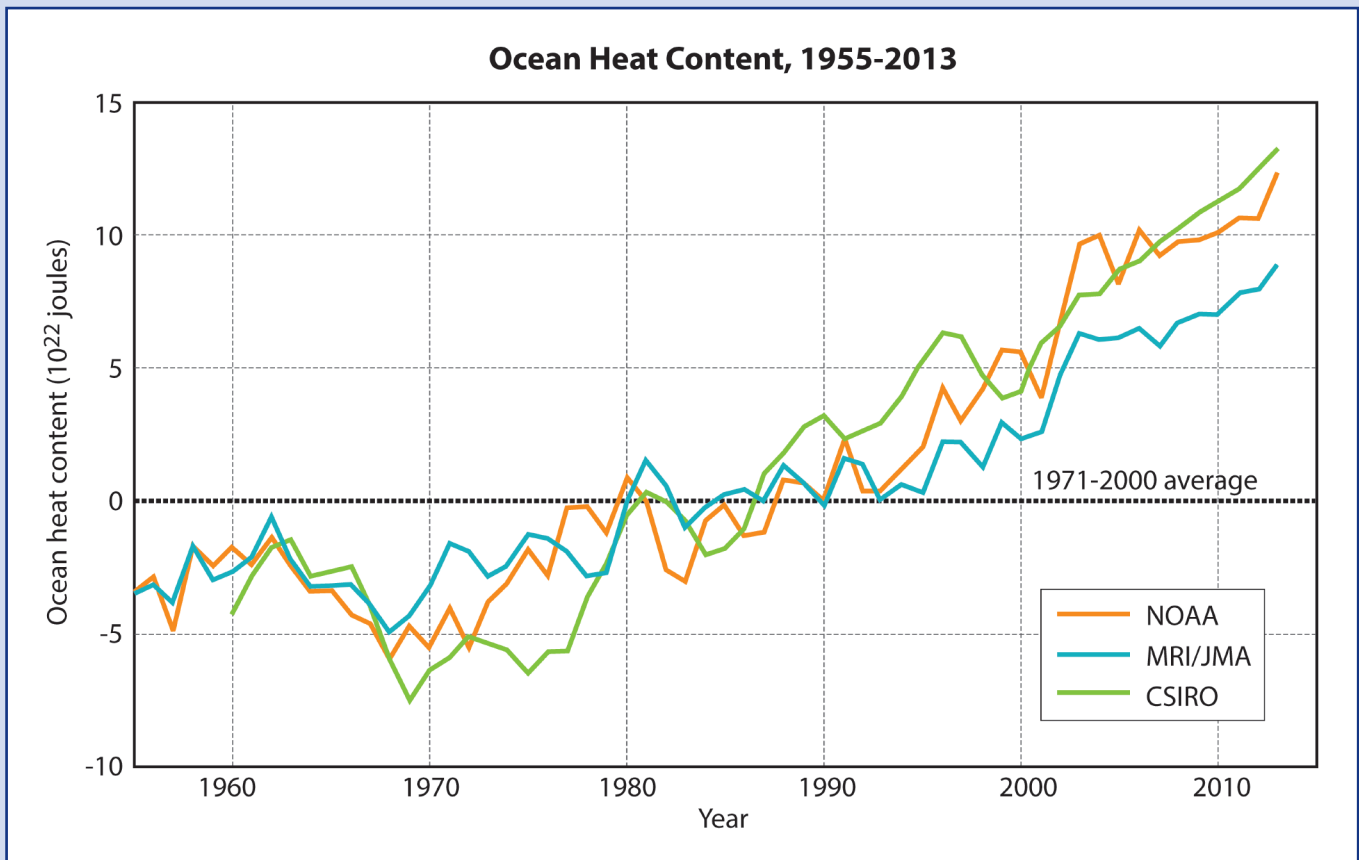
Figure 7.4. *Change in ocean heat content, 1960-2010. From*
http://www.epa.gov/climatechange/science/indicators/oceans/ocean-heat.html

Ainslie, M.A. 2012. Potential causes of increasing low frequency ocean noise levels. *Journal of the Acoustical Society of America* 129: 2497-2497.

Ainslie, M.A. Ainslie, M.A., C.A.F. de Jong, and J. Dreschler. 2011. Effects of bladdered fish on ambient noise measurements close to the Port of Rotterdam. Pages 723-730 in *Proceedings 4th International Conference and Exhibition on Underwater Acoustic Measurements: Technologies and Results*. 20-24 June 2011, Kos, Greece.

Ainslie, M.A., C.A.F. de Jong, H.S. Dol, G. Blacquière, and C. Marasini, C. 2009. Assessment of natural and anthropogenic sound sources and acoustic propagation in the North Sea, TNO-report C085, pp., available from [http://www.noordzeeloket.nl/ overig/bibliotheek.asp (Nota's en rapporten)]

Ainslie, M.A., and R. Dekeling. 2011. The environmental cost of marine sound sources. Pp. 703-710 in *Proceedings 4th International Conference and Exhibition on Underwater Acoustic Measurements: Technologies and Results*. 20-24 June 2011, Kos, Greece.

André, M., M. van der Schaar, S. Zaugg, L. Houégnigan, A.M. Sánchez, and J.V. Castell. 2011. Listening to the deep: live monitoring of ocean noise and cetacean acoustic signals. *Marine Pollution Bulletin* 63:18-26.

Andrew, R.K., B.M. Howe, and J.A. Mercer. 2011. Long-time trends in ship traffic noise for four sites off the North American West Coast. *Journal of the Acoustical Society of America* 129(2):642-651.

Andrew, R.K., B.M. Howe, J.A. Mercer, and M.A. Dzieciuch. 2002. Ocean ambient sound: Comparing the 1960s with the 1990s for a receiver off the California coast. *Acoustic Research Letters Online* 3:65-70.

Au, W.W.L., D.A. Carder, R.H. Penner, and B.L. Scronce. 1985. Demonstration of adaptation in beluga whale echolocation signals. *Journal of the Acoustical Society of America* 77:726-730.

Ausubel, J. 2009. Rethinking sound and light. *Seed*: November 23, 2009. http://seedmagazine.com/ content/article/rethinking_light_and_sound/.

Bakun, A., and S.J. Weeks. 2006. Adverse feedback sequences in exploited marine systems: Are deliberate interruptive actions warranted? *Fish and Fisheries* 7:316-333.

Boebel, O., M. Breitzke, E. Burkhardt, and H. Bornemann. 2009. Strategic assessment of the risk posed to marine mammals by the use of airguns in the Antarctic Treaty area, Information Paper IP 51, Agenda Item: CEP 8c, Antarctic Treaty Consultative Meeting XXXII, Baltimore, USA. hdl:10013/epic.32056. http://epic.awi.de/20201/1/Boe2009c.pdf

Boyd, I.L., R. Brownell, D. Cato, C. Clark, D. Costa, P. Evans, J. Gedamke, R. Gentry, R. Gisiner, J. Gordon, P. Jepson, P. Miller, L. Rendell, M. Tasker, P. Tyack, E. Vos, H. Whitehead, D. Wartzok, and W. Zimmer. 2008. The effects of anthropogenic sound on marine mammals -- A draft research strategy. European Science Foundation Marine Board Position Paper 13, June 2008, www.esf.org/marineboard.

Boyd, I.L., D.E. Claridge, C.W. Clark, B.L. Southall, and P.L. Tyack. 2007. Behavioral Response Study Cruise Report (BRS-2007). http://www.sea-inc.net/resources/brs_08_finalcruisereport.pdf.

Boyd, I., G. Frisk, E. Urban, P. Tyack, J. Ausubel, S. Seeyave, D. Cato, B. Southall, M. Weise, R. Andrew, T. Akamatsu, R. Dekeling, C. Erbe, D. Farmer, R. Gentry, T. Gross, A. Hawkins, F. Li, K. Metcalf, J.H. Miller, D. Moretti, C. Rodrigo, and T. Shinke. 2011. An International Quiet Ocean Experiment. *Oceanography* 24(2):174–181. doi:10.5670/oceanog.2011.37.

Brewer, P.G., and K. Hester. 2009. Ocean acidification and the increasing transparency of the ocean to low-frequency sound. *Oceanography* 22:86-93.

Bucker, H. 1994. A simple 3-D Gaussian beam sound propagation model for shallow water. *Journal of the Acoustical Society of America* 95:2437-2440.

Buckingham, M.J., B.V. Berkhout, and S.A.L. Glegg. 1992. Imaging the ocean with ambient sound. *Nature* 356:327-329.

Budelmann, B. 1992. Hearing in nonarthropod invertebrates. Pp. 141–155 in *The Evolutionary Biology of Hearing,* D.B. Webster, R.R. Fay and A.N. Popper (eds.), Springer Verlag, New York.

Burtenshaw, J.C., E.M. Oleson, J.A. Hildebrand, M.A. McDonald, R.K. Andrew, B.M. Howe, and J.A. Mercer. 2004. Acoustic and satellite remote sensing of blue whale seasonality and habitat in the northeast Pacific. *Deep-Sea Research II* 51:967-986.

Carey, W.M., and R.B. Evans. 2011. *Ocean Ambient Noise.* The Underwater Acoustics Series, Springer. 263 pp.

Castellote, M., T.A. Mooney, L. Quakenbush, R. Hobbs, C. Goertz, and E. Gaglione. 2014. Baseline hearing abilities and variability in wild beluga whales (*Delphinapterus leucas*). *The Journal of Experimental Biology* 217:1682-1691. doi:10.1242/jeb.093252.

Cato, D.H. 1997. Ambient sea sound in Australian waters. Pp. 2813-2818 in. *Proc. Fifth International Congress on Sound and Vibration*, Adelaide, Casual Productions, Adelaide, Vol. 5.

Cato, D.H. 2008. Ocean ambient sound: Its measurement and its significance to marine animals. *Proc. Institute of Acoustics* 30 (5).

Chapman, C.J., and A.D. Hawkins. 1973. A field study of hearing in the cod, *Gadus morhua L. Journal of Comparative Physiology* 85:147-167.

Chapman, N.R., and A. Price. 2011. Low frequency deep ocean ambient noise trend in the Northeast Pacific Ocean. *Journal of the Acoustical Society of America* 129(5):EL161-EL165.

Clark, C.W., W.T. Ellison, B.L. Southall, L. Hatch, S.M. Van Parijs, A. Frankel, and D. Ponirakis. 2009. Acoustic masking in marine ecosystems: Intuitions, analysis, and implication. *Marine Ecology Progress Series* 395:201-222.

Cotter, A.J.R. 2008. The "soundscape" of the sea, underwater navigation, and why we should be listening more. Pp 451-471 in *Advances in Fisheries Science: 50 Years on From Beverton and Holt*. A. Payne, J. Cotter, and T. Potter (eds.), Blackwell, Oxford. doi: 10.1002/9781444302653.ch19.

Cox, T.M., T.J. Ragen, A.J. Read, E. Vos, R.W. Baird, K. Balcomb, J. Barlow, J. Caldwell, T. Cranford, L. Crum, A. D'Amico, G. D'Spain, A. Fernández, J. Finneran, R. Gentry, W. Gerth, F. Gulland, J. Hildebrand, D. Houser, T. Hullar, P.D. Jepson, D. Ketten, C.D. Macleod, P. Miller, S. Moore, D.C. Mountain, D. Palka, P. Ponganis, S. Rommel, T. Rowles, B. Taylor, P. Tyack, D. Wartzok, R. Gisiner, J. Mead, and L. Benner. 2006. Understanding the impacts of anthropogenic sound on beaked whales. *Journal of Cetacean Research and Management* 7:177-187.

D'Amico, A.D., R. Gisiner, D.R. Ketten, J.A. Hammock, C. Johnson, P. Tyack, and J. Mead. 2009. Beaked whale strandings and naval exercises. *Aquatic Mammals* 35:452-472.

De Jong C.A.F., and M.A. Ainslie. 2008. Underwater radiated noise due to the piling for the offshore wind park. Acoustic 08, June 29-July 4, 2008, Paris.

Depraetere, M., D. Pavoine, F. Jiguet, A. Gasc, S. Duvail, and J. Sueur. 2012. Monitoring animal diversity using acoustic indices: Implementation in a temperate woodland, *Ecological Indicators* 13:46-54. http://dx.doi.org/10.1016/j.ecolind.2011.05.006.

DeRuiter, S.L., B.L. Southall, J. Calambokidis, W.M.X. Zimmer, D. Sadykova, E.A. Falcone, A.S. Friedlaender, J.E. Joseph, D. Moretti, G.S. Schorr, L. Thomas, and P.L. Tyack. 2013. First direct measurements of behavioural responses by Cuvier's beaked whales to mid-frequency active sonar. *Biology Letters* 9: 20130223. http://dx.doi.org/10.1098/rsbl.2013.0223.

Dumyahn, S.L., and B.C. Pijanowski. 2011. Soundscape conservation. *Landscape Ecology* 26(9):1327-1344.

Dushaw, B., W. Au, A. Beszczynska-Möller, R. Brainard, B.D. Cornuelle, T. Duda, M. Dzieciuch, A. Forbes, L. Freitag, J.-C. Gascard, A. Gavrilov, J. Gould, B. Howe, S.R. Jayne, O.M. Johannessen, J.F. Lynch, D. Martin, D. Menemenlis, P. Mikhalevsky, J.H. Miller, S.E. Moore, W.H. Munk, J. Nystuen, R.I. Odom, J. Orcutt, T. Rossby, H. Sagen, S. Sandven, J. Simmen, E. Skarsoulis, B. Southall, K. Stafford, R. Stephen, K.J. Vigness Raposa, S. Vinogradov, K.B. Wong, P.F. Worcester, and C. Wunsch. 2010. A Global Ocean Acoustic Observing Network in *Proceedings of OceanObs'09: Sustained Ocean Observations and Information for Society* (Vol. 2), Venice, Italy, 21-25 September 2009, J. Hall, D.E. Harrison, and D. Stammer, Eds., ESA Publication WPP-306. doi:10.5270/OceanObs09.cwp.25.

Ellison, W.T., B.L. Southall, C.W. Clark, and A.S. Frankel. 2012. A new context-based approach to assess marine mammal behavioral responses to anthropogenic sounds. *Conservation Biology* 26(1):21-28.

Erbe, C., C. McPherson, and A. Craven. 2011. Acoustic Investigation of Bycatch Mitigation Pingers. JASCO Applied Sciences report to the Australian Marine Mammal Centre, Kingston, Australia. 89 pp.

Fay, R.R. 1969. Behavioural audiogram for the goldfish. *Journal of Auditory Research* 9:112-121.

Fay, R.R., and A.N. Popper. 2000. Evolution of hearing in vertebrates: the inner ears and processing. *Hearing Research* 149:1-10.

Filadelfo, R., J. Mintz, E. Michlovich, A.D. D'Amico, P. Tyack, and D.R. Ketten. 2009. Correlating military sonar use with beaked whale mass strandings: what do these historical data show? *Aquatic Mammals* 35:435-444.

Foote, A.D., R.W. Asborne, and A.R. Hoelzel. 2004. Whale-call response to masking boat sound. *Nature* 428:910.

Frisk, G.V. 1994. *Ocean and Seabed Acoustics: A Theory of Wave Propagation*. Prentice-Hall (Englewood Cliffs, NJ). 299 pp.

Frisk, G.V. 2012. Noiseonomics: The relationship between ambient noise levels in the sea and global economic trends. *Nature Scientific Reports 2*, Article number 437. doi:10.1038/srep00437.

Gervaise, C., S. Vallez, C. Ioana, Y. Stephan, and Y. Simard. 2007. Passive acoustic tomography: New concepts and applications using marine mammals: A review. *Journal of the Marine Biological Association of the United Kingdom* 87:5-10.

Gillespie, A. 2007. The precautionary principle in the 21st century: A case study of sound pollution in the oceans. *The International Journal of Marine and Coastal Law* 22:61-87.

Gillespie, D., M. Caillat, J. Gordon, and P. White. 2013. Automatic detection and classification of odontocete whistles. *J. Acoust. Soc. Am*. 134:2427. http://dx.doi.org/10.1121/1.4816555

Goldbogen, J.A., B.L. Southall, S.L. DeRuiter, J. Calambokidis, A.S. Friedlaender, E.L. Hazen, E.A. Falcone, G.S. Schorr, A. Douglas, D.J. Moretti, C. Kyburg, M.F. McKenna, and P.L. Tyack. 2013. Blue whales respond to simulated mid-frequency military sonar. *Proceedings of the Royal Society B* 280:20130657. http://dx.doi.org/10.1098/rspb.2013.0657.

Götz, T., and V.M. Janik. 2011. Repeated elicitation of the acoustic startle reflex leads to sensitisation in subsequent avoidance behaviour and induces fear conditioning. *BMC Neuroscience* 12:30 http://www.biomedcentral.com/1471-2202/12/30.

Grist, J.P., S.A. Josey, L. Boehme, M.P. Meredith, F.J.M. Davidson, G.B. Stenson, and M.O. Hammill. 2011. Temperature signature of high latitude Atlantic boundary currents revealed by marine mammal-borne sensor and Argo data. *Geophysical Research Letters* 38:L15601. doi:10.1029/2011GL048204.

Gunn, J., A. Rogers, and E. Urban. 2010. Observation of Ocean Biology on a Global Scale: Implementing Bio-GOOS in *Proceedings of OceanObs'09: Sustained Ocean Observations and Information for Society (Vol. 1)*, Venice, Italy, 21-25 September 2009, J. Hall, D.E. Harrison, and D. Stammer, Eds., ESA Publication WPP-306. doi:10.5270/OceanObs09.pp.20.

Halpern, B.S., S. Walbridge, K.A. Selkoe, C.V. Kappel, F. Micheli, C. D'Agrosa J.F. Bruno, K.S. Casey, C. Ebert, H.E. Fox, R. Fujita, D. Heinemann, H.S.

Lenihan, E.M.P. Madin, M.T. Perry, E.R. Selig, M. Spalding, R. Steneck, and R. Watson. 2008. A global map of human impact on marine ecosystems. *Science* 319:948-952.

Hatch, L., C. Clark, R. Merrick, S. Van Parijs, D. Ponirakis, K. Schwehr, M. Thompson, and D. Wiley. 2008. Characterizing the relative contributions of large vessels to total ocean noise fields: a case study using the Gerry E. Studds Stellwagen Bank National Marine Sanctuary. *Environmental Management* 42:735-752.

Hatch, L.T., and K.M. Fristrup. 2009. No barrier at the boundaries: Implementing regional frameworks for noise management in protected natural areas. *Marine Ecology Progress Series* 395:223-244.

Hester, K.C., E.T. Peltzer, and P.G. Brewer. 2008. Unanticipated consequences of ocean acidification: A noisier ocean at lower pH. *Geophysical Research Letters* 35:L19601.

Hildebrand, J.A. 2009. Anthropogenic and natural sources of ambient sound in the ocean. *Marine Ecology Progress Series* 395:5-20.

Holt, M.M., D.P. Noren, V. Veirs, C.K. Emmonds, and S. Veirs. 2008. Speaking up: Killer whales (*Orcinus orca*) increase their call amplitude in response to vessel sound. *Journal of the Acoustical Society of America Express Letters* 125:EL27-EL32.

Ilyina, T., R.E. Zeebe, and P.G. Brewer. 2009. Future ocean increasingly transparent to low-frequency sound owing to carbon dioxide emissions. *Nature Geoscience* 3:18–22. doi:10.1038/ngeo719.

Johnson, C.S. 1967. Sound detection thresholds in marine mammals. In W.N. Tavolga (ed.), *Marine Bio-acoustics*, vol. 2. Pergamon, Oxford, U.K.

Johnson, K.S., W.M. Berelson, E.S. Boss, Z. Chase, H. Claustre, S.R. Emerson, N. Gruber, A. Kortzinger, M.J. Perry, and S.C. Riser. 2009. Observing biogeochemical cycles at global scales with profiling floats and gliders: Prospects for a global array. *Oceanography* 22:216-225.

Johnson, M., and P.L. Tyack. 2003. A digital acoustic recording tag for measuring the response of wild marine mammals to sound. *IEEE Journal of Oceanic Engineering* 28:3-12.

Joseph, J.E., and C.-S. Chiu. 2010. A computational assessment of the sensitivity of ambient noise level to ocean acidification. *Journal of the Acoustical Society of America* 128:EL144-EL149.

Kastak, D., and R.J. Schusterman. 1995. Aerial and underwater hearing thresholds for 100 Hz pure tones in two pinniped species. In: *Sensory Systems of Aquatic Mammals*, R.A. Kastelein et al. (eds.). De Spil Publ., Woerden, Netherlands.

Kastak, D., and R.J. Schusterman. 1998. Low-frequency amphibious hearing in pinnipeds: Methods, measurements, noise and ecology. *Journal of the Acoustical Society of Americ*a 103(4):2216-2228.

Kastelein, R.A., P. Bunskoek, M. Hagedoorn, W.L.W. Au, and D. de Haan. 2002. Audiogram of a harbor porpoise (*Phocoena phocoena*) measured with narrow-band frequency-modulated signals. *Journal of the Acoustical Society of America* 112(1):334-344.

Keeling, C.D. 1960. The concentration and isotopic abundances of carbon dioxide in the atmosphere. *Tellus* 12:200-203.

Ketten, D.R. 2010. Underwater ears and potential impacts: How to see what whales can hear. *Israel Journal of Ecology and Evolution* 56:87.

Kite-Powell, H.L. 2009. Economic Considerations in the Design of Ocean Observing Systems. *Oceanography* 22:44-49.

Knutson, T.R., J.L. McBride, J. Chan, K. Emanuel, G. Holland, C. Landsea, I. Held, J.P. Kossin, A.K. Srivastava, and Masato Sugi. 2010. Tropical cyclones and climate change. *Nature Geoscience* 3:157-163.

Kroodsma, D.E. 1989. Suggested experimental designs for song playbacks. *Animal Behaviour* 37:600–609.

Kroodsma, D.E. 1990. Using appropriate experimental designs for intended hypotheses in song playbacks, with examples for testing effects of song repertoire sizes. *Animal Behaviour* 40:1138–1150.

Kroodsma, D.E., B.E. Byers, E. Goodale, S. Johnson, and W.-C. Liu. 2001. Pseudoreplication in playback experiments, revisited a decade later. *Animal Behaviour* 61:1029–1033.

Lammers, M.O., R.E. Brainard, W.W.L. Au, T.A. Mooney, and K.B. Wong. 2008. An ecological acoustic recorder (EAR) for long-term monitoring of biological and anthropogenic sounds on coral reefs and other habitats. *Journal of the Acoustical Society of America* 123(3). doi: 10.1121/1.2836780.

Lengagne, T. 2008. Traffic sound affects communication behaviour in a breeding anuran, *Hyla arborea. Biological Conservation* 141:2023-2031. doi: 10.1016/j.biocon.2008.05.017.

Lombard, E. 1911. Le signe de le elevation de la voix. Ann. *Malad.I'Orielle. Larynx. Nez. Pharynx* 37:101-119.

Makris, N.C., P. Ratilal, D. Symonds, S. Jagannathan, S. Lee, and R. Nero. 2006. Fish population and behavior revealed by instantaneous continental-shelf-scale imaging. *Science* 311:660-663.

Mann, D.A., D.M. Higgs, W.N. Tavolga, M.J. Souza, and A.N. Popper. 2001. Ultrasound detection by clupeiform fishes. *The Journal of the Acoustical Society of America* 109(6):3048-3054.

Mann, D.A., Z. Lu, and A.N. Popper. 1997. A clupeid fish can detect ultrasound. *Nature* 48:341.

Marine Strategy Framework Directive (MSFD); Task Group 11 Report: Underwater sound and other forms of energy, April 2010, M.L. Tasker, M. Amundin, M. Andre, A. Hawkins, W. Lang, T. Merck, A. Scholik-Schlomer, J. Teilmann, F. Thomsen, S. Werner and M. Zakharia. Publications Office of the European Union. http://publications.jrc.ec.europa.eu/repository/handle/JRC58105.

Marques, T.A., L. Thomas, S. Martin, D. Mellinger, J. Ward, P. Tyack, and D. Moretti. 2012. Estimating animal population density using passive acoustics. *Biological Reviews*. doi: 10.1111/brv.12001.

Marques, T.A., L. Thomas, J. Ward, N. DiMarzio, and P.L. Tyack. 2009. Estimating cetacean population density using fixed passive acoustic sensors: An example with Blainville's beaked whales. *Journal of the Acoustical Society of America* 125:1982-1994.

McDonald, M.A., J.A. Hildebrand, S.M. Wiggins, and D. Ross. 2008. A 50 Year comparison of ambient ocean sound near San Clemente Island: A bathymetrically complex coastal region off Southern California. *Journal of the Acoustical Society of America* 124:1985-1992.

McGregor, P.K. 1992. *Playback and Studies of Animal Communication.* New York: Plenum Press.

McGregor, P.K. 2000. Playback experiments: design and analysis. *Acta Ethologica* 3:3-8.

McKenna, M.F., S.L. Katz, S.M. Wiggins, D. Ross, and J.A. Hildebrand. 2012. A quieting ocean: Unintended consequence of a fluctuating economy. *Journal of the Acoustical Society of America* 132(3):EL169-EL175.

Mellinger, D.K., and C.W. Clark. 2006. MobySound: A reference archive for studying automatic recognition of marine mammal sounds. *Applied Acoustics* 67(11):1226-1242.

Mellinger, D.K., K.M. Stafford, S.E. Moore, R.P. Dziak, and H. Matsumoto. 2007. An overview of fixed passive acoustic observation methods for cetaceans. *Oceanography* 20:36-45.

Miller, P., R. Antunes, P. Wensveen, F.I.P. Samarra, A.C. Alves, P.L. Tyack, P. Kvadsheim, L. Kleivane, F.P. Lam, M. Ainslie, and L. Thomas. 2014. Dose–response relationships for avoidance of sonar by free-ranging killer whales (*Orcinus orca*). *Journal of the Acoustical Society of America* 135: 975–993.

Miller, P.J.O., N. Biassoni, A. Samuels, and P.L. Tyack. 2000. Whale songs lengthen in response to sonar. *Nature* 405:903.

Miller, P.J.O, M.P. Johnson, P.T. Madsen, N. Biassoni, M.E. Quero, and P.L. Tyack. 2009. Using at-sea

experiments to study the effects of airguns on the foraging behavior of sperm whales in the Gulf of Mexico. *Deep-Sea Research* 56:1168-1181.

Møhl, B. 1968. Auditory sensitivity of the common seal in air and water. *Journal of Auditory Research* 8:27-38.

Montgomery, J.C., A. Jeffs, S.D. Simpson, M. Meekan, and C. Tindle. 2006. Sound as an orientation cue for the pelagic larvae of reef fishes and decapod crustaceans. *Advances in Marine Biology* 51:143-196. doi:10.1016/S0065-2881(06)51003-X.

Moretti, D., L. Thomas, T. Marques, J. Harwood, A. Dilley, B. Neales, J. Shaffer, E. McCarthy, L. New, S. Jarvis, and R. Morrissey. 2014. A Risk Function for Behavioral Disruption of Blainville's Beaked Whales (*Mesoplodon densirostris*) from Mid-Frequency Active Sonar. *PLoS One* 9(1): e85064. doi:10.1371/journal.pone.0085064.

Nachtigall, P.E., T.A. Mooney, K.A. Taylor, and M.M.L. Yuen. 2007. Hearing and auditory evoked potential methods applied to odontocete cetaceans. *Aquatic Mammals* 33:6-13.

Nachtigall, P.E., M.M.L. Yuen, T.A. Mooney, and K.A. Taylor. 2005. Hearing measurements from a stranded infant Risso's dolphin, *Grampus griseus*. *Journal of Experimental Biology* 208:4181-4188.

NRC (National Research Council). 2000. *Low-Frequency Sound and Marine Mammals: Progress Since 1994*. National Academy Press, Washington, D.C.

NRC. 2003. *Ocean Sound and Marine Mammals*. National Academy Press, Washington, D.C.

NRC. 2005. *Marine Mammal Populations and Ocean Sound: Determining When Sound Causes Biologically Significant Effects*. National Academy Press, Washington, D.C.

Nicholls, K.W., E.P. Abrahamsen, K.J. Heywood, K. Stansfield, and S. Osterhus. 2008. High-latitude oceanography using the Autosub autonomous underwater vehicle. *Limnology and Oceanography* 53:2309-2320.

NOAA (National Oceanic and Atmospheric Administration). 2005. Regulations governing the taking and importing of marine mammals. Subchapter C: Marine Mammal Protection Act regulations (50 CFR 216).

NOAA. 2012. Mapping Cetaceans and Sound: Modern Tools for Ocean Management. Final Symposium Report of a Technical Workshop held May 23-24 in Washington, D.C. 83 pp. <available online at: http://cetsound.noaa.gov>

Nystuen, J.A., E. Amitai, E.N. Anagnostou, and M.N. Anagnostou. 2008. Spatial averaging of oceanic rainfall variability using underwater sound: Ionian sea rainfall experiment 2004. *Journal of the Acoustical Society of America* 123:1952-1962 doi: 10.1121/1.2871485.

Nystuen, J.A., S.E. Moore, and P.J. Stabeno. 2010. A sound budget for the southeastern Bering Sea: Measuring wind, rainfall, shipping, and other sources of underwater sound. *Journal of the Acoustical Society of America* 128:58-65. doi: 10.1121/1.3436547.

OSPAR. 2009. Overview of the impacts of anthropogenic underwater sound in the marine environment. OSPAR Commission, 2009. Publication number 441/2009.

Parks, S.E., C. Clark, and P.L. Tyack. 2007. Short and long-term changes in right whale calling behavior: The potential effects of noise on acoustic communication. *Journal of Acoustical Society of America* 122:3725-3731.

Parks, S.E., M. Johnson, D. Nowacek, and P.L. Tyack. 2010. Individual right whales call louder in increased environmental sound. *Biology Letters* 7:33-35. doi:10.1098/rsbl.2010.0451.

Parks, S.E., J.L. Miksis-Olds, and S.L. Denes. 2013. Assessing marine ecosystem acoustic diversity across ocean basins. *Ecological Informatics*. doi: 10.1016/j.ecoinf.2013.11.003.

Pijanowski, B.C., L.J. Villanueva-Rivera, S.L. Dumyahn, A. Farina, B.L. Krause, B.M. Napoletano, S.H. Gage, and N. Pieretti. 2011. Soundscape ecology: The science of sound in the landscape. *BioScience* 61:203-216.

Popper, A.N., and R.R. Fay. 2011. Rethinking sound detection by fishes. *Hearing Research* 273:25-36.

Popper A.N., and M.C. Hastings. 2009. The effect of anthropogenic sound on fishes. *Journal of Fish Biology* 75:455-489.

Prior, M.K., D.J. Brown, G. Haralabus, and J. Stanley. 2012. Long-term monitoring of ambient noise at CTBTO hydrophone stations. Pp. 1018-1025 in *Proceedings of the 11th European Conference on Underwater Acoustics*. Volume 2. Institute of Acoustics, St. Albans Hertfordshire, United Kingdom.

Radford, C.A., J.A. Stanley, S.D. Simpson, and A.G. Jeffs. 2011. Juvenile coral reef fish use sound to locate habitats. *Coral Reefs* 30:295-305.

Reeder, D.B., E. Sheffield, and S.M. Mach. 2011. Wind-generated ambient noise in a topographically isolated basin: A pre-industrial era proxy. *Journal of the Acoustical Society of America* 129:64-73.

Ridgway, S.H., D.A. Carder, T. Kamolnick, R.R. Smith, C.E. Schlundt, and W.R. Elsberry. 2001. Hearing and whistling in the deep sea: Depth influences whistle spectra but does not attenuate hearing by

white whales (*Delphinapterus leucas*) (Odontoceti, Cetacea). *Journal of Experimental Biology* 204:3829-3841.

Roemmich, D., G.C. Johnson, S. Riser, R. Davis, J. Gilson, W.B. Owens, S.L. Garzoli, C. Schmid, and M. Ignaszewski. 2009. The Argo Program Observing the Global Ocean with Profiling Floats. *Oceanography* 22:34-43.

Rolland, R.M., S. Parks, K. Hunt, M. Castolette, P.J. Corkeron, D.P. Nowacek, S.K. Wasser, and S.D. Kraus. 2012. Evidence that ship noise increases stress in right whales. *Proceedings of the Royal Society, B*. doi:10.1098/rspb.2011.2429.

Ross, D.G. 2005. Ship sources of ambient noise. *Journal of Oceanic Engineering* 30:257–261.

Ruttenberg, B.I., S.L. Hamilton, S.M. Walsh, M.K. Donovan, A. Fiedlander, E. DeMartini, E. Sala, and S.A. Sandin. 2011. Predator-Induced Demographic Shifts in Coral Reef Fish Assemblages. *PLoS ONE* 6: e21062 doi: 10.1371/journal.pone.0021062.

Simpson, S.D., M. Meekan, J. Montgomery, R. McCauley, and A. Jeffs. 2005. Homeward sound. *Science* 308:221.

Simpson, S.D., J. Purser, and A.N. Radford. 2014. Anthropogenic noise compromises antipredator behavior in European eels. *Global Change Biology* 1-8. doi:10.;1111/gcb.12685.

Slabbekoorn, H., and N. Bouton. 2008. Soundscape orientation: A new field in need of sound investigation. *Animal Behaviour* 76.4:e5-e8.

Slabbekoorn, H., N. Bouton, I. van Opzeeland, A. Coers, C. ten Cate, and A.N. Popper. 2010. A noisy spring: The impact of globally rising underwater sound levels on fish. *Trends in Ecology & Evolution* 25:419-427. doi:10.1016/ j.tree.2010.04.005.

Smith, W.H.F., and D.T. Sandwell. 1997. Global seafloor topography from satellite altimetry and ship depth soundings. *Science* 277:1957-1962.

Southall, B.L., A.E. Bowles, W.T. Ellison, J.J. Finneran, R.L. Gentry, C.R. Greene, D. Kastak, D.R. Ketten, J.H. Miller, P.E. Nachtigall, W.J. Richardson, J.A. Thomas, and P.L. Tyack. 2007. Marine mammal sound exposure criteria: Initial scientific recommendations. *Aquatic Mammals* 33:411-522.

Stafford, K.M., D.K. Mellinger, S.E. Moore, and C.G. Fox. 2007. Seasonal variability and detection range modeling of baleen whale calls in the Gulf of Alaska, 1999–2002. *The Journal of the Acoustical Society of America* 122(6):3378-3390.

Sueur, J., S. Pavoine, O. Hamerlynck, and S. Duvail. 2008. Rapid acoustic survey for biodiversity appraisal. *PLoS ONE* 3, e4065.

Tasker, M.L., M. Amundin, M. Andre, A. Hawkins, W.

Lang, T. Merck, A. Scholik-Schlomer, J. Teilmann, F. Thomsen, S. Werner, and M. Zakharia. 2010. Marine Strategy Framework Directive Task Group 11 Report: Underwater noise and other forms of energy. European Commission and ICES, EUR24341 EN – 2010.

Teilmann, J., and J. Carstensen. 2012. Negative long term effects on harbor porpoises from a large scale offshore wind farm in the Baltic—evidence of slow recovery. *Environmental Research Letters 7*. doi:10.1088/1748-9326/7/4/045101.

Thurstan, R.H., and C.M. Roberts. 2010. Ecological Meltdown in the Firth of Clyde, Scotland: Two Centuries of Change in a Coastal Marine Ecosystem. *PLoS ONE* 5:e11767. doi:10.1371/journal.pone.0011767.

Tougaard, J., A.J. Wright, and P.T. Madsen. 2015. Cetacean noise criteria revisited in the light of proposed exposure limits for harbour porpoises. *Marine Pollution Bulletin* 90(1-2):196-208. doi:10.1016/j.marpolbul.2014.10.051.Epub2014 Nov. 20.

Tyack, P.L. 2008. Implications for marine mammals of large-scale changes in the marine acoustic environment. *Journal of Mammalogy* 89:549-558. doi: 10.1644/07-MAMM-S-307R.1.

Tyack, P.L., W.X.M. Zimmer, D. Moretti, B.L. Southall, D.E. Claridge, J. Durban, C.W. Clark, A. D'Amico, N. DiMarzio, S. Jarvis, E.M. McCarthy, R. Morrissey, J. Ward, and I.L. Boyd. 2011. Beaked Whales Respond to Simulated and Actual Navy Sonar. *PLoS ONE* 6(3):e17009. doi:10.1371/journal.pone.0017009.

Udovydchenkov, I.A., T.F. Duda, S.C. Doney, and I.D. Lima. 2010. Modeling deep ocean shipping noise in varying acidity conditions. *Journal of the Acoustical Society of America*, 128(3), EL130-EL136.

Van der Graaf, A.J., M.A. Ainslie, M. André, K. Brensing, J. Dalen, R.P.A. Dekeling, S. Robinson, M.L. Tasker, F. Thomsen, and S. Werner. 2012. European Marine Strategy Framework Directive – Good Environmental Status (MSFD GES): Report of the Technical Subgroup on Underwater noise and other forms of energy.

Van Parijs, S.M., C.W. Clark, R.S. Sousa-Lima, S.E. Parks, S. Rankin, D. Risch, and I.C. Van Opzeeland. 2009. Management and research applications of real-time and archival passive acoustic sensors over varying temporal and spatial scales. *Marine Ecology Progress Series* 395:21–36.

Wenz, G.M. 1962. Acoustic ambient noise in the ocean: Spectra and sources. *Journal of the Acoustical*

Society of America 34:1936-1956.

Wenz, G.M. 1969. Low-frequency deep-water ambient noise along the Pacific Coast of the United States. *U.S. Navy Journal of Underwater Acoustics* 19:423-444 (recently declassified).

Weston, D.E., and P.A. Ching. 1989. Wind effects in shallow-water transmission. *Journal of the Acoustical Society of America* 86:1530-1545.

Wiley, R.H. 2003. Is there an ideal behavioural experiment? *Animal Behaviour* 66:585–588. doi:10.1006/anbe.2003.2231.

Williams, R., and E. Ashe. 2007. Killer whale evasive tactics vary with boat number. *Journal of Zoology* 272:390-397.

Yuen, M.M.L., P.E. Nachtigall, M. Breese, and A.Y. Supin. 2005. Behavioral and auditory evoked potential audiograms of a false killer whale (*Pseudorca crassidens*). *Journal of the Acoustical Society of America* 118:2688-2695.

Young, I.R., S. Zieger, and A.V. Babanin. 2011. Global trends in wind speed and wave height. *Science* 332:451-455.

Acronyms

AITP	Acoustic Ice Tethered Platforms
AUTEC	Atlantic Undersea Test and Evaluation Center
CEDA	Central Dredging Association
CEEs	controlled exposure experiments
CTBTO	Comprehensive Test Ban Treaty Organization
CTD	conductivity-temperature-depth
DMAC	data management and communication
DOSITS	Discovery of Sound in the Sea project
E&P	exploration and production
EARs	Ecological Acoustic Recorders
EIAs	Environmental Impact Assessments
ESA	Endangered Species Act (U.S.)
ESTOC	European Station for Time Series in the Ocean
FOAM	Fast Ocean Atmosphere Model
GC	glucocorticoid
GOOS	Global Ocean Observing System
HPA	hypothalamic–pituitary–adrenal
HYCOM	Hybrid Coordinate Ocean Model
IGY	International Geophysical Year
IMO	International Maritime Organization
IPO	International Project Office
IPY	International Polar Year
IQOE	International Quiet Ocean Experiment
ISO	International Organization for Standardization
IYQO	International Year of the Quiet Ocean

MEPC	Marine Environmental Protection Committee (IMO)
MMPA	Marine Mammal Protection Act (U.S.)
MSFD	Marine Strategy Framework Directive
NAVOCEANO	Naval Oceanographic Office (U.S.)
NOAA	National Oceanic and Atmospheric Administration (U.S.)
NRC	National Research Council (U.S.)
NSL	noise spectral density level
OGP-JIP	International Oil and Gas Producers-Joint Industry Program
ONR	Office of Naval Research (U.S.)
OOSs	ocean observing systems
PAM	passive acoustic monitoring
PAMBuoy	Passive Acoustic Monitoring Buoy
PCAD	Population Consequences of Acoustic Disturbance
PLOCAN	Oceanic Platform of the Canary Islands
POGO	Partnership for Observation of the Global Oceans
PSA	Particularly Sensitive Areas
PTS	permanent threshold shift
SC	Steering Committee
SCOR	Scientific Committee on Oceanic Research
SEL	sound exposure level
SOFAR	Sound Fixing and Ranging
SOSUS	Sound Surveillance System (U.S.)
SPL	sound pressure level
TTS	temporary threshold shift

Appendix I
Contributors to Science Plan

Editors
These individuals transformed the outputs from the IQOE Open Science Meeting into the Science Plan, based on experience with previous projects: Peter Tyack, George Frisk, Ian Boyd, Ed Urban, and Sophie Seeyave.

Discussion Session Participants
Most of the time at the IQOE Open Science Meeting was devoted to discussion sessions. Each group was led by two cochairs and two rapporteurs. These groups are responsible for the good ideas and much of the text in this Science Plan. The full list of participants is given in Appendix III.

Theme 1: Doug Cato and Manell Zakharia (chairs) and Christine Erbe and Tony Hawkins (rapporteurs).
Other contributors: Michael Ainslie, Caroline Carter, Ross Chapman, Thomas Folegot, Lars Kindermann, David Mann, Jeffrey Nystuen, Michael Porter, Mark Prior, and George Shillinger.

Theme 2 (this theme was created from the outputs from two different discussion groups): Christopher Clark, Robert Gisiner, Vincent Janik and Jakob Tougaard (chairs) and Sophie Brasseur, Peter Evans, Roger Gentry, and Patrick Miller (rapporteurs).
Other contributors: Tomonari Akamatsu, Clara Amorim, Susannah Buchan, Dan Costa, Yong-Min Jiang, Darlene Ketten, Megan McKenna, Andy Radford, Steve Simpson, Peter Tyack, Michael Weise, and Rob Williams.

Theme 3: Brian Dushaw and Brandon Southall (chairs) and Rex Andrew and Jennifer Miksis-Olds (rapporteurs).
Other contributors: Michel Andre, Olaf Boebel, Del Dakin, Eric Delory, Richard Dewey, Albert Fischer, Lee Freitag, George Frisk, Tom Gross, Zygmunt Klusek, Fenghua Li, Ellen Livingston, David Moretti, Sophie Seeyave, Yvan Simard, Alexander Vedenev, Ed Urban, and Peter Worcester.

Theme 4: Frank Thomsen and John Young (chairs) and René Dekeling and Jason Gedamke (rapporteurs).
Other contributors: Hussein Alidina, Aurélien Carbonnière, David Farmer, Paul Holthus, Gail Scowcroft, Michael Stocker, Anne-Isabelle Vichot, and Dietrich Wittekind.

Others who did not attend the Open Science Meeting but contributed comments: Jesse Ausubel, Gerrit Blacquiere, Christ de Jong, and Bruce Howe.

Appendix 2
Matrix of Acoustic Capabilities of Existing Observing Systems

Table 1 *(on three pages)* presents cabled systems.

Table 2 *(on three pages)* presents fixed autonomous systems

Table 3 *(on three pages)* presents mobile autonomous systems

The following descriptions apply to the columns in the table:

Time synch/precision relates to time synchrony between elements and between the GPS time.

Data download specifies the time interval between data downloads.

Depth is the depth at which the sensors are located.

Calibration" indicates whether or not the acoustic system is calibrated.

Ancillary Data highlights other data availble or planned from the same region of the acoustic sensors.

Data Availability conveys how accessible the data are to the public.

Sponsor refers to the original and/or current sponsor providing funding support for the system.

Society Value indicates the societal purpose for which the system was originally designed

Installation & Life Expectancy reports the years of system installation and projected life expectancy of the system.

Table 1 - Cabled Systems

System	Geographical Scale	Location	Coordinates	Human Activity	Natural Activity	Projected Change	Acoustics Operational
CTBTO	basin	Wake Island					yes
		Cape Leewin					yes
		Ascension					yes
		Diego Garcia					yes
		Juan Fernandez		low			yes
		Crozet Island		low			yes
ALOHA	100 km	Hawaii					yes
NEPTUNE	100 km	Juan de Fuca British Columbia		shipping	whales, geophysical		yes
VENUS	50 km	Strait of Georgia British Columbia		shipping	whales, fish, geophysical		yes
ANTARES	50 km	Ligurian Sea	43.0846N, 5.2115E	shipping, Navy, seismic	whales, geophysical		yes
OBSEA	10 km	Northwest Mediterranean Sea	41.1819N, 1.7523E	shipping	whales, fish		yes
NEMO	25 km	East Sicily	37.3211N, 15.3625E	shipping, Navy, seismic	whales, geophysical		yes
JAMSTEC	100 km	Hatsushima, Japan	35.0031N, 139.2247E	shipping	whales		yes
	100 km	Kushiro 1, Japan	41.6870N, 144.3945E	shipping	whales		yes
	100 km	Kushiro 2, Japan	45.9408N, 145.0562E	shipping	whales		yes
	100 km	Kushiro 3, Japan	49.2528N, 144.8107E	shipping	whales		yes
	50 km	DONET					yes
OOI RSN	1000 km	Juan de Fuca Plate (Oregon/ Washington USA)		shipping, fishing, some Navy	whales, odontocetes, pinnipeds, hydrothermal vents	climate changes in animal distributions possible	yes, but limited - opportunity for expanded capabilities
SOSUS	~3000 km^2	Northeast Pacific	various	shipping	whales		yes/no
AUTEC	~1250 km^2	Bahamas		military	beaked whale, odontocetes		yes
SOCAL	~1350 km^2	Southern California		military/shipping	beaked whale, odontocetes, mysticetes		yes
PMRF	~2500 km^2	Hawaii		military/shipping	beaked whale, odontocetes, mysticetes		yes
PALAOA	100s km	Antarctica		low/none	whales, geophysical		yes
ARGOMARINE	regional	Ligurian Sea		shipping			yes
GOOS							no
IOOS							no
OOS							no
PLOCAN	coastal	Canary Islands	27.9833N 15.3667W	ocean renewable energy, shipping	beaked whale, odontocetes, mysticetes	ocean renewable energy	none planned (2012-2013)

Table 1 - Cabled Systems (continued)

System	Units (Auto) Mode (Mobile)	Frequency Bandwidth	Directionality	Time synch/ Precision	Duty Cycle	Data Downloads	# Elements	Depth	Calibrated
CTBTO		<100 Hz	H		continuous	continuous	6 (2 triads)	sound channel	yes
		<100 Hz	H		continuous	continuous	3 (1 triad)	sound channel	yes
		<100 Hz	H		continuous	continuous	6 (2 triads)	sound channel	yes
		<100 Hz	H		continuous	continuous	6 (2 triads)	sound channel	yes
		<100 Hz	H		continuous	continuous	6 (2 triads)	sound channel	yes
		<100 Hz	H		continuous	continuous	6 (2 triads)	sound channel	yes
ALOHA		broadband	omni		continuous	continuous	1	4750 m (bottom)	yes
NEPTUNE		10 Hz-50 kHz hydrophones 1 - 200 Hz seismometers 360 s - 50 Hz seismometers	omni	ms in use 10 μs capable	continuous	continuous	5 4 5	100-3000 m (bottom)	no
VENUS		10 Hz-50 kHz	H	ms	continuous	continuous	9	100-300 m (bottom)	no
ANTARES		100 Hz-125 kHz	omni	ms	continuous	continuous	36	2000 m (bottom)	yes
OBSEA		10 Hz-200 kHz	omni	ms	continuous	continuous	1	20 m	yes
NEMO		10 Hz-96 kHz	omni	ms	continuous	continuous	2 x 4	2500 m	yes
JAMSTEC		1-50 Hz	omni	ms	continuous	continuous	1	2500 m	yes
		1-50 Hz	omni	msec	continuous	continuous	1	2500 m	yes
		1-50 Hz	omni	msec	continuous	continuous	1	2500 m	yes
		1-50 Hz	omni	msec	continuous	continuous	1	2500 m	yes
OOI RSN	7 planned nodes - each with seismic sensors and broadband phones	5 Hz-1 kHz (seismic); 100 Hz-90 kHz (two overlapping broadband phones sampled 250 kHz)	omni	1s	continuous	real-time (data transmission rate 10 kB/s)	notionally 7 nodes each with multiple sensors on each	variable (4 on shelf in 500-1000 m, 1 mid-plate in >3000 m and 2 on JdF Ridge in ~3000 m	yes - broadband phones
SOSUS		10 Hz - 500 Hz	omni	1s	continuous	semi-annual	1	deep bottom, exact N/A	yes, legacy
AUTEC		~50 Hz-45 kHz	N	500 μs	continuous	continuous	91	~1200-2000 m	mixed
SOCAL		~50 Hz-45 kHz	N	501 μs	continuous	continuous	170	~1100-2500 m	mixed
PMRF		~50 Hz-45 kHz	N	502 μs	continuous	continuous	200	~150-4000 m	mixed
PALAOA		10 Hz-198 kHz	H	ms	continuous	continuous	2	200 m	yes
ARGOMARINE		10 Hz-70 kHz	tetra array		continuous	continuous	4	20 m (bottom)	yes
GOOS									
IOOS									
OOS									
PLOCAN		under definition	under definition	under definition	continuous	continuous	under definition	100m	yes

Table 1 - Cabled Systems (continued)

System	Ancillary Data	Data Available	Integration Possibility	Sponsor	Society Value	Installation Life Expectancy
CTBTO	no	approval needed	no	CTBTO	nuclear monitoring	early 2000s + decades
	no	approval needed	no	CTBTO	nuclear monitoring	early 2000s + decades
	no	approval needed	no	CTBTO	nuclear monitoring	early 2000s + decades
	no	approval needed	no	CTBTO	nuclear monitoring	early 2000s + decades
	no	approval needed	no	CTBTO	nuclear monitoring	early 2000s + decades
	no	approval needed	no	CTBTO	nuclear monitoring	early 2000s + decades
ALOHA	HOT site	open	yes	NSF	exploration	2011 + decades
NEPTUNE	CTD, ADCP, echo, cameras, chemical, BPR, fluorometer	open	yes	CFI/Canada	ecosystems, biodiversity	2009 + decades
VENUS	CTD, ADCP, echo, sediment, irradiance, fluorometer	open	yes	CFI/Canada	ecosystems, biodiversity	2006 + decades
ANTARES	telescope	upon request	yes	ANTARES collaboration	Neutrino Observatory	2000 + decades
OBSEA	CTD, video, meteorology	upon request	yes	UPC	meteorology	2009 + decades
NEMO	HOT site	upon request	no	LFN/INGV	geo-hazards	2005 + decades
JAMSTEC	seismometers	open	no	JAMSTEC	geo-hazards	2005 + decades
	seismometers	open	no	JAMSTEC	geo-hazards	2005 + decades
	seismometers	open	no	JAMSTEC	geo-hazards	2005 + decades
	seismometers	open	no	JAMSTEC	geo-hazards	2005 + decades
						2012
OOI RSN	various oceanographic and geophysical	possible once operational (2013)	yes	NSF - OOI	ecosystem monitoring, research, education	2011-12 laying cables; 2013 operational with possible additional acoustic elements later
SOSUS	no	TBD; request required	no	U.S. Navy / APL-UW	military	1950s - ???
AUTEC	SVP	screened upon request	yes	U.S. Navy		>2020
SOCAL	SVP	screened upon request	yes	U.S. Navy		>2021
PMRF	SVP	screened upon request	yes	U.S. Navy		>2022
PALAOA	CTD, video, meteorology	upon request	no	AWI	ecosystems, biodiversity	2006 + decade
ARGOMARINE	compass	NATO countries	yes	NURC	communication, security	2011 + decade
GOOS						
IOOS						
OOS						
PLOCAN						

Table 2 - Fixed Autonomous Systems

System	Geographical Scale	Location	Coordinates	Human Activity	Natural Activity	Projected Change	Acoustics Operational
HAFOS	basin	Weddell Sea		low/none	whale migration	no	yes
HARP	regional	Pacific Ocean, Atlantic Ocean, Gulf of Mexico, Gulf of Alaska, Hawaiian Islands, Chukchi Sea, etc.	30 deployments, see http://cetus,ucsd.edu/projects_Main.htm	shipping, sonar, oil & gas exploration	marine mammals fish, ice, wind, rain, eathquakes	biological and human sound sources	yes
SBNMS	regional	SBNMS		shipping	whales		yes
EARS	regional	Arctic Ligurian Sea		shipping	whales		yes
NOAA EcoFOCI	regional	Bering Sea		low	seasonal ice	climate, shipping, fishing	yes
	regional	Bering		low	seasonal ice	climate, shipping, fishing	yes
PAL	regional	Station PAPA, Pacific Ocean		low			yes
	regional	Ionian Sea		shipping	whales		yes
POI	100 km	Sakhalin Island (Russia)		oil exploration/production	whales	increased industrial activity	yes
Hydra	regional	Ligurian Sea		shipping	whales		yes
IOPAS	regional	Baltic Sea		shipping, oil platform	fish migrations		yes
		Spitsbergen Fjord		shipping	diving birds		yes
BIMET	coastal	N. Atlantic (Spain)		shipping, geophysics	whales		yes
SEAWAYS	regional	St. Lawrence Seaway	Lower St. Lawrence Estuary	shipping	whales	shipping	yes
ARCTIC-NET+	regional	Eastern Beaufort Sea Canadian Archipelago Hudson Strait, Hudson Bay		none to occasional shipping and airgun seismic	whales, Arctic marine life	climate, shipping, fishing	yes
PMEL	large scale	Pacific Ocean, Atlantic Ocean, Davis Strait			whales	climate, shipping	
DASAR	regional	Arctic Ocean	Beaufort Sea	oil & gas	whales	climate, shipping, fishing	
AURALs	regional	Arctic Ocean	Beaufort Sea, Chukchi Sea	oil & gas	whales	climate, shipping, fishing	
ESTOC-PLOCAN	regional	Central-Eastern Atlantic (ESTOC site)	29.1667N, 15.3000W	shipping, volcanic tremor	whales (migratory and permanent)		no, but planned
IMOS Perth Canyon	regional	Perth Canyon, Western Australia		shipping, seismic surveys	whales	shipping, increase from whales	yes
IMOS Portland	regional	shelf break south Portland		shipping, seismic surveys	whales, fish, ocean noise		yes
IMOS NSW Australia	regional	shelf break west Cape Howe		shipping	fish, whales	unknown	yes
IMOS Northwest WA	regional	northwest shelf, Western Australia		shipping, seismic surveys	fish, whales	unknown	yes
JASCO-AMARs	regional	Chukchi Sea	8-160 km offshore	oil & gas exploration	mysticetes, odontocetes, pinnipeds		yes
ABB (SIO RAS)	regional	Black and Baltic seas		climate, shipping, fishing			yes
AUSOMS	regional	Andaman Sea, Okinawa Island		variable	variable		yes
PAMBUOY	100 to 100s kms	Sakhalin Island variable	n/a	shipping, oil platform, shipping, sonar, pile driving, seismic	whales and other marine mammals	biological and human sound sources	yes

Table 2 - Fixed Autonomous Systems (continued)

System	Units (Auto) Mode (Mobile)	Frequency Bandwidth	Directionality	Time synch/ Precision	Duty Cycle	Data Downloads	# Elements	Depth	Calibrated
HAFOS	sonovault, AURAL, cPOD	10-5000 Hz	omni		continuous	3 years	10	850 m	no
HARP	bottom mounted, mooring, WaveGlider	10 Hz-160 kHz	omni and 4-sensor directional array	5-10 ms	continuous and programmable	4-18 months	1-4 sensors per deployment	100-1000 m	yes
SBNMS	MARU								yes
EARS		0-40 kHz	omni		up to 50%	40 days	5	850 m	yes
NOAA EcoFOCI	PAL	20 Hz-50 kHz	omni	10s s	adaptive (2-5 min)	6-12 months	2	70 m	yes
	AURAL		omni		16%	6-12 months	3-4	70 m	
PAL		20 Hz-50 kHz	omni	10s s	adaptive (2-5 min)	2 years	1	500 m	yes
		20 Hz-50 kHz	omni	10s s	adaptive (2-5 min)	6 months	1	500 m	yes
POI	AUR	2 Hz - 15 kHz	omni		continuous	weeks to months	15-20	10 & 20 m (up to 100 m)	yes
Hydra		10 Hz-70 kHz	tetra array		continuous	53 days	4	1000 m	yes
IOPAS		100 Hz-50 kHz	V, H	ms	adaptive	6 months	up to 8	150 m	yes
		100 Hz-50 kHz	V, H	ms	adaptive	6 months	up to 8	150 m	yes
BIMET		10 Hz-120 kHz	omni	ms	continuous	continuous	1	100 m	yes
SEAWAYS	AURAL + cabled/shore	1 Hz-100000 kHz	omni +H	µs to s	programmable to continuous	3 to 12 months per year	up to 10	75-300 m	yes
ARCTIC-NET+	AURALs	1Hz-16 kHz	omni	s	programmable to continuous	3 to 12 months per year	up to 8	50-250 m	yes
PMEL	PMEL autonomous hydrophone		omni H	s					
DASAR	DASAR	1-500 Hz	directional				~40	50-100 m	
AURALs	AURAL	1 Hz-16 kHz	omni		programmable		~30	50-100 m	
ESTOC-PLOCAN	under definition	under definition	under definition	under definition	under definition	6 months	under definition	sound channel	
IMOS Perth Canyon	Curtin Univ. Loggers CMST-DSTO	1 Hz - 6 kHz	omni	ms	200 to 500 s / 900 s	12 months	4	430-500 m	yes
IMOS Portland	Curtin Univ. Loggers CMST-DSTO	1 Hz - 6 kHz	omni	ms	200 to 500 s / 900 s	12 months	4	130 - 160 m	yes
IMOS NSW Australia	Curtin Univ. Loggers CMST-DSTO	1 Hz - 6 kHz	omni	ms	200-500 s / 900 s	12 months	4	150-190 m	yes
IMOS Northwest WA	Curtin Univ. Loggers CMST-DSTO	1 Hz - 6 kHz	omni	ms	200-500 s / 900 s	12 months	4 + 2	250-300m	yes
JASCO-AMARs	JASCO-AMARs	5 Hz - 8 kHz	omni & synchronised arrays	ms	continuous & 17%	every July & Oct	35 AMARs & 9 AURALs	20-50 m	yes
ABB (SIO RAS)	AURAL	1 Hz-32 kHz	omni+V	ms	programmable and continuous	3-4 months	2	6000 m	yes
AUSOMS	bottom mounted and mooring	20 Hz-22 kHz, max: 20 Hz-96 kHz	stereo	22 µs	programmable and continuous	15 days	2	60 m	
PAMBUOY		10-150 Hz	omni		continuous	continuous	1	5-50 m	yes

Table 2 - Fixed Autonomous Systems (continued)

System	Ancillary Data	Data Available	Integration Possibility	Sponsor	Society Value	Installation Life Expectancy
HAFOS	CTD, ADCP, echosounder	yes	yes	AWI	whale migration monitoring	2011 + 10 yrs
HARP SBNMS	CTD	upon request and approval		Navy, NOAA, BP	marine mammals, ecosystem, shipping	2005-2020
EARS		NATO countries	yes	NURC	MMRM	2011
NOAA EcoFOCI	CTD, ADCP, echo, chl, oxygen, nutrients	yes	yes	ONR/PMEL	ecosystems, biodiversity	2008 + 5 years
	CTD, ADCP, echo, chl, oxygen, nutrients		yes	PMEL/NMML	ecosystems, biodiversity	2008 + 5 years
PAL	meteorology, waves	yes	yes	NOAA	climate	2006 + 5 years
		yes	no	Poseidon	rainfall	2008 + 5 years
POI	SVP measurements, current measurements	very limited	no	SEIC, ExxonMobile	industry monitoring	2005 - deployed annually
Hydra	compass, tilt	NATO countries	yes	NURC	MMRM	2011
IOPAS	pressure, temperature, echo	upon request	yes	Polish national programs	exploration, weather, physical research	2005 + decade
	pressure, temperature, echo	upon request	yes	Norwegian Funds	exploration, weather, physical research	2006-2009, lost
BIMET	no	upon request	no	AZTI	MMRM	2011 + decades
SEAWAYS	hydrography, ADCPs, hydroacoustics, circulation modeling	research program	yes	DFO UQAR	shipping MPA, marine park, whale watching	2003 - + eventual permanent SEAWAYS observatory
ARCTIC-NET+	oceanographic sensors, ADCPs, hydroacoustics	research programs	yes	Arctic-Net DFO UQAR	Arctic pre-industrial background, Inuit communities, climate change, ice melting, whale monitoring	2003-2013+
PMEL		PMEL		PMEL/NMML	earthquakes, whales, ocean basin	
DASAR		oil & gas		oil & gas		2008-2009 +
AURALs		oil & gas		oil & gas		2008-2009 +
ESTOC-PLOCAN	ESTOC station suite of instruments: including current, wind, salinity, CTD profiles, chl, oxygen, nutrients	data policy under definition	in progress	Spain Ministry of Science and Innovation and Canary Islands govt	exploration, weather, physical research	1995 until 2025
IMOS Perth Canyon	temperature	IMOS		Australian govt	various	2008-2013
IMOS Portland	temperature	IMOS		Australian govt	various	2009-2013
IMOS NSW Australia	temperature	IMOS		Australian govt	various	2010-2013
IMOS Northwest WA	temperature & nearby oceanography	IMOS		Western Australian govt	various	2012-2014
JASCO-AMARs	temperature	request approval	yes	Shell, Conoco Phillips, Statoil	marine mammal migration, distribution, density; baseline ambient noise	2006-2016
ABB (SIO RAS)		upon request	yes	Russian Academy of Science	exploration, weather, physical research	2003 + decade
AUSOMS						

Table 3 - Mobile Autonomous Systems

System	Geographical Scale	Location	Coordinates	Human Activity	Natural Activity	Projected Change	Acoustics Operational
WaveGlider HARP	regional	Pacific Ocean, Atlantic Ocean, Gulf of Mexico, Gulf of Alaska, Hawaiian Islands, Chuckchi Sea, etc.	30 existing deployments	shipping, sonar, oil & gas exploration	marine mammals, fish, ice, wind, rain, earthquakes	biological and human sources	yes
Argo	basin	global		variable	variable		no
AQARIUS	basin	global		variable	variable		yes
SPURS	basin	North Atlantic Ocean		variable	variable		yes
CPAM	local	Ligurian Sea		shipping	whales		yes
NURC-Gliders	regional	Ligurian Sea		shipping	whales		yes
PLOCAN-Gliders	basin	global		shipping, volcanic tremor	whales		no, but planned

System	Units (Auto) Mode (Mobile)	Frequency Bandwidth	Directionality	Time synch/ Precision	Duty Cycle	Data Downloads	# Elements	Depth	Calibrated
HARP	WaveGlider	10 Hz-160 kHz	omni and 4-sensor directional array	5-10 ms	continuous and programmable	4-18 months	1-4 sensors per deployment	100-1000 m	yes
Argo	drifting								
AQARIUS	drifting, Argo-like	50 kHz	omni	ms	adaptive	7-10 days	45	1000 m	yes
SPURS	drifting, Argo-like	50 kHz	omni	ms	adaptive	7-10 days	25	1000 m	yes
CPAM	towed	20 Hz-80 kHz			continuous	continuous	6	150 m	yes
NURC-Gliders	gliding								
PLOCAN-Gliders	gliding	under definition	under definition	under definition	under definition	under definition		1000 m	

System	Ancillary Data	Data Available	Integration Possibility	Sponsor	Society Value	Installation Life Expectancy
HARP	CTD	upon request and approval		Navy, NOAA, BP	marine mammals, ecosystems, shipping	2005-2020
Argo	CTD		yes			
AQARIUS	CTD	open	no	NASA	water budget/ salinity/rainfall	2011 + 2
SPURS	CTD	open	no	NASA	water budget	2012
CPAM	pitch, roll, compass	NATO countries	yes	NURC	MMRM	2011
NURC-Gliders						
PLOCAN-Gliders	CTD	data policy under definition	depending on system	Spanish Ministry of Science and Innovation	exploration, weather, physical research	2011-2025

Appendix 2
Acronym Definitions

ADCP	Acoustic Doppler Current Profiler	**CTD**	conductivity-temperature-depth
ABB-SIO RAS	Autonomous Bottom Buoys Shirshov Institute of Oceanology, Russian Academy of Sciences	**DASAR**	Directional Autonomous Seafloor Acoustic Recorders
APL-UW	Applied Physics Laboratory, University of Washington	**DFO**	Department of Fisheries and Oceans (Canada)
ARCTIC-NET+	Network of Centres of Excellence of Canada to study the coastal Canadian Arctic	**DONET**	Dense Oceanfloor Network for Earthquakes and Tsunamis
ARGOMARINE	Automated Oil Spill Recognition and Geopositioning Integrated in a Marine Monitoring Network (European Union Framework 7 Programme project	**EARS**	Ecological Acoustic Recorder
		ESTOC	European Station for Time Series in the Ocean
ALOHA	Cabled observatory 100 km north of Oahu, owned and operated by the University of Hawaii	**GOOS**	Global Ocean Observing System
AMAR	Advanced Multi-channel Acoustic Recorder (JASCO)	**HAFOS**	Hybrid Arctic/Antarctic Float Observing System
ANTARES	Astronomy with a Neutrino Telescope and Abyss environmental RESearch (an installation of the EuroSITES European Ocean Observatory Network	**HARP**	High-frequency Acoustic Recording Packages
		HOT	Hawaiian Ocean Time-series
		Hydra	Acoustic telemetry service on the U.S. Pacific Coast
AUR	Autonomous Underwater Recorder	**IMOS**	Integrated Marine Observing System (Australia)
AURALs	Autonomous Underwater Recorder for Acoustic Listening	**IOOS**	Integrated Ocean Observing System (U.S.)
AUSOMS	automatic underwater sound monitoring systems	**IOPAS**	Institute of Oceanology, Polish Academy of Sciences
AUTEC	Atlantic Undersea Test and Evaluation Center (U.S. Navy)		
AWI	Alfred-Wegener-Institut (Germany)	**JAMSTEC**	Japan Agency for Marine-Earth Science and Technology
AZTI	an expert technology center in marine and food research	**JdF Ridge**	Juan de Fuca Ridge
BP	British Petroleum	**LFN/INGV**	Low-Frequency Noise System of the Istituto Nazionale di Geofisica e Vulcanologia
BPR	bottom pressure recorder		
CFI	Canada Foundation for Innovation		
Chl	chlorophyll	**MARU**	marine acoustic recording unit
CMST-DSTO	Centre for Marine Science and Technology-Defense Science and Technology Organisation (Curtin University, Australia)	**MMRM**	marine mammal risk mitigation
		MPA	marine protected area
		NASA	National Aeronautics and Space Administration (U.S.)
CPAM	compact passive acoustic monitor		
cPOD	click detection and passive acoustic monitoring	**NATO**	North Atlantic Treaty Organization
		NEMO	NEutrino Mediterranean Observatory
CTBTO	Comprehensive Test Ban Treaty Organization	**NEPTUNE**	NorthEast Pacific Time-Series Undersea Networked Experiments

NMML	National Marine Mammal Laboratory (U.S.)	**PLOCAN**	Plataforma Oceánica de Canarias
NOAA	National Oceanic and Atmospheric Administration (U.S.)	**PMEL**	Pacific Marine Environmental Laboratory (NOAA)
NOAA EcoFOCI	NOAA Ecosystems & Fisheries-Oceanography Coordinated Investigations	**PMRF**	Pacific Missile Range Facility
		POI	Pacific Oceanological Institute
NSF	National Science Foundation (U.S.)	**SBNMS**	Stellwagen Bank National Marine Sanctuary (U.S.)
NSW	New South Wales (Australia)	**SEAWAYS**	SEAWAYS Ocean Innovation (France)
NURC	NATO Undersea Research Centre	**SEIC**	Sakhalin Energy Investment Company
		SOCAL	Southern California Range Complex
OBSEA	Expandable Seafloor Observatory (Spain)	**SOSUS**	Sound Surveillance System (U.S.)
		SPURS	Salinity Processes in the Upper Ocean Regional Study
ONR	Office of Naval Research (U.S.)		
OOI	Ocean Observatories Initiative (U.S.)	**SVP**	sound velocity profile
OOI RSN	OOI Regional Scale Nodes		
OOS	Ocean Observing System	**UPC**	Universitat Politetécnica de Catalunya
		UQAR	Université du Québec à Rimouski (Canada)
PAL	Passive Acoustic Listener		
PALAOA	Perennial Aco ustic Observatory in the Antarctic Ocean (AWI)	**VENUS**	Victoria Experimental Network Under the Sea (Canada)
PAMBuoy	Passive Acoustic Monitoring Buoy		
Station PAPA	Ocean Station P at 50°N, 145°W	**WA**	Western Australia

Appendix 3
List of Participants

Michael Ainslie, TNO, NETHERLANDS
Tomonari Akamatsu, National Research Institute of Fisheries Engineering, JAPAN
Hussein Alidina, WWF Canada, CANADA
Clara Amorim, ISPA, PORTUGAL
Michel Andre, Technical Univ. of Catalonia, SPAIN
Rex Andrew, Univ. of Washington, USA
Olaf Boebel, Alfred Wegener Institute for Polar and Marine Research, GERMANY
Nicolas Bousquie, CGGVeritas, FRANCE
Ian Boyd, Univ. of St Andrews, UK
Sophie Brasseur, IMARES, NETHERLANDS
Susannah Buchan, Universidad de Concepcion, CHILE
Aurélien Carbonnière, Marine Board-ESF, BELGIUM
Caroline Carter, Scottish Association for Marine Science, UK
Douglas Cato, Defence Science & Technology Organisation/Univ. of Sydney, AUSTRALIA
Ross Chapman, Univ. of Victoria, CANADA
Christopher Clark, Cornell Univ., USA
Daniel Costa, UC Santa Cruz, USA
Sarika Cullis-Suzuki, Univ. of York, UK, CANADA
Del Dakin, Ocean Networks Canada, CANADA
René Dekeling, Defence Materiel Organisation, NETHERLANDS
Eric Delory, PLOCAN - Oceanic Platform of the Canary Islands, SPAIN
Richard Dewey, Univ. of Victoria, CANADA
Brian Dushaw, Univ. of Washington, USA
Christine Erbe, JASCO Applied Sciences, USA
Peter Evans, Sea Watch Foundation, UK
David Farmer, Univ. of Rhode Island, USA
Albert Fischer, IOC/UNESCO, FRANCE
Thomas Folegot, Quiet-Oceans, FRANCE
Lee Freitag, Woods Hole Oceanographic Institution, USA
George Frisk, Florida Atlantic Univ./Woods Hole Oceanographic Institution, USA
Jason Gedamke, NOAA, USA
Roger Gentry, ProScience Consulting LLC, USA
Robert Gisiner, U.S. Navy, USA
Tom Gross, IOC / UNESCO, FRANCE
Anthony Hawkins, Loughine Ltd., UK
Paul Holthus, World Ocean Council, USA
Vincent Janik, Univ. of St Andrews, UK

Yong-Min Jiang, NURC, ITALY
Darlene Ketten, Harvard Medical School/Woods Hole Oceanographic Institution, USA
Lars Kindermann, Alfred Wegener Institute for Polar and Marine Research, GERMANY
Zygmunt Klusek, Institute of Oceanology Polish Academy of Sciences, POLAND
Fenghua Li, Institute of Acoustics, Chinese Academy of Sciences, CHINA
Ellen Livingston, ONR Global, UK
David Mann, Univ. of South Florida, USA
Megan McKenna, U.S. Marine Mammal Commission, USA
Jennifer Miksis-Olds, Pennsylvania State Univ., USA
Patrick Miller, Univ. of St Andrews, UK
David Moretti, Naval Undersea Warfare Center, USA
Jeffrey Nystuen, Univ. of Washington, USA
Michael Porter, Heat, Light, and Sound Research, USA
Mark Prior, Comprehensive Test Ban Treaty Organisation, AUSTRIA
Andy Radford, Univ. of Bristol, UK
Stephen Robinson, NPL, UK
Gail Scowcroft, Univ. of Rhode Island, USA
Sophie Seeyave, POGO, UK
George Shillinger, Stanford Univ., USA
Yvan Simard, Fisheries & Oceans Canada, CANADA
Steve Simpson, Univ. of Bristol, UK
Brandon Southall, SEA, Inc., USA
Michael Stocker, Ocean Conservation Research, USA
Frank Thomsen, DHI, DENMARK
Jakob Tougaard, Aarhus Univ., DENMARK
Peter Tyack, Woods Hole Oceanographic Institution, USA
Ed Urban, Scientific Committee on Oceanic Research, USA
Alexander Vedenev, Shirshov Institute of Oceanology, RAS, RUSSIA
Anne-Isabelle Vichot, French Navy, FRANCE
Wendy Watson-Wright, IOC/UNESCO, FRANCE
Michael Weise, Office of Naval Research, USA
Rob Williams, Univ. of St Andrews, UK
Dietrich Wittekind, DW-ShipConsult GmbH/ Okeanos Foundation, GERMANY
Peter Worcester, UC San Diego, USA
John Young, Resource Access International, USA
Manell Zakharia, NURC, ITALY

REPORT DOCUMENTATION PAGE		*Form Approved* *OMB No. 0704-0188*

The public reporting burden for this collection of information is estimated to average 1 hour per response, including the time for reviewing instructions, searching existing data sources, gathering and maintaining the data needed, and completing and reviewing the collection of information. Send comments regarding this burden estimate or any other aspect of this collection of information, including suggestions for reducing the burden, to Department of Defense, Washington Headquarters Services, Directorate for Information Operations and Reports (0704-0188), 1215 Jefferson Davis Highway, Suite 1204, Arlington, VA 22202-4302. Respondents should be aware that notwithstanding any other provision of law, no person shall be subject to any penalty for failing to comply with a collection of information if it does not display a currently valid OMB control number.
PLEASE DO NOT RETURN YOUR FORM TO THE ABOVE ADDRESS.

1. REPORT DATE *(DD-MM-YYYY)* 10/15/2015	**2. REPORT TYPE** Final Report	**3. DATES COVERED** *(From - To)* 1 Dec 2012 - 31 July 2015

4. TITLE AND SUBTITLE APL-UW Deep Water Propagation: Philippine Sea Signal Physics and North Pacific Ambient Noise	**5a. CONTRACT NUMBER**
	5b. GRANT NUMBER N00014-13-1-0009
	5c. PROGRAM ELEMENT NUMBER
6. AUTHOR(S) Rex K. Andrew	**5d. PROJECT NUMBER**
	5e. TASK NUMBER
	5f. WORK UNIT NUMBER

7. PERFORMING ORGANIZATION NAME(S) AND ADDRESS(ES) Applied Physics Laboratory University of Washington 1013 NE 40th Street Seattle, W 98105-6698	**8. PERFORMING ORGANIZATION REPORT NUMBER**
9. SPONSORING/MONITORING AGENCY NAME(S) AND ADDRESS(ES) Robert H. Headrick, Code 322 Office of Naval Research 875 North Randolph Street Arlington, VA 22203-1995	**10. SPONSOR/MONITOR'S ACRONYM(S)** ONR
	11. SPONSOR/MONITOR'S REPORT NUMBER(S)

12. DISTRIBUTION/AVAILABILITY STATEMENT
Approved for Public Release: distribution is unlimited

13. SUPPLEMENTARY NOTES

14. ABSTRACT
Grant involved two inter-related ASW components: signal and noise. Analysis of signal datasets from PhilSea09 and PhilSea10 showed (1) small biases in Munk-Zachariasen and Flatte-Dashen predictions of log-amplitude variance at 284~Hz at 107~km, (2) Flatte-Dashen prediction of pulse spread at 200~Hz and 300~Hz at 510~km was quite accurate (vice findings at lower frequencies and larger ranges) (3) observed pulse intensity distribution at 200~Hz and 510~km (near exponential) not consistent with observed pulse spread (very small). Low-Frequency ambient noise from 1994-2007 is decreasing at seven receivers throughout the N. Pacific. Further ambient noise collection suspended by USNavy.

15. SUBJECT TERMS
Underwater acoustic, long-range propagation, low-frequency, random media, pulse spread, log-amplitude variance, intensity, ambient noise, North Pacific, Philippine Sea

16. SECURITY CLASSIFICATION OF:			**17. LIMITATION OF ABSTRACT**	**18. NUMBER OF PAGES**	**19a. NAME OF RESPONSIBLE PERSON** Rex K. Andrew
a. REPORT	**b. ABSTRACT**	**c. THIS PAGE**			**19b. TELEPHONE NUMBER** *(Include area code)*
U	U	U	UU	314	206-543-1250